ISSN 1007-9327 (print)
ISSN 2219-2840 (online)

World Journal of *Gastroenterology*

World J Gastroenterol 2012 June 21; 18(23): 2887-3034

Baishideng Publishing Group
www.wjgnet.com

WJG World Journal of Gastroenterology

A peer-reviewed, online, open-access journal of gastroenterology and hepatology

Editorial Board

2010-2013

The *World Journal of Gastroenterology* Editorial Board consists of 1352 members, representing a team of worldwide experts in gastroenterology and hepatology. They are from 64 countries, including Albania (1), Argentina (8), Australia (33), Austria (15), Belgium (14), Brazil (13), Brunei Darussalam (1), Bulgaria (2), Canada (21), Chile (3), China (82), Colombia (1), Croatia (2), Cuba (1), Czech (6), Denmark (9), Ecuador (1), Egypt (4), Estonia (2), Finland (8), France (29), Germany (87), Greece (22), Hungary (11), India (32), Indonesia (2), Iran (10), Ireland (6), Israel (13), Italy (124), Japan (140), Jordan (2), Kuwait (1), Lebanon (4), Lithuania (2), Malaysia (1), Mexico (11), Morocco (1), Moldova (1), Netherlands (32), New Zealand (2), Norway (13), Pakistan (2), Poland (11), Portugal (6), Romania (4), Russia (1), Saudi Arabia (3), Serbia (3), Singapore (11), Slovenia (1), South Africa (3), South Korea (46), Spain (43), Sri Lanka (1), Sweden (17), Switzerland (12), Thailand (1), Trinidad and Tobago (1), Turkey (30), United Arab Emirates (2), United Kingdom (95), United States (285), and Uruguay (1).

Phillip S Oates, *Perth*
Ross C Smith, *Sydney*
Kevin J Spring, *Brisbane*
Philip G Dinning, *Koagarah*
Christopher Christophi, *Melbourne*
Cuong D Tran, *North Adelaide*
Shan Rajendra, *Tasmania*
Rajvinder Singh, *Adelaide*
William Kemp, *Melbourne*
Phil Sutton, *Melbourne*
Richard Anderson, *Victoria*
Vance Matthews, *Melbourne*
Alexander G Heriot, *Melbourne*
Debbie Trinder, *Fremantle*
Ian C Lawrance, *Perth*
Adrian G Cummins, *Adelaide*
John K Olynyk, *Fremantle*
Alex Boussioutas, *Melbourne*
Emilia Prakoso, *Sydney*
Robert JL Fraser, *Daw Park*

Austria

Wolfgang Mikulits, *Vienna*
Alfred Gangl, *Vienna*
Dietmar Öfner, *Salzburg*
Georg Roth, *Vienna*
Herwig R Cerwenka, *Graz*
Ashraf Dahaba, *Graz*
Markus Raderer, *Vienna*
Alexander M Hirschl, *Wien*
Thomas Wild, *Kapellerfeld*
Peter Ferenci, *Vienna*
Valentin Fuhrmann, *Vienna*
Kurt Lenz, *Linz*
Markus Peck-Radosavljevic, *Vienna*
Michael Trauner, *Vienna*
Stefan Riss, *Vienna*

Belgium

Rudi Beyaert, *Gent*
Inge I Depoortere, *Leuven*
Olivier Detry, *Liège*
Benedicte Y De Winter, *Antwerp*
Etienne M Sokal, *Brussels*
Marc Peeters, *De Pintelaan*
Eddie Wisse, *Keerbergen*
Jean-Yves L Reginster, *Liège*
Mark De Ridder, *Brussel*
Freddy Penninckx, *Leuven*
Kristin Verbeke, *Leuven*
Lukas Van Oudenhove, *Leuven*
Leo van Grunsven, *Brussels*
Philip Meuleman, *Ghent*

Brazil

Heitor Rosa, *Goiania*
Roberto J Carvalho-Filho, *Sao Paulo*
Damiao Carlos Moraes Santos, *Rio de Janeiro*
Marcelo Lima Ribeiro, *Braganca Paulista*
Eduardo Garcia Vilela, *Belo Horizonte*
Jaime Natan Eisig, *São Paulo*
Andre Castro Lyra, *Salvador*
José Liberato Ferreira Caboclo, *Brazil*
Yukie Sato-Kuwabara, *São Paulo*
Raquel Rocha, *Salvador*
Paolo R Salvalaggio, *Sao Paulo*
Ana Cristina Simões e Silva, *Belo Horizonte*
Joao Batista Teixeira Rocha, *Santa Maria*

Brunei Darussalam

Vui Heng Chong, *Bandar Seri Begawan*

Bulgaria

Zahariy Krastev, *Sofia*
Mihaela Petrova, *Sofia*

Canada

Eldon Shaffer, *Calgary*
Nathalie Perreault, *Sherbrooke*
Philip H Gordon, *Montreal*
Ram Prakash Galwa, *Ottawa*
Baljinder Singh Salh, *Vancouver*
Claudia Zwingmann, *Montreal*
Alain Bitton, *Montreal*
Pingchang Yang, *Hamilton*
Michael F Byrne, *Vancouver*
Andrew L Mason, *Alberta*
John K Marshall, *Hamilton Ontario*
Kostas Pantopoulos, *Montreal*
Waliul Khan, *Ontario*
Eric M Yoshida, *Vancouver*
Geoffrey C Nguyen, *Toronto*
Devendra K Amre, *Montreal*
Tedros Bezabeh, *Winnipeg*
Wangxue Chen, *Ottawa*
Qiang Liu, *Saskatoon*

Chile

De Aretxabala Xabier, *Santiago*
Marcelo A Beltran, *La Serena*
Silvana Zanlungo, *Santiago*

China

Chi-Hin Cho, *Hong Kong*
Chun-Qing Zhang, *Jinan*
Ren Xiang Tan, *Nanjing*
Fei Li, *Beijing*
Hui-Jie Bian, *Xi'an*
Xiao-Peng Zhang, *Beijing*
Xing-Hua Lu, *Beijing*
Fu-Sheng Wang, *Beijing*
An-Gang Yang, *Xi'an*
Xiao-Ping Chen, *Wuhan*
Zong-Jie Cui, *Beijing*
Ming-Liang He, *Hong Kong*
Yuk-Tong Lee, *Hong Kong*
Qin Su, *Beijing*
Jian-Zhong Zhang, *Beijing*
Paul Kwong-Hang Tam, *Hong Kong*
Wen-Rong Xu, *Zhenjiang*
Chun-Yi Hao, *Beijing*
San-Jun Cai, *Shanghai*
Simon Law, *Hong Kong*
Yuk Him Tam, *Hong Kong*
De-Liang Fu, *Shanghai*
Eric WC Tse, *Hong Kong*
Justin CY Wu, *Hong Kong*
Nathalie Wong, *Hong Kong*
Jing Yuan Fang, *Shanghai*
Yi-Min Mao, *Shanghai*
Wei-Cheng You, *Beijing*
Xiang-Dong Wang, *Shanghai*
Xuan Zhang, *Beijing*
Zhao-Shen Li, *Shanghai*
Guang-Wen Cao, *Shanghai*
En-min Li, *Shantou*
Yu-Yuan Li, *Guangzhou*
Fook Hong Ng, *Hong Kong*
Hsiang-Fu Kung, *Hong Kong*
Wai Lun Law, *Hong Kong*
Eric CH Lai, *Hong Kong*
Jun Yu, *Hong Kong*
Ze-Guang Han, *Shanghai*
Bian zhao-xiang, *Hong Kong*
Wei-Dong Tong, *Chongqing*

Colombia

Germán Campuzano-Maya, *Medellín*

Croatia

Tamara Cacev, *Zagreb*
Marko Duvnjak, *Zagreb*

Cuba

Damian C Rodriguez, *Havana*

Czech

Milan Jirsa, *Praha*
Pavel Trunečka, *Prague*
Jan Bures, *Hradec Kralove*
Marcela Kopacova, *Hradec Kralove*
Ondrej Slaby, *Brno*
Radan Bruha, *Prague*

Denmark

Asbjørn M Drewes, *Aalborg*
Leif Percival Andersen, *Copenhagen*
Jan Mollenhauer, *Odense C*
Morten Frisch, *Copenhagen S*
Jorgen Rask-Madsen, *Skodsborg*
Morten Hylander Møller, *Holte*
Søren Rafaelsen, *Vejle*
Vibeke Andersen, *Aabenraa*
Ole Haagen Nielsen, *Herlev*

Ecuador

Fernando E Sempértegui, *Quito*

Egypt

Zeinab Nabil Ahmed Said, *Cairo*
Hussein M Atta, *El-Minia*
Asmaa Gaber Abdou, *Shebein Elkom*

Maha Maher Shehata, *Mansoura*

Estonia

Riina Salupere, *Tartu*
Tamara Vorobjova, *Tartu*

Finland

Saila Kauhanen, *Turku*
Pauli Antero Puolakkainen, *Turku*
Minna Nyström, *Helsinki*
Juhani Sand, *Tampere*
Jukka-Pekka Mecklin, *Jyvaskyla*
Lea Veijola, *Helsinki*
Kaija-Leena Kolho, *Helsinki*
Thomas Kietzmann, *Oulu*

France

Boris Guiu, *Dijon*
Baumert F Thomas, *Strasbourg*
Alain L Servin, *Châtenay-Malabry*
Patrick Marcellin, *Paris*
Jean-Jacques Tuech, *Rouen*
Francoise L Fabiani, *Angers*
Jean-Luc Faucheron, *Grenoble*
Philippe Lehours, *Bordeaux*
Stephane Supiot, *Nantes*
Lionel Bueno, *Toulouse*
Flavio Maina, *Marseille*
Paul Hofman, *Nice*
Abdel-Majid Khatib, *Paris*
Annie Schmid-Alliana, *Nice cedex 3*
Frank Zerbib, *Bordeaux Cedex*
Rene Gerolami Santandera, *Marseille*
Sabine Colnot, *Paris*
Catherine Daniel, *Lille Cedex*
Thabut Dominique, *Paris*
Laurent Huwart, *Paris*
Alain Braillon, *Amiens*
Bruno Bonaz, *Grenoble*
Evelyne Schvoerer, *Strasbourg*
M Coeffier, *Rouen*
Mathias Chamaillard, *Lille*
Hang Nguyen, *Clermont-Ferrand*
Veronique Vitton, *Marseille*
Alexis Desmoulière, *Limoges*
Juan Iovanna, *Marseille*

Germany

Hans L Tillmann, *Leipzig*
Stefan Kubicka, *Hannover*
Elke Cario, *Essen*
Hans Scherubl, *Berlin*
Harald F Teutsch, *Ulm*
Peter Konturek, *Erlangen*
Thilo Hackert, *Heidelberg*
Jurgen M Stein, *Frankfurt*
Andrej Khandoga, *Munich*
Karsten Schulmann, *Bochum*
Jutta Elisabeth Lüttges, *Riegelsberg*
Wolfgang Hagmann, *Heidelberg*
Hubert Blum, *Freiburg*
Thomas Bock, *Berlin*
Christa Buechler, *Regensburg*
Christoph F Dietrich, *Bad Mergentheim*
Ulrich R Fölsch, *Kiel*
Nikolaus Gassler, *Aachen*
Markus Gerhard, *Munich*
Dieter Glebe, *Giessen*
Klaus R Herrlinger, *Stuttgart*
Eberhard Hildt, *Berlin*
Joerg C Hoffmann, *Ludwigshafen*
Joachim Labenz, *Siegen*
Peter Malfertheiner, *Magdeburg*
Sabine Mihm, *Göttingen*
Markus Reiser, *Bochum*
Steffen Rickes, *Magdeburg*
Andreas G Schreyer, *Regensburg*
Henning Schulze-Bergkamen, *Heidelberg*
Ulrike S Stein, *Berlin*
Wolfgang R Stremmel, *Heidelberg*
Fritz von Weizsäcker, *Berlin*
Stefan Wirth, *Wuppertal*
Dean Bogoevski, *Hamburg*
Bruno Christ, *Halle/Saale*
Peter N Meier, *Hannover*
Stephan Johannes Ott, *Kiel*
Arndt Vogel, *Hannover*
Dirk Haller, *Freising*
Jens Standop, *Bonn*
Jonas Mudter, *Erlangen*
Jürgen Büning, *Lübeck*
Matthias Ocker, *Erlangen*
Joerg Trojan, *Frankfurt*
Christian Trautwein, *Aachen*
Jorg Kleeff, *Munich*
Christian Rust, *Munich*
Claus Hellerbrand, *Regensburg*
Elke Roeb, *Giessen*
Erwin Biecker, *Siegburg*
Ingmar Königsrainer, *Tübingen*
Jürgen Borlak, *Hannover*
Axel M Gressner, *Aachen*
Oliver Mann, *Hamburg*
Marty Zdichavsky, *Tübingen*
Christoph Reichel, *Bad Brückenau*
Nils Habbe, *Marburg*
Thomas Wex, *Magdeburg*
Frank Ulrich Weiss, *Greifswald*
Manfred V Singer, *Mannheim*
Martin K Schilling, *Homburg*
Philip D Hard, *Giessen*
Michael Linnebacher, *Rostock*
Ralph Graeser, *Freiburg*
Rene Schmidt, *Freiburg*
Robert Obermaier, *Freiburg*
Sebastian Mueller, *Heidelberg*
Andrea Hille, *Goettingen*
Klaus Mönkemüller, *Bottrop*
Elfriede Bollschweiler, *Köln*
Siegfried Wagner, *Deggendorf*
Dieter Schilling, *Mannheim*
Joerg F Schlaak, *Essen*
Michael Keese, *Frankfurt*
Robert Grützmann, *Dresden*
Ali Canbay, *Essen*
Dirk Domagk, *Muenster*
Jens Hoeppner, *Freiburg*
Frank Tacke, *Aachen*
Patrick Michl, *Marburg*
Alfred A Königsrainer, *Tübingen*
Kilian Weigand, *Heidelberg*
Mohamed Hassan, *Duesseldorf*
Gustav Paumgartner, *Munich*
Philipe N Khalil, *Munich*
Martin Storr, *Munich*

Greece

Andreas Larentzakis, *Athens*
Tsianos Epameinondas, *Ioannina*
Elias A Kouroumalis, *Heraklion*
Helen Christopoulou-Aletra, *Thessaloniki*
George Papatheodoridis, *Athens*
Ioannis Kanellos, *Thessaloniki*
Michael Koutsilieris, *Athens*
T Choli-Papadopoulou, *Thessaloniki*
Emanuel K Manesis, *Athens*
Evangelos Tsiambas, *Ag Paraskevi Attiki*
Konstantinos Mimidis, *Alexandroupolis*
Spilios Manolakopoulos, *Athens*
Spiros Sgouros, *Athens*
Ioannis E Koutroubakis, *Heraklion*
Stefanos Karagiannis, *Athens*
Spiros Ladas, *Athens*
Elena Vezali, *Athens*
Dina G Tiniakos, *Athens*
Ekaterini Chatzaki, *Alexandroupolis*
Dimitrios Roukos, *Ioannina*
George Sgourakis, *Athens*
Maroulio Talieri, *Athens*

Hungary

Peter L Lakatos, *Budapest*
Yvette Mándi, *Szeged*
Ferenc Sipos, *Budapest*
György M Buzás, *Budapest*
László Czakó, *Szeged*
Peter Hegyi, *Szeged*
Zoltan Rakonczay, *Szeged*
Gyula Farkas, *Szeged*
Zsuzsa Szondy, *Debrecen*
Gabor Veres, *Budapest*
Zsuzsa Schaff, *Budapest*

India

Philip Abraham, *Mumbai*
Sri P Misra, *Allahabad*
Ramesh Roop Rai, *Jaipur*
Nageshwar D Reddy, *Hyderabad*
Rakesh Kumar Tandon, *New Delhi*
Jai Dev Wig, *Chandigarh*
Uday C Ghoshal, *Lucknow*
Pramod Kumar Garg, *New Delhi*
Barjesh Chander Sharma, *New Delhi*
Gopal Nath, *Varanasi*
Bhupendra Kumar Jain, *Delhi*
Devinder Kumar Dhawan, *Chandigarh*
Ashok Kumar, *Lucknow*
Benjamin Perakath, *Tamil Nadu*
Debidas Ghosh, *Midnpore*
Pankaj Garg, *Panchkula*
Samiran Nundy, *New Delhi*
Virendra Singh, *Chandigarh*
Bikash Medhi, *Chandigarh*
Radha K Dhiman, *Chandigarh*
Vandana Panda, *Mumbai*
Vineet Ahuja, *New Delhi*
SV Rana, *Chandigarh*

Deepak N Amarapurkar, *Mumbai*
Abhijit Chowdhury, *Kolkata*
Jasbir Singh, *Kurukshetra*
B Mittal, *Lucknow*
Sundeep Singh Saluja, *New Delhi*
Pradyumna Kumar Mishra, *Mumbai*
Runu Chakravarty, *Kolkata*
Nagarajan Perumal, *New Delhi*

Indonesia

David handojo Muljono, *Jakarta*
Andi Utama, *Tangerang*

Iran

Seyed-Moayed Alavian, *Tehran*
Reza Malekzadeh, *Tehran*
Peyman Adibi, *Isfahan*
Alireza Mani, *Tehran*
Seyed Mohsen Dehghani, *Shiraz*
Mohammad Abdollahi, *Tehran*
Majid Assadi, *Bushehr*
Arezoo Aghakhani, *Tehran*
Marjan Mohammadi, *Tehran*
Fariborz Mansour-Ghanaei, *Rasht*

Ireland

Ross McManus, *Dublin*
Billy Bourke, *Dublin*
Catherine Greene, *Dublin*
Ted Dinan, *Cork*
Marion Rowland, *Dublin*

Israel

Abraham R Eliakim, *Haifa*
Simon Bar-Meir, *Tel Hashomer*
Ami D Sperber, *Beer-Sheva*
Boris Kirshtein, *Beer Sheva*
Mark Pines, *Bet Dagan*
Menachem Moshkowitz, *Tel-Aviv*
Ron Shaoul, *Haifa*
Shmuel Odes, *Beer Sheva*
Sigal Fishman, *Tel Aviv*
Alexander Becker, *Afula*
Assy Nimer, *Safed*
Eli Magen, *Ashdod*
Amir Shlomai, *Tel-Aviv*

Italy

Mauro Bortolotti, *Bologna*
Gianlorenzo Dionigi, *Varese*
Fiorucci Stefano, *Perugia*
Roberto Berni Canani, *Naples*
Ballarin Roberto, *Modena*
Bruno Annibale, *Roma*
Vincenzo Stanghellini, *Bologna*
Giovanni B Gaeta, *Napoli*
Claudio Bassi, *Verona*
Mauro Bernardi, *Bologna*
Giuseppe Chiarioni, *Valeggio*
Michele Cicala, *Rome*
Dario Conte, *Milano*
Francesco Costa, *Pisa*
Giovanni D De Palma, *Naples*
Giammarco Fava, *Ancona*
Francesco Feo, *Sassari*
Edoardo G Giannini, *Genoa*
Fabio Grizzi, *Milan*
Salvatore Gruttadauria, *Palermo*
Pietro Invernizzi, *Milan*
Ezio Laconi, *Cagliari*
Giuseppe Montalto, *Palermo*
Giovanni Musso, *Torino*
Gerardo Nardone, *Napoli*
Valerio Nobili, *Rome*
Raffaele Pezzilli, *Bologna*
Alberto Piperno, *Monza*
Anna C Piscaglia, *Roma*
Piero Portincasa, *Bari*
Giovanni Tarantino, *Naples*
Cesare Tosetti, *Porretta Terme*
Alessandra Ferlini, *Ferrara*
Alessandro Ferrero, *Torino*
Donato F Altomare, *Bari*
Giovanni Milito, *Rome*
Giuseppe Sica, *Rome*
Guglielmo Borgia, *Naples*
Giovanni Latella, *L'Aquila*
Salvatore Auricchio, *Naples*
Alberto Biondi, *Rome*
Alberto Tommasini, *Trieste*
Antonio Basoli, *Roma*
Giuliana Decorti, *Trieste*
Marco Silano, *Roma*
Michele Reni, *Milan*
Pierpaolo Sileri, *Rome*
Achille Iolascon, *Naples*
Alessandro Granito, *Bologna*
Angelo A Izzo, *Naples*
Giuseppe Currò, *Messina*
Pier Mannuccio Mannucci, *Milano*
Marco Vivarelli, *Bologna*
Massimo Levrero, *Rome*
Massimo Rugge, *Padova*
Paolo Angeli, *Padova*
Silvio Danese, *Milano*
Antonello Trecca, *Rome*
Antonio Gasbarrini, *Rome*
Cesare Ruffolo, *Treviso*
Massimo Falconi, *Verona*
Fausto Catena, *Bologna*
Francesco Manguso, *Napoli*
Giancarlo Mansueto, *Verona*
Luca Morelli, *Trento*
Marco Scarpa, *Padova*
Mario M D'Elios, *Florence*
Francesco Luzza, *Catanzaro*
Franco Roviello, *Siena*
Guido Torzilli, *Rozzano Milano*
Luca Frulloni, *Verona*
Lucia Malaguarnera, *Catania*
Lucia Ricci Vitiani, *Rome*
Mara Massimi, *L'Aquila*
Mario Pescatori, *Rome*
Mario Rizzetto, *Torino*
Mirko D'Onofrio, *Verona*
Nadia Peparini, *Rome*
Paola De Nardi, *Milan*
Paolo Aurello, *Rome*
Piero Amodio, *Padova*
Riccardo Nascimbeni, *Brescia*
Vincenzo Villanacci, *Brescia*
Vittorio Ricci, *Pavia*
Silvia Fargion, *Milan*
Luigi Bonavina, *Milano*
Oliviero Riggio, *Rome*
Fabio Pace, *Milano*
Gabrio Bassotti, *Perugia*
Giulio Marchesini, *Bologna*
Roberto de Franchis, *Milano*
Giovanni Monteleone, *Rome*
C armelo Scarpignato, *Parma*
Luca VC Valenti, *Milan*
Urgesi Riccardo, *Rome*
Marcello Persico, *Naples*
Antonio Moschetta, *Bari*
Luigi Muratori, *Bologna*
Angelo Zullo, *Roma*
Vito Annese, *Florence*
Simone Lanini, *Rome*
Alessandro Grasso, *Savona*
Giovanni Targher, *Verona*
Domenico Girelli, *Verona*
Alessandro Cucchetti, *Bologna*
Fabio Marra, *Florence*
Michele Milella, *Rome*
Francesco Franceschi, *Rome*
Giuseppina De Petro, *Brescia*
Salvatore Leonardi, *Catania*
Cristiano Simone, *Santa Maria Imbaro*
Bernardino Rampone, *Salerno*
Francesco Crea, *Pisa*
Walter Fries, *Messina*
Antonio Craxì, *Palermo*
Gerardo Rosati, *Potenza*
Mario Guslandi, *Milano*
Gianluigi Giannelli, *Bari*
Paola Loria, *Modena*
Paolo Sorrentino, *Avellino*
Armando Santoro, *Rozzano*
Gabriele Grassi, *Trieste*
Antonio Orlacchio, *Rome*

Japan

Tsuneo Kitamura, *Chiba*
Katsutoshi Yoshizato, *Higashihiroshima*
Masahiro Arai, *Tokyo*
Shinji Tanaka, *Hiroshima*
Keiji Hirata, *Kitakyushu*
Yoshio Shirai, *Niigata*
Susumu Ohmada, *Maebashi*
Kenichi Ikejima, *Tokyo*
Masatoshi Kudo, *Osaka*
Yoshiaki Murakami, *Hiroshima*
Masahiro Tajika, *Nagoya*
Kentaro Yoshika, *Toyoake*
Kyoichi Adachi, *Izumo*
Yasushi Adachi, *Sapporo*
Takafumi Ando, *Nagoya*
Akira Andoh, *Otsu*
Hitoshi Asakura, *Tokyo*
Mitsuhiro Fujishiro, *Tokyo*
Toru Hiyama, *Higashihiroshima*
Yutaka Inagaki, *Kanagawa*
Hiromi Ishibashi, *Nagasaki*
Shunji Ishihara, *Izumo*
Toru Ishikawa, *Niigata*
Yoshiaki Iwasaki, *Okayama*
Terumi Kamisawa, *Tokyo*

Norihiro Kokudo, *Tokyo*
Shin Maeda, *Tokyo*
Yasushi Matsuzaki, *Ibaraki*
Kenji Miki, *Tokyo*
Hiroto Miwa, *Hyogo*
Yoshiharu Motoo, *Kanazawa*
Kunihiko Murase, *Tusima*
Atsushi Nakajima, *Yokohama*
Yuji Naito, *Kyoto*
Hisato Nakajima, *Tokyo*
Hiroki Nakamura, *Yamaguchi*
Shotaro Nakamura, *Fukuoka*
Mikio Nishioka, *Niihama*
Hirohide Ohnishi, *Akita*
Kazuichi Okazaki, *Osaka*
Morikazu Onji, *Ehime*
Satoshi Osawa, *Hamamatsu*
Hidetsugu Saito, *Tokyo*
Yutaka Saito, *Tokyo*
Yasushi Sano, *Kobe*
Tomohiko Shimatani, *Kure*
Yukihiro Shimizu, *Toyama*
Shinji Shimoda, *Fukuoka*
Masayuki Sho, *Nara*
Hidekazu Suzuki, *Tokyo*
Shinji Togo, *Yokohama*
Satoshi Yamagiwa, *Niigata*
Takayuki Yamamoto, *Yokkaichi*
Hiroshi Yoshida, *Tokyo*
Norimasa Yoshida, *Kyoto*
Akihito Nagahara, *Tokyo*
Hiroaki Takeuchi, *Kochi*
Keiji Ogura, *Tokyo*
Kotaro Miyake, *Tokushima*
Mitsunori Yamakawa, *Yamagata*
Naoaki Sakata, *Sendai*
Naoya Kato, *Tokyo*
Satoshi Mamori, *Hyogo*
Shogo Kikuchi, *Aichi*
Shoichiro Sumi, *Kyoto*
Susumu Ikehara, *Osaka*
Taketo Yamaguchi, *Chiba*
Tokihiko Sawada, *Tochigi*
Tomoharu Yoshizumi, *Fukuoka*
Toshiyuki Ishiwata, *Tokyo*
Yasuhiro Fujino, *Akashi*
Yasuhiro Koga, *Isehara city*
Yoshihisa Takahashi, *Tokyo*
Yoshitaka Takuma, *Okayama*
Yutaka Yata, *Maebashi-city*
Itaru Endo, *Yokohama*
Kazuo Chijiiwa, *Miyazaki*
Kouhei Fukushima, *Sendai*
Masahiro Iizuka, *Akita*
Mitsuyoshi Urashima, *Tokyo*
Munechika Enjoji, *Fukuoka*
Takashi Kojima, *Sapporo*
Takumi Kawaguchi, *Kurume*
Yoshiyuki Ueno, *Sendai*
Yuichiro Eguchi, *Saga*
Akihiro Tamori, *Osaka*
Atsushi Masamune, *Sendai*
Atsushi Tanaka, *Tokyo*
Hitoshi Tsuda, *Tokyo*
Takashi Kobayashi, *Tokyo*
Akimasa Nakao, *Nagogya*
Hiroyuki Uehara, *Osaka*
Masahito Uemura, *Kashihara*
Satoshi Tanno, *Sapporo*
Toshinari Takamura, *Kanazawa*
Yohei Kida, *Kainan*

Masanori Hatakeyama, *Tokyo*
Satoru Kakizaki, *Gunma*
Shuhei Nishiguchi, *Hyogo*
Yuichi Yoshida, *Osaka*
Manabu Morimoto, *Japan*
Mototsugu Kato, *Sapporo*
Naoki Ishii, *Tokyo*
Noriko Nakajima, *Tokyo*
Nobuhiro Ohkohchi, *Tsukuba*
Takanori Kanai, *Tokyo*
Kenichi Goda, *Tokyo*
Mitsugi Shimoda, *Mibu*
Zenichi Morise, *Nagoya*
Hitoshi Yoshiji, *Kashihara*
Takahiro Nakazawa, *Nagoya*
Utaroh Motosugi, *Yamanashi*
Nobuyuki Matsuhashi, *Tokyo*
Yasuhiro Kodera, *Nagoya*
Takayoshi Ito, *Tokyo*
Yasuhito Tanaka, *Nagoya*
Haruhiko Sugimura, *Hamamatsu*
Hiroki Yamaue, *Wakayama*
Masao Ichinose, *Wakayama*
Takaaki Arigami, *Kagoshima*
Nobuhiro Zaima, *Nara*
Naoki Tanaka, *Matsumoto*
Satoru Motoyama, *Akita*
Tomoyuki Shibata, *Toyoake*
Tatsuya Ide, *Kurume*
Tsutomu Fujii, *Nagoya*
Osamu Kanauchi, *Toky*
Atsushi Irisawa, *Aizuwakamatsu*
Hikaru Nagahara, *Tokyo*
Keiji Hanada, *Onomichi*
Keiichi Mitsuyama, *Fukuoka*
Shin Maeda, *Yokohama*
Takuya Watanabe, *Niigata*
Toshihiro Mitaka, *Sapporo*
Yoshiki Murakami, *Kyoto*
Tadashi Shimoyama, *Hirosaki*

Jordan

Ismail Matalka, *Irbid*
Khaled Jadallah, *Irbid*

Kuwait

Islam Khan, *Safat*

Lebanon

Bassam N Abboud, *Beirut*
Rami Moucari, *Beirut*
Ala I Sharara, *Beirut*
Rita Slim, *Beirut*

Lithuania

Giedrius Barauskas, *Kaunas*
Limas Kupcinskas, *Kaunas*

Malaysia

Andrew Seng Boon Chua, *Ipoh*

Mexico

Saúl Villa-Trevio, *México*
Omar Vergara-Fernandez, *Mexico*
Diego Garcia-Compean, *Monterrey*
Arturo Panduro, *Jalisco*
Miguel Angel Mercado, *Distrito Federal*
Richard A Awad, *Mexico*
Aldo Torre Delgadillo, *México*
Paulino Martínez Hernández Magro, *Celaya*
Carlos A Aguilar-Salinas, *Mexico*
Jesus K Yamamoto-Furusho, *Mexico*

Morocco

Samir Ahboucha, *Khouribga*

Moldova

Igor Mishin, *Kishinev*

Netherlands

Ulrich Beuers, *Amsterdam*
Albert Frederik Pull ter Gunne, *Tilburg*
Jantine van Baal, *Heidelberglaan*
Wendy Wilhelmina Johanna de Leng, *Utrecht*
Gerrit A Meijer, *Amsterdam*
Lee Bouwman, *Leiden*
J Bart A Crusius, *Amsterdam*
Frank Hoentjen, *Haarlem*
Servaas Morré, *Amsterdam*
Chris JJ Mulder, *Amsterdam*
Paul E Sijens, *Groningen*
Karel van Erpecum, *Utrecht*
BW Marcel Spanier, *Arnhem*
Misha Luyer, *Sittard*
Pieter JF de Jonge, *Rotterdam*
Robert Christiaan Verdonk, *Groningen*
John Plukker, *Groningen*
Maarten Tushuizen, *Amsterdam*
Wouter de Herder, *Rotterdam*
Erwin G Zoetendal, *Wageningen*
Robert J de Knegt, *Rotterdam*
Albert J Bredenoord, *Nieuwegein*
Annemarie de Vries, *Rotterdam*
Astrid van der Velde, *Ede*
Lodewijk AA Brosens, *Utrecht*
James CH Hardwick, *Leiden*
Loes van Keimpema, *Nijmegen*
WJ de Jonge, *Amsterdam*
Zuzana Zelinkova, *Rotterdam*
LN van Steenbergen, *Eindhoven*
Frank G Schaap, *Amsterdam*
Jeroen Maljaars, *Leiden*

New Zealand

Andrew S Day, *Christchurch*
Max S Petrov, *Auckland*

Norway

Espen Melum, *Oslo*

Trine Olsen, *Tromsø*
Eyvind J Paulssen, *Tromsø*
Rasmus Goll, *Tromsø*
Asle W Medhus, *Oslo*
Jon Arne Søreide, *Stavanger*
Kjetil Soreide, *Stavanger*
Reidar Fossmark, *Trondheim*
Trond Peder Flaten, *Trondheim*
Olav Dalgard, *Oslo*
Ole Høie, *Arendal*
Magdy El-Salhy, *Bergen*
Jørgen Valeur, *Oslo*

Pakistan

Shahab Abid, *Karachi*
Syed MW Jafri, *Karachi*

Poland

Beata Jolanta Jablońska, *Katowice*
Halina Cichoż-Lach, *Lublin*
Tomasz Brzozowski, *Cracow*
Hanna Gregorek, *Warsaw*
Marek Hartleb, *Katowice*
Stanislaw J Konturek, *Krakow*
Andrzej Dabrowski, *Bialystok*
Jan Kulig, *Kraków*
Julian Swierczynski, *Gdansk*
Marek Bebenek, *Wroclaw*
Dariusz M Lebensztejn, *Bialystok*

Portugal

Ricardo Marcos, *Porto*
Guida Portela-Gomes, *Estoril*
Ana Isabel Lopes, *Lisboa Codex*
Raquel Almeida, *Porto*
Rui Tato Marinho, *Lisbon*
Ceu Figueiredo, *Porto*

Romania

Dan L Dumitrascu, *Cluj*
Adrian Saftoiu, *Craiova*
Andrada Seicean, *Cluj-Napoca*
Anca Trifan, *Iasi*

Russia

Vasiliy I Reshetnyak, *Moscow*

Saudi Arabia

Ibrahim A Al Mofleh, *Riyadh*
Abdul-Wahed Meshikhes, *Qatif*
Faisal Sanai, *Riyadh*

Serbia

Tamara M Alempijevic, *Belgrade*
Dusan M Jovanovic, *Sremska Kamenica*
Zoran Krivokapic, *Belgrade*

Singapore

Brian Kim Poh Goh, *Singapore*
Khek-Yu Ho, *Singapore*
Fock Kwong Ming, *Singapore*
Francis Seow-Choen, *Singapore*
Kok Sun Ho, *Singapore*
Kong Weng Eu, *Singapore*
Madhav Bhatia, *Singapore*
London Lucien Ooi, *Singapore*
Wei Ning Chen, *Singapore*
Richie Soong, *Singapore*
Kok Ann Gwee, *Singapore*

Slovenia

Matjaz Homan, *Ljubljana*

South Africa

Rosemary Joyce Burnett, *Pretoria*
Michael Kew, *Cape Town*
Roland Ndip, *Alice*

South Korea

Byung Chul Yoo, *Seoul*
Jae J Kim, *Seoul*
Jin-Hong Kim, *Suwon*
Marie Yeo, *Suwon*
Jeong Min Lee, *Seoul*
Eun-Yi Moon, *Seoul*
Joong-Won Park, *Goyang*
Hoon Jai Chun, *Seoul*
Myung-Gyu Choi, *Seoul*
Sang Kil Lee, *Seoul*
Sang Yeoup Lee, *Gyeongsangnam-do*
Won Ho Kim, *Seoul*
Dae-Yeul Yu, *Daejeon*
Donghee Kim, *Seoul*
Sang Geon Kim, *Seoul*
Sun Pyo Hong, *Geonggi-do*
Sung-Gil Chi, *Seoul*
Yeun-Jun Chung, *Seoul*
Ki-Baik Hahm, *Incheon*
Ji Kon Ryu, *Seoul*
Kyu Taek Lee, *Seoul*
Yong Chan Lee, *Seoul*
Seong Gyu Hwang, *Seongnam*
Seung Woon Paik, *Seoul*
Sung Kim, *Seoul*
Hong Joo Kim, *Seoul*
Hyoung-Chul Oh, *Seoul*
Nayoung Kim, *Seongnam-si*
Sang Hoon Ahn, *Seoul*
Seon Hahn Kim, *Seoul*
Si Young Song, *Seoul*
Young-Hwa Chung, *Seoul*
Hyo-Cheol Kim, *Seoul*
Kwang Jae Lee, *Swon*
Sang Min Park, *Seoul*
Young Chul Kim, *Seoul*
Do Hyun Park, *Seoul*
Dae Won Jun, *Seoul*
Dong Wan Seo, *Seoul*
Soon-Sun Hong, *Incheon*
Hoguen Kim, *Seoul*
Ho-Young Song, *Seoul*
Joo-Ho Lee, *Seoul*
Jung Eun Lee, *Seoul*
Jong H Moon, *Bucheon*

Spain

Eva Vaquero, *Barcelona*
Andres Cardenas, *Barcelona*
Laureano Fernández-Cruz, *Barcelona*
Antoni Farré, *Spain*
Maria-Angeles Aller, *Madrid*
Raul J Andrade, *Málaga*
Fernando Azpiroz, *Barcelona*
Josep M Bordas, *Barcelona*
Antoni Castells, *Barcelona*
Vicente Felipo, *Valencia*
Isabel Fabregat, *Barcelona*
Angel Lanas, *Zaragoza*
Juan-Ramón Larrubia, *Guadalajara*
María IT López, *Jaén*
Jesús M Prieto, *Pamplona*
Mireia Miquel, *Sabadell*
Ramon Bataller, *Barcelona*
Fernando J Corrales, *Pamplona*
Julio Mayol, *Madrid*
Matias A Avila, *Pamplona*
Juan Macías, *Seville*
Juan Carlos Laguna Egea, *Barcelona*
Juli Busquets, *Barcelona*
Belén Beltrán, *Valencia*
José Manuel Martin-Villa, *Madrid*
Lisardo Boscá, *Madrid*
Luis Grande, *Barcelona*
Pedro Lorenzo Majano Rodriguez, *Madrid*
Adolfo Benages, *Valencia*
Domínguez-Muñoz JE, *Santiago de Compostela*
Gloria González Aseguinolaza, *Navarra*
Javier Martin, *Granada*
Luis Bujanda, *San Sebastián*
Matilde Bustos, *Pamplona*
Luis Aparisi, *Valencia*
José Julián calvo Andrés, *Salamanca*
Benito Velayos, *Valladolid*
Javier Gonzalez-Gallego, *León*
Ruben Ciria, *Córdoba*
Francisco Rodriguez-Frias, *Barcelona*
Manuel Romero-Gómez, *Sevilla*
Albert Parés, *Barcelona*
Joan Roselló-Catafau, *Barcelona*

Sri Lanka

Arjuna De Silva, *Kelaniya*

Sweden

Stefan G Pierzynowski, *Lund*
Hanns-Ulrich Marschall, *Stockholm*
Lars A Pahlman, *Uppsala*
Helena Nordenstedt, *Stockholm*
Bobby Tingstedt, *Lund*
Evangelos Kalaitzakis, *Gothenburg*
Lars Erik Agréus, *Huddinge*
Annika Lindblom, *Stockholm*

Roland Andersson, *Lund*
Zongli Zheng, *Stockholm*
Mauro D'Amato, *Huddinge*
Greger Lindberg, *Stockholm*
Pär Erik Myrelid, *Linköping*
Sara Lindén, *Göteborg*
Sara Regnér, *Malmö*
Åke Nilsson, *Lund*

Switzerland

Jean L Frossard, *Geneva*
Andreas Geier, *Zürich*
Bruno Stieger, *Zürich*
Pascal Gervaz, *Geneva*
Paul M Schneider, *Zurich*
Felix Stickel, *Berne*
Fabrizio Montecucco, *Geneva*
Inti Zlobec, *Basel*
Michelangelo Foti, *Geneva*
Pascal Bucher, *Geneva*
Andrea De Gottardi, *Berne*
Christian Toso, *Geneva*

Thailand

Weekitt Kittisupamongkol, *Bangkok*

Trinidad and Tobago

Shivananda Nayak, *Mount Hope*

Turkey

Tarkan Karakan, *Ankara*
Yusuf Bayraktar, *Ankara*
Ahmet Tekin, *Mersin*
Aydin Karabacakoglu, *Konya*
Osman C Ozdogan, *Istanbul*
Özlem Yilmaz, *Izmir*
Bülent Salman, *Ankara*
Can GONEN, *Kutahya*
Cuneyt Kayaalp, *Malatya*
Ekmel Tezel, *Ankara*
Eren Ersoy, *Ankara*
Hayrullah Derici, *Balıkesir*
Mehmet Refik Mas, *Etlik-Ankara*
Sinan Akay, *Tekirdag*
A Mithat Bozdayi, *Ankara*
Metin Basaranoglu, *Istanbul*
Mesut Tez, *Ankara*
Orhan Sezgin, *Mersin*
Mukaddes Esrefoglu, *Malatya*
Ilker Tasci, *Ankara*
Kemal Kismet, *Ankara*
Selin Kapan, *Istanbul*
Seyfettin Köklü, *Ankara*
Murat Sayan, *Kocaeli*
Sabahattin Kaymakoglu, *Istanbul*
Yucel Ustundag, *Zonguldak*
Can Gonen, *Istanbul*
Yusuf Yilmaz, *Istanbul*
Müge Tecder-Ünal, *Ankara*
İlhami Yüksel, *Ankara*

United Arab Emirates

Fikri M Abu-Zidan, *Al-Ain*
Sherif M Karam, *Al-Ain*

United Kingdom

Anastasios Koulaouzidis, *Edinburgh*
Sylvia LF Pender, *Southampton*
Hong-Xiang Liu, *Cambridge*
William Dickey, *Londonderry*
Simon D Taylor-Robinson, *London*
James Neuberger, *Birmingham*
Frank I Tovey, *London*
Kevin Robertson, *Glasgow*
Chew Thean Soon, *Manchester*
Geoffrey Burnstock, *London*
Vamsi R Velchuru, *United Kingdom*
Simon Afford, *Birmingham*
Navneet K Ahluwalia, *Stockport*
Lesley A Anderson, *Belfast*
Anthony TR Axon, *Leeds*
Jim D Bell, *London*
Alastair D Burt, *Newcastle*
Tatjana Crnogorac-Jurcevic, *London*
Daniel R Gaya, *Edinburgh*
William Greenhalf, *Liverpool*
Indra N Guha, *Southampton*
Stefan G Hübscher, *Birmingham*
Robin Hughes, *London*
Pali Hungin, *Stockton*
Janusz AZ Jankowski, *Oxford*
Peter Karayiannis, *London*
Patricia F Lalor, *Birmingham*
Giorgina Mieli-Vergani, *London*
D Mark Pritchard, *Liverpool*
Marco Senzolo, *Padova*
Roger Williams, *London*
M H Ahmed, *Southampton*
Christos Paraskeva, *Bristol*
Emad M El-Omar, *Aberdeen*
A M El-Tawil, *Birmingham*
Anne McCune, *Bristol*
Charles B Ferguson, *Belfast*
Chin Wee Ang, *Liverpool*
Clement W Imrie, *Glasgow*
Dileep N Lobo, *Nottingham*
Graham MacKay, *Glasgow*
Guy Fairbairn Nash, *Poole*
Ian Lindsey, *Oxford*
Jason CB Goh, *Birmingham*
Jeremy FL Cobbold, *London*
Julian RF Walters, *London*
Jamie Murphy, *London*
John Beynon, *Swansea*
John B Schofield, *Kent*
Anil George, *London*
Aravind Suppiah, *East Yorkshire*
Basil Ammori, *Salford*
Catherine Walter, *Cheltenham*
Chris Briggs, *Sheffield*
Jeff Butterworth, *Shrewsbury*
Nawfal Hussein, *Nottingham*
Patrick O'Dwyer, *Glasgow*
Rob Glynne-Jones, *Northwood*
Sharad Karandikar, *Birmingham*
Venkatesh Shanmugam, *Derby*
Yeng S Ang, *Wigan*
Alberto Quaglia, *London*
Andrew Fowell, *Southampton*
Gianpiero Gravante, *Leicester*
Piers Gatenby, *London*
Kondragunta Rajendra Prasad, *Leeds*
Sunil Dolwani, *Cardiff*
Andrew McCulloch Veitch, *Wolverhampton*
Brian Green, *Belfast*
Noriko Suzuki, *Middlesex*
Richard Parker, *North Staffordshire*
Shahid A Khan, *London*
Akhilesh B Reddy, *Cambridge*
Jean E Crabtree, *Leeds*
John S Leeds, *Sheffield*
Paul Sharp, *London*
Sumita Verma, *Brighton*
Thamara Perera, *Birmingham*
Donald Campbell McMillan, *Glasgow*
Kathleen B Bamford, *London*
Helen Coleman, *Belfast*
Eyad Elkord, *Manchester*
Mohammad Ilyas, *Nottingham*
Simon R Carding, *Norwich*
Ian Chau, *Sutton*
Claudio Nicoletti, *Norwich*
Hendrik-Tobias Arkenau, *London*
Muhammad Imran Aslam, *Leicester*
Giuseppe Orlando, *Oxford*
John S Leeds, *Aberdeen*
S Madhusudan, *Nottingham*
Amin Ibrahim Amin, *Dunfermline*
David C Hay,*Edinburgh*
Alan Burns, *London*

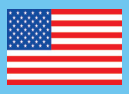

United States

Tauseef Ali, *Oklahoma City*
George Y Wu, *Farmington*
Josef E Fischer, *Boston*
Thomas Clancy, *Boston*
John Morton, *Stanford*
Luca Stocchi, *Cleveland*
Kevin Michael Reavis, *Orange*
Shiu-Ming Kuo, *Buffalo*
Gary R Lichtenstein, *Philadelphia*
Natalie J Torok, *Sacramento*
Scott A Waldman, *Philadelphia*
Georgios Papachristou, *Pittsburgh*
Carla W Brady, *Durham*
Robert CG Martin, *Louisville*
Eugene P Ceppa, *Durham*
Shashi Bala, *Worcester*
Imran Hassan, *Springfield*
Klaus Thaler, *Columbia*
Andreas M Kaiser, *Los Angeles*
Shawn D Safford, *Norfolk*
Massimo Raimondo, *Jacksonville*
Kazuaki Takabe, *Richmond VA*
Stephen M Kavic, *Baltimore*
T Clark Gamblin, *Pittsburgh*
BS Anand, *Houston*
Ananthanarayanan M, *New York*
Anthony J Bauer, *Pittsburgh*
Edmund J Bini, *New York*
Xian-Ming Chen, *Omaha*
Ramsey Chi-man Cheung, *Palo Alto*
Parimal Chowdhury, *Arkansas*
Mark J Czaja, *New York*

Conor P Delaney, *Cleveland*
Sharon DeMorrow, *Temple*
Bijan Eghtesad, *Cleveland*
Alessandro Fichera, *Chicago*
Glenn T Furuta, *Aurora*
Jean-Francois Geschwind, *Baltimore*
Shannon S Glaser, *Temple*
Ajay Goel, *Dallas*
James H Grendell, *New York*
Anna S Gukovskaya, *Los Angeles*
Jamal A Ibdah, *Columbia*
Atif Iqbal, *Omaha*
Hajime Isomoto, *Rochester*
Hartmut Jaeschke, *Kansas*
Leonard R Johnson, *Memphis*
Rashmi Kaul, *Tulsa*
Ali Keshavarzian, *Chicago*
Miran Kim, *Providence*
Burton I Korelitz, *New York*
Richard A Kozarek, *Seattle*
Alyssa M Krasinskas, *Pittsburgh*
Ming Li, New *Orleans*
Zhiping Li, *Baltimore*
Chen Liu, *Gainesville*
Michael R Lucey, *Madison*
James D Luketich, *Pittsburgh*
Patrick M Lynch, *Houston*
Willis C Maddrey, *Dallas*
Mercedes Susan Mandell, *Aurora*
Wendy M Mars, *Pittsburgh*
Laura E Matarese, *Pittsburgh*
Lynne V McFarland, *Washington*
Stephan Menne, *New York*
Didier Merlin, *Atlanta*
George Michalopoulos, *Pittsburgh*
James M Millis, *Chicago*
Pramod K Mistry, *New Haven*
Emiko Mizoguchi, *Boston*
Peter L Moses, *Burlington*
Masaki Nagaya, *Boston*
Robert D Odze, *Boston*
Stephen JD O'Keefe, *Pittsburgh*
Zhiheng Pei, *New York*
Raymund R Razonable, *Minnesota*
Basil Rigas, *New York*
Richard A Rippe, *Chapel Hill*
Philip Rosenthal, *San Francisco*
Stuart Sherman, *Indianapolis*
Christina Surawicz, *Seattle*
Wing-Kin Syn, *Durham*
Yvette Taché, *Los Angeles*
K-M Tchou-Wong, *New York*
George Triadafilopoulos, *Stanford*
Chung-Jyi Tsai, *Lexington*
Andrew Ukleja, *Florida*
Arnold Wald, *Wisconsin*
Irving Waxman, *Chicago*
Steven D Wexner, *Weston*
Jackie Wood, *Ohio*
Jian Wu, *Sacramento*
Zobair M Younossi, *Virginia*
Liqing Yu, *Winston-Salem*
Ruben Zamora, *Pittsburgh*
Michael E Zenilman, *New York*
Michael A Zimmerman, *Colorado*
Beat Schnüriger, *California*
Clifford S Cho, *Madison*

R Mark Ghobrial, *Texas*
Anthony T Yeung, *Philadelphia*
Chang Kim, *West Lafayette*
Balamurugan N Appakalai, *Minneapolis*
Aejaz Nasir, *Tampa*
Ashkan Farhadi, *Irvine*
Kevin E Behrns, *Gainesville*
Joseph J Cullen, *Iowa City*
David J McGee, *Shreveport*
Anthony J Demetris, *Pittsburgh*
Dimitrios V Avgerinos, *New York*
Dong-Hui Li, *Houston*
Eric S Hungness, *Chicago*
Giuseppe Orlando, *Winston Salem*
Hai-Yong Han, *Phoenix*
Huanbiao Mo, *Denton*
Jong Park, *Tampa*
Justin MM Cates, *Nashville*
Charles P Heise, *Madison*
Craig D Logsdon, *Houston*
Ece A Mutlu, *Chicago*
Jessica A Davila, *Houston*
Rabih M Salloum, *Rochester*
Amir Maqbul Khan, *Marshall*
Bruce E Sands, *Boston*
Chakshu Gupta, *Saint Joseph*
Ricardo Alberto Cruciani, *New York*
Mariana D Dabeva, *Bronx*
Edward L Bradley III, *Sarasota*
Martín E Fernández-Zapico, *Rochester*
Henry J Binder, *New Haven*
John R Grider, *Richmond*
Ronnie Fass, *Tucson*
Dinesh Vyas, *Washington*
Wael El-Rifai, *Nashville*
Craig J McClain, *Louisville*
Christopher Mantyh, *Durham*
Daniel S Straus, *Riverside*
David A Brenner, *San Diego*
Eileen F Grady, *San Francisco*
Ekihiro Seki, *La Jolla*
Fang Yan, *Nashville*
Fritz Francois, *New York*
Giamila Fantuzzi, *Chicago*
Guang-Yin Xu, *Galveston*
Jianyuan Chai, *Long Beach*
JingXuan Kang, *Charlestown*
Le Shen, *Chicago*
Lin Zhang, *Pittsburgh*
Mitchell L Shiffman, *Richmond*
Douglas K Rex, *Indianapolis*
Bo Shen, *Cleveland*
Edward J Ciaccio, *New York*
Jean S Wang, *Saint Louis*
Bao-Ting Zhu, *Kansas*
Tamir Miloh, *Phoenix*
Eric R Kallwitz, *Chicago*
Yujin Hoshida, *Cambridge*
C Chris Yun, *Atlanta*
Alan C Moss, *Boston*
Oliver Grundmann, *Gainesville*
Linda A Feagins, *Dallas*
Chanjuan Shi, *Nashville*
Xiaonan Han, *Cincinnati*
William R Brugge, *Boston*
Richard W McCallum, *El Paso*
Lisa Ganley-Leal, *Boston*
Lin-Feng Chen, *Urbana*

Elaine Y Lin, *New York*
Julian Abrams, *New York*
Arun Swaminath, *New York*
Huiping Zhou, *Richmond*
Korkut Uygun, *Boston*
Anupam Bishayee, *Signal Hill*
C Bart Rountree, *Hershey*
Avinash Kambadakone, *Boston*
Courtney W Houchen, *Oklahoma*
Joshua R Friedman, *Philadelphia*
Justin H Nguyen, *Jacksonville*
Sophoclis Alexopoulos, *Los Angeles*
Suryakanth R Gurudu, *Scottsdale*
Wei Jia, *Kannapolis*
Yoon-Young Jang, *Baltimore*
Ourania M Andrisani, *West Lafayette*
Roderick M Quiros, *Bethlehem*
Timothy R Koch, *Washington*
Adam S Cheifetz, *Boston*
Lifang Hou, *Chicago*
Thiru vengadam Muniraj, *Pittsburgh*
Dhiraj Yadav, *Pittsburgh*
Ying Gao, *Rockville*
John F Gibbs, *Buffalo*
Aaron Vinik, *Norfolk*
Charles Thomas, *Oregon*
Robert Jensen, *Bethesda*
John W Wiley, *Ann Arbor*
Jonathan Strosberg, *Tampa*
Randeep Singh Kashyap, *New York*
Kaye M Reid Lombardo, *Rochester*
Lygia Stewart, *San Francisco*
Martin D Zielinski, *Rochester*
Matthew James Schuchert, *Pittsburgh*
Michelle Lai, *Boston*
Million Mulugeta, *Los Angeles*
Patricia Sylla, *Boston*
Pete Muscarella, *Columbus*
Raul J Rosenthal, *Weston*
Robert V Rege, *Dallas*
Roberto Bergamaschi, *New York*
Ronald S Chamberlain, *Livingston*
Alexander S Rosemurgy, *Tampa*
Run Yu, *Los Angeles*
Samuel B Ho, *San Diego*
Sami R Achem, *Florida*
Sandeep Mukherjee, *Omaha*
Santhi Swaroop Vege, *Rochester*
Scott Steele, *Fort Lewis*
Steven Hochwald, *Gainesville*
Udayakumar Navaneethan, *Cincinnati*
Radha Krishna Yellapu, *New York*
Rupjyoti Talukdar, *Rochester*
Shi-Ying Cai, *New Haven*
Thérèse Tuohy, *Salt Lake City*
Tor C Savidge, *Galveston*
William R Parker, *Durham*
Xiaofa Qin, *Newark*
Zhang-Xu Liu, *Los Angeles*
Adeel A Butt, *Pittsburgh*
Dean Y Kim, *Detroit*
Denesh Chitkara, *East Brunswick*
Mohamad A Eloubeidi, *Alabama*
JiPing Wang, *Boston*
Oscar Joe Hines, *Los Angeles*
Jon C Gould, *Madison*
Kirk Ludwig, *Wisconsin*
Mansour A Parsi, *Cleveland*

World Journal of Gastroenterology

Contents

Weekly Volume 18 Number 23 June 21, 2012

World Journal of Gastroenterology
Volume 18 Number 23 June 21, 2012

Contents

NAME OF JOURNAL
World Journal of Gastroenterology

ISSN AND EISSN
ISSN 1007-9327 (print)
ISSN 2219-2840 (online)

LAUNCH DATE
October 1, 1995

FREQUENCY
Weekly

RESPONSIBLE INSTITUTION
Department of Science and Technology of Shanxi Province

SPONSOR
Taiyuan Research and Treatment Center for Digestive Diseases, 77 Shuangta Xijie, Taiyuan 030001, Shanxi Province, China

EDITING
Editorial Board of *World Journal of Gastroenterology*
Room 903, Building D, Ocean International Center, No. 62 Dongsihuan Zhonglu, Chaoyang District, Beijing 100025, China
Telephone: +86-10-59080039
Fax: +86-10-85381893
E-mail: wjg@wjgnet.com
http://www.wjgnet.com

EDITORIAL OFFICE
Jian-Xia Cheng, Director
World Journal of Gastroenterology
Room 903, Building D, Ocean International Center, No. 62 Dongsihuan Zhonglu, Chaoyang District, Beijing 100025, China
Telephone: +86-10-59080039
Fax: +86-10-85381893
E-mail: wjg@wjgnet.com
http://www.wjgnet.com

PUBLISHER
Baishideng Publishing Group Co., Limited
Room 1701, 17/F, Henan Building,
No.90 Jaffe Road, Wanchai, Hong Kong, China
Fax: +852-31158812
Telephone: +852-58042046
E-mail: bpg@baishideng.com
http://www.wjgnet.com

PRINT SUBSCRIPTION
RMB 300 Yuan for each issue, RMB 14400 Yuan for one year.

PUBLICATION DATE
June 21, 2012

INSTRUCTIONS TO AUTHORS
Full instructions are available online at http://www.wjgnet.com/1007-9327/g_info_20100315215714.htm

ONLINE SUBMISSION
http://www.wjgnet.com/1007-9327office/

World Journal of Gastroenterology

Online Submissions: http://www.wjgnet.com/1007-9327office
wjg@wjgnet.com
doi:10.3748/wjg.v18.i23.2887

World J Gastroenterol 2012 June 21; 18(23): 2887-2894
ISSN 1007-9327 (print) ISSN 2219-2840 (online)

EDITORIAL

New perspectives in occult hepatitis C virus infection

Vicente Carreño, Javier Bartolomé, Inmaculada Castillo, Juan Antonio Quiroga

Vicente Carreño, Javier Bartolomé, Inmaculada Castillo, Juan Antonio Quiroga, Foundation for the Study of Viral Hepatitis, C/Guzmán el Bueno 72, 28015 Madrid, Spain
Author contributions: Carreño V, Bartolomé J, Castillo I and Quiroga JA equally contributed to generating the ideas for this review and writing this manuscript.
Supported by Fundación de Investigaciones Biomédicas (Madrid, Spain); and the Fundación Mutua Madrileña (Madrid, Spain)
Correspondence to: Vicente Carreño, MD, PhD, Foundation for the Study of Viral Hepatitis, C/Guzmán el Bueno 72, 28015 Madrid, Spain. fehvhpa@fehv.org
Telephone: +34-91-5446013 Fax: +34-91-5449228
Received: August 5, 2011 Revised: December 12, 2011
Accepted: April 28, 2012
Published online: June 21, 2012

Abstract

Occult hepatitis C virus (HCV) infection, defined as the presence of HCV RNA in liver and in peripheral blood mononuclear cells (PBMCs) in the absence of detectable viral RNA in serum by standard assays, can be found in anti-HCV positive patients with normal serum levels of liver enzymes and in anti-HCV negative patients with persistently elevated liver enzymes of unknown etiology. Occult HCV infection is distributed worldwide and all HCV genotypes seem to be involved in this infection. Occult hepatitis C has been found not only in anti-HCV positive subjects with normal values of liver enzymes or in chronic hepatitis of unknown origin but also in several groups at risk for HCV infection such as hemodialysis patients or family members of patients with occult HCV. This occult infection has been reported also in healthy populations without evidence of liver disease. Occult HCV infection seems to be less aggressive than chronic hepatitis C although patients affected by occult HCV may develop liver cirrhosis and even hepatocellular carcinoma. Thus, anti-HCV negative patients with occult HCV may benefit from antiviral therapy with pegylated-interferon plus ribavirin. The persistence of very low levels of HCV RNA in serum and in PBMCs, along with the maintenance of specific T-cell responses against HCV-antigens observed during a long-term follow-up of patients with occult hepatitis C, indicate that occult HCV is a persistent infection that is not spontaneously eradicated. This is an updated report on diagnosis, epidemiology and clinical implications of occult HCV with special emphasis on anti-HCV negative cases.

Key words: Occult hepatitis C virus; Hepatitis C virus RNA; Liver; Peripheral blood mononuclear cells; T-cell response

Peer reviewer: Munechika Enjoji, MD, PhD, Department of Clinical Pharmacology, Fukuoka University, 8-17-1 Nanakuma, Jonan-ku, Fukuoka 814-0180, Japan

Carreño V, Bartolomé J, Castillo I, Quiroga JA. New perspectives in occult hepatitis C virus infection. *World J Gastroenterol* 2012; 18(23): 2887-2894 Available from: URL: http://www.wjgnet.com/1007-9327/full/v18/i23/2887.htm DOI: http://dx.doi.org/10.3748/wjg.v18.i23.2887

INTRODUCTION

The hepatitis C virus (HCV), an enveloped single-stranded RNA virus, was identified in 1989 and it was classified within the Flaviviridae family as a separate genus (Hepacivirus)[1]. The virus replicates by the synthesis of the complementary RNA strand (the so-called negative or antigenomic strand)[2]. So far, six major genotypes (HCV-1 to HCV-6) have been described, each containing multiple subtypes[3], with significant differences in their global distribution and prevalence[4]. It is estimated that about 170 million people, 3% of the world's population, are infected with HCV[5] and it is a leading cause of chronic liver disease worldwide including cirrhosis and hepatocellular carcinoma[6,7]. The diagnosis of HCV infection is made by the detection of antibodies against HCV (anti-HCV) and/or by detecting the presence of the HCV RNA in serum[7,8].

However, a new entity of HCV infection was first described in 2004 in patients with persistently elevated liver function tests and who were anti-HCV and serum HCV RNA negative[9]. Despite the absence of conventional HCV markers, 57% of these patients had HCV RNA in the liver and so this clinical situation was termed "occult HCV infection". Moreover, it was proven that the antigenomic HCV RNA strand could be detected also in the hepatocytes of a high proportion of those patients with occult HCV infection, this indicating an active viral replication. Occult HCV infection has also been described in two other different clinical settings. One of these is in anti-HCV positive, serum HCV-RNA negative subjects with persistent normal values of liver enzymes (asymptomatic HCV carriers), of whom nearly 90% have detectable viral RNA in liver and in peripheral blood mononuclear cells (PBMCs)[10-12]. The second one is in anti-HCV positive individuals who resolved HCV infection either spontaneously or after antiviral treatment[13-16]. In these patients, HCV RNA is detected in liver and in PBMCs years after apparent recovery from the disease (normalization of liver enzyme values and loss of serum HCV RNA). This occult HCV infection is related to the persistence of necroinflammation activity in the liver of the sustained responders. Thus, there are two types of occult HCV infection: one can be found among anti-HCV seropositive individuals with normal values of liver enzymes and the other is found among anti-HCV seronegative patients with abnormal levels of liver enzymes. The present review focuses on the latest studies of occult HCV infection performed in anti-HCV negative and serum HCV RNA negative patients.

IDENTIFICATION OF OCCULT HCV INFECTION

Occult HCV infection was first identified in liver of anti-HCV and serum HCV RNA negative patients with abnormal liver function tests and it was also found that viral RNA could be present in the PBMCs of nearly 70% of these patients[9]. Furthermore, it was demonstrated that occult HCV replicates in these cells[17]. By detecting HCV RNA in liver biopsies or in PBMCs, other groups in Japan, Italy, Egypt, Colombia, Pakistan and Iran[18-23] have confirmed the existence of occult HCV infection in patients with elevated liver enzymes and without conventional HCV markers (Table 1). Occult HCV infection has also been found in hemodialysis patients who were persistently anti-HCV and serum HCV RNA negative but with abnormal values of liver enzymes[24], in the family setting of patients with occult hepatitis C[25] and even in healthy subjects with normal alanine aminotransferase (ALT) levels and no clinical evidence of liver disease[26].

Since HCV was replicating in the liver and PBMCs of patients with occult HCV infection, it was speculated that it should exist as circulating viral particles but at such low levels that the virions could not be detected even using the most sensitive reverse-transcription polymerase chain reaction (RT-PCR) techniques. This hypothesis was tested by concentrating HCV virions by ultracentrifugation of 2 mL of serum from patients with occult HCV prior to HCV RNA detection by RT-PCR[27]. In this way, serum viral RNA was found in nearly 60% of the patients. In addition, it was found that the density of the viral particles isolated from patients with occult HCV infection was similar to the highly-infectious lipoviral particles present in the serum of patients with classical chronic hepatitis C[27,28], suggesting that serum from patients with occult HCV is potentially infectious.

HCV-SPECIFIC T-CELL RESPONSES AND THE OCCULT INFECTION

Functional virus-specific memory $CD4^+$ and $CD8^+$ T-cells have been documented in the circulation of patients with HCV RNA persistence in the liver and so assaying cellular immunity has been proposed as a surrogate marker of occult HCV infection[29,30]. To test HCV-specific T-cell responses, PBMCs isolated from fresh heparinized venous blood by gradient centrifugation are washed twice in phosphate-buffered saline and resuspended in RPMI-1640 medium, supplemented with 10% heat-inactivated fetal bovine serum, 20 mmol/L HEPES, 2 mmol/L glutamine and antibiotics. PBMCs are cultured in triplicate (1.0×10^5 viable cells/100 μL) in flat-bottomed 96-well culture plates at 37 ℃, 5% CO_2 and humidity in the presence or absence of 1 μg/mL HCV proteins core, NS3 and NS4; *Staphylococcus aureus* enterotoxin B (10 μg/mL) is used as positive control. On day 6, cultures are pulsed with 1 μCi/well of 3H-thymidine for 16 h and then harvested and transferred to filters and the incorporated radioactivity measured[31].

T-cell responses found in occult HCV infection are similar to those described in anti-HCV-positive patients following spontaneous or treatment-induced recovery[32-34]. HCV-specific T-cell responses have been detected often among occult HCV-infected hemodialysis patients[35], family members of patients with occult or overt HCV infection[36] and among HCV-seronegative sexual partners of patients with chronic hepatitis C (Aguilar-Reina J, personal communication), supporting exposure to trace amounts of HCV RNA. The maintenance of such immune responses may require only a low level productive infection. In fact, sporadic reappearance of minute amounts of HCV RNA stimulates cellular immunity[37]. However, persistence of occult HCV in face of adaptive cellular responses indicates that the latter do not ultimately result in sterilising immunity. The actual impact on the natural history of the occult infection is still a matter of debate. Indeed, HCV-specific T-cell responses have been described in apparently healthy persons, as well as in those who likely have resolved the infection or who have been exposed to, but who apparently did not became infected by, HCV[30]. To summarize, T-cell responses are more frequent and stronger compared with chronic hepatitis C patients[29], contributing to control the

Table 1 Prevalence and hepatitis C virus genotype distribution of occult hepatitis C virus infection

Type	Country	Prevalence[1]	Genotype	Cohort/setting	Ref.
Anti-HCV negative					
	Spain	57/100 (57%)	1b	Cryptogenic chronic hepatitis	[9]
	Japan	Not applicable	Not reported	Cryptogenic cirrhosis with HCC	[18]
	Italy	2/5 (40%)	Not reported	Cryptogenic cirrhosis with HCC	[19]
	Egypt	4/40 (10%)	Not reported	Cryptogenic chronic hepatitis	[20]
	Colombia	Not applicable	1a	Liver retransplantation	[21]
	Pakistan	23/31 (74%)	1a, 3a, 3b	Cryptogenic chronic hepatitis	[22]
	Iran	7/69 (10%)	1a, 1b, 3a	Cryptogenic chronic hepatitis	[23]
	Italy	9/276 (3.3%)	1a, 1b, 2a	General population without liver disease	[26]
Anti-HCV positive					
	United States/Poland	11/11 (100%)[2]	1a, 1b	Asymptomatic anti-HCV carrier	[10]
	Cuba/Mexico	17/18 (94%)	Not reported	Asymptomatic HCV carrier and therapy response	[11]
	Spain	10/12 (83%)	1b	Asymptomatic anti-HCV carrier	[12]
	Canada	16/16 (100%)[2]	1a, 1b, 2a	Spontaneous recovery and therapy response	[13]
	United States/Poland	15/17 (88%)[2]	1a, 1b, 2a, 3a	Therapy response	[14]
	Spain	19/20 (95%)	1b, 2, 3	Therapy response	[15]
	Canada	24/24 (100%)[2]	1, 1a, 3a	Therapy response	[16]
	Egypt	7/62 (11%)	Not reported	Therapy response	[20]

[1]Hepatitis C virus (HCV) RNA detection in liver and/or peripheral blood mononuclear cells; [2]Including HCV RNA detection in serum with nested reverse-transcription polymerase chain reaction-nucleic acid hybridization assay. HCC: Hepatocellular carcinoma.

extent of the infection and thus prevent HCV RNA detection in serum.

HUMORAL IMMUNITY TO HCV DURING THE OCCULT INFECTION

It is unknown how HCV persists in persons who remain anti-HCV non-reactive by currently available antibody screening tests[38]. Antibodies to HCV proteins usually develop within 4-12 wk following exposure to the virus, those directed to the core and non-structural-3 region being the earliest and more frequently detected. Anti-HCV continues to be detectable throughout the duration of the infection although antibody reactivity declines over time after apparent clinical recovery of chronic hepatitis C[39-41]. In immunocompetent individuals, the etiology of the primary occult HCV infection is most likely explained by the sporadic exposure to low infective virus doses resulting in a latent seronegative infection. Thus, anti-HCV reactivity remains undetectable due to prolonged very low antibody titres[38], excluding persons with immunodeficiencies, immunosuppressed or suffering from a concomitant chronic infection.

Isolated reactivity to single proteins or peptides has been reported on supplemental anti-HCV assays in blood donors in samples which are either HCV RNA-positive or -negative[42,43]. Such pattern of anti-HCV indeterminate results resembles the profile of antibody reactivity documented in some international seroconversion panels when tested on supplemental anti-HCV assays. These panels are composed of sequential samples from a single-source donor obtained throughout the antibody development which frequently show single-antigen reactivity at the initial stages of anti-HCV seroconversion. In addition, reactivity recorded as "faint band(s)" has been shown among at risk persons but seronegative by screening anti-HCV tests[44]. At this point the criteria recommended by the supplier of the supplemental assay to validate the testing as reactive or anti-HCV-positive *vs* indeterminate result should be discussed. But this issue would require a thorough comparison of the HCV antigens employed by the licensed tests and the interpretation of their reactivity in particular populations, which is out of the scope of this review and deserves future investigation.

The majority of persons exposed to HCV who become infected and seroconvert to anti-HCV remain asymptomatic. Up to 80% of seropositive infections are not diagnosed because persons belong to low, or supposedly null, risk groups. Screening programs in the general population would promote awareness and prevention of HCV spread because seropositive persons may be identified and offered appropriate counselling. However, this strategy still will not identify the seronegative infections using the current screening anti-HCV tests, as evidenced by the existence of the primary occult HCV infection.

In an attempt to overcome this, an anti-HCV assay based on a well-conserved core-derived epitope has been reported recently[45]. Briefly, wells of a microtitre plate are coated overnight with HCV-core 5-19-peptide. Wells are washed and non-specific sites are blocked with phosphate buffer saline containing Tween-20 plus heat-inactivated fetal bovine serum. Diluted serum samples are added to the HCV-core coated wells and after incubation for 1 h, wells are washed five times and incubated with horseradish peroxidase-conjugated rabbit polyclonal anti-human IgG for 1 h. After five washings wells are reacted in the dark with 2, 20-azinobis-[3-ethylbenzthiazoline-6-sulfonic acid]-diammonium salt. Absorbance is measured at 405 nm with a reference at 620 nm. In contrast to the NS3 sequence which shows considerable inter-genotypic heterogeneity[46], the core sequence is largely conserved

among genotypes 1 through 6[47]. Antibody to HCV core was tested in a cohort of 145 anti-HCV screening-negative patients with occult HCV infection of whom 40% were found to be anti-HCV core-positive, including 10% of individuals who were antibody non-reactive at the time of the first sample testing. Also, the anti-HCV core was detected in 99% of chronic hepatitis C patients but in none of the patients with HCV-unrelated liver disease. Thus, anti-HCV core testing allowed serological identification of up to 40% of the anti-HCV screening-negative infections on repeated testing[45]. The finding that a number of patients with occult infection who were initially nonreactive for anti-HCV core antibodies became positive upon subsequent testing underscores the necessity of screening serial samples as proposed by other authors[32,48].

In addition, the anti-HCV core assay has been able to track HCV exposure among relatives of patients with occult HCV. Intrafamilial spread of occult HCV infection seems to occur as often as that of chronic hepatitis C[25]. So, anti-HCV core was detected in 23% anti-HCV-screening-negative relatives of patients with occult HCV infection. Thus, antibody testing to HCV core detected frequent exposure to and possible transmission of HCV among family members of HCV-infected patients compared with screening anti-HCV tests[36]. On the other hand, because patients undergoing hemodialysis are at risk of occult HCV infection[24,35], testing for anti-HCV core has been evaluated in repeatedly anti-HCV screening-negative and serum HCV RNA-negative hemodialysis patients with abnormal liver enzymes. Anti-HCV core antibodies were detectable in 34% hemodialysis patients who have been exposed to HCV and who might have developed occult HCV infection (unpublished results).

Therefore, anti-HCV fails to be detected by screening tests available in some populations of at-risk patients[49], including those individuals multi-exposed such as intravenous drug users or prison inmates[44,50-52]. The ultimate utility of the anti-HCV core-based antibody assay in those cases and other settings such as blood donors warrants further investigation.

MAY OCCULT HCV INFECTION BE DIAGNOSED WITHOUT A LIVER BIOPSY?

Detection of HCV RNA in the liver biopsy is the gold-standard method for the diagnosis of an occult HCV infection. However, as commented before, viral RNA is detectable in the PBMCs and in ultracentrifuged serum of patients with occult HCV[9,27] and anti-core HCV tested by a non-commercial enzyme-linked immunosorbent assay (ELISA) is also found in a substantial proportion of these patients[45]. Therefore, in a recent report it was determined whether all cases of occult HCV infection could be diagnosed without performing a liver biopsy by combining these methods[53]. A total of 122 patients, who were diagnosed of an occult HCV infection by the presence of viral RNA in a liver biopsy and with available serum samples and PBMCs were included in the study. Anti-core HCV (tested with the non-commercial ELISA) was found positive in 44/122 (36%) of the patients. After ultracentrifugation of serum samples, HCV RNA was found in 70/122 (57%) of the patients, while 74/122 (61%) had viral RNA in PBMCs. When combining the detection of anti-core HCV and the detection of HCV RNA in ultracentrifuged serum and in PBMCs, 91% of the patients (111/122) were positive for at least one of these markers. So, in the light of these results, occult HCV infection may be properly diagnosed in up to 91% of the patients without the need to perform a liver biopsy by testing for anti-core HCV and for HCV RNA in ultracentrifuged serum and in PBMCs.

In summary, when occult HCV infection is suspected and a liver biopsy is not available for HCV RNA detection, the diagnosis can be made by testing, with a highly sensitive real-time PCR technique, for the presence of viral RNA in PBMCs (that identifies between 60%-70% of the cases)[9,53] or in ultracentrifuged serum (that allows identification of occult HCV in around 60% of the patients)[27,53]. The combination of these two approaches along with the detection of anti-core HCV improves the diagnosis of occult HCV infection in more than 90% of the cases. Nevertheless, in order to increase the percentage of patients diagnosed of occult HCV infection with non-invasive methods, more studies should be done in the future to improve the sensitivity of the above mentioned techniques.

CHARACTERISTICS OF OCCULT HCV INFECTION AND RESPONSE TO ANTIVIRAL TREATMENT

Clinical characteristics of patients with occult HCV infection have been compared to those of patients with chronic hepatitis C matched with respect to age, gender and known duration of the disease[54]. In the study it was found that patients with occult HCV presented significantly lower values of iron, alanine aminotransferase, γ-glutamyl transpeptidase and α-fetoprotein whereas triglycerides and cholesterol levels were significantly higher than those of patients with chronic hepatitis C. In the liver biopsies, patients with chronic hepatitis C frequently had more necroinflammation activity (96%) and fibrosis (75%) than patients with occult HCV infection (31% and 15%, respectively), but liver cirrhosis was diagnosed with a similar frequency in both groups (4.4% in occult HCV *vs* 7.2% in chronic hepatitis C). Although cholesterol and triglyceride levels were significantly higher in patients with occult HCV infection than in patients with chronic hepatitis C, the percentage of cases with liver steatosis did not differ significantly between these two groups, suggesting that dyslipidemic disorders did not play a predominant role in the development of steatosis in patients with occult HCV. So, occult HCV infection seems to be a milder form of the disease caused by HCV with less liver damage. However, it is important to point out that

occult HCV may lead to liver cirrhosis and therefore to the development of hepatocellular carcinoma. Regarding this issue, the presence of viral RNA in the tumour and non-tumour tissue of anti-HCV and serum HCV RNA negative patients with liver cancer has been reported[18,19]. Nevertheless, the number of patients analyzed in these reports was low and further studies are needed to ascertain the role of occult HCV in causing hepatocellular carcinoma.

Taking into account that patients with occult HCV present with abnormal liver function tests and may have histological damage, a study was conducted to determine whether these patients could respond to antiviral treatment with pegylated-interferon (PEG-IFN) plus ribavirin[55]. A total of 10 patients with occult HCV genotype 1b infection (anti-HCV and serum HCV-RNA negative but HCV RNA positive in liver) who were HCV RNA positive in PBMCs, had abnormal values of alanine aminotransferase for at least 12 mo and had necroinflammatory activity in a liver biopsy performed within one year before the study entry, were treated with standard doses of PEG-IFN plus ribavirin for 24 wk. The patients received a 24-wk treatment course instead of the recommended 48-wk course for HCV genotype 1 because they were serum HCV RNA negative[56-58]. After treatment, patients were followed for 24 wk. At the end of therapy, 80% of the patients had normalized ALT values and were HCV RNA negative in PBMCs, but at the end of the post-treatment follow-up, only 3 cases remained with normal ALT values and without HCV RNA in PBMCs (complete responders). Five of the patients (2 of them with a complete response) underwent a second liver biopsy at the end of the follow-up period. Necroinflammatory activity and fibrosis scores had decreased in the post-treatment liver biopsy of 3 patients, while scores in the other 2 cases remained unchanged. Viral RNA persisted in the liver of the 5 patients but HCV RNA load was significantly lower in the post-treatment biopsy than in the basal one. Thus, treatment with PEG-IFN plus ribavirin may be beneficial in patients with occult HCV because intrahepatic HCV RNA load decreases and histological liver damage may improve but, as it has been described for chronic hepatitis C[13-16], occult HCV infection is not eradicated.

In conclusion, although occult HCV infection appears to be milder than "classical" chronic hepatitis C, liver fibrosis is present in up to 5% of the patients[4,42]. In addition, necroinflammatory activity is detected in the liver of nearly 35% of the cases[9,54]. This suggests that occult HCV infection may progress to a more serious chronic liver injury. Supporting this notion is the fact that occult HCV infection has been identified in patients with liver cirrhosis and even in hepatocellular carcinoma[18,19]. Thus, the treatment of patients with occult HCV infection with PEG-IFN plus ribavirin is a reasonable option, as it is proven for chronic hepatitis C[59] because the histological liver damage may improve with treatment. However, the infection is not completely eradicated, as described for patients with chronic hepatitis C who respond to antiviral treatment[13-16].

IS OCCULT HCV A TRANSIENT OR A PERSISTENT INFECTION?

In order to determine whether occult HCV infection remains over time, we have performed a study including 37 patients who were anti-HCV and serum HCV RNA negative but with viral RNA in the liver biopsy[60]. Patients were followed for a mean time of 55 mo and serum and PBMCs samples were collected periodically for HCV RNA testing. Evidence of viral persistence in patients with occult HCV infection was found by the detection (over the observational period) of intermittent or persistent HCV RNA positivity in the ultracentrifuged serum or in PBMCs in all but one patient. These results suggest that anti-HVC negative occult HCV is a permanent infection as it has been reported in anti-HCV positive patients who resolved HCV infection[16,61]. Nevertheless, in order to extend the knowledge in the natural history and the pathogenesis of occult HCV infection, a more prolonged follow-up is needed.

GENOTYPES OF OCCULT HCV INFECTION

In the initial studies of occult HCV infection the only HCV genotype detected was 1b[4,19,22]. This result was predictable because HCV genotype 1b is the most prevalent genotype in Spain[62,63]. However, later studies performed worldwide (Table 1) have reported occult HCV infection belonging to HCV genotypes 1a, 2a, 3a and 3b[21-23,26]. So, it can be assumed that occult HCV infection is a universal phenomenon and all genotypes may be involved in this infection. This hypothesis should be proven with several studies performed in countries with different prevalence of HCV genotypes.

ROLE OF OCCULT HCV INFECTION IN LIVER TRANSPLANTATION

In anti-HCV positive patients with occult HCV, the reactivation of HCV infection (with reappearance of serum HCV-RNA) is well documented in special clinical situations, such as immunocompromised patients, patients on long term chemotherapy for cancer or patients receiving immunosuppressive therapy (including those who have undergone liver, kidney or bone marrow transplant)[64-69]. By contrast, there are no studies of the serologically silent (anti-HCV negative) occult HCV infection in these settings, except for a reported case of occult HCV infection as the cause of a liver transplantation and retransplantation[21]. The patient was a 29-year-old man who was transplanted due to liver cirrhosis of unknown etiology. Ten months after the first liver transplant, the patient was retransplanted because of liver failure secondary to severe chronic cholestasis of unknown origin. Liver

samples of both explants were available for study. The patient has remained anti-HCV and HCV RNA negative in serum and plasma since the initial diagnosis, but viral RNA was detected in the liver tissue samples from the two explants. Furthermore, a phylogenetic analysis demonstrated that the HCV RNA isolated from the two liver samples belonged to genotype 1a. Although HCV RNA was undetectable in the PBMCs of the patient, he had an occult HCV infection and probably, the liver graft was infected by PBMCs.

This case suggests that occult HCV infection may play a role as an etiological agent of liver failure in transplanted patients. Also, this report strongly supports the need for performing studies not only in liver transplant, but also in other immunocompromised patients with unexplained elevation of liver enzymes to determine the real magnitude, clinical significance and long-term consequences of occult HCV infection.

OCCULT HCV INFECTION IN HEALTHY POPULATION WITH NORMAL LIVER ENZYMES

Although occult HCV infection was identified in patients with abnormal values of liver function tests, a recent work by De Marco *et al*[26] describes the existence of occult HCV infection among healthy people with normal alanine aminotransferase and normal aminotransferase values. These healthy subjects were enrolled in the frame of three different epidemiological studies: the Italy cohort series of the European Prospective Investigation into Cancer and Nutrition, the Turin Case-Control Bladder Cancer Study and the Italian project in Cervical Cancer Screening. Subjects were tested for anti-HCV and for HCV RNA in plasma and in PBMCs. All of them were anti-HCV and serum HCV RNA negative, but viral RNA was detected in the PBMCs of 9/276 (3.3%) healthy controls with normal liver enzymes. Interestingly, in the studied population, blood donors were over-sampled but the authors do not indicate if any of these blood donors had an occult HCV infection.

So, this work potentially has important implications. Thus, the frequency of occult HCV infection may be underestimated since until now this infection has been exclusively studied among patients with abnormal values of liver enzymes. In this sense, in the study of De Marco *et al*[26] the frequency of occult HCV infection in their health population was 3.3% *vs* the 2.7% prevalence of anti-HCV positivity detected in the general Italian population. Although the number of participants in the former study (276 subjects) should be increased, there is a potential risk for HCV spread from an occult HCV healthy population. Thus in blood donations, despite approaches to reduce the risk of leukocyte-related disease, such as leukodepletion, the efficacy in reducing the risk of transmitting viruses is still under debate[70]. Furthermore, as HCV RNA may be detected after ultracentrifugation of serum samples in more than 50% of patients with occult HCV infection[27] and this test was not performed in the Italian study, it may be possible that healthy blood donors have HCV RNA in serum undetectable by conventional PCR assays. If this is the case, blood donors with occult HCV infection may potentially transmit this occult infection as it is undetectable by the current applied screening tests for HCV in blood banks. However, more studies should be performed in healthy subjects with normal liver enzymes and especially among blood donors to definitively establish the possible magnitude of this infection.

CONCLUSION

Occult HCV infection has been found in two different settings: in anti-HCV positive, serum HCV RNA negative patients with normal levels of liver enzymes and in anti-HCV negative, serum HCV RNA negative patients with abnormal liver function tests of unknown etiology. Occult HCV is distributed worldwide and all viral genotypes may be involved. Although seronegative occult HCV infection seems to be less aggressive than classical chronic hepatitis C, it has been detected in patients with liver cirrhosis and even in hepatocellular carcinoma. Occult HCV infection has been described also in a healthy population with no evidence of liver disease, indicating that this infection may be present in a wide spectrum of clinical situations. Further studies on the natural history and the clinical significance of occult HCV infection are needed to determine its global prevalence, infectivity, implication in causing extrahepatic diseases and its long-term complications in special circumstances such as immunocompromised patients.

REFERENCES

1 **Bartenschlager R**, Lohmann V. Replication of hepatitis C virus. *J Gen Virol* 2000; **81**: 1631-1648
2 **Poenisch M**, Bartenschlager R. New insights into structure and replication of the hepatitis C virus and clinical implications. *Semin Liver Dis* 2010; **30**: 333-347
3 **Bukh J**, Miller RH, Purcell RH. Genetic heterogeneity of hepatitis C virus: quasispecies and genotypes. *Semin Liver Dis* 1995; **15**: 41-63
4 **Bostan N**, Mahmood T. An overview about hepatitis C: a devastating virus. *Crit Rev Microbiol* 2010; **36**: 91-133
5 **Shepard CW**, Finelli L, Alter MJ. Global epidemiology of hepatitis C virus infection. *Lancet Infect Dis* 2005; **5**: 558-567
6 **Alberti A**, Chemello L, Benvegnù L. Natural history of hepatitis C. *J Hepatol* 1999; **31** Suppl 1: 17-24
7 **Ghany MG**, Strader DB, Thomas DL, Seeff LB. Diagnosis, management, and treatment of hepatitis C: an update. *Hepatology* 2009; **49**: 1335-1374
8 **Pawlotsky JM**, Lonjon I, Hezode C, Raynard B, Darthuy F, Remire J, Soussy CJ, Dhumeaux D. What strategy should be used for diagnosis of hepatitis C virus infection in clinical laboratories? *Hepatology* 1998; **27**: 1700-1702
9 **Castillo I**, Pardo M, Bartolomé J, Ortiz-Movilla N, Rodríguez-Iñigo E, de Lucas S, Salas C, Jiménez-Heffernan JA, Pérez-Mota A, Graus J, López-Alcorocho JM, Carreño V. Occult hepatitis C virus infection in patients in whom the etiology of persistently abnormal results of liver-function tests is unknown. *J Infect Dis* 2004; **189**: 7-14
10 **Radkowski M**, Horban A, Gallegos-Orozco JF, Pawelczyk A,

Jablonska J, Wilkinson J, Adair D, Laskus T. Evidence for viral persistence in patients who test positive for anti-hepatitis C virus antibodies and have normal alanine aminotransferase levels. *J Infect Dis* 2005; **191**: 1730-1733
11 **Falcón V**, Acosta-Rivero N, Shibayama M, Luna-Munoz J, Miranda-Sanchez M, de la Rosa MC, Menéndez I, Gra B, Dueñas-Carrera S, García W, Vilar E, Silva J, Lopez D, González-Bravo M, Fernández-Ortega C, Casillas D, Morales J, Kouri J, Tsutsumi V. Evidences of hepatitis C virus replication in hepatocytes and peripheral blood mononuclear cells from patients negative for viral RNA in serum. *Am J Infect Dis* 2005; **1**: 34-42
12 **Carreño V**, Pardo M, López-Alcorocho JM, Rodríguez-Iñigo E, Bartolomé J, Castillo I. Detection of hepatitis C virus (HCV) RNA in the liver of healthy, anti-HCV antibody-positive, serum HCV RNA-negative patients with normal alanine aminotransferase levels. *J Infect Dis* 2006; **194**: 53-60
13 **Pham TN**, MacParland SA, Mulrooney PM, Cooksley H, Naoumov NV, Michalak TI. Hepatitis C virus persistence after spontaneous or treatment-induced resolution of hepatitis C. *J Virol* 2004; **78**: 5867-5874
14 **Radkowski M**, Gallegos-Orozco JF, Jablonska J, Colby TV, Walewska-Zielecka B, Kubicka J, Wilkinson J, Adair D, Rakela J, Laskus T. Persistence of hepatitis C virus in patients successfully treated for chronic hepatitis C. *Hepatology* 2005; **41**: 106-114
15 **Castillo I**, Rodríguez-Iñigo E, López-Alcorocho JM, Pardo M, Bartolomé J, Carreño V. Hepatitis C virus replicates in the liver of patients who have a sustained response to antiviral treatment. *Clin Infect Dis* 2006; **43**: 1277-1283
16 **Pham TN**, Coffin CS, Churchill ND, Urbanski SJ, Lee SS, Michalak TI. Hepatitis C virus persistence after sustained virological response to antiviral therapy in patients with or without past exposure to hepatitis B virus. *J Viral Hepat* 2012; **19**: 103-111
17 **Castillo I**, Rodríguez-Iñigo E, Bartolomé J, de Lucas S, Ortíz-Movilla N, López-Alcorocho JM, Pardo M, Carreño V. Hepatitis C virus replicates in peripheral blood mononuclear cells of patients with occult hepatitis C virus infection. *Gut* 2005; **54**: 682-685
18 **Esaki T**, Suzuki N, Yokoyama K, Iwata K, Irie M, Anan A, Nakane H, Yoshikane M, Nishizawa S, Ueda S, Sohda T, Watanabe H, Sakisaka S. Hepatocellular carcinoma in a patient with liver cirrhosis associated with negative serum HCV tests but positive liver tissue HCV RNA. *Intern Med* 2004; **43**: 279-282
19 **Comar M**, Dal Molin G, D'Agaro P, Crocè SL, Tiribelli C, Campello C. HBV, HCV, and TTV detection by in situ polymerase chain reaction could reveal occult infection in hepatocellular carcinoma: comparison with blood markers. *J Clin Pathol* 2006; **59**: 526-529
20 **Zaghloul H**, El-Sherbiny W. Detection of occult hepatitis C and hepatitis B virus infections from peripheral blood mononuclear cells. *Immunol Invest* 2010; **39**: 284-291
21 **Cortés-Mancera FM**, Restrepo JC, Osorio G, Hoyos S, Correa G, Navas MC. Occult hepatitis C virus infection in a retransplanted patients with liver failure of unknown etiology. *Rev Col Gastroenterol* 2010; **25**: 72-80
22 **Idrees M**, Lal A, Malik FA, Hussain A, Rehman I, Akbar H, Butt S, Ali M, Ali L, Malik FA. Occult hepatitis C virus infection and associated predictive factors: the Pakistan experience. *Infect Genet Evol* 2011; **11**: 442-445
23 **Bokharaei-Salim F**, Keyvani H, Monavari SH, Alavian SM, Madjd Z, Toosi MN, Alizadeh AH. Occult hepatitis C virus infection in Iranian patients with cryptogenic liver disease. *J Med Virol* 2011; **83**: 989-995
24 **Barril G**, Castillo I, Arenas MD, Espinosa M, Garcia-Valdecasas J, Garcia-Fernández N, González-Parra E, Alcazar JM, Sánchez C, Diez-Baylón JC, Martinez P, Bartolomé J, Carreño V. Occult hepatitis C virus infection among hemodialysis patients. *J Am Soc Nephrol* 2008; **19**: 2288-2292
25 **Castillo I**, Bartolomé J, Quiroga JA, Barril G, Carreño V. Hepatitis C virus infection in the family setting of patients with occult hepatitis C. *J Med Virol* 2009; **81**: 1198-1203
26 **De Marco L**, Gillio-Tos A, Fiano V, Ronco G, Krogh V, Palli D, Panico S, Tumino R, Vineis P, Merletti F, Richiardi L, Sacerdote C. Occult HCV infection: an unexpected finding in a population unselected for hepatic disease. *PLoS One* 2009; **4**: e8128
27 **Bartolomé J**, López-Alcorocho JM, Castillo I, Rodríguez-Iñigo E, Quiroga JA, Palacios R, Carreño V. Ultracentrifugation of serum samples allows detection of hepatitis C virus RNA in patients with occult hepatitis C. *J Virol* 2007; **81**: 7710-7715
28 **Nielsen SU**, Bassendine MF, Burt AD, Martin C, Pumeechockchai W, Toms GL. Association between hepatitis C virus and very-low-density lipoprotein (VLDL)/LDL analyzed in iodixanol density gradients. *J Virol* 2006; **80**: 2418-2428
29 **Quiroga JA**, Llorente S, Castillo I, Rodríguez-Iñigo E, Pardo M, Carreño V. Cellular immune responses associated with occult hepatitis C virus infection of the liver. *J Virol* 2006; **80**: 10972-10979
30 **Carreño V**, Bartolomé J, Castillo I, Quiroga JA. Occult hepatitis B virus and hepatitis C virus infections. *Rev Med Virol* 2008; **18**: 139-157
31 **Rico MA**, Ruiz S, Subirá D, Barril G, Cigarrán S, Castañón S, Quiroga JA, Selgas R, Carreño V. Virus-specific effector CD4+ T-cell responses in hemodialysis patients with hepatitis C virus infection. *J Med Virol* 2004; **72**: 66-74
32 **Pham TN**, Coffin CS, Michalak TI. Occult hepatitis C virus infection: what does it mean? *Liver Int* 2010; **30**: 502-511
33 **Pham TN**, Mercer SE, Michalak TI. Chronic hepatitis C and persistent occult hepatitis C virus infection are characterized by distinct immune cell cytokine expression profiles. *J Viral Hepat* 2009; **16**: 547-556
34 **Quiroga JA**, Llorente S, Castillo I, Rodríguez-Iñigo E, López-Alcorocho JM, Pardo M, Carreño V. Virus-specific T-cell responses associated with hepatitis C virus (HCV) persistence in the liver after apparent recovery from HCV infection. *J Med Virol* 2006; **78**: 1190-1197
35 **Barril G**, Quiroga JA, Espinosa M, Arenas D, García-Valdecasas J, González-Parra E, García-Fernández N, Alcazar JN, Sánchez-González MC, Martínez-Rubio P, Llorente S, Castillo I, Bartolomé J, Carreño V. Hepatitis C virus (HCV)-specific T-cell responses are often detectable among hemodialysis patients at risk of occult HCV infection. *Clinical Kideney Journal* 2009; **2** (suppl 2): 1353
36 **Quiroga JA**, Llorente S, Castillo I, Bartolome J, Barril G, Carreño V. Tracking intrafamilial spread of serologically silent occult HCV infection through humoral and cellular HCV-specific responses. *J Hepatol* 2009; **50**; S149
37 **Veerapu NS**, Raghuraman S, Liang TJ, Heller T, Rehermann B. Sporadic reappearance of minute amounts of hepatitis C virus RNA after successful therapy stimulates cellular immune responses. *Gastroenterology* 2011; **140**: 676-685.e1
38 **Quiroga JA**, Castillo I, Pardo M, Rodríguez-Iñigo E, Carreño V. Combined hepatitis C virus (HCV) antigen-antibody detection assay does not improve diagnosis for seronegative individuals with occult HCV infection. *J Clin Microbiol* 2006; **44**: 4559-4560
39 **Takaki A**, Wiese M, Maertens G, Depla E, Seifert U, Liebetrau A, Miller JL, Manns MP, Rehermann B. Cellular immune responses persist and humoral responses decrease two decades after recovery from a single-source outbreak of hepatitis C. *Nat Med* 2000; **6**: 578-582
40 **Toyoda H**, Kumada T, Kiriyama S, Sone Y, Tanikawa M, Hisanaga Y, Kuzuya T, Honda T, Hayashi K, Nakano I, Katano Y, Goto H. Changes in hepatitis C virus (HCV) antibody status in patients with chronic hepatitis C after eradication of HCV infection by interferon therapy. *Clin Infect Dis*

2005; **40**: e49-e54
41 **Umemura T**, Wang RY, Schechterly C, Shih JW, Kiyosawa K, Alter HJ. Quantitative analysis of anti-hepatitis C virus antibody-secreting B cells in patients with chronic hepatitis C. *Hepatology* 2006; **43**: 91-99
42 **Semmo N**, Barnes E, Taylor C, Kurtz J, Harcourt G, Smith N, Klenerman P. T-cell responses and previous exposure to hepatitis C virus in indeterminate blood donors. *Lancet* 2005; **365**: 327-329
43 **Echevarría JM**, Avellón A, Jonas G, Hausmann M, Vockel A, Kapprell HP. Sensitivity of a modified version of the ARCHITECT Anti-HCV test in detecting samples with immunoblot-confirmed, low-level antibody to hepatitis C virus. *J Clin Virol* 2006; **35**: 368-372
44 **Post JJ**, Pan Y, Freeman AJ, Harvey CE, White PA, Palladinetti P, Haber PS, Marinos G, Levy MH, Kaldor JM, Dolan KA, Ffrench RA, Lloyd AR, Rawlinson WD. Clearance of hepatitis C viremia associated with cellular immunity in the absence of seroconversion in the hepatitis C incidence and transmission in prisons study cohort. *J Infect Dis* 2004; **189**: 1846-1855
45 **Quiroga JA**, Castillo I, Llorente S, Bartolomé J, Barril G, Carreño V. Identification of serologically silent occult hepatitis C virus infection by detecting immunoglobulin G antibody to a dominant HCV core peptide epitope. *J Hepatol* 2009; **50**: 256-263
46 **Lodrini S**, Bagaglio S, Canducci F, De Mitri MS, Andreone P, Loggi E, Lazzarin A, Clementi M, Morsica G. Sequence analysis of NS3 protease gene in clinical strains of hepatitis C virus. *J Biol Regul Homeost Agents* 2003; **17**: 198-204
47 **Bukh J**, Purcell RH, Miller RH. Sequence analysis of the core gene of 14 hepatitis C virus genotypes. *Proc Natl Acad Sci USA* 1994; **91**: 8239-8243
48 **Pham TN**, Mulrooney-Cousins PM, Mercer SE, MacParland SA, Inglot M, Zalewska M, Simon K, Michalak TI. Antagonistic expression of hepatitis C virus and alpha interferon in lymphoid cells during persistent occult infection. *J Viral Hepat* 2007; **14**: 537-548
49 **Kubitschke A**, Bahr MJ, Aslan N, Bader C, Tillmann HL, Sarrazin C, Greten T, Wiegand J, Manns MP, Wedemeyer H. Induction of hepatitis C virus (HCV)-specific T cells by needle stick injury in the absence of HCV-viraemia. *Eur J Clin Invest* 2007; **37**: 54-64
50 **Freeman AJ**, Ffrench RA, Post JJ, Harvey CE, Gilmour SJ, White PA, Marinos G, van Beek I, Rawlinson WD, Lloyd AR. Prevalence of production of virus-specific interferon-gamma among seronegative hepatitis C-resistant subjects reporting injection drug use. *J Infect Dis* 2004; **190**: 1093-1097
51 **Mizukoshi E**, Eisenbach C, Edlin BR, Newton KP, Raghuraman S, Weiler-Normann C, Tobler LH, Busch MP, Carrington M, McKeating JA, O'Brien TR, Rehermann B. Hepatitis C virus (HCV)-specific immune responses of long-term injection drug users frequently exposed to HCV. *J Infect Dis* 2008; **198**: 203-212
52 **Zeremski M**, Shu MA, Brown Q, Wu Y, Des Jarlais DC, Busch MP, Talal AH, Edlin BR. Hepatitis C virus-specific T-cell immune responses in seronegative injection drug users. *J Viral Hepat* 2009; **16**: 10-20
53 **Castillo I**, Bartolomé J, Quiroga JA, Barril G, Carreño V. Diagnosis of occult hepatitis C without the need for a liver biopsy. *J Med Virol* 2010; **82**: 1554-1559
54 **Pardo M**, López-Alcorocho JM, Rodríguez-Iñigo E, Castillo I, Carreño V. Comparative study between occult hepatitis C virus infection and chronic hepatitis C. *J Viral Hepat* 2007; **14**: 36-40
55 **Pardo M**, López-Alcorocho JM, Castillo I, Rodríguez-Iñigo E, Perez-Mota A, Carreño V. Effect of anti-viral therapy for occult hepatitis C virus infection. *Aliment Pharmacol Ther* 2006; **23**: 1153-1159
56 **Poynard T**, Marcellin P, Lee SS, Niederau C, Minuk GS, Ideo G, Bain V, Heathcote J, Zeuzem S, Trepo C, Albrecht J. Randomised trial of interferon alpha2b plus ribavirin for 48 weeks or for 24 weeks versus interferon alpha2b plus placebo for 48 weeks for treatment of chronic infection with hepatitis C virus. International Hepatitis Interventional Therapy Group (IHIT). *Lancet* 1998; **352**: 1426-1432
57 **Manns MP**, McHutchison JG, Gordon SC, Rustgi VK, Shiffman M, Reindollar R, Goodman ZD, Koury K, Ling M, Albrecht JK. Peginterferon alfa-2b plus ribavirin compared with interferon alfa-2b plus ribavirin for initial treatment of chronic hepatitis C: a randomised trial. *Lancet* 2001; **358**: 958-965
58 EASL International Consensus Conference on Hepatitis C. Paris, 26-28, February 1999, Consensus Statement. European Association for the Study of the Liver. *J Hepatol* 1999; **30**: 956-961
59 **Alberti A**. Impact of a sustained virological response on the long-term outcome of hepatitis C. *Liver Int* 2011; **31** Suppl 1: 18-22
60 **Castillo I**, Bartolomé J, Quiroga JA, Barril G, Carreño V. Long-term virological follow up of patients with occult hepatitis C virus infection. *Liver Int* 2011; **31**: 1519-1524
61 **Castillo I**, Bartolomé J, Quiroga JA, Barril G, Carreño V. Presence of HCV-RNA after ultracentrifugation of serum samples during the follow-up of chronic hepatitis C patients with a sustained virological response may predict reactivation of hepatitis C virus infection. *Aliment Pharmacol Ther* 2009; **30**: 477-486
62 **Basaras M**, Lombera N, de las Heras B, López C, Arrese E, Cisterna R. Distribution of HCV genotypes in patients infected by different sources. *Res Virol* 1997; **148**: 367-373
63 **Ramos B**, Núñez M, Toro C, Sheldon J, García-Samaniego J, Ríos P, Soriano V. Changes in the distribution of hepatitis C virus (HCV) genotypes over time in Spain according to HIV serostatus: implications for HCV therapy in HCV/HIV-coinfected patients. *J Infect* 2007; **54**: 173-179
64 **Vento S**, Cainelli F, Longhi MS. Reactivation of replication of hepatitis B and C viruses after immunosuppressive therapy: an unresolved issue. *Lancet Oncol* 2002; **3**: 333-340
65 **Melisko ME**, Fox R, Venook A. Reactivation of hepatitis C virus after chemotherapy for colon cancer. *Clin Oncol* (R Coll Radiol) 2004; **16**: 204-205
66 **Zekri AR**, Mohamed WS, Samra MA, Sherif GM, El-Shehaby AM, El-Sayed MH. Risk factors for cytomegalovirus, hepatitis B and C virus reactivation after bone marrow transplantation. *Transpl Immunol* 2004; **13**: 305-311
67 **Melon S**, Galarraga MC, Villar M, Laures A, Boga JA, de Oña M, Gomez E. Hepatitis C virus reactivation in anti-hepatitic C virus-positive renal transplant recipients. *Transplant Proc* 2005; **37**: 2083-2085
68 **Lee WM**, Polson JE, Carney DS, Sahin B, Gale M. Reemergence of hepatitis C virus after 8.5 years in a patient with hypogammaglobulinemia: evidence for an occult viral reservoir. *J Infect Dis* 2005; **192**: 1088-1092
69 **Lin A**, Thadareddy A, Goldstein MJ, Lake-Bakaar G. Immune suppression leading to hepatitis C virus re-emergence after sustained virological response. *J Med Virol* 2008; **80**: 1720-1722
70 **Kopko PM**, Holland PV. Universal leukocyte reduction. *Curr Opin Hematol* 2000; **7**: 397-401

S- Editor Shi ZF **L- Editor** O'Neill M **E- Editor** Zheng XM

World Journal of Gastroenterology

Online Submissions: http://www.wjgnet.com/1007-9327office
wjg@wjgnet.com
doi:10.3748/wjg.v18.i23.2895

World J Gastroenterol 2012 June 21; 18(23): 2895-2901
ISSN 1007-9327 (print) ISSN 2219-2840 (online)

EDITORIAL

Potential prospects of nanomedicine for targeted therapeutics in inflammatory bowel diseases

Madharasi VA Pichai, Lynnette R Ferguson

Madharasi VA Pichai, Lynnette R Ferguson, Discipline of Nutrition, Faculty of Medical and Health Sciences, University of Auckland, Auckland 1142, New Zealand
Author contributions: All authors have contributed equally to this paper.
Correspondence to: Lynnette R Ferguson, Professor, Discipline of Nutrition, Faculty of Medical and Health Sciences, University of Auckland, 85 Park Road, Grafton Private Bag 92019, Auckland Mail Centre, Auckland 1142, New Zealand. l.ferguson@auckland.ac.nz
Telephone: +64-9-9236372 Fax: +64-9-3035962
Received: October 29, 2011 Revised: April 5, 2012
Accepted: April 10, 2012
Published online: June 21, 2012

Peer reviewers: Dr. Pingchang Yang, MD, PhD, Department of Pathology and Molecular Medicine, McMaster University, BBI-T3330, 50 Charlton Ave East, Hamilton, L8N 4A6, Canada; Emiko Mizoguchi, MD, PhD, Department of Medicine, Gastrointestinal Unit, GRJ 702, Massachusetts General Hospital, Boston, MA 02114, United States

Pichai MVA, Ferguson LR. Potential prospects of nanomedicine for targeted therapeutics in inflammatory bowel diseases. *World J Gastroenterol* 2012; 18(23): 2895-2901 Available from: URL: http://www.wjgnet.com/1007-9327/full/v18/i23/2895.htm DOI: http://dx.doi.org/10.3748/wjg.v18.i23.2895

Abstract

Inflammatory bowel diseases (IBDs) such as Crohn's disease are highly debilitating. There are inconsistencies in response to and side effects in the current conventional medications, failures in adequate drug delivery, and the lack of therapeutics to offer complete remission in the presently available treatments of IBD. This suggests the need to explore beyond the horizons of conventional approaches in IBD therapeutics. This review examines the arena of the evolving IBD nanomedicine, studied so far in animal and *in vitro* models, before comprehensive clinical testing in humans. The investigations carried out so far in IBD models have provided substantial evidence of the nanotherapeutic approach as having the potential to overcome some of the current drawbacks to conventional IBD therapy. We analyze the pros and cons of nanotechnology in IBD therapies studied in different models, aimed at different targets and mechanisms of IBD pathogenesis, in an attempt to predict its possible impact in humans.

Key words: Inflammatory bowel disease; Crohn's disease; Ulcerative colitis; Tumor necrosis factor-α; Nanomedicine

INTRODUCTION

Crohn's disease (CD) and ulcerative colitis (UC) constitute the two principal components of inflammatory bowel diseases (IBDs), which occur as a result of dysregulated immune responses in genetically predisposed individuals due to various environmental conditions[1]. There are sufficient similarities in the pathological conditions in CD and UC that cause about 10% of IBD cases to be diagnosed as indeterminate IBD[2]. Nevertheless, CD and UC show discrete risk factors and dissimilar gene and protein expressions, which manifest distinctive pathophysiological mechanisms. CD exhibits a transmural inflammatory response and can be associated with granulomas, whereas UC usually shows mucosa-confined inflammation[2-8]. Genomic technologies are now being used to separate the effects of different susceptibility genes in the two diseases. For example, Wu *et al*[6] have studied 36 expression profiles of colonoscopic pinch biopsies from CD and UC patients. Affected genes, mostly related to interferon (IFN)-γ inducible T helper cell 1 (TH1) process and antigen presentation in CD patients, were differentially regulated, with the upregulation of 47 genes and downregulation of 30 genes. In contrast, the expression of genes from UC biopsies showed upregulation of 51 genes and downregulation of 81 other genes,

associated with biosynthesis, metabolism and electrolyte transport[6].

The common conventional medications currently in use to treat both CD and UC involve 5-aminosalicylic acid drugs, corticosteroids, immunosuppressive agents, biologic therapies and antibiotics[9], with a customary "step up" approach of starting with aminosalicylates and rising to corticosteroids and immunosuppressive agents in response to the persisting conditions of the disease. The more effective biological therapies are usually considered as a last option and only in case of refractory diseases, because their systemic action in the host often leads to adverse effects[10,11].

Nanomedicines are precise therapeutics established with the aid of nanotechnology to treat diseases at the molecular level[12]. The application of nanotechnology in medicine can be termed as nanomedicine. It is an evolving face of medicine that uses nanoparticulate carriers to deliver therapeutics targeted to specific cells, or constituents of cells or tissues. Studies have shown nanomedicines to be more beneficial than conventional medications, because their size leads to more effecting targeting, better availability at diseased tissues, and decreased adverse effects. Moreover, nanomedicines have been found to have similar or even better therapeutic impacts at lower drug concentrations than their conventional counterparts[12]. However, although the arena of nanomedicine appears to be encouraging for IBD therapy, concerns related to the impact of the nature of nanoparticles due to their size, shape, aggregation potential, and surface chemistry on the IBD gut need to be scrutinized[12,13], and investigations on the impact of nanomedicine in IBD therapy is currently in early stages. As targeted drug or biological delivery to sites of inflammation remains a crucial challenge in the current treatment of IBD[14], nanostrategies involving short interfering RNAs (siRNAs), antisense oligonucleotides, nanomedicines delivered to the sites of malfunction in IBD can be a valuable therapeutic approach.

The RNA interference technique, notable for specificity, can be speculated to regulate the expression of proinflammatory cytokines and genes related to IBD at the mRNA level[15]. As the impact of noncoding RNAs and RNA silencing in gene modulation is known to be great[16], the use of siRNAs as drugs to silence proinflammatory genes is being scrutinized in various animal models of IBD. This strategy also reduces the chances of immune reactions usually associated with viral vectors[15,17,18]. Due to the potential importance of targeted therapy in IBD, this review is presented to explore the advancements in the prospects of nanomedicine in the modulation of gene expression and targeted therapeutics in IBD (Figure 1).

GENE AND PROTEIN MODULATIONS WITH NANO PROSPECTS

Amongst the key genes involved in IBD pathogenesis,

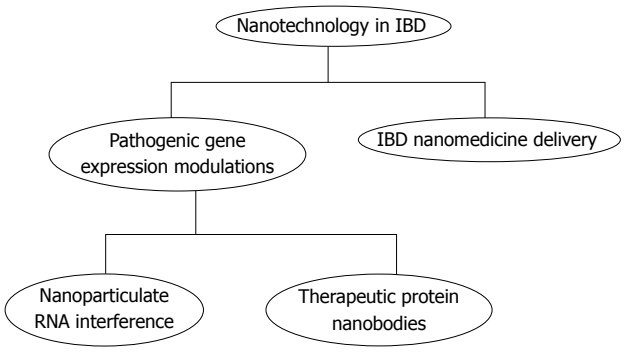

Figure 1 Graphical representation of nanoinvestigations in inflammatory bowel diseases models. IBD: Inflammatory bowel disease.

the function of tumor necrosis factor (TNF)-α in the mediation of inflammation in IBD is extensively acknowledged. Therefore, many biological therapies comprising monoclonal antibodies or soluble receptors are intended to reduce TNF-α activity, and have been extensively tested in many clinical trials[19-24]. However, there are adverse side effects due to the systemic depletion of TNF-α. These adverse effects involve amplified infusion reactions, immunosuppression, opportunistic infections and decreased efficacy of the biologics due to antibody formation against them[24-26].

The gene silencing nanostrategy, in which orally delivered TNF-α siRNA is encapsulated in thioketal nanoparticles (TKNs) made from the polymer poly-PPADT (1, 4-phenyleneacetone dimethylene thioketal), effectively decreases the levels of TNF-α mRNA levels at sites of intestinal inflammation in dextran sulfate sodium (DSS)-induced mouse models of UC. In this study, the site specific delivery of siRNA was made possible due to the ability of TKNs to degrade in the presence of higher levels of reactive oxygen species (ROS) present in regions of inflammation in the intestinal tissue[27]. In another study, TNF-α siRNA/polyethyleneimine (PEI) nanocomplex was shown to inhibit TNF-α secretion by macrophages *in vitro*, whereas the oral administration of TNF-α siRNA/PEI nanocomplexes in lipopolysaccharides (LPS)-treated mice models was found to reduce specifically the synthesis and secretion of TNF-α in the colon[28]. Nanoparticles in a microsphere oral system (Ni-MOS), comprised of TNF-α siRNA entrapped in type B gelatin enclosed in poly(ε-caprolactone) (PCL) microspheres, were found to exhibit favorable gene silencing in the colon tissues of DSS-treated murine models of UC. This treatment results in the suppression of proinflammatory cytokines such as interleukin (IL)-1β, IFN-γ, chemokine monocyte chemoattractant protein (MCP)-1, permitting an increase in body weight and diminished action of tissue myeloperoxidase in mouse models[29]. A protein modulation nanostrategy involving monovalent and bivalent murine TNF-α neutralizing nanobody proteins has been investigated in DSS-induced murine chronic colitis models. *Lactococcus lactis* engineered to produce the therapeutic nanobodies was orally administered, which

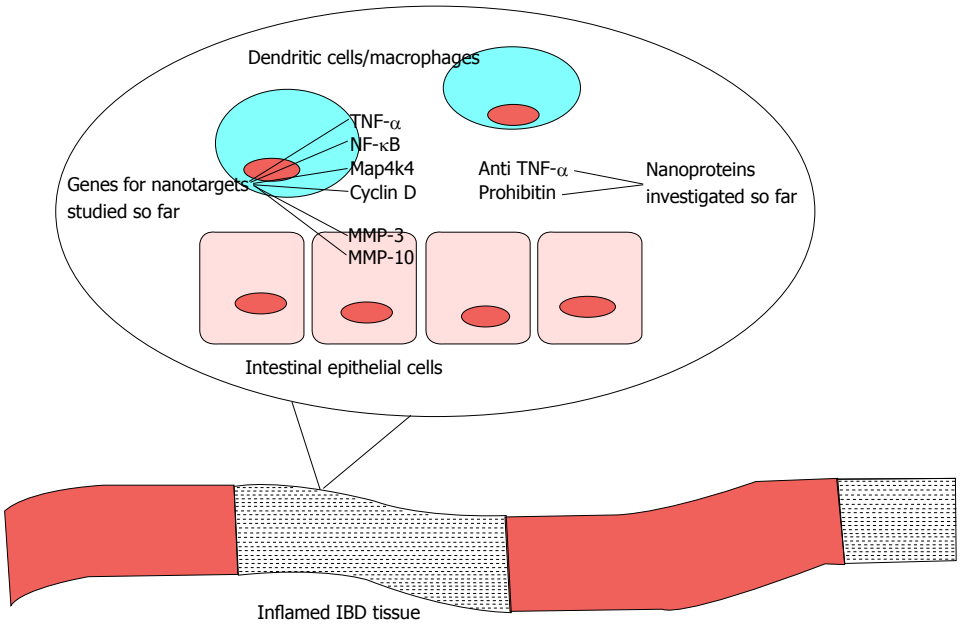

Figure 2 Nanomodulations whose efficacy has been validated in animal models of inflammatory bowel diseases. Genes regulated therapeutically by nano gene silencing in intestinal tissues and macrophages and protein nanobodies that have been investigated to have therapeutic impacts to help control inflammation and tissue destruction in animal models relevant to inflammatory bowel diseases (IBDs). TNF: Tumor necrosis factor; Map4k4: Mitogen-activated protein kinase kinase kinase kinase 4; MMP: Matrix metalloproteinase; NF-κB: Nuclear factor kappa B.

resulted in a significant reduction in the TNF-α driven inflammation in the mucosa of the colon in mouse models, without affecting considerable TNF-α levels in the systemic circulation[30].

Increased TNF-α suppresses the expression of the anti-inflammatory protein prohibitin (PHB) in IBD[31,32], therefore, a study by Theiss *et al*[33] considered the oral delivery of PHB entrapped in poly (lactic acid) nanoparticles in mouse models of DSS-induced colitis. This strategy inhibited the TNF-α-induced nuclear factor (NF)-κB activation; consequently curtailing inflammatory reactions and reducing the severity of colitis. Double-stranded decoy oligonucleotides (ODNs) against the proinflammatory NF-κB gene were enclosed in chitosan-modified poly (D,L-lactide-co-glycolide) nanospheres (CS-PLGA NSs) and delivered orally to DSS-induced murine colitis models. This study showed the absorption of the ODN-CS-PLGA NSs in inflamed mucosal regions, producing considerable curative effects on DSS-induced diarrhea, bloody feces, shortening of colon length, and myeloperoxidase activity[34].

Besides directly inhibiting the TNF-α gene in macrophages, macrophages more generally play a role in inducing the pathogenic inflammatory reactions[35]. This study has revealed the importance of mitogen-activated protein kinase kinase kinase kinase 4 (Map4k4) gene in macrophages in mediating the production of inflammatory cytokines. Map4k4 siRNA encapsulated in β1,3-D-glucan shells silenced Map4k4 expression *in vivo* in mice treated with LPS, protecting them from LPS-induced systemic inflammation by suppressing the production of TNF-α and IL-1β[35].

Matrix metalloproteinases (MMPs) play a vital role in tissue remodeling by regulating the intestinal tissue architecture during the inflammatory reactions and wound healing in IBD[36,37]. Studies have indicated the increased expression of MMP-3 (stromelysin-1) and MMP-10 (stromelysin-2) in causing enhanced tissue injury in DSS-induced murine colitis[38,39]. Furthermore, IBD patients have shown increased MMP-3 and MMP-10 expression in the gut and intestinal ulcer tissues[39-42]. Polymorphisms in various MMP genes may be susceptibility factors for IBD risk, at least in some populations[43]. A study by Kobayashi *et al*[39] demonstrated the specific inhibition of MMP-3 and MMP-10 by siRNA targeted against MMP-3 and MMP-10, having a therapeutic benefit in protecting the colon tissue and reducing the severity of colitis in DSS-treated murine models, which could therefore be a valuable gene silencing option to prevent intestinal damage in IBD (Figure 2).

Cyclin D1 (CyD1) is a cell cycle regulatory protein that is upregulated in IBD in both epithelial and immune cells[44]. A leukocyte-directed siRNA against CyD1 mRNA inhibits the intestinal inflammatory responses in murine models of DSS-induced colitis. Silencing the CyD1 gene decreases the induction of TH1 cell inflammatory cytokines TNF-α and IL-12, but has no impact on the production of TH2 cell cytokine IL-10[45]. Therapeutic efforts to enhance the action of the anti-inflammatory cytokine IL-10, which is known to be critically involved in maintaining mucosal immune balance due to its potent impact on immunosuppression[46] and involvement in CD pathogenesis[47,48], have been largely unsuccessful to date. This is thought to be due to the adverse side effects caused by systemic action of the IL-10 therapies, and the low concentrations of IL-10 delivered to the intestinal tissues[49]. Therefore, biologics intend-

ing to enhance cytokine IL-10 action have been dropped from the current IBD therapies[50]. However, because the involvement of IL-10 and its genetic variations in IBD is great[47,48,51], a consideration of the targeted study by Bhavsar *et al*[52], which involved the nanodelivery of IL-10-producing plasmid to the mucosa in murine models mimicking IBD intestinal epithelial pathogenesis[53] can be scrutinized. According to this study, trinitrobenzene sulfonic acid (TNBS)-induced acute colitis models in Balb/c mice were treated with NiMOS intended for oral gene therapy. This comprised the pORF5-mIL-10 plasmid DNA encapsulated in type B gelatin nanoparticles in PCL. This strategy directed the local transfection of IL-10 plasmid in inflamed intestinal tissues and caused its enhanced expression, which led to suppression of predominant proinflammatory cytokines such as IFN-γ, TNF-α, IL-1α, IL-1β and IL-12, consequently causing the therapeutic benefits of restored colon length and weight, increased body weight, and beneficial clinical activity score[52].

IMPLICATIONS OF IBD DRUGS GOING NANO

Nanomedicines comprising IBD drugs loaded onto nanoparticles, designed to cope and act in accordance with the pathophysiological changes in the intestinal tissues of IBD, can be an intelligent mode of targeted drug delivery. This approach offers the possibility of eliminating undesirable side effects usually caused by systemic action of the drugs[14]. The usual pathophysiological conditions related to inflamed intestinal tissues in IBD predominantly involve abnormal intestinal permeability, increased presence of immune cells, and higher levels of mucus production[54-56].

Cellular interaction of nanoparticles in the IBD gut

Nanomedicines in IBD can potentially be more efficient in their mechanism due to the cellular intake of the nanoparticles by the cells at the targeted sites of delivery. This means that they are not eliminated from the intestinal tract by diarrhea, as are many current conventional medications. This is an important IBD symptom[57,58]. Nanoparticles in the gastrointestinal tract are usually found to be adsorbed either by paracellular transport or endocytosis by regular epithelial cells[59]. Specialized differentiated epithelial cells called M cells, which form major populations of Peyer's patches are involved in the predominant uptake of nanoparticles through transcytosis[60,61]. Predominant CD mutations such as R702W, G908R and 3020insC have been associated with ileal-specific disease[62,63], which show an enhanced presence in Peyer's patches and M cells, which may cause an increase in the uptake of dietary and nanoparticulate substances[13]. In addition to these, translocation of nanoparticles in the intestinal tract can also occur by persorption through gaps or holes at the villous tips[64,65]. Cells involve the autophagic mechanism to cause the clearance of nanoparticles[66], and Powell *et al*[13] have indicated that mutations in the autophagy gene *Atg16L1* in IBD subjects can be susceptible to possible alterations in the clearance of nanoparticles.

Investigations of IBD drugs in nanomodes

Furthermore, IBD drugs delivered in nanomodes have been shown to have greater therapeutic impacts as compared to their conventional delivery studied in animal models, For example, the anti-inflammatory IBD drug mesalamine (5-ASA) covalently linked to the PCL nanoparticles was found to be 60 times more efficient as a nanomedicine at much lower doses (0.5 mg/kg) than the free solution of 5-ASA (30 mg/kg) in treating TNBS-induced colitis in BALB/c murine models[67]. Moulari *et al*[68] have established that silicon nanoparticles have a sixfold increased ability to adhere to inflamed tissues when compared to tissues in healthy controls. In this study, 5-ASA loaded in its methylated form in silicon nanoparticles was shown to collect in inflamed regions in TNBS-induced murine colitis models, inducing a positive impact on clinical activity score and myeloperoxidase activity at reduced drug doses, as compared to conventional delivery[68]. An immunosuppressive drug tacrolimus, used to treat UC, was encapsulated in polylactic-co-glycolic acid (PLGA) nanoparticles and used to treat murine models of TNBS- and oxazolone-induced colitis. This study showed that nanomedicine had an augmented and specific action with a threefold increased penetration in inflamed tissues when compared to healthy tissues[69]. Also, tacrolimus-loaded PLGA nanoparticles and tacrolimus-loaded pH-sensitive Eudragit P-4135F nanoparticles showed diminished side effects in DSS-induced murine colitis models when compared to the free tacrolimus which causes nephrotoxicity in traditional delivery[70]. An anti-inflammatory tripeptide Lys-Pro-Val (KPV) loaded into polylactide (PLA) nanoparticles delivered in combination with a polysaccharide hydrogel had a similar anti-inflammatory effect at 12 000-fold lower doses (25.2 ng/d) to that of KPV in free solution (200 μg/d), thus demonstrating the greater therapeutic efficiency of the nanomode of the drug in treating DSS-induced colitis in murine models[71]. Nakase *et al*[72] demonstrated that dexamethasone, encapsulated in poly-DL-lactic acid (PDLLA) microspheres was more effective in ameliorating DSS-induced murine colitis when compared to the free solution of the same drug, because the microsphere form was engulfed by the immune cells in the inflamed colonic tissue, which resulted in increased efficiency of the drug in mouse models. An *ex vivo* study by Serpe *et al*[73] showed solid lipid nanoparticles (SLNs) comprising the anti-inflammatory molecule cholesteryl butyrate (chol-but) showed a greater impact than butyrate alone in significantly reducing proinflammatory cytokines such as IL-1β and TNF-α and increasing IL-10 production in whole blood *ex vivo* models of peripheral blood mononuclear cells (PBMCs) obtained from IBD patients taking no anti-inflammatory medications. Furthermore, this study demonstrated SLNs, consisting of the immunosuppres-

Table 1 Comparison of therapeutic parameters

Experimental system	Drug in nano mode	Comparison of differences in certain distinct therapeutic parameters		Ref.
		Nano mode	Controls	
In vivo TNBS-induced murine colitis	5-ASA covalently linked to PCL nanoparticles	Myeloperoxidase (MPO) activity of 5-ASA-NP at 0.5 mg/kg: 15.2 ± 5.6 U/mg	MPO activity of 5-ASA free solution at 30 mg/kg: 16.2 ± 3.6 U/mg	[67]
In vivo TNBS-induced murine colitis	5-ASA in silicon nanoparticles	MPO activity of 5-ASA-Si NP at 25 mg/kg: 5.2 ± 2.4 U/mg	MPO activity of 5-ASA-free solution at 100 mg/kg: 8.2 ± 3.4 U/mg	[68]
In vivo TNBS-induced murine colitis/oxazolone-induced murine colitis	Tacrolimus in PLGA NPs	Enhanced penetration into the inflamed tissue-FK506-NP, 105 ± 24 nmol/cm^2	Healthy tissue penetration-FK506-NP, 51 ± 13 nmol/cm^2	[69]
In vivo DSS- induced murine colitis	Tacrolimus in PLGA/or pH sensitive Eudragit P-4135F NPs	Diminished side effects	Increased susceptibility to nephrotoxicity	[70]
In vivo DSS-induced murine colitis	Anti-inflammatory tripeptide KPV in PLA NPs	Nanomode with lowered doses at 25.2 ng/d	Free solution has the similar anti-inflammatory impact at 200 μg/d	[71]
Whole blood *ex vivo* models of PBMCs	Dexamethasone in SLNs	90% reduction in proinflammatory cytokines IL-1β and TNF-α	25% reduction in TNF-α by the free solution	[73]
Whole blood *ex vivo* models of PBMCs	chol-but in SLNs	Significant decrease in IL-1β, and TNF-α increase in IL-10	-	[73]

NP: Nanoparticle; TNBS: Trinitrobenzene sulfonic acid; DSS: Dextran sulfate sodium; PBMCs: Peripheral blood mononuclear cells; 5-ASA: Mesalamine; KPV: Lys-Pro-Val; PLA: Polylactide; SLNs: Solid lipid nanoparticles; IL: Interleukin; TNF: Tumor necrosis factor; MPO: Myeloperoxidase; PLGA: Polylactic-co-glycolic acid.

sive corticosteroid dexamethasone, suppressed TNF-α by 90% when the free solution of dexamethasone showed a TNF-α suppression of 25% at the highest concentrations in similar whole blood IBD *ex vivo* models. These studies provide preliminary support for the effects of SLNs chol-but and SLN dexamethasone in inducing an enhanced anti-inflammatory activity, due to the more effective cellular intake of the nanodrug forms, as compared to the free drugs in solution (Table 1).

LIKELY CONCERNS OF GOING NANO

The general concern associated with the nano approach is due to the fact that nano-sized materials display altered physicochemical properties[74] as compared to their larger counterparts, with chances of causing possible toxicity, since nonbiological nanoparticulate carriers above a particle size of 100-200 nm can alter normal cellular activity, because they can invoke cell membrane ruffling, cytoskeletal rearrangement and stimulate endocytic machinery causing their ingression in phagocytic cells[75]. However, reliable data on the adverse impacts of nanomedicine in IBD is unavailable, whereas the impact of nanoparticles themselves in the gastrointestinal tract might vary according to the nanoparticle polymer material and nanoparticle size, as surface interactions and surface chemistry differ for different nanoparticle sizes. Also, different nanoparticle sizes can cause different mechanisms of cellular uptake, due to which, nanoparticle sizes can be modulated to cause different intracellular effects[13,76,77]. The studies on the effects of nanoparticles themselves in the human gastrointestinal tract in IBD have been limited and need to be explored further.

Although nanostrategies for IBD therapeutics investigated in animal and *in vitro* models of IBD have shown promise, it is still only the dawn of the era of interest in IBD nanomedicine, and there is a definite need for further extensive investigations on many issues related to the safety and uptake of the different nanomedical therapeutics acting on various pathways and phases in the human gastrointestinal tract. It is essential to be confident of their consequent impact on immune responses and therapeutic effects in the different genotypic populations, before recommending the clinical use of nanomedicines to treat IBD in humans.

REFERENCES

1 **Xavier RJ**, Podolsky DK. Unravelling the pathogenesis of inflammatory bowel disease. *Nature* 2007; **448**: 427-434
2 **Podolsky DK**. Inflammatory bowel disease. *N Engl J Med* 2002; **347**: 417-429
3 **Barrett JC**, Hansoul S, Nicolae DL, Cho JH, Duerr RH, Rioux JD, Brant SR, Silverberg MS, Taylor KD, Barmada MM, Bitton A, Dassopoulos T, Datta LW, Green T, Griffiths AM, Kistner EO, Murtha MT, Regueiro MD, Rotter JI, Schumm LP, Steinhart AH, Targan SR, Xavier RJ, Libioulle C, Sandor C, Lathrop M, Belaiche J, Dewit O, Gut I, Heath S, Laukens D, Mni M, Rutgeerts P, Van Gossum A, Zelenika D, Franchimont D, Hugot JP, de Vos M, Vermeire S, Louis E, Cardon LR, Anderson CA, Drummond H, Nimmo E, Ahmad T, Prescott NJ, Onnie CM, Fisher SA, Marchini J, Ghori J, Bumpstead S, Gwilliam R, Tremelling M, Deloukas P, Mansfield J, Jewell D, Satsangi J, Mathew CG, Parkes M, Georges M, Daly MJ. Genome-wide association defines more than 30 distinct susceptibility loci for Crohn's disease. *Nat Genet* 2008; **40**: 955-962
4 **Parkes M**, Jewell D. Ulcerative colitis and Crohns disease: molecular genetics and clinical implications. *Expert Rev Mol Med* 2001; **2001**: 1-18
5 **McGovern DP**, Gardet A, Törkvist L, Goyette P, Essers J, Taylor KD, Neale BM, Ong RT, Lagacé C, Li C, Green T, Stevens CR, Beauchamp C, Fleshner PR, Carlson M, D'

Amato M, Halfvarson J, Hibberd ML, Lördal M, Padyukov L, Andriulli A, Colombo E, Latiano A, Palmieri O, Bernard EJ, Deslandres C, Hommes DW, de Jong DJ, Stokkers PC, Weersma RK, Sharma Y, Silverberg MS, Cho JH, Wu J, Roeder K, Brant SR, Schumm LP, Duerr RH, Dubinsky MC, Glazer NL, Haritunians T, Ippoliti A, Melmed GY, Siscovick DS, Vasiliauskas EA, Targan SR, Annese V, Wijmenga C, Pettersson S, Rotter JI, Xavier RJ, Daly MJ, Rioux JD, Seielstad M. Genome-wide association identifies multiple ulcerative colitis susceptibility loci. *Nat Genet* 2010; **42**: 332-337

6 **Wu F**, Dassopoulos T, Cope L, Maitra A, Brant SR, Harris ML, Bayless TM, Parmigiani G, Chakravarti S. Genome-wide gene expression differences in Crohn's disease and ulcerative colitis from endoscopic pinch biopsies: insights into distinctive pathogenesis. *Inflamm Bowel Dis* 2007; **13**: 807-821

7 **Shkoda A**, Werner T, Daniel H, Gunckel M, Rogler G, Haller D. Differential protein expression profile in the intestinal epithelium from patients with inflammatory bowel disease. *J Proteome Res* 2007; **6**: 1114-1125

8 **Lawrance IC**, Fiocchi C, Chakravarti S. Ulcerative colitis and Crohn's disease: distinctive gene expression profiles and novel susceptibility candidate genes. *Hum Mol Genet* 2001; **10**: 445-456

9 **Talley NJ**, Abreu MT, Achkar JP, Bernstein CN, Dubinsky MC, Hanauer SB, Kane SV, Sandborn WJ, Ullman TA, Moayyedi P. An evidence-based systematic review on medical therapies for inflammatory bowel disease. *Am J Gastroenterol* 2011; **106** Suppl 1: S2-S25; quiz S26

10 **Desilva S**, Kaplan G, Panaccione R. Sequential therapies for Crohn's disease: optimizing conventional and biologic strategies. *Rev Gastroenterol Disord* 2008; **8**: 109-116

11 **Schmidt KJ**, Büning J, Jankowiak C, Lehnert H, Fellermann K. Crohn's targeted therapy: myth or real goal? *Curr Drug Discov Technol* 2009; **6**: 290-298

12 **Hock SC**, Ying YM, Wah CL. A review of the current scientific and regulatory status of nanomedicines and the challenges ahead. *PDA J Pharm Sci Technol* 2011; **65**: 177-195

13 **Powell JJ**, Faria N, Thomas-McKay E, Pele LC. Origin and fate of dietary nanoparticles and microparticles in the gastrointestinal tract. *J Autoimmun* 2010; **34**: J226-J233

14 **Lamprecht A**. IBD: selective nanoparticle adhesion can enhance colitis therapy. *Nat Rev Gastroenterol Hepatol* 2010; **7**: 311-312

15 **Plevy SE**, Targan SR. Future therapeutic approaches for inflammatory bowel diseases. *Gastroenterology* 2011; **140**: 1838-1846

16 **Ferguson LR**. RNA silencing: Mechanism, biology and responses to environmental stress. *Mutat Res* 2011; **714**: 93-94

17 **Pellish RS**, Nasir A, Ramratnam B, Moss SF. Review article: RNA interference--potential therapeutic applications for the gastroenterologist. *Aliment Pharmacol Ther* 2008; **27**: 715-723

18 **Lieberman J**, Song E, Lee SK, Shankar P. Interfering with disease: opportunities and roadblocks to harnessing RNA interference. *Trends Mol Med* 2003; **9**: 397-403

19 **Mueller C**. Tumour necrosis factor in mouse models of chronic intestinal inflammation. *Immunology* 2002; **105**: 1-8

20 **Holtmann MH**, Neurath MF. Anti-TNF strategies in stenosing and fistulizing Crohn's disease. *Int J Colorectal Dis* 2005; **20**: 1-8

21 **D'Haens G**. Anti-TNF therapy for Crohn's disease. *Curr Pharm Des* 2003; **9**: 289-294

22 **Oldenburg B**, Hommes D. Biological therapies in inflammatory bowel disease: top-down or bottom-up? *Curr Opin Gastroenterol* 2007; **23**: 395-399

23 **Sandborn WJ**. Strategies for targeting tumour necrosis factor in IBD. *Best Pract Res Clin Gastroenterol* 2003; **17**: 105-117

24 **van Deventer SJ**. New biological therapies in inflammatory bowel disease. *Best Pract Res Clin Gastroenterol* 2003; **17**: 119-130

25 **Van Assche G**, Vermeire S, Rutgeerts P. Safety issues with biological therapies for inflammatory bowel disease. *Curr Opin Gastroenterol* 2006; **22**: 370-376

26 **Hoentjen F**, van Bodegraven AA. Safety of anti-tumor necrosis factor therapy in inflammatory bowel disease. *World J Gastroenterol* 2009; **15**: 2067-2073

27 **Wilson DS**, Dalmasso G, Wang L, Sitaraman SV, Merlin D, Murthy N. Orally delivered thioketal nanoparticles loaded with TNF-α-siRNA target inflammation and inhibit gene expression in the intestines. *Nat Mater* 2010; **9**: 923-928

28 **Laroui H**, Theiss AL, Yan Y, Dalmasso G, Nguyen HT, Sitaraman SV, Merlin D. Functional TNFα gene silencing mediated by polyethyleneimine/TNFα siRNA nanocomplexes in inflamed colon. *Biomaterials* 2011; **32**: 1218-1228

29 **Kriegel C**, Amiji M. Oral TNF-α gene silencing using a polymeric microsphere-based delivery system for the treatment of inflammatory bowel disease. *J Control Release* 2011; **150**: 77-86

30 **Vandenbroucke K**, de Haard H, Beirnaert E, Dreier T, Lauwereys M, Huyck L, Van Huysse J, Demetter P, Steidler L, Remaut E, Cuvelier C, Rottiers P. Orally administered L. lactis secreting an anti-TNF Nanobody demonstrate efficacy in chronic colitis. *Mucosal Immunol* 2010; **3**: 49-56

31 **Theiss AL**, Idell RD, Srinivasan S, Klapproth JM, Jones DP, Merlin D, Sitaraman SV. Prohibitin protects against oxidative stress in intestinal epithelial cells. *FASEB J* 2007; **21**: 197-206

32 **Hsieh SY**, Shih TC, Yeh CY, Lin CJ, Chou YY, Lee YS. Comparative proteomic studies on the pathogenesis of human ulcerative colitis. *Proteomics* 2006; **6**: 5322-5331

33 **Theiss AL**, Laroui H, Obertone TS, Chowdhury I, Thompson WE, Merlin D, Sitaraman SV. Nanoparticle-based therapeutic delivery of prohibitin to the colonic epithelial cells ameliorates acute murine colitis. *Inflamm Bowel Dis* 2011; **17**: 1163-1176

34 **Tahara K**, Samura S, Tsuji K, Yamamoto H, Tsukada Y, Bando Y, Tsujimoto H, Morishita R, Kawashima Y. Oral nuclear factor-κB decoy oligonucleotides delivery system with chitosan modified poly(D,L-lactide-co-glycolide) nanospheres for inflammatory bowel disease. *Biomaterials* 2011; **32**: 870-878

35 **Aouadi M**, Tesz GJ, Nicoloro SM, Wang M, Chouinard M, Soto E, Ostroff GR, Czech MP. Orally delivered siRNA targeting macrophage Map4k4 suppresses systemic inflammation. *Nature* 2009; **458**: 1180-1184

36 **Naito Y**, Yoshikawa T. Role of matrix metalloproteinases in inflammatory bowel disease. *Mol Aspects Med* 2005; **26**: 379-390

37 **Ravi A**, Garg P, Sitaraman SV. Matrix metalloproteinases in inflammatory bowel disease: boon or a bane? *Inflamm Bowel Dis* 2007; **13**: 97-107

38 **von Lampe B**, Barthel B, Coupland SE, Riecken EO, Rosewicz S. Differential expression of matrix metalloproteinases and their tissue inhibitors in colon mucosa of patients with inflammatory bowel disease. *Gut* 2000; **47**: 63-73

39 **Kobayashi K**, Arimura Y, Goto A, Okahara S, Endo T, Shinomura Y, Imai K. Therapeutic implications of the specific inhibition of causative matrix metalloproteinases in experimental colitis induced by dextran sulphate sodium. *J Pathol* 2006; **209**: 376-383

40 **Gordon JN**, Pickard KM, Di Sabatino A, Prothero JD, Pender SL, Goggin PM, MacDonald TT. Matrix metalloproteinase-3 production by gut IgG plasma cells in chronic inflammatory bowel disease. *Inflamm Bowel Dis* 2008; **14**: 195-203

41 **Louis E**, Ribbens C, Godon A, Franchimont D, De Groote D, Hardy N, Boniver J, Belaiche J, Malaise M. Increased production of matrix metalloproteinase-3 and tissue inhibitor of metalloproteinase-1 by inflamed mucosa in inflammatory bowel disease. *Clin Exp Immunol* 2000; **120**: 241-246

42 **Vaalamo M**, Karjalainen-Lindsberg ML, Puolakkainen P, Kere J, Saarialho-Kere U. Distinct expression profiles of

stromelysin-2 (MMP-10), collagenase-3 (MMP-13), macrophage metalloelastase (MMP-12), and tissue inhibitor of metalloproteinases-3 (TIMP-3) in intestinal ulcerations. *Am J Pathol* 1998; **152**: 1005-1014
43 **Morgan AR**, Han DY, Lam WJ, Triggs CM, Fraser AG, Barclay M, Gearry RB, Meisner S, Stokkers P, Boeckxstaens GE, Ferguson LR. Genetic variations in matrix metalloproteinases may be associated with increased risk of ulcerative colitis. *Hum Immunol* 2011; **72**: 1117-1127
44 **Maclachlan I**. siRNAs with guts. *Nat Biotechnol* 2008; **26**: 403-405
45 **Peer D**, Park EJ, Morishita Y, Carman CV, Shimaoka M. Systemic leukocyte-directed siRNA delivery revealing cyclin D1 as an anti-inflammatory target. *Science* 2008; **319**: 627-630
46 **Li MC**, He SH. IL-10 and its related cytokines for treatment of inflammatory bowel disease. *World J Gastroenterol* 2004; **10**: 620-625
47 **Correa I**, Veny M, Esteller M, Piqué JM, Yagüe J, Panés J, Salas A. Defective IL-10 production in severe phenotypes of Crohn's disease. *J Leukoc Biol* 2009; **85**: 896-903
48 **Santaolalla R**, Mañé J, Pedrosa E, Lorén V, Fernández-Bañares F, Mallolas J, Carrasco A, Salas A, Rosinach M, Forné M, Espinós JC, Loras C, Donovan M, Puig P, Mañosa M, Gassull MA, Viver JM, Esteve M. Apoptosis resistance of mucosal lymphocytes and IL-10 deficiency in patients with steroid-refractory Crohn's disease. *Inflamm Bowel Dis* 2011; **17**: 1490-1500
49 **Herfarth H**, Schölmerich J. IL-10 therapy in Crohn's disease: at the crossroads. Treatment of Crohn's disease with the anti-inflammatory cytokine interleukin 10. *Gut* 2002; **50**: 146-147
50 **Buruiana FE**, Solà I, Alonso-Coello P. Recombinant human interleukin 10 for induction of remission in Crohn's disease. *Cochrane Database Syst Rev* 2010: CD005109
51 **Wang AH**, Lam WJ, Han DY, Ding Y, Hu R, Fraser AG, Ferguson LR, Morgan AR. The effect of IL-10 genetic variation and interleukin 10 serum levels on Crohn's disease susceptibility in a New Zealand population. *Hum Immunol* 2011; **72**: 431-435
52 **Bhavsar MD**, Amiji MM. Oral IL-10 gene delivery in a microsphere-based formulation for local transfection and therapeutic efficacy in inflammatory bowel disease. *Gene Ther* 2008; **15**: 1200-1209
53 **Wirtz S**, Neurath MF. Mouse models of inflammatory bowel disease. *Adv Drug Deliv Rev* 2007; **59**: 1073-1083
54 **Bruewer M**, Luegering A, Kucharzik T, Parkos CA, Madara JL, Hopkins AM, Nusrat A. Proinflammatory cytokines disrupt epithelial barrier function by apoptosis-independent mechanisms. *J Immunol* 2003; **171**: 6164-6172
55 **Allison MC**, Cornwall S, Poulter LW, Dhillon AP, Pounder RE. Macrophage heterogeneity in normal colonic mucosa and in inflammatory bowel disease. *Gut* 1988; **29**: 1531-1538
56 **Seldenrijk CA**, Drexhage HA, Meuwissen SG, Pals ST, Meijer CJ. Dendritic cells and scavenger macrophages in chronic inflammatory bowel disease. *Gut* 1989; **30**: 484-491
57 **Ulbrich W**, Lamprecht A. Targeted drug-delivery approaches by nanoparticulate carriers in the therapy of inflammatory diseases. *J R Soc Interface* 2010; **7** Suppl 1: S55-S66
58 **Laroui H**, Wilson DS, Dalmasso G, Salaita K, Murthy N, Sitaraman SV, Merlin D. Nanomedicine in GI. *Am J Physiol Gastrointest Liver Physiol* 2011; **300**: G371-G383
59 **Mohanraj VJ**, Chen Y. Nanoparticles-A Review. *Trop J Pharm Res* 2006; **5**: 561-573
60 **des Rieux A**, Ragnarsson EG, Gullberg E, Préat V, Schneider YJ, Artursson P. Transport of nanoparticles across an in vitro model of the human intestinal follicle associated epithelium. *Eur J Pharm Sci* 2005; **25**: 455-465
61 **Seifert J**, Sass W. Intestinal absorption of macromolecules and small particles. *Dig Dis* 1990; **8**: 169-178
62 **Cuthbert AP**, Fisher SA, Mirza MM, King K, Hampe J, Croucher PJ, Mascheretti S, Sanderson J, Forbes A, Mansfield J, Schreiber S, Lewis CM, Mathew CG. The contribution of NOD2 gene mutations to the risk and site of disease in inflammatory bowel disease. *Gastroenterology* 2002; **122**: 867-874
63 **Ahmad T**, Armuzzi A, Bunce M, Mulcahy-Hawes K, Marshall SE, Orchard TR, Crawshaw J, Large O, de Silva A, Cook JT, Barnardo M, Cullen S, Welsh KI, Jewell DP. The molecular classification of the clinical manifestations of Crohn's disease. *Gastroenterology* 2002; **122**: 854-866
64 **Volkheimer G**. [Persorption of microparticles]. *Pathologe* 1993; **14**: 247-252
65 **Hillyer JF**, Albrecht RM. Gastrointestinal persorption and tissue distribution of differently sized colloidal gold nanoparticles. *J Pharm Sci* 2001; **90**: 1927-1936
66 **Zabirnyk O**, Yezhelyev M, Seleverstov O. Nanoparticles as a novel class of autophagy activators. *Autophagy* 2007; **3**: 278-281
67 **Pertuit D**, Moulari B, Betz T, Nadaradjane A, Neumann D, Ismaïli L, Refouvelet B, Pellequer Y, Lamprecht A. 5-amino salicylic acid bound nanoparticles for the therapy of inflammatory bowel disease. *J Control Release* 2007; **123**: 211-218
68 **Moulari B**, Pertuit D, Pellequer Y, Lamprecht A. The targeting of surface modified silica nanoparticles to inflamed tissue in experimental colitis. *Biomaterials* 2008; **29**: 4554-4560
69 **Lamprecht A**, Yamamoto H, Takeuchi H, Kawashima Y. Nanoparticles enhance therapeutic efficiency by selectively increased local drug dose in experimental colitis in rats. *J Pharmacol Exp Ther* 2005; **315**: 196-202
70 **Meissner Y**, Pellequer Y, Lamprecht A. Nanoparticles in inflammatory bowel disease: particle targeting versus pH-sensitive delivery. *Int J Pharm* 2006; **316**: 138-143
71 **Laroui H**, Dalmasso G, Nguyen HT, Yan Y, Sitaraman SV, Merlin D. Drug-loaded nanoparticles targeted to the colon with polysaccharide hydrogel reduce colitis in a mouse model. *Gastroenterology* 2010; **138**: 843-853.e1-2
72 **Nakase H**, Okazaki K, Tabata Y, Chiba T. Biodegradable microspheres targeting mucosal immune-regulating cells: new approach for treatment of inflammatory bowel disease. *J Gastroenterol* 2003; **38** Suppl 15: 59-62
73 **Serpe L**, Canaparo R, Daperno M, Sostegni R, Martinasso G, Muntoni E, Ippolito L, Vivenza N, Pera A, Eandi M, Gasco MR, Zara GP. Solid lipid nanoparticles as anti-inflammatory drug delivery system in a human inflammatory bowel disease whole-blood model. *Eur J Pharm Sci* 2010; **39**: 428-436
74 **Nel AE**, Mädler L, Velegol D, Xia T, Hoek EM, Somasundaran P, Klaessig F, Castranova V, Thompson M. Understanding biophysicochemical interactions at the nano-bio interface. *Nat Mater* 2009; **8**: 543-557
75 **Harding CV**, Song R. Phagocytic processing of exogenous particulate antigens by macrophages for presentation by class I MHC molecules. *J Immunol* 1994; **153**: 4925-4933
76 **Lamprecht A**, Schäfer U, Lehr CM. Size-dependent bioadhesion of micro- and nanoparticulate carriers to the inflamed colonic mucosa. *Pharm Res* 2001; **18**: 788-793
77 **Paulo CS**, Pires das Neves R, Ferreira LS. Nanoparticles for intracellular-targeted drug delivery. *Nanotechnology* 2011; **22**: 494002

S- Editor Cheng JX **L- Editor** Kerr C **E- Editor** Zheng XM

World Journal of Gastroenterology

Online Submissions: http://www.wjgnet.com/1007-9327office
wjg@wjgnet.com
doi:10.3748/wjg.v18.i23.2902

World J Gastroenterol 2012 June 21; 18(23): 2902-2908
ISSN 1007-9327 (print) ISSN 2219-2840 (online)

TOPIC HIGHLIGHT

Luis Bujanda, PhD, Professor, *Series Editor*

Spontaneous regression of pancreatic cancer: Real or a misdiagnosis?

Marta Herreros-Villanueva, Elizabeth Hijona, Angel Cosme, Luis Bujanda

Marta Herreros-Villanueva, Schulze Center for Novel Therapeutics, Division of Oncology Research, Department of Medicine, Mayo Clinic, Rochester, MN 55905, United States
Elizabeth Hijona, Angel Cosme, Luis Bujanda, Department of Gastroenterology, Centro de Investigación Biomédica en Red en Enfermedades Hepáticas y Digestivas, University of the Basque Country, Donostia Hospital-Biodonostia Institute, 20014 San Sebastian, Spain
Author contributions: Herreros-Villanueva M and Hijona E designed and wrote the paper; Cosme A and Bujanda L designed and reviewed the paper.
Supported by Instituto Salud Carlos Ⅲ
Correspondence to: Luis Bujanda, MD, PhD, Department of Gastroenterology, Centro de Investigación Biomédica en Red en Enfermedades Hepáticas y Digestivas, University of the Basque Country, Donostia Hospital-Biodonostia Institute, Paseo Dr. Beguiristain S/N, 20014 San Sebastian, Spain. luis.bujanda@osakidetza.net
Telephone: +34-94-3007173 Fax: +34-94-3007065
Received: January 1, 2012 Revised: March 4, 2012
Accepted: March 20, 2012
Published online: June 21, 2012

Abstract

Spontaneous tumor regression has been subject of numerous studies and speculations for many years. This phenomenon is exceptional, but well reported, in some types of tumors, but not in pancreatic cancer. Pancreatic cancer has the worst five-year survival rate of any cancer. Despite numerous molecular studies and clinical approaches, using several mouse models, this cancer responds poorly to the existing chemotherapeutic agents and progress on treatment remains elusive. Although pancreatic cancer tumors seldom undergo spontaneous regression, and some authors take that with skepticism, there are some cases reported in the literature. However, the variability in the description of the reports and technical details could make this process susceptible to misdiagnosis. Distinguishing between different types of pancreatic carcinoma should be taken with caution as they have wide differences in malignant potential. Diseases such as pancreatic benign tumors, insulinomas, or autoimmune pancreatitis could be responsible for this misdiagnosis as a pancreatic cancer. Here we review different cases reported, their clinical characteristics, and possible mechanisms leading to spontaneous regression of pancreatic cancer. We also discuss the possibilities of misdiagnosis.

Key words: Autoimmune pancreatitis; Insulinoma; Pancreatic cancer; Pancreatic ductal adenocarcinoma; Spontaneous regression

Peer reviewers: Dr. Alexander S Rosemurgy, Tampa General Medical Group, 409 Bayshore Blvd, Tampa, FL 33606, United States; Keiji Hanada, Center for Gastroendoscopy, Onomichi General Hospital, 1-10-25 Hirahara, Onomichi 722-8508, Japan; Massimo Falconi, Department of Surgery, Policlinico GB Rossi Piazzale Scuro 10, 37134 Verona, Italy

Herreros-Villanueva M, Hijona E, Cosme A, Bujanda L. Spontaneous regression of pancreatic cancer: Real or a misdiagnosis? *World J Gastroenterol* 2012; 18(23): 2902-2908 Available from: URL: http://www.wjgnet.com/1007-9327/full/v18/i23/2902.htm DOI: http://dx.doi.org/10.3748/wjg.v18.i23.2902

INTRODUCTION

Spontaneous tumor regression has been the subject of great interest and speculation for many years. It is an exceptional and well-documented biological event in some types of tumors, but not in pancreatic cancer.

Pancreatic cancer is a special form of cancer with the worst five-year survival rate of any cancer[1]. Despite numerous molecular studies and clinical approaches, using several mouse models[2], this cancer responds poorly to the existing chemotherapeutic agents and progress on

treatment remains elusive[3].

Pancreatic cancer is seldom described as undergoing spontaneous regression, but there are some cases reported in the literature.

In this review, the historical background, clinical features, and possible mechanisms are discussed for spontaneous regression of pancreatic cancer. In addition, we discuss whether it is a real phenomenon or a misdiagnosis.

Further understanding of this process and harnessing of the mechanisms involved will have significant diagnostic, preventative, and therapeutic implications.

HISTORICAL BACKGROUND AND CASES REPORTED FOR PANCREATIC CANCER

Spontaneous regression of cancer (SRC) is defined as the partial or complete disappearance of a malignant tumor in the absence of therapy that is capable of inducing anti-neoplastic effects. Although SRC has often been questioned, the literature reveals different cases showing this phenomenon. In 1966, Everson *et al*[4] published a classical monograph review describing 176 cases of SRC published from 1900 to 1964. In 1990, Challis *et al*[5] reported cases from 1900 to 1987, the majority of which occurred in renal cell carcinoma, choriocarcinoma, neuroblastoma, melanoma, breast cancer, and leukemia and lymphomas. Later, in 1993, O'Regan *et al*[6] agreed that the five most common tumors to undergo spontaneous regression are renal cell carcinoma, leukemia and lymphoma, neuroblastoma, carcinoma of breast and melanoma.

In these three main reviews, only three cases of pancreatic cancer were cited, and none of them were described in detail. Here, we review the most important cases of spontaneous regression of pancreatic cancer that have been reported in the literature. The first reported case was described in 1934 and published in 1967, describing a patient admitted to hospital presenting jaundice, severe pain, nausea, chills, and a high fever[7]. Laparotomy and biopsy confirmed pancreatic carcinoma. The patient's recovery spanned two months, after which she could return to work. She remained in good health, dying seven and a half years later of a pulmonary embolism. An autopsy did not find any tumors.

The second case was reported in 1973 by Lokich *et al*[8] and described a 42-year-old man with progressive diarrhea and weight loss. An upper image suggested a mass in the head of the pancreas. The patient underwent total pancreatectomy and microscopic examination reveled a moderately well differentiated ductal adenocarcinoma arising in the head of the pancreas. Adenocarcinoma was also found in the body of the pancreas, but the tail had only pancreatitis with fibrosis.

Although the patient was stabilized with insulin treatment, one year later he presented with rectal carcinomatosis consistent with adenocarcinoma of pancreatic cancer. Postoperatively, the patient received a combined chemotherapeutic program based on 5-fluorouracil (5-FU) and carmustine or bis-chloroethylnitrosourea, experiencing a gradual regression. Twenty-six months following onset of therapy treatment, there was no evidence of tumor recurrence.

The third case[9] was a male with a two-month history of ulcer pain and diarrhea. At exploration, he was diagnosed with a large tumor of the pancreatic head, extending into the liver with involved lymph nodes. The disease was confirmed by biopsy but no further manipulation was performed. By the fourth month following surgery, he was asymptomatic. Examined six years later, the patient remained symptom-free and a gastrointestinal exam demonstrated healing of the ulcer.

The fourth case, published in 1974, reported one case in 1962 of a 21-year-old male who presented with jaundice, anorexia, and fever of three months duration[10]. A liver biopsy was followed by abdominal pain, fever, tachycardia, and a decrease in blood pressure. Exploratory surgery to repair bile peritonitis revealed acute cholangitis and pericholangitis. When he was re-operated on seven weeks later, and was diagnosed with pancreatic adenocarcinoma. A T tube placed in the common duct improved symptoms and he made a slow recovery with no recurrence at the time of reporting. Unfortunately, details on the duration and intensity of fever or infection over the course of the illness in most of these cases were not provided.

In 2003, Hoption Cann *et al*[11] reported a case of a 50-year-old man with a three-month history of weight loss, anorexia, and discomfort after meals. By ultrasound and computed tomography (CT) identified a hypoechoic mass of 6.5 cm × 4 cm × 4 cm in the body of the pancreas. The posterior CT-guided biopsy was positive for pancreatic adenocarcinoma (T2N1M0, stage Ⅲb). A subsequent CT scan revealed a further 50%-60% increase in tumor volume and the tumor was considered inoperable. The patient received chemotherapy based on gemcitabine, mytomycin, and radiotherapy. As CA19-9 levels increased from 38 to 140 U/mL and the patient's health declined, the treatment was considered a failure. Some days later, the patient developed acute abdominal pain and fever and, after surgery, he had a perforated duodenal ulcer with contamination of the abdomen. Recovery was considered doubtful. However 90 d later, the patient's recuperation and weight gain were surprisingly rapid, while the CA19-9 level was normal and a positron emission tomography (PET) scan was negative for any focal disease. An ultrasound, however, confirmed residual tumor, although it had regressed by approximately 70%. However, five months later, an elevated CA19-9 and subsequent PET scan confirmed a relapse. Although the patient was treated with chemotherapy based on oxaliplatin and 5-FU initially, then gemcitabine, his health progressively deteriorated and he died one year later, almost two years following his febrile infection.

Apart from the infection, the authors suggested other factors could be relevant to this tumor regression. Some of them are the vegetarian diet based on Chinese herbs,

high-dose vitamin C and other antioxidant vitamins, hydrogen peroxide, and ginseng, followed by this patient. However, regression presented in this case appeared mostly to coincide with a prolonged febrile infection, similar to that often observed in many other cases of SRC[11,12].

BENIGN TUMORS

Some special types of pancreatic tumors are considered benign or their malignant potential is not well determined. Specifically, solid-pseudopapillary tumors are classified in this category and were often previously described in the literature as being related to spontaneous regression.

In 2008, Nakahara *et al*[13] described a 18-year-old healthy woman who was admitted to hospital for evaluation of a pancreatic mass. A solid-pseudopapillary tumor was suspected from the findings of diagnostic images, and surgery was recommended. However, the patient refused surgery and a later ultrasound-guided transcutaneous biopsy revealed proliferation of tumoral cells with small nuclei showing a pseudopapillary arrangement. periodic acid-Schiff positive granules and alpha-1-antitrypsin positive cells were proven, which led to confirmed diagnosis of pseudopapillary pancreatic tumor. The maximum diameter of the tumor gradually decreased over 10 years from 45 mm to 15 mm. This was the first report describing marked spontaneous shrinkage of this particular type of pancreatic tumor. The authors did not report details of whether the patient took any medication, antioxidant agent, or vitamins.

In this case, the authors showed histological findings and CT images suggesting that the shrinkage of the tumor may be attributable to continued degenerative change, including minor hemorrhage, necrosis, and absorption as the tumor was classified hypovascular.

In 2010, Suzuki *et al*[14] described a 13-year-old boy showing a demarcated hypovascular round mass of 50 mm in diameter in the head of the pancreas, presenting abdominal pain, nauseas, and elevated serum amylase and serum lipase. CT demonstrated a partially enhanced encapsulated tumoral mass with cystic components and calcification, without evidence of invasion to the surrounding organs, which was diagnosed as solid pseudopapillary tumor (SPT) and treated for acute pancreatitis. Six weeks later, the mass had decreased to 43 mm in diameter, and nine weeks after admission, concentrations of tumor markers, such as alpha-fetoprotein, carcinoembryonic antigen, carbohydrate antigen-199, and elastase-I, were not elevated, although the level of neuron-specific enolase (NSE) was slightly increased. Follow-up included routine laboratory tests and CT demonstrated that the size of the tumor slowly decreased to non-measurable size. After 4 years, the patient's NSE level was within the normal range. The authors presented CT images indicating that the tumor was highly likely to be SPT, based on the typical CT finding of a tumor bulging from the contour of the pancreas with eggshell-like calcification, the existence of both solid and cystic components with hypovascularity, and the patient's age. The rapid shrinkage of the tumor may be attributable to continued degenerative changes, including minor hemorrhage due to trauma, necrosis, and absorption. The authors did not report the administration of any medication or different agents to the patient. The authors suggest spontaneous tumor shrinkage, although they were unable to obtain pathology for the tumor and are conscious that there have been reports of recurrence and metastasis that developed more than 10 years after tumor resection in this type of neoplasm.

Considering all of the cases reported above, we can distinguish a wide variation in the description of the data presented. The first cases reported, until 1980, do not show images or acute laboratory test results that could verify the real entity of spontaneous regression of pancreatic carcinoma. In some cases, they do not specify the type of pancreatic tumor or give details about the biopsy, making it difficult to determine if it would be classified as a different entity, based in current diagnostic criteria.

However, considering the difference in the availability of medical technology more than 30 years ago compared with the present, this data should be taken with caution, and it is difficult to conclude whether these cases would be considered as genuine spontaneous regression of pancreatic adenocarcinoma today or would be considered as misdiagnoses.

The most recent cases, published since 2000, are more accurate in the presentation of images and blood test values, although they also show variability.

Finally, the most recent report concludes a diagnosis of SPT and not adenocarcinoma of pancreas. All of these data show that there are no recent cases reported of spontaneous regression of adenocarcinoma of the pancreas, unlike pseudopapillary tumors, which represent 1% of primary pancreatic tumors and are characterized by low malignant potential[13,14].

Some other types of pancreatic tumors with spontaneous regression, rather than adenocarcinomas and peudopapillary tumors, have been described. The most common neuroendocrine tumor with spontaneous regression is an insulinoma.

Insulinoma is a rare endocrine tumor developed from pancreatic beta cells. Eighty-seven percent are benign tumors, seven percent belong to multiendocrine neoplasia syndrome, and only six percent are considered malignant, as defined by the presence of metastasis[15].

The diagnosis of insulinoma is established by demonstrating inappropriately high serum insulin concentrations during a spontaneous or induced episode of hypoglycemia. Imaging techniques are then used to localize the tumor[16]. In 2008, Groselj *et al*[17] described a 64-year-old patient presenting with paroxysmal episodes. Electroencephalography finding suggested metabolic encephalopathy and laboratory tests showed hypoglycemia, and high insulin and C-peptide. Finally, ultrasonography and gagnetic resonance imaging (MRI) confirmed an

insulinoma in the head of the pancreas. The authors pointed out that the patient had a spontaneous recovery of the pancreatic tumor.

The overall survival rate of patients with benign insulinoma do not differ from that expected in the general population, and a misdiagnosis could be a reasonable justification for reporting SRC, even if it is not considered a malignant phenotype. Malignant insulinomas are rare, and patients have prolonged survival, even in the presence of liver or lymph node metastasis. It has been reported that some patients with malignant insulinoma who developed metastatic disease 4 years to 12 years after initial diagnosis, remained alive for up to 25 years[18]. This better outcome compared to the acinar or ductal adenocarcinoma could be a reason for a misdiagnosis, or it could also be reported as a spontaneous regression of pancreatic cancer.

AUTOIMMUNE PANCREATITIS MIMICKING PANCREATIC CANCER

Autoimmune pancreatitis (AIP) was described by Sarles *et al*[19] in 1961 and then proposed by Yoshida *et al*[20] in 1995 as a type of chronic pancreatitis occurring secondary to an autoimmune process, which may cause permanent structural and functional damage of the pancreas.

AIP represents approximately 6% of the patients with chronic pancreatitis[21,22] and is a heterogeneous manifestation associated with elevated serum levels of the immunoglobulin G subtype 4 (IgG4), which decreases with corticosteroid therapy. The most common site of extrapancreatic involvement is the bile duct, where distal biliary or mass-forming AIP mimics pancreatic cancer and proximal biliary involvement[23]. Recently, two types of AIP have been described, type 1 (or lymphoplasmacytic sclerosing pancreatitis) and type 2 (idiopathic duct centric pancreatitis or granulocyte epithelial lesion). Although clinically these two entities have comparable presentations, they differ significantly in their demography, serological characteristics, other organ involvement, and relapse rate[24].

While type 1 is associated with elevation of nonspecific autoantibodies and serum IgG4 levels, type 2 does not have definitive serologic autoimmune markers. In addition, high serum IgG4 may also be found in patients with pancreatic cancer[25], and tumoral markers such as CA19-9, SPAN-1, and DUPAN-2 may also be elevated in patients with AIP[26]. These findings can make the diagnosis of AIP confusing. AIP, in contrast to other benign chronic pancreatic diseases, can be cured with immunosuppressant drugs[27]; therefore, the differentiation of AIP from pancreatic cancer is of particular interest in clinical practice[28]. Two studies have also pointed out the possibility that some patients with AIP may develop pancreatic cancer[29,30], and this contributes to increasing misdiagnosis. However, the synchronous presence of adenocarcinoma and AIP can not be excluded, as some cases have been reported[31] and pancreatic cancer can develop after histologically confirmed AIP diagnosis[32].

Attempting to establish applicable diagnostic guidelines, the Japan Pancreas Society[33], the Korean Society[34], and more recently American criteria by Chari *et al*[24] in the Mayo Clinic at the Honolulu consensus proposed specific criteria to distinguished the two histological types of AIP and pancreatic cancer. The five important diagnostic criteria include imaging, histology, serology, other organ involvement and response to therapy, leading to an improvement in the diagnostic yield for AIP and avoidance of misdiagnosis of pancreatic cancer[35]. Nevertheless, several cases have been reported that suspect pancreatic cancer rather than AIP[36-38].

In 2005, Ozden *et al*[39] described a 58-year-old woman with jaundice referred for pancreatic head carcinoma and diagnosed by MRI. By laparotomy, a pancreatic head mass involving the mesocolon, pancreatic body, and tail was found. Pancreatic biopsies revealed cholecystitis and pancreatitis with lymphoplasmacytic infiltration. Two months after the surgery there was no parenchymal lesion on MRI. Serum immunoglobulin G, G4, and E levels were increased.

The authors report this as a spontaneous regression of a pancreatic head mass and biliary obstruction because of autoimmune pancreatitis. In this and other cases of a patient with autoimmune pancreatitis that were initially misdiagnosed as pancreatic cancer, the response to steroid therapy could appear to be a spontaneous resolution of a malignant pancreatic tumor. Patients operated on for pancreatic adenocarcinoma could represent a false spontaneous regression of pancreatic cancer instead of lack of malignancy.

MECHANISMS LEADING TO SPONTANEOUS REGRESSION

Most of the SRC cases reported do not provide a discussion regarding possible explanatory mechanisms. In pancreatic cancer reports, only the most recent publications show data in detail (images and laboratory test) and finally suggest some possible biological mechanisms leading to the spontaneous regression.

The prevalent hypotheses regarding mechanisms leading to spontaneous regression include the immunological response in the host as the most important factor[40-43]. Other mechanisms causing spontaneous regression include increased apoptosis and necrosis, epigenetic modifications, hormonal responses, role of oncogenes and tumoral suppressors, cytokines and growth factors, and psychological mechanisms (Table 1). All of these mechanisms were reviewed in 1996 by Papac[44], who specifically described some cancers, but not pancreatic tumors.

Today, the activation of these mechanisms in spontaneous regression of cancer occurs infrequently[5,40,45,46] and remains not well documented in pancreatic cancer. In other related tumors, like hepatocellular carcinoma, several mechanisms leading to the spontaneous regression of these tumors have been described, such as absti-

Table 1 Possible mechanisms for spontaneous regression in pancreatic cancer

Immunological response
Hormonal response
Induction of spontaneous differentiation
Elimination of the carcinogen
Modification in expression of oncogenes and tumoral suppressor genes
Angiogenesis inhibition
Apoptosis
Necrosis
Epigenetic mechanisms
Psychological mechanisms

nence from alcohol[47], persistent fever[48], withdrawal of androgen[49], blood transfusion[50], massive bleeding[51], and use of herbal medicine[52]. However, in the small number of reported pancreatic cancer cases, no evidence of clear and specific events was observed during the period of spontaneous regression.

Renal cell carcinoma accounts for the largest number of patients with spontaneous regression with acceptable histology and radiological confirmation[53,54]; therefore, this disease offers the best system to study the immunological response in spontaneous regression. The increased incidence of some tumors in immunosuppressed individuals, and regression following reduction of immunosupressive agents, suggests an important role for immunological factors[55,56]. Cytokines, interferon, and interleukin 2 (IL-2), IL-6 and IL-8[57,58], exert antitumor effects. While cytokines could activate T-lymphocytes, natural killer, lymphocyte-activated killer cells, and tumor infiltrating lymphocyte cells as a mechanism of action, interferons are capable of multiple immunomodulatory effects, involving monocytes, macrophages, and B-cells, as well as induction of IL-2 receptors[59,60].

Regression often occurs in the setting of febrile illness (bacterial or viral), other, different, cytokines associated with the host response to infections could mediate the regression as tumor necrosis factors[61]. Patients diagnosed with pancreatic cancer frequently suffer infections and all of these cytokines could play an important role in the spontaneous regression of pancreatic cancer; however, there is no evidence of this phenomena in the literature. Angiogenesis, as an essential component of the malignant process, has also been investigated as a mechanism contributing to regression. Several cytokines are known to inhibit this process, such as tumor necrosis factor-alpha and transforming growth factor beta, which could play a role in spontaneous regression[62]. Regarding hormonal mechanisms that could exert a role in pancreatic cancer, there is no data suggesting specific effects in spontaneous regression, although studies should be made because the endocrine pancreas could be exerting an important role.

A mechanism that has received more attention for spontaneous regression in the literature is the apoptotic process inside the tumor. The activation of this programmed cell death was proposed as the basis for spontaneous regression, especially in neuroblastoma[63] and renal cell carcinoma. Several authors suggest that the neoplastic cells, in response to different stimuli, such as T-cell mediated survival signals or cytokine regulation, could undergo apoptosis, followed by clinical remission.

As several data have demonstrated, vascular endothelial growth factor receptor blockade leads to rapid, robust, and progressive regression of tumor vasculature, increased intratumoral hypoxia, and apoptosis, and reduced tumor invasiveness and metastasis in pancreatic islet cancer[64]. Thus, this process could also be implicated in tumor regression. This apoptotic process is driven by oncogenes and tumoral suppressor gene expression and, although there is no specific, documented examples on the role of changes in the expression of regulator genes, this possibility has been cited in leukemia[65].

The expression of these oncogenes or tumoral suppressors could be switched by mutations and by epigenetic mechanisms, leading to apoptosis inside the tumor. The cited epigenetic changes have been demonstrated in retinoblastoma tumors[66] by abnormalities in methylation levels[67]. Some authors have suggested that loss of hypermethylation may be involved in the spontaneous regression of some retinoblastomas, but there is no confirmed evidence. In addition, repression of telomerase activity has been proposed as a possible mechanism for regression[68-70]. Some studies showed that patients whose tumors do not show telomerase activity underwent spontaneous regression, suggesting repression of telomerase activity as a possible mechanism for regression, although it has not yet been demonstrated in any type of pancreatic cancer.

Differentiation, a mechanism by which malignant cells develop a non-malignant phenotype, has been shown to occur in several types of cancer, such as retinoblastoma, neuroblastoma, choriocarcinoma, teratocarcinoma, and leukemias[71,72], where differentiation is possibly the major factor contributing to spontaneous regression, but this is still unknown in pancreatic cancer. Finally, related to the immunological response in tumors, psychological mechanisms have been proposed as a possible phenomenon in some cancers, but this is still regarded with skepticism. Although authors have reported psychological reasons, corroborating biological studies are lacking[73,74] and are not approved by most investigators.

This lack of information forces us to conclude that spontaneous regression in pancreatic cancer is not a well-documented phenomenon, the mechanisms leading to the regression remains unknown, and only hypotheses can be made based on some other types of tumors. In recent reports, where the radiological and histological confirmation of pancreatic disease are more precise, only an immunological response has been suggested as the most probable mechanism leading to regression of pancreatic cancer. Most of the causative factors leading to this phenomenon remain speculative.

In conclusion, it is very difficult to determine the characteristics of pancreatic cancer patients who experi-

ence spontaneous regression and the mechanisms leading to such spontaneous regression.

Currently, the existence of spontaneous regression of pancreatic cancer is a matter of debate. The small number of cases cited in the literature as a possible spontaneous regression could represent a nonmalignant disease, such as AIP or specific pseudopapillary tumor of the pancreas. In the cases described many years ago, the data presented make it difficult evaluate the diagnosis because of the lack of advanced images techniques or laboratory tests to distinguish pancreatic cancer from other diseases. In addition, many cases are not completely well documented, the presence of metastasis is questionable, therapy may have played a role, or the temporary or permanent regression of tumor growth was not defined.

Therefore, cases of spontaneous regression of pancreatic cancer described in the literature should be taken caution. Biological and molecular findings cannot provide a complete explanation of the underlying mechanisms and accumulation of such cases and further investigations of regression will contribute to better understanding of this intriguing phenomenon.

Elucidation of the mechanism could lead to better understanding and replication of the process, and to improved therapies for pancreatic cancer treatment.

REFERENCES

1 **Jemal A**, Siegel R, Xu J, Ward E. Cancer statistics, 2010. *CA Cancer J Clin* 2010; **60**: 277-300
2 **Herreros-Villanueva M**, Hijona E, Cosme A, Bujanda L. Mouse model of pancreatic cancer. *World J Gastroenterol* 2012; **18**: 1286-1294
3 **Herreros-Villanueva M**, Hijona E, Cosme A, Bujanda L. Adjuvant and neoadjuvant treatment in pancreatic cancer. *World J Gastroenterol* 2012; **18**: 1565-1572
4 **Everson TC**, Cole WH. Spontaneous regression of cancer. Philadelphia, PA: WB Saunders, 1966: 6-7
5 **Challis GB**, Stam HJ. The spontaneous regression of cancer. A review of cases from 1900 to 1987. *Acta Oncol* 1990; **29**: 545-550
6 **O'Regan B**, Hirschberg C. Spontaneous Remission. An Annotated Bibliography. Sausalito, California: Institute of Noetic Sciences, 1993
7 **Shapiro SL**. Spontaneous regression of cancer. *Eye Ear Nose Throat Mon* 1967; **46**: 1306-1310
8 **Lokich JJ**, Brooks JR. Disappearance of disseminated pancreatic carcinoma with combined chemotherapy. *Ann Surg* 1973; **177**: 13-14
9 **Eidemiller LR**, Fletcher WS, Dennis DL, Krippaehne WW. Spontaneous remission of proven cancer. *Northwest Med* 1971; **70**: 539-543
10 **Tchertkoff V**, Hauser AD. Carcinoma of head of pancreas with spontaneous regression. *N Y State J Med* 1974; **74**: 1814-1817
11 **Hoption Cann SA**, van Netten JP, van Netten C. Dr William Coley and tumour regression: a place in history or in the future. *Postgrad Med J* 2003; **79**: 672-680
12 **Maywald O**, Buchheidt D, Bergmann J, Schoch C, Ludwig WD, Reiter A, Hastka J, Lengfelder E, Hehlmann R. Spontaneous remission in adult acute myeloid leukemia in association with systemic bacterial infection-case report and review of the literature. *Ann Hematol* 2004; **83**: 189-194
13 **Nakahara K**, Kobayashi G, Fujita N, Noda Y, Ito K, Horaguchi J, Takasawa O, Obana T. Solid-pseudopapillary tumor of the pancreas showing a remarkable reduction in size over the 10-year follow-up period. *Intern Med* 2008; **47**: 1335-1339
14 **Suzuki M**, Shimizu T, Minowa K, Ikuse T, Baba Y, Ohtsuka Y. Spontaneous shrinkage of a solid pseudopapillary tumor of the pancreas: CT findings. *Pediatr Int* 2010; **52**: 335-336
15 **Service FJ**, McMahon MM, O'Brien PC, Ballard DJ. Functioning insulinoma--incidence, recurrence, and long-term survival of patients: a 60-year study. *Mayo Clin Proc* 1991; **66**: 711-719
16 **Placzkowski KA**, Vella A, Thompson GB, Grant CS, Reading CC, Charboneau JW, Andrews JC, Lloyd RV, Service FJ. Secular trends in the presentation and management of functioning insulinoma at the Mayo Clinic, 1987-2007. *J Clin Endocrinol Metab* 2009; **94**: 1069-1073
17 **Groselj LD**, Butinar D. Insulinoma presenting itself as a night paroxysmal disorder with spontaneous recovery. *Lijec Vjesn* 2008; **130**: 104-105
18 **Hirshberg B**, Cochran C, Skarulis MC, Libutti SK, Alexander HR, Wood BJ, Chang R, Kleiner DE, Gorden P. Malignant insulinoma: spectrum of unusual clinical features. *Cancer* 2005; **104**: 264-272
19 **Sarles H**, Sarles JC, Muratore R, Guien C. Chronic inflammatory sclerosis of the pancreas--an autonomous pancreatic disease? *Am J Dig Dis* 1961; **6**: 688-698
20 **Yoshida K**, Toki F, Takeuchi T, Watanabe S, Shiratori K, Hayashi N. Chronic pancreatitis caused by an autoimmune abnormality. Proposal of the concept of autoimmune pancreatitis. *Dig Dis Sci* 1995; **40**: 1561-1568
21 **Kim KP**, Kim MH, Lee SS, Seo DW, Lee SK. Autoimmune pancreatitis: it may be a worldwide entity. *Gastroenterology* 2004; **126**: 1214
22 **Kim KP**, Kim MH, Song MH, Lee SS, Seo DW, Lee SK. Autoimmune chronic pancreatitis. *Am J Gastroenterol* 2004; **99**: 1605-1616
23 **Church NI**, Pereira SP, Deheragoda MG, Sandanayake N, Amin Z, Lees WR, Gillams A, Rodriguez-Justo M, Novelli M, Seward EW, Hatfield AR, Webster GJ. Autoimmune pancreatitis: clinical and radiological features and objective response to steroid therapy in a UK series. *Am J Gastroenterol* 2007; **102**: 2417-2425
24 **Chari ST**, Kloeppel G, Zhang L, Notohara K, Lerch MM, Shimosegawa T. Histopathologic and clinical subtypes of autoimmune pancreatitis: the honolulu consensus document. *Pancreatology* 2010; **10**: 664-672
25 **Morselli-Labate AM**, Pezzilli R. Usefulness of serum IgG4 in the diagnosis and follow up of autoimmune pancreatitis: A systematic literature review and meta-analysis. *J Gastroenterol Hepatol* 2009; **24**: 15-36
26 **Mishima S**, Mizuta Y, Yamao T, Yamakawa M, Akazawa Y, Mishima R, Ohba K, Masuda JI, Ohnita K, Isomoto H, Shikuwa S, Omagari K, Kohno S. Autoimmune pancreatitis with extreme elevation of DUPAN-2. *Intern Med* 2007; **46**: 377-381
27 **Pezzilli R**, Cariani G, Santini D, Calculli L, Casadei R, Morselli-Labate AM, Corinaldesi R. Therapeutic management and clinical outcome of autoimmune pancreatitis. *Scand J Gastroenterol* 2011; **46**: 1029-1038
28 **Pezzilli R**, Casadei R, Calculli L, Santini D. Autoimmune pancreatitis. A case mimicking carcinoma. *JOP* 2004; **5**: 527-530
29 **Uchida K**, Yazumi S, Nishio A, Kusuda T, Koyabu M, Fukata M, Miyoshi H, Sakaguchi Y, Fukui T, Matsushita M, Takaoka M, Okazaki K. Long-term outcome of autoimmune pancreatitis. *J Gastroenterol* 2009; **44**: 726-732
30 **Ghazale A**, Chari S. Is autoimmune pancreatitis a risk factor for pancreatic cancer? *Pancreas* 2007; **35**: 376
31 **Pezzilli R**, Vecchiarelli S, Di Marco MC, Serra C, Santini D, Calculli L, Fabbri D, Rojas Mena B, Imbrogno A. Pancreatic ductal adenocarcinoma associated with autoimmune pancreatitis. *Case Rep Gastroenterol* 2011; **5**: 378-385
32 **Loos M**, Esposito I, Hedderich DM, Ludwig L, Fingerle A,

Friess H, Klöppel G, Büchler P. Autoimmune pancreatitis complicated by carcinoma of the pancreatobiliary system: a case report and review of the literature. *Pancreas* 2011; **40**: 151-154
33 **Okazaki K**, Kawa S, Kamisawa T, Naruse S, Tanaka S, Nishimori I, Ohara H, Ito T, Kiriyama S, Inui K, Shimosegawa T, Koizumi M, Suda K, Shiratori K, Yamaguchi K, Yamaguchi T, Sugiyama M, Otsuki M. Clinical diagnostic criteria of autoimmune pancreatitis: revised proposal. *J Gastroenterol* 2006; **41**: 626-631
34 **Choi EK**, Kim MH, Kim JC, Han J, Seo DW, Lee SS, Lee SK. The Japanese diagnostic criteria for autoimmune chronic pancreatitis: is it completely satisfactory? *Pancreas* 2006; **33**: 13-19
35 **Agrawal S**, Daruwala C, Khurana J. Distinguishing autoimmune pancreatitis from pancreaticobiliary cancers: current strategy. *Ann Surg* 2012; **255**: 248-258
36 **Lo RS**, Singh RK, Austin AS, Freeman JG. Autoimmune pancreatitis presenting as a pancreatic mass mimicking malignancy. *Singapore Med J* 2011; **52**: e79-e81
37 **Matsumoto I**, Shinzeki M, Toyama H, Asari S, Goto T, Yamada I, Ajiki T, Fukumoto T, Ku Y. A focal mass-forming autoimmune pancreatitis mimicking pancreatic cancer with obstruction of the main pancreatic duct. *J Gastrointest Surg* 2011; **15**: 2296-2298
38 **Efeovbokhan N**, Makol A, Cuison RV, Minter RM, Kotaru VP, Conley BA, Chandana SR. An unusual case of autoimmune pancreatitis presenting as pancreatic mass and obstructive jaundice: a case report and review of the literature. *J Med Case Reports* 2011; **5**: 253
39 **Ozden I**, Dizdaroğlu F, Poyanli A, Emre A. Spontaneous regression of a pancreatic head mass and biliary obstruction due to autoimmune pancreatitis. *Pancreatology* 2005; **5**: 300-303
40 **Cole WH**. Efforts to explain spontaneous regression of cancer. *J Surg Oncol* 1981; **17**: 201-209
41 **Wooff JC**, Trites JR, Walsh NM, Bullock MJ. Complete spontaneous regression of metastatic merkel cell carcinoma: a case report and review of the literature. *Am J Dermatopathol* 2010; **32**: 614-617
42 **Kalialis LV**, Drzewiecki KT, Klyver H. Spontaneous regression of metastases from melanoma: review of the literature. *Melanoma Res* 2009; **19**: 275-282
43 **Bir AS**, Fora AA, Levea C, Fakih MG. Spontaneous regression of colorectal cancer metastatic to retroperitoneal lymph nodes. *Anticancer Res* 2009; **29**: 465-468
44 **Papac RJ**. Spontaneous regression of cancer. *Cancer Treat Rev* 1996; **22**: 395-423
45 **Everson TC**. Spontaneous regression of cancer. *Prog Clin Cancer* 1967; **3**: 79-95
46 **Bodey B**, Bodey B, Siegel SE, Kaiser HE. The spontaneous regression of neoplasms in mammals: possible mechanisms and their application in immunotherapy. *In Vivo* 1998; **12**: 107-122
47 **Grossmann M**, Hoermann R, Weiss M, Jauch KW, Oertel H, Staebler A, Mann K, Engelhardt D. Spontaneous regression of hepatocellular carcinoma. *Am J Gastroenterol* 1995; **90**: 1500-1503
48 **Stoelben E**, Koch M, Hanke S, Lossnitzer A, Gaertner HJ, Schentke KU, Bunk A, Saeger HD. Spontaneous regression of hepatocellular carcinoma confirmed by surgical specimen: report of two cases and review of the literature. *Langenbecks Arch Surg* 1998; **383**: 447-452
49 **McCaughan GW**, Bilous MJ, Gallagher ND. Long-term survival with tumor regression in androgen-induced liver tumors. *Cancer* 1985; **56**: 2622-2626
50 **Tocci G**, Conte A, Guarascio P, Visco G. Spontaneous remission of hepatocellular carcinoma after massive gastrointestinal haemorrhage. *BMJ* 1990; **300**: 641-642
51 **Gaffey MJ**, Joyce JP, Carlson GS, Esteban JM. Spontaneous regression of hepatocellular carcinoma. *Cancer* 1990; **65**: 2779-2783
52 **Takeda Y**, Togashi H, Shinzawa H, Miyano S, Ishii R, Karasawa T, Takeda Y, Saito T, Saito K, Haga H, Matsuo T, Aoki M, Mitsuhashi H, Watanabe H, Takahashi T. Spontaneous regression of hepatocellular carcinoma and review of literature. *J Gastroenterol Hepatol* 2000; **15**: 1079-1086
53 **Kavoussi LR**, Levine SR, Kadmon D, Fair WR. Regression of metastatic renal cell carcinoma: a case report and literature review. *J Urol* 1986; **135**: 1005-1007
54 **Abubakr YA**, Chou TH, Redman BG. Spontaneous remission of renal cell carcinoma: a case report and immunological correlates. *J Urol* 1994; **152**: 156-157
55 **Cole WH**. Spontaneous regression of cancer. *CA Cancer J Clin* 1974; **24**: 274-279
56 **Baker HW**. Biologic control of cancer. The James Ewing lecture. *Arch Surg* 1986; **121**: 1237-1241
57 **Lu C**, Vickers MF, Kerbel RS. Interleukin 6: a fibroblast-derived growth inhibitor of human melanoma cells from early but not advanced stages of tumor progression. *Proc Natl Acad Sci USA* 1992; **89**: 9215-9219
58 **Gutman M**, Singh RK, Xie K, Bucana CD, Fidler IJ. Regulation of interleukin-8 expression in human melanoma cells by the organ environment. *Cancer Res* 1995; **55**: 2470-2475
59 **Hawkins MJ**. Interleukin-2 antitumor and effector cell responses. *Semin Oncol* 1993; **20**: 52-59
60 **Kirkwood JM**, Ernstoff MS. Interferons in the treatment of human cancer. *J Clin Oncol* 1984; **2**: 336-352
61 **Balkwill FR**, Naylor MS, Malik S. Tumour necrosis factor as an anticancer agent. *Eur J Cancer* 1990; **26**: 641-644
62 **Broder S**, Karp JE. Progress against cancer. *J Cancer Res Clin Oncol* 1995; **121**: 633-647
63 **Pritchard J**, Hickman JA. Why does stage 4s neuroblastoma regress spontaneously? *Lancet* 1994; **344**: 869-870
64 **You WK**, Sennino B, Williamson CW, Falcón B, Hashizume H, Yao LC, Aftab DT, McDonald DM. VEGF and c-Met blockade amplify angiogenesis inhibition in pancreatic islet cancer. *Cancer Res* 2011; **71**: 4758-4768
65 **Bedi A**, Griffin CA, Barber JP, Vala MS, Hawkins AL, Sharkis SJ, Zehnbauer BA, Jones RJ. Growth factor-mediated terminal differentiation of chronic myeloid leukemia. *Cancer Res* 1994; **54**: 5535-5538
66 **Greger V**, Passarge E, Höpping W, Messmer E, Horsthemke B. Epigenetic changes may contribute to the formation and spontaneous regression of retinoblastoma. *Hum Genet* 1989; **83**: 155-158
67 **Baylin SB**, Makos M, Wu JJ, Yen RW, de Bustros A, Vertino P, Nelkin BD. Abnormal patterns of DNA methylation in human neoplasia: potential consequences for tumor progression. *Cancer Cells* 1991; **3**: 383-390
68 **Hiyama E**, Hiyama K, Yokoyama T, Matsuura Y, Piatyszek MA, Shay JW. Correlating telomerase activity levels with human neuroblastoma outcomes. *Nat Med* 1995; **1**: 249-255
69 **Tabori U**, Vukovic B, Zielenska M, Hawkins C, Braude I, Rutka J, Bouffet E, Squire J, Malkin D. The role of telomere maintenance in the spontaneous growth arrest of pediatric low-grade gliomas. *Neoplasia* 2006; **8**: 136-142
70 **Pathak S**, Multani AS, McConkey DJ, Imam AS, Amoss MS. Spontaneous regression of cutaneous melanoma in sinclair swine is associated with defective telomerase activity and extensive telomere erosion. *Int J Oncol* 2000; **17**: 1219-1224
71 **Stoll BA**. Spontaneous regression of cancer: new insights. *Biotherapy* 1992; **4**: 23-30
72 **Castaigne S**, Chomienne C, Daniel MT, Ballerini P, Berger R, Fenaux P, Degos L. All-trans retinoic acid as a differentiation therapy for acute promyelocytic leukemia. I. Clinical results. *Blood* 1990; **76**: 1704-1709
73 **Meares A**. Psychological mechanisms in the regression of cancer. *Med J Aust* 1983; **1**: 583-584
74 **Weinstock C**. Further evidence on psychobiological aspects of cancer. *Int J Psychosom* 1984; **31**: 20-22

S- Editor Gou SX **L- Editor** Stewart GJ **E- Editor** Li JY

World Journal of Gastroenterology

Online Submissions: http://www.wjgnet.com/1007-9327office
wjg@wjgnet.com
doi:10.3748/wjg.v18.i23.2909

World J Gastroenterol 2012 June 21; 18(23): 2909-2913
ISSN 1007-9327 (print) ISSN 2219-2840 (online)

REVIEW

Animal models for the study of hepatitis C virus infection and replication

Kristin L MacArthur, Catherine H Wu, George Y Wu

Kristin L MacArthur, Department of Medicine, Beth Israel Deaconess Medical Center, Boston, MA 02215, United States
Catherine H Wu, George Y Wu, Department of Medicine, Division of Gastroenterology-Hepatology, University of Connecticut Health Center, Farmington, CT 06030-1845, United States
Author contributions: MacArthur KL contributed to the literature search, manuscript writing and final revision of the article; Wu CH revised and edited the manuscript; Wu GY conceived of the idea, wrote some sections and edited the final version.
Correspondence to: George Y Wu, MD, PhD, Department of Medicine, Division of Gastroenterology-Hepatology, University of Connecticut Health Center, 263 Farmington Avenue, Farmington, CT 06030-1845, United States. wu@nso.uchc.edu
Telephone: +1-860-6792509 Fax: +1-860-6793159
Received: November 18, 2011 Revised: March 1, 2012
Accepted: April 9, 2012
Published online: June 21, 2012

Abstract

Hepatitis C virus (HCV) hepatitis, initially termed non-A, non-B hepatitis, has become one of the leading causes of cirrhosis and hepatocellular carcinoma worldwide. With the help of animal models, our understanding of the virus has grown substantially from the time of initial discovery. There is a paucity of available animal models for the study of HCV, mainly because of the selective susceptibility limited to humans and primates. Recent work has focused modification of animals to permit HCV entry, replication and transmission. In this review, we highlight the currently available models for the study of HCV including chimpanzees, tupaia, mouse and rat models. Discussion will include methods of model design as well as the advantages and disadvantages of each model. Particular focus is dedicated to knowledge of pathophysiologic mechanisms of HCV infection that have been elucidated through animal studies. Research within animal models is critically important to establish a complete understanding of HCV infection, which will ultimately form the basis for future treatments and prevention of disease.

Key words: Hepatitis C virus; Infection; Replication; Vaccine; Hepatitis A virus

Peer reviewer: Dr. Harry Hua-Xiang Xia, Novartis Pharmaceuticals Corporation, One Health Plaza, East Hanover, NJ 07936, United States

MacArthur KL, Wu CH, Wu GY. Animal models for the study of hepatitis C virus infection and replication. *World J Gastroenterol* 2012; 18(23): 2909-2913 Available from: URL: http://www.wjgnet.com/1007-9327/full/v18/i23/2909.htm DOI: http://dx.doi.org/10.3748/wjg.v18.i23.2909

INTRODUCTION

The hepatitis C virus (HCV) is a positive-sense, single stranded RNA virus of the family Flaviviridae. There are six distinct genotypes with several subgenotypes that have been identified. The World Health Organization estimates that the virus affects approximately 3% of people worldwide. Approximately 170 million people are chronic carriers of the virus. There is higher prevalence in the Far East, Mediterranean countries and in certain African and eastern European areas. HCV infects primarily liver cells causing an acute hepatitis. Of those acutely infected, roughly 15% will clear the virus without medical intervention while the remainder will develop chronic hepatitis C. Approximately 30% of chronic hepatitis C will progress to cirrhosis, of which 20% will develop hepatocellular carcinoma. Thus, HCV infection remains a global health problem requiring continued research efforts to understand viral infection and to develop improved drug therapies.

Efforts to obtain information regarding the intricacies of hepatitis C viral entry, lifecycle and replication have been limited by the lack of model organisms available to serve as experimental hosts to the virus. Hu-

mans and other primates are the only known organisms naturally permissive to HCV infection. Costs and ethical concerns, thus, limit the study of the disease in chimpanzees. Recently, novel animal systems have permitted detailed examination of HCV infection, replication, and host responses. In this review, the status of HCV animal models is summarized, and the advantages as well as disadvantages, are discussed in terms of the potential impact on the development of future novel anti-HCV therapies.

ANIMAL MODELS

Chimpanzees and immune responses to HCV infection

The path leading to the discovery of HCV began in 1975 when some patients with viral hepatitis were found to lack markers for hepatitis A virus or hepatitis B virus (HBV) in serum. This led to the recognition that a separate unrelated hepatitis virus was responsible. This entity was initially termed non-A non-B hepatitis (NANBH). Thus began a wide body of research to isolate and identify the virus using chimpanzees as hosts for infection with human NANBH-infected serum. In 1989, Choo *et al*[1] and Houghton *et al*[2] created a complementary DNA clone of NANBH (clone 5-1-1) derived from positive-strand RNA, and confirmed that it encoded an antigen specific to NANBH infections. The cDNA was used to create antigens (c100-3) subsequently used as substrates to detect circulating serum antibodies *via* enzyme immunoassay. Through these discoveries in chimpanzees, antibody testing enabled screening of blood for the presence of the agent, now named HCV.

The study of HCV in chimpanzees has provided a wealth of knowledge regarding the mechanism of infection, replication, and both innate and humoral antiviral immune responses. Chimpanzees infected with HCV display elevations of aminotransferases and liver biopsies show necroinflammatory changes after acute infection. However, chimpanzees differ from humans in that their course of infection is milder; chronic carriers do not develop cirrhosis or fibrosis and only one chimpanzee has been reported to have developed HCV-related hepatocellular carcinoma[3]. Other differences include lack of efficacy of interferon (IFN) treatment as evidenced by constant viral loads despite administration of this agent. Alternative studies of direct antiviral agents are currently being studied in chimpanzees. For example, Olsen *et al*[4] showed that administration of a nucleoside analogue and protease inhibitor resulted in viral load decline in HCV-infected chimpanzees. Together with recent clinical trials and use of novel HCV protease inhibitors, success in the treatment of HCV-infected chimpanzees has potential to spark new human clinical trials using antiviral agents without concurrent use of pegylated-IFN and ribavirin.

Chimpanzees offer a valuable animal model for active immunization studies as well as for investigating mechanisms of innate and cell-mediated antiviral activity. Through studies on chimpanzees that have naturally cleared infection, Nascimbeni *et al*[5] have described the role of memory T-cell (both CD4 and CD8) responses that may help prevent infection upon re-challenge with virus. The varying quantity and quality of this cell mediated response helps explain differing responses to re-infection among individual chimpanzees. Barth *et al*[6] recently highlighted the importance of neutralizing antibodies to prevent early viral replication. They also showed that heightened CD8+ and natural killer (NK) cell activity increased production of IFN stimulating genes and IFN Ⅰ/Ⅱ, thus further supporting the role of adaptive immunity in limiting viral re-infection. Results of vaccination studies in HCV-infected chimpanzees have proven difficult to interpret for a variety of reasons including heterogeneity of genotypes, the error-prone RNA polymerase that creates mutations resistant to neutralizing antibodies, and downregulation of NK and T-cell responses *via* gpE2 interaction with CD81. Important information can nonetheless be gathered from both therapeutic and prophylactic vaccination studies[7]. Meta-analyses of HCV therapeutic vaccination studies in chimpanzees by Dahari *et al*[8] concluded that vaccinations that included non-structural HCV proteins were less effective in achieving HCV clearance in comparison to inclusion of structural proteins in vaccines, which were hypothesized to heighten T-cell responses. However, successful vaccination data should be interpreted carefully, because most studies use endpoints as reduction in clinical disease rather than sustained virological response. The search for a prophylactic vaccination for HCV has been challenging. The mechanism of protective vaccination is usually the generation of neutralizing antibodies. In HCV, neutralizing antibodies have been observed to coexist with high HCV titers, thus suggesting their presence does not limit HCV entry into cells *in vivo*. Neutralizing antibody levels also tend to decrease after infection resolves, indicating a lack of a memory response or capability to prevent re-infection. More recent work has subsequently focused on generating a reliable T-cell (CD4+ and CD8+) response in attempts to protect against the development of infection with exposure to the virus. Folgori *et al*[9] developed a prophylactic vaccination strategy in chimpanzees using adenoviral vectors and electroporated plasmid DNA encoding the HCV non-structural region. Through stimulation of a cross-reactive T-cell response, chimpanzees were capable of resolving infection when challenged with virus differing from the vaccine by more than 13% at the amino acid level. Vaccination studies in chimpanzees are ongoing. There are many disadvantages to the use chimpanzees as models, including cost, ethics, and most recently, an NIH ban on the use of chimpanzees for biomedical research[10].

Tupaia infection with HCV

Tupaia belangeri is a tree shrew native to Southeast Asia. Tupaia has been shown to be susceptible to a variety of human viruses including herpes simplex virus, rotavirus,

and HBV. In 2002, Zhao *et al*[11] demonstrated effective hepatitis C replication and virion synthesis in primary tupaia hepatocytes. This group plated and infected primary tupaia hepatocytes with serum or plasma derived HCV from infected humans. Infection and effective replication was confirmed by reverse transcription polymerase chain reaction detection of negative strand RNA in hepatocytes as well as secretion of viral particles in culture medium. HCV RNA could be detected up to 14 d after plating. The enveloped virions produced were shown to be resistant to degradation by ribonuclease and could infect previously uninfected tupaia hepatocytes.

In 2010, Amako *et al*[12] reported a longitudinal study which followed HCV-infected tupaia over a three year period after inoculation with hepatitis C from a patient or viral particles from full length cDNA. The animals demonstrated mild inflammation and viremia during the acute infection followed later by development of liver steatosis, cirrhotic nodules and tumorigenesis. Moreover, serum from infected tupaia was harvested and inoculated into naïve tupaia resulting in acute infection, demonstrating effective replication and potential transmission of HCV.

HCV entry in tupaia has been shown to support current knowledge of human essential entry receptors. In 2011, Tong *et al*[13] cloned tupaia CD81, scavenger receptor class B member 1 (SCARB- I or SR-B I), claudin-1 (CLDN1) and occludin and demonstrated that entry of HCV pseudoparticles or cell culture-derived HCV was permitted by these molecules. Inhibition of CD81 or SR-B I blocked HCV entry. However, there may be structural variations between human and tupaia receptors that may allow for differences in efficiency of viral entry. For example, the subtle structural difference between human and tupaia CD81 was shown to alter the ability of the extracellular loop to bind to HCV glycoprotein E2 in a study by Tian *et al*[14]. This information may be helpful in elucidating potential drug targets to block viral entry in humans. Tupaia is, therefore, a promising and effective model for the ongoing study of HCV entry and replication. A disadvantage of the tupaia model is that unlike humans with HCV, these animals rarely maintain sustained virema[12,15].

Mouse models for HCV replication

Much research has been devoted to understanding why murine hepatic cells are naturally resistant to hepatitis C viral cell entry, and permit only inefficient replication in cell culture and in animals. Ultimately, overcoming this resistance could provide a valuable mouse model for HCV replication as well as development of potential immune strategies to block HCV entry and replication in humans.

Mouse hepatocytes have been shown to allow HCV entry in cell culture in cells genetically engineered to express human HCV-specific entry molecules including CD81 and occludin. However, in addition to the barrier to entry, murine cells also have a resistance towards replication, assembly and release of HCV. This was demonstrated by Long *et al*[16] who used a transcomplementation system of mouse hepatoma cell lines that contained a subgenomic HCV replicon for ectopic expression of HCV structural proteins, p7, NS2 and apolipoprotein E (ApoE). They were able to demonstrate that assembly and release occurred successfully in murine cells with expression of the aforementioned proteins including ApoE.

In order to overcome the barrier to murine infection by HCV, Washburn *et al*[17] developed a model consisting of a humanized mouse engineered by engraftment of human hepatocyte progenitors and human CD34+ human hematopoietic stem cells. This model was generated by the use of a fusion of the FK506 binding protein and caspase 8 under the control of the albumin promoter. This construct induced apoptotic elimination of host hepatocytes in Balb/C Rag2 (-/-) C-null mice. Ultimately these humanized mice were shown to harbor both human hepatocytes and T cells. Upon infection with HCV, the mice developed liver inflammation and fibrosis. A human T-cell immune response to HCV was observed. This study was limited by low levels of HCV infection demonstrated by absence of HCV RNA in the serum, and a lack of a B cell immune response due to absence of an engraftment of a complete immune system.

Similarly, Mercer *et al*[18] and Kneteman *et al*[19] developed a chimeric severe combined immune deficient (SCID)/urokinase-type plasminogen activator mouse model. This immune deficient mouse model has been shown to support proliferation of transplanted human hepatocytes, and more importantly, sustained HCV infection as demonstrated by detection of viral RNA within hepatocytes after intravenous inoculation. Production and release of viral particles were demonstrated by successful passage of infection through three generations of mice. The studies showed that when the human hepatocytes comprise the majority of liver cells (at least 80% of total hepatocytes) within chimeric SCID mice, infection with HCV can occur, and can result in liver failure. Further research revealed that human apolipoprotein (ApoB) and cholesterol ester transfer protein may play a role in allowing HCV infection in the chimeric SCID mice, and thus may offer a target to prevent viral entry within humans[20]. HCV-infected SCID mice have also been used to study direct antiviral agents including IFN alpha-2 anti-NS3 and anti-NS5B proteases. Responses were shown to parallel that of humans. More recently, Kamiya *et al*[21] tested anti-NS3-4A (telaprevir) in HCV-infected SCID mice to evaluate the pharmacokinetics and dynamics of the drug as it related to a dose-dependent reduction in HCV serum RNA. Studies on SCID mice thus offer the potential to serve as a bridge between *in vitro* and clinical trials for HCV antiviral agents. Limiting factors of the SCID mouse model include a lack of a complex immune system, and inability to achieve a fully humanized liver. Recent studies have shown promise with use of a herpes simplex virus type-1 thymidine kinase/ganciclovir system

for cell specific ablation as means of obtaining exclusive growth of human hepatocytes in the SCID mouse[22].

In order to create a mouse model permissive to HCV infection while maintaining complex immunity, Dorner *et al*[23] developed a humanized mouse model using genetic engineering to study viral entry and immunity. Mice were genetically engineered to express HCV-specific entry factors including CD81, occludin, SCARB-Ⅰ, and CLDN1. Using this model, it was demonstrated that human-specific CD81 and occludin were essential to all HCV entry into murine hepatocytes. Expression of SCARB- I heightened HCV entry when expressed in combination with CD81 and occludin. Because this model used an immunocompetent mouse, viral replication and persistence of infection was limited. However, this model was also used to study passive immunization by administration of anti-CD81 antibodies and anti-E2 antibodies both of which decreased HCV infection. This model may offer future study of passive immunization or vaccination strategies to prevent acute infection of HCV before or after exposure.

Rat model for HCV infection

As discussed above, the search for an immunocompetent rodent host for HCV infection has been difficult. Although transplantation of human hepatocytes has been possible in mice, long-term HCV infection has only been shown in the setting of immunodeficiency, which limits study of immune responses. Ouyang *et al*[24] sought to overcome these barriers by creating an immunocompetent rat model that was tolerant to human hepatocytes. In order to achieve this, Huh7 human hepatoma cells were injected into the peritoneal cavities of fetal rats between gestation ages of 15-17 d. By injecting human hepatocytes during the development of the fetal immune system of the rat, specific tolerance to that specific cell type was achieved. Subsequent transplantation of human Huh7 cells into newborn tolerant rats resulted in survival and limited growth of the human cells without evidence of rejection as demonstrated by mixed lymphocyte assays. Colonies of cells bearing human liver cell markers increased in size, and were visualized within rat livers by immunohistochemical staining. Human albumin was detected in liver cells and in serum, and human hepatic mRNA was detected in hepatocytes, thus demonstrating active synthetic function of transplanted human Huh7 cells.

To study HCV infection, HCV isolated from human serum was inoculated into immunocompetent, tolerant, Huh7 cell-transplanted rats[25]. HCV RNA levels of 7.0×10^3 copies/mL were detectable in serum by week 4, and peaked at 20×10^3 copies/mL by week 12 after infection. Levels decreased thereafter. Moreover, biochemical evidence of hepatic inflammation was demonstrated by elevations of serum alanine aminotransferase beginning at 4 wk, and peaked at 3× the baseline level by the 13th week, after which levels declined. Light microscopy of liver sections showed mononuclear infiltrates in portal and central regions at times coinciding with detectable viremia. Controls without transplanted cells, tolerization, or HCV inoculation lacked any markers of HCV infection or hepatitis. The limitations of this rat model include low numbers of transplanted human hepatocytes as well as relatively low levels of viremia (22 500 copies/mL), in comparison to that in a typical human infection. However, this model offers a rodent model large enough to tolerate repeated blood and tissue sampling to study viral entry, replication, and immune-mediated hepatic injury as well as a screening tool to evaluate novel antiviral agents.

PROSPECTIVE

Hepatitis C viral infection is a growing health concern that leads to liver failure and hepatocellular carcinoma. The study of HCV has been limited due to a lack of appropriate and reliable animal models. However, much of our understanding of viral infection, replication and host immune responses has been gathered from animal data. Animal studies have historically utilized chimpanzees, but alternative models such as tupaia, mice and rats are now viable models for research.

Chimpanzees are advantageous models given their close genetic resemblance to humans, intact immune system which offers potential for study of innate and adaptive immune responses, and potential to study both treatments and prophylactic vaccinations. Additionally, important research with chimpanzees has resulted in the development of molecular clones of the virus for use in molecular and cellular research. Disadvantages include high cost, ethical constraints, and low susceptibility to chronic infection, thus limiting the study of HCV-related cirrhosis and hepatocellular carcinoma. Currently, chimpanzees are not available for biomedical research[10].

Advantages of the tupaia model include low cost, ease of propagation, immunocompetence, and capability to study cirrhosis and tumorigenesis. On the other hand, tupaia and humans are genetically very different, potentially limiting the applicability of tupaia data on viral infectivity and disease to humans. Reliability and reproducibility of infection with tupaia have been also been debated.

Xenograft mice constructed with human hepatocytes are useful models given the demonstrated persistent viremia, and development of cirrhosis. These models provide a unique opportunity to study viral activity within human hepatocytes in a living host. Limitations include difficulty with mouse reproduction for repeated sampling, and immunodeficiency that limits the study of the natural immunological response.

The immunocompetent mouse and rat are promising models given their relatively low cost, ease of propagation, and intact immune system. There is great potential for the study of immunologic mechanisms as well as treatment and vaccination agents using these models. Disadvantages include relatively low levels of viremia,

and possible limitation of persistent infection by a competent immune response.

Our knowledge of HCV and related disease has grown significantly from its discovery nearly three decades ago. Together with molecular and cellular approaches, continued animal research will undoubtedly play a critical role in development of new antiviral therapies, and our understanding of mechanisms involved in the pathogenesis of both acute and chronic HCV infections. Further research is needed to enhance the potential of the currently available models in order to optimize the cost of maintenance and propagation, viremia, and maximize the similarity of infection models as they relate to human infection.

REFERENCES

1 **Choo QL**, Kuo G, Weiner AJ, Overby LR, Bradley DW, Houghton M. Isolation of a cDNA clone derived from a blood-borne non-A, non-B viral hepatitis genome. *Science* 1989; **244**: 359-362

2 **Houghton M**. The long and winding road leading to the identification of the hepatitis C virus. *J Hepatol* 2009; **51**: 939-948

3 **Muchmore E**, Popper H, Peterson DA, Miller MF, Lieberman HM. Non-A, non-B hepatitis-related hepatocellular carcinoma in a chimpanzee. *J Med Primatol* 1988; **17**: 235-246

4 **Olsen DB**, Davies ME, Handt L, Koeplinger K, Zhang NR, Ludmerer SW, Graham D, Liverton N, MacCoss M, Hazuda D, Carroll SS. Sustained viral response in a hepatitis C virus-infected chimpanzee via a combination of direct-acting antiviral agents. *Antimicrob Agents Chemother* 2011; **55**: 937-939

5 **Nascimbeni M**, Mizukoshi E, Bosmann M, Major ME, Mihalik K, Rice CM, Feinstone SM, Rehermann B. Kinetics of CD4+ and CD8+ memory T-cell responses during hepatitis C virus rechallenge of previously recovered chimpanzees. *J Virol* 2003; **77**: 4781-4793

6 **Barth H**, Rybczynska J, Patient R, Choi Y, Sapp RK, Baumert TF, Krawczynski K, Liang TJ. Both innate and adaptive immunity mediate protective immunity against hepatitis C virus infection in chimpanzees. *Hepatology* 2011; **54**: 1135-1148

7 **Houghton M**. Prospects for prophylactic and therapeutic vaccines against the hepatitis C viruses. *Immunol Rev* 2011; **239**: 99-108

8 **Dahari H**, Feinstone SM, Major ME. Meta-analysis of hepatitis C virus vaccine efficacy in chimpanzees indicates an importance for structural proteins. *Gastroenterology* 2010; **139**: 965-974

9 **Folgori A**, Capone S, Ruggeri L, Meola A, Sporeno E, Ercole BB, Pezzanera M, Tafi R, Arcuri M, Fattori E, Lahm A, Luzzago A, Vitelli A, Colloca S, Cortese R, Nicosia A. A T-cell HCV vaccine eliciting effective immunity against heterologous virus challenge in chimpanzees. *Nat Med* 2006; **12**: 190-197

10 **Harrington M**. State of the (research) chimp. *Lab Anim* (NY) 2012; **41**: 31

11 **Zhao X**, Tang ZY, Klumpp B, Wolff-Vorbeck G, Barth H, Levy S, von Weizsäcker F, Blum HE, Baumert TF. Primary hepatocytes of Tupaia belangeri as a potential model for hepatitis C virus infection. *J Clin Invest* 2002; **109**: 221-232

12 **Amako Y**, Tsukiyama-Kohara K, Katsume A, Hirata Y, Sekiguchi S, Tobita Y, Hayashi Y, Hishima T, Funata N, Yonekawa H, Kohara M. Pathogenesis of hepatitis C virus infection in Tupaia belangeri. *J Virol* 2010; **84**: 303-311

13 **Tong Y**, Zhu Y, Xia X, Liu Y, Feng Y, Hua X, Chen Z, Ding H, Gao L, Wang Y, Feitelson MA, Zhao P, Qi ZT. Tupaia CD81, SR-BI, claudin-1, and occludin support hepatitis C virus infection. *J Virol* 2011; **85**: 2793-2802

14 **Tian ZF**, Shen H, Fu XH, Chen YC, Blum HE, Baumert TF, Zhao XP. Interaction of hepatitis C virus envelope glycoprotein E2 with the large extracellular loop of tupaia CD81. *World J Gastroenterol* 2009; **15**: 240-244

15 **Xu X**, Chen H, Cao X, Ben K. Efficient infection of tree shrew (Tupaia belangeri) with hepatitis C virus grown in cell culture or from patient plasma. *J Gen Virol* 2007; **88**: 2504-2512

16 **Long G**, Hiet MS, Windisch MP, Lee JY, Lohmann V, Bartenschlager R. Mouse hepatic cells support assembly of infectious hepatitis C virus particles. *Gastroenterology* 2011; **141**: 1057-1066

17 **Washburn ML**, Bility MT, Zhang L, Kovalev GI, Buntzman A, Frelinger JA, Barry W, Ploss A, Rice CM, Su L. A humanized mouse model to study hepatitis C virus infection, immune response, and liver disease. *Gastroenterology* 2011; **140**: 1334-1344

18 **Mercer DF**, Schiller DE, Elliott JF, Douglas DN, Hao C, Rinfret A, Addison WR, Fischer KP, Churchill TA, Lakey JR, Tyrrell DL, Kneteman NM. Hepatitis C virus replication in mice with chimeric human livers. *Nat Med* 2001; **7**: 927-933

19 **Kneteman NM**, Weiner AJ, O'Connell J, Collett M, Gao T, Aukerman L, Kovelsky R, Ni ZJ, Zhu Q, Hashash A, Kline J, Hsi B, Schiller D, Douglas D, Tyrrell DL, Mercer DF. Anti-HCV therapies in chimeric scid-Alb/uPA mice parallel outcomes in human clinical application. *Hepatology* 2006; **43**: 1346-1353

20 **Steenbergen RH**, Joyce MA, Lund G, Lewis J, Chen R, Barsby N, Douglas D, Zhu LF, Tyrrell DL, Kneteman NM. Lipoprotein profiles in SCID/uPA mice transplanted with human hepatocytes become human-like and correlate with HCV infection success. *Am J Physiol Gastrointest Liver Physiol* 2010; **299**: G844-G854

21 **Kamiya N**, Iwao E, Hiraga N, Tsuge M, Imamura M, Takahashi S, Miyoshi S, Tateno C, Yoshizato K, Chayama K. Practical evaluation of a mouse with chimeric human liver model for hepatitis C virus infection using an NS3-4A protease inhibitor. *J Gen Virol* 2010; **91**: 1668-1677

22 **Douglas DN**, Kawahara T, Sis B, Bond D, Fischer KP, Tyrrell DL, Lewis JT, Kneteman NM. Therapeutic efficacy of human hepatocyte transplantation in a SCID/uPA mouse model with inducible liver disease. *PLoS One* 2010; **5**: e9209

23 **Dorner M**, Horwitz JA, Robbins JB, Barry WT, Feng Q, Mu K, Jones CT, Schoggins JW, Catanese MT, Burton DR, Law M, Rice CM, Ploss A. A genetically humanized mouse model for hepatitis C virus infection. *Nature* 2011; **474**: 208-211

24 **Ouyang EC**, Wu CH, Walton C, Promrat K, Wu GY. Transplantation of human hepatocytes into tolerized genetically immunocompetent rats. *World J Gastroenterol* 2001; **7**: 324-330

25 **Wu GY**, Konishi M, Walton CM, Olive D, Hayashi K, Wu CH. A novel immunocompetent rat model of HCV infection and hepatitis. *Gastroenterology* 2005; **128**: 1416-1423

S- Editor Gou SX **L- Editor** A **E- Editor** Li JY

World Journal of Gastroenterology

Online Submissions: http://www.wjgnet.com/1007-9327office
wjg@wjgnet.com
doi:10.3748/wjg.v18.i23.2914

World J Gastroenterol 2012 June 21; 18(23): 2914-2928
ISSN 1007-9327 (print) ISSN 2219-2840 (online)

ORIGINAL ARTICLE

Proteome profiling of spinal cord and dorsal root ganglia in rats with trinitrobenzene sulfonic acid-induced colitis

Xiao-Jun Zhang, Feung Ping Leung, Wendy WL Hsiao, Shun Tan, Shao Li, Hong-Xi Xu, Joseph JY Sung, Zhao-Xiang Bian

Xiao-Jun Zhang, Feung Ping Leung, Wendy WL Hsiao, Shun Tan, Zhao-Xiang Bian, School of Chinese Medicine, Hong Kong Baptist University, Hong Kong, China
Shao Li, Ministry of Education Key Laboratory of Bioinformatics and Bioinformatics Division, TNLIST/Department of Automation, Tsinghua University, Beijing 100084, China
Hong-Xi Xu, Shanghai University of Traditional Chinese Medicine, Shanghai 200032, China
Joseph JY Sung, Faculty of Medicine, The Chinese University of Hong Kong, Hong Kong, China
Author contributions: Xu HX, Sung JJY and Bian ZX designed the research; Zhang XJ, Hsiao WWL and Tan S performed the research; Zhang XJ wrote the paper, Leung FP and Li S provided helpful suggestions and revised the paper.
Supported by The Research Grants Council of Hong Kong, RGC-HKBU2/07C; and The Hong Kong Jockey Club Institute of Chinese Medicine, JCICM4-07
Correspondence to: Zhao-Xiang Bian, MD, PhD, Professor, School of Chinese Medicine, Hong Kong Baptist University, Hong Kong, China. bzxiang@hkbu.edu.hk
Telephone: +86-852-34112905 Fax: +86-852-34112929
Received: August 15, 2011 Revised: September 24, 2011
Accepted: April 12, 2012
Published online: June 21, 2012

Abstract

AIM: To investigate proteomic changes in spinal cord and dorsal root ganglia (DRG) of rats with trinitrobenzene sulfonic acid (TNBS)-induced colitis.

METHODS: The colonic myeloperoxidase (MPO) activity and tumor necrosis factor-α (TNF-α) level were determined. A two-dimensional electrophoresis (2-DE)-based proteomic technique was used to profile the global protein expression changes in the DRG and spinal cord of the rats with acute colitis induced by intracolonic injection of TNBS.

RESULTS: TNBS group showed significantly elevated colonic MPO activity and increased TNF-α level. The proteins derived from lumbosacral enlargement of the spinal cord and DRG were resolved by 2-DE; and 26 and 19 proteins that displayed significantly different expression levels in the DRG and spinal cord were identified respectively. Altered proteins were found to be involved in a number of biological functions, such as inflammation/immunity, cell signaling, redox regulation, sulfate transport and cellular metabolism. The overexpression of the protein similar to potassium channel tetramerisation domain containing protein 12 (Kctd 12) and low expression of proteasome subunit α type-1 (psma) were validated by Western blotting analysis.

CONCLUSION: TNBS-induced colitis has a profound impact on protein profiling in the nervous system. This result helps understand the neurological pathogenesis of inflammatory bowel disease.

Key words: Inflammatory bowel disease; Trinitrobenzene sulfonic acid; Two-dimensional electrophoresis-based proteomic technique; Dorsal root ganglia; Spinal cord

Peer reviewers: Masahiro Iizuka, MD, PhD, Director, Akita Health Care Center, Akita Red Cross Hospital, 3-4-23, Nakadori, Akita 010-0001, Japan; Mohammad Abdollahi, Professor, Faculty of Pharmacy and Pharmaceutical Sciences Research Center, Tehran University of Medical Sciences, Tehran 1417614411, Iran

Zhang XJ, Leung FP, Hsiao WWL, Tan S, Li S, Xu HX, Sung JJY, Bian ZX. Proteome profiling of spinal cord and dorsal root ganglia in rats with trinitrobenzene sulfonic acid-induced colitis. *World J Gastroenterol* 2012; 18(23): 2914-2928 Available from: URL: http://www.wjgnet.com/1007-9327/full/v18/i23/2914.htm DOI: http://dx.doi.org/10.3748/wjg.v18.i23.2914

INTRODUCTION

Inflammatory bowel disease (IBD) is defined as a group

of inflammatory conditions in the colon and small intestine, mainly including ulcerative colitis and Crohn's disease. The cause of IBD is suggested to be a nebulous combination of not only host genetic factors, but also immune dysfunction, dysbiosis, cellular oxidative stress and leakage of intestinal barrier[1]. Fundamental therapy for this condition has not yet been established because its etiology remains obscure. Unfortunately, the prevalence of IBD is continuing to increase in both Eastern and Western countries, causing enormous medical costs[2,3]. Beside intestinal disorders, many organs outside the gastrointestinal tract, such as the central nervous system, are involved in IBD[4]. Neuropathies, cerebrovascular events, white matter lesions, and visceral pain are common neurological manifestations[4]. These alterations may help explain some of the underlying comorbidities, such as hyperalgesia, seizure and anorexia[5,6]. Unfortunately, the exact mechanism for IBD needs further investigations.

This study focuses on the spinal cord and dorsal root ganglia (DRG) to reveal the neurological dimension in a trinitrobenzene sulfonic acid (TNBS)-induced active colitis model. Unlike previous studies that were based mainly on investigations of specifically selected gene/proteins, proteomic approach was applied in this study to reveal the global changes of proteins. The two-dimensional electrophoresis (2-DE) in combination with matrix-assisted laser desorption-time-of-flight/time-of-flight mass spectrometer (MALDI-TOF/TOF MS) have been widely used to probe into changes of protein profiles accompanied with diseases like cancer and hyperalgesia[7,8]. In the present study, this approach was applied to analyze the proteomic differences in lumbar enlargement of spinal cord and DRG in the rat model of TNBS-induced colitis. This study aimed to investigate whether changed protein profiles in the nervous system are in any way associated with neurological dimensions in IBD animal model.

MATERIALS AND METHODS

Animals and tissue processing

Male Sprague-Dawley rats (180-200 g in weight) were obtained from the Laboratory Animal Services Centre, The Chinese University of Hong Kong. Rats were kept at room temperature 23 ℃ ± 2 ℃ with an alternating 12 h light-dark cycle, and were allowed access to food and water *ad libitum*. All of the experimental protocols were carried out with the approval of the Committee on Use of Human and Animal Subjects in Teaching and Research of Hong Kong Baptist University and according to the Regulations of the Department of Health, Hong Kong, China.

Induction of colitis

Induction of colitis was adapted from the previously reported methods[9,10]. Briefly, under chloral hydrate (350 mg/kg, ip) anesthesia, colitis was induced in overnight-fasted rats (n = 5) by intra-colonic administration of 30 mg/kg of TNBS (Sigma, St. Louis, United States) dissolved in 50% ethanol solution at 8 cm from the anal verge using a rubber catheter. The rats were kept upside-down for 1 min to ensure that the TNBS solution was not expelled immediately. The rats in control group (n = 4) received intra-colonic injection of saline.

Tissue preparation

On the 7th day after TNBS instillation, the rats were anesthetized with chloral hydrate (350 mg/kg, ip). Distal colon tissue was excised in two pieces. One piece was fixed in 4% paraformaldehyde, routinely embedded in paraffin, cut into 5 μm sections, mounted on glass slides and stained with hematoxylin and eosin to reveal structural features. The other piece of colon sample was frozen in liquid nitrogen and stored at -80 ℃ for measurement of myeloperoxidase (MPO) activity and tumor necrosis factor-α (TNF-α) level. The rat was then perfused with ice-cold normal saline. The spinal cord and DRG of the lumbosacral enlargement were dissected, immediately frozen and stored at -80 ℃ until use. Samples were firstly lysed in buffer (8 mol/L urea, 2 mol/L thiourea, 2% 3-[(3-cholamidopropyl) dimethylammonio]-1-propanesulfonate (CHAPS), 1% NP-40, 2 mmol/L tribromophenol (TBP), 1 × protease inhibitor mix, 1 × nuclease mix, 1 mmol/L phenylmethanesulfonylfluoride or phenylmethylsulfonyl fluoride (PMSF), and 2% immobilized pH gradient (IPG) buffer, and then incubated on ice for 45 min. The lysed mixtures were centrifuged at 14 000 × g for 15 min at 4 ℃. The supernatant samples were determined by Bradford protein assay (BioRad, California, United States) and stored at -80 ℃.

Two-dimensional gel electrophoresis and image analysis

2-DE and image analysis were performed as previously described with some modifications[11]. Isoelectric focusing (IEF) was performed using IPGphor Ⅱ apparatus (Amersham, Sweden). Samples (150 μg protein/group, containing an equal amount of protein from each animal) were diluted in 250 μL rehydration solution (8 mol/L urea, 2% CHAPS, 0.4% dithiothreitol (DTT), 0.5% IPG buffer, 0.002% bromophenol blue) and loaded onto the IPG strips (13 cm, pH 3-10, NL) by 10 h rehydration at 30 V. Proteins were focused by using a step-wise voltage ramp: 500 V for 1 h, 1000 V for 1 h, and finally 8000 V for 6 h. The IPG strips were then incubated in the equilibration buffer (6 mol/L urea, 2% SDS, 30% glycerol, 0.002% bromophenol blue, 50 mmol/L Tris-HCl, pH 6.8) containing 1% DTT for 15 min with gentle agitation. The strips were then transferred to the equilibrating solution containing 2.5% iodoacetamide and agitated for 15 min, and subsequently were placed on top of a 12.5% uniform SDS-PAGE gel (150 mm × 158 mm × 1.5 mm). Separation in the second dimension was performed in Tris-glycine buffer (25 mmol/L Tris, 0.2 mol/L glycine, 0.1% SDS) at a constant current setting of 15 mA/gel initially for 30 min and 30 mA/gel thereafter. SDS-PAGE was terminated when the bromophenol blue dye front reached the lower ends of the gels. After 2-DE, gels were visualized using silver-staining[11]. All the raw images were digitalized using

a scanner (GS-800 calibrated densitometer, BioRad) and the Quantity One software (BioRad). Further analysis was completed using PDQuest (version 8.0, BioRad) mainly for spots' detection and quantification. The protein spots where the peak-volume ratio in the TNBS group changed more than 3-folds in comparison with the matched spots in the control group, were considered as differentially expressed, and were picked out for identification by tandem mass spectrometer (MS-MS).

In-gel digestion

Protein spots of interest were manually excised from the 2-D gels, and digested as previously described with small modification[12-14]. Briefly, the gel plugs were washed in 30 mmol/L potassium ferricyanide and 100 mmol/L sodium thiosulfate (1:1 v/v) for 5 min, and then washed in water twice. Subsequently, the gel plugs were equilibrated in 50 mmol/L ammonium bicarbonate for 20 min, then in 25 mmol/L ammonium bicarbonate and 50% acetonitrile (ACN), and finally soaked in 100% ACN until gel plugs became opaque. Thereafter, vacuum-dried gel plugs were rehydrated with 10 mg/mL of trypsin in 25 mmol/L ammonium bicarbonate (pH 8.0). Proteolysis of proteins was performed at 37 ℃ for 16-18 h. Supernatants were transferred into a new tube, and mixed with 1/2 volume of 1% trifluoroacetic acid to stop digestion. The samples were then vacuum dried at 45 ℃ for 1-2 h.

Protein identification by MS/MS

Protein identification was performed using a Autoflex Ⅲ MALDI-TOF/TOF mass spectrometer (Bruker, Germany) equipped with a 200 Hz N2 laser operating at 337 nm. Data were acquired in the positive ion reflector mode over a mass range of 800-4000 m/z using Bruker calibration mixture as an external standard. Bruker calibration mixture consists of the following peptides (monoisotopic mass of the singly protonated ion is given in parenthesis in Da); bradykinin (757.3992), angiotensin Ⅱ (1046.5420), angiotensin I (1296.6853), substance P (1347.7361), bombesin (1619.8230), renin substrate (1758.9326), ACTH clip 1-17 (2093.0868), ACTH clip 18-39 (2465.1990) and somatostatin 28 (3147.4714). Keratin contamination peaks, matrix ion peaks and trypsin ion peaks were excluded from spectra. Typically 400 shots were accumulated per spectrum in MS mode and 2000 shots in MS/MS mode. The spectra were processed using the FlexAnalysis 3.0 and BioTools 3.1 software tools (Bruker, Germany). Protein identification was performed using Mascot (2.2.04, http://www.matrixscience.com) to search the international protein index (IPI) database. Peptide masses were matched with the theoretical peptides of all proteins in the IPI database using the Mascot search program. The following parameters were used for database searches: monoisotopic mass accuracy < 100 ppm, missed cleavages 1, carbamidomethylation of cysteine as fixed modification, oxidation of methionine as variable modifications. In MS/MS mode, the fragment ion mass accuracy was set at < 0.5 Da.

Determination of MPO activity and TNF-α level

The MPO activity was measured following the method as previously described[15,16]. Colonic TNF-α was determined using an enzyme-linked immunosorbent assay kit (Leinco Technologies, United States). The protein was quantified using a bicinchoninic acid protein assay kit (Thermo Scientific, United States).

Immunoblotting analysis

Two identified proteins: (1) similar to potassium channel tetramerisation domain containing protein 12 (Kctd12); and (2) proteasome subunit α type-1 (Psma1), were selected for the confirmation study. For Western-blot analysis, protein lysates were diluted in sample buffer and denatured at 100 ℃ for 5 min. Proteins (15 μg/lane) of interest were separated by 12% SDS-PAGE, and transferred onto polyvinylidene fluoride (PVDF) membranes (Bio-Rad). Nonspecific binding sites were blocked with 5% nonfat milk for 1 h at room temperature, then the blots were incubated at 4 ℃ overnight with rabbit antibody against mouse antibody against Psma1 (1:250 in TBST, Santa Cruz) or Kctd12 (1:500 in TBST, Santa Cruz). After washing, the membranes were incubated in horseradish peroxidase (HRP)-conjugated secondary antibodies (1:2000) in Tris-Buffered Saline and Tween 20 (TBST) with 5% nonfat milk against the primary antibody species for 1 h at room temperature. The immunoreaction was detected with the enhanced chemiluminescence (ECL) Western blotting kit (Invitrogen). Bands were visualized on Bio-max X-ray film (Kodak, Japan) and captured by a scanner. The optical densities of protein blots were analyzed using Image J software. The results were presented as the ratio of optical density of Kctd12 or Psma1 standardized to optical density of β-actin.

RESULTS

Establishment of IBD model

Rats developed hypomotility and diarrhea 1 d after TNBS treatment. Hematoxylin and eosin staining of distal colon revealed incrassation and edema in the mucosa and submucosa, hyperaemia and dilation of the blood vessel, and prominent neutrophilic infiltrates in the submucosal layer, indicating severe colonic inflammation (Figure 1A). TNBS group showed significantly elevated MPO activity (Figure 1B) and TNF-α level (Figure 1C), suggesting increased granulocyte recruitment and macrophage activation in the acute phase of inflammation.

Identified proteins by 2-DE-based proteomic technique

The representative 2-DE images of protein profiling changes in DRG and spinal cord is shown in Figure 2. Overall, a total of 26 spots differentially expressed in the DRG of these two groups were identified by the mass spectrometry (MS) analysis, 12 of which were up-regulated and 14 of which were down-regulated (Table 1). A total of 19 spots differentially expressed in the spinal cord of the two groups were identified by MS analysis, 9 of which

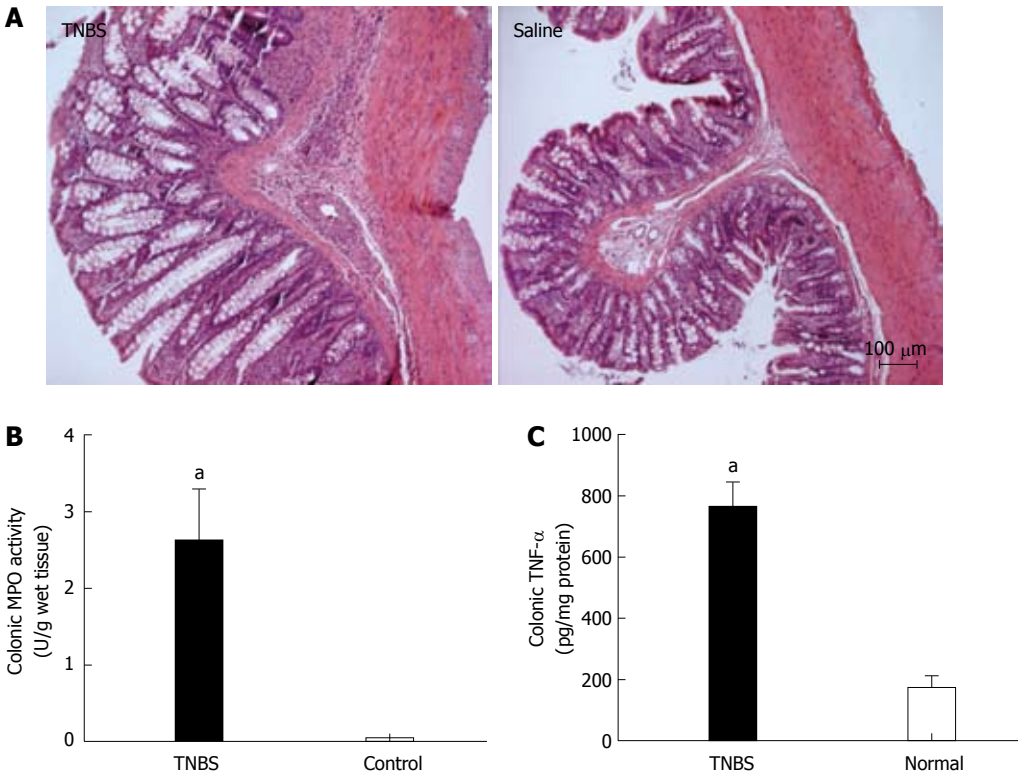

Figure 1 The establishment of colitis in trinitrobenzene sulfonic acid rats. Representative hematoxylin and eosin microscopic photos of the colon tissue (A) revealed inflammation in the sub-mucosa layer of trinitrobenzene sulfonic acid (TNBS) rats; measurement of myeloperoxidase (MPO) activity in wet colon tissue (B, 2.61 ± 2.47 *vs* 0.03 ± 0.01) and tumor necrosis factor-α (TNF-α) level in colonic total protein (C, 759.80 ± 81.07 *vs* 174.00 ± 31.92) revealed significantly elevated MPO activity and TNF-α level in TNBS treated group in comparison with saline control group. $^{a}P < 0.05$ *vs* saline group.

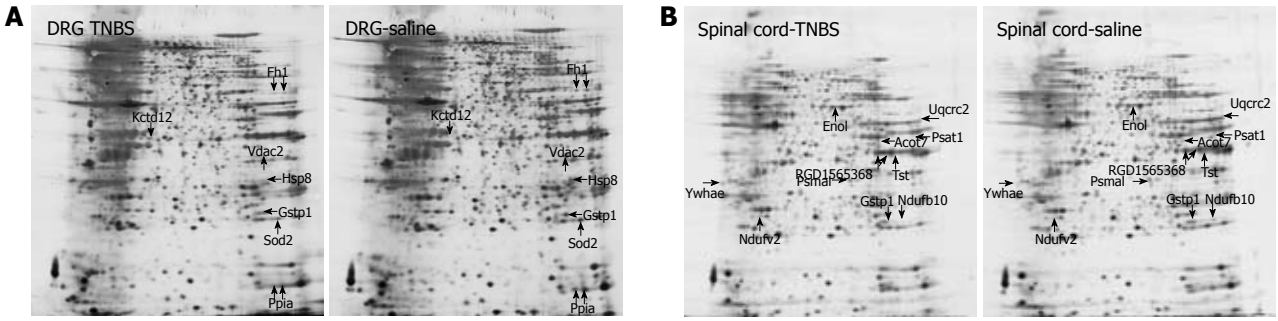

Figure 2 Representative examples of the silver-stained two-dimensional electrophoresis gels show expression maps of proteins in dorsal root ganglia (A) and spinal cord (B) of trinitrobenzene sulfonic acid colitis group and saline control groups. TNBS: Trinitrobenzene sulfonic acid; DRG: Dorsal root ganglia; Gstp1: Glutathione S-transferase P; Sod2: Superoxide dismutase; Ndufv2: NADH dehydrogenase (ubiquinone) flavoprotein 2; Ndufb10: NADH dehydrogenase (ubiquinone) 1 β subcomplex 10; Fh1: Fumarate hydratase; Psat1: Phosphoserine aminotransferase; Kctd12: Potassium channel tetramerisation domain containing protein 12; Vdac2: Voltage-dependent anion-selective channel protein 2; Ywhae: The 14-3-3 protein epsilon; Tst: Thiosulfate sulfurtransferase; Hspa8: Heat shock cognate 71 kDa protein.

were up-regulated and 10 of which were down-regulated (Table 2). In particular, we found altered expression of (1) proteins involved in inflammatory/immune responses, such as Isoform B0a of heterogeneous nuclear ribonucleoproteins A2/B1 (Hnrnpa2b1) and proteasome subunit α type-1 (Psma1); (2) signal-related proteins, such as adenylyl cyclase-associated protein 1 (Cap1) and voltage-dependent anion-selective channel protein 2 (Vdac2); (3) proteins involved in sulfate transport, thiosulfate sulfurtransferase (Tst); (4) cellular enzymes involved in cell redox homeostasis, such as glutathione S-transferase P (Gstp1) and superoxide dismutase (Sod2); (5) metabolic enzymes, such as fructose-bisphosphate aldolase C (Aldoc); (6) structure protein Lamin C2 (Lmna); and (7) chaperonins, such as heat shock cognate 71 kDa protein (Hspa8, or HSC70) and stress-induced phosphoprotein 1 (Stip1). Although previous studies have reported the contribution of a few proteins, such as down-regulated glutathione peroxiredoxin-1 (Prdx1) and malate dehydrogenase (Mdh2)[12], most of the proteins were first identified in TNBS-induced colitis (Table 3). Most importantly, the samples analyzed in previous studies were usually mucosa or submucosa of the colon, whereas this paper firstly investigated the global protein expression changes in the spinal cord and DRG of

Table 1 Significantly regulated proteins after trinitrobenzene sulfonic acid-induced colitis in dorsal root ganglia

Function	Cell component	Protein name	Abbreviation	Accession No.	Theoretical PI/Mr (kDa)	Sequence coverage (%)	MASSOT score	Change (TNBS)
Proteins involved in inflammatory/immune response								
Autoantigen in many autoimmune diseases	Cytoplasm, nucleus spliceosome	Isoform B0a of heterogeneous nuclear ribonucleoproteins A2/B1	Hnrnpa2b1	IPI00923129	8.74/32 572	16	220	↑
Hemopexin	Secreted	Hemopexin	Hpx	IPI00195516	7.58/52 060	22	597	↑
1. Accelerate the folding of protein 2. Immunosuppression	Cytosol, nucleus	Peptidyl-prolyl cis-trans isomerase A	Ppia	IPI00387771	8.34/18 091	32	363	↓
Proteins involved in cell signaling								
Growth protein	Membrane	Adenylyl cyclase-associated protein 1	Cap1	IPI00555187	7.16/51 899	5	145	↑
Cytoplasmic tetramerisation domain of voltage-gated K+ channel		Similar to potassium channel tetramerisation domain containing protein 12	Kctd12	IPI00359734	8.95/47 077	16	192	↑
1. Ion channel 2. Mitochondrial apoptosis	Mitochondrial outer membrane	Voltage-dependent anion-selective channel protein 2	Vdac2	IPI00198327	7.44/32 353	9	76	↓
Proteins involved in redox regulation								
Cell redox homeostasis	Mitochondria	Dihydrolipoyl dehydrogenase, mitochondrial	Dld	IPI00365545	7.96/54 574	5	141	↑
Antioxidant	Mitochondria	Superoxide dismutase [Mn], mitochondrial	Sod2	IPI00211593	8.96/24 887	22	130	↓
Xenobiotic metabolism and cellular defense	Nucleus	Glutathione S-transferase P	Gstp1	IPI00231229	6.89/23 652	12	255	↓
Eliminating peroxides	Mitochondria, cytosol	Peroxiredoxin-1	Prdx1	IPI00211779	8.27/22 323	9	108	↓
Proteins involved in chaperone function								
Chaperonins/heat shock proteins	Mitochondria	Heat shock cognate 71 kDa protein	Hspa8	IPI00208205	5.37/71 055	18	304	↓
Chaperonins/heat shock proteins	Nucleus, cytoplasm	Stress-induced-phosphoprotein 1	Stip1	IPI00213013	6.40/63 158	9	156	↑
Proteins involved in cellular structure								
Component of the nuclear lamina	Insoluble fraction, lamin filament, nuclear matrix	Lamin C2	Lmna	IPI00188879	6.22/52 661	16	136	↑
Proteins involved in cellular metabolism								
Oxidoreductase in valine and pyrimidine catabolic pathways	Mitochondria	Methylmalonate-semialdehyde dehydrogenase [acylating],mitochondrial	Aldh6a1	IPI00205018	8.44/58 396	4	68	↓
Glycolytic enzyme	Mitochondria	Fructose-bisphosphate aldolase A	Aldoc	IPI00231734	8.31/39 783	11	148	↓
Glycolytic enzyme	Axon, mitochondria	Aldoc 17 kDa protein	Aldoc	IPI00561972	6.84/16 666	14	88	↓
Glycolytic enzyme	Mitochondria	Dihydrolipoyllysine-residueacetyltransferase component of pyruvate dehydrogenase complex	Dlat	IPI00231714	8.76/67 637	7	79	↑
Glycolytic enzyme	Cytoplasm	Phosphoglycerate kinase 1	Pgk1	IPI00231426	8.02/44 909	16	184	↓
Glycolytic enzyme		Similar to pyruvate kinase 3		IPI00561880	7.15/58 264	17	231	↓
Glycolytic enzyme	Nucleus cytoplasm	Isoform M1 of pyruvate kinase isozymes M1/M2	Pkm2	IPI00231929	6.63/58 452	22	491	↑
1. Glycolytic enzyme 2. Transcription activation 3. Initiation of apoptosis	Cytoplasm	Similar to glyceraldehyde-3-phosphate dehydrogenase	RGD1565368	IPI00554039	8.44/36 045	14	347	↑
ATP energy transduction	Cytoplasm	Creatine kinase M-type	Ckm	IPI00211053	6.58/43 246	19	361	↑
ATP transducing	Mitochondria	Creatine kinase, mitochondrial 1, ubiquitous	Ckmt1	IPI00555166	8.58/47 331	21	231	↓

TCA cycle	Mitochondria	Isoform mitochondrial of fumarate hydratase, mitochondrial	Fh1	IPI00231611	9.06/54 714	5	115	↓
1. TCA cycle 2. Gluconeogenesis 3. Antioxidant	Mitochondria	Malate dehydrogenase, mitochondrial	Mdh2	IPI00197696	8.93/36 117	11	90	↓
Extrahepatic ketone body catabolism	Mitochondria	3-ketoacid-coenzyme A transferase 1, mitochondrial	Oxct1 Succinyl-CoA	IPI00766788	8.7/56 624	6	116	↑

↑: Elevated protein expression in TNBS group compared with saline group; ↓: Decreased protein expression in TNBS group in comparison with saline group. DRG: Dorsal root ganglia; TNBS: Trinitrobenzene sulfonic acid; Hnrnpa2b1: Heterogeneous nuclear ribonucleoproteins A2/B1; Cap1: Cyclase-associated protein 1; Kctd12: Potassium channel tetramerisation domain containing protein 12; Vdac2: Voltage-dependent anion-selective channel protein 2; Dld: Dihydrolipoyl dehydrogenase; Sod2: Superoxide dismutase; Gstp1: Glutathione S-transferase P; Prdx1: Peroxiredoxin-1; Stip1: Stress-induced phosphoprotein 1; Lmna: Lamin C2; Ckm: Creatine kinase M-type; Ckmt1: Creatine kinase, mitochondrial 1, ubiquitous; Fh1: Fumarate hydratase; Mdh2: Malate dehydrogenase; Oxct1 Succinyl-CoA: 3-ketoacid-coenzyme A transferase 1.

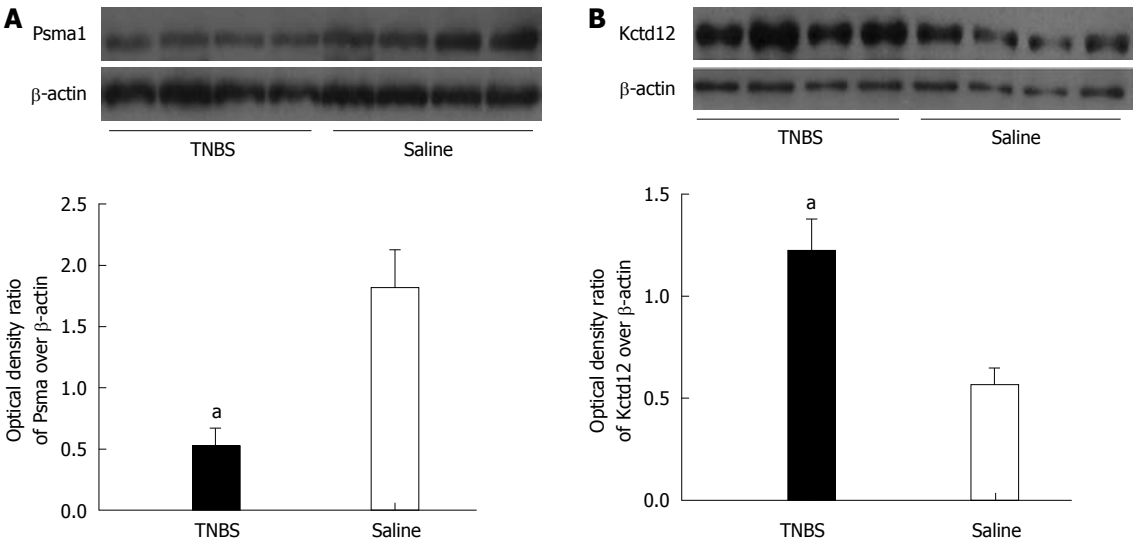

Figure 3 Immunoblotting analyses to validate the differential expression of proteasome subunit α type-1 (A, 0.53 ± 0.14 *vs* 1.81 ± 0.53) and potassium channel tetramerisation domain containing protein 12 (B, 1.21 ± 0.20 *vs* 0.56 ± 0.07) between trinitrobenzene sulfonic acid treated group and saline control group. The relative expression ratio standardized to β-actin. $^{a}P < 0.05$ *vs* saline group. TNBS: Trinitrobenzene sulfonic acid; Psma1: Proteasome subunit α type-1; Kctd12: Potassium channel tetramerisation domain containing protein 12.

rats with TNBS-induced acute colitis.

Validation by Western blotting analysis

In order to validate the proteomic data, two of the protein spots: Psma1, a protein involved in immunity, and Kctd12, a protein involved in voltage-gated potassium channel activity, were chosen for validation by Western blotting analysis. The comparison of samples derived from TNBS rats (lanes 1-4) and samples derived from saline control (lanes 5-8) revealed down-regulation of Psma1 (Figure 3A) in the spinal cord and up-regulation of Kctd12 (Figure 3B) in the DRG. These results confirmed the changed protein levels concluded from 2-DE.

DISCUSSION

Colitis persists for at least 28 d after TNBS colonic administration[17,18]. For the study of TNBS-induced colitis, rats were usually sacrificed 7 d after TNBS treatment[19], since TNBS-caused changes of gene expression profile were maximal at day 5 and day 7 after induction[20]. Consistent with previous studies, on day 7 after TNBS intraluminal treatment, we observed macroscopic and microscopic damage of the distal colon, demonstrating the presence of acute colitis. By using 2-DE in combination with MALDI-TOF/TOF MS based proteomic approach, we observed changed expression profiles not only in proteins participating in the immune/inflammatory response, but also in a broad range of proteins involved in cell signaling, sulfate transport, redox homeostasis, and cell metabolism. This result is consistent with previous studies revealing that in addition to inflammation/immunity response, TNBS-colitis affects the gene expression related to a numerous biological functions, such as signal transduction and cell metabolism[21,22]. The identified proteins from the spinal cord and DRG could be categorized into seven groups as follows.

Group 1: Proteins involved in inflammatory/immune responses

Consistent with previous results[23,24], the current study

Table 2 Proteins significantly regulated after trinitrobenzene sulfonic acid-induced colitis in spinal cord

Function	Cell component	Protein name	Abbreviation	Accession No.	Theoretical PI/Mr (kDa)	Sequence coverage (%)	MASSOT score	Change (TNBS)
Proteins involved in inflammatory/immune response								
1. Fatty acid catabolic process 2. Play a role in eicosanoid synthesis and inflammation	Cytoplasm	Isoform 1 of cytosolic acyl coenzyme A thioester hydrolase	Acot7	IPI00213571	7.16/37 936	14	167	↓
1. Glycolytic enzyme 2. Autoantigen	Cell membrane, cytoplasm	α-enolase	Eno1	IPI00464815	6.16/47 440	13	183	↓
Immunity	Cytoplasm, nucleus	Proteasome subunit α type-1	Psma1	IPI00191748	6.15/29 784	17	193	↓
Proteins involved in cell signaling								
1. Growth protein 2. Modulate calcium influx 3. Regulate the release of ICGRP	Cytoplasm	Dihydropyrimidinase-related protein 2	Dpysl2	IPI00870112	5.95/62 638	16	270	↑
Calcium ion signaling	Cytoplasm, cytoskeleton	Troponin C-like protein		gi223036	4.12/16 696	10	91	↓
1. Cell division 2. Apoptosis 3. Regulate insulin sensitivity	Melanosome, cytoplasm	14-3-3 protein epsilon	Ywhae	IPI00325135	4.63/29 326	15	165	↑
Proteins involved in sulfate transport								
Transferase detoxification	Mitochondrial matrix	Thiosulfate sulfurtransferase	Tst	IPI00366293	7.71/33 614	25	333	↓
Proteins involved in redox regulation								
Xenobiotic metabolism and cellular defense	Nucleus	Glutathione S-transferase P	Gstp1	IPI00231229	6.89/23 652	20	263	↓
Proteins involved in chaperone function								
Assist protein folding	Cytoplasm	T-complex protein 1 subunit γ	Cct3	IPI00372388	6.23/61 179	8	122	↑
Chaperonins/heat shock proteins	Mitochondria	Heat shock cognate 71 kDa protein	Hspa8	IPI00208205	5.37/71 055	11	172	↑
Chaperonins/heat shock proteins	Cytoplasm, nucleus	Stress-induced-phosphoprotein 1	Stip1	IPI00213013	6.4/63 158	7	143	↑
Proteins involved in cellular metabolism								
Glycolytic enzyme	Axon, mitochondria	Fructose-bisphosphate aldolase C	Aldoc	IPI00231736	6.67/39 658	10	189	↓
Glycolytic enzyme	Cytoplasm	Similar to phosphoglycerate kinase 1	RGD1560402	IPI00372910	6.15/43 604	10	151	↑
1. Glycolytic enzyme 2. Transcription activation 3. Initiation of apoptosis	Cytoplasm	Similar to glyceraldehyde-3-phosphate dehydrogenase	RGD1565368	IPI00554039	8.44/36 045	18	454	↑
ATP transducing	Mitochondria	Creatine kinase, mitochondrial 1, ubiquitous	Ckmt1	IPI00555166	8.58/47 331	12	155	↑
1. Electron transport in respiratory chain 2. Oxidoreductase	Mitochondria	NADH dehydrogenase [ubiquinone] flavoprotein 2, mitochondrial	Ndufv2	IPI00367152	6.23/27 703	24	253	↑
Electron transport in respiratory chain	Membrane, mitochondria	NADH dehydrogenase (ubiquinone) 1 β subcomplex, 10	Ndufb10	IPI00202238	7.57/21 131	32	306	↓
1. Electron transport in respiratory chain 2. Mitochondrial dysfunction	Mitochondrial	Cytochrome b-c1 complex subunit 2, mitochondrial	Uqcrc2	IPI00188924	9.16/48 423	8	222	↓
Amino-acid (serine) biosynthesis		Phosphoserine aminotransferase	Psat1	IPI00331919	7.57/40 943	8	97	↓

↑: Elevated protein expression in TNBS group compared with saline group; ↓: Decreased protein expression in TNBS group in comparison with saline group; TNBS: Trinitrobenzene sulfonic acid; NADH: Nicotinamide adenine dinucleotide; Psma1: Proteasome subunit α type-1; Dpysl2: Dihydropyrimidinase-related protein 2; Ywhae: The 14-3-3 protein epsilon; Tst: Thiosulfate sulfurtransferase; Gstp1: Glutathione S-transferase P; Hspa8: Heat shock cognate 71 kDa protein; Stip1: Stress-induced phosphoprotein 1; Aldoc: Aldolase C; Ckmt1: Creatine kinase mitochondrial 1 ubiquitous; Ndufv2: NADH dehydrogenase (ubiquinone) flavoprotein 2; Ndufb10: NADH dehydrogenase (ubiquinone) 1 β subcomplex 10; Uqcrc2: Cytochrome b-c1 complex subunit 2; Psat1: Phosphoserine aminotransferase.

demonstrated immune regulation in the nervous system following peripheral inflammation. Hnrnpa2b1 hinders the double strand DNA break repair process by binding the DNA-dependent protein kinase complex[25], and is an autoantigen in autoimmune diseases such as rheumatoid arthritis and autoimmune hepatitis[26,27]. Thus, the up-

Table 3 Differentially expressed proteins identified in cellular and animal models of inflammatory bowel disease and in clinical samples of inflammatory bowel disease patients

Ref.	Animal model	Cell	Patient	Sample	Analytical technique (S)	No. of regulated proteins	Major findings	Protein name	Change
[68]		Human adenocarcinoma cells Dld-1 exposed to interferon-γ, interleukin-1 and interleukin-6			2D PAGE-MALDI-TOF-MS/MS	5	Protein biosynthesis	Tryptophanyl-tRNA synthetase	Up
							Redox regulation	Indoleamine-2, 3-Dioxygenase	Up
[14]		HT29 Cl.16E cell treated with interferon-γ			1D PAGE-LC ESI/QTOF-MS/MS	7	Structure protein	Histone H2A type-1B	Up
							Metabolic enzymes	Adenosylhomocysteinase	Up
							Redox regulation	Peroxiedonxin-1	Down
			CD patients	Intestinal epithelial cells		14	Structure protein	Histone H1.2, H2A.V, H2B Type 1-C/E/F/G/I, H3 Like, H4	Up
							Chaperone	Heat shock 70 kDa protein 5	Up
							Annexin	Annexin A1	Down
[69]			CD and UC patients	Endoscopic biopsies of colonic mucosa	Multi-epitope-ligand-cartographic immunofluorescence microscopy		Apoptosis	Caspase-3	Down
							Transcription regulation	NF-κ B	Up
[12]			UC patients	Colon biopsies	2D-MALDI-TOF-MS/MS	19	Negative regulation of cell proliferation and DNA replication	Prohibitin (PHB)	Down
							1. TCA Cycle 2. Gluconeogenesis 3. Antioxidant	Mitochondrial malate dehydrogenase (Mdh2)	Down
							Eliminating Peroxides	Thioredoxin peroxidase (Prdx1)	Down
							1. Ion Channel 2. Apoptosis	Voltage-dependent anion-selective channel protein 1 (Vdac1)	Down
							1. Intracellular signal transduction 2. Regulation of transcription, DND-dependent	Nuclear factor of activated T-cells cytoplasmic (NFAT C1)	Up
							Protein folding	Tumor rejection antigen 1 (TRA1)	Up
							Cell adhesion Host-virus interaction	Poliovirus receptor related protein 1 (PVRL1)	Up
[70]			CD and UC patients	Serum	SELDI-TOF-MS	4	Cytokine-mediated signaling	Platelet factor 4	Up
							Chronic inflammation	Myeloid related protein 8	Up
							Fibrin producing and inflammation	FIBA	Up
							Transferase	Haptoglobin alph2	Up
[71]			CD and UC patients	Intestinal epithelial cells	2D PAGE-MALDI-TOF-MS	17	Regulation of GTPase activity	Rho gdp dissociation inhibitor (GDI) α chain	Up
							Differentiation	Nicotinamide phosphor-ribosyltransferase	Up
							Calcium ion binding	Myosin regulatory light chain 2, nonsarcomeric	Up
[72]			CD patients	Serum	RP NANO-LC ESI/Q-TOF MS	8	Immunity	Complement C3	Up
							Blood coagulation	Fibrinogen α chain	Up
							Lipid transport	Apolipoprotein E	Down

[73]		UC patients	Mucosa/ submucosa	2D PAGE-LC-MS/MS	7	Cell adhesion	Protocadherin 17 precursor	Up
						Acute-phase response	α-1-Antitrypsin (precursor)	Up
						Muscle protein	Caldesmon	Up
						Structural molecule activity	Mutant desmin	Up
[74]	DSS treated Balb/C mice		Mucosa	2D-DIGE-MALTI-TOF	5	Isomerase	Protein disulfide isomerase family A, member 3	Down
						Redox regulation	Peroxiredoxin 6 (Prx6)	Down
[13]	TNBS treated SD rats		Lymphocytes	2D-MALDI-TOF-MS/MS	42	Apoptosis-related proteins	PYD and Card domain containing protein	Down
						DNA damage response	Proteasome activator complex subunit 2	Down
						Glycolysis	Phosphoglycerate mutase type B subunit	Down
						Xenobiotic metabolism and cellular defense	Glutathione S-transferase, Pi 2	Down
						Cytokine	Interleukin-12 p40 precursor	Up
						Proteins involved in cell growth, differentiation and signal trransduction	Nucleoside diphosphate kinases β isoform	Up
						Inflammatory factors	Myeloid-related protein	Up
						ATP transduction	ATP-citrate synthase	Up
						Redox regulation	Dismutase	Up
[49]	TNBS treated SD Rats		DRG	2D-MALDI-TOF-MS/MS	26	Xenobiotic metabolism and cellular defense	Glutathione S-transferase P (Gstp1)	Down
						Eliminating peroxides	Peroxiredoxin-1 (Prdx1)	Down
						1. Accelerate the folding of protein 2. Immunosuppression	Peptidyl-prolyl cis-trans isomerase A (Ppia)	Down
						1. Ion channel 2. Mitochondrial apoptosis	Voltage-dependent anion-selective channel protein 2 (Vdac2)	Down
						Cytoplasmic tetramerisation domain of voltage-gated K+ channel	similar to Potassium channel tetramerisation domain containing protein 12	Up
			Spinal cord		19	Xenobiotic metabolism and cellular defense	Glutathione S-transferase P (Gstp1)	Down
						1. Glycolytic enzyme 2. Autoantigen in many diseases	α-enolase (Eno1)	Down
						Immunity	Proteasome subunit α type-1 (Psma1)	Down

DRG: Dorsal root ganglia; TNBS: Trinitrobenzene sulfonic acid; CD: Crohn's disease; UC: Ulcerative colitis; DSS: Dextran sulfate sodium; NF: Nuclear factor.

regulated Hnrnpa2b1 in DRG of TNBS rats may suggest reduced DNA repair efficiency of neurons and activated autoimmunity in DRG. Ppia (also known as cyclophilin A) contributes to the pathogenesis of inflammation-mediated diseases by directly inducing leukocyte chemotaxis and expression of proinflammatory cytokine/chemokines through a NF-κB dependent pathway[28,29]. In addition, Ppia is a novel paracrine and autocrine modulator of endothelial cell functions in immune-mediated diseases[30]. The down-regulated expression of Ppia in DRG of TNBS rats might associate with impaired immune modulation following acute colitis. Eno1 is a multifunctional enzyme that plays a part in various processes such as glycolysis, growth control and allergic responses. It is an autoantigen in many diseases, however, its diagnostic value in IBD is still controversial[31]. The underexpressed Eno1 may suggest that glycolysis is blocked and gluconeogenesis is dominant, which may associate with diarrhea and emaciation caused by colitis. Psma1 and Acot7 may be associated with the anti-inflammatory effect of macrophages. Psma1 mediates lipopolysaccharide-induced signal transduction in the macrophage proteasome[32]. Acot7 hydrolyzes the CoA thioester of palmitoyl-CoA, an important precursor for proinflammatory and immunoactive eicosanoids. Acot7 gene is highly expressed in macrophages and up-regulated by lipopolysaccharide[33]. The down-regulated Psma1 and Acot7 expression in the spinal cord of TNBS rats may be associated with inhibited anti-inflammatory responses.

Group 2: Proteins involved in cell signaling

Group 2 consists of proteins involved in ion channel

function, cell growth and division. Potassium channels are important in shaping the action potential, excitability and plasticity of neurons[34]. Changes in the properties of potassium channels at the soma accompanied with hyperexcitability in nociceptive DRG neurons in animal with TNBS-induced ileitis[35]. We observed overexpressed kctd12 protein in DRG of the TNBS rats. This might be related to altered function of potassium channel in DRG and hyperalgesia in colitis rats. Voltage-dependent anion-selective channel protein 2 (Vdac2) inhibits mitochondrial apoptosis[36]. It is interesting that a significantly down-regulated Vdac2 protein expression was observed in the DRG of TNBS rats, indicating an up-regulated apoptosis signaling. Adenylyl cyclase-associated protein 1 (Cap1) is a growth protein involved in the cyclic AMP (cAMP) pathway. Inflammatory signals can activate cAMP-protein kinase A pathways, which correlates with electrophysiological hyperexcitability of DRG neuron[37]. And, cAMP plays a role in DRG axon regeneration[38]. The up-regulated Cap1 in DRG of TNBS rats is probably a sign of neuronal hyperexcitability and/or axon regeneration. The 14-3-3 protein epsilon (Ywhae) is a splice variant of the 14-3-3 protein, which modulates cell division and apoptosis[39]. Elevated Ywhae expression was observed in the spinal cord of injury rats[40]. Consistent with down-regulated Vdac2 expression in DRG, the elevated Ywhae expression in spinal cord of TNBS rats may also indicate enhanced apoptosis signaling. Dihydropyrimidinase-related protein 2 (Dpysl2) plays a role in axon guidance, neuronal growth cone collapse and cell migration. In rat brain after ischemic stroke, up-regulated Dpysl2 indicates an early neuronal defense mechanism involving active neuronal repair, regeneration and development[41]. The up-regulated Dpysl2 in the spinal cord of TNBS rats may be related to the neurite outgrowth/plasticity associated with immunoreaction.

Group 3: Proteins involved in sulfate transport

Thiosulfate sulfurtransferase (Tst) can detoxify H_2S. Dysregulation of Tst expression associates with inability to detoxify detrimental H_2S and could be a factor in cell loss and inflammation[42]. The down-regulated Tst expression in spinal cord of TNBS rats may indicate dysfunction of the Tst detoxification that is possibly related to cell damage and inflammation in acute colitis.

Group 4: Proteins involved in cell redox homeostasis

Glutathione S-transferase P (Gstp1) functions in xenobiotic metabolism and plays a central role in the cellular defense against harmful endogenous compounds and xenobiotics[43,44]. Gstp1 is distributed in neuronal perikarya and oligodendrocytes in the central nervous system (CNS), and in neuronal perikarya and satellite cells of the DRG[45]. Reduced level of Gstp1 indicates a declined antioxidative capacity which may contribute to the damage to motor neurons in the process of immune-mediated motor neuron injury[46]. The underexpression of Gstp1 in both spinal cord and DRG of TNBS rats might suggest oxidative stress and damage in neuronal cells. Prdx1 may participate in the signaling cascades of growth factors and TNF-α by regulating the intracellular concentrations of H_2O_2. A recent study revealed that in dextran sulfate sodium (DSS) mice, the inflamed intestinal mucosa has a down-regulated Prdx6 expression in comparison with normal mucosa[13]. Consistently, down-regulated Prdx1 in DRG of rats with TNBS colitis suggesting oxidative stress occurred in DRG. Superoxide dismutase (Mn), mitochondrial (Sod2) is an important antioxidant defenser in nearly all cells exposed to oxygen[47]. Ulcerative colitis involves intestinal mucosal damage driven by reactive oxygen species (ROS), in particular, superoxide anion. At the stage of severe inflammation, suppression of superoxide dismutase activity and elevation of nitrous oxide systems activity occur concomitantly. The underexpression of Sod2 protein indicates oxidative stress existing in the DRG of TNBS rats. Taken together, the down-regulated Gstp1 expression in spinal cord and DRG of TNBS rats, along with decreased expression of Prdx1 and Sod2 in DRG of TNBS rats, suggest that TNBS rats may have a significantly declined antioxidative and cellular defense capacity in the nervous system. Interestingly, another protein involved in cell redox homeostasis, dihydrolipoyl dehydrogenase (Dld), has a higher expression in the DRG of TNBS rats. Dld is a source of ROS, capable of scavenging nitric oxide, and can serve as an antioxidant by protecting other proteins against oxidative inactivation[48].

Group 5: Chaperonins

In both the spinal cord and DRG of TNBS rats, we observed significant up-regulation of Stip1. It is a chaperone that mediates the association of the molecular chaperones, heat shock cognate 71 kDa protein (Hspa8) and heat shock protein 90. Hspa8 is a key component of stress responses induced by various noxious conditions[49]. It regulates protein biosynthesis and refolding of denatured proteins, and plays an essential role in protecting cells in intestinal mucosal inflammation, potentially by lessening the extent and severity of injury[50,51]. The up-regulated Stip1 expression was observed in both the DRG and spinal cord of TNBS rats, indicating stress responses in primary afferent and CNS. Hspa8 is up-regulated in the spinal cord and down-regulated in DRG of TNBS rats. As Hspa8 exhibits both protective and antigenic properties, and the Hspa8 expression may stem from neuron, satellite or immune cells[49,52], the conflicting Hspa8 expression in spinal cord and DRG merits further investigation.

Group 6: Structure protein

Lamins are components of the nuclear lamina, providing a framework for the nuclear envelope. The mechanical properties of the cytoskeleton and cytoskeleton-based processes (such as cell motility and cell polarization), depend critically on the integrity of the nuclear lamina[53]. The overexpressed Lmna protein was observed in DRG of TNBS rats, which may suggest altered cytoskeleton.

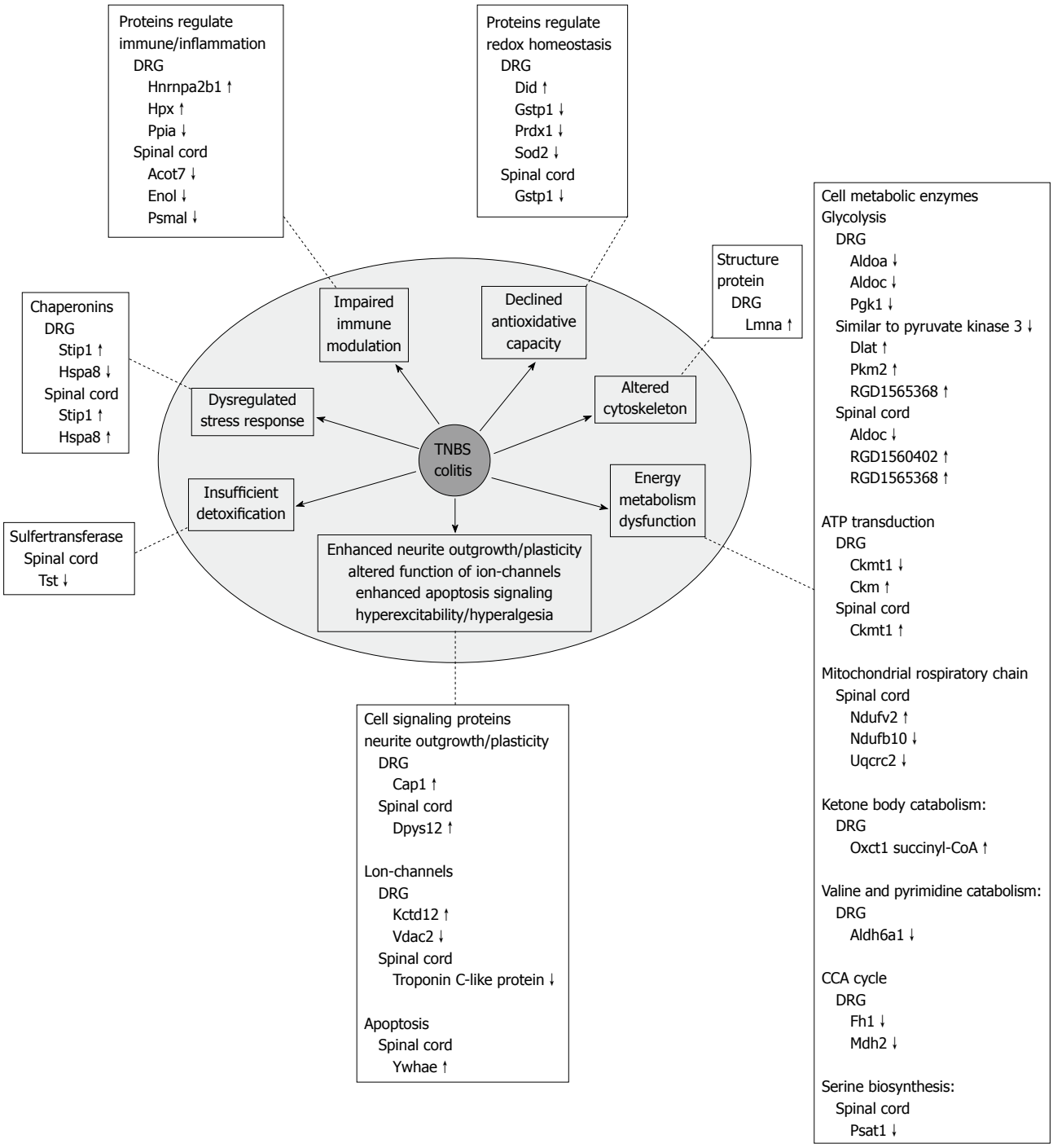

Figure 4 Schematic drawing summarizes the major findings that might associate with pathophysiological changes in rat nervous system caused by trinitrobenzene sulfonic acid-induced colitis. TNBS: Trinitrobenzene sulfonic acid; DRG: Dorsal root ganglia; Hnrnpa2b1: Heterogeneous nuclear ribonucleoproteins A2/B1; Gstp1: Glutathione S-transferase P; Prdx1: Peroxiredoxin-1; Sod2: Superoxide dismutase; Lmna: Lamin C2; Aldoa: Aldolase A; Aldoc: Aldolase C; Ckmt1: Creatine kinase, mitochondrial 1, ubiquitous; Ckm: Creatine kinase M-type; Ndufv2: NADH dehydrogenase (ubiquinone) flavoprotein 2; Ndufb10: NADH dehydrogenase (ubiquinone) 1 β subcomplex 10; Oxct1 succinyl-CoA: 3-ketoacid-coenzyme A transferase 1; Fh1: Fumarate hydratase; Mdh2: Malate dehydrogenase; Psat1: Phosphoserine aminotransferase; Cap1: Cyclase-associated protein 1; Kctd12: Potassium channel tetramerisation domain containing protein 12; Vdac2: Voltage-dependent anion-selective channel protein 2; Ywhae: The 14-3-3 protein epsilon; Tst: Thiosulfate sulfurtransferase; Stip1: Stress-induced phosphoprotein 1; Hspa8: heat shock cognate 71 kDa protein.

Group 7: Cell metabolic enzymes

Proteins involved in glycolysis: Significant down-regulation of glycolysis enzymes, for example, Aldoc 17 kDa protein, fructose-bisphosphate aldolase A (Aldoa), and a third enzyme similar to pyruvate kinase 3, was observed in the DRG of TNBS group. Consistent with this, decreased expression of Aldoc was observed in spinal cord of TNBS rats. Aldoc and Aldoa regulate the stability of the light-neurofilament mRNA[54], and Aldoc provides marked neuroprotection to Purkinje cells after trauma and AMPA-

mediated excitotoxicity[55]. The down-regulated Aldoc in spinal cord and DRG together with decreased Aldoa expression in DRG may suggest down-regulated neuroprotection in TNBS rats. In addition, inhibition or activation of other glycolysis enzymes may result in speeding up or slowing down certain steps in the glycolysis pathway, and reflecting adjustment to physiological/pathological changes compensating for the cellular energy or neuron apoptosis[49].

Proteins involved in adenosine triphosphate transduction: Creatine kinase serves as an energy reservoir for the rapid buffering and regeneration of adenosine triphosphate (ATP) to sites with high, fluctuating energy demands, such as the synapse[55]. In the present study, expression of creatine kinase, mitochondrial 1, ubiquitous (Ckmt1) in the spinal cord was significantly up-regulated in TNBS rats. In contrast, Ckmt1 expression was decreased but the expression of creatine kinase M-type (Ckm) was up-regulated in the DRG of TNBS rats. Given that selective localization of Ckm in neurons was postulated to reflect the specific energy requirements of the specialized cells, these alterations may indicate enhanced phosphocreatine energy shuttles in spinal cord and remodelled energy shuttles/circles in the DRG[56,57].

Proteins involved in mitochondrial respiratory chain: Cytochrome b-c1 complex subunit 2, mitochondrial (Uqcrc2) is implicated in mitochondrial ROS generation and inflammation. Uqcrc2 deficiency causes mitochondrial dysfunction and exacerbates allergic airway inflammation[58]. The down-regulated Uqcrc2 expression in the spinal cord of TNBS rats might associate with inflammatory responses. Nicotinamide adenine dinucleotide (NADH) dehydrogenase is a potent source of reactive oxygen species such as superoxide and hydrogen peroxide[59]. It is interesting that, in contrast to the up-regulated protein expression of NADH dehydrogenase (ubiquinone) flavoprotein 2 (Ndufv2) in the spinal cord of the TNBS group, the NADH dehydrogenase (ubiquinone) 1 β subcomplex 10 (Ndufb10) was down-regulated. As the specific cellular functions of these subcomplexs are still not well known, further investigation is warranted.

Proteins involved in ketone body catabolism: 3-keto-acid-coenzyme A transferase 1 (Oxct1 Succinyl-CoA) is a mitochondrial matrix enzyme that plays a central role in extrahepatic ketone body catabolism. In the DRG of TNBS rats, Oxct1 Succinyl-CoA showed a 4-fold higher expression than in control rats. This observation is consistent with accelerated hepatic gluconeogenesis as well as ketogenesis in patients with chronic IBD, which probably is a consequence of the altered hormonal milieu[60].

Proteins involved in tricarboxylic acid cycle: Malate dehydrogenase, mitochondrial (Mdh2) is a cellular antioxidant, an enzyme in the tricarboxylic acid (TCA) cycle and gluconeogenesis. Mdh2 was down-regulated in experimental autoimmune uveitis oxidative stress, and in colon mucosa of ulcerative colitis patients[12,61]. Similarly, the down-regulated Mdh2 and isoform mitochondrial of fumarate hydratase (Fh1) expression in DRG of TNBS rats may indicate a TCA metabolic dysregulation under disease condition.

Proteins involved in serine biosynthesis: Phosphoserine aminotransferase (Psat1) is an active serine biosynthesis enzyme in the mammal brain. Patients with Psat1 deficiency present with intractable seizures and psychomotor retardation[62]. The significantly down-regulated Psat1 expression in spinal cord of the TNBS group may indicate dysregulation of serine biosynthesis and may be associated with seizure susceptibility in TNBS rats.

Our analysis provides an overview profiling the proteomic changes in the spinal cord and DRG of rats with TNBS-induced colitis. As summarized in Figure 4, intracolonal instillation of TNBS not only induces inflammatory/immune responses in the DRG and spinal cord, but also triggers broad alterations of protein involving cell signaling, cellular metabolism, redox regulation, stress response *etc*. The TNBS-induced colitis in rodents is an immunologically mediated colitis that accompanies with an increase in proinflammatory factors and systemic endotoxaemia[63]. Besides colonic and systematic changes, a series of alterations in the nervous system have been described, such as transient disruption of blood-brain-barrier to small molecules[64]; a marked inflammatory response within the CNS[22]; and neurosignaling activation in rodent primary afferent nerve as well as in DRG and spinal cord neurons[20,65,66]. These neurological alterations may relate to intrinsic neuronal excitability and help explain some of the underlying comorbidities, such as hyperalgesia, seizure and anorexia[5,6]. The neurologic manifestations of IBD are most likely primary immune-mediated disorders, possibly caused by proinflammatory cytokines that diminish neuron proliferation, increase apoptosis, increase neuronal excitability, exacerbate sickness and/or result in psychological symptoms[21,67]. Our results delineated a dramatic deviation of protein profiling from the carefully orchestrated physiological balance in the DRG and spinal cord of TNBS rats. These findings provide useful proteins for further investigation on the neurological manifestations of IBD.

COMMENTS

Background

Inflammatory bowel disease (IBD) is a systematic illness, whose etiology and pathophysiology is incompletely understood. Many organs outside the gastrointestinal tract are involved in IBD, including the nervous system (neuropathies, cerebrovascular events, white matter lesions). These pathological changes may associate with a variety of comorbidities, such as hyperalgesia, seizure, and anorexia, but the underlying mechanism remains poorly understand.

Research frontiers

Proteomics keeps a rapidly expanding field, with a wealth of reports regularly appearing on technology enhancements and scientific studies using these new instruments.

Innovations and breakthroughs

This study demonstrated that trinitrobenzene sulfonic acid (TNBS) colitis profoundly changed expression of not only proteins involved in inflammatory/immune responses, but also proteins involved in cell signaling, sulfate transport, redox homeostasis and cell metabolism.

Applications

This study provides an overview profiling the proteomic changes in the spinal cord and dorsal root ganglia (DRG) of rats with TNBS-induced experimental colitis. These findings provide useful proteins for further investigation on the neurological manifestations of IBD.

Peer review

In this study, the authors profiled the global protein expression changes in the DRG and spinal cord in rats with acute colitis induced by TNBS using a two-dimensional electrophoresis-based proteomic technique. They found that altered proteins were involved in a number of biological functions including inflammation/immunity, cell signaling, redox regulation, sulfate transport and cellular metabolism. Although the number of the samples examined in this study was small, this paper is well written and the results are interesting.

REFERENCES

1 **Strober W**, Fuss I, Mannon P. The fundamental basis of inflammatory bowel disease. *J Clin Invest* 2007; **117**: 514-521
2 **Shanahan F**, Bernstein CN. The evolving epidemiology of inflammatory bowel disease. *Curr Opin Gastroenterol* 2009; **25**: 301-305
3 **Goh K**, Xiao SD. Inflammatory bowel disease: a survey of the epidemiology in Asia. *J Dig Dis* 2009; **10**: 1-6
4 **de Lau LM**, de Vries JM, van der Woude CJ, Kuipers EJ, Siepman DA, Sillevis Smitt PA, Hintzen RQ. Acute CNS white matter lesions in patients with inflammatory bowel disease. *Inflamm Bowel Dis* 2009; **15**: 576-580
5 **El-Haj T**, Poole S, Farthing MJ, Ballinger AB. Anorexia in a rat model of colitis: interaction of interleukin-1 and hypothalamic serotonin. *Brain Res* 2002; **927**: 1-7
6 **Medhi B**, Prakash A, Avti PK, Chakrabarti A, Khanduja KL. Intestinal inflammation and seizure susceptibility: understanding the role of tumour necrosis factor-alpha in a rat model. *J Pharm Pharmacol* 2009; **61**: 1359-1364
7 **Tseng CW**, Yang JC, Chen CN, Huang HC, Chuang KN, Lin CC, Lai HS, Lee PH, Chang KJ, Juan HF. Identification of 14-3-3β in human gastric cancer cells and its potency as a diagnostic and prognostic biomarker. *Proteomics* 2011; **11**: 2423-2439
8 **Fujisawa H**, Ohtani-Kaneko R, Naiki M, Okada T, Masuko K, Yudoh K, Suematsu N, Okamoto K, Nishioka K, Kato T. Involvement of post-translational modification of neuronal plasticity-related proteins in hyperalgesia revealed by a proteomic analysis. *Proteomics* 2008; **8**: 1706-1719
9 **Messaoudi M**, Desor D, Grasmück V, Joyeux M, Langlois A, Roman FJ. Behavioral evaluation of visceral pain in a rat model of colonic inflammation. *Neuroreport* 1999; **10**: 1137-1141
10 **Friedrich AE**, Gebhart GF. Effects of spinal cholecystokinin receptor antagonists on morphine antinociception in a model of visceral pain in the rat. *J Pharmacol Exp Ther* 2000; **292**: 538-544
11 **Li G**, Zhang XA, Wang H, Wang X, Meng CL, Chan CY, Yew DT, Tsang KS, Li K, Tsai SN, Ngai SM, Han ZC, Lin MC, He ML, Kung HF. Comparative proteomic analysis of mesenchymal stem cells derived from human bone marrow, umbilical cord, and placenta: implication in the migration. *Proteomics* 2009; **9**: 20-30
12 **Hsieh SY**, Shih TC, Yeh CY, Lin CJ, Chou YY, Lee YS. Comparative proteomic studies on the pathogenesis of human ulcerative colitis. *Proteomics* 2006; **6**: 5322-5331
13 **Liu BG**, Cao YB, Cao YY, Zhang JD, An MM, Wang Y, Gao PH, Yan L, Xu Y, Jiang YY. Altered protein profile of lymphocytes in an antigen-specific model of colitis: a comparative proteomic study. *Inflamm Res* 2007; **56**: 377-384
14 **Nanni P**, Mezzanotte L, Roda G, Caponi A, Levander F, James P, Roda A. Differential proteomic analysis of HT29 Cl.16E and intestinal epithelial cells by LC ESI/QTOF mass spectrometry. *J Proteomics* 2009; **72**: 865-873
15 **Krawisz JE**, Sharon P, Stenson WF. Quantitative assay for acute intestinal inflammation based on myeloperoxidase activity. Assessment of inflammation in rat and hamster models. *Gastroenterology* 1984; **87**: 1344-1350
16 **Grisham MB**, Benoit JN, Granger DN. Assessment of leukocyte involvement during ischemia and reperfusion of intestine. *Methods Enzymol* 1990; **186**: 729-742
17 **Miranda A**, Nordstrom E, Mannem A, Smith C, Banerjee B, Sengupta JN. The role of transient receptor potential vanilloid 1 in mechanical and chemical visceral hyperalgesia following experimental colitis. *Neuroscience* 2007; **148**: 1021-1032
18 **Gao D**, Wagner AH, Fankhaenel S, Stojanovic T, Schweyer S, Panzner S, Hecker M. CD40 antisense oligonucleotide inhibition of trinitrobenzene sulphonic acid induced rat colitis. *Gut* 2005; **54**: 70-77
19 **Martínez-Augustin O**, Merlos M, Zarzuelo A, Suárez MD, de Medina FS. Disturbances in metabolic, transport and structural genes in experimental colonic inflammation in the rat: a longitudinal genomic analysis. *BMC Genomics* 2008; **9**: 490
20 **Yang X**, Han JQ, Liu R. Effects of experimental colitis on the expressions of calcitonin gene-related peptide and vanilloid receptor 1 in rat spinal cord sensory neurons. *Shengli Xuebao* 2008; **60**: 143-148
21 **Riazi K**, Galic MA, Kuzmiski JB, Ho W, Sharkey KA, Pittman QJ. Microglial activation and TNFalpha production mediate altered CNS excitability following peripheral inflammation. *Proc Natl Acad Sci USA* 2008; **105**: 17151-17156
22 **Wang K**, Yuan CP, Wang W, Yang ZQ, Cui W, Mu LZ, Yue ZP, Yin XL, Hu ZM, Liu JX. Expression of interleukin 6 in brain and colon of rats with TNBS-induced colitis. *World J Gastroenterol* 2010; **16**: 2252-2259
23 **Dumortier H**, Monneaux F, Jahn-Schmid B, Briand JP, Skriner K, Cohen PL, Smolen JS, Steiner G, Muller S. B and T cell responses to the spliceosomal heterogeneous nuclear ribonucleoproteins A2 and B1 in normal and lupus mice. *J Immunol* 2000; **165**: 2297-2305
24 **Yukitake M**, Sueoka E, Sueoka-Aragane N, Sato A, Ohashi H, Yakushiji Y, Saito M, Osame M, Izumo S, Kuroda Y. Significantly increased antibody response to heterogeneous nuclear ribonucleoproteins in cerebrospinal fluid of multiple sclerosis patients but not in patients with human T-lymphotropic virus type I-associated myelopathy/tropical spastic paraparesis. *J Neurovirol* 2008; **14**: 130-135
25 **Iwanaga K**, Sueoka N, Sato A, Hayashi S, Sueoka E. Heterogeneous nuclear ribonucleoprotein B1 protein impairs DNA repair mediated through the inhibition of DNA-dependent protein kinase activity. *Biochem Biophys Res Commun* 2005; **333**: 888-895
26 **Huguet S**, Labas V, Duclos-Vallee JC, Bruneel A, Vinh J, Samuel D, Johanet C, Ballot E. Heterogeneous nuclear ribonucleoprotein A2/B1 identified as an autoantigen in autoimmune hepatitis by proteome analysis. *Proteomics* 2004; **4**: 1341-1345
27 **Goëb V**, Thomas-L'Otellier M, Daveau R, Charlionet R, Fardellone P, Le Loët X, Tron F, Gilbert D, Vittecoq O. Candidate autoantigens identified by mass spectrometry in early rheumatoid arthritis are chaperones and citrullinated glycolytic enzymes. *Arthritis Res Ther* 2009; **11**: R38
28 **Song F**, Zhang X, Ren XB, Zhu P, Xu J, Wang L, Li YF, Zhong N, Ru Q, Zhang DW, Jiang JL, Xia B, Chen ZN. Cyclophilin A (CyPA) induces chemotaxis independent of its peptidylprolyl cis-trans isomerase activity: direct binding between CyPA and the ectodomain of CD147. *J Biol Chem*

2011; **286**: 8197-8203
29 **Kim H**, Kim WJ, Jeon ST, Koh EM, Cha HS, Ahn KS, Lee WH. Cyclophilin A may contribute to the inflammatory processes in rheumatoid arthritis through induction of matrix degrading enzymes and inflammatory cytokines from macrophages. *Clin Immunol* 2005; **116**: 217-224
30 **Kim SH**, Lessner SM, Sakurai Y, Galis ZS. Cyclophilin A as a novel biphasic mediator of endothelial activation and dysfunction. *Am J Pathol* 2004; **164**: 1567-1574
31 **Vermeulen N**, Arijs I, Joossens S, Vermeire S, Clerens S, Van den Bergh K, Michiels G, Arckens L, Schuit F, Van Lommel L, Rutgeerts P, Bossuyt X. Anti-alpha-enolase antibodies in patients with inflammatory Bowel disease. *Clin Chem* 2008; **54**: 534-541
32 **Qureshi N**, Perera PY, Shen J, Zhang G, Lenschat A, Splitter G, Morrison DC, Vogel SN. The proteasome as a lipopolysaccharide-binding protein in macrophages: differential effects of proteasome inhibition on lipopolysaccharide-induced signaling events. *J Immunol* 2003; **171**: 1515-1525
33 **Forwood JK**, Thakur AS, Guncar G, Marfori M, Mouradov D, Meng W, Robinson J, Huber T, Kellie S, Martin JL, Hume DA, Kobe B. Structural basis for recruitment of tandem hotdog domains in acyl-CoA thioesterase 7 and its role in inflammation. *Proc Natl Acad Sci USA* 2007; **104**: 10382-10387
34 **Tempel BL**, Jan YN, Jan LY. Cloning of a probable potassium channel gene from mouse brain. *Nature* 1988; **332**: 837-839
35 **Moore BA**, Stewart TM, Hill C, Vanner SJ. TNBS ileitis evokes hyperexcitability and changes in ionic membrane properties of nociceptive DRG neurons. *Am J Physiol Gastrointest Liver Physiol* 2002; **282**: G1045-G1051
36 **Cheng EH**, Sheiko TV, Fisher JK, Craigen WJ, Korsmeyer SJ. VDAC2 inhibits BAK activation and mitochondrial apoptosis. *Science* 2003; **301**: 513-517
37 **Zheng JH**, Walters ET, Song XJ. Dissociation of dorsal root ganglion neurons induces hyperexcitability that is maintained by increased responsiveness to cAMP and cGMP. *J Neurophysiol* 2007; **97**: 15-25
38 **Qiu J**, Cai D, Dai H, McAtee M, Hoffman PN, Bregman BS, Filbin MT. Spinal axon regeneration induced by elevation of cyclic AMP. *Neuron* 2002; **34**: 895-903
39 **Springer JE**, Azbill RD, Nottingham SA, Kennedy SE. Calcineurin-mediated BAD dephosphorylation activates the caspase-3 apoptotic cascade in traumatic spinal cord injury. *J Neurosci* 2000; **20**: 7246-7251
40 **Afjehi-Sadat L**, Brejnikow M, Kang SU, Vishwanath V, Walder N, Herkner K, Redl H, Lubec G. Differential protein levels and post-translational modifications in spinal cord injury of the rat. *J Proteome Res* 2010; **9**: 1591-1597
41 **Indraswari F**, Wong PT, Yap E, Ng YK, Dheen ST. Upregulation of Dpysl2 and Spna2 gene expression in the rat brain after ischemic stroke. *Neurochem Int* 2009; **55**: 235-242
42 **Ramasamy S**, Singh S, Taniere P, Langman MJ, Eggo MC. Sulfide-detoxifying enzymes in the human colon are decreased in cancer and upregulated in differentiation. *Am J Physiol Gastrointest Liver Physiol* 2006; **291**: G288-G296
43 **Berkhout M**, Friederich P, van Krieken JH, Peters WH, Nagengast FM. Low detoxification capacity in the ileal pouch mucosa of patients with ulcerative colitis. *Inflamm Bowel Dis* 2006; **12**: 112-116
44 **Edalat M**, Mannervik B, Axelsson LG. Selective expression of detoxifying glutathione transferases in mouse colon: effect of experimental colitis and the presence of bacteria. *Histochem Cell Biol* 2004; **122**: 151-159
45 **Philbert MA**, Beiswanger CM, Manson MM, Green JA, Novak RF, Primiano T, Reuhl KR, Lowndes HE. Glutathione S-transferases and gamma-glutamyl transpeptidase in the rat nervous systems: a basis for differential susceptibility to neurotoxicants. *Neurotoxicology* 1995; **16**: 349-362
46 **Guo Y**, Liu Y, Xu L, Wu D, Wu H, Li CY. Reduced Nrf2 and Phase II enzymes expression in immune-mediated spinal cord motor neuron injury. *Neurol Res* 2010; **32**: 460-465
47 **Ishihara T**, Tanaka K, Tasaka Y, Namba T, Suzuki J, Ishihara T, Okamoto S, Hibi T, Takenaga M, Igarashi R, Sato K, Mizushima Y, Mizushima T. Therapeutic effect of lecithinized superoxide dismutase against colitis. *J Pharmacol Exp Ther* 2009; **328**: 152-164
48 **Yan LJ**, Thangthaeng N, Forster MJ. Changes in dihydrolipoamide dehydrogenase expression and activity during postnatal development and aging in the rat brain. *Mech Ageing Dev* 2008; **129**: 282-290
49 **Zhang Y**, Wang YH, Zhang XH, Ge HY, Arendt-Nielsen L, Shao JM, Yue SW. Proteomic analysis of differential proteins related to the neuropathic pain and neuroprotection in the dorsal root ganglion following its chronic compression in rats. *Exp Brain Res* 2008; **189**: 199-209
50 **Tao Y**, Hart J, Lichtenstein L, Joseph LJ, Ciancio MJ, Hu S, Chang EB, Bissonnette M. Inducible heat shock protein 70 prevents multifocal flat dysplastic lesions and invasive tumors in an inflammatory model of colon cancer. *Carcinogenesis* 2009; **30**: 175-182
51 **Hu S**, Ciancio MJ, Lahav M, Fujiya M, Lichtenstein L, Anant S, Musch MW, Chang EB. Translational inhibition of colonic epithelial heat shock proteins by IFN-gamma and TNF-alpha in intestinal inflammation. *Gastroenterology* 2007; **133**: 1893-1904
52 **Ludwig D**, Stahl M, Ibrahim ET, Wenzel BE, Drabicki D, Wecke A, Fellermann K, Stange EF. Enhanced intestinal expression of heat shock protein 70 in patients with inflammatory bowel diseases. *Dig Dis Sci* 1999; **44**: 1440-1447
53 **Lee JS**, Hale CM, Panorchan P, Khatau SB, George JP, Tseng Y, Stewart CL, Hodzic D, Wirtz D. Nuclear lamin A/C deficiency induces defects in cell mechanics, polarization, and migration. *Biophys J* 2007; **93**: 2542-2552
54 **Cañete-Soler R**, Reddy KS, Tolan DR, Zhai J. Aldolases a and C are ribonucleolytic components of a neuronal complex that regulates the stability of the light-neurofilament mRNA. *J Neurosci* 2005; **25**: 4353-4364
55 **Slemmer JE**, Haasdijk ED, Engel DC, Plesnila N, Weber JT. Aldolase C-positive cerebellar Purkinje cells are resistant to delayed death after cerebral trauma and AMPA-mediated excitotoxicity. *Eur J Neurosci* 2007; **26**: 649-656
56 **Hamburg RJ**, Friedman DL, Olson EN, Ma TS, Cortez MD, Goodman C, Puleo PR, Perryman MB. Muscle creatine kinase isoenzyme expression in adult human brain. *J Biol Chem* 1990; **265**: 6403-6409
57 **Hemmer W**, Zanolla E, Furter-Graves EM, Eppenberger HM, Wallimann T. Creatine kinase isoenzymes in chicken cerebellum: specific localization of brain-type creatine kinase in Bergmann glial cells and muscle-type creatine kinase in Purkinje neurons. *Eur J Neurosci* 1994; **6**: 538-549
58 **Aguilera-Aguirre L**, Bacsi A, Saavedra-Molina A, Kurosky A, Sur S, Boldogh I. Mitochondrial dysfunction increases allergic airway inflammation. *J Immunol* 2009; **183**: 5379-5387
59 **Murphy MP**. How mitochondria produce reactive oxygen species. *Biochem J* 2009; **417**: 1-13
60 **Eriksson LS**. Splanchnic exchange of glucose, amino acids and free fatty acids in patients with chronic inflammatory bowel disease. *Gut* 1983; **24**: 1161-1168
61 **Saraswathy S**, Rao NA. Mitochondrial proteomics in experimental autoimmune uveitis oxidative stress. *Invest Ophthalmol Vis Sci* 2009; **50**: 5559-5566
62 **Hart CE**, Race V, Achouri Y, Wiame E, Sharrard M, Olpin SE, Watkinson J, Bonham JR, Jaeken J, Matthijs G, Van Schaftingen E. Phosphoserine aminotransferase deficiency: a novel disorder of the serine biosynthesis pathway. *Am J Hum Genet* 2007; **80**: 931-937
63 **Neilly PJ**, Gardiner KR, Kirk SJ, Jennings G, Anderson NH, Elia M, Rowlands BJ. Endotoxaemia and cytokine production in experimental colitis. *Br J Surg* 1995; **82**: 1479-1482

64 **Natah SS**, Mouihate A, Pittman QJ, Sharkey KA. Disruption of the blood-brain barrier during TNBS colitis. *Neurogastroenterol Motil* 2005; **17**: 433-446
65 **De Schepper HU**, De Winter BY, Van Nassauw L, Timmermans JP, Herman AG, Pelckmans PA, De Man JG. TRPV1 receptors on unmyelinated C-fibres mediate colitis-induced sensitization of pelvic afferent nerve fibres in rats. *J Physiol* 2008; **586**: 5247-5258
66 **Birder LA**, Kiss S, de Groat WC, Lecci A, Maggi CA. Effect of nepadutant, a neurokinin 2 tachykinin receptor antagonist, on immediate-early gene expression after trinitrobenzenesulfonic acid-induced colitis in the rat. *J Pharmacol Exp Ther* 2003; **304**: 272-276
67 **Dantzer R**, O'Connor JC, Freund GG, Johnson RW, Kelley KW. From inflammation to sickness and depression: when the immune system subjugates the brain. *Nat Rev Neurosci* 2008; **9**: 46-56
68 **Barceló-Batllori S**, André M, Servis C, Lévy N, Takikawa O, Michetti P, Reymond M, Felley-Bosco E. Proteomic analysis of cytokine induced proteins in human intestinal epithelial cells: implications for inflammatory bowel diseases. *Proteomics* 2002; **2**: 551-560
69 **Berndt U**, Bartsch S, Philipsen L, Danese S, Wiedenmann B, Dignass AU, Hämmerle M, Sturm A. Proteomic analysis of the inflamed intestinal mucosa reveals distinctive immune response profiles in Crohn's disease and ulcerative colitis. *J Immunol* 2007; **179**: 295-304
70 **Meuwis MA**, Fillet M, Geurts P, de Seny D, Lutteri L, Chapelle JP, Bours V, Wehenkel L, Belaiche J, Malaise M, Louis E, Merville MP. Biomarker discovery for inflammatory bowel disease, using proteomic serum profiling. *Biochem Pharmacol* 2007; **73**: 1422-1433
71 **Shkoda A**, Werner T, Daniel H, Gunckel M, Rogler G, Haller D. Differential protein expression profile in the intestinal epithelium from patients with inflammatory bowel disease. *J Proteome Res* 2007; **6**: 1114-1125
72 **Nanni P**, Levander F, Roda G, Caponi A, James P, Roda A. A label-free nano-liquid chromatography-mass spectrometry approach for quantitative serum peptidomics in Crohn's disease patients. *J Chromatogr B Analyt Technol Biomed Life Sci* 2009; **877**: 3127-3136
73 **Fogt F**, Jian B, Krieg RC, Wellmann A. Proteomic analysis of mucosal preparations from patients with ulcerative colitis. *Mol Med Report* 2008; **1**: 51-54
74 **Naito Y**, Takagi T, Okada H, Omatsu T, Mizushima K, Handa O, Kokura S, Ichikawa H, Fujiwake H, Yoshikawa T. Identification of inflammation-related proteins in a murine colitis model by 2D fluorescence difference gel electrophoresis and mass spectrometry. *J Gastroenterol Hepatol* 2010; **25** Suppl 1: S144-S148

S- Editor Cheng JX **L- Editor** Ma JY **E- Editor** Zheng XM

World Journal of Gastroenterology

Online Submissions: http://www.wjgnet.com/1007-9327office
wjg@wjgnet.com
doi:10.3748/wjg.v18.i23.2929

World J Gastroenterol 2012 June 21; 18(23): 2929-2937
ISSN 1007-9327 (print) ISSN 2219-2840 (online)

ORIGINAL ARTICLE

Stem cell factor-mediated wild-type KIT receptor activation is critical for gastrointestinal stromal tumor cell growth

Chen-Guang Bai, Xiao-Wei Hou, Feng Wang, Cen Qiu, Yan Zhu, Ling Huang, Jing Zhao, Jing-Jing Xu, Da-Lie Ma

Chen-Guang Bai, Xiao-Wei Hou, Cen Qiu, Yan Zhu, Da-Lie Ma, Department of Pathology, Changhai Hospital, Second Military Medical University, Shanghai 200433, China
Feng Wang, Institute of Surgery, Changhai Hospital, Second Military Medical University, Shanghai 200433, China
Ling Huang, Jing Zhao, Jing-Jing Xu, Laboratory of Molecular Pathology, Changhai Hospital, Second Military Medical University, Shanghai 200433, China
Author contributions: Bai CG, Hou XW and Wang F contributed equally to this work; Bai CG and Ma DL designed the research; Bai CG, Hou XW, Wang F, Qiu C, Zhu Y, Huang L, Zhao J and Xu JJ performed the research; Bai CG, Hou XW and Ma DL analyzed the data; Bai CG, Hou XW and Wang F wrote the paper; Ma DL revised the manuscript.
Supported by The National Natural Science Foundation of China, No.30700809 and No.30972876
Correspondence to: Da-Lie Ma, Professor, Department of Pathology, Changhai Hospital, Second Military Medical University, 168 Changhai Road, Shanghai 200433, China. madalie@126.com
Telephone: +86-21-81873692 Fax: +86-21-81873690
Received: October 17, 2011 Revised: February 27, 2012
Accepted: March 19, 2012
Published online: June 21, 2012

Abstract

AIM: To clarify the biological role of stem cell factor (SCF)-mediated wild-type KIT receptor activation in gastrointestinal stromal tumor (GIST) growth.

METHODS: The co-expression of wild-type KIT receptor and SCF was evaluated in 51 GIST samples using mutation analysis and immunohistochemistry, and the results were correlated with clinicopathological parameters, including the mitotic count, proliferative index (Ki-67 immunohistochemical staining), mitotic index (phospho-histone H3 immunohistochemical staining) and apoptotic index (terminal deoxynucleotidyl transferase-mediated dUTP-biotin nick end labeling). Using primary cultured GIST cells, the effect of SCF-mediated wild-type KIT receptor activation was determined by western blotting, methyl thiazolyl tetrazolium (MTT), and apoptosis assays.

RESULTS: We found that wild-type KIT receptor and SCF protein were expressed in 100% and 76.5% of the 51 GIST samples, respectively, and the co-expression of wild-type KIT receptor and SCF was associated with known indicators of poor prognosis, including larger tumor size (P = 0.0118), higher mitotic count (P = 0.0058), higher proliferative index (P = 0.0012), higher mitotic index (P = 0.0282), lower apoptosis index (P = 0.0484), and increased National Institutes of Health risk level (P = 0.0012). We also found that the introduction of exogenous SCF potently increased KIT kinase activity, stimulated cell proliferation (P < 0.01) and inhibited apoptosis (P < 0.01) induced by serum starvation, while a KIT immunoblocking antibody suppressed proliferation (P = 0.01) and promoted apoptosis (P < 0.01) in cultured GIST cells.

CONCLUSION: SCF-mediated wild-type KIT receptor activation plays an important role in GIST cell growth. The inhibition of SCF-mediated wild-type KIT receptor activation may prove to be particularly important for GIST therapy.

Key words: Gastrointestinal stromal tumor; Stem cell factor; Wild-type KIT receptor; Cell growth; *In vitro*

Peer reviewer: Dina G Tiniakos, Laboratory of Histology and Embryology, Medical School, University of Athens, 75, M. Asias str, Goudi, 11527 Athens, Greece

Bai CG, Hou XW, Wang F, Qiu C, Zhu Y, Huang L, Zhao J, Xu JJ, Ma DL. Stem cell factor-mediated wild-type KIT receptor activation is critical for gastrointestinal stromal tumor cell growth. *World J Gastroenterol* 2012; 18(23): 2929-2937 Available from: URL: http://www.wjgnet.com/1007-9327/full/v18/i23/2929.htm DOI: http://dx.doi.org/10.3748/wjg.v18.i23.2929

INTRODUCTION

The KIT receptor, encoded by the oncogene *c-kit*[1], is characterised structurally by five immunoglobulin-like extracellular domains and an intracytoplasmic domain that contains an adenosine triphosphate (ATP)-binding domain and a phosphotransferase domain, which are separated by an interkinase sequence[2-5]. Under physiological conditions, the stem cell factor (SCF) binds to KIT and induces KIT homodimerisation, resulting in the phosphorylation of its tyrosine residues. The tyrosine-phosphorylated KIT receptor subsequently becomes a new docking site for signal transduction molecules and induces substrate binding and phosphorylation[6]. Thus, the interaction between SCF and the KIT receptor is essential for normal hematopoiesis, melanogenesis, gametogenesis, and the growth and differentiation of mast cells and interstitial cells of Cajal (ICCs)[7,8]. Notably, mutations in the *c-kit* gene have been implicated in neoplasms arising from these cell lineages. Oncogenic mutations in *c-kit* cause a constitutive phosphorylation of the KIT receptor that is independent of SCF binding, leading to a cascade of intracellular signalling events that contribute to the abnormal proliferation and survival of these neoplastic cells[9,10].

Gastrointestinal stromal tumors (GISTs) are the most common mesenchymal neoplasms of the gastrointestinal tract, and they are believed to originate from ICC progenitor cells[11-13]. It has also been noted that approximately 90% of GIST cases have activating mutations in either the *c-kit* or platelet-derived growth factor receptor (PDGFR) A genes[14-16]. In addition, the emerging role of SCF in *c-kit*-mutant GISTs indicates that an autocrine-paracrine loop serves as a further mechanism of wild-type KIT receptor activation[17,18].

In this study, we demonstrated the co-existence of wild-type KIT receptor and SCF in primary GISTs by analysing the entire coding sequence of *c-kit* and the protein expression of KIT and SCF in these tumors, as suggested in a previous study[19]. Based on *ex vivo* assays, we further demonstrated that SCF-mediated wild-type KIT receptor activation affected GIST growth in a dual manner by stimulating proliferation and inhibiting the apoptosis of GIST primary cells. These data suggest that the inhibition of SCF-mediated wild-type KIT receptor activation may be particularly important for GIST therapy.

MATERIALS AND METHODS

Patients

Samples from 51 consecutive patients with GISTs who underwent surgery at Changhai Hospital (Shanghai, China) between January and October 2006 were subjected to histological analysis. In addition, GIST primary cells were isolated from three fresh GIST specimens from patients who underwent surgery at Changhai Hospital in 2009. The GIST diagnosis was confirmed as previously described[20-22], and all tumors were KIT protein (CD117)-positive. No patients had received imatinib prior to the surgical resection of the tumor. Demographic data and clinical and histological features for all of the GISTs analysed in this study are summarised in Table 1.

Table 1 Correlations between the co-expression of wild-type KIT receptor and stem cell factor and clinicopathological factors in gastrointestinal stromal tumors

	Co-expression of wild-type KIT receptor and stem cell factor		
	Absent (n = 12)	Present (n = 39)	P value
Age (yr)	58.9 ± 13.2	52.8 ± 10.5	0.0524
Sex			
Male	6	18	0.8154
Female	6	21	
Tumor size (cm)	3.69 ± 1.68	6.21 ± 3.94	0.0118
Histological phenotype			
Spindle type	8	26	0.7262
Epithelioid/mixed type	4	13	
Cellularity			
Sparse	1	6	0.8000
Moderate/dense	11	33	
Tumor location			
Gastric	6	25	0.5931
Non-gastric	6	14	
Proliferative index	2.92 ± 2.23	7.21 ± 4.93	0.0012
pHH3			
≤ 5	12	24	0.0282
> 5	0	15	
Mitotic counts	3 ± 2.37	7.36 ± 6.36	0.0058
≤ 5	10	14	0.0004
> 5	2	25	
Apoptosis index	44.58 ± 19.00	32.59 ± 17.63	0.0484
c-kit mutation			
Presence	5	27	0.1659
Absence	7	12	
National Institutes of Health risk group			
Very low or low	10	10	0.0012
Intermediate or high	2	29	

The use of all human tissues was approved by the hospital's institutional committee for human research, and informed consent was obtained from all of the subjects.

Immunohistochemistry

Immunohistochemical staining was performed using the labelled streptavidin-biotin method (DAKO LSAB-2 Kit, Peroxidase, DAKO) according to the manufacturer's instructions. The following primary antibodies were used: CD117 (DAKO), Ki-67 (DAKO), SCF (Cell Signaling Technology, Inc.) and phospho-histone H3 (pHH3, Cell Signaling Technology). Parallel sections were used to examine the co-expression of KIT and SCF. For Ki-67 and pHH3, positive cells were counted in five randomised regions in the tumor component of each lesion, and the labelling index was calculated as follows: Labelling index (%) = (positive cell number/total cell number) × 100%.

In situ apoptosis

In situ apoptosis was assessed by terminal deoxynucleotidyl transferase-mediated dUTP nick-end labelling (TUNEL, Roche Diagnostics) staining, which was performed according to the manufacturer's instructions. The apoptotic index was calculated as follows: Apoptotic index (%) = (apoptotic cell number/total cell number) × 100%.

Polymerase chain reaction amplification and sequencing

Genomic DNA was extracted from cryopreserved (n = 51) or fresh (n = 3) specimens using a commercial kit (BBI, Canada). Next, *c-kit* exons 9, 11, 13, 14 and 17, as well as PDGFRA exons 12 and 18, were amplified using the following primer sequences and annealing temperatures (designed): *c-kit* exon 9 (5'TTTATTTTCCTAGAGTAAGCCAGGG-3' and 5'-ATCATGACTGATATGGTAGACAGAGC-3', at 56 ℃), *c-kit* exon 11 (5'-ATTATTAAAAGGTGAT CTATTTTT-3' and 5'-ACTGTTATGTGTACCCAAAAAG-3', at 60 ℃), *c-kit* exon 13 (5'-CACCATCACCACTTACTTGTTGTCT-3' and 5'-GACAGACAAT AAAAGGCAGCTTGGAC-3', at 67 ℃), *c-kit* exon 14 (5'-TCTCACCTTC TTTCTAACCTTTTC-3' and 5'-AACCCTTATGACCCCATGAA-3', at 54 ℃), *c-kit* exon 17 (5'GAACATCATTCAAGGCGTACTTTTG-3' and 5'-TTGAAA CTAAAAATCCTTTGCAGGAC-3', at 65 ℃), PDGFRA exon 12 (5'-CTCTGGTGCACTGGGACTTT-3' and 5'-GCAAGGGAAAAGGGAGTCT T-3', at 60 ℃), and PDGFRA exon 18 (5'-ATGGCTTGATCCTGAGTCATT-3' and 5'-GTGTGGGAAGTGTGGACG-3', at 60 ℃). Gene mutations were analysed through the direct sequencing of uncloned polymerase chain reaction (PCR) fragments. Samples that appeared to contain mutations were further examined for the presence of the wild-type *c-kit* gene by subcloning the purified PCR products using a TA cloning vector system (Stratagene, CA). Five independent subclones from each PCR were sequenced.

Cell isolation and short-term primary cell culture

GIST primary cells were isolated and cultured as described in the literature with minor modifications[23]. The nonnecrotic tissue was separated from fresh GIST samples and finely minced with curved scissors. The minced tissue was homogenised by being passed through a 15-gauge needle with a syringe five times and subsequently being passed through a stainless steel mesh (200 wires/inch). The cells were counted with a haemocytometer, and cell viability was determined by propidium iodide staining.

After centrifugation in phosphate buffered solution (PBS) at 4 ℃, cell pellets were resuspended in 1640 RPMI medium supplemented with 20% heat-inactivated foetal bovine serum (FBS), 1.0 mmol/L nonessential amino acids, 1.0 mmol/L sodium pyruvate, and 0.5 mmol/L 3-isobutyl-1- methylxanthine to inhibit fibroblast growth. Medium changes were performed at 24 h after seeding and every two or three days before cell analysis.

Enzyme-linked immunosorbent assay for stem cell factor production

For the measurement of SCF production, the concentration of GIST primary cells was adjusted to 5×10^6 cells/mL, and the supernatants were collected 24 h later. Samples were stored at -80 ℃ for further analysis. SCF concentration was determined by enzyme-linked immunosorbent assay (ELISA) using 96-well plates coated with catching antibody (diluted to 5 μg/mL in PBS, 100 μL/well) at 4 ℃ overnight according to the manufacturer's instructions.

Western blotting

Protein extracts were separated by sodium dodecyl sulphate-polyacrylamide gel electrophoresis, transferred to nitrocellulose membranes, and incubated with a specific antibody to demonstrate protein loading. Anti-phospho-KIT (pY703) antibody was purchased from Abcam (United Kingdom). Glyceraldehyde-3-phosphate dehydrogenase mouse monoclonal antibody (Santa Cruz Biotechnology) was used as an internal control. To examine the effects of exogenous SCF on KIT phosphorylation, GIST primary cells were incubated overnight with medium containing 0.5% FBS. Cells were subsequently stimulated with various concentrations of SCF for 15 min, and phospho-KIT was examined as described above.

In vitro proliferation assay

Cell proliferation was determined using a methyl thiazolyl tetrazolium (MTT) assay (Roche, United States) according to the manufacturer's instructions. In brief, GIST primary cells were seeded at a density of 8×10^3 cells/100 μL into 96-well plates and allowed to adhere. After 24 h, the original media were replaced with fresh media containing various concentrations of SCF (PeproTech, United States) or KIT immunoblocking antibody (Sigma, United States) with 0.5% FBS. After 48 h of incubation, MTT was added to each well. The quantity of the formazan product measured at 572 nm was directly proportional to the number of live cells in the culture.

Flow cytometric analysis of apoptosis

GIST primary cells were subjected to serum withdrawal for 12 h in the presence or absence of exogenous SCF or KIT immunoblocking antibody to induce apoptosis. Subsequently, apoptosis was detected using an annexin V-fluorescein isothiocyanate staining kit (R and D Systems). The apoptotic index was reported as the percentage of annexin V-positive cells in the early and late stages of apoptosis.

Statistical analysis

Data are expressed as the mean ± SD or the median and 25th and 75th percentiles [median (Q1, Q3)] for continuous variables and as percentages for categorical variables. Continuous variables were compared using Student's t test or the Wilcoxon rank sum test for nonnormally distributed data. Correlations between categorical and continuous variables were assessed using the χ^2 or Fisher's exact test and t test, respectively. P values of less than 0.05 were considered to be significant. All analysis were performed with SPSS version 17.0 (SPSS, Chicago, IL).

RESULTS

Tumor genotypes

All 51 cryopreserved specimens were screened for mutations in the *c-kit* gene. Overall, 32 of 51 (62.7%) tumors

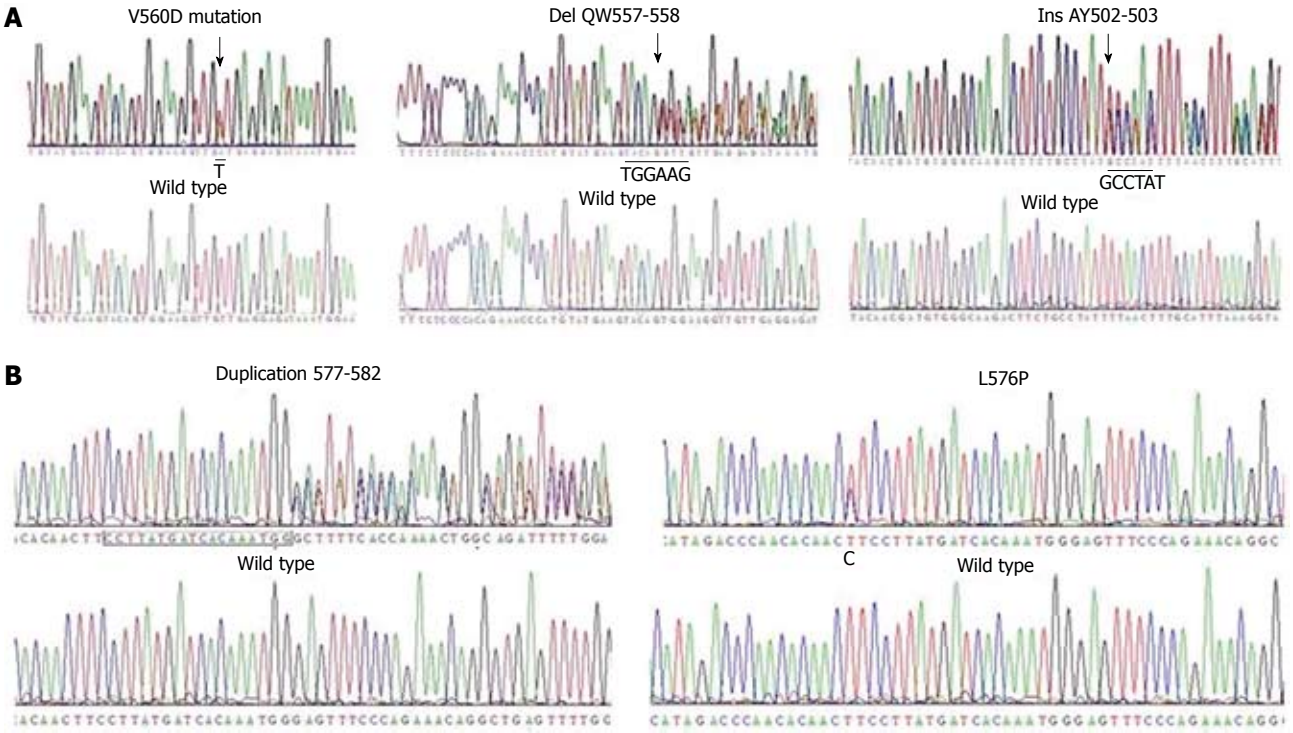

Figure 1 Heterozygous *c-kit* mutations in primary gastrointestinal stromal tumors. The mutant nucleotide sequence is indicated in the upper diagram, and the wild-type nucleotide sequence is indicated in the lower diagram. Nucleotide changes are shown in red capital letters. A: Cryopreserved specimens; B: Fresh specimens.

harboured *c-kit* mutations. Among the GISTs with *c-kit* mutations, 27 (52.9%) had mutations in exon 11 of *c-kit,* five had mutations in exon 9 (Figure 1), and none had mutations in exon 13, 14 or 17. The amino acid changes observed in the 27 tumors with exon 11 mutations were as follows: deletion in 16 (59.3%) tumors, substitution in 7 (25.9%), both deletion and substitution in 2 (7.4%), insertion in 1 (3.7%), and duplication in 1 (3.7%). Five cases harboured exon 9 *c-kit* mutations, including in-frame insertions (3 tumors; 60.0%) and missense mutations (2 tumors; 40%). GISTs without *c-kit* mutations were further examined for PDGFRA mutations; only four (7.8%) tumors harboured substitution mutations in PDGFRA exon 18. All *c-kit* mutations were heterozygous, as indicated by the presence of a wild-type *c-kit* allele in the nucleotide sequence (Figure 1A).

In the three fresh specimens analysed in this experiment, sequencing showed that GIST1 and GIST3 each harboured heterozygous *c-kit* exon 11 mutations, while GIST2 had no mutations in either *c-kit* or PDGFRA (Figure 1B).

Expression of stem cell factor in primary GISTS

The immunohistochemistry experiments shown in Figure 2 demonstrated that SCF expression was observed in both GIST cells and fibroblasts, while KIT and SCF were co-expressed in tumor cells. Given that GISTs contains only a small number of fibroblasts, a specimen was considered "positive" for SCF expression if only the tumor cells showed distinct cytoplasmic or membrane staining; otherwise, the specimen was considered "negative" for SCF expression. SCF protein was present in 39 (76.5%) of the 51 GIST samples. A morphometric study revealed more pHH3 and Ki-67 positive cells and lower apoptotic cells in SCF-positive GIST cases compared with SCF-negative GIST cases (Figure 2). These results suggest that SCF may participate in an autocrine-paracrine stimulatory loop within primary GISTs.

Correlations between SCF and clinicopathological variables

As shown in Table 1, the co-expression of wild-type KIT receptor and SCF was associated with known prognostic variables, including larger tumor size ($P = 0.0118$), higher mitotic count ($P = 0.0058$), higher proliferative index ($P = 0.0012$), higher mitotic index ($P = 0.0282$), lower apoptosis index ($P = 0.0484$), and an increased NIH risk level ($P = 0.0012$). These results suggest that the SCF-mediated activation of wild-type KIT may play an important role in tumor cell growth by directly promoting cell proliferation and inhibiting apoptosis. The co-expression of the wild-type KIT receptor and SCF was not associated with any other variable tested, including patient's age, sex, histological phenotype, cellularity, tumor location and *c-kit* gene mutation.

KIT activation in primary GISTS

In line with other published findings[24,25], KIT was phosphorylated at tyrosine 703 in 74.5% (38/51) of GISTs (Figure 3A), although the levels of phosphorylated KIT varied substantially from tumor to tumor, even between those with identical *c-kit* gene mutations.

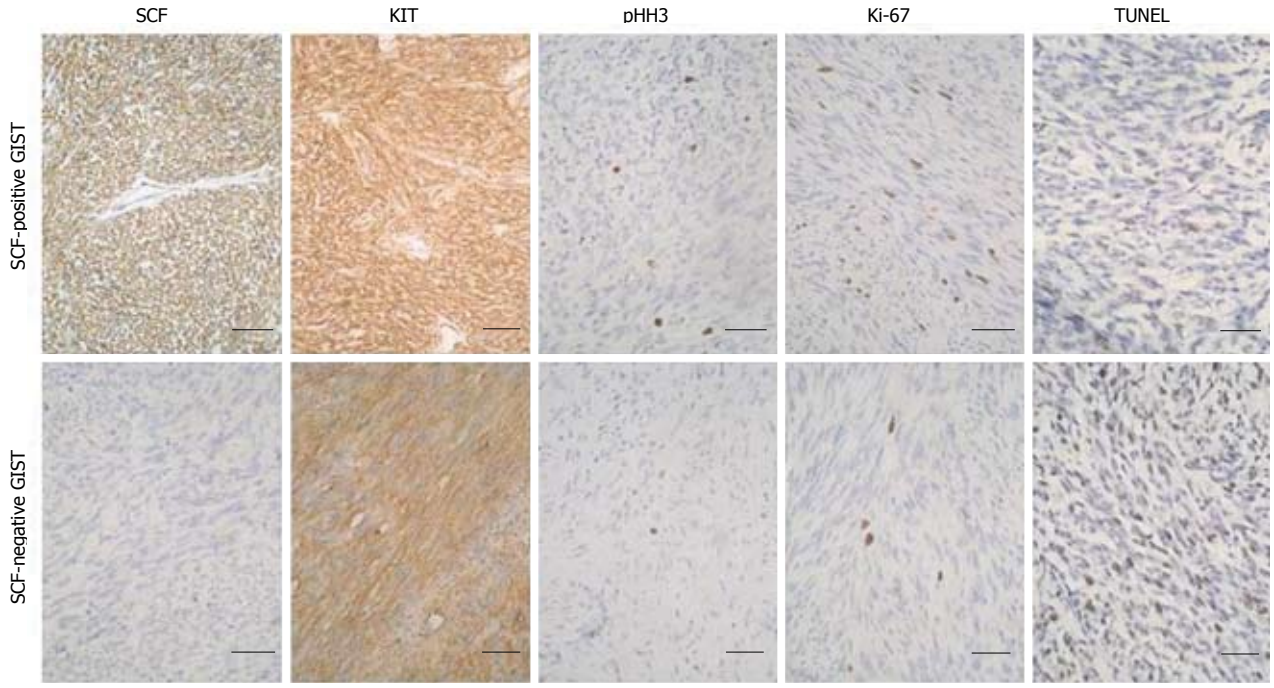

Figure 2 The expression of stem cell factor in primary gastrointestinal stromal tumors. Sections of gastrointestinal stromal tumors (GISTs) (n = 51) were immunostained with stem cell factor (SCF), KIT (CD117), pHH3 and Ki-67 antibodies (magnification, ×200). Apoptosis was assessed *in situ* by terminal deoxynucleotidyl transferase-mediated dUTP-biotin nick end labeling (TUNEL) staining (magnification, ×200). Representative images are shown. Bar = 50 μm.

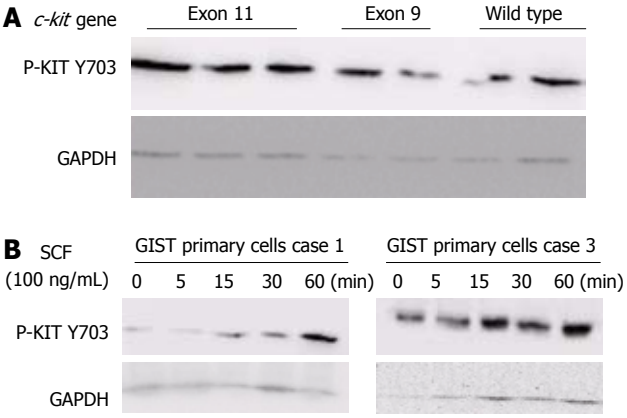

Figure 3 Western blotting analysis of phosphorylated KIT. A: KIT phosphorylation (p-KIT Y703) was analysed in gastrointestinal stromal tumor (GIST) samples (n = 51). A representative western blotting of p-KIT Y703 (top) and glyceraldehyde 3-phosphate dehydrogenase (GAPDH) (bottom) in patients with exon 11 or 9 mutations or wild-type c-kit-bearing tumors; B: GIST primary cells were incubated with 100 ng/mL stem cell factor (SCF) for the indicated times. KIT phosphorylation (p-KIT Y703) was analysed by western blotting.

Furthermore, KIT phosphorylation was not significantly associated with the presence of *c-kit* mutations (P = 0.6625). Thirteen tumors without detectable *c-kit* mutations showed strong KIT phosphorylation, which was consistent with a nonmutational mechanism of KIT activation.

To determine whether the KIT receptor was activated due to the presence of the wild-type KIT receptor in *c-kit*-mutant GISTs, we cultivated GIST primary cells in the presence of various concentrations of exogenous SCF. KIT was rapidly phosphorylated in response to exogenous SCF in a time-dependent manner in GIST primary cells (Figure 3B). These findings suggest that the hyperphosphorylation of the wild-type KIT receptor was induced by exogenous SCF, confirming that SCF mediated the activation of the wild-type KIT receptor in *c-kit*-mutant GISTs.

Effects of wild-type KIT receptor activation on proliferation in GIST primary cells

To assess whether SCF-mediated wild-type KIT activation participated in the proliferation of GIST tumor cells, we analysed the proliferation rate of GIST primary cells exposed to exogenous SCF. Consistent with the finding that SCF induced KIT phosphorylation, exogenous SCF significantly increased cell proliferation in a dose-dependent manner after 72 h of treatment (Figure 4A).

The ELISA results showed that all three primary cell lines produced significant amounts of SCF (3.5 ± 2.33 pg/mL per 10^6 cells). Therefore, we examined the effect of SCF-mediated wild-type KIT activation on cell proliferation by inhibiting the interactions between the KIT receptor and endogenous SCF. As shown in Figure 4B, cell proliferation was significantly inhibited (by > 50%) after 72 h of treatment with a KIT immunoblocking antibody, suggesting that SCF-mediated wild-type KIT receptor activation plays a key role in controlling GIST cell proliferation through the SCF/KIT autocrine-paracrine loop.

Effects of wild-type KIT receptor activation on apoptosis in GIST primary cells

The capacity to regulate survival is an important feature of tumor cells. Therefore, we tested whether wild-type

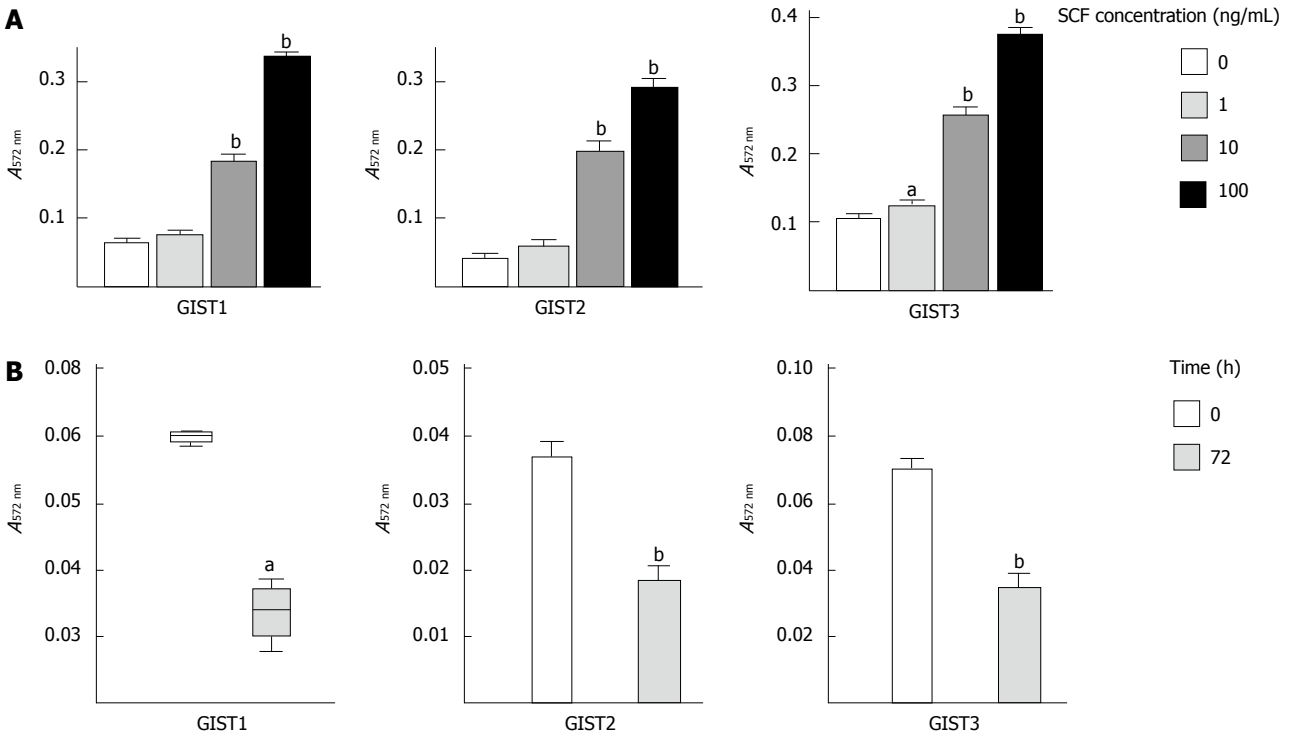

Figure 4 Stem cell factor stimulates gastrointestinal stromal tumors cell proliferation *in vitro*. Gastrointestinal stromal tumor (GIST) primary cells were incubated for 72 h with exogenous stem cell factor (SCF) (0-100 ng/mL, A) or KIT immunoblocking antibody (100 ng/mL, B), cell proliferation was analysed by methyl thiazolyl tetrazolium assay. The data are presented as the mean ± SD (n = 4 for each). $^{a}P < 0.05$, $^{b}P < 0.01$ *vs* untreated cells.

KIT receptor activation could rescue GIST primary cells from serum deprivation-induced death. As shown in Figure 5, the addition of exogenous SCF (100 ng/mL, 12 h) significantly reduced the percentage of apoptotic cells, from 32.05% ± 2.65% to 18.55% ± 1.83% ($P < 0.01$) in GIST primary cells. In contrast, treatment with KIT immunoblocking antibody significantly increased the percentage of apoptotic cells from 32.05% ± 2.65% to 43.58% ± 2.94% ($P < 0.01$).

DISCUSSION

The present study showed that *c-kit* gene mutations occurred in 32 (62.7%) of the 51 GIST clinical samples, which is consistent with previous results[14-16]. All of these mutations were heterozygous, i.e., at least one wild-type *c-kit* allele was present in all tumors, which is consistent with a previous report that most GIST mutations were heterozygous[26]. The heterozygous nature of the receptor status in GISTs suggests that KIT receptor activation is not induced by *c-kit* gene mutations alone but rather by other mechanisms, such as the activation of ligand-dependent signal transduction pathways. Indeed, we noted that KIT activation, as manifested by receptor tyrosine phosphorylation, is a general phenomenon in GISTs, even those without *c-kit* mutations.

Constitutive receptor tyrosine kinase activation is believed to be important for tumor proliferation and progression, and in GISTs, KIT activation can serve as an initiating event in oncogenesis[27-29]. However, the results obtained in our study showed that SCF expression was positively correlated with mitotic activity. KIT was rapidly phosphorylated upon stimulation with exogenous SCF, suggesting that ligand-dependent hyperactivation is also a strong mitogen in GIST cells. This observation is consistent with the data reported by Hirano *et al*[18], who found that SCF-positive GIST cases had a significantly higher average MIB-1 labelling index and a larger average tumor size than did the SCF-negative cases. Similarly, Théou-Anton *et al*[17] detected SCF in up to 93% of the GISTs studied and speculated that KIT activation in GISTs may be caused partly by the presence of SCF within the tumors. However, no *in vitro* measurements were conducted in either of these two studies, and the possible role of SCF-mediated wild-type KIT receptor activation in GIST proliferation should be explored *in vitro* to assess its independent contribution to cell growth. Accordingly, we further examined the mitogenic activity of this molecule on GIST primary cells harbouring a heterozygous c-kit mutation. It was found that exogenous SCF markedly stimulated cell proliferation and KIT phosphorylation in all GIST primary cells, while the inhibition of the SCF/KIT interaction reduced cell proliferation, confirming that exogenous or endogenous SCF-mediated activation of wild-type KIT provided an important signal for GIST cell proliferation. Further, GIST882, which has a homozygous activating *c-kit* mutation[30], did not exhibit increased proliferation in response to supplemental SCF, and the exogenous SCF stimulation of GIST544 cells, which express a heterozy-

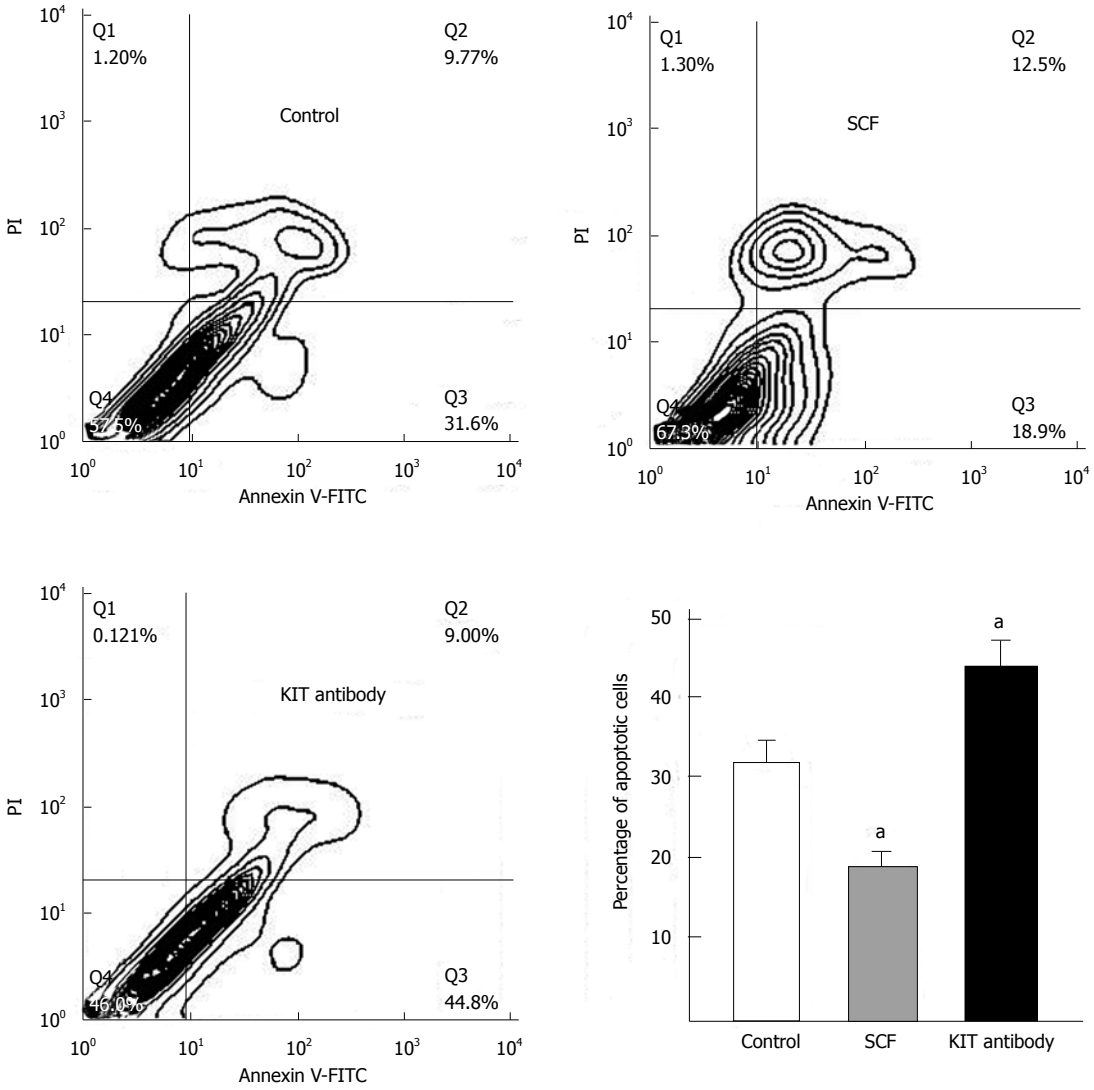

Figure 5 Stem cell factor inhibits gastrointestinal stromal tumor cell apoptosis *in vitro*. Representative flow cytometric contour of annexin V-fluorescein isothiocyanate (FITC)/propidium iodide (PI) dual-colour flow cytometry after 12 h of treatment with exogenous stem cell factor (SCF) or KIT immunoblocking antibody. The lower right quadrant represents early apoptotic cells. The data are presented as the mean ± SD (n = 4 for each). $^{a}P < 0.01$ *vs* untreated cells.

gous *c-kit* mutation, induces stronger KIT phosphorylation and cell growth[31]; these observations further validate our results.

Apoptosis is an active process that plays a key role in the development and maintenance of tissue homeostasis. The tumor growth rate partly depends on an excess of proliferation over apoptosis[32]. Indeed, the relationship between SCF-mediated wild-type KIT receptor activation and apoptosis has been explored extensively. For example, *c-kit* activation was found to suppress the apoptosis of normal murine melanocyte precursors[33], soft tissue sarcomas of neuroectodermal origin[34], neuroblastomas[35], and normal and malignant human haematopoietic cells[36]. Our results also support a role for SCF mediated wild-type KIT receptor activation in the survival of GIST primary cells because exogenous SCF rescues GIST primary cells from serum deprivation-induced death and may consequently prolong cell survival, while blocking the interactions between KIT receptor and endogenous SCF markedly reduces the viability of these cells.

In summary, our results demonstrated that the SCF-dependent activation of the wild-type KIT receptor is specifically involved in promoting the cell growth of GISTs *via* autocrine-paracrine loop activation. Therefore, drugs targeted against GISTs should switch off the activation of both mutant and wild-type receptors to achieve an effective response.

COMMENTS

Background

Gastrointestinal stromal tumor (GIST) is the most common sarcoma of the intestinal tract. Imatinib has shown remarkable efficacy in the treatment of GISTs, which are notoriously refractory to conventional chemotherapy or radiation. However, a considerable proportion of GIST patients show primary or acquired resistance to Imatinib.

Innovations and breakthroughs

In this study, the authors showed that the co-expression of the wild-type KIT receptor and stem cell factor (SCF) was associated with known prognostic variables in a series of 51 patients. Authors further demonstrated that SCF-

mediated wild-type KIT receptor activation participated in GIST growth by stimulating the proliferation and inhibiting the apoptosis of GIST primary cells. These results suggest that SCF-mediated wild-type KIT receptor activation represents a new and potentially promising target for GIST therapy. Therefore, to achieve an effective response, drugs targeted against GISTs should switch off the activation of both mutant and wild-type receptors.

Applications

The study demonstrated that the SCF-dependent activation of the wild-type KIT receptor is specifically involved in promoting the cell growth of GISTs *via* autocrine-paracrine loop activation. Therefore, drugs that target wild-type receptor activation may be viable candidates for the treatment of GISTs and should be explored in future studies.

Peer review

This is a well written manuscript. The use of confocal microscopy would have been ideal for studying both KIT and SCF expression.

REFERENCES

1 **Yarden Y**, Kuang WJ, Yang-Feng T, Coussens L, Munemitsu S, Dull TJ, Chen E, Schlessinger J, Francke U, Ullrich A. Human proto-oncogene c-kit: a new cell surface receptor tyrosine kinase for an unidentified ligand. *EMBO J* 1987; **6**: 3341-3351

2 **Anderson DM**, Lyman SD, Baird A, Wignall JM, Eisenman J, Rauch C, March CJ, Boswell HS, Gimpel SD, Cosman D. Molecular cloning of mast cell growth factor, a hematopoietin that is active in both membrane bound and soluble forms. *Cell* 1990; **63**: 235-243

3 **Flanagan JG**, Leder P. The kit ligand: a cell surface molecule altered in steel mutant fibroblasts. *Cell* 1990; **63**: 185-194

4 **Martin FH**, Suggs SV, Langley KE, Lu HS, Ting J, Okino KH, Morris CF, McNiece IK, Jacobsen FW, Mendiaz EA. Primary structure and functional expression of rat and human stem cell factor DNAs. *Cell* 1990; **63**: 203-211

5 **Zsebo KM**, Williams DA, Geissler EN, Broudy VC, Martin FH, Atkins HL, Hsu RY, Birkett NC, Okino KH, Murdock DC. Stem cell factor is encoded at the Sl locus of the mouse and is the ligand for the c-kit tyrosine kinase receptor. *Cell* 1990; **63**: 213-224

6 **Blechman JM**, Lev S, Givol D, Yarden Y. Structure-function analyses of the kit receptor for the steel factor. *Stem Cells* 1993; **11** Suppl 2: 12-21

7 **Fleischman RA**. From white spots to stem cells: the role of the Kit receptor in mammalian development. *Trends Genet* 1993; **9**: 285-290

8 **Huizinga JD**, Thuneberg L, Klüppel M, Malysz J, Mikkelsen HB, Bernstein A. W/kit gene required for interstitial cells of Cajal and for intestinal pacemaker activity. *Nature* 1995; **373**: 347-349

9 **Boissan M**, Feger F, Guillosson JJ, Arock M. c-Kit and c-kit mutations in mastocytosis and other hematological diseases. *J Leukoc Biol* 2000; **67**: 135-148

10 **Testa U**. Membrane Tyrosine Kinase Receptors are an Important Target for the Therapy of Acute Myeloid Leukemia. *Current Cancer Therapy Reviews* 2008; **4**: 31-49

11 **Sircar K**, Hewlett BR, Huizinga JD, Chorneyko K, Berezin I, Riddell RH. Interstitial cells of Cajal as precursors of gastrointestinal stromal tumors. *Am J Surg Pathol* 1999; **23**: 377-389

12 **Miettinen M**, Lasota J. Gastrointestinal stromal tumors: review on morphology, molecular pathology, prognosis, and differential diagnosis. *Arch Pathol Lab Med* 2006; **130**: 1466-1478

13 **Kindblom LG**, Remotti HE, Aldenborg F, Meis-Kindblom JM. Gastrointestinal pacemaker cell tumor (GIPACT): gastrointestinal stromal tumors show phenotypic characteristics of the interstitial cells of Cajal. *Am J Pathol* 1998; **152**: 1259-1269

14 **Hirota S**, Ohashi A, Nishida T, Isozaki K, Kinoshita K, Shinomura Y, Kitamura Y. Gain-of-function mutations of platelet-derived growth factor receptor alpha gene in gastrointestinal stromal tumors. *Gastroenterology* 2003; **125**: 660-667

15 **Antonescu CR**, Sommer G, Sarran L, Tschernyavsky SJ, Riedel E, Woodruff JM, Robson M, Maki R, Brennan MF, Ladanyi M, DeMatteo RP, Besmer P. Association of KIT exon 9 mutations with nongastric primary site and aggressive behavior: KIT mutation analysis and clinical correlates of 120 gastrointestinal stromal tumors. *Clin Cancer Res* 2003; **9**: 3329-3337

16 **Rubin BP**, Heinrich MC, Corless CL. Gastrointestinal stromal tumour. *Lancet* 2007; **369**: 1731-1741

17 **Théou-Anton N**, Tabone S, Brouty-Boyé D, Saffroy R, Ronnstrand L, Lemoine A, Emile JF. Co expression of SCF and KIT in gastrointestinal stromal tumours (GISTs) suggests an autocrine/paracrine mechanism. *Br J Cancer* 2006; **94**: 1180-1185

18 **Hirano K**, Shishido-Hara Y, Kitazawa A, Kojima K, Sumiishi A, Umino M, Kikuchi F, Sakamoto A, Fujioka Y, Kamma H. Expression of stem cell factor (SCF), a KIT ligand, in gastrointestinal stromal tumors (GISTs): a potential marker for tumor proliferation. *Pathol Res Pract* 2008; **204**: 799-807

19 **Tamborini E**, Bonadiman L, Negri T, Greco A, Staurengo S, Bidoli P, Pastorino U, Pierotti MA, Pilotti S. Detection of overexpressed and phosphorylated wild-type kit receptor in surgical specimens of small cell lung cancer. *Clin Cancer Res* 2004; **10**: 8214-8219

20 **West RB**, Corless CL, Chen X, Rubin BP, Subramanian S, Montgomery K, Zhu S, Ball CA, Nielsen TO, Patel R, Goldblum JR, Brown PO, Heinrich MC, van de Rijn M. The novel marker, DOG1, is expressed ubiquitously in gastrointestinal stromal tumors irrespective of KIT or PDGFRA mutation status. *Am J Pathol* 2004; **165**: 107-113

21 **Rubin BP**. Gastrointestinal stromal tumours: an update. *Histopathology* 2006; **48**: 83-96

22 **Fletcher CD**, Berman JJ, Corless C, Gorstein F, Lasota J, Longley BJ, Miettinen M, O'Leary TJ, Remotti H, Rubin BP, Shmookler B, Sobin LH, Weiss SW. Diagnosis of gastrointestinal stromal tumors: A consensus approach. *Hum Pathol* 2002; **33**: 459-465

23 **Prenen H**, Cools J, Mentens N, Folens C, Sciot R, Schöffski P, Van Oosterom A, Marynen P, Debiec-Rychter M. Efficacy of the kinase inhibitor SU11248 against gastrointestinal stromal tumor mutants refractory to imatinib mesylate. *Clin Cancer Res* 2006; **12**: 2622-2627

24 **Janeway KA**, Liegl B, Harlow A, Le C, Perez-Atayde A, Kozakewich H, Corless CL, Heinrich MC, Fletcher JA. Pediatric KIT wild-type and platelet-derived growth factor receptor alpha-wild-type gastrointestinal stromal tumors share KIT activation but not mechanisms of genetic progression with adult gastrointestinal stromal tumors. *Cancer Res* 2007; **67**: 9084-9088

25 **Rubin BP**, Singer S, Tsao C, Duensing A, Lux ML, Ruiz R, Hibbard MK, Chen CJ, Xiao S, Tuveson DA, Demetri GD, Fletcher CD, Fletcher JA. KIT activation is a ubiquitous feature of gastrointestinal stromal tumors. *Cancer Res* 2001; **61**: 8118-8121

26 **Théou N**, Tabone S, Saffroy R, Le Cesne A, Julié C, Cortez A, Lavergne-Slove A, Debuire B, Lemoine A, Emile JF. High expression of both mutant and wild-type alleles of c-kit in gastrointestinal stromal tumors. *Biochim Biophys Acta* 2004; **1688**: 250-256

27 **Nishida T**, Hirota S, Taniguchi M, Hashimoto K, Isozaki K, Nakamura H, Kanakura Y, Tanaka T, Takabayashi A, Matsuda H, Kitamura Y. Familial gastrointestinal stromal tumours with germline mutation of the KIT gene. *Nat Genet* 1998; **19**: 323-324

28 **Maeyama H**, Hidaka E, Ota H, Minami S, Kajiyama M, Kuraishi A, Mori H, Matsuda Y, Wada S, Sodeyama H, Nakata S, Kawamura N, Hata S, Watanabe M, Iijima Y, Katsuyama T. Familial gastrointestinal stromal tumor with

hyperpigmentation: association with a germline mutation of the c-kit gene. *Gastroenterology* 2001; **120**: 210-215
29 **Corless CL**, McGreevey L, Haley A, Town A, Heinrich MC. KIT mutations are common in incidental gastrointestinal stromal tumors one centimeter or less in size. *Am J Pathol* 2002; **160**: 1567-1572
30 **Lux ML**, Rubin BP, Biase TL, Chen CJ, Maclure T, Demetri G, Xiao S, Singer S, Fletcher CD, Fletcher JA. KIT extracellular and kinase domain mutations in gastrointestinal stromal tumors. *Am J Pathol* 2000; **156**: 791-795
31 **Duensing A**, Medeiros F, McConarty B, Joseph NE, Panigrahy D, Singer S, Fletcher CD, Demetri GD, Fletcher JA. Mechanisms of oncogenic KIT signal transduction in primary gastrointestinal stromal tumors (GISTs). *Oncogene* 2004; **23**: 3999-4006
32 **Henson PM**, Hume DA. Apoptotic cell removal in development and tissue homeostasis. *Trends Immunol* 2006; **27**: 244-250
33 **Ito M**, Kawa Y, Ono H, Okura M, Baba T, Kubota Y, Nishikawa SI, Mizoguchi M. Removal of stem cell factor or addition of monoclonal anti-c-KIT antibody induces apoptosis in murine melanocyte precursors. *J Invest Dermatol* 1999; **112**: 796-801
34 **Ricotti E**, Fagioli F, Garelli E, Linari C, Crescenzio N, Horenstein AL, Pistamiglio P, Vai S, Berger M, di Montezemolo LC, Madon E, Basso G. c-kit is expressed in soft tissue sarcoma of neuroectodermic origin and its ligand prevents apoptosis of neoplastic cells. *Blood* 1998; **91**: 2397-2405
35 **Timeus F**, Crescenzio N, Valle P, Pistamiglio P, Piglione M, Garelli E, Ricotti E, Rocchi P, Strippoli P, Cordero di Montezemolo L, Madon E, Ramenghi U, Basso G. Stem cell factor suppresses apoptosis in neuroblastoma cell lines. *Exp Hematol* 1997; **25**: 1253-1260
36 **Hassan HT**, Zander A. Stem cell factor as a survival and growth factor in human normal and malignant hematopoiesis. *Acta Haematol* 1996; **95**: 257-262

S- Editor Gou SX **L- Editor** A **E- Editor** Li JY

World Journal of Gastroenterology

Online Submissions: http://www.wjgnet.com/1007-9327office
wjg@wjgnet.com
doi:10.3748/wjg.v18.i23.2938

World J Gastroenterol 2012 June 21; 18(23): 2938-2947
ISSN 1007-9327 (print) ISSN 2219-2840 (online)

ORIGINAL ARTICLE

Hepatocellular carcinoma and macrophage interaction induced tumor immunosuppression *via* Treg requires TLR4 signaling

Jing Yang, Jin-Xiang Zhang, Hui Wang, Guo-Liang Wang, Qing-Gang Hu, Qi-Chang Zheng

Jing Yang, Qing-Gang Hu, Qi-Chang Zheng, Department of Hepatobiliary Surgery, Union Hospital of Tongji Medical College, Huazhong University of Science and Technology, Wuhan 430022, Hubei Province, China
Jin-Xiang Zhang, Guo-Liang Wang, Department of Emergency Surgery, Union Hospital of Tongji Medical College, Huazhong University of Science and Technology, Wuhan 430022, Hubei Province, China
Hui Wang, Department of Medical Genetics, Tongji Medical College, Huazhong University of Science and Technology, Wuhan 430030, Hubei Province, China
Author contributions: Yang J, Zhang JX and Wang GL performed the majority of experiments; Zhang JX, Wang H and Zheng QC provided vital reagents and analytical tools and revised the manuscript; Yang J and Hu QG collected the human materials and provided financial support for this work; Yang J designed the study and wrote the manuscript.
Correspondence to: Qi-Chang Zheng, Professor, Department of Hepatobiliary Surgery, Union Hospital of Tongji Medical College, Huazhong University of Science and Technology, Wuhan 430022, Hubei Province, China. qc_zheng@mail.hust.edu.cn
Telephone: +86-27-62900023 Fax: +86-27-62900023
Received: May 13, 2011 Revised: March 26, 2012
Accepted: April 2, 2012
Published online: June 21, 2012

Abstract

AIM: To investigated the interaction between toll-like receptor 4 (TLR4)-activated hepatoma cells and macrophages in the induction of tumor-immune suppression mediated by CD4+CD25^{high} family of transcription factor P3 (FOXP3) regulatory T cells (Tregs).

METHODS: The proportion of FOXP3+ Tregs was identified in peripheral blood and tumor tissues of 60 hepatocellular carcinoma (HCC) patients. TLR4 expression was examined in tumor tissues and cell lines. The correlation was examined between FOXP3+ Tregs in peripheral blood and TLR4 expression of HCC tissues. Following activation of TLR4 in H22 murine hepatoma cells pre-incubated with lipopolysaccharide (LPS) and co-cultured with macrophage cell line RAW246.7, the synthesis of cytokines tumor necrosis factor-α, CCL22, and interleukin (IL)-10 by the two cell lines was detected and analyzed.

RESULTS: FOXP3+ Tregs were enriched in tumor sites, and circulating FOXP3+ Tregs were increased in HCC patients in correlation with multiple tumor foci and up-regulated TLR4 expression in HCC tissues. Semi-quantitative analysis indicated that TLR4 was over-expressed in HCC compared with the matched normal tissues. Cell cultivation experiments indicated that the mRNAs of IL-10 and CCL22 were significantly up-regulated in the RAW246.7 cell line when co-cultured with LPS pre-incubated H22 cells.

CONCLUSION: In hepatoma cell lines, TLR4 may indirectly facilitate the recruitment of Tregs to the tumor site and promote intrahepatic metastasis through its interaction with macrophages.

Key words: CD4+CD25^{high}FOXP3+ regulatory T cell; Toll-like receptor; Tumor immunity; Hepatocellular carcinoma; Macrophage

Peer reviewer: Dr. Fabrizio Montecucco, Internal Medicine, University of Geneva, avenue de la Roseraie, 64, 1211 Geneva, Switzerland

Yang J, Zhang JX, Wang H, Wang GL, Hu QG, Zheng QC. Hepatocellular carcinoma and macrophage interaction induced tumor immunosuppression *via* Treg requires TLR4 signaling. *World J Gastroenterol* 2012; 18(23): 2938-2947 Available from: URL: http://www.wjgnet.com/1007-9327/full/v18/i23/2938.htm DOI: http://dx.doi.org/10.3748/wjg.v18.i23.2938

INTRODUCTION

Hepatocellular carcinoma (HCC) is the fifth most com-

mon cancer worldwide, and is the third most common cause of cancer related deaths[1]. Previous studies have demonstrated that the majority of HCC patients develop tumor-specific immune responses; however, in most patients, tumors progress despite tumor-specific humoral and cellular immune responses. These findings imply that HCC escapes the anti-tumor immune response through various strategies.

Recently, many studies have suggested that the tumor microenvironment plays an important role in the establishment and progression of tumors. Lymphocytes contribute to the tumor microenvironment through immunity and inflammation. Through diverse strategies, tumor cells play an important role in the suppression of anti-tumor immunity in the surrounding microenvironment *via* interactions with infiltrated immune cells or macrophages, which in turn potentially facilitates growth of the tumor itself. Moreover, induction of the differentiation and/or recruitment of regulatory T cells (Tregs), a unique population of CD4+ T cells, potentially comprises one of the key mechanisms. Tregs are defined based on their expression of CD4, CD25 and forkhead, or winged helix family of transcription factor P3 (FOXP3), which is critical for the development and function of Tregs in mice and humans[2]. Tregs play a critical role in immunologic self-tolerance and suppression in the tumor immune response[3,4]. Early evidence indicates that Tregs (not FOXP3+ T cells but CD4+CD25+ T cells) are increased in patients with various types of cancer[5-7]. It is hypothesized that their systemic and/or local accumulation promotes tumor growth through suppression of the host anti-tumor response[8]. However, considerable uncertainty remains regarding the characteristics, functions, and regulation of Tregs. Therefore, we investigated the clinicopathologic significance of CD4+CD25^{high}FOXP3+ Tregs in HCC patients, and analyzed their ability to suppress the immune response. Elucidation of the mechanisms underlying Treg elevation is essential for the development of new approaches that aim to modulate the frequency and function of Tregs in order to enhance the efficacy of cancer immune-based therapies.

Toll-like receptors (TLRs) recognize specific structural regions of invading pathogens and initiate innate and adaptive immune responses; their expression has been detected in immune cells and also in many cancer cells[9]. Lipopolysaccharide (LPS), a ligand for TLR4, stimulates immune cells and triggers the production of inflammatory cytokines and other mediators *via* TLR4, which in turn regulates the host immune defense system and eliminates pathogens[10,11]. It has been reported that inflammatory cytokines induced by inflammatory stimuli counteract immune surveillance and facilitate tumor growth[12,13]. However, various other reports have suggested that diverse TLRs potentially exhibit different effects on Tregs due to differences in pathogens and immune environment, resulting in either increased suppression or abrogation of suppression[14-17]. The suppressive function of Tregs is tightly regulated to respond to the different requirements of immunity. The mechanism underlying the selective control of Treg function remains obscure. Precise modulation of the suppressive function of Tregs is crucial for the development of effective cancer immunotherapy. Thus, in this study we investigated whether TLR4 is expressed in HCC, and whether tumor TLR4 is functionally active in inducing cytokines, and we also examined the clinicopathological correlation between tumor TLR4 signaling and CD4+CD25^{high}FOXP3+ Tregs in tumor immune escape.

Currently, the roles of CD4+CD25^{high}FOXP3+ Tregs and TLR4 in HCC and their regulatory activity in the tumor microenvironment remain unclear. In the present study, we described the clinicopathological significance of Tregs in 60 HCC patients, and the expression of TLR4 in hepatic cancer cells. Our findings indicated that TLR4 ligation promotes the secretion of inhibitory cytokine interleukin (IL)-10 and chemokine CCL22 from co-cultured macrophages, but not from the tumor cells themselves. Furthermore, the prevalence of Tregs significantly correlated with the presence of multifocal tumor. Our results suggest a mechanistic path for the indirect modulation of CD4+CD25^{high}FOXP3+ Tregs *via* tumor TLR4 signaling, and demonstrate that interactions between hepatoma cells and macrophages induce anti-tumor immune suppression *via* Tregs.

MATERIALS AND METHODS

Ethics

This study was conducted in accordance with the Declaration of Helsinki (2000) of the World Medical Association. The Ethics Committee of Tongji Medical College (Wuhan, China) approved the study protocol. All patients provided informed written consent before blood and tumor sampling.

Patient and samples

Blood samples were collected from 60 HCC patients who underwent hepatic resection in the Center of Hepatobiliary Surgery, Union Hospital, Wuhan, China from March 2008 to October 2008. Control blood samples were obtained from 20 healthy volunteers. HCC patients were pathologically diagnosed following surgical resection. Among the 60 HCC patients, there were 51 males and nine females aged 17-77 years (mean, 51.3 years). According to the International Union against Cancer tumor-node-metastasis classification[18], there were 19 (31.7%), 24 (40%) and 17 (28.3%) cases at stage Ⅰ, Ⅱ and Ⅲ, respectively. No patient was treated with local ablative therapy, chemotherapy, or immunotherapy prior to surgery. Clinical and laboratory characteristics of the HCC patients are shown in Table 1. Blood samples (3 mL) were collected 2-3 d before operation from each patient in the early morning. Samples were placed in ethylenediaminetetraacetic acid anticoagulant tubes for flow cytometric detection in our hospital. Next, 1 cm × 1 cm × 1 cm tumor and normal tissues were obtained from each patient intraoperatively, avoiding

Table 1 Clinical and laboratory characteristics of the 60 hepatocellular carcinoma patients

Items	Results
Age (yr) median (range)	53.5 (17-77)
Gender (male/female)	51/9
Virus (HBV/HCV)	48/4
TNM stage (Ⅰ/Ⅱ/Ⅲ/Ⅳ)	19/24/17/0
AFP (μg/L), median (range)	350 (1.8-127 278)
Blood neutrophil (%)	62.29 ± 10.96
Blood monocyte (%)	7.21 ± 1.69
Hemoglobin concentration (g/L)	124.47 ± 17.04

TNM: Tumor-node-metastasis; HBV: Hepatitis B virus; HCV: Hepatitis C virus; AFP: α-fetoprotein.

areas of necrosis, hemorrhage, and/or adipose tissues. One portion of each specimen was snap frozen in liquid nitrogen and the other part was fixed in 10% polyformaldehyde solution and embedded in paraffin.

Flow cytometric analysis

Peripheral blood mononuclear cells from each patient (100 μL) was separated into a heparinized container. Twenty microliters anti-human CD25-fluorescein isothiocyanate and anti-human CD4-PerCP was added to each tube, and incubated at room temperature in the dark for 15 min. After washing in 1 × phosphate-buffered saline, fixed broken membrane buffer 1 mL (1% paraformaldehyde and 70% ice-alcohol; pH 7.4) was added. The remaining lymphocytes were incubated in 20 μL FOXP3-PE at 4 ℃ for 30 min. Subsequently, cells were analyzed by flow cytometry (FACS Calibur, BD) with Cellquest software (Version 3.3, BD Biosciences-Pharmingen, United States). All conjugated antibodies described above and their isotype-matched monoclonal antibodies were purchased from BD, United States.

Lymphocytes were gated on forward and side scatter profiles followed by gating on CD4+ T cells, and these cells were then analyzed for CD25 expression. For FOXP3 expression analysis, cells inside the CD4+CD25^{high} gate were analyzed.

Western blotting

Nuclear protein extracts were prepared in sodium dodecyl sulfate (SDS) lysis buffer containing protease inhibitors, pre-stained molecular weight markers were denatured in laemmli buffer (10% glycerol, 2% SDS, 0.1 mol/L dithiothreitol, 50 mmol/L Tris, 0.01 mg/mL bromphenol blue; pH 6.8) at 90 ℃, and were separated by SDS-polyacrylamide gel electrophoresis. Resolved proteins were transferred onto polyvinylidene fluoride membrane in Trans-blot wet buffer (Bio-Rad Laboratories, United States). The membranes were blocked with 5% nonfat dry milk in 1 × tris-buffered saline (TBS), then incubated with 2 μg/mL mouse monoclonal anti-FoxP3 antibody (clone 22510; Abcam, United States) overnight at 4 ℃ followed by horseradish peroxidase-conjugated goat anti-mouse immunoglobulin G (IgG) for 1 h at room temperature, and washed with 1 × TBS. Membranes were treated with enhanced chemiluminescence plus Western blotting detection kit (Transgen, Beijing, China), and bands were detected using STORM 840v2005 with ImageQuant software (GE, United States).

Cell lines and reagents

If not indicated otherwise, all substances were purchased from Gibco, United States. The H22 (murine) and HepG2 (human) hepatic cancer cell lines were a gift from Dr. Huang Bo (Tongji Medical College, Huazhong University of Science and Technology, Wuhan, China). The immortalized murine macrophage line RAW246.7 was preserved in our laboratory. The cell lines were cultured in RPMI-1640 medium supplemented with 10% fetal bovine serum. All experiments were performed under endotoxin-free conditions.

Co-culture assay

The various cellular components were grown in an artificial basement membrane in a modified Polyster-Transwell (Costar, United States) plate without direct cell-to-cell contact. 1 × 10^5 RAW246.7 cells/mL were seeded into the upper well of the Transwell plate (0.4 μm pore diameter), which consisted of a membrane permeable to liquids but not cells, whereas the lower well was filled to the top with RPMI + 10% fetal calf serum. H22 cells (1 × 10^6 cells/mL RPMI) were seeded into a 12-well plate. To activate TLR4 in H22 cells, LPS (Gibco, United States) was used at 1 μg/mL. The culture medium was removed after LPS-stimulating the H22 cells for 12 h. Next, the Transwells were inserted into the 12-well plate. Gene expression was compared between control and macrophages co-cultured with H22 cells after 24 h, and macrophages with or without conditioned tumor medium were analyzed using reverse transcriptase polymerase chain reaction (RT-PCR). All experiments were performed at least in triplicate.

RNA extraction and RT-PCR

Total RNA was extracted from patient samples, H22, HepG2, and RAW246.7 cells, using Trizol reagent (Invitrogen, United States). Using a first strand cDNA synthesis kit (ToYoBo, Shanghai, China), cDNA was generated with Oligo dT primer. Primers for TLR4, tumor necrosis factor-α (TNF-α), IL-10, CCL22 and β-actin were designed using Premier 5.0 software (Table 2). Primers were synthesized by Sangon Inc. Shanghai, China.

Each reaction mixture contained 2.5 μL 10 × buffer, 2.5 μL 2.5 mmol $MgCl_2$, 0.5 μL 10 mmol of dNTP, 0.2 μL 5 U/μL Taq DNA polymerase, 1 μL each of sense and antisense primer, and 1 μL cDNA in a final volume of 25 μL (Fermentas, United States). Reaction mixtures were incubated at 94 ℃ for 5 min to activate the Taq DNA polymerase, and then amplified using 40 cycles of 30 s at 94 ℃ (denaturation) and 40 s at annealing temperature for TLR4, TNF-α, IL-10, CCL22, and β-actin, respectively. PCR was performed using the Agarose Gel Electrophoresis Imaging Analysis System (Beijing, China).

Table 2 Primer sequences and conditions used for reverse transcription-polymerase chain reaction

Gene	Sequence	Product size (bp)	Annealing temperature (℃)
mTLR4	5′-GCTTTCACCTCTGCCTTCAC-3′ 3′-AGGCGATACAATTCCACCTG-5′	259	57
HuTLR4	5′-GAAATGGAGGCACCCCTTC-3′ 3′-GAATATTCCTTTGCATAGGT-5′	506	52
CCL22	5′-AAGACAGTATCTGCTGCCAGG-3′ 3′-GATCGGCACAGATATCTCGG-5′	141	57
IL-10	5′-GGTTGCCAAGCCTTATCGGA-3′ 3′-ACCTGCTCCACTGCCTTGCT-5′	190	60
TNF-α	5′-CATCTTCTCAAAATTCGAGTG ACAA-3′ 3′-TGGGAGTAGACAAGGTACAA CCC-5′	175	58
β-actin	5′-TCACCCACACTGTGCCCATCT ACGA-3′ 3′-GATAACCGTTGCTCGCCAAG GCTAC-5′	300	50

TNF: Tumor necrosis factor; IL: Interleukin; TLR: Toll-like receptor.

Immunohistochemistry

To assess TLR4 protein expression in HCC and normal tissues, a polyclonal rabbit anti-human TLR4 (ab47093; Abcam, United States) was used. Paraffin-embedded sections (5-μm thick) were fixed in freshly prepared 10% paraformaldehyde for 5 min. After blocking the endogenous peroxidase activity with 0.3% hydrogen peroxide in TBS for 15 min, the sections were immersed in horse serum diluted 1:10 in TBS for 30 min to reduce nonspecific binding, and then incubated with the primary antibody overnight at 4 ℃ after washing in TBS. Next, the sections were incubated in biotinylated horse anti-mouse or goat anti-rabbit IgG for 30 min, and avidin-biotin-peroxidase complex for 30 min. After each step of the staining procedure, the sections were given three 5-min washes in TBS. Immunoreactivity (IR) was visualized using 1 mg/mL diaminobenzidine as chromogen and 0.01% hydrogen peroxide as substrate. The peroxidase reaction was stopped after 5 min with distilled water, and the sections were counter-stained with Toluidine blue, dehydrated, and then mounted with Entellan.

Slides were evaluated under a light microscope (× 400 magnification). For digital image analysis, the software Adobe Photoshop version 7.0 was used. Results were scored by two independent investigators as positive, heterogeneous, or negative. The two scores were averaged.

Statistical analysis

SPSS version 10.0 (SPSS Inc., United States) was used for statistical analysis. All data were expressed as mean ± SE. Statistical analyses were performed using the Student's *t* test. If there was evidence of non-normality, Kruskal-Wallis one-way analysis of variance was used to test the difference in median among the groups. To analyze the correlation between Tregs and TLR4, Spearman's rank correlation coefficients were performed. Difference was considered statistically significant at $P < 0.05$.

RESULTS

$CD4+CD25^{high}FOXP3+$ Tregs accumulation in HCC tumor and peripheral blood

The prevalence of $CD4+CD25^{high}$ and $CD4+CD25^{high}$ FOXP3+ Tregs was analyzed in the peripheral blood of 60 patients with HCC. The population of $CD4+CD25^{high}$ and FOXP3+ Tregs as a percentage of total CD4+ T and $CD4+CD25^{high}$ T cells, respectively, was identified by flow cytometry. Representative dot plots of HCC patients and controls are shown in Figure 1A. The frequency of $CD4+CD25^{high}$ and FOXP3+ Tregs in HCC patients was significantly higher than in the healthy controls (Figure 1B). The expression of FOXP3 in HCC patients was detected using Western blotting analysis. As shown in Figure 1C and D, both tumor and normal tissues exhibited FOXP3 protein expression, although the expression was weaker in normal tissues.

Clinicopathologic characteristics of HCC patients and prevalence of circulating $CD4+CD25^{high}FOXP3+$ Tregs

We analyzed the correlation between the proportion of $CD4+CD25^{high}FOXP3+$ Tregs in the peripheral blood and the clinicopathological characteristics of the subjects (Table 3). The proportion of $CD4+CD25^{high}FOXP3+$ Tregs was significantly higher in patients with high serum AFP levels and multiple tumor foci ($P = 0.009$). The proportion of $CD4+CD25^{high}FOXP3+$ Tregs did not correlate with other clinicopathological characteristics of HCC patients ($P > 0.05$).

Considering the potential impact of multifocal tumor on tumor size, the correlation of the proportion of $CD4+CD25^{high}FOXP3+$ Tregs with different tumor diameters was analyzed in 52 patients with a single lesion. Our findings indicated that the proportion of Tregs was low in patients with a small tumor (< 5 cm in diameter) (Figure 2).

Expression of TLR4 in patient samples and hepatoma cell lines

The expression of TLR4 in patient tumor samples and hepatoma cell lines was examined using RT-PCR. Tumor and normal tissues, as well as HepG2 and H22 cells, expressed TLR4 mRNA (Figure 3). We determined the relative expression of TLR4 mRNA (TLR4 mRNA level/β-actin mRNA level × 100%) and found that TLR4 mRNA expression level in HCC tissues was higher than in the normal tissues ($P = 0.01$) (Figure 3A). Additionally, immunohistochemical analysis confirmed the expression of TLR4 protein. TLR4 positive hepatocytes were present in paraffin-embedded sections. Moderate and strong IR for TLR4 was detected in 63.4% (38/60) of HCC specimens, and normal tissues displayed positive staining in 10% (6/60). TLR4 in cancer cells was stained more intensely than in the normal cells (Figure 3C). The distribution of TLR4 in a given HCC specimen was uneven, and the majority of positive hepatocytes exhibited expression on the membrane and in the cytoplasm. Scattered expression of TLR4 protein was also observed in a small number of liver sections derived from normal tissues.

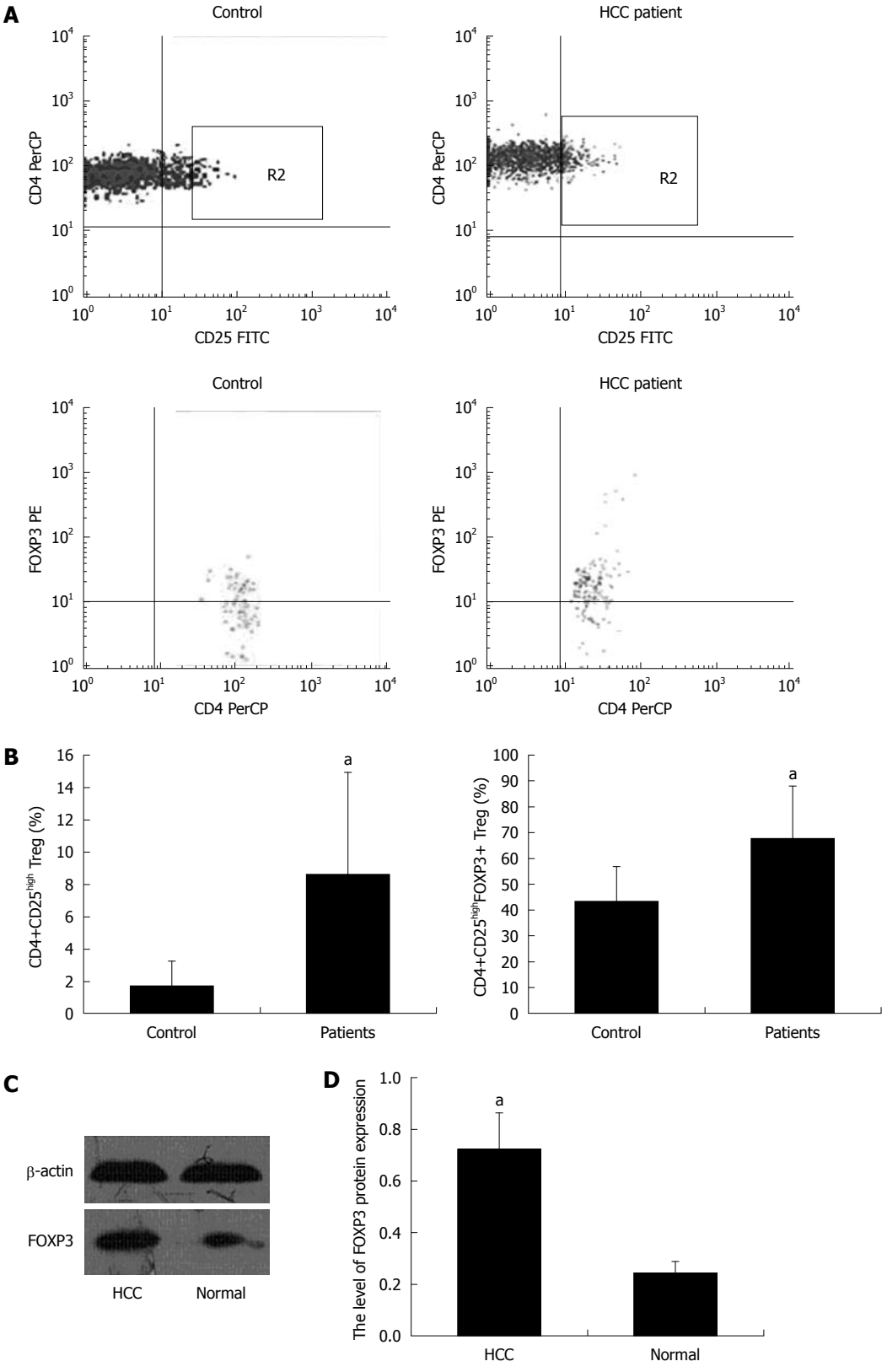

Figure 1 CD4+CD25^{high}FOXP3^{+} regulatory T cells accumulation in hepatocellular carcinoma and peripheral blood. A: Representative flow cytometry plots of CD4+CD25^{high} regulatory T cell (Treg) (region R2) and family of transcription factor P3 (FOXP3)+ Treg cells in peripheral blood from a healthy donor and hepatocellular carcinoma (HCC) patient; B: Percentage of CD4+CD25^{high} Treg and FOXP3+ Treg cells in peripheral blood from HCC patients and controls; C: The prevalence of CD4+CD25^{high} Treg (8.57% ± 6.31%, P = 0.002) and FOXP3+ Treg cells (67.51% ± 20.59%, P < 0.05) in peripheral blood from HCC patients was significantly higher than that of healthy donors (1.71% ± 1.59% and 43.35% ± 13.91%, respectively). Western blotting analysis of nuclear extracts prepared from HCC and normal tissues; D: The relative expression of FOXP3 protein (FOXP3 protein/β-actin protein × 100%). The FOXP3 protein expression in HCC tissues was stronger (0.72 ± 0.14) as compared with normal tissues (0.24 ± 0.05) (^{a}P < 0.05). FITC: Fluorescein isothiocyanate.

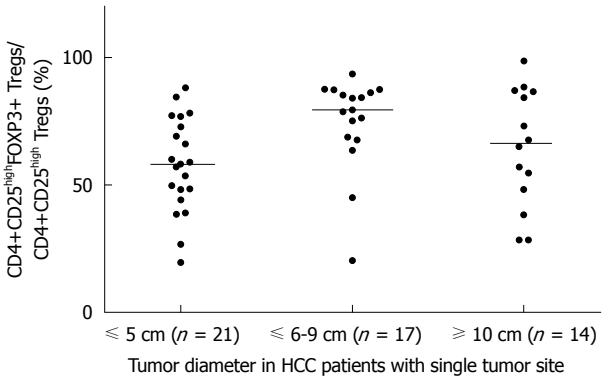

Figure 2 Correlation of regulatory T cells with tumor size of a single tumor. Circulating levels of CD4+CD25^{high}FOXP3+ regulatory T cells (Tregs) was low in patients with a small tumor (less than 5 cm in diameter). Comparisons of data of Tregs among 3 tumor size groups using a Kruskal-Wallis test. Statistically significant differences were found in all comparisons between the 3 groups (χ^2: 7.365, P = 0.0252). HCC: Hepatocellular carcinoma.

Upregulation of IL-10 and CCL22 expression in RAW246.7 cells elicited by co-cultivation with LPS preincubated hepatoma cells

Hepatoma cell line H22 cells were pre-incubated with LPS. The RAW246.7 cells and the H22 cells were co-cultured in a transwell system for 24 h. Semiquantitative RT-PCR was performed to detect the expression of TNF-α, IL-10, and CCL22 in different cell lines. RAW246.7 cells co-cultured with LPS pre-treated H22 cells exhibited significant up-regulation of mRNA for genes IL-10 and CCL22 ($P < 0.001$), whereas expression of TNF-α remained unchanged (Figure 4). Tumor cells without LPS pre-incubation induced negligible gene expression changes in co-cultured RAW246.7 cells. H22 cells alone did not produce IL-10 and CCL22 under conditions of TLR4 activation following LPS stimuli or not (data not shown). These findings, taken together, suggested that activated TLR4 on H22 cells facilitated the induction of cytokine secretion of IL-10 and CCL22 by RAW246.7 cells.

Correlation between proportion of CD4+CD25^{high}FOXP3+ Tregs in peripheral blood of HCC patients and TLR4 in HCC tissues

We investigated the associations between tumor Union for International Cancer Control (UICC) stage, circulating CD4+CD25^{high}FOXP3+ Tregs, and TLR4 in the HCC tissues. The expression level of TLR4 protein in 60 HCC specimens was positively correlated with the frequency of CD4+CD25^{high}FOXP3+ Tregs in peripheral blood (Figure 5A). There was an increased frequency of Tregs in the peripheral blood of HCC patients, which exhibited a high level of expression of TLR4 protein. However, there was no significant correlation between the number of CD4+CD25^{high}FOXP3+ Tregs and tumor UICC stage (Figure 5B).

DISCUSSION

Increased FOXP3+ Tregs in HCC tissues and peripheral blood

T cells play an essential role in the immunosurveillance and destruction of cancer cells. Among CD4+ T lymphocytes, CD4+CD25+ Tregs are thought to comprise a functionally unique subpopulation of T cells that act to maintain immune homeostasis. The lack of CD4+CD25+ Tregs results in various autoimmune syndromes. Alternatively, Tregs-mediated suppression potentially hinders an effective immune response, which is crucial for elimination of tumors and infection[19]. Humans with cancer exhibit increased numbers of peripherally circulating and tumor Tregs[5,20,21]. Ormandy *et al*[22] found that in HCC patients the number of Tregs in the peripheral blood was significantly increased. However, Yang *et al*[23] found that the proportion of CD4+CD25+ Tregs in the peripheral blood of HCC patients was significantly decreased. Too few samples and different patient inclusion criteria has potentially led to conflicting results in previous studies. This study presents evidence of an accumulation of FOXP3+ Tregs in HCC tumor tissues and peripheral blood. A few previous studies have also investigated the clinicopathologic significance of Tregs, but conclusions regarding correlations with various clinicopathologic features were contradictory. Our results demonstrated

Table 3 Correlation between the proportion of CD4+ CD25^{high}FOXP3+ regulatory T cells in peripheral blood and clinicopathological characteristics of hepatocellular carcinoma

Items	*n*	Treg (%)	*P* values
Sex			0.201
Male	51	68.95 ± 20.71	
Female	9	59.37 ± 18.97	
UICC/TNM stage			0.781
I	19	66.41 ± 20.28	
II-III	41	68.02 ± 20.97	
AFP (μg/L)			<0.001
≤ 20	23	53.13 ± 17.96	
> 20	37	76.45 ± 16.84	
HBsAg			0.611
Positive	48	68.20 ± 19.69	
Negative	12	64.78 ± 24.66	
Margin			0.981
Clear	29	67.45 ± 19.74	
Unclear	31	67.57 ± 21.69	
Capsule			0.058
Complete	28	62.14 ± 21.92	
Incomplete	32	72.22 ± 18.43	
Tumor diameter (cm)			0.245
≤ 5	23	59.84 ± 19.06	
6-9	18	75.94 ± 18.43	
≥ 10	19	68.81 ± 21.84	
Tumor number			0.009
Single	52	63.83 ± 20.55	
≥ 2	8	86.41 ± 6.18	
Cirrhosis			0.881
Presence	23	68.02 ± 20.42	
Absence	37	67.19 ± 20.98	
Tumor differentiation			0.152
WD	11	56.61 ± 24.98	
MD	7	69.60 ± 20.45	
PD	42	70.02 ± 18.59	

MD: Moderately differentiated; WD: Well differentiated; PD: Poorly differentiated; AFP: α-fetoprotein; Tregs: Regulatory T cells; TNM: Tumor-node-metastasis; UICC: Union for International Cancer Control.

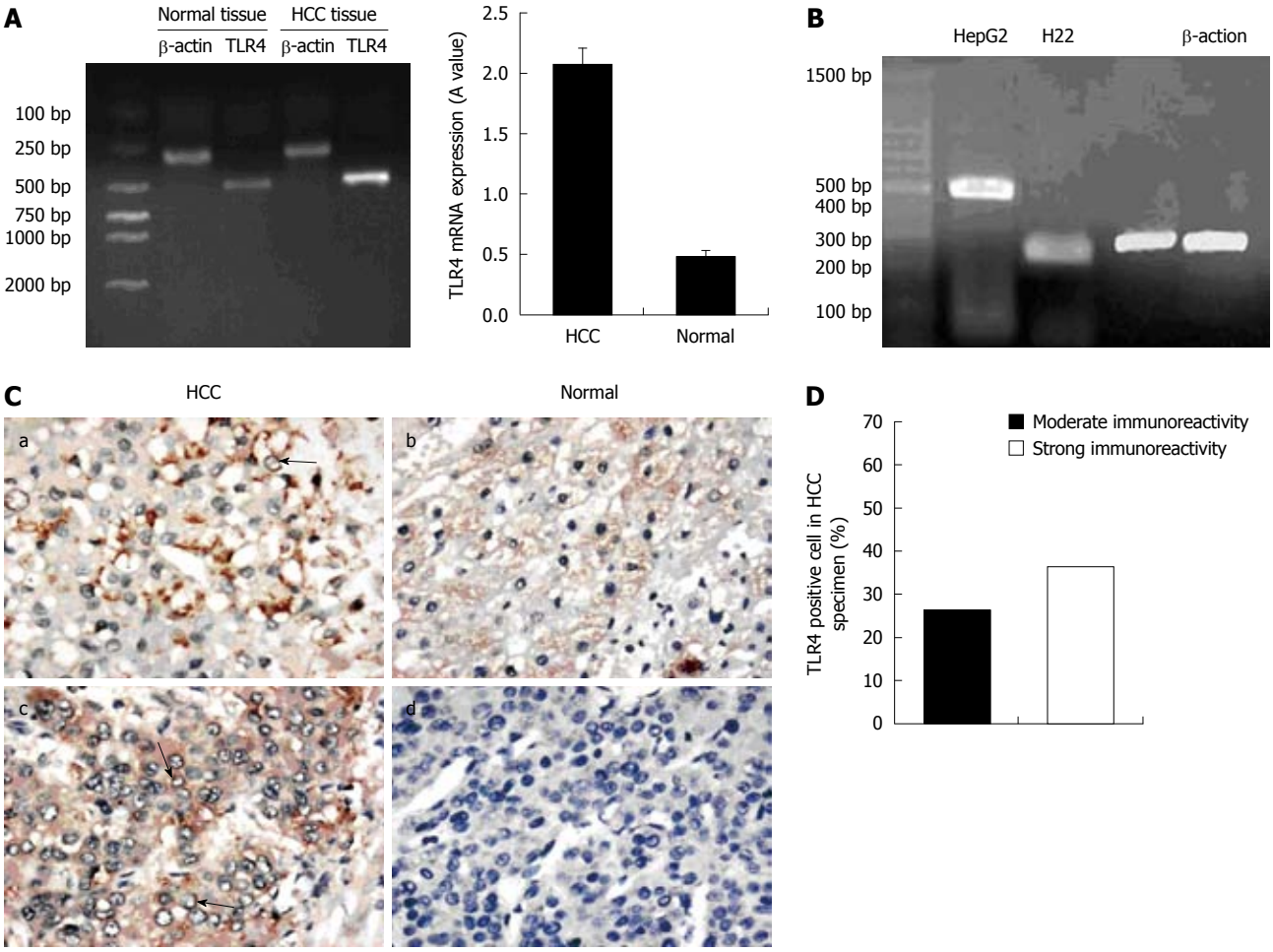

Figure 3 Expression of toll-like receptor 4 mRNA in hepatocellular carcinoma patients and hepatoma cell lines. A: Reverse transcriptase polymerase chain reaction analysis of total RNA from hepatocellular carcinoma (HCC) and normal tissues. The toll-like receptor 4 (TLR4) mRNA expression in HCC tissues was stronger (2.08 ± 0.14) compared to normal tissues (0.48 ± 0.05) (P = 0.01); B: TLR4 mRNA expressed in human HepG2 and murine H22 hepatoma cell lines; C: Expression of TLR4 protein in HCC and normal tissues by immunohistochemistry. a, c: Paraffin-embedded sections of HCC exhibiting positive expression on the membrane and in the cytoplasm in several positive hepatocytes (arrows) [diaminobenzidine (DAB) ×400]; b, d: Paraffin-embedded sections of normal tissues showing weaker expression (DAB ×400); D: TLR4 was detected by immunohistochemistry in tissue sections of patients with HCC (frequency of positive hepatocytes for TLR4 in paraffin-embedded sections).

that the proportion of Tregs was not correlated with hepatitis and cirrhosis, which was in concordance with other studies[22,24]. Shen *et al*[25] indicated that the increased prevalence and expanded function of Tregs in the tumor microenvironment of HCC correlated with cancer stage. However, no significant differences between number of Tregs and tumor UICC stage were observed in our HCC patients; other research groups also confirmed our findings[26,27]. The discrepancy among different research groups potentially results from differences in patient profiles, e.g., Shen *et al*[25] selected 31 patients who had undergone hepatectomy for their study. Moreover, we demonstrated a positive correlation between the number of Tregs and serum AFP levels and multifocal tumor. In order to exclude the influence of multifocal tumor, we separately analyzed 52 HCC patients with a single lesion, and found that the proportion of Tregs was higher in patients with a larger tumor size (Figure 3, P = 0.0252). Our results suggested that the number of Tregs in HCC potentially contributes to the inhibition of effective anti-tumor immune responses and promotes intrahepatic tumor metastasis.

Correlation between Tregs levels and expression of TLR4 in HCC tissues

Despite the important role of Tregs in controlling immune responses to self-antigen and non-self-antigens and their natural ligands, the molecular mechanisms underlying the regulation and recruitment of Tregs in the tumor microenvironment remain poorly understood. One family of receptors involved in immune regulation is TLRs, a class of receptors that recognizes pathogen-associated molecular patterns or endogenous inflammation-associated molecules[28]. Recently, TLRs were identified on cancer cells and T cells, including Tregs[9,11]. Thus, TLR-signaling directly or indirectly regulates the immunosuppressive function of Tregs in the immune response[29-32]. A few studies concerning indirect regulatory function have been conducted to clarify the complex cross-talk between TLRs and Tregs in tumors. Our data provide

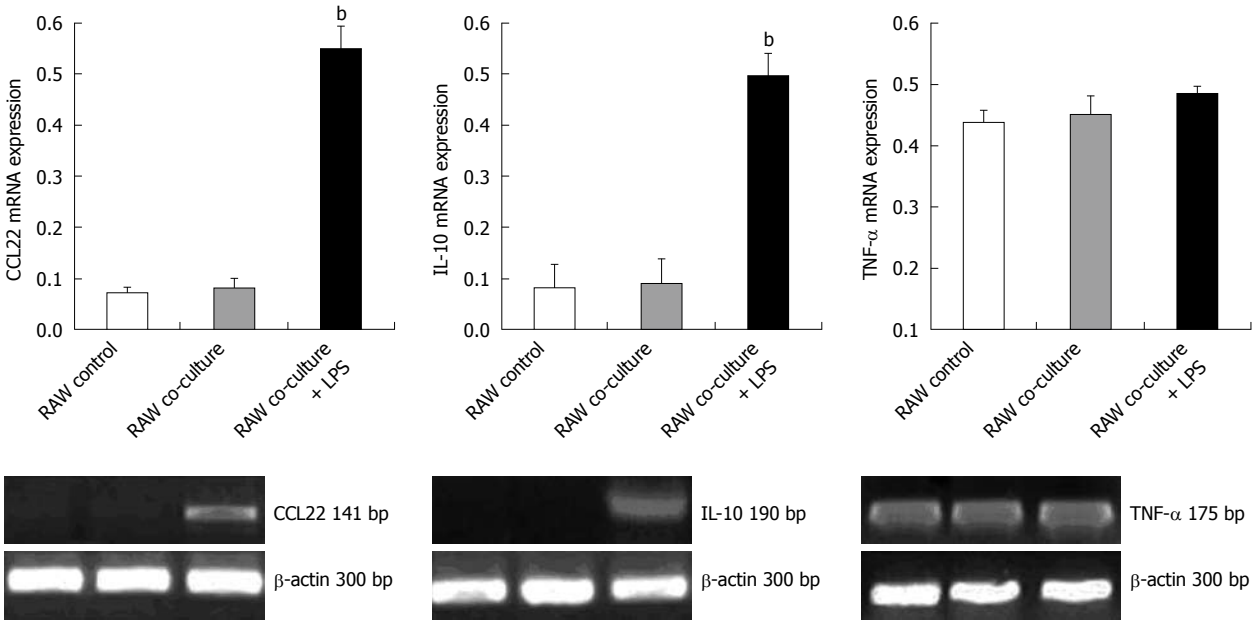

Figure 4 Tumor necrosis factor-α, interleukin-10, and CCL22 mRNA expression in RAW246.7 and RAW246.7 cells co-cultured with H22 cells ± lipopolysaccharide. The bars indicate the relative amount of tumor necrosis factor (TNF)-α, interleukin (IL)-10 and CCL22 mRNA expression (reverse transcriptase polymerase chain reaction). LPS: Lipopolysaccharide. $^{b}P < 0.001$ *vs* RAW co-culture.

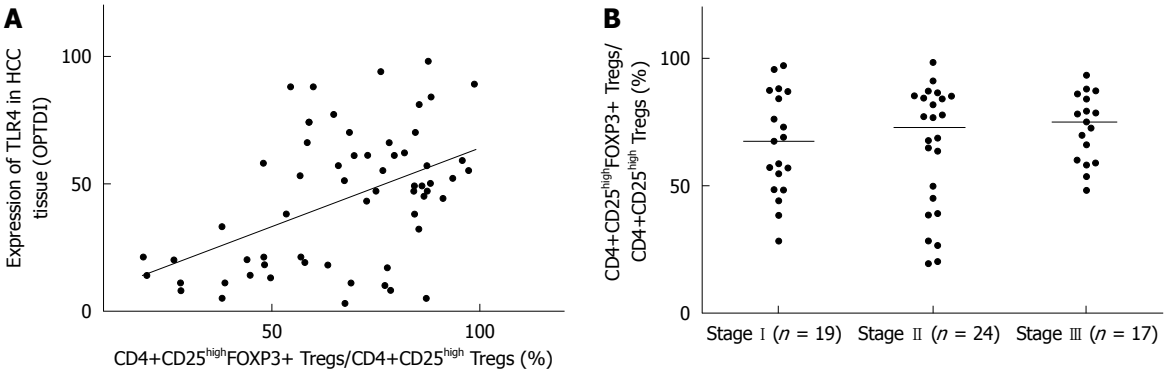

Figure 5 Correlation between the expression of toll-like receptor 4 in hepatocellular carcinoma specimens, tumor Union for International Cancer Control stage, and CD4+CD25^{high}FOXP3+ regulatory T cell. A: Toll-like receptor 4 expression was positively correlated with the number of CD4+CD25^{high}FOXP3+ regulatory T cells (Tregs) in peripheral blood. Analysis of data was performed using Spearman's rank correlation coefficients ($n = 60$, $r = 0.411$, $P < 0.001$); B: According to Union for International Cancer Control/tumor-node-metastasis classification, there were 19 cases, 24 cases, and 17 cases at stage Ⅰ, Ⅱ and Ⅲ hepatocellular carcinoma, respectively. Statistically negative correlations were found in all comparisons between the 3 groups ($\chi^2 = 0.921$, $P = 0.631$) using the Kruskal-Wallis test.

some important clues regarding the interaction of TLR4 expression in tumor tissues and the number of Tregs in hepatocellular cancer. We demonstrated that TLR4 was expressed in diverse hepatoma cells and enriched in HCC tumor tissues, and that the expression of TLR4 in HCC positively correlated with the frequency of FOXP3+ Tregs in both circulation and tumor tissues ($P < 0.001$). These results suggest that the recruitment and proliferation of Tregs are indirectly regulated *via* TLR4 signaling.

Activation of TLR4 on tumor cells and its interaction with macrophages indirectly suppress anti-tumor immune response via recruitment of Tregs

Although some evidence implicates Tregs in the immunopathogenesis of cancer, suppressive mechanisms in the tumor microenvironment and the underlying mechanisms of regulation remain poorly understood[33]. Early evidence suggests that CCL22 preferentially attracts activated antigen-specific T cells to dendritic cells[34]. Curiel recently demonstrated that tumor cells and microenvironmental macrophages in ovarian carcinoma produce the chemokine CCL22, which mediates Treg trafficking to the tumor[35]. Therefore, tumor cells potentially utilize this effect to attract Tregs to the microenvironment. Our data suggested that co-culture of macrophages with a hepotoma cell line leads to a significant increase in the expression of IL-10 and CCL22 ($P < 0.001$). The source of this CCL22 is co-cultured macrophages and hepatoma cells preincubated with LPS. IL-10 is a pleiotropic cytokine produced by myeloid cells and lymphocytes that displays immunoregulatory effects[36]. IL-10 inhibits the production of other cytokines such as IL-2, IL-12 and TNF-α

and plays an important role in suppression of T cell anti-tumor responses[37-39]. In this study, we demonstrated that co-cultured macrophages and LPS pre-treated hepatoma cells significantly up-regulate IL-10 expression. Our findings indicated that the activation of TLR4 on hepatoma cells indirectly modulates the suppressive function of Tregs and enhances Tregs recruitment by inducing cytokines, resulting in the immune escape of HCC.

The accumulation of FOXP3+ Tregs in HCC suggests a trend toward intrahepatic metastasis. The modulation of TLR4 activation on tumor cells links between Tregs suppressive function and the immunopathogenesis of human cancer. The association between TLR4-signaling and functional control of CD4+CD25^{high}FOXP3+ Tregs indicates intriguing potential opportunities to suppress anti-HCC immunity and improve therapeutic effectiveness for the patients. Our study provides the evidence which is useful for the development of an improved immunotherapeutic approach to HCC, and further studies are warranted.

ACKNOWLEDGMENTS

We thank Ms. Yanli He for her technical assistance in flow cytometric detection.

COMMENTS

Background

The survival of hepatocellular carcinoma (HCC) is limited in the majority of such cases. The active suppression of immune responses against tumor is a major barrier to the likely success of cancer immunotherapy. There is now compelling evidence implicating CD4+CD25^{high} family of transcription factor P3 (FOXP3)+ regulatory T cells (Tregs) as being key players driving immune suppression. However, precise function regulation of CD4+CD25^{high}FOXP3+ Tregs remains obscure.

Research frontiers

Toll-like receptors (TLRs) have recently emerged as a critical pathogen-associated molecular pattern of the innate immune system for detecting microbial infection and activation of dendritic cell maturation programs to induce adaptive immune responses. TLR4, an important member of TLRs family, plays a central role in phagocytosis, signal transduction and cell apoptosis. New evidence suggests that TLR signaling may directly or indirectly regulate the suppressive function of Treg cells. TLR4 signaling pathway activation induces production of massive cytokines, and finally intrigues the downstream nuclear factor kappa B to shift the balance between CD4+ T-helper and Treg cells, in ways that may facilitate tumor evasion of immune surveillance.

Innovations and breakthroughs

Currently, the roles of CD4+CD25^{high}FOXP3+ Tregs and TLR4 in HCC and their regulatory activity in the tumor microenvironment remain unclear. In the present study, authors described the clinicopathological significance of Tregs in 60 HCC patients, and the expression of TLR4 in hepatic cancer cells. The findings indicated that TLR4 ligation promotes the secretion of inhibitory cytokine interleukin-10 and chemokine CCL22 from co-cultured macrophages, not from the tumor cells themselves. Furthermore, the prevalence of Tregs significantly correlated with the presence of multifocal tumor. The results suggest a mechanistic path for the indirect modulation of CD4+CD25^{high}FOXP3+ Tregs *via* tumor TLR4 signaling, and demonstrate that interactions between hepatoma carcinoma cells and macrophages induce anti-tumor immune suppression *via* Tregs.

Applications

The authors report that activation of TLR4 on hepatoma cells followed by its interaction with macrophages may indirectly facilitate the recruitment of Tregs into tumor site and promote the intrahepatic metastasis, which suggests innate immunity mediated cellular interference maybe an effective therapeutic target in the treatment of HCC patients.

Terminology

CD4+CD25^{high}FOXP3+ Treg: Tregs are defined based on their expression of CD4, CD25 and forkhead, or winged helix FOXP3, which is critical for the development and function of Tregs in mice and humans. Tregs play a critical role in immunologic self-tolerance and suppression in the tumor immune response; TLR: To recognize specific structural regions of invading pathogens and initiate innate and adaptive immune responses; their expression has been detected in immune cells and also in many cancer cells. TLR4, an important member of TLRs family, plays a central role in phagocytosis, signal transduction and cell apoptosis.

Peer review

The article shows that TLR on hepatoma cell lines may indirectly facilitate the recruitment of Treg cells within tumor site *via* the potential activation of macrophages. This is a good exploratory study in which authors analyze the relationship of tumor TLR4 signaling pathway and CD4+CD25^{high}FOXP3+ Treg cells in tumor immune escape.

REFERENCES

1 **Llovet JM**, Burroughs A, Bruix J. Hepatocellular carcinoma. *Lancet* 2003; **362**: 1907-1917
2 **Fontenot JD**, Rudensky AY. A well adapted regulatory contrivance: regulatory T cell development and the forkhead family transcription factor Foxp3. *Nat Immunol* 2005; **6**: 331-337
3 **Sakaguchi S**, Sakaguchi N, Shimizu J, Yamazaki S, Sakihama T, Itoh M, Kuniyasu Y, Nomura T, Toda M, Takahashi T. Immunologic tolerance maintained by CD25+ CD4+ regulatory T cells: their common role in controlling autoimmunity, tumor immunity, and transplantation tolerance. *Immunol Rev* 2001; **182**: 18-32
4 **Nishikawa H**, Sakaguchi S. Regulatory T cells in tumor immunity. *Int J Cancer* 2010; **127**: 759-767
5 **Wolf AM**, Wolf D, Steurer M, Gastl G, Gunsilius E, Grubeck-Loebenstein B. Increase of regulatory T cells in the peripheral blood of cancer patients. *Clin Cancer Res* 2003; **9**: 606-612
6 **Sasada T**, Kimura M, Yoshida Y, Kanai M, Takabayashi A. CD4+CD25+ regulatory T cells in patients with gastrointestinal malignancies: possible involvement of regulatory T cells in disease progression. *Cancer* 2003; **98**: 1089-1099
7 **Schaefer C**, Kim GG, Albers A, Hoermann K, Myers EN, Whiteside TL. Characteristics of CD4+CD25+ regulatory T cells in the peripheral circulation of patients with head and neck cancer. *Br J Cancer* 2005; **92**: 913-920
8 **Khazaie K**, von Boehmer H. The impact of CD4+CD25+ Treg on tumor specific CD8+ T cell cytotoxicity and cancer. *Semin Cancer Biol* 2006; **16**: 124-136
9 **Huang B**, Zhao J, Li H, He KL, Chen Y, Chen SH, Mayer L, Unkeless JC, Xiong H. Toll-like receptors on tumor cells facilitate evasion of immune surveillance. *Cancer Res* 2005; **65**: 5009-5014
10 **Akira S**, Takeda K. Toll-like receptor signalling. *Nat Rev Immunol* 2004; **4**: 499-511
11 **Caramalho I**, Lopes-Carvalho T, Ostler D, Zelenay S, Haury M, Demengeot J. Regulatory T cells selectively express toll-like receptors and are activated by lipopolysaccharide. *J Exp Med* 2003; **197**: 403-411
12 **He W**, Liu Q, Wang L, Chen W, Li N, Cao X. TLR4 signaling promotes immune escape of human lung cancer cells by inducing immunosuppressive cytokines and apoptosis resistance. *Mol Immunol* 2007; **44**: 2850-2859
13 **Yang H**, Zhou H, Feng P, Zhou X, Wen H, Xie X, Shen H, Zhu X. Reduced expression of Toll-like receptor 4 inhibits human breast cancer cells proliferation and inflammatory cytokines secretion. *J Exp Clin Cancer Res* 2010; **29**: 92
14 **Peng G**, Guo Z, Kiniwa Y, Voo KS, Peng W, Fu T, Wang DY, Li Y, Wang HY, Wang RF. Toll-like receptor 8-mediated reversal of CD4+ regulatory T cell function. *Science* 2005; **309**: 1380-1384

15 **Sutmuller RP**, den Brok MH, Kramer M, Bennink EJ, Toonen LW, Kullberg BJ, Joosten LA, Akira S, Netea MG, Adema GJ. Toll-like receptor 2 controls expansion and function of regulatory T cells. *J Clin Invest* 2006; **116**: 485-494

16 **van Maren WW**, Jacobs JF, de Vries IJ, Nierkens S, Adema GJ. Toll-like receptor signalling on Tregs: to suppress or not to suppress? *Immunology* 2008; **124**: 445-452

17 **Forward NA**, Furlong SJ, Yang Y, Lin TJ, Hoskin DW. Signaling through TLR7 enhances the immunosuppressive activity of murine CD4+CD25+ T regulatory cells. *J Leukoc Biol* 2010; **87**: 117-125

18 **Greene FL**, Page DL, Fleming ID, Fritz AG, Balch CM, Haller DG, Morrow M. AJCC cancer staging manual. 6th ed. New York: Springer, 2002: 131-144

19 **Fu J**, Xu D, Liu Z, Shi M, Zhao P, Fu B, Zhang Z, Yang H, Zhang H, Zhou C, Yao J, Jin L, Wang H, Yang Y, Fu YX, Wang FS. Increased regulatory T cells correlate with CD8 T-cell impairment and poor survival in hepatocellular carcinoma patients. *Gastroenterology* 2007; **132**: 2328-2339

20 **Miller AM**, Lundberg K, Ozenci V, Banham AH, Hellström M, Egevad L, Pisa P. CD4+CD25high T cells are enriched in the tumor and peripheral blood of prostate cancer patients. *J Immunol* 2006; **177**: 7398-7405

21 **Frey DM**, Droeser RA, Viehl CT, Zlobec I, Lugli A, Zingg U, Oertli D, Kettelhack C, Terracciano L, Tornillo L. High frequency of tumor-infiltrating FOXP3(+) regulatory T cells predicts improved survival in mismatch repair-proficient colorectal cancer patients. *Int J Cancer* 2010; **126**: 2635-2643

22 **Ormandy LA**, Hillemann T, Wedemeyer H, Manns MP, Greten TF, Korangy F. Increased populations of regulatory T cells in peripheral blood of patients with hepatocellular carcinoma. *Cancer Res* 2005; **65**: 2457-2464

23 **Yang XH**, Yamagiwa S, Ichida T, Matsuda Y, Sugahara S, Watanabe H, Sato Y, Abo T, Horwitz DA, Aoyagi Y. Increase of CD4+ CD25+ regulatory T-cells in the liver of patients with hepatocellular carcinoma. *J Hepatol* 2006; **45**: 254-262

24 **Unitt E**, Rushbrook SM, Marshall A, Davies S, Gibbs P, Morris LS, Coleman N, Alexander GJ. Compromised lymphocytes infiltrate hepatocellular carcinoma: the role of T-regulatory cells. *Hepatology* 2005; **41**: 722-730

25 **Shen X**, Li N, Li H, Zhang T, Wang F, Li Q. Increased prevalence of regulatory T cells in the tumor microenvironment and its correlation with TNM stage of hepatocellular carcinoma. *J Cancer Res Clin Oncol* 2010; **136**: 1745-1754

26 **Kobayashi N**, Hiraoka N, Yamagami W, Ojima H, Kanai Y, Kosuge T, Nakajima A, Hirohashi S. FOXP3+ regulatory T cells affect the development and progression of hepatocarcinogenesis. *Clin Cancer Res* 2007; **13**: 902-911

27 **Zhou J**, Ding T, Pan W, Zhu LY, Li L, Zheng L. Increased intratumoral regulatory T cells are related to intratumoral macrophages and poor prognosis in hepatocellular carcinoma patients. *Int J Cancer* 2009; **125**: 1640-1648

28 **Akira S**, Hemmi H. Recognition of pathogen-associated molecular patterns by TLR family. *Immunol Lett* 2003; **85**: 85-95

29 **Wang RF**, Peng G, Wang HY. Regulatory T cells and Toll-like receptors in tumor immunity. *Semin Immunol* 2006; **18**: 136-142

30 **Kubo T**, Hatton RD, Oliver J, Liu X, Elson CO, Weaver CT. Regulatory T cell suppression and anergy are differentially regulated by proinflammatory cytokines produced by TLR-activated dendritic cells. *J Immunol* 2004; **173**: 7249-7258

31 **Liu H**, Komai-Koma M, Xu D, Liew FY. Toll-like receptor 2 signaling modulates the functions of CD4+ CD25+ regulatory T cells. *Proc Natl Acad Sci USA* 2006; **103**: 7048-7053

32 **Pasare C**, Medzhitov R. Toll pathway-dependent blockade of CD4+CD25+ T cell-mediated suppression by dendritic cells. *Science* 2003; **299**: 1033-1036

33 **Wang RF**. Regulatory T cells and innate immune regulation in tumor immunity. *Springer Semin Immunopathol* 2006; **28**: 17-23

34 **Tang HL**, Cyster JG. Chemokine Up-regulation and activated T cell attraction by maturing dendritic cells. *Science* 1999; **284**: 819-822

35 **Curiel TJ**, Coukos G, Zou L, Alvarez X, Cheng P, Mottram P, Evdemon-Hogan M, Conejo-Garcia JR, Zhang L, Burow M, Zhu Y, Wei S, Kryczek I, Daniel B, Gordon A, Myers L, Lackner A, Disis ML, Knutson KL, Chen L, Zou W. Specific recruitment of regulatory T cells in ovarian carcinoma fosters immune privilege and predicts reduced survival. *Nat Med* 2004; **10**: 942-949

36 **Salazar-Onfray F**, López MN, Mendoza-Naranjo A. Paradoxical effects of cytokines in tumor immune surveillance and tumor immune escape. *Cytokine Growth Factor Rev* 2007; **18**: 171-182

37 **Matsuda M**, Salazar F, Petersson M, Masucci G, Hansson J, Pisa P, Zhang QJ, Masucci MG, Kiessling R. Interleukin 10 pretreatment protects target cells from tumor- and allo-specific cytotoxic T cells and downregulates HLA class I expression. *J Exp Med* 1994; **180**: 2371-2376

38 **Petersson M**, Charo J, Salazar-Onfray F, Noffz G, Mohaupt M, Qin Z, Klein G, Blankenstein T, Kiessling R. Constitutive IL-10 production accounts for the high NK sensitivity, low MHC class I expression, and poor transporter associated with antigen processing (TAP)-1/2 function in the prototype NK target YAC-1. *J Immunol* 1998; **161**: 2099-2105

39 **Zeng L**, O'Connor C, Zhang J, Kaplan AM, Cohen DA. IL-10 promotes resistance to apoptosis and metastatic potential in lung tumor cell lines. *Cytokine* 2010; **49**: 294-302

S- Editor Gou SX **L- Editor** Ma JY **E- Editor** Zheng XM

World Journal of Gastroenterology

Online Submissions: http://www.wjgnet.com/1007-9327office
wjg@wjgnet.com
doi:10.3748/wjg.v18.i23.2948

World J Gastroenterol 2012 June 21; 18(23): 2948-2955
ISSN 1007-9327 (print) ISSN 2219-2840 (online)

ORIGINAL ARTICLE

Pyogenic liver abscesses associated with nonmetastatic colorectal cancers: An increasing problem in Eastern Asia

Kai Qu, Chang Liu, Zhi-Xin Wang, Feng Tian, Ji-Chao Wei, Ming-Hui Tai, Lei Zhou, Fan-Di Meng, Rui-Tao Wang, Xin-Sen Xu

Kai Qu, Chang Liu, Zhi-Xin Wang, Feng Tian, Ji-Chao Wei, Ming-Hui Tai, Lei Zhou, Fan-Di Meng, Rui-Tao Wang, Xin-Sen Xu, Department of Hepatobiliary Surgery, First Affiliated Hospital, School of Medicine, Xi'an Jiaotong University, Xi'an 710061, Shaanxi Province, China

Author contributions: Qu K and Liu C designed the research; Qu K and Wang ZX performed the majority of experiments; Qu K, Tian F, Wei JC and Tai MH provided analytical tools; Qu K, Zhou L, Meng FD and Wang RT analyzed the data; Qu K and Xu XS were involved in editing the manuscript.

Supported by The National Natural Science Foundation of China, No. 30872482 and No. 81072051

Correspondence to: Chang Liu, Professor, Department of Hepatobiliary Surgery, First Affiliated Hospital, School of Medicine, Xi'an Jiaotong University, No.277 West Yan-ta Road, Xi'an 710061, Shaanxi Province, China. liuchangdoctor@163.com
Telephone: +86-29-82653900 Fax: +86-29-82653905

Received: October 19, 2011 Revised: December 15, 2011
Accepted: March 10, 2012
Published online: June 21, 2012

Abstract

AIM: To elaborate the clinicopathologic features of colorectal cancer-related pyogenic liver abscess (PLA).

METHODS: Reported cases of colorectal cancer-related PLAs were collected from the literature published up to October 2011 and evaluated for their clinicopathologic features. Data of collected cases included demographics, clinical presentation, microbial findings and treatment. Categorical variables were compared by χ^2 analysis and continuous variables were evaluated using Student's *t* test.

RESULTS: A total 96 cases of colorectal cancer-related PLA were collected from the previous literature. Most patients (60%) were male and 40% cases occurred in the age group of 61-70 years. Apart from some special types of PLA, there were significant differences in the microbiological spectrum between Eastern Asia and non-Eastern Asian countries, which implied different risk factors and courses of the disease. Gram negative bacteria especially *Klebsiella pneumoniae* (*K. pneumoniae*) PLA was predominant in Eastern Asia (80.0%) in contrast to non-Eastern Asian countries ($P < 0.01$). Meanwhile, most of the Eastern Asian patients exhibited smaller size of liver abscess and atypical presentation. Sigmoid colon and rectum (72.73%) were the main sites of tumor in Eastern Asian patients, whereas tumor sites were uneven among most of the non-Easter Asian PLA patients.

CONCLUSION: *K. pneumoniae* PLA was strongly associated with colorectal cancer, especially those occurring in sigmoid colon and rectum, in elderly Eastern Asian male patients.

Key words: Colorectal cancer; Pyogenic liver abscess; Etiology; Microbiology; Treatment

Peer reviewers: Michael A Fink, MBBS, FRACS, Department of Surgery, The University of Melbourne, Austin Hospital, Melbourne, Victoria 3084, Australia; Robert V Rege, MD, Department of Surgery, University of Texas Southwestern Medical Center, 5323 Harry Hines Boulevard, Dallas, Texas, TX 75390-9031, United States

Qu K, Liu C, Wang ZX, Tian F, Wei JC, Tai MH, Zhou L, Meng FD, Wang RT, Xu XS. Pyogenic liver abscesses associated with nonmetastatic colorectal cancers: An increasing problem in Eastern Asia. *World J Gastroenterol* 2012; 18(23): 2948-2955 Available from: URL: http://www.wjgnet.com/1007-9327/full/v18/i23/2948.htm DOI: http://dx.doi.org/10.3748/wjg.v18.i23.2948

INTRODUCTION

Liver is the most common organ to develop abscesses.

Pyogenic liver abscess (PLA), once predominantly a disease of young adults as a consequence of post-appendicitis pylephlebitis, nowadays occurs more frequently in elderly patients, with hepatobiliary tract diseases or intra-abdominal infections including cholecystitis, suppurative cholangitis, suppurative pylephlebitis, diverticulitis and peritonitis[1]. Meanwhile, as we cannot find significant underlying causes of PLA, the term "cryptogenic abscesses" is used. For all types of PLA, mucosal defect present within digestive tract lesions or a compromised mucosal barrier allowing a route for bacteria invasion into the portal system with subsequent hematogenous spread to the liver is regarded as the key process[2].

Previous studies revealed that a few cryptogenic PLA patients were related to neoplasms[3]. This type of PLA was regarded as a warning indicator of silent cancers. Recently, many cases of PLA associated with nonmetastatic colorectal carcinoma have been reported worldwide. Interestingly, this PLA in Eastern Asia seems to have greater morbidity and exhibits differences in clinical characteristics. However, there were few studies which analyzed this phenomenon, neither was there any recommendation or consensus for treatment. Therefore, we reviewed published case reports from worldwide literature and retrospectively investigated the etiology, clinical characteristics and treatment of PLA complicated with nonmetastatic colorectal carcinoma.

MATERIALS AND METHODS

Source of data

Data from the available medical literature were systematically reviewed and pooled to analyze. MEDLINE (United States National Library of Medicine, Bethesda, MD), EMBASE (Elsevier Science, New York, NY) and CNKI National Knowledge Infrastructure) bibliographic databases were searched and relevant studies in form of case-control studies, case series or case report published in English language were retrieved using the keywords: "hepatic/liver abscess", "malignant cancer", "colorectal cancer" or "bacterium". The relevant article references in English and other languages were also collected.

Data extraction and quality control

A medical information scientist performed the literature retrieval and the initial screening of relevant studies, and a medical doctor reviewed and coded all studies. Cases were scrutinized to exclude any duplicate reports of the same patients. Many studies reported only aggregate results. Whenever possible, data were extracted both at an aggregate level within each study and at a patient level. The individual cases without individual identification were also excluded. We excluded studies or individuals with missing data from specific analyses. As a result, the number of patients in each analysis varied.

Database

The collected cases were evaluated individually, and details were extracted and computerized for further analysis. Coded potential prognostic determinants included patient demographics, microbial, clinical and laboratory findings, and the authors' affiliations. The data were pooled at both the aggregate and patient levels to determine the distribution of the underlying disease, site of infection, and other pertinent variables.

Statistical analysis

All collected data were transcribed into a Microsoft Excel spreadsheet and analyzed using SPSS software, version 14.0 (SPSS). Continuous variables were compared using analysis of variance, and categorical variables were compared using the χ^2 test. $P < 0.05$ was regarded as significantly different.

RESULTS

Removing irrelevant articles, and articles published in internal journal and reviews, we collected a total of 32 articles with 96 cases from 623 publications in the international literature up to September 2011. Two case-control studies[4,5] and 30 case reports[3,6-34] were included. Most of articles were single case report (26/32). Sixteen cases included in aggregate series[2,15,27-31,33] and 32 cases with individual information summarized in one article published in Japanese were also extracted[7]. Among the 32 collected articles, 25 articles were in English, 2 were in Japanese, 1 was in Chinese, 1 was in Spanish, 1 was in French and 1 was in Hebrew.

Global distribution of reported cases

Although cases of colorectal cancer-related PLA were originally reported in Western countries[2,27-31,33], most of reported cases (80.21%) were published in the Eastern Asian countries/regions, especially in Japan (40 cases), China (26 cases) and Korea (8 cases) (Table 1). The reported number of colorectal cancer-related PLA has increased significantly over the past two decades. Approximately, 90% patients have been reported since 1990 after colonoscopy and percutaneous transhepatic abscess drainage (PTAD) became common in clinical practice. In Eastern Asian countries/regions, the number of cases was increasing rapidly, with a growth rate of approximately 4-5 times every decade from 1981 to 2011 (Figure 1).

Demographical evaluation

The average age of the patients in the present series was 64.4 ± 10.1 years. A male-to-female ratio of 1.5:1 was calculated for the overall series and for patients of different areas. There was no significant difference in the average age between gender groups (male 65.0 years *vs* female 63.4 years, $P > 0.05$) and geographical groups (Eastern Asia 64.6 years *vs* non-Eastern Asia 63.3 years, $P > 0.05$). In the overall series from both Eastern Asia and non-Eastern Asian groups, approximately 40% patients fell into the age groups of 61-70 years (Figure 2).

Table 1 Documented cases collected from the international literature

Country/region	No. of cases	No. of articles
Eastern Asia		
Japan	40	36[6-10]1
China	26	6[4,5,11-14]
Korea	8	1[15]
Singapore	3	1[16]
Middle East and Europe		
Israel	3	3[17-19]
Italy	2	2[20,21]
Spain	2	2[22,23]
Portugal	1	1[24]
France	1	1[25]
United Kingdom	1	1[26]
North and Central America		
United States	7	7[2,27-32]
Canada	1	1[33]
Netherlands Antilles	1	1[34]
Total	96	63

[1]Other 33 cases reported in a Japanese article reference were included[8].

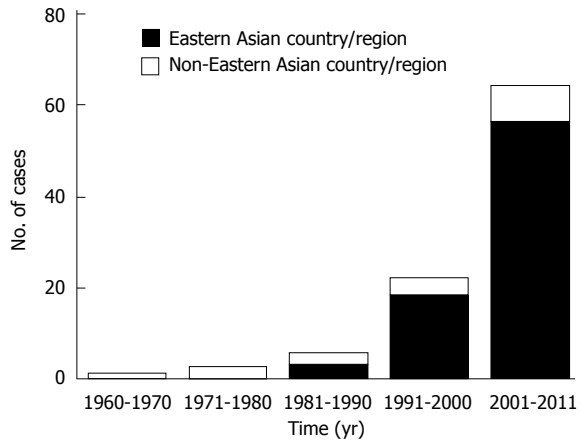

Figure 1 Growth trend of reported cases in different countries/regions from 1960 to 2011.

Table 2 Constituent ratio of pus bacterial cultures *n* (%)

Pathogens	Eastern Asia (*n* = 49)	Non-Eastern Asia (*n* = 9)	Total (*n* = 58)
Bacteria			
Gram negative bacteria			
Klebsiella pneumoniae	28 (57.14)	1 (11.1)	29 (50.0)
Fusobacterium species	4 (8.16)	0	4 (6.90)
Bacteroides species	2 (4.08)	1 (11.1)	3 (5.17)
Escherichia coli	0	1 (11.1)	1 (1.72)
Pseudomonas aeruginosa	1 (2.04)	0	1 (1.72)
Gram positive bacteria			
Streptococcus species	1 (2.04)	3 (33.3)	4 (6.90)
Enterococcus faecium	2 (4.08)	0	2 (3.44)
Polymicrobial	0	2 (22.2)[1]	2 (3.44)
Amoebae	2 (4.08)	0	2 (3.44)
Negative	9 (18.37)	1 (11.1)	10 (17.24)

[1]Pus cultures showed mixed infection in two patients: *E. corrodens*, *Candida albicans* and *Candida glabrata*; *Peptostreptococcus anaerobius*, *Bacteroides melaninogenicus* and *Peptostreptococcus spp*.

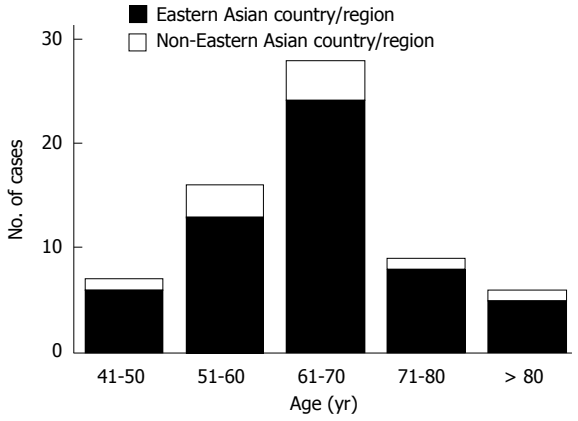

Figure 2 Age distribution of reported cases in different countries/regions.

Microbiology

According to bacteria culture results from 58 patients, *Klebsiella pneumoniae* (*K. pneumoniae*) was the most common pathogen (50.0%), followed by *Fusobacterium species* (6.90%), *Streptococcus species* (6.90%), *Bacteroides species* (5.17%), *Enterococcus faecium* (3.44%), *Escherichia coli* (3.44%) and *Pseudomonas aeruginosa* (3.44%). There were two cases of amoebic liver abscess and two cases with mixed infection. In addition, 10 patients had negative results of pus cultures (Table 2). There was a significant difference between Eastern Asian and non-Eastern Asian groups in gram stains of pathogens. Among the gram-negative pathogens, *K. pneumoniae* was more dominant in Eastern Asian than in non-Eastern Asian groups (Figure 3).

Morphologic characteristics of liver abscess

All liver abscess cases were finally diagnosed with B-mode ultrasonic and/or computed tomography scanning. According to the image results of the 66 patients, 66.7% abscesses formed in the right liver lobe, 18.2% in the left lobe and 12.1% in two lobes (Figure 4). There was no significant difference in the location of liver abscess between Eastern Asian and non-Eastern Asian groups (Figure 5). Thirty-one reported cases had individual data of liver abscess size, which was 5.31 ± 2.11 cm on average. The average abscess size of Eastern Asian patients was smaller than that of non- Eastern Asian patients ($P < 0.05$). Moreover, there was no significant difference in the average size between gender groups, age groups and pathogen groups (Figure 6).

Clinical manifestations and diagnosis

The clinical manifestation of 25 patients was pyogenic liver abscess, including fever and chill (92.0%), abdominal pain (68.0%), abdominal tenderness (64.0%) and nausea/vomiting (45.0%). No more than 40% patients had the chief complaint of atypical symptoms of tumor, which included anemia (40.0%) and weight loss (32.0%). Only approximately 10% of the patients had bowl cancer symptoms, including bloody stool (12.0%) and alterations

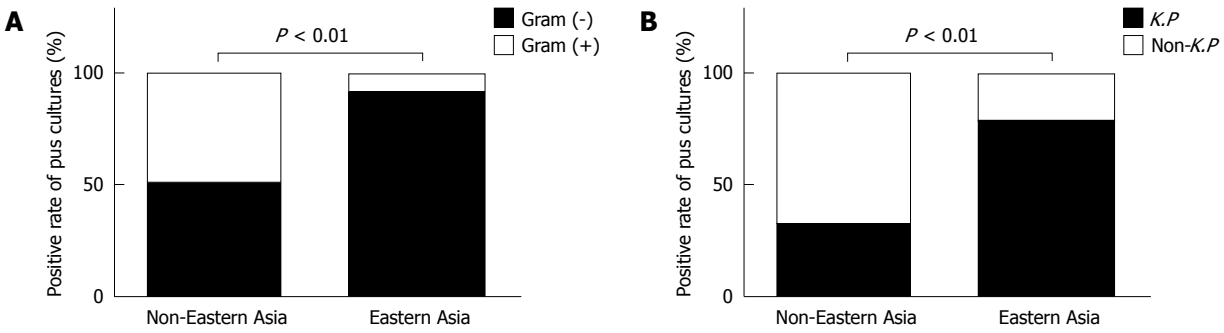

Figure 3 Categorization of pathogens in Eastern Asian and non-Eastern Asian patients. A: Distribution of Gram-negative and Gram-positive pathogens; B: Distribution of *Klebsiella pneumoniae* (*K.P*) and non-*K.P*. There were significant differences in categories of pathogens between Eastern Asian and non-Eastern Asian patients ($P < 0.01$).

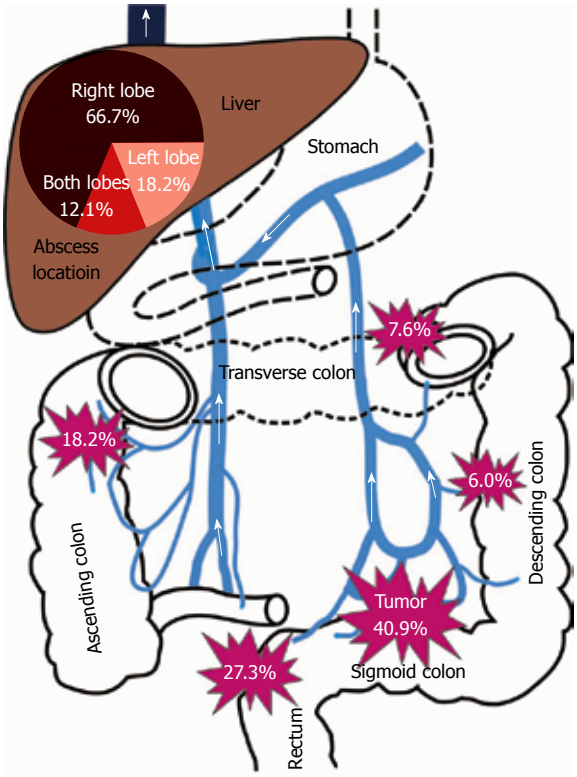

Figure 4 Distribution of colorectal cancer and liver abscesses.

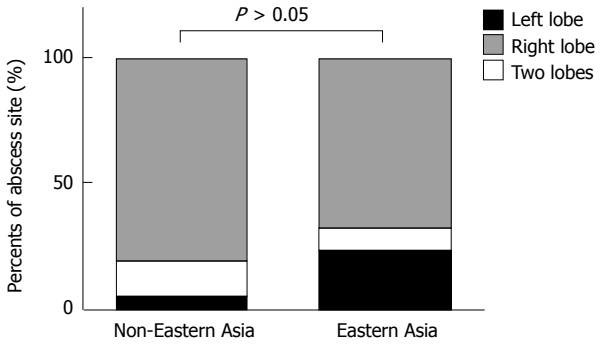

Figure 5 Probability of abscess in different liver lobes in Eastern Asian and non-Eastern Asian patients. There was no significant difference between the two groups ($P > 0.05$).

in bowel habits (4.0%) (Figure 7). None of the cases had abdominal mass, and the digital rectal examinations were negative. Infection indices of the 25 patients with details of laboratory examination revealed a significantly increased level of white blood cell count (17.9-5.22 × 10^9/L) and C-reactive protein (17.8 ± 7.49 mg/dL); and a moderately elevated level of alanine aminotransferase and total bilirubin. However, colorectal cancer-related biomarkers (including CA19-9 and carcinoembryonic antigen) did not elevate in most of the patients.

Monitoring of occult colorectal cancers

Most of the diagnoses of colorectal cancer were made by coloscopy (77.3%) and barium enema (29.2%). The most common site of tumor formation was sigmoid colon (40.9%), followed by rectum (27.3%), ascending (18.2%), transverse (7.6%) and descending colon (6.0%) (Figure 4). Among the 23 patients with pathological reports, colorectal adenocarcinoma (81.8%) and medium differentiation degree (66.7%) were the most common pathological type and differentiation degree, respectively. There was no difference between Eastern Asian and non-Eastern Asian groups in the sites of colon tumors. However, tumors occurred more often in sigmoid colon and rectum in Eastern Asia group (Figure 8).

Treatment for colorectal cancer-related PLA

All of the patients were treated with broad-spectrum antibiotics. The most commonly used antibiotics were cephalosporins with or without metronidazole, followed by fluoroquinolones with or without metronidazole, ampicillin and gentamicin, carbapenems, and gentamicin (Table 3). PTAD was extremely successful as initial treatment for liver abscess. The type of treatment (antibiotics combined with/without PTAD) chosen may have been influenced by several factors (e.g., clinician/radiologist's decision and others). There was no significant difference in the distribution of demographic characteristics (age, gender, geographic distribution and pathogens) between the study and the comparison groups (Table 4). Until the date of the submission of the report, 17 patients had been followed up for an average of 15.4 ± 15.44 mo, all

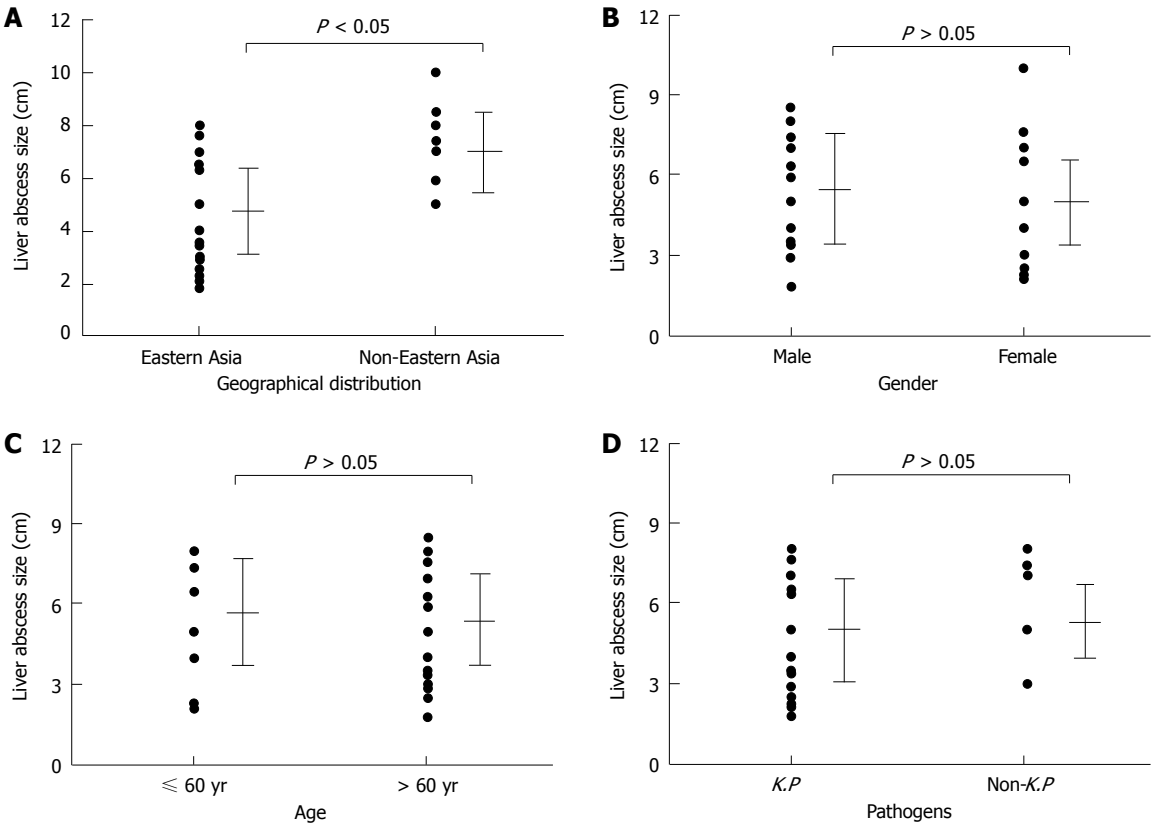

Figure 6 Univariate analysis of abscess size in colorectal cancer related pyogenic liver abscess patients. A: Abscess sizes in different geographical groups; B: Abscess sizes in different gender groups; C: Abscess sizes in different age groups; D: Abscess sizes in different pathogenic groups. There was significant difference in liver abscess sizes between Eastern Asian and non-Eastern Asian patients ($P < 0.05$). *K.P*: *Klebsiella pneumoniae*.

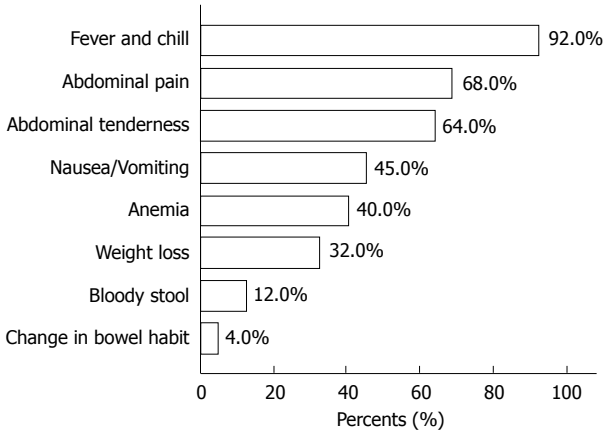

Figure 7 Clinical presentations of colorectal cancer related pyogenic liver abscess patients.

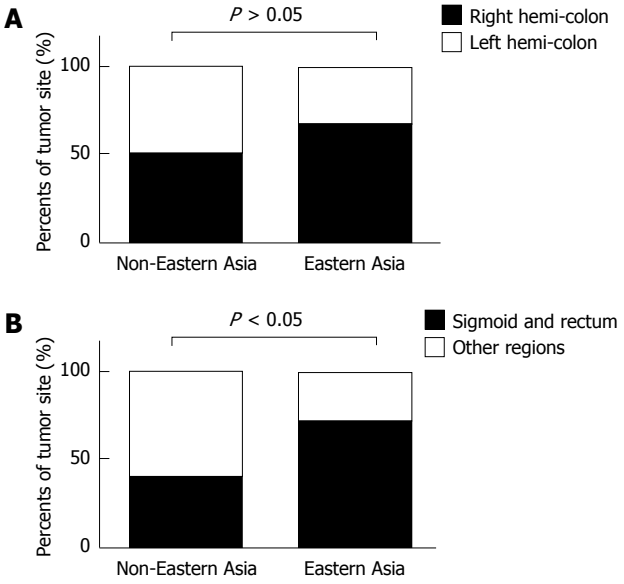

Figure 8 Probability of cancer in different colorectal regions in Eastern Asian and non-Eastern Asian patients. A: Probability of cancer appeared in the right and left hemi-colon; B: Probability of cancer in sigmoid and rectum and other regions. Sigmoid and rectum were the more common cancer sites, compared with other regions ($P < 0.05$).

were kept stable with no tumor recurrence.

DISCUSSION

Colorectal cancer is the fourth most common cancer in men and the third most common cancer in women all over the world. Previous studies have reported rapid increases in colorectal cancer incidence rates, especially in economically transitioning countries[35,36]. Many Eastern Asian countries, such as China, Japan, South Korea, and Singapore, have experienced a 2-4 folds increase in the incidence of colorectal cancer during the past few decades[37]. Common manifestations of colon cancer are

Table 3 Treatment for liver abscess complicated with colorectal carcinoma

Sex	Age, yr	Count of abscess	Anti-infection treatment	Surgical treatment	Ref.
Female	46	Mutiple[1]	Cephalosporin	Sigmoidectomy	[4]
Female	79	Single	Carbapenem	PTAD + low anterior rectal resection	[5]
Male	66	Single	Broad spectrum antibiotic[6]	PTAD + low anterior rectal resection	[6]
Male	73	Single	Broad spectrum antibiotic[6]	PTAD + sigmoidectomy	[7]
Male	65	Single	Broad spectrum antibiotic[6]	PTAD	[7]
Male	67	Single	Broad spectrum antibiotic[6]	PTAD	[7]
Male	81	Mutiple	Broad spectrum antibiotic[6]	Laparoscopic-assisted sigmoidectomy	[8]
Male	67	Mutiple[2]	Cephalosporin	PTAD + polypectomy under colonscopy	[11]
Male	67	Single	Broad spectrum antibiotic[6]	PTAD + polypectomy under colonscopy	[12]
Female	84	Single	Broad spectrum antibiotic[6]	None[7]	[12]
Female	82	Mutiple[3]	Cephalosporin	PTAD + sigmoidectomy	[13]
Female	57	Single	Cephalosporin + carbapenem + moxifloxacin + gentamicin	PTAD + sigmoidectomy + chemotherapy	[14]
Female	68	Single	Cephalosporin	PTAD + low anterior rectal resection	[16]
Male	67	Single	Cephalosporin	Polypectomy under colonscopy	[16]
Male	77	Single[4]	Cephalosporin + ciprofloxacin + gentamicin	PTAD[7]	[16]
Female	66	Single	Broad spectrum antibiotic[6]	PTAD + sigmoidectomy	[18]
Male	64	Single	Broad spectrum antibiotic[6]	PTAD + right hemi-colectomy + partial hepatectomy	[19]
Male	60	Mutiple	Piperacillin + aminoglycoside	Right hemi-colectomy	[20]
Female	50	Single	Broad spectrum antibiotic[6]	Right hemi-colectomy + partial hepatectomy + chemotherapy	[21]
Male	68	Three	Amoxicillin + clavulanic acid	PTAD + sigmoidectomy	[22]
Male	72	Single	Cephalosporin + metronidazole + gentamicin	PTAD + right hemi-colectomy	[23]
Male	64	Two	Cephalosporin + metronidazole	Sigmoidectomy and radiotherapy	[24]
Female	82	Single	Cephalosporin +metronidazole	PTAD	[26]
Male	52	Mutiple[5]	Broad spectrum antibiotic[6]	Sigmoidectomy + chemotherapy + gemcitabine	[32]
Male	55	Single	Ampicillin + sulbactam + gentamicin	PTAD + sigmoidectomy	[34]

[1]Patient had endophthalmitis with brain, lung abscesses complicated with liver abscesses; [2]Patient developed *S. bovis* bacteremia with complications of endocarditis, osteomyelitis and silent splenic abscess after four episodes of *Klebsiella pneumoniae* liver abscess within 3 years; [3]Patient experienced three episodes of liver abscess within 1 year; [4]Complicated with pulmonary infections; [5]Patient experienced two episodes of liver abscess within 3 mo; [6]Details were not recorded; [7]Patients refused to have further treatments. PTAD: Percutaneous transhepatic abscess drainage.

Table 4 Different therapy for colorectal cancer related liver abscess patients *n* (%)

	No. of patients		*P* value
	Antibiotics alone (*n* = 16)	Antibiotics + drainage (*n* = 42)	
Gender			0.057
Male	13 (81.2)	23 (54.8)	
Female	3 (18.8)	19 (45.2)	
Age (yr)			0.631
< 60	2 (12.5)	5 (11.9)	
> 60	14 (87.5)	37 (88.1)	
Geographic distribution			0.564
Eastern Asia	13 (81.2)	35 (83.3)	
Non-Eastern Asia	3 (18.8)	7 (16.7)	
Pathogen			0.498
K. pneumoniae	6 (37.5)	14 (33.3)	
Non-*K. pneumoniae*	16 (62.5)	28 (66.7)	

K. pneumoniae: *Klebsiella pneumoniae*.

alteration in bowel habit, rectal bleeding and abdominal pain. Besides, liver abscess during the course of an undiagnosed colon cancer may also occur as the initial manifestation of the disease, even without associated metastasis. This PLA had been reported worldwide and was regarded as the herald of colorectal cancers.

Recently, the number of new cases of colorectal cancer-related PLA is soaring in Eastern Asia, and this trend is worthy of concern. We found that 80% of the reported cases in the whole world occurred in the Eastern Asian countries, especially in Japan, China and Korea. The demographic features of the Eastern Asian and non-Eastern Asian patients in this study were non-specific. The mean age was 64.4 years, and male to female ratio was about 1.5:1. However, microbiological feature was different between Eastern Asian and non-Eastern Asian patients. The bacteriologic analysis in our series revealed that *K. pneumoniae* was the most common pathogen in Eastern Asian patients. Our observation was also consistent with the entire incidence of *K. pneumoniae* PLA in Eastern Asian population[38-40].

Clinical features of the colorectal cancer-related PLA patients in this study were non-specific. The most common clinical presentations were fever, chills, abdominal pain, and nausea or vomiting. In contrast, only 10% patients had bowl cancer symptoms and the diagnosis of colorectal cancer was extremely difficult. Colonoscopy was considered as an effective screening method for diagnosis of colorectal cancer. Most (77.3%) of colorectal cancer patients in our study were confirmed by colonoscopy. The colon site of tumor mostly involved was the sigmoid colon (40.9%), followed by the rectum (27.3%), ascending colon (18.2%), transverse colon (7.6%) and descending colon (6.0%). There was significant difference of tumor site between Eastern Asian and non-Eastern Asian patients. Thus, Eastern Asian physicians should be vigilant in monitoring colorectal cancers, especially in the sigmoid colon and rectum.

In our case series, before colorectal cancers were found,

several patients had experienced recurrence of PLA after PTAD treatment[13,15,32]. Destruction of the mucosal barrier of colon and the repeated bacterial translocation was the pathogenesis of liver abscesses in such patients. Thus, although broad spectrum antibiotics combined with PTAD as first-line treatment for the management of PLA had been accepted by most physicians[41], operative intervention for colorectal lesions remains crucial. Meanwhile, in the elderly with recurrent cryptogenic PLA, colonoscopy is suggested and required to avoid misdiagnosis of colorectal cancer.

To our knowledge, this is the first attempt to systemically review the cases of colorectal cancer-related PLA worldwide. However, there still remain limitations to our retrospective study. Incomplete data collection was found during our review of literatures. Some clinical features appeared to have been overlooked; in particular, the relatively non-specific clinical symptoms were missing. In addition, although more reported cases were observed in Eastern Asian than non Eastern Asian countries, the real incidence of colorectal cancer-related PLA is still unknown. Epidemiological investigation with a larger sample size is needed for further analysis.

In conclusion, colorectal cancer-related PLA is an increasing life-threatening disease in Eastern Asia in the recent two decades. In the absence of significant manifestation, the search for the underlying cause of the pyogenic liver abscess should be an integral part of the management of liver abscesses. The association with a colorectal cancer is rare but should be taken into consideration. Early and appropriate surgical treatment can achieve good prognosis.

ACKNOWLEDGMENTS

We thank Dr. Ying Yang from Tangdu Hospital for her critical review and revision of the manuscript. This study was done as a collaborative work of researchers who have long been involved in the field of liver abscess complicated with colorectal cancers. Therefore, sincere thanks for those who supported all prior pilot studies in this field.

COMMENTS

Background

Colorectal cancers related-pyogenic liver abscess (PLA) is a special hepatic infection and regarded as the herald of colon cancer. Recent publications from Eastern Asia revealed a considerable morbidity in this region. Knowledge of etiology and clinical features, when possible, play an important role in the successful treatment of colorectal cancers-related PLA patients.

Research frontiers

PLA, once occurs more frequently in elderly patients with hepatobiliary tract disease or intra-abdominal infections. Recently, many cases of PLA associated with nonmetastatic colorectal carcinomas have been reported in the worldwide. Interestingly, this PLA in Eastern Asia seems to have a greater morbidity and exhibits differences in clinical characteristics. However, there have been few studies to analyze this phenomenon.

Innovations and breakthroughs

This is the first attempt to systemically review the cases of colorectal cancer-related PLA worldwide. A total of 96 cases of colorectal cancers-related PLAs were collected from the international literature and evaluated in clinicopathologic features. This study results revealed that *Klebsiella pneumoniae* (*K. pneumoniae*) PLA was tightly related with colorectal cancer (especially those located in sigmoid colon and rectum) in elderly Eastern Asian males.

Applications

By understanding the different clinicopathological features between patients from Eastern Asia and non-Eastern Asia countries, this study may represent a future strategy for therapeutic intervention in the treatment of patients with colorectal cancer-related PLA.

Terminology

PLA, occurs more frequently in elderly patients with hepatobiliary tract diseases or intra-abdominal infections. For all types of PLA, mucosal defects present within digestive tract lesions are regarded to be the key process. Recent studies revealed that a few PLA patients were related to neoplasms. This type of PLA exhibited different features and was regarded as a warning indicator of silent cancers.

Peer review

The authors reviewed the literature to evaluate features of colorectal cancer-related pyogenic liver abscess. It revealed that there was clear differences in the microbiological spectrum between Asian and non-Asian cases. Gram-negative bacteria especially *K. pneumoniae* PLA was predominant in Eastern Asia. Meanwhile, most of the Eastern Asian patients exhibited smaller size of liver abscess and atypical presentation. Sigmoid colon and rectum were the main sites of tumor in these patients. The results are interesting and may represent a clear understanding of colorectal cancer-related PLA in Eastern Asian patients.

REFERENCES

1 **Branum GD**, Tyson GS, Branum MA, Meyers WC. Hepatic abscess. Changes in etiology, diagnosis, and management. *Ann Surg* 1990; **212**: 655-662
2 **Cohen JL**, Martin FM, Rossi RL, Schoetz DJ. Liver abscess. The need for complete gastrointestinal evaluation. *Arch Surg* 1989; **124**: 561-564
3 **Marcus SG**, Walsh TJ, Pizzo PA, Danforth DN. Hepatic abscess in cancer patients. Characterization and management. *Arch Surg* 1993; **128**: 1358-1364; discussion 1364
4 **Yeh TS**, Jan YY, Jeng LB, Hwang TL, Chao TC, Chien RN, Chen MF. Pyogenic liver abscesses in patients with malignant disease: a report of 52 cases treated at a single institution. *Arch Surg* 1998; **133**: 242-245
5 **Lai HC**, Lin HC. Cryptogenic pyogenic liver abscess as a sign of colorectal cancer: a population-based 5-year follow-up study. *Liver Int* 2010; **30**: 1387-1393
6 **Matsushita M**, Hajiro K, Okazaki K, Takakuwa H, Nishio A. Endophthalmitis with brain, lung, and liver abscesses associated with an occult colon cancer. *Am J Gastroenterol* 2000; **95**: 3664-3665
7 **Ryo Yoshida**, Norio Yokoigawa, Hideho Takada, A Hon Kwon. A rare case of concomitant cardiac insufficiency, and rectal cancer with liver abscess. *Jpn J Clin Surg* 2009; **70**: 1449-1453
8 **Tomonari Katayama**, Takeshi Kikuchi, Kazuhito Uemura, Yoshio Ito, Yoshie Une. A case of rectal cancer complicated with liver abscess. *Jpn J Clin Surg* 2009; **70**: 3074-3079
9 **Hiraoka A**, Yamashita Y, Uesugi K, Koizumi Y, Yamamoto Y, Doi H, Hasebe A, Ichikawa S, Yano M, Miyamoto Y, Ninomiya T, Matsuura B, Horiike N, Michitaka K, Hiasa Y, Nishikage S, Onji M. Three cases of liver abscesses complicated with colon cancer without liver metastasis: importance of screening for digestive disease. *Intern Med* 2007; **46**: 2013-2017
10 **Yokota T**, Iwamoto K, Watanabe Y, Yamauchi H, Kikuchi S, Hatori M. Pyogenic liver abscesses secondary to carcinoma of the sigmoid colon: a case report and clinical features of 20 cases in Japan. *Ups J Med Sci* 2005; **110**: 241-244
11 **Weng SW**, Liu JW, Chen WJ, Wang PW. Recurrent Klebsiella pneumoniae liver abscess in a diabetic patient followed by Streptococcus bovis endocarditis--occult colon tumor

plays an important role. *Jpn J Infect Dis* 2005; **58**: 70-72
12 **Lai HC**, Chan CY, Peng CY, Chen CB, Huang WH. Pyogenic liver abscess associated with large colonic tubulovillous adenoma. *World J Gastroenterol* 2006; **12**: 990-992
13 **Hsu WH**, Yu FJ, Chuang CH, Chen CF, Lee CT, Lu CY. Occult colon cancer in a patient with diabetes and recurrent Klebsiella pneumoniae liver abscess. *Kaohsiung J Med Sci* 2009; **25**: 98-103
14 **Jizheng L**, Congjun H, Hongyi L, Lun W. Liver abscess as initial presentation in colon carcinoma: a case report. *Zhonghua Baojian Yixue Zazhi* 2011; **13**: 259-260
15 **Jeong SW**, Jang JY, Lee TH, Kim HG, Hong SW, Park SH, Kim SG, Cheon YK, Kim YS, Cho YD, Kim JO, Kim BS, Lee EJ, Kim TH. Cryptogenic pyogenic liver abscess as the herald of colon cancer. *J Gastroenterol Hepatol* 2012; **27**: 248-255
16 **Lim WC**, Lim CC. Silent colorectal carcinoma and pyogenic liver abscess. *J Gastroenterol Hepatol* 2004; **19**: 945-946
17 **Leiba A**, Apter S, Avni I, Osherov A, Thaler M, Grossman E. [Pyogenic liver abscess--an unusual presentation of colonic villous adenoma]. *Harefuah* 2003; **142**: 336-337, 399
18 **Teitz S**, Guidetti-Sharon A, Manor H, Halevy A. Pyogenic liver abscess: warning indicator of silent colonic cancer. Report of a case and review of the literature. *Dis Colon Rectum* 1995; **38**: 1220-1223
19 **Tzur T**, Liberman S, Felzenstein I, Cohen R, Rivkind AI, Almogy G. Liver abscesses caused by Streptococcus milleri: an uncommon presenting sign of silent colonic cancer. *Isr Med Assoc J* 2003; **5**: 206-207
20 **Lonardo A**, Grisendi A, Pulvirenti M, Della Casa G, Melini L, Di Gregorio C, Nasi G, Sarti M, Tamborrino E, Lonardo F. Right colon adenocarcinoma presenting as Bacteroides fragilis liver abscesses. *J Clin Gastroenterol* 1992; **14**: 335-338
21 **Giuliani A**, Caporale A, Demoro M, Scimò M, Galati F, Galati G. Silent colon carcinoma presenting as a hepatic abscess. *Tumori* 2007; **93**: 616-618
22 **Fernández Ruiz M**, Guerra Vales JM, Castelbón Fernández FJ, Llenas García J. [Pyogenic liver abscess as presenting manifestation of silent colon adenocarcinoma]. *Rev Esp Enferm Dig* 2007; **99**: 303-305
23 **Alvarez JA**, Baldonedo RF, Bear IG, Alvarez P, Jorge JL. Anaerobic liver abscesses as initial presentation of silent colonic cancer. *HPB* (Oxford) 2004; **6**: 41-42
24 **Zakout R**, Santos JM, Ferreira C, Victorino RM. Colonoscopy for 'cryptogenic' pyogenic liver abscess? *Colorectal Dis* 2010; **12**: 71-72
25 **Pierrugues R**, Taourel P, Avril P. [Liver abscess revealing adenocarcinoma of the right colon]. *J Chir* (Paris) 1994; **131**: 521-522
26 **Abbas SZ**, Cunningham R, Wilkinson SP. An unusual polymicrobial liver abscess. *J Infect* 2000; **40**: 291-292
27 **SHERMAN JD**, ROBBINS SL. Changing trends in the casuistics of hepatic abscess. *Am J Med* 1960; **28**: 943-950
28 **Rubin RH**, Swartz MN, Malt R. Hepatic abscess: changes in clinical, bacteriologic and therapeutic aspects. *Am J Med* 1974; **57**: 601-610
29 **Pitt HA**, Zuidema GD. Factors influencing mortality in the treatment of pyogenic hepatic abscess. *Surg Gynecol Obstet* 1975; **140**: 228-234
30 **Verlenden WL**, Frey CF. Management of liver abscess. *Am J Surg* 1980; **140**: 53-59
31 **Herbert DA**, Fogel DA, Rothman J, Wilson S, Simmons F, Ruskin J. Pyogenic liver abscesses: successful non-surgical therapy. *Lancet* 1982; **1**: 134-136
32 **Lee JK**, Kum J, Ghosh P. Nonmetastatic cancer of the colon associated with pyogenic liver abscess. *Am J Gastroenterol* 2008; **103**: 798-799
33 **Wilson SR**, Arenson AM. Sonographic evaluation of hepatic abscesses. *J Can Assoc Radiol* 1984; **35**: 174-177
34 **Millichap JJ**, McKendrick AI, Drelichman VS. Streptococcus intermedius liver abscesses and colon cancer: a case report. *West Indian Med J* 2005; **54**: 341-342
35 **Cress RD**, Morris C, Ellison GL, Goodman MT. Secular changes in colorectal cancer incidence by subsite, stage at diagnosis, and race/ethnicity, 1992-2001. *Cancer* 2006; **107**: 1142-1152
36 **Center MM**, Jemal A, Ward E. International trends in colorectal cancer incidence rates. *Cancer Epidemiol Biomarkers Prev* 2009; **18**: 1688-1694
37 **Sung JJ**, Lau JY, Goh KL, Leung WK. Increasing incidence of colorectal cancer in Asia: implications for screening. *Lancet Oncol* 2005; **6**: 871-876
38 **Rahimian J**, Wilson T, Oram V, Holzman RS. Pyogenic liver abscess: recent trends in etiology and mortality. *Clin Infect Dis* 2004; **39**: 1654-1659
39 **Lin YT**, Jeng YY, Chen TL, Fung CP. Bacteremic community-acquired pneumonia due to Klebsiella pneumoniae: clinical and microbiological characteristics in Taiwan, 2001-2008. *BMC Infect Dis* 2010; **10**: 307
40 **Cerwenka H**. Pyogenic liver abscess: differences in etiology and treatment in Southeast Asia and Central Europe. *World J Gastroenterol* 2010; **16**: 2458-2462
41 **Mezhir JJ**, Fong Y, Jacks LM, Getrajdman GI, Brody LA, Covey AM, Thornton RH, Jarnagin WR, Solomon SB, Brown KT. Current management of pyogenic liver abscess: surgery is now second-line treatment. *J Am Coll Surg* 2010; **210**: 975-983

S- Editor Cheng JX **L- Editor** Ma JY **E- Editor** Li JY

World Journal of Gastroenterology

Online Submissions: http://www.wjgnet.com/1007-9327office
wjg@wjgnet.com
doi:10.3748/wjg.v18.i23.2956

World J Gastroenterol 2012 June 21; 18(23): 2956-2965
ISSN 1007-9327 (print) ISSN 2219-2840 (online)

ORIGINAL ARTICLE

Targeting X-linked inhibitor of apoptosis protein inhibits pancreatic cancer cell growth through p-Akt depletion

Chun Jiang, Xiao-Ping Yi, Hong Shen, Yi-Xiong Li

Chun Jiang, Department of Gynaecology and Obstetrics, Xiang Ya Hospital, Central South University, Changsha 410008, Hunan Province, China
Xiao-Ping Yi, Department of Radiology, Xiang Ya Hospital, Central South University, Changsha 410008, Hunan Province, China
Hong Shen, Medical Research Center, Xiang Ya Hospital, Central South University, Changsha 410008, Hunan Province, China
Yi-Xiong Li, Department of General Surgery, Xiang Ya Hospital, Central South University, Changsha 410008, Hunan Province, China
Author contributions: Jiang C and Yi XP performed the majority of the experiments; Shen H provided analytical tools and was also involved in editing the manuscript; Li YX provided financial support for this work and designed the study; Jiang C wrote the manuscript.
Supported by National Natural Science Foundation of China, No. 30872492; and Natural Science Foundation of Hunan Province, No. 088JJ3042
Correspondence to: Dr. Yi-Xiong Li, Department of General Surgery, Xiang Ya Hospital, Central South University, 87 Xiang Ya Road, Changsha 410008, Hunan Province, China. liyixiong2011@hotmail.com
Telephone: +86-731-84327021 Fax: +86-731-84327332
Received: October 17, 2011 Revised: April 5, 2012
Accepted: April 10, 2012
Published online: June 21, 2012

Abstract

AIM: To determine whether lentivirus-mediated shRNA targeting the X-linked inhibitor of apoptosis protein (XIAP) gene could be exploited in the treatment of pancreatic cancer.

METHODS: Human pancreatic cancer cells Panc-1, Mia-paca2, Bxpc-3 and SW1990, infected with lentivirus, were analyzed by real-time polymerase chain reaction (PCR). Western blotting was used to examine XIAP protein levels, survivin and p-Akt to confirm the result of real-time PCR and determine the possible mechanism. The 3-(4,5-cimethylthiazol-2-yl)-2,5-diphenyl tetrazolium bromide (MTT) assay was used to measure IC_{50} to determine chemosensitivity to the chemotherapeutic drugs 5-fluorouracil (5-FU) and gemcitabine. A colony assay, MTT assay and a tumorigenicity experiment were used to study cell proliferation *in vitro* and *in vivo*. Caspase-3/7 activity, 4',6-diamidino-2-phenylindole-staining and flow cytometric measurements were used to study apoptosis in SW1990 cells.

RESULTS: XIAP proteins were found to be differentially expressed among pancreatic cancer cell lines Panc-1, Mia-paca2, Bxpc-3 and SW1990. Data of real-time PCR and Western blotting showed that XIAP was reduced persistently and markedly by lentivirus-mediated shRNA. Downregulation of XIAP by transfection with XIAP shRNA resulted in decreased p-Akt expression. XIAP shRNA also inhibited the growth of pancreatic cancer cells *in vitro* and *in vivo*, enhanced drug-induced apoptosis and increased chemosensitivity to 5-FU and gemcitabine. Results also suggest that inhibition of XIAP and subsequent p-Akt depletion may have an anti-tumor effect through attenuating the ability of cancer cells to survive.

CONCLUSION: Lentivirus-mediated gene therapy is an attractive strategy in the treatment of pancreatic cancer and justifies the use of lentivirus in pancreatic cancer gene therapy studies.

Key words: Pancreatic cancer; Lentivirus-mediated shRNA; X-linked inhibitor of apoptosis protein; p-Akt; Gene therapy; Proliferation; Apoptosis

Peer reviewer: Run Yu, MD, PhD, Division of Endocrinology, Diabetes and Metabolism, Cedars-Sinai Medical Center, 8700 Beverly Blvd, B-131, Los Angeles, CA 90048, United States

Jiang C, Yi XP, Shen H, Li YX. Targeting X-linked inhibitor of apoptosis protein inhibits pancreatic cancer cell growth through

p-Akt depletion. *World J Gastroenterol* 2012; 18(23): 2956-2965 Available from: URL: http://www.wjgnet.com/1007-9327/full/v18/i23/2956.htm DOI: http://dx.doi.org/10.3748/wjg.v18.i23.2956

INTRODUCTION

Pancreatic cancer is one of the most aggressive human malignancies, with an extremely poor prognosis and a 5-year survival rate of only approximately 5%[1], partially due to the very little possibility of surgical resection and resistance to chemo-radiotherapy. Disordered apoptosis and abnormal proliferation have been linked with development of malignancy and treatment resistance[2,3]. Apoptosis, also termed programmed cell death, occurs *via* extrinsic or intrinsic signal transduction pathways[4,5]. Therefore, further understanding of the molecular mechanisms, the relationship between pancreatic cancer chemoresistance and disordered apoptosis and abnormal proliferation, can be important in trying to circumvent resistance to cancer therapy[6].

To date, 8 human inhibitor of apoptosis protein (IAP) family members [X-linked IAP (XIAP), cIAP1, cIAP2, IAP-like protein 2, melanoma IAP, neuronal apoptosis inhibitory protein, survivin and baculovirus IAP repeats repeat-containing ubiquitin conjugating enzyme] have been identified. XIAP, a member of the IAP family, plays an important role in regulating both apoptosis and cell proliferation. XIAP is one of the most important members of the IAP family. It is highly expressed in malignant tumor cells and promotes tumor cell invasion, metastasis, growth, survival and chemoresistance. It is reported that XIAP antagonists such as second mitochondria-derived activator of caspase/direct inhibitor of apoptosis-binding protein with low pI increase caspase activity, and not only directly induce apoptosis of many types of tumor cell lines *in vitro*, but also suppress growth of established tumors in xenograft models in mice *in vivo*, while displaying little toxicity to normal tissues. These findings validate XIAP as a target for cancer gene therapy. XIAP is a key factor in malignancy development and treatment resistance, which is associated with disordered cell apoptosis and abnormal proliferation. It is clear that XIAP is one of the most efficient caspase inhibitors of the 8 proteins, and inhibition of apoptosis by XIAP is mainly coordinated through binding to initiator caspase-9 and effector caspase-3 and caspase-7[7-9]. In addition to caspase inhibition, XIAP induces nuclear factor-κB and mitogen-activated protein kinase activation during transforming growth factor-β and bone morphogenetic protein receptor signaling and overexpression. Akt (protein kinase B) represents a subfamily of serine/threonine kinases that promotes cell survival[10]. XIAP and Akt are functionally linked in maintaining homeostasis between cell death and cell proliferation[11]. XIAP may be a core link between the cell apoptosis signaling pathway and the cell survival signaling pathway. Targeting XIAP might simultaneously influence cell apoptosis and proliferation.

RNA interference (RNAi) is a sequence specific post-transcriptional gene silencing factor, which has been extensively used in the study of gene function and gene therapy for cancer[12]. The use of chemically synthesized small interfering RNA (siRNA) or siRNA-encoding plasmids to produce RNAi in mammalian cells by transfection is still limited in clinical application due to some disadvantages including transient expression, and low transfection efficiency especially in non-dividing cells and when it is necessary to generate long-time gene silencing *in vivo*. A lentivirus-based vector is considered to be a promising gene delivery tool because of its ability for specific, highly stable and functional knockout of gene expression in both dividing and non-dividing cells compared with retroviral vectors. In addition, there is minimal immunogenicity associated with lentivirus vectors compared with adenoviral vectors[13-15].

In this study, we constructed lentivirus vectors encoding shRNA targeting the human XIAP gene to study the possible mechanisms of the XIAP gene in regulating apoptosis and proliferation in pancreatic cancer. There was an inhibitory effect of XIAP gene shRNA on the growth of SW1990 cells *in vitro* and *in vivo*, which would be useful for the development of gene therapy approaches for pancreatic cancer treatment in clinical application.

MATERIALS AND METHODS

Construction and production of lentivirus vectors

Three self-complementary hairpin DNA oligos targeting XIAP mRNA and a negative control were synthesized and cloned into a lentivirus vector. A self-inactivating lentivirus vector pGCSIL-PUR (Genechem, Shanghai, China) containing a cytomegalovirus-driven puromycin and a U6 promoter upstream of the cloning restriction sites (*Age*I and *Eco*RI) was used. Three coding regions corresponding to targeting human XIAP (GenBank Accession No: NM_001167) were selected as shRNA target sequences under the guide of the shRNA design protocol. We constructed 3 shRNA-XIAP and negative control lentivirus vectors, namely Lv-X1, Lv-X2, Lv-X3 and Lv-Xnc, respectively (Table 1). Oligonucleotides were annealed and inserted between the *Age*I and *Eco*RI restriction sites of the lentivirus vector. They were confirmed by restriction mapping and DNA sequencing. Lentivirus vector DNA and packaging vectors (pHelper1.0, pHelper2.0) were then transfected into 293T cells. Forty-eight hours later, the supernatant containing the lentivirus particles was collected, filtered through the 0.45 μm cellulose acetate filters, and the titer of lentiviruses was determined by hole-by-dilution titer assay. The virus titers produced was approximately 10^9 TU/mL.

Cell culture and infection

SW1990, Panc-1, Mia-paca2 and Bxpc-3 human pancre-

Table 1 Sequences selected as target sequences of RNA interference against human X-linked inhibitor of apoptosis protein (NM_001167)

Name	Target sequences selected	Sequence cloned into the vector
Lv-X1	GGTGAAGGTGATAAAGTAA	f: 5′-CCGGTAGGTGAAGGTGATAAAGTAATTCAAGAGATTACTTTATCACCTTCACCTA TTTTTG-3′ r: 5′-AATTCAAAAATAGGTGAAGGTGATAAAGTAATCTCTTGAATTACTTTATCACCTTCACCTA-3′
Lv-X2	CTTGAGGAGTGTCTGGTAA	f: 5′-CCGGCACTTGAGGAGTGTCTGGTAATTCAAGAGATTACCAGACACTCCTCAAGTGTTTTTG-3′ r: 5′-AATTCAAAAACACTTGAGGAGTGTCTGGTAATCTCTTGAATTACCAGACACTCCTCAAGTG-3′
Lv-X3	GTGGTAGTCCTGTTTCAGC	f: 5′-CCGGAAGTGGTAGTCCTGTTTCAGCTTCAAGAGAGCTGAAACAGGACTACCACTTTTTTTG-3′ r: 5′-AATTCAAAAAAAGTGGTAGTCCTGTTTCAGCTCTCTTGAAGCTGAAACAGGACTACCACTT-3′
Lv-Xnc	TTCTCCGAACGTGTCACGT	f: 5′-CCGGTTCTCCGAACGTGTCACGTTTCAAGAGAACGTGACACGTTCGGAGAATTTTTG-3′ r: 5′-AATTCAAAAATTCTCCGAACGTGTCACGTTCTCTTGAAACGTGACACGTTCGGAGAA-3′

atic cancer cells were maintained in Dulbecco's modified Eagle's medium (DMEM) containing 10% fetal bovine serum and antibiotics (100 mg/mL streptomycin and 100 U/mL penicillin) at 37 ℃ in a humidified incubator containing 5% CO_2. SW1990 cells were maintained in DMEM and was plated into 6-well plates at 1×10^5 cells per well. Overnight when the cells reached 30%-50% confluence, they were infected with viral particles in the presence of polybrene (5 μg/mL final concentration) and ENi.S (Genechem) for 8 h at a multiplicity of infection (MOI) of 50, and then added to fresh medium. The transfected SW1990 cells were subcultured at an appropriate density in fresh DMEM and 90% of the cells were transfected at 5 d post-transfection as indicated by the expression of green fluorescent protein (GFP) (pGCSIL-GFP empty vector was used to observe the transfection efficiency of lentivirus particles). Pooled stable transfectants were established using puromycin (Sigma-Aldrich, St Louis, MI, United States) selection. Puromycin was added into the medium to select stably transfected cells at a concentration of 1 μg/mL. Puromycin-resistant colonies were picked up 14 d after transfection and stable transfectant cells were maintained in medium containing 0.5 μg/mL puromycin.

Quantification by real-time polymerase chain reaction

Total RNA was isolated using Trizol (Invitrogen). M-MLV reverse transcriptase (Fermentas) was used to create cDNA according to the manufacturer's instructions: 1 μg RNA, Oligo dt18 as primer, 42 ℃ for 60 min, 70 ℃ for 5 min. Quantitative real-time polymerase chain reaction (RT-PCR) assays were carried out using SYBR TAQ real-time kits (TaKaRa Biotechnology, Otsu, Japan) and RT-PCR amplification equipment ABI PRISM 7900HT (Applied Biosystems, Foster City, CA, United States). The PCR primers used to detect XIAP and β-actin were as follows: XIAP, upstream primer 5'-GACAGTATGCAAGATGAGTCAAGTCA-3', downstream primer 5'-GCAAAGCTTCTCCTCTTGCAG-3', with a product length of 93 bp; β-actin, upstream primer 5'-ACTCTTCCAGCCTTCCTTCC-3', downstream primer 5'-GTACTTGCGCTCAGGAGGAG-3', with a product length of 232 bp. The quantitative RT-PCR parameters and analysis of results were performed as normal.

Western blotting analysis

The cell extracts were prepared with lysis buffer radio immunoprecipitation assay containing 50 mmol/L Tris-HCl, pH 7.3, 150 mmol/L NaCl, 2% NP-40, 0.5% deoxycholate, 2 mmol/L ethylenediaminetetraacetic acid, 2 mmol/L NaF, and 1% Protease Inhibitor Cocktail (Pierce, Rockford, IL, United States). Total protein concentration was measured using the BCA assay kit (Sigma, Inc.) with bovine serum albumin as a standard according to the manufacturer's instructions. Western blotting was performed with primer and secondary antibodies: (1) Goat antihuman XIAP polyclonal antibody (R and D Systems Inc., Minneapolis, MN, United States) 1:2000, secondary antibody, 1:10 000; (2) Rabbit antihuman survivin antibody (Novus Biologicals, Inc.) 1:1000, secondary antibody, 1:10 000; (3) Rabbit antihuman p-Akt antibody (Abcam, Inc.) 1:300, secondary antibody, 1:10 000; and (4) Mouse antihuman β-actin monoclonal antibody (Sigma, Inc.) 1:10 000, secondary antibody, 1:10 000. Densitometry was performed by Quantity One image analysis software.

3-(4,5-cimethylthiazol-2-yl)-2,5-diphenyl tetrazolium bromide assay

Cells were plated in 96-well plates at 5×10^3 (to test drug sensitivity) or 1×10^3 (for the growth curves) per well. Cell growth was examined by 3-(4,5-cimethylthiazol-2-yl)-2,5-diphenyl tetrazolium bromide (MTT) assay after lentivirus transfection once a day for 8 d. The cells were cultured in DMEM overnight to ensure that they adhered to the wall of the plates. Various concentrations of 5-fluorouracil (5-FU) or gemcitabine were added to the medium. After incubation for 72 h, 20 μL of 5 mg/mL MTT (Sigma, Inc.) was added to the medium and cultured for another 4 h, then 150 μL of dimethyl sulfoxide (Sigma, Inc.) was added into each well and shaken for 10 min. Absorbance of each well was read using a Bio-Rad model 550-microplate reader (Bio-Rad Co., CA, United States) at a wavelength of 490 nm. Semilogarithmic curves were drawn for cell survival and the logarithm of the drug concentration by SPSS16.0. The 50% inhibitory concentration (IC_{50}) was determined according to the curves.

Colony assay

Approximately 1×10^3 non-transfected control cells and SW1990 cells stably transfected with Lv-Xnc, Lv-X1, Lv-X2, Lv-X3 were plated in 10-cm culture dishes. After 28 d, cells were fixed with methanol and stained with 0.1% crystal violet. Colonies were counted by visual inspection.

Caspase-3/7 activity

Caspase-3/7 activity was evaluated using the Caspase-Glo 3/7 Assay (Promega, Madison, United States) according to the manufacturer's instructions. Cells (1×10^5 cells per well) were seeded in a 6-well plate incubated at 37 ℃ overnight, then specific concentrations of 5-FU or gemcitabine were added into the medium. The ultimate concentrations for both 5-FU and gemcitabine were 1, 10 and 0.1, 1 μg/mL. Plates were further incubated at 37 ℃ for 72 h and luminescence was measured at 3 s delay-time, 10 s duration using SIRIUS Luminometer V3.2 (Berthold, Inc., Germany). Caspase-3/7 activity was normalized to the number of viable cells (as determined by trypan blue staining). Caspase-3/7-fold induction was determined as the ratio between caspase-3/7 activities in treated and control cells.

4',6-diamidino-2-phenylindole staining

Cells were seeded into 24-well plates on sterile round glass coverslips at a density of 2×10^4 cells per well. The cells were incubated in the medium with various concentration of 5-FU or gemcitabine for 72 h. Cells were then washed once with phosphate-buffered saline (PBS) and fixed in PBS containing 4% paraformaldehyde and 10% sucrose at room temperature for 15 min in the dark. Cells were labeled with 4',6-diamidino-2-phenylindole (DAPI) in PBS (1 μg DAPI/mL) at room temperature for 2 min in the dark. Thereafter, cells were washed twice with PBS and once with distilled water, and mounted in glycergel (60%, 4 μL). Staining was visualized *via* fluorescence microscope. The apoptosis index (AI) of cultured SW1990 cells with different lentivirus transfection was calculated using the following formula. AI (%) = apoptotic cells/total cells × 100%.

Flow cytometric measurements

Apoptosis was measured with an annexin V-fluorescein isothiocyanate Apoptosis Detection Kit (Beyotime institute of biotechnology, China). Cells were seeded in 6-well culture plates and divided into the following groups: non-transfected control, SW1990 cells stably transfected with Lv-Xnc, Lv-X1; SW1990 + 5-FU, Lv-Xnc + 5-FU, Lv-X1 + 5-FU; SW1990 + gemcitabine, Lv-Xnc + gemcitabine, Lv-X1 + gemcitabine. Each group contained three culture flasks. When the cells were 70%-80% confluent, cells were added with 1 μg/mL 5-FU or 0.1 μg/mL gemcitabine. After 72 h, the cells were harvested and washed in cold PBS. Annexin V and PI staining were carried out using the Annexin V-FITC Apoptosis Detection Kit according to the manufacturer's protocol. Apoptotic cells were immediately analyzed by fluorescence-activated cell sorting analysis.

Tumorigenicity experiments

To determine whether the Lv-X1 silence XIAP gene could inhibit tumor development *in vivo*, non-transfected control cells, Lv-Xnc control, Lv-X1 transfected SW1990 cells (1.5×10^7 cells in 200 μL DMEM) were injected subcutaneously into the left axilla of BALB/c nude mice (6 mice per group). Tumor growth was monitored every 4 d in 2 dimensions with a vernier caliper, and tumor size was calculated according to the formula $V = a^2b/2$, where a and b are the shortest and longest diameters, respectively.

Statistical analysis

All data are expressed as mean ± SD. Analysis was performed using analysis of variance or the Student *t* test. The relationship between XIAP protein level and IC_{50} was analyzed by Pearson linear correlation analysis. The criterion for significance was $P < 0.05$. All the statistical analysis was performed by SPSS16.0.

RESULTS

XIAP overexpression is associated with greater chemotherapeutic drug chemoresistance

Levels of XIAP expression were highest in Panc-1 and SW1990 cell lines with a higher degree of 5-FU and gemcitabine chemoresistance than Mia-paca2 and Bxpc-3, which expressed XIAP at relatively lower levels (Figure 1A and B).

Selection of the most effective suppression XIAP specific shRNA vector

In order to exclude an off-target silencing effect mediated by specific shRNA, we designed 3 different sequences targeting XIAP and selected the most effective Lv-shRNA in this study. Real-time RT-PCR was performed after transfection and selection with puromycin. The XIAP mRNA expression in Lv-X1, Lv-X2 and Lv-X3 transfected SW1990 cells were reduced by 62.48% ± 7.67%, 49.62% ± 4.7% and 54.47% ± 2.7%, respectively, compared with the Lv-Xnc transfected control ($P < 0.05$). In addition, no difference was observed between the Lv-Xnc control and the SW1990 control ($P > 0.05$) (Figure 1C). Western blotting revealed that the inhibition efficiencies on XIAP protein expression by Lv-X1, Lv-X2, and Lv-X3 lentivirus were consistent with that on the targeted genes' mRNA expression. XIAP protein was knocked down in Lv-X1, Lv-X2 and Lv-X3 transfected SW1990 cells, its expression demonstrated a significant reduction in Lv-X1 (5.98% ± 0.7%), Lv-X2 (12.32% ± 0.9%) and Lv-X3 (13.52% ± 2.2%) transfected SW1990 cells compared with the Lv-Xnc transfected control ($P < 0.05$). In addition, no difference was observed between the Lv-Xnc control and the SW1990 control ($P > 0.05$) (Figure 1D). According to the results of RT-PCR and Western blotting, Lv-X1 was the most effective lentivirus vector and thus we used it in the following research. To validate the specificity of RNAi targeting XIAP, we also determined the level of anther IAP family protein, survivin. The results showed that survivin was not affected by any constructed lentivirus (Figure 1D).

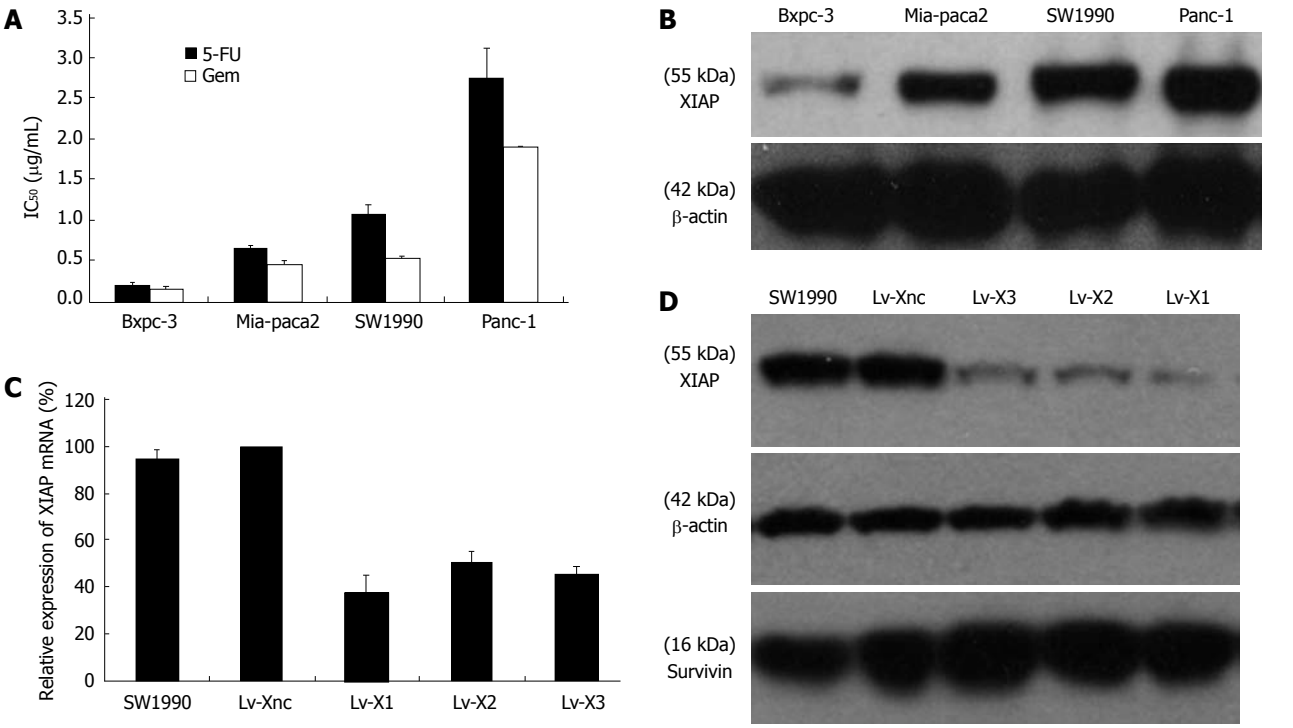

Figure 1 X-linked inhibitor of apoptosis protein expression analysis and selection of the RNAi target for X-linked inhibitor of apoptosis protein. A, B: The X-linked inhibitor of apoptosis protein (XIAP) protein level and IC_{50} for Panc-1, SW1990, Mia-paca2 and Bxpc-3 cell lines. R^2 = 0.87 (Spearman correlation) between IC_{50} and relative XIAP expression, $P < 0.05$; C: Relative expression of XIAP mRNA after transfection and selection with puromycin; D: Downregulatory effect of lentivirus-mediated RNAi on XIAP in SW1990 cells. Lv-X1, Lv-X2, Lv-X3 efficiently suppressed XIAP expression. The results also showed that survivin was not affected by any lentivirus. Lv-Xnc, which was transfected with the non-sense lentivirus vector, was set as the calibrator with the relative expression value of "1". β-actin was used as the internal loading control in three independent experiments. 5-FU: 5-fluorouracil.

Suppression of XIAP expression enhances drug-induced cytotoxicity and inhibits cell proliferation in vitro and in vivo

To determine the IC_{50}, cells were exposed to 1000, 100, 10, 1, 0.1, 0.01 and 0.001 μg/mL 5-FU or gemcitabine for 72 h. The IC_{50} was calculated from MTT cytotoxicity assay data. Lv-X1 (0.2 ± 0.01 μg/mL for 5-FU, 0.14 ± 0.03 μg/mL for gemcitabine), Lv-X2 (0.72 ± 0.08 μg/mL for 5-FU, 0.42 ± 0.02 μg/mL for gemcitabine), Lv-X3 (0.5 ± 0.05 μg/mL for 5-FU, 0.28 ± 0.01 μg/mL for gemcitabine) inhibited the IC_{50} significantly ($P < 0.05$ *vs* Lv-Xnc), and Lv-X1 was the most effective. Lv-Xnc control had no effect on the IC_{50} ($P > 0.05$ *vs* SW1990 control) (Figure 2A). When compared with SW1990 and Lv-Xnc control cells, Lv-X1, Lv-X2 and Lv-X3 infected SW1990 transfected cells showed much slower growth, especially Lv-X1 infected SW1990 transfected cells. XIAP shRNA lentivirus transfection knockdown of XIAP significantly inhibited the proliferation of cultured SW1990 cells *in vitro* at the time points from day 4 to day 8 ($P < 0.05$) (Figure 2B). The result of the colony formation assay indicated that the number of colonies of Lv-X1 cells (55.26% ± 3.74%) were much less than that of Lv-Xnc (100.6% ± 5.07%) and non-transfected cells (100% ± 6.04%) ($P < 0.05$) (Figure 2C). To determine whether Lv-X1 knockout of the XIAP gene could inhibit tumor development *in vivo*, SW1990 control cells, Lv-Xnc control, and Lv-X1 infected SW1990 cells were injected into BALB/c nude mice and tumor growth was monitored every 4 d. At the time points of day 16 to day 28 after SW1990 implantation, the tumorigenicity experiments revealed that suppression of XIAP in the Lv-X1 group significantly inhibited the growth of the transplanted tumor in nude mice, which was consistent with the results achieved from the experiments *in vitro* ($P < 0.05$). For example, the tumor volume in nude mice at day 28 after the inoculation of SW1990 cells in groups of non-transfected, Lv-Xnc and Lv-X1 were 1223.28 ± 176.14, 1173.45 ± 149.61 and 532.83 ± 84.59 mm^3, respectively. When compared with SW1990 and Lv-Xnc control cells, Lv-X1 infected SW1990 transfected cells developed much smaller tumors in the nude mice ($P < 0.05$) (Figure 2D).

XIAP specific silencing enhances drug-induced activation of caspase-3/7 and enhances drug-induced apoptosis

5-FU or gemcitabine induced apoptosis in cancer cells, *via* caspase activation and inhibition of apoptosis by XIAP, was mainly coordinated through binding to effector caspase-3 and caspase-7. Thus, we sought to determine the effect of XIAP silencing on caspase activities after exposure to different concentrations of 5-FU or gemcitabine for 72 h. 5-FU or gemcitabine-induced caspase-3/7 activity was markedly increased after transfection of Lv-X1 (4.41 ± 0.51-fold, 23.31 ± 8.14-fold at 1,

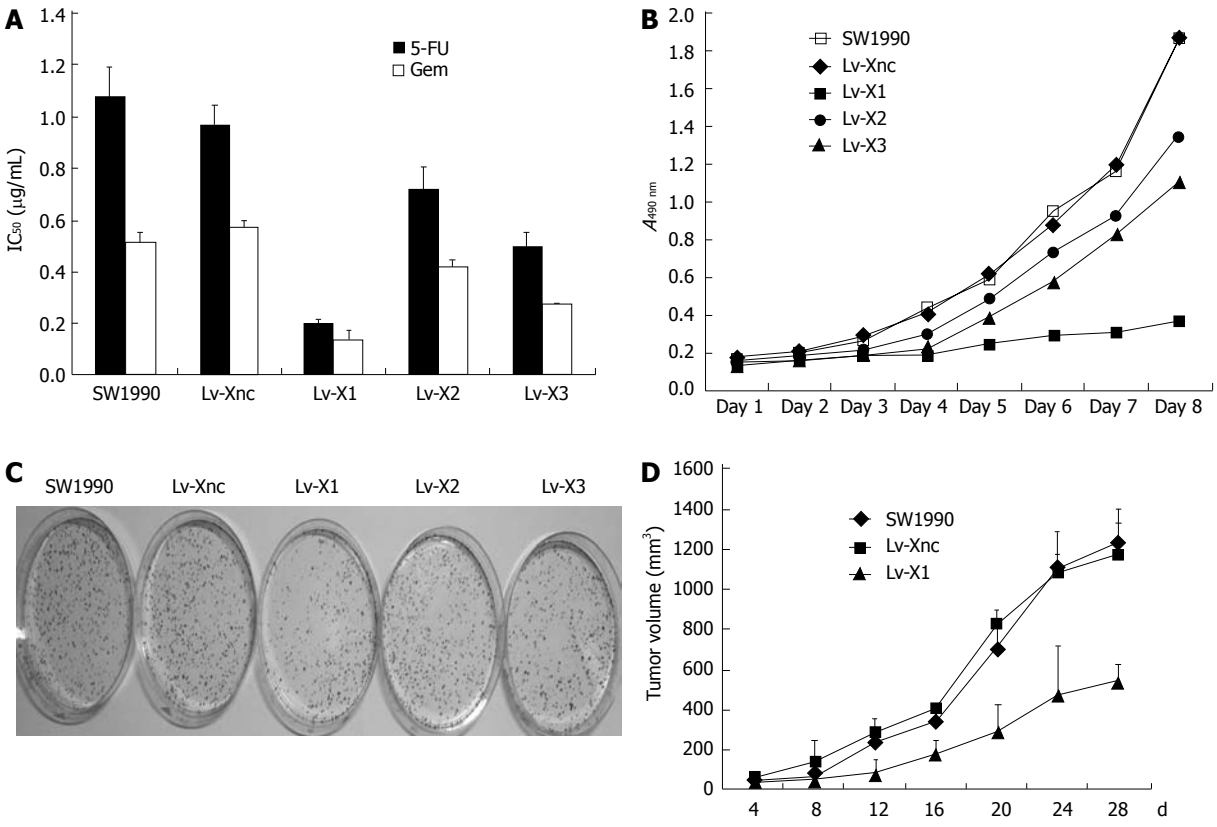

Figure 2 Lentivirus-mediated shRNA targeting the X-linked inhibitor of apoptosis protein gene inhibits the growth of human pancreatic cancer SW1990 cells *in vitro* and *in vivo* and promotes chemosensitivity to drugs. A: Lv-X1, Lv-X2, Lv-X3 promoted 5-fluorouracil (5-FU) or gemcitabine-induced cytotoxicity. The IC_{50} was determined by 3-(4,5-cimethylthiazol-2-yl)-2,5-diphenyl tetrazolium bromide assay after exposure to 5-FU or gemcitabine for 72 h; B: The growth curves of different stably transfected cell lines; C: Results of colony formation assay. Lv-X1 had much fewer colonies than Lv-Xnc and untransfected cells. These experiments were performed 3 times; D: SW1990, Lv-Xnc and Lv-X1 cells growth in BALB/c nude mice ($P < 0.05$, from day 12 to day 28).

10 μg/mL 5-FU, respectively; 20.26 ± 0.96-fold, 36.62 ± 3.77-fold at 0.1, 1 μg/mL gemcitabine, respectively), but was unaffected after transfection of Lv-Xnc control. In addition, blank Lv-X1 (1.07 ± 0.03-fold) and Lv-Xnc (1.03 ± 0.01-fold) caspase-3/7 activity, although slightly increased, were not significantly different compared with SW1990 control (Figure 3A), which was also confirmed by DAPI staining and flow cytometry (FCM) (Figure 3B and C). We used DAPI staining to observe the morphological changes of apoptosis and the apoptosis index of DAPI staining analysis was consistent with caspase-3/7 activity (Figure 3B). To validate the results of DAPI staining, SW1990 and stably transfected SW1990 cells (Lv-Xnc, Lv-X1) were stained with annexin V and PI and analyzed by FCM. Cell apoptosis analysis indicated that downregulation of XIAP was not associated with a significantly increased spontaneous apoptosis rate (there were no obvious differences in apoptosis rates among SW1990 (3.03% ± 0.49%), Lv-X1 (5.06% ± 0.54%) and Lv-Xnc (4.21% ± 0.36%) ($P > 0.05$)), while the apoptosis of Lv-X1 + 5-FU (12.7% ± 0.50%) or Lv-X1 + Gem (13.68% ± 0.56%) was significantly increased compared with SW1990 and Lv-Xnc control cells ($P < 0.05$) (Figure 3C). All these results showed that the lentivirus-mediated inhibition of XIAP expression did not lead to acceleration of the apoptosis of SW1990 cells.

Downregulation of XIAP with Lv-X1 decreased p-Akt levels

We observed that decreased expression of XIAP resulted in inhibition of cell proliferation according to the results of the growth curves and colony formation assay of different stably transfected cell lines (Figure 2B-D). Caspase-3/7 activity, DAPI staining and FCM analysis of Lv-X1 groups although slightly increased, showed no significant differences compared with controls (Figure 3A-C). It is reported that apoptotic pathways in cancer functionally crossover with survival pathways PI3K/Akt, and compared with the Lv-Xnc group, XIAP protein expression levels in cells transfected with Lv-X1 were reduced by 92.55% ± 0.78% ($P < 0.05$), and p-Akt protein expression in Lv-X1 transfection groups was reduced by 94.63% ± 0.32% ($P < 0.05$) (Figure 4). We found that downregulation of XIAP with Lv-X1 decreased p-Akt levels, which might explain the phenomenon.

DISCUSSION

It has been reported that XIAP is overexpressed in many human malignancies such as ovarian carcinoma, laryngeal cancer, esophageal cancer, breast cancer, hepatoma cells, colon cancer, and pancreatic cancer. Upregulated levels of XIAP expression have been correlated with

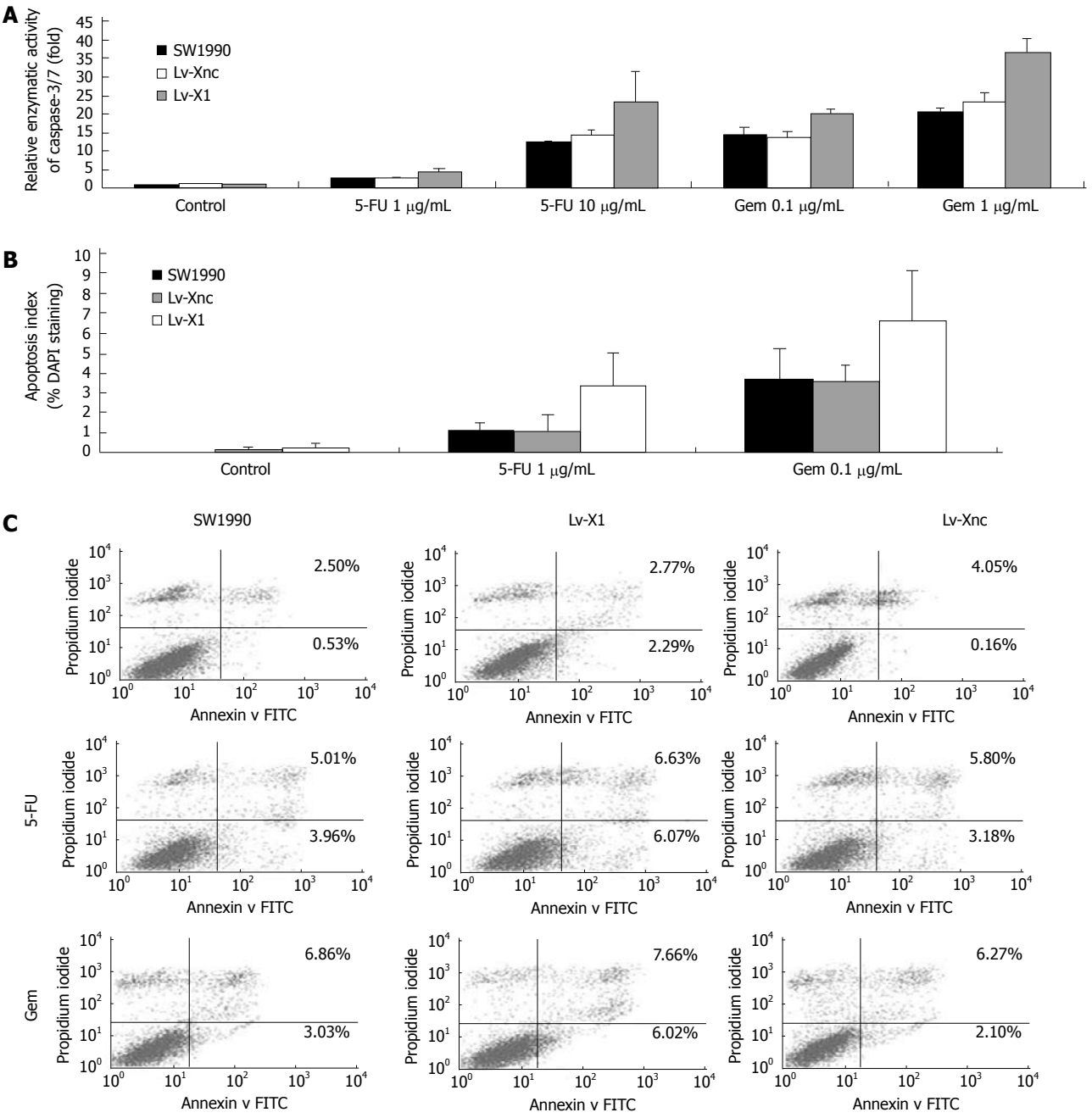

Figure 3 Apoptosis analysis. A: Relative enzymatic activity of caspase-3/7; B: Apoptosis examined by 4',6-diamidino-2-phenylindole (DAPI) staining (200×), apoptosis index (%) = Apoptotic cells/Total cells × 100% (Seen in a same microscopic field and 3 randomized microscopic fields chosen for counting) using DAPI staining. Either gemcitabine or 5-fluorouracil (5-FU) kills cancer cells by inducing apoptosis, and X-linked inhibitor of apoptosis protein knocked out by Lv-X1 can enhance the capacity of the 2 drugs; C: Flow cytometry: The apoptotic rate of Lv-X1 and Lv-Xnc slightly increased but there was no significant difference among SW1990, Lv-X1 and Lv-Xnc. While the apoptotic rate of Lv-X1 + 5-FU and Lv-X1 + gemcitabine increased (12.7% and 13.68%, respectively, $P < 0.05$). FITC: Fluorescein isothiocyanate.

tumor resistance to chemotherapy or radiotherapy, and some researchers have reported that inhibition of XIAP by siRNA, plasmid or adenovirus mediated-shRNA can reduce tumor cell growth, induce apoptosis and enhance the sensitivity of tumor cells to chemotherapeutic or radiotherapeutic agents[16-21]. Though chemically synthesized siRNA can be introduced into cells *via* traditional delivery strategies including liposomes, polyethyleneimine, or electroporation, these methods have short gene silencing effects and the effects cannot be passed to cell progeny. Other gene delivery systems such as adenovirus showed transient expression of the transgene and immunogenicity. Lentivirus vectors were developed to overcome these disadvantages. Recently, the lentivirus vector-mediated gene therapy including RNAi or overexpression has shown great promise in pancreatic cancer and other tumors because of its long-term gene expression and high efficiency in transducing dividing and non-dividing cells[22-25].

As we know, Panc-1 and Mia-paca2 are poorly differentiated; SW1990 and Bxpc-3 are moderately differentiated. In our study, human pancreatic cancer cell lines

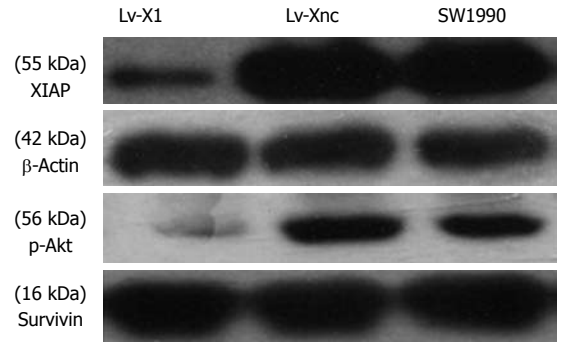

Figure 4 Immunoblot analysis for p-Akt in SW1990 cells after stable transfection. Downregulation of X-linked inhibitor of apoptosis protein with Lv-X1 largely decreased p-Akt protein levels and survivin was not affected (6 mo in culture).

with higher levels of XIAP protein displayed greater 5-FU or gemcitabine chemoresistance (Figure 1A and B).

In this study, we found that lentivirus-based vectors were extremely efficient in transducing SW1990 cells. *In vitro*, 79% of the cells expressed GFP at a MOI of 50. In addition, GFP expression was stable up to 6 mo in culture (data was not shown). To determine whether lentivirus-mediated shRNA could stably inhibit the expression of XIAP, pooled clones were expanded, and stably transfected cells were lysed for Western blotting analysis 6 mo later. The results showed that the expression of XIAP in Lv-X1 cell was still markedly reduced (Figure 4). It indicated that lentivirus-based shRNA resulted in a persistent gene knockdown instead of a transient inhibitory effect.

Furthermore, the strong inhibition of XIAP by lentivirus could inhibit proliferation of SW1990 cells (Figure 2B-D), enhance drug-induced apoptosis and promote chemosensitivity to chemotherapeutic drugs, which also were reported in other studies (Figure 3A-C)[26,27], and some drugs induce apoptosis through downregulation of cell survival proteins and upregulation of death receptors *via* the reactive oxygen species-mediated upregulation of the CHOP (CCAAT/enhancer-binding protein-homologous protein) pathway[28]. Some studies showed that silencing the XIAP gene resulted in a significant induction of apoptosis in pancreatic cancer cells Mia-paca2 and AsPC-1[29]. In this study, we did not find that downregulation of XIAP was associated with a significantly increased spontaneous apoptosis rate (Figure 3A-C), which was consistent with some other previous studies[30]. To validate the specificity of RNAi targeting XIAP and to avoid off-target phenomenon, we transfected the cells with lentivirus carrying 3 different shRNA sequences against XIAP and determined the level of another IAP family protein survivin (Figures 1-4). The results showed that survivin was not affected by any constructed lentivirus, which was not consistent with previous studies[31].

One of the greatest challenges for researchers in new treatment strategies for pancreatic cancer is the obvious need to test them in preclinical *in vivo* animal models that have a good probability of being predictive of similar activity in humans. The most used models are xenografts of human tumors grown subcutaneously in immunodeficient mice such as BALB/c nude mice[32]. In this study, we determined whether SW1990 cells stably transfected with lentivirus have reduced tumorigenicity. In the xenograft model, BALB/c nude mice that received injection of Lv-X1 cells developed tumors of a smaller size compared with control, and also showed higher levels of XIAP protein and greater tumorigenicity (Figure 2D). These findings were consistent with some previous studies in xenograft models, in which tumors from the parental pancreatic carcinoma cells with stable XIAP knockdown clones showed growth retardation[33].

Akt, which has been shown to have both prosurvival and antiapoptotic functions, is a serine/threonine kinase that is known to have at least 3 isoforms (Akt1, Akt2 and Akt3), all of which are activated by phosphoinositide 3-kinase (PI3K), and p-Akt is an activity form of Akt. It is reported that total Akt (phosphorylated + non-phosphorylated) was not altered by XIAP, nor was the expression of the p85 subunit of PI3K, suggesting a direct influence of XIAP upon Akt activation rather than an upregulation of Akt expression[34]. One of the Akt substrates identified to have antiapoptotic effects is Bad, which is the proapoptotic Bcl-2 family member that initiates apoptosis *via* binding antiapoptotic Bcl-2 family members and results in the release of cytochrome c from mitochondria. Akt has also been shown to directly phosphorylate and inactivate caspase-9[10,35], which is coordinated through binding to XIAP. Recently, XIAP was added to the list of Akt substrates. Akt has been shown to prevent the ubiquitination and degradation of XIAP *via* phosphorylation both *in vitro* and *in vivo*, and XIAP is a downstream target of Akt and a potentially important mediator of the effect of Akt on cell survival[36]. XIAP is also thought to promote Akt activity, XIAP acting as an E3 ubiquitin ligase for PTEN and promotes Akt activity by regulating PTEN content and compartmentalization, while XIAP silencing reduces constitutive mono- and poly-ubiquitination of PTEN, increases PTEN protein levels, and prevents nuclear accumulation of PTEN[37]. Furthermore, it has been reported that suppression of XIAP by either siRNA or antisense adenovirus of XIAP induced apoptosis and inhibited Akt-stimulated cell survival in ovarian cancer cells and uterine cancer cells[11,34]. These results are significant because they suggest a feedback regulation of XIAP and Akt. In this study, we found stable downregulation of XIAP with Lv-X1 in SW1990 pancreatic cancer cells markedly decreased the p-Akt protein level (Figure 4). Perhaps XIAP is a potentially important mediator of the effect of Akt on cell survival in pancreatic cancer cells as well as in ovarian and uterine cancer cells. While XIAP upregulates Akt phosphorylation and requires Akt for its function, so stable downregulation of XIAP markedly decreases the p-Akt protein level in SW1990 pancreatic cancer cells. Thus, it appears that there is an intricate, coordinated regulatory system at play between XIAP and the PI3K/Akt signaling pathway. Additional studies are necessary

to determine the precise molecular mechanism by which XIAP regulates the Akt survival pathway.

In summary, our findings demonstrate for the first time that suppression of XIAP expression *via* lentivirus-mediated shRNA represents a novel strategy for chemosensitizing pancreatic cancer cells to chemotherapeutic drugs. Our study indicates that lentivirus-mediated inhibition of XIAP is an attractive therapeutic strategy in the treatment of pancreatic cancer and justifies the use of lentivirus in cancer gene therapy studies. However, emergence of replication competent lentivirus *in vivo*, transcriptional targeting affected by the chromosomal integration site and risk of oncogene activation by the lentivirus are current problems, and an effective and safe protocol should be developed. Thus, there remains a long road before lentivirus-mediated shRNA targeting XIAP can be introduced into clinical use.

COMMENTS

Background

Pancreatic cancer is one of the most aggressive human malignancies with an extremely poor prognosis and a 5-year survival rate of only approximately 5%, partially because of the low possibility of surgical resection and resistance to chemo-radiotherapy.

Research frontiers

It has been reported that X-linked inhibitor of apoptosis protein (XIAP) is overexpressed in many human malignancies. The upregulated levels of XIAP expression have been correlated with tumor resistance to chemotherapy or radiotherapy. Lentivirus vector-mediated gene therapy has great promise in pancreatic cancer because of its long-term gene expression and high efficiency. Thus it is necessary to determine whether lentivirus-mediated shRNA targeting XIAP gene could be exploited in the treatment of pancreatic cancer.

Innovations and breakthroughs

XIAP proteins were found to be differentially expressed among pancreatic cancer cell lines. Downregulation of XIAP by transfection with XIAP shRNA resulted in decreased p-Akt expression. Moreover, it could inhibit the growth of pancreatic cancer cells *in vitro* and *in vivo* and enhance drug-induced apoptosis and promote chemosensitivity to chemotherapeutic drugs 5-fluorouracil and gemcitabine. Results also suggest that inhibition of XIAP and subsequent p-Akt depletion may have an anti-tumor effect through attenuating the ability of cancer cells to survive. Perhaps XIAP is a potentially important mediator of the effect of Akt on cell survival in pancreatic cancer cells. It appears that there is an intricate, coordinated regulatory system at play between XIAP and the phosphatidylinositol 3-kinases/Akt signaling pathway.

Applications

The results suggest that suppression of XIAP expression *via* lentivirus-mediated shRNA represents a novel strategy for chemosensitizing pancreatic cancer to chemotherapeutic drugs. Lentivirus-mediated inhibition of XIAP is an attractive therapeutic strategy in the treatment of pancreatic cancer and justifies the use of lentivirus in cancer gene therapy studies.

Terminology

XIAP: A member of the IAP family, plays an important role in regulating both apoptosis and cell proliferation; Apoptosis or programmed cell death: Disordered apoptosis and abnormal proliferation have been linked to malignancy development and treatment resistance; Akt: Also termed protein kinase B, represents a subfamily of serine/threonine kinases that promotes cellular survival. RNAi: RNA interference, a sequence specific posttranscriptional gene silencing process, which has been extensively used in the study of gene function and gene therapy for cancer.

Peer review

This is an interesting manuscript. The data is solid, but it is still a long way from lentivirus-mediated shRNA targeting XIAP to clinical use.

REFERENCES

1 **Jemal A**, Siegel R, Xu J, Ward E. Cancer statistics, 2010. *CA Cancer J Clin* 2010; **60**: 277-300
2 **Hanahan D**, Weinberg RA. Hallmarks of cancer: the next generation. *Cell* 2011; **144**: 646-674
3 **Ghavami S**, Hashemi M, Ande SR, Yeganeh B, Xiao W, Eshraghi M, Bus CJ, Kadkhoda K, Wiechec E, Halayko AJ, Los M. Apoptosis and cancer: mutations within caspase genes. *J Med Genet* 2009; **46**: 497-510
4 **Qiao L**, Wong BC. Targeting apoptosis as an approach for gastrointestinal cancer therapy. *Drug Resist Updat* 2009; **12**: 55-64
5 **Schimmer AD**. Inhibitor of apoptosis proteins: translating basic knowledge into clinical practice. *Cancer Res* 2004; **64**: 7183-7190
6 **Kim R**, Tanabe K, Uchida Y, Emi M, Inoue H, Toge T. Current status of the molecular mechanisms of anticancer drug-induced apoptosis. The contribution of molecular-level analysis to cancer chemotherapy. *Cancer Chemother Pharmacol* 2002; **50**: 343-352
7 **Danson S**, Dean E, Dive C, Ranson M. IAPs as a target for anticancer therapy. *Curr Cancer Drug Targets* 2007; **7**: 785-794
8 **Hunter AM**, LaCasse EC, Korneluk RG. The inhibitors of apoptosis (IAPs) as cancer targets. *Apoptosis* 2007; **12**: 1543-1568
9 **Lopes RB**, Gangeswaran R, McNeish IA, Wang Y, Lemoine NR. Expression of the IAP protein family is dysregulated in pancreatic cancer cells and is important for resistance to chemotherapy. *Int J Cancer* 2007; **120**: 2344-2352
10 **Datta SR**, Brunet A, Greenberg ME. Cellular survival: a play in three Akts. *Genes Dev* 1999; **13**: 2905-2927
11 **Gagnon V**, Van Themsche C, Turner S, Leblanc V, Asselin E. Akt and XIAP regulate the sensitivity of human uterine cancer cells to cisplatin, doxorubicin and taxol. *Apoptosis* 2008; **13**: 259-271
12 **Hannon GJ**. RNA interference. *Nature* 2002; **418**: 244-251
13 **Manjunath N**, Wu H, Subramanya S, Shankar P. Lentiviral delivery of short hairpin RNAs. *Adv Drug Deliv Rev* 2009; **61**: 732-745
14 **Rubinson DA**, Dillon CP, Kwiatkowski AV, Sievers C, Yang L, Kopinja J, Rooney DL, Zhang M, Ihrig MM, McManus MT, Gertler FB, Scott ML, Van Parijs L. A lentivirus-based system to functionally silence genes in primary mammalian cells, stem cells and transgenic mice by RNA interference. *Nat Genet* 2007; **39**: 803
15 **Waehler R**, Russell SJ, Curiel DT. Engineering targeted viral vectors for gene therapy. *Nat Rev Genet* 2007; **8**: 573-587
16 **Wang R**, Li B, Wang X, Lin F, Gao P, Cheng SY, Zhang HZ. Inhibiting XIAP expression by RNAi to inhibit proliferation and enhance radiosensitivity in laryngeal cancer cell line. *Auris Nasus Larynx* 2009; **36**: 332-339
17 **Zhang S**, Ding F, Luo A, Chen A, Yu Z, Ren S, Liu Z, Zhang L. XIAP is highly expressed in esophageal cancer and its downregulation by RNAi sensitizes esophageal carcinoma cell lines to chemotherapeutics. *Cancer Biol Ther* 2007; **6**: 973-980
18 **Zhang Y**, Wang Y, Gao W, Zhang R, Han X, Jia M, Guan W. Transfer of siRNA against XIAP induces apoptosis and reduces tumor cells growth potential in human breast cancer in vitro and in vivo. *Breast Cancer Res Treat* 2007; **103**: 129
19 **Yamaguchi Y**, Shiraki K, Fuke H, Inoue T, Miyashita K, Yamanaka Y, Saitou Y, Sugimoto K, Nakano T. Targeting of X-linked inhibitor of apoptosis protein or survivin by short interfering RNAs sensitize hepatoma cells to TNF-related apoptosis-inducing ligand- and chemotherapeutic agent-induced cell death. *Oncol Rep* 2005; **14**: 1311-1316
20 **Dai Y**, Qiao L, Chan KW, Yang M, Ye J, Zhang R, Ma J, Zou B, Lam CS, Wang J, Pang R, Tan VP, Lan HY, Wong BC. Adenovirus-mediated down-regulation of X-linked inhibi-

tor of apoptosis protein inhibits colon cancer. *Mol Cancer Ther* 2009; **8**: 2762-2770
21 **Li Y**, Jian Z, Xia K, Li X, Lv X, Pei H, Chen Z, Li J. XIAP is related to the chemoresistance and inhibited its expression by RNA interference sensitize pancreatic carcinoma cells to chemotherapeutics. *Pancreas* 2006; **32**: 288-296
22 **Jiang G**, Li J, Zeng Z, Xian L. Lentivirus-mediated gene therapy by suppressing survivin in BALB/c nude mice bearing oral squamous cell carcinoma. *Cancer Biol Ther* 2006; **5**: 435-440
23 **Wang F**, Chen L, Mao ZB, Shao JG, Tan C, Huang WD. Lentivirus-mediated short hairpin RNA targeting the APRIL gene suppresses the growth of pancreatic cancer cells in vitro and in vivo. *Oncol Rep* 2008; **20**: 135-139
24 **Liau SS**, Ashley SW, Whang EE. Lentivirus-mediated RNA interference of HMGA1 promotes chemosensitivity to gemcitabine in pancreatic adenocarcinoma. *J Gastrointest Surg* 2006; **10**: 1254-1262; discussion 1263
25 **Ravet E**, Lulka H, Gross F, Casteilla L, Buscail L, Cordelier P. Using lentiviral vectors for efficient pancreatic cancer gene therapy. *Cancer Gene Ther* 2010; **17**: 315-324
26 **Shrikhande SV**, Kleeff J, Kayed H, Keleg S, Reiser C, Giese T, Büchler MW, Esposito I, Friess H. Silencing of X-linked inhibitor of apoptosis (XIAP) decreases gemcitabine resistance of pancreatic cancer cells. *Anticancer Res* 2006; **26**: 3265-3273
27 **Vogler M**, Walczak H, Stadel D, Haas TL, Genze F, Jovanovic M, Gschwend JE, Simmet T, Debatin KM, Fulda S. Targeting XIAP bypasses Bcl-2-mediated resistance to TRAIL and cooperates with TRAIL to suppress pancreatic cancer growth in vitro and in vivo. *Cancer Res* 2008; **68**: 7956-7965
28 **Sung B**, Park B, Yadav VR, Aggarwal BB. Celastrol, a triterpene, enhances TRAIL-induced apoptosis through the down-regulation of cell survival proteins and up-regulation of death receptors. *J Biol Chem* 2010; **285**: 11498-11507
29 **Rückert F**, Samm N, Lehner AK, Saeger HD, Grützmann R, Pilarsky C. Simultaneous gene silencing of Bcl-2, XIAP and Survivin re-sensitizes pancreatic cancer cells towards apoptosis. *BMC Cancer* 2010; **10**: 379
30 **McManus DC**, Lefebvre CA, Cherton-Horvat G, St-Jean M, Kandimalla ER, Agrawal S, Morris SJ, Durkin JP, Lacasse EC. Loss of XIAP protein expression by RNAi and antisense approaches sensitizes cancer cells to functionally diverse chemotherapeutics. *Oncogene* 2004; **23**: 8105-8117
31 **Zhu Y**, Roshal M, Li F, Blackett J, Planelles V. Upregulation of survivin by HIV-1 Vpr. *Apoptosis* 2003; **8**: 71-79
32 **Céspedes MV**, Casanova I, Parreño M, Mangues R. Mouse models in oncogenesis and cancer therapy. *Clin Transl Oncol* 2006; **8**: 318-329
33 **Mohr A**, Albarenque SM, Deedigan L, Yu R, Reidy M, Fulda S, Zwacka RM. Targeting of XIAP combined with systemic mesenchymal stem cell-mediated delivery of sTRAIL ligand inhibits metastatic growth of pancreatic carcinoma cells. *Stem Cells* 2010; **28**: 2109-2120
34 **Asselin E**, Mills GB, Tsang BK. XIAP regulates Akt activity and caspase-3-dependent cleavage during cisplatin-induced apoptosis in human ovarian epithelial cancer cells. *Cancer Res* 2001; **61**: 1862-1868
35 **Straszewski-Chavez SL**, Abrahams VM, Aldo PB, Romero R, Mor G. AKT controls human first trimester trophoblast cell sensitivity to FAS-mediated apoptosis by regulating XIAP expression. *Biol Reprod* 2010; **82**: 146-152
36 **Dan HC**, Sun M, Kaneko S, Feldman RI, Nicosia SV, Wang HG, Tsang BK, Cheng JQ. Akt phosphorylation and stabilization of X-linked inhibitor of apoptosis protein (XIAP). *J Biol Chem* 2004; **279**: 5405-5412
37 **Van Themsche C**, Leblanc V, Parent S, Asselin E. X-linked inhibitor of apoptosis protein (XIAP) regulates PTEN ubiquitination, content, and compartmentalization. *J Biol Chem* 2009; **284**: 20462-20466

S- Editor Cheng JX **L- Editor** Cant MR **E- Editor** Li JY

World Journal of Gastroenterology

Online Submissions: http://www.wjgnet.com/1007-9327office
wjg@wjgnet.com
doi:10.3748/wjg.v18.i23.2966

World J Gastroenterol 2012 June 21; 18(23): 2966-2972
ISSN 1007-9327 (print) ISSN 2219-2840 (online)

BRIEF ARTICLE

Impact of ribavirin dose on retreatment of chronic hepatitis C patients

Christiane Stern, Michelle Martinot-Peignoux, Marie Pierre Ripault, Nathalie Boyer, Corinne Castelnau, Dominique Valla, Patrick Marcellin

Christiane Stern, Michelle Martinot-Peignoux, Marie Pierre Ripault, Nathalie Boyer, Corinne Castelnau, Dominique Valla, Patrick Marcellin, Service d'Hépatologie and INSERM U773-CRB3, Hôpital Beaujon, University Paris-Diderot, 92110 Clichy, France

Author contributions: Stern C, Martinot-Peignoux M and Marcellin P designed the study; Stern C and Ripault MP collected the data; Martinot-Peignoux M performed the measurements and analyses; Stern C performed statistical analyses; Boyer N, Castelnau C and Valla D contributed to the interpretation of data; Stern C and Marcellin P drafted the manuscript; and all authors have read and approved the final manuscript.

Supported by Assistance publique-Hôpitaux de Paris, INSERM U773-CRB3 and University Paris-Diderot; Fees from Roche, Schering Plough, Novartis, Gilead Sciences, BMS, MSD, Vertex, Tibotec, Biolex, to Marcellin P; Zymmogenetics and grants from Gilead Sciences, Roche and Schering Plough

Correspondence to: Patrick Marcellin, MD, Service d'Hépatologie and INSERM U773-CRB3, Hôpital Beaujon, University Paris-Diderot, Pavillon Abrami, 100 Boulevard du Général Leclerc, 92110 Clichy, France. patrick.marcellin@bjn.aphp.fr
Telephone: +33-1-40875338 Fax: +33-1-47309440

Received: October 2, 2011 Revised: February 15, 2012
Accepted: February 26, 2012
Published online: June 21, 2012

Abstract

AIM: To study the efficacy and factors associated with a sustained virological response (SVR) in chronic hepatitis C (CHC) relapsing patients.

METHODS: Out of 1228 CHC patients treated with pegylated interferon (PEG-IFN) and ribavirin (RBV), 165 (13%) had a relapse. Among these, 62 patients were retreated with PEG-IFN-α2a or -α2b and RBV. Clinical, biological, virological and histological data were collected. Initial doses and treatment modifications were recorded. The efficacy of retreatment and predictive factors for SVR were analyzed.

RESULTS: An SVR was achieved in 42% of patients. SVR was higher in young (< 50 years) (61%) than old patients (27%) (P = 0.007), and in genotype 2 or 3 (57%) than in genotype 1 or 4 (28%) patients (P = 0.023). Prolonging therapy for at least 24 wk more than the previous course was associated with higher SVR rates (53% *vs* 28%, P = 0.04). Also, a better SVR rate was observed with RBV dose/body weight > 15.2 mg/kg per day (70% *vs* 35%, P = 0.04). In logistic regression, predictors of a response were age (P = 0.018), genotype (P = 0.048) and initial RBV dose/body weight (P = 0.022). None of the patients without a complete early virological response achieved an SVR (negative predictive value = 100%).

CONCLUSION: Retreatment with PEG-IFN/RBV is effective in genotype 2 or 3 relapsers, especially in young patients. A high dose of RBV seems to be important for the retreatment response.

Key words: Chronic hepatitis C; Relapse; Retreatment; Ribavirin; Pegylated interferon

Peer reviewers: Eric R Kallwitz, Assistant Professor, University of Illinois, 840 S Wood Street MC 787, Chicago, IL 60612, United States; Satoshi Yamagiwa, MD, PhD, Division of Gastroenterology and Hepatology, Niigata University Graduate School of Medical and Dental Sciences, 757 Asahimachi-dori 1, Chuo-ku, Niigata 951-8510, Japan

Stern C, Martinot-Peignoux M, Ripault MP, Boyer N, Castelnau C, Valla D, Marcellin P. Impact of ribavirin dose on retreatment of chronic hepatitis C patients. *World J Gastroenterol* 2012; 18(23): 2966-2972 Available from: URL: http://www.wjgnet.com/1007-9327/full/v18/i23/2966.htm DOI: http://dx.doi.org/10.3748/wjg.v18.i23.2966

INTRODUCTION

Major advances have been made in the treatment of chronic hepatitis C (CHC) over the last decade. However, only 50% of patients will achieve a sustained virological response (SVR) with the combination of pegylated interferon (PEG-IFN)-α and ribavirin (RBV), the reference standard of care[1,2]. Hence, non-response and relapse are major issues. Approximately 30% of CHC patients with undetectable hepatitis C virus (HCV) RNA at the end of therapy (EOT) will experience relapse[3].

Although its mode of action is not completely understood, RBV is clearly needed to improve SVR rates when combination therapy with PEG-IFN is prescribed[4]. The optimal dose of RBV to maintain the highest SVR rates differs according to genotype. The recommended RBV dose is 1000/1200 mg/d and 800 mg/d in HCV genotype-1 and genotype-2 or -3 infected patients, respectively[2,5]. Controversial studies showed that RBV dose, as well as RBV reduction and/or discontinuation during the first 12-24 wk of treatment could have an impact on the treatment response[6-12].

In addition to RBV dose and cumulative exposure, viral and host factors associated with a virological response were identified in naïve patients. The likelihood of a response is higher when patients have an early and long period of undetectable HCV RNA[13]. Patients who attain a rapid virological response and early virological response (EVR) have lower rates of relapse[14]. Also, older age, advanced liver fibrosis, high baseline viral load, infection with HCV genotype 1 and co-infection with human immunodeficiency virus (HIV) are known factors associated with treatment failure[2,13,15,16]. Recent data suggests that the type of PEG-IFN also has an impact on the outcome of HCV treatment. In the IDEAL trial, PEG-IFN-α2a and PEG-IFN-α2b in combination with RBV were compared. Although the EOT response was lower with PEG-IFN-α2b, higher relapse rates were observed with PEG-IFN-α2a. Therefore, the rates of SVR did not differ between the two types of PEG-IFN[13].

In contrast to the well-defined management of new HCV patients, relapsers are a challenge nowadays. There are no proven guidelines for retreatment of relapsers. Retreatment studies have been made based on heterogeneous groups. The majority of reports included both non-responders and relapsers and different previous therapies: IFN monotherapy, IFN plus RBV or PEG-IFN monotherapy. Overall SVR rates of 13%-50% were obtained in retreatment of patients who failed previous IFN-based therapy, with a higher SVR in former relapsers than in non-responders[17-21].

Thus, retreatment of relapsers with PEG-IFN plus RBV has not been well studied. The aim of this study was to evaluate, outside of trials, the efficacy of retreatment, and predictors of response, in a population of CHC relapsers after a previous course of PEG-IFN and RBV.

MATERIALS AND METHODS

Patient selection

Patients with CHC who relapsed after a previous course of PEG-IFN-α2a or PEG-IFN-α2b in combination with RBV were eligible. Patients previously treated for at least 12 wk, with undetectable HCV RNA at the end of treatment and recurrence of viremia during 24-wk post-treatment follow-up were included in this retrospective cohort study. Exclusion criteria were co-infection with human immunodeficiency virus or HBV, the presence of any other cause of liver disease, decompensated liver disease and a history of hepatocellular carcinoma.

Study design

Patients were treated with PEG-IFN-α2a at a dose of 180 μg per week, plus weight-based oral RBV as previously described or PEG-IFN-α2b at the standard dose of 1.5 μg/kg body weight per week, in combination with oral RBV at a dose of 800-1200 mg per day, according to genotype and body weight[2,22]. The duration of therapy was determined according to genotype, duration of previous therapy, initial virological response and tolerability. Treatment prolongation and high RBV dose administration were decided case by case according to the physicians' discretion. All patients had a post-treatment follow-up of at least 24 wk.

Assessments

Serum HCV RNA level was measured at treatment initiation, treatment week 4, every 12 wk during the treatment period; and during post-treatment follow-up at weeks 4, 12 and 24. HCV RNA was detected qualitatively with the use of transcription-mediated assay (VERSANT HCV RNA Qualitative Assay; Siemens Medical Solution Diagnosis), which has a sensitivity of 9.6 IU/mL. A rapid virological response (RVR) was defined as undetectable HCV RNA at week 4 of treatment. An EVR was defined according to HCV viral load at week 12 and categorized as: no EVR (reduction of less than 2 log in HCV viral load compared with the baseline level); partial EVR (pEVR): reduction greater than 2 log; and complete EVR (cEVR): undetectable HCV RNA. Response to treatment was based on HCV RNA measurement at the end of therapy and at week 24 of follow-up. Non-responders were defined as detectable HCV RNA at EOT. Relapsers were defined as HCV RNA undectable at EOT but detectable within the 24-wk follow-up period. An SVR was defined as negative HCV RNA 24 wk after cessation of therapy. Pretreatment liver biopsies were analyzed by a single pathologist using the METAVIR scoring system.

Patients were evaluated for tolerability and safety by physical examination and laboratory evaluation, including hematological and biochemical analyses. Dose reductions or discontinuation of PEG-IFN or RBV (or both)

Table 1 Baseline characteristics *n* (%)

	All patients (*n* = 62)
Male gender	45 (72.6)
Mean age, yr ± SD	52 ± 9
Mean weight, kg ± SD	76 ± 14
Mean BMI, kg/m^2 ± SD	26 ± 4
Abnormal ALT	54 (90)
Abnormal GGT	36 (67)
Mean hemoglobin, g/dL ± SD	14.8 ± 1.5
HCV RNA	
> 600 000 IU/mL	11 (28)
METAVIR fibrosis score	
F2	20 (34)
F3	11 (19)
F4	23 (39)
Steatosis	
< 5%	13 (21)
5%-30%	23 (37)
> 30%	26 (42)

BMI: Body mass index; ALT: Alanine aminotransferase; GGT: γ-glutamyl transferase; HCV: Hepatitis C virus.

were performed when appropriate, in accordance with guideline recommendations.

Statistical analysis

Univariate analysis was performed to evaluate treatment response and baseline characteristics. Categorical variables were compared using χ^2 or *F* tests. Continuous variables were analyzed with the Student *t* test or Mann-Whitney *U* test as appropriate. Predictors of response were identified and entered in a stepwise logistic regression in order to assess their association with SVR. Statistical significance was defined as $P < 0.05$ and all comparisons were two-tailed. Statistical analysis was performed using SPSS, version 12.0 (SPSS Inc., Chigago, IL).

RESULTS

Patient population

Of 1228 CHC patients treated with a combination of PEG-IFN-α plus RBV in the Hepatology Department of Hôpital Beaujon, 165 (13%) patients were identified as relapsers and were eligible for this study. Retreatment was proposed for 75 patients. Among these, 62 consecutive patients were retreated between April 2003 and June 2008 and finished their follow-up period. Retreatment was prescribed with the same type of PEG-IFN-α used in the prior PEG-IFN combination treatment in 53% of patients. Median duration of therapy was 48 wk (16-72 wk). Retreatment was at least 24 wk longer than previous therapy in 51% of patients. Initial dose of RBV was >13.3 mg/kg per day in 54%. A high dose of RBV (daily doses > 15.2 mg/kg[22]) was prescribed in 16% of patients.

Baseline demographic, clinical, biochemical, virological and histological characteristics are summarized in Table 1. The mean age of the patients was 52 years, and approximately 73% were male; 57% had a body mass index (BMI) > 25 kg/m^2. Serum alanine aminotransferase and γ-glutamyl transferase (GGT) levels were abnormal in 90% and 67% of patients, respectively. Forty-eight patients were infected with HCV genotype 1. High viral load (> 600 000 IU/mL) was observed in 28%. Necro-inflammatory activity was mild (A1) in 51% of patients, 34% had F2 fibrosis, 19% had advanced fibrosis (F3) and 39% had cirrhosis (F4). Steatosis was absent (< 5%) in 21%, mild (5%-30%) in 37%, and moderate or severe (> 30%) in 42% of patients.

Table 2 Treatment characteristics

	No. of patients, *n* (%)	SVR (%)
Overall population	62 (100)	42
Type of PEG-IFN (retreatment)		
PEG-IFN-α2a	43 (69)	40
PEG-IFN-α2b	19 (31)	47
RBV ⩾ 13.3 mg/kg per day	34 (54)	35
RBV ⩾ 15.2 mg/kg per day	10 (16)	70
Treatment duration 24 wk longer than previous course	31 (51)	53
Patients with RBV ⩾ 15.2 mg/kg per day and 24 wk longer duration	6 (10)	67

Sustained virological response (SVR) according to different types of pegylated interferon (PEG-IFN), dose of ribavirin (RBV) and duration of therapy.

Response to treatment

After retreatment with PEG-IFN and RBV, the overall SVR rate was 42%. An EOT response was achieved by 77% of patients (48/62); among them, 46% (22/48) again experienced a relapse. Patients < 50 years achieved a higher SVR rate (61%) when compared to older patients (27%) ($P = 0.007$). Female and male patients had SVR rates of 53% and 38%, respectively, but with no significant difference ($P = 0.28$). There was a trend for higher SVR rates in patients with normal baseline GGT (61% *vs* 36%, $P = 0.081$) and lower BMI (mean BMI 24.6 in SVR *vs* 26.5 in non responder, $P = 0.071$). In addition, patients infected with genotype 2 or 3 had higher SVR than those with genotype 1 or 4 (57% *vs* 28%, $P = 0.023$) (Figure 1A). SVR rates were similar regarding low and high viral load (41% *vs* 36%, $P = 0.77$). Necro-inflammatory activity, fibrosis and steatosis did not influence SVR rates.

Treatment responses according to dose and duration are summarized in Table 2. There was no difference between retreatment response with PEG-IFN-α2a or PEG-IFN-α2b regarding EOT (74% *vs* 84%, $P = 0.52$) and SVR rate (40% *vs* 47%, $P = 0.56$). Relapse rates were similar between groups (35% *vs* 37%, $P = 0.68$). In patients retreated with a different type of PEG-IFN-α from prior therapy, SVR was achieved in 36%, similar to that in patients retreated with the same PEG-IFN, who attained an SVR rate of 46% ($P = 0.39$). Retreatment for at least 24 wk longer than the previous therapy was associated with a higher SVR rate (53% *vs* 28%, $P = 0.044$). A high initial dose of RBV was associated with a higher likelihood of SVR. Although EOT response rates

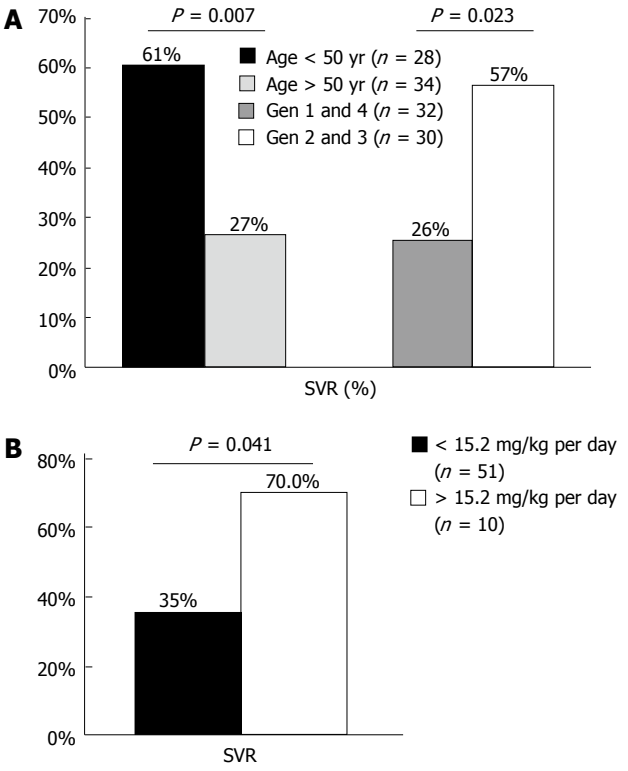

Figure 1 Sustained virological response rates according to age, genotype and initial ribavirin dose. A: Sustained virological response (SVR) rates according to age, genotype; B: SVR rates according to initial ribavirin dose.

were not statistically different between groups (90% *vs* 75%, $P = 0.43$), patients who received > 15.2 mg/kg per day had a superior SVR rate when compared to patients receiving lower doses (70% *vs* 35%, $P = 0.041$) (Figure 1B). These results were related to a lower rate of relapse among patients with a high dose of RBV (20% *vs* 39%). Regarding RBV dose reduction, no impact on SVR rates was observed (43% among those patients without a reduction *vs* 33% with a dose reduction, $P = 0.75$).

Tolerability and dose reduction

Retreatment with combination therapy was well tolerated. Seventy-nine percent of patients did not reduce their initial dose of PEG-IFN and/or RBV. Only 4 patients (6.6%) had a reduction in PEG-IFN dose, 3 of whom had clinical intolerance with asthenia, and one had marked neutropenia. The reduction in RBV dose was necessary in 12 patients (19.7%), with anemia being the major reason (58%). Among all patients, only 2 had cumulative RBV doses lower than 80% of the predicted dose. High initial doses of RBV did not seem to influence RBV reduction. In patients with an initial dose of RBV > 13.3 mg/kg per day and in those with > 15.2 mg/kg per day, 26% and 30% of patients needed RBV dose reduction. The treatment was stopped earlier than the proposed therapy duration in 11 patients (18%). Among these, 10% did not achieve a virological response at week 24, and treatment was discontinued.

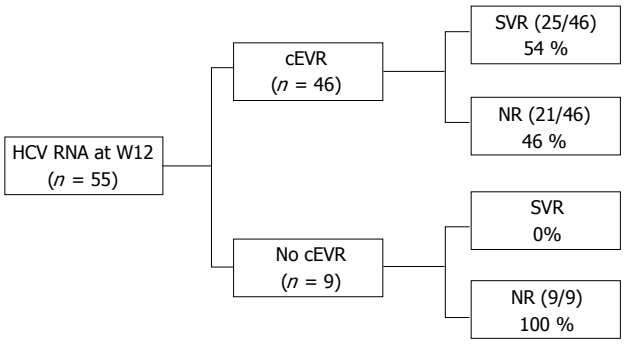

Figure 2 Predictive value of complete early virological response. Among 46 patients with complete early virological response (cEVR), 25 (54%) patients achieved an sustained virological response (SVR) and 21 (46%) were non-responders (17 patients had a relapse and 4 patients had a non-response). Positive predictive value of cEVR for SVR = 54% ($P = 0.003$). Negative predictive value of cEVR for SVR = 100% ($P = 0.003$). HCV: Hepatitis C virus; NR: Non response.

Predictors of response

The factors identified in bivariate analysis as possibly associated with SVR and entered in a logistic regression model were: age, genotype, and high dose RBV. In the stepwise logistic regression analysis, the predictors of SVR were age [< 50 years *vs* ⩾ 50 years; odds ratio (OR), 4.26; 95% CI: 1.28-14.19], genotype (G2/3 *vs* G1/4; OR, 3.55; 95% CI: 1.01-12.46), and high dose RBV (> 15.2 mg/kg per day *vs* <15.2 mg/kg per day; OR, 6.99; 95% CI: 1.32-36.97). Younger patients with genotype 2 or 3 can attain an SVR of 59%, while older patients, infected with genotype 1 or 4 only had an SVR of 10%. None of the patients of older age, genotype 1 or 4, and RBV initial dose < 15.2 mg/kg per day achieved an SVR.

Predictive value of rapid virological response and early virological response

RVR was assessed in 39 patients; 18% (7/39) achieved an RVR, and 5 of these achieved an SVR [positive predictive value (PPV) = 71%]. In addition, RVR had a negative predictive value (NPV) for SVR of 88% ($P = 0.007$).

At week 12, 55 patients were classified according to the 3 categories of EVR described earlier. pEVR and cEVR were observed in 11% and 84% of patients. Patients with no EVR (3/55) or pEVR (6/55) did not attain an SVR (NPV = 100%). Among the 46 patients with cEVR, 4 (9%) were non-responders, 17 (37%) were relapsers and 25 (54%) had an SVR. cEVR had a PPV and a NPV for SVR of 54% and 100%, respectively ($P = 0.003$) (Figure 2).

DISCUSSION

Retreatment of CHC patients who have failed prior antiviral therapy is an important clinical issue. Our study evaluated the efficacy of retreatment of CHC patients who relapsed after combination therapy with PEG-IFN

plus RBV. The overall SVR rate achieved was 42%. An important point of our study is the inclusion of a homogeneous population of prior relapsers to the PEG-IFN-α plus RBV combination therapy. Most previous studies analyzed the efficacy of retreatment with PEG-IFN plus RBV based on groups composed mainly of patients who failed conventional IFN-based therapy without distinguishing between non-responders and relapsers, or between monotherapy and combination therapy. Jacobson *et al*[21] demonstrated that SVR rates decreased according to previous conventional IFN-based therapy status: 42% in conventional IFN (cIFN) plus RBV relapsers, 21% in cIFN monotherapy non-responders, and 8% in cIFN plus RBV non-responders. These data were also confirmed by several other studies: retreatment of previous relapsers to cIFN plus RBV could achieve SVR rates of 41%-58%, while for patients who were non-responders, only 4%-26% achieved an SVR[17-21]. The same relationship was observed in previous failures to PEG-IFN and RBV: 33% in prior relapsers and 14% in prior non-responders, with an overall SVR of 22%[23].

The SVR rate of 42% observed in our study was slightly higher than that described in the EPIC3 clinical trial, where prior PEG-IFN plus RBV relapsers attained an SVR of 33%[23]. In our study, HCV genotype was an important predictor for SVR. Patients infected with genotype 2 or 3 attained the highest rates of SVR (60% in genotype 2 and 56% in genotype 3). Thus, a higher proportion of genotype non-1 infected patients in the current study (52% *vs* 20% in EPIC3 trial) could account for this difference. In addition, the EPIC trial used less sensitive qualitative assays that could result in misclassification of EOT responders, increasing the number of relapsers that were in fact non-responders, with a lower probability of SVR.

Young age and genotype 2 or 3 were factors associated with treatment response as previously reported[2,13,15]. We did not find a relationship between low baseline viral load or low fibrosis stage and better response to therapy. These factors have been described in controversial studies with the treatment of naïve and IFN-experienced patients, and their impact on the response in relapsers could have less strength[7,13,19,23,24].

Retreatment with only PEG-IFN-α in patients who failed to respond to the other PEG-IFN-α has been described as an alternative strategy. However, in our study no gain was observed in patients who received a different type of PEG-IFN-α. This finding is consistent with the REPEAT trial, where prior non-responders to PEG-IFN-α2b were retreated with PEG-IFN-α2a. Only 9% of SVR was observed in the regimen of 48 wk retreatment[25]. Besides, this trial demonstrated higher SVR rates in the group retreated for 72 wk (14%)[26]. In the current study, the SVR rate was also improved with longer duration of therapy. Thus, retreatment for at least 24 wk longer than the previous course is important to increase the probability of SVR in relapsers and non-responders.

Some controversial studies have suggested that exposure to RBV is critical for attaining an SVR. At first, adherence to therapy was considered extremely important. McHutchison *et al*[8] demonstrated that at least 80% adherence to therapy enhanced SVR. They found a continuous, increasing relationship between adherence and SVR in genotype 1. These findings were also observed in another study with genotype 1-naïve patients, where a linear relationship between exposure and the SVR rate was observed at the first 12 wk of treatment[7]. Also, a study with RBV discontinuation in a subset of HCV RNA-negative patients at week 24 showed an increase in the rate of virological breakthrough and relapse[9]. In contrast, in our study no relation was found between dose reduction of RBV and SVR. However, the rate of RBV reduction was 20% and only 2 patients did not have at least 80% of the predicted RBV doses.

Recent studies suggested that high-dose RBV schedules reduced relapse rates and increased SVR in difficult-to-treat selected patients[10-12]. In a pilot study with 10 genotype 1 patients, higher RBV doses were associated with more frequent and serious adverse events, but the SVR rate was 90%[11]. Also, Fried *et al*[10] reported a study with 188 treatment-naïve, genotype 1 and high viral load patients. Patients who received an RBV dose of 1600 mg/d had superior SVR rates when compared with standard doses (1200 mg/d). Our data demonstrated a clear relation between high initial dose of RBV[22] and SVR rates. Patients with RBV dose >15.2 mg/kg per day achieved an SVR rate of 70%, while only 26% of patients with lower doses attained an SVR.

Our study demonstrates that an RVR in a relapser retreatment population is attained by 18%, of whom 71% achieved an SVR. Prediction of non response on treatment was more marked with EVR analyses. If the patient did not achieve a cEVR, no SVR was observed (NPV = 100%). Hence, the presence of detectable HCV RNA at week 12 is a good indication to stop treatment in relapsers and it is as relevant as for naïve or non-responding patients[3,19,25].

Specifically targeted antiviral therapies for hepatitis C are currently under evaluation in clinical trials. These new drugs are mostly effective and have been studied in genotype 1 patients[27-29]. Telaprevir, an antiprotease NS3-NS4A, increases SVR rates in genotype 1 naïve and non-responding patients, but it has limited activity against genotype 2 and 3[30]. Besides, even when these medications will be available outside trials, they will not be accessible worldwide. For these reasons, PEG-IFN and RBV still have a role on hepatitis C retreatment, in particular in young patients infected with non genotype 1.

In conclusion, our study shows that retreatment of prior relapsers after treatment with a combination of PEG-IFN plus RBV may be effective. As observed with naïve patients, genotype is crucial for a treatment response. Better results of retreatment are obtained in patients with genotype 2 or 3 and of younger age. In addition, in this subset of patients, higher SVR rates

are achieved with increased doses of RBV, without a marked increase in adverse events or dose reductions. Thus, a high dose schedule of RBV is recommended if retreatment is proposed. Also, prolonging therapy for at least 24 wk more than the previous course enhances SVR rates. Finally, the absence of a cEVR as defined by detectable HCV RNA at week 12 should be considered a stopping rule in the retreatment of relapsers.

COMMENTS

Background

Only 50% of chronic hepatitis C (CHC) patients treated with the combination of pegylated interferon (PEG-IFN)-α and ribavirin (RBV), the standard treatment, will achieve a sustained virological response (SVR). Therefore, patients with no response or relapse after PEG-IFN and RBV treatment are a major issue. Approximately 30% of CHC patients with undetectable hepatitis C virus (HCV) RNA at end of therapy (EOT) will experience relapse.

Research frontiers

Retreatment of CHC patients with relapse to antiviral therapy is a current clinical issue. There are no specific recommendations about type, dose and duration of retreatment in this particular situation. In this research area, different dose schedules and duration of PEG-IFN and RBV therapy have been evaluated in order to increase the SVR in patients with a previous relapse to this antiviral therapy.

Innovations and breakthroughs

This study shows in a real life cohort that retreatment of relapsers after prior treatment with a combination of PEG-IFN plus RBV may be effective. Better results of retreatment are obtained in patients with genotype 2 or 3 and of younger age as is observed in naïve patients. Moreover, in this subset of patients, higher SVR rates are achieved with increased doses of RBV (> 15.2 mg/kg per day), without a marked increase in adverse events or dose reductions. Also, lengthening therapy for at least 24 wk more than the previous course enhances SVR rates.

Applications

The study suggests that retreatment of patients with a relapse after treatment with PEG-IFN and RBV may be effective, especially in patients with genotype 2 or 3 who are of younger age. In order to increase SVR in this particular situation, high dose RBV and longer duration of therapy should be proposed.

Terminology

In CHC patients, treatment responses to the combination of PEG-IFN and RBV are defined by a virological parameter (HCV RNA analysis) rather than a clinical endpoint. The most important definitions are: SVR if HCV RNA remains undetectable 24 wk after EOT, non response if HCV RNA is positive at EOT, and relapse if HCV RNA is undetectable at EOT but detectable within 24-wk follow-up period.

Peer review

The authors revealed that SVR was achieved in 42% of the retreated patients, and that initial dose/weight of RBV was an important predictor of SVR.

REFERENCES

1 **Marcellin P**. Hepatitis B and hepatitis C in 2009. *Liver Int* 2009; **29** Suppl 1: 1-8
2 **Ghany MG**, Strader DB, Thomas DL, Seeff LB. Diagnosis, management, and treatment of hepatitis C: an update. *Hepatology* 2009; **49**: 1335-1374
3 **Martinot-Peignoux M**, Stern C, Maylin S, Ripault MP, Boyer N, Leclere L, Castelnau C, Giuily N, El Ray A, Cardoso AC, Moucari R, Asselah T, Marcellin P. Twelve weeks post-treatment follow-up is as relevant as 24 weeks to determine the sustained virologic response in patients with hepatitis C virus receiving pegylated interferon and ribavirin. *Hepatology* 2010; **51**: 1122-1126
4 **Dusheiko G**, Nelson D, Reddy KR. Ribavirin considerations in treatment optimization. *Antivir Ther* 2008; **13** Suppl 1: 23-30
5 **Hadziyannis SJ**, Sette H, Morgan TR, Balan V, Diago M, Marcellin P, Ramadori G, Bodenheimer H, Bernstein D, Rizzetto M, Zeuzem S, Pockros PJ, Lin A, Ackrill AM. Peginterferon-alpha2a and ribavirin combination therapy in chronic hepatitis C: a randomized study of treatment duration and ribavirin dose. *Ann Intern Med* 2004; **140**: 346-355
6 **Shiffman ML**, Ghany MG, Morgan TR, Wright EC, Everson GT, Lindsay KL, Lok AS, Bonkovsky HL, Di Bisceglie AM, Lee WM, Dienstag JL, Gretch DR. Impact of reducing peginterferon alfa-2a and ribavirin dose during retreatment in patients with chronic hepatitis C. *Gastroenterology* 2007; **132**: 103-112
7 **Bain VG**, Lee SS, Peltekian K, Yoshida EM, Deschênes M, Sherman M, Bailey R, Witt-Sullivan H, Balshaw R, Krajden M. Clinical trial: exposure to ribavirin predicts EVR and SVR in patients with HCV genotype 1 infection treated with peginterferon alpha-2a plus ribavirin. *Aliment Pharmacol Ther* 2008; **28**: 43-50
8 **McHutchison JG**, Manns M, Patel K, Poynard T, Lindsay KL, Trepo C, Dienstag J, Lee WM, Mak C, Garaud JJ, Albrecht JK. Adherence to combination therapy enhances sustained response in genotype-1-infected patients with chronic hepatitis C. *Gastroenterology* 2002; **123**: 1061-1069
9 **Bronowicki JP**, Ouzan D, Asselah T, Desmorat H, Zarski JP, Foucher J, Bourlière M, Renou C, Tran A, Melin P, Hézode C, Chevalier M, Bouvier-Alias M, Chevaliez S, Montestruc F, Lonjon-Domanec I, Pawlotsky JM. Effect of ribavirin in genotype 1 patients with hepatitis C responding to pegylated interferon alfa-2a plus ribavirin. *Gastroenterology* 2006; **131**: 1040-1048
10 **Fried MW**, Jensen DM, Rodriguez-Torres M, Nyberg LM, Di Bisceglie AM, Morgan TR, Pockros PJ, Lin A, Cupelli L, Duff F, Wang K, Nelson DR. Improved outcomes in patients with hepatitis C with difficult-to-treat characteristics: randomized study of higher doses of peginterferon alpha-2a and ribavirin. *Hepatology* 2008; **48**: 1033-1043
11 **Lindahl K**, Stahle L, Bruchfeld A, Schvarcz R. High-dose ribavirin in combination with standard dose peginterferon for treatment of patients with chronic hepatitis C. *Hepatology* 2005; **41**: 275-279
12 **Snoeck E**, Wade JR, Duff F, Lamb M, Jorga K. Predicting sustained virological response and anaemia in chronic hepatitis C patients treated with peginterferon alfa-2a (40KD) plus ribavirin. *Br J Clin Pharmacol* 2006; **62**: 699-709
13 **McHutchison JG**, Lawitz EJ, Shiffman ML, Muir AJ, Galler GW, McCone J, Nyberg LM, Lee WM, Ghalib RH, Schiff ER, Galati JS, Bacon BR, Davis MN, Mukhopadhyay P, Koury K, Noviello S, Pedicone LD, Brass CA, Albrecht JK, Sulkowski MS. Peginterferon alfa-2b or alfa-2a with ribavirin for treatment of hepatitis C infection. *N Engl J Med* 2009; **361**: 580-593
14 **Farnik H**, Mihm U, Zeuzem S. Optimal therapy in genotype 1 patients. *Liver Int* 2009; **29** Suppl 1: 23-30
15 **Heathcote J**. Retreatment of chronic hepatitis C: who and how? *Liver Int* 2009; **29** Suppl 1: 49-56
16 **Martinot-Peignoux M**, Boyer N, Pouteau M, Castelnau C, Giuily N, Duchatelle V, Aupérin A, Degott C, Benhamou JP, Erlinger S, Marcellin P. Predictors of sustained response to alpha interferon therapy in chronic hepatitis C. *J Hepatol* 1998; **29**: 214-223
17 **Parise E**, Cheinquer H, Crespo D, Meirelles A, Martinelli A, Sette H, Gallizi J, Silva R, Lacet C, Correa E, Cotrim H, Fonseca J, Paraná R, Spinelli V, Amorim W, Tatsch F, Pessoa M. Peginterferon alfa-2a (40KD) (PEGASYS) plus ribavirin (COPEGUS) in retreatment of chronic hepatitis C patients, nonresponders and relapsers to previous conventional interferon plus ribavirin therapy. *Braz J Infect Dis* 2006; **10**: 11-16
18 **Basso M**, Torre F, Grasso A, Percario G, Azzola E, Artioli S, Blanchi S, Pelli N, Picciotto A. Pegylated interferon and rib-

avirin in re-treatment of responder-relapser HCV patients. *Dig Liver Dis* 2007; **39**: 47-51
19 **Moucari R**, Ripault MP, Oulès V, Martinot-Peignoux M, Asselah T, Boyer N, El Ray A, Cazals-Hatem D, Vidaud D, Valla D, Bourlière M, Marcellin P. High predictive value of early viral kinetics in retreatment with peginterferon and ribavirin of chronic hepatitis C patients non-responders to standard combination therapy. *J Hepatol* 2007; **46**: 596-604
20 **Sagir A**, Heintges T, Akyazi Z, Oette M, Erhardt A, Häussinger D. Relapse to prior therapy is the most important factor for the retreatment response in patients with chronic hepatitis C virus infection. *Liver Int* 2007; **27**: 954-959
21 **Jacobson IM**, Gonzalez SA, Ahmed F, Lebovics E, Min AD, Bodenheimer HC, Esposito SP, Brown RS, Bräu N, Klion FM, Tobias H, Bini EJ, Brodsky N, Cerulli MA, Aytaman A, Gardner PW, Geders JM, Spivack JE, Rahmin MG, Berman DH, Ehrlich J, Russo MW, Chait M, Rovner D, Edlin BR. A randomized trial of pegylated interferon alpha-2b plus ribavirin in the retreatment of chronic hepatitis C. *Am J Gastroenterol* 2005; **100**: 2453-2462
22 **Shiffman ML**, Salvatore J, Hubbard S, Price A, Sterling RK, Stravitz RT, Luketic VA, Sanyal AJ. Treatment of chronic hepatitis C virus genotype 1 with peginterferon, ribavirin, and epoetin alpha. *Hepatology* 2007; **46**: 371-379
23 **Poynard T**, Colombo M, Bruix J, Schiff E, Terg R, Flamm S, Moreno-Otero R, Carrilho F, Schmidt W, Berg T, McGarrity T, Heathcote EJ, Gonçales F, Diago M, Craxi A, Silva M, Bedossa P, Mukhopadhyay P, Griffel L, Burroughs M, Brass C, Albrecht J. Peginterferon alfa-2b and ribavirin: effective in patients with hepatitis C who failed interferon alfa/ribavirin therapy. *Gastroenterology* 2009; **136**: 1618-1628.e2
24 **Fried MW**, Shiffman ML, Reddy KR, Smith C, Marinos G, Gonçales FL, Häussinger D, Diago M, Carosi G, Dhumeaux D, Craxi A, Lin A, Hoffman J, Yu J. Peginterferon alfa-2a plus ribavirin for chronic hepatitis C virus infection. *N Engl J Med* 2002; **347**: 975-982
25 **Jensen DM**, Freilich B, Andreone P, Adrian DiBisceglie, Carlos E. Brandao-Mello, K. Rajender Reddy, Antonio Craxi, Antonio Olveira Martin, Gerlinde Teuber, Diethelm Messinger, Greg Hooper, Matei Popescu and Patrick Marcellin. Pegylated interferon alfa-2a (40kD) plus ribavirin (RBV) in prior non-responders to pegylated interferon alfa-2b (12kD)/RBV: final efficacy and safety outcomes of the REPEAT study. *Hepatology* 2007; **46** Suppl 1: 291A-292A
26 **Jensen DM**, Marcellin P, Freilich B, Andreone P, Di Bisceglie A, Brandão-Mello CE, Reddy KR, Craxi A, Martin AO, Teuber G, Messinger D, Thommes JA, Tietz A. Re-treatment of patients with chronic hepatitis C who do not respond to peginterferon-alpha2b: a randomized trial. *Ann Intern Med* 2009; **150**: 528-540
27 **Mchutchison JG**, Everson GT, Gordon SC, Jacobson I, Kauffman R, McNair L, Muir A. Prove1: results from a phase 2 study of Telaprevir with peginterfeon alfa-2a and ribavirin in treatment-naive subjects with hepatitis C. *J Hepatol* 2008; **48** Suppl 2: S4
28 **Asselah T**, Benhamou Y, Marcellin P. Protease and polymerase inhibitors for the treatment of hepatitis C. *Liver Int* 2009; **29** Suppl 1: 57-67
29 **Hézode C**, Forestier N, Dusheiko G, Ferenci P, Pol S, Goeser T, Bronowicki JP, Bourlière M, Gharakhanian S, Bengtsson L, McNair L, George S, Kieffer T, Kwong A, Kauffman RS, Alam J, Pawlotsky JM, Zeuzem S. Telaprevir and peginterferon with or without ribavirin for chronic HCV infection. *N Engl J Med* 2009; **360**: 1839-1850
30 **Foster GR**, Hezode C, Bronowicki JP, Carosi G, Weiland O, Verlinden L, van Heeswijk R, Van Baelen B, Picchio G, Beumont-Mauviel M. Activity of telaprevir alone or in combination with peginterferon alfa-2a and ribavirin in treatment-naive genotype 2 and 3 hepatitis-c patients: final results of study C209. *J Hepatol* 2010; **52** Suppl 1: S27

S- Editor Gou SX **L- Editor** Cant MR **E- Editor** Li JY

World Journal of Gastroenterology

Online Submissions: http://www.wjgnet.com/1007-9327office
wjg@wjgnet.com
doi:10.3748/wjg.v18.i23.2973

World J Gastroenterol 2012 June 21; 18(23): 2973-2978
ISSN 1007-9327 (print) ISSN 2219-2840 (online)

BRIEF ARTICLE

Investigation of compensatory postures with videofluoromanometry in dysphagia patients

Antonio Solazzo, Luigi Monaco, Lucia Del Vecchio, Stefania Tamburrini, Francesca Iacobellis, Daniela Berritto, Nunzia Luisa Pizza, Alfonso Reginelli, Natale Di Martino, Roberto Grassi

Antonio Solazzo, Francesca Iacobellis, Daniela Berritto, Nunzia Luisa Pizza, Alfonso Reginelli, Roberto Grassi, Department of Radiology Magrassi-Lanzara, Second University of Naples, 80138 Napoli, Italy
Luigi Monaco, Natale Di Martino, Department of Gerontology, Geriatrics and Metabolic Diseases, Second University of Naples, 80138 Napoli, Italy
Lucia Del Vecchio, Department of Pathology of the Head and Neck, Oral Cavity and Audio-verbal Communication, Second University of Naples, 80138 Napoli, Italy
Stefania Tamburrini, UOC Diagnostic Imaging, PO Pellegrini, 80134 Napoli, Italy
Author contributions: Solazzo A, Monaco L and Del Vecchio L designed and drafted the article; Reginelli A, Tamburrini S and Pizza NL analyzed and interpreted the data; Iacobellis F and Berritto D acquired and analyzed the data and critically revised the intellectual content of the article; Grassi R and Di Martino N approved the final version of the manuscript; and all authors approved the version for publication.
Correspondence to: Dr. Antonio Solazzo, Department of Radiology Magrassi-Lanzara, Second University of Naples, 80138 Napoli, Italy. antoniosolazzo@hotmail.it
Telephone: +39-81-5665203 Fax: +39-81-5665200
Received: August 20, 2011 Revised: September 26, 2011
Accepted: February 27, 2012
Published online: June 21, 2012

Abstract

AIM: To investigate the effectiveness of head compensatory postures to ensure safe oropharyngeal transit.

METHODS: A total of 321 dysphagia patients were enrolled and assessed with videofluoromanometry (VFM). The dysphagia patients were classified as follows: safe transit; penetration without aspiration; aspiration before, during or after swallowing; multiple aspirations and no transit. The patients with aspiration or no transit were tested with VFM to determine whether compensatory postures could correct their swallowing disorder.

RESULTS: VFM revealed penetration without aspiration in 71 patients (22.1%); aspiration before swallowing in 17 patients (5.3%); aspiration during swallowing in 32 patients (10%); aspiration after swallowing in 21 patients (6.5%); multiple aspirations in six patients (1.9%); no transit in five patients (1.6%); and safe transit in 169 patients (52.6%). Compensatory postures guaranteed a safe transit in 66/75 (88%) patients with aspiration or no transit. A chin-down posture achieved a safe swallow in 42/75 (56%) patients, a head-turned posture in 19/75 (25.3%) and a hyperextended head posture in 5/75 (6.7%). The compensatory postures were not effective in 9/75 (12%) cases.

CONCLUSION: VFM allows the speech-language therapist to choose the most effective compensatory posture without a trial-and-error process and check the effectiveness of the posture.

Key words: Aspiration; Compensatory postures; Oropharyngeal dysphagia; Videofluoromanometry; Chin-down posture; Head-turned; Hyperextended head

Peer reviewer: Richard A Awad, Professor, Experimental Medicine and Motility Unit, Mexico City General Hospital, Dr. Balmis 148, Mexico DF 06726, Mexico

Solazzo A, Monaco L, Del Vecchio L, Tamburrini S, Iacobellis F, Berritto D, Pizza NL, Reginelli A, Di Martino N, Grassi R. Investigation of compensatory postures with videofluoromanometry in dysphagia patients. *World J Gastroenterol* 2012; 18(23): 2973-2978 Available from: URL: http://www.wjgnet.com/1007-9327/full/v18/i23/2973.htm DOI: http://dx.doi.org/10.3748/wjg.v18.i23.2973

INTRODUCTION

Swallowing is a coordinated activity that enables solids and liquids to pass uninterrupted from the mouth to the

stomach. Dysphagia occurs when this process is altered by organic or functional alterations at the level of swallow initiation or esophageal emptying[1].

Oropharyngeal dysphagia can manifest as one or more symptoms that are specific for oropharyngeal dysfunction, which help the clinician distinguish it from esophageal dysphagia. Typical symptoms include the inability to chew, a delayed or absent swallow initiation, a bolus delay located in the neck, nasal regurgitation, a need to swallow repeatedly to clear food or fluid from the pharynx, coughing after aspiration, and dysphonia[2,3].

Oropharyngeal dysphagia is usually a manifestation of a systemic disease rather than a disease specific to the oropharynx. This manifestation occurs in one-third of all stroke patients and has a 20%-50% prevalence in conditions such as Parkinson's disease, Alzheimer's disease, and amyotrophic lateral sclerosis[3-5].

Videofluoroscopy (VFS) is the gold standard in the study of oropharyngeal dysphagia because it provides information on the presence and severity of the major categories of dysfunction, including the presence, timing and severity of aspiration[6,7].

Videofluoromanometry (VFM) correlates fluoroscopic events with manometric data. For example, the narrow upper esophageal sphincter (UES) opening can be distinguished from uncoordinated UES relaxation, and the weak propulsive pharyngeal forces can be distinguished from an increased outflow resistance. Moreover, VFM is especially useful for subsequent treatment planning[2].

Characterization of a swallowing disorder allows the patient to adopt compensatory swallowing postures, change their diet to permit safe oral feeding, and delay the use of percutaneous endoscopic gastrostomy in degenerative diseases[8]. The aim of our study was to evaluate the effectiveness of compensatory postures to ensure safe oropharyngeal transit with videofluoromanometric guidance.

MATERIALS AND METHODS

From January 2008 to December 2010, 321 dysphagia patients (171 male, 150 female, aged 18-87 years, mean age: 57 years) were enrolled in this study. All patients gave their written consent. The past medical history, present symptoms, and alimentary status were obtained from all patients. All patients underwent a morphofunctional logopedic evaluation according to recent guidelines[9,10].

Through the VFM assessment, the dysphagia patients were classified as follows: safe transit; penetration without aspiration; aspiration before, during, or after swallowing; multiple aspirations and no transit. The patients with aspiration or no transit were investigated to determine whether compensatory postures could correct the swallowing disorder. Based on manometric data, a chin-down posture, head-turned posture or hyperextended head posture was tested to obtain safe swallowing. Patients with multiple aspirations were excluded from the search for compensatory postures. These patients, who are often in an advanced disease stage, do not follow the operator commands during the VFM assessment and do not cooperatively assume the compensatory postures. Additionally, these subjects may only somewhat benefit from these compensatory postures[11]. The VFM study consisted of a parallel execution of VFS and manometry. A simultaneous manometric evaluation analyzed the tongue base pressure (the contact pressure between the posterior tongue thrust and the pharyngeal wall), UES tone (resting pressure, contraction pressure and residual pressure) and the bolus transit coordination, which are useful for selecting the compensatory postures[12,13] (Table 1).

Table 1 Normal values of videofluoromanometry

	Normal values measured with VFM
Tongue base pressure	130 ± 70 mmHg
UES	
Resting pressure	90 ± 30 mmHg
Contraction pressure	240 ± 80 mmHg
Residual pressure	< 10 mmHg
Relaxation duration	1.5 ± 0.4 s
Bolus progression	> 4 cm/s
Pharyngeal pressure	60 ± 20 mmHg

VFM: Videofluoromanometry; UES: Upper esophageal sphincter.

A Dyno Compact computerized system (MENFIS Biomedica s.r.l., Bologna, Italy) was used. This system was equipped with the following: (1) A graphics card for managing radiographic images; and (2) AVIUS-dedicated software, which enables digital-quality recording (PAL/NTSC, composite video or S-video) of the VFS study in AVI format with a 320 × 240 resolution and 25 Hz acquisition frequency. The delay introduced by the image digitization process was approximately 200 ms; therefore, for analytical purposes, the images could be considered synchronized with the manometric recordings. The concurrent pressure measurements were performed with a manometry catheter with endoluminal five-channel, solid-state microtransducers 2 cm apart at an angle of 120°-90°. The catheter was inserted through the nasal cavity into the stomach. The value recorded was used for the calibration of 0. Afterwards, a pull through was performed and the catheter was withdrawn to allow for the positioning of the transducers. Transducer 1 was placed at Passavant's ridge to evaluate the correct closure of the rhinopharynx during swallowing and phonation. Transducers 2, 3 and 4 were placed in the pharynx. Transducer 5 was placed at the UES, and the correct placement was determined by the appearance of the characteristic M wave. During image acquisition, the video images and manometric trace were displayed in real time as a full screen image on the personal computer monitor. A cursor indicated the exact correspondence between the video images and the traces. Following the acquisition, the video and manometric trace could be analyzed during real-time reproduction or at reduced or increased speed, or it could be paused for a frame-by-frame analysis. The examinations were acquired with the patient standing or

Table 2 Results of videofluoromanometry

	ALS	Stroke	MS	PD	Post-surgery	AD	Others	Total
Safe transit	41	21	22	28	3	14	40	169
Penetration without aspiration	22	14	8	10	-	7	10	71
Aspiration before swallowing	4	5	1	3	1	3	-	17
Aspiration during swallowing	12	5	3	5	4	3	-	32
Aspiration after swallowing	10	2	2	3	2	2	-	21
Multiple aspirations	4	-	-	-	-	2	-	6
No transit	1	-	-	2	-	2	-	5
Total	94	47	36	51	10	33	50	321

ALS: Amyotrophic lateral sclerosis; MS: Multiple sclerosis; PD: Parkinson's disease; AD: Alzheimer's disease. Others: Gastroesophageal reflux disease, achalasia, chest pain, diverticula.

seated if the patient was unable to remain standing.

VFM began with a baseline evaluation (without contrast) to study the motility of the vocal chords and soft palate. The VFM proceeded with barium contrast medium (Prontobario HD suspension, Bracco SpA, Milan; 250% w/v) at a dose of 5-15 mL that was optimized for the patient to evaluate swallowing, with particular attention paid to aspiration. This was made possible by previous evaluation by a speech therapist. The patients were asked to hold the bolus in their mouth for several seconds and to swallow when asked by the operator. All phases of the process were video-recorded first in the anteroposterior and then the laterolateral view[9,14]. If an impaired bolus transit or aspiration in the airways was detected, an evaluation of the ideal bolus size and monitoring the effectiveness of the compensatory postures were used to investigate correcting the dysfunction.

The compensatory posture was selected for each patient based on the specific swallowing dysfunction that was considered to have caused the aspiration. For an effective oropharyngeal bolus transit while swallowing, the following compensatory postures were tested. The chin-down posture involved tucking the chin to the neck. The change in head position inverted the epiglottis into a more protective position over the airway entry, which reduced the airway entrance space and increased the size of the vallecular spaces[12,15,16]. The head-turned posture narrowed the ipsilateral piriform sinus and sent the bolus to the contralateral sinus. In addition, it determined the decrease in UES pressure, delayed its closure during swallowing, and optimized the bolus propulsion[17,18]. The hyperextended head posture facilitated the bolus transit using the force of gravity. This posture is indicated for reduced pharyngeal peristalsis[4].

RESULTS

VFM in 169 (52.6%) of 321 enrolled patients showed safe transit of the contrast medium. In 71/321 cases (22.1%), penetration of the contrast medium into the laryngeal lumen without aspiration below the glottic level was observed, and we did not suggest compensatory postures for these patients. In 5/321 (1.5%) cases, there was no transit.

In 76/321 patients (23.7%), aspiration was observed. In 70/76 (92.1%) patients, VFM revealed a single aspiration, and in 17/70 (24.3%) cases, aspiration occurred before swallowing, in 32/70 (45.7%) during swallowing, and in 21/70 (30%) after swallowing. In 6/76 cases (7.9%), there were multiple aspirations, and compensatory postures were not sought in these patients.

Compensatory postures (Figures 1 and 2) through VFM guidance were tested in the 70 patients with a single aspiration and the five with no transit (Table 2). Among the aspiration cases, 24 (34%) had no spontaneous reflex cough. The 17 patients with aspiration before swallowing suffered from disorders of the oral phase, such as a deficit of lip closure (17.6%), reduced lifting of the soft palate (41.2%), and reduced (29.4%) or disorganized tongue movement (11.8%). The tongue-palate contact was incomplete in 4/17 (23.5%), with leakage and aspiration before voluntary swallowing due to a fraction of the bolus moving into the pharynx and being aspired without manometric alterations. In 8/17 cases (47%), the manometric evaluation showed that the tongue base pressure was < 60 mmHg during swallowing. In all 17 patients, a total resolution of the disorder was obtained by adopting the chin-down posture.

Aspiration during swallowing occurred in 32 (45.7%) cases. Eighteen of these (56.3%) were related to a reduced laryngeal closure (10/32) or elevation (8/32), and 14 were related to a UES disorder, with a residual pressure during relaxation of > 10 mmHg (9/14, 28.1%) and an early closure of the UES compared to the end of the pharyngeal contraction (5/14, 15.6%).

In 14/18 (78%) patients with reduced laryngeal closure or elevation, the chin-down posture (Figure 2) resolved the aspiration, whereas in 10/14 (71%) patients with UES disorders, the aspiration was corrected with the head-turned posture.

The compensatory postures were not effective in 8/32 (25%) patients. In the 21 cases of aspiration after swallowing, the bolus was inhaled due to stagnant contrast medium in the pharynx. The contrast medium was noted in 5/21 (23.8%) cases at the piriform sinuses, in 4/21 (19.1%) at the glossoepiglottic valleys, and in 12 (57.1%) at both locations. Aspiration after swallowing in 4/21 (19.1%) cases resulted from incomplete release

Table 3 Results of compensatory postures in selected patients

	ALS	Stroke	MS	PD	Post-surgery	AD	Others	Total
Swallowing disorders								
Aspiration before swallowing	4	5	1	3	1	3	-	17
Aspiration during swallowing	12	5	3	5	4	3	-	32
Aspiration after swallowing	10	2	2	3	2	2	-	21
No transit	1	-	-	2	-	2	-	5
Compensation postures								
Chin down	13	6	5	6	5	7	0	42
Head turned	10	4	1	3	0	1	0	19
Head hyperextended	1	0	0	2	0	2	0	5
No compensation	3	2	0	2	2	0	0	9

ALS: Amyotrophic lateral sclerosis; MS: Multiple sclerosis; PD: Parkinson's disease; AD: Alzheimer's disease.

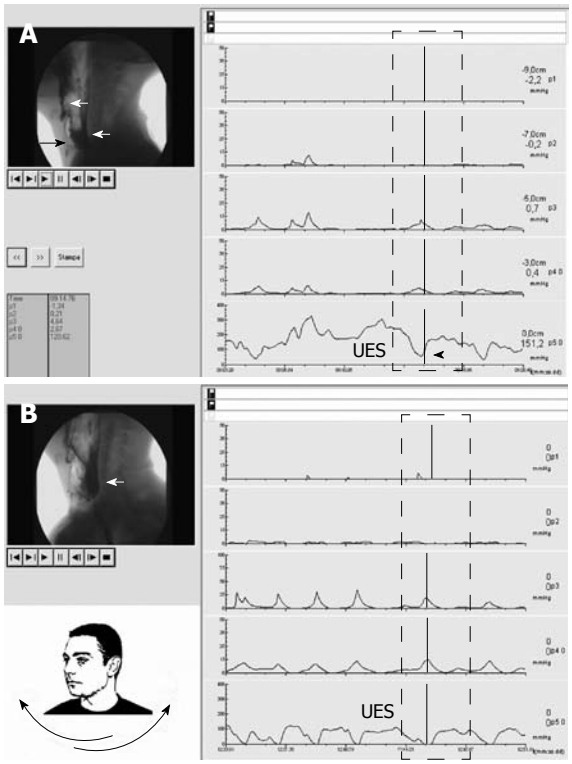

Figure 1 Videofluoromanometry study. A: Aspiration after swallowing (black arrow) with stagnation in the glossoepiglottic valleys and piriform sinuses (white arrows). Incomplete upper esophageal sphincter (UES) release (arrow); B: The same occurred with the head-rotated posture; stasis persisted at the pharyngo-esophageal junction (white arrow), but there was no aspiration of the contrast medium. The UES was fully open (dashed box).

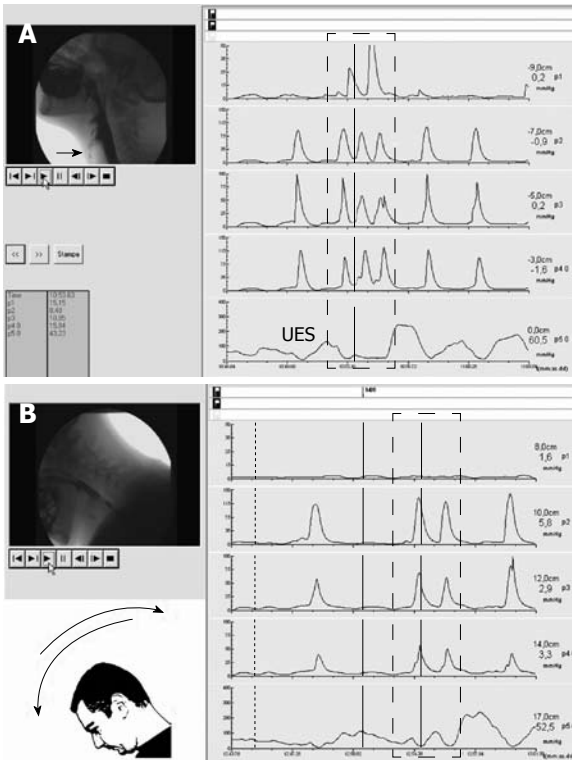

Figure 2 Videofluoromanometry study. A: Aspiration during swallowing (arrow) for the reduced laryngeal closure with an incomplete upper esophageal sphincter (UES) release; B: The same occurred in the course of the chin-down posture; this posture resolved the aspiration because it placed the epiglottis in a more protective position of the airways and restricted the airway entrance.

of the UES, with a residual pressure of > 10 mmHg. In 4/21 (19.1%) cases, the resting pressure of the UES was > 150 mmHg. In 1/21 (4.8%) cases, the pharyngeal dysfunction and stagnation of contrast medium was unilateral. The chin-down posture solved the aspiration in 11/21 cases (52.4%), and the head-turned posture was useful in 9/21 patients (42.9%). In 1/21 (4.7%) cases, there was no discomfort reduction.

In the five cases of dysphagia with no transit, the disorder was characterized by alterations in the initiation of the swallowing reflex without a peristaltic wave from the tongue base; all of these cases benefited from the hyperextended head posture (Table 3).

DISCUSSION

Swallowing therapy has the primary goal of maintaining oral feeding and achieving safe and efficient swallowing, which is important to ensure a good quality of life. Different swallowing techniques have been adopted rapidly during the past decade and are used almost worldwide. However, few studies have investigated how each technique affects swallowing[13,15,19].

When treating patients with oropharyngeal dysfunction, an ideal approach to the assessment and treatment

is working in a team with a radiologist, gastroenterologist and a speech-language pathologist. In the present study, a multi-specialist assessment team evaluated each enrolled patient to assess the swallowing dysfunction and test the adequacy of therapy to ensure safe transit. VFM provides a parallel acquisition of videofluoroscopic and manometric data and plays a crucial role in therapeutic planning.

We did not employ dietary modifications, including increases in the volume or density of food, for radioprotection reasons, but a single bolus of contrast medium was optimized for the patient.

Three different compensatory postures, including chin down, head turned and head hyperextended, were adopted. Each patient was tested before the posture was deemed appropriate. The compensatory postures restored a safe transit in 66/75 patients (88%). The chin-down posture was effective in 42/66 patients (63.6%). This posture was useful in all patients with aspiration before swallowing because it promoted bolus control in the oral cavity until the swallowing reflex was elicited. In patients with aspiration during swallowing and reduced laryngeal closure or elevation, the chin-down posture protected the airway from aspiration. In patients with aspiration after swallowing, dropping the tongue base and the contrast medium stasis in the pharynx fostered the bolus flow into the esophagus.

The head-turned posture was useful in 19/66 (28.8%) patients with both aspiration during swallowing and aspiration after swallowing with a residual pressure or uncoordinated UES relaxation due to the decrease in UES pressure and increase in UES opening time. This posture was useful also in one patient with stroke and unilateral pharyngeal failure because it excluded the affected side from the bolus transit.

The hyperextended head posture was effective in all five patients without transit. This posture uses gravity to aid swallowing; therefore, this posture is recommended for all cases with impaired lingual propulsion but should be suggested only after verifying that the transit occurs safely[4].

The compensatory postures were not effective in 9/75 patients (12%). This finding was related to a massive aspiration in 3/9 cases, poor compliance due to an advanced stage of disease in 4/9 cases, and surgery in 2/9 cases.

Silent aspiration, defined as aspiration in the absence of reflex cough, should also be mentioned. This event occurred in 24/70 (34.3%) patients with a single aspiration; specifically, three with aspiration before swallowing, 10 during swallowing, and 11 after swallowing. In other studies, this phenomenon occurred in approximately half of those patients who aspirated and was significantly more frequent in those with a history of laryngeal pathology[20].

Silent aspiration has major importance[21] because it promotes the early onset of complications, such as aspiration pneumonia. Aspiration pneumonia is three times more frequent in dysphagia patients than those without[22], and is the most common cause of death in patients with neurological disorders associated with dysphagia[23].

The present study had some limitations, including the use of an intraluminal manometric catheter, which is considered a non-altering device for swallowing, and the poor availability and high cost of this imaging method.

Compared to other studies[13,15], this study included the largest number of patients. The effectiveness of the compensatory postures in the oropharyngeal dysphagia patients was evaluated with combined videofluorography and manometry. In our experience, manometry has extensively evaluated deglutition disorders. Consequently, this method has chosen the better posture and defined the more effective therapeutic strategy.

In conclusion, there is not a single compensatory posture for each type of aspiration. Only VFM accurately defines the pathogenic mechanism of the swallowing deficit; helps the speech-language therapist choose the most effective compensation posture without a trial-and-error process; and checks the effectiveness at the same time. The chin-down, head-turned and head hyperextension postures are efficacious in several swallowing disorders. These postures can be evaluated during the examination itself, are easy to learn, and ensure good patient compliance. This study, complemented by a professional treatment team, guarantees a more accurate diagnosis and greater therapeutic efficacy than the individual modalities for evaluating dysphagia patients.

COMMENTS

Background

Choking, aspiration pneumonia, malnutrition and dehydration can complicate dysphagia. An exact characterization of the pathogenetic mechanisms of dysphagia helps define the therapeutic approach to reduce the risk of complications.

Research frontiers

Videofluoromanometry (VFM) is the gold standard for swallowing studies and analyzing the mechanisms underlying dysphagia.

Innovations and breakthroughs

There is not a single compensatory posture for each type of aspiration. Only VFM accurately defines the pathogenic mechanism of the swallowing deficit; helps the speech-language therapist choose the most effective compensation posture without a trial-and-error process; and checks the effectiveness at the same time.

Applications

VFM explores the effectiveness of the compensatory postures. This method may help manage dysphagia.

Peer review

This is a novel approach for the assessment of swallowing and the anatomy and physiology of the laryngopharyngeal segment. The authors seem to know the radiological aspects of the subject.

REFERENCES

1 **Merlo A**, Cohen S. Swallowing disorders. *Annu Rev Med* 1988; **39**: 17-28
2 **Cook IJ**, Kahrilas PJ. AGA technical review on management of oropharyngeal dysphagia. *Gastroenterology* 1999; **116**: 455-478
3 **Cook IJ**. Oropharyngeal dysphagia. *Gastroenterol Clin North Am* 2009; **38**: 411-431

4 **Rofes L**, Arreola V, Romea M, Palomera E, Almirall J, Cabré M, Serra-Prat M, Clavé P. Pathophysiology of oropharyngeal dysphagia in the frail elderly. *Neurogastroenterol Motil* 2010; **22**: 851-858, e230

5 **Eslick GD**, Talley NJ. Dysphagia: epidemiology, risk factors and impact on quality of life--a population-based study. *Aliment Pharmacol Ther* 2008; **27**: 971-979

6 **Lo Re G**, Galia M, La Grutta L, Russo S, Runza G, Taibbi A, D'Agostino T, Lo Greco V, Bartolotta TV, Midiri M, Cardinale AE, De Maria M, Lagalla R. Digital cineradiographic study of swallowing in patients with amyotrophic lateral sclerosis. *Radiol Med* 2007; **112**: 1173-1187

7 **Barbiera F**, Condello S, De Palo A, Todaro D, Mandracchia C, De Cicco D. Role of videofluorography swallow study in management of dysphagia in neurologically compromised patients. *Radiol Med* 2006; **111**: 818-827

8 Società Italiana di Nutrizione Artificiale e Metabolismo (SINPE) Linee Guida per la Nutrizione Artificiale Ospedaliera, 2002. Available from: URL: http//: www.sinpe.it

9 **Cappabianca S**, Reginelli A, Monaco L, Del Vecchio L, Di Martino N, Grassi R. Combined videofluoroscopy and manometry in the diagnosis of oropharyngeal dysphagia: examination technique and preliminary experience. *Radiol Med* 2008; **113**: 923-940

10 American Speech-Language Hearing Association (ASHA) Revisione medica delle linee guida per interventi sulla disfagia, 2004. Available from: URL: http//: www.asha.org

11 **Ohmae Y**, Karaho T, Hanyu Y, Murase Y, Kitahara S, Inouye T. [Effect of posture strategies on preventing aspiration]. *Nihon Jibiinkoka Gakkai Kaiho* 1997; **100**: 220-226

12 **Bülow M**, Olsson R, Ekberg O. Supraglottic swallow, effortful swallow, and chin tuck did not alter hypopharyngeal intrabolus pressure in patients with pharyngeal dysfunction. *Dysphagia* 2002; **17**: 197-201

13 **Olsson R**, Castell JA, Castell DO, Ekberg O. Solid-state computerized manometry improves diagnostic yield in pharyngeal dysphagia: simultaneous videoradiography and manometry in dysphagia patients with normal barium swallows. *Abdom Imaging* 1995; **20**: 230-235

14 **Solazzo A**, Del Vecchio L, Reginelli A, Monaco L, Sagnelli A, Monsorrò M, Di Martino N, Tedeschi G, Grassi R. Search for compensation postures with videofluoromanometric investigation in dysphagic patients affected by amyotrophic lateral sclerosis. *Radiol Med* 2011; **116**: 1083-1094

15 **Rasley A**, Logemann JA, Kahrilas PJ, Rademaker AW, Pauloski BR, Dodds WJ. Prevention of barium aspiration during videofluoroscopic swallowing studies: value of change in posture. *AJR Am J Roentgenol* 1993; **160**: 1005-1009

16 **Baylow HE**, Goldfarb R, Taveira CH, Steinberg RS. Accuracy of clinical judgment of the chin-down posture for dysphagia during the clinical/bedside assessment as corroborated by videofluoroscopy in adults with acute stroke. *Dysphagia* 2009; **24**: 423-433

17 **Logemann JA**, Kahrilas PJ, Kobara M, Vakil NB. The benefit of head rotation on pharyngoesophageal dysphagia. *Arch Phys Med Rehabil* 1989; **70**: 767-771

18 **Nagaya M**, Kachi T, Yamada T, Igata A. Videofluorographic study of swallowing in Parkinson's disease. *Dysphagia* 1998; **13**: 95-100

19 **Logemann JA**. Dysphagia: evaluation and treatment. *Folia Phoniatr Logop* 1995; **47**: 140-164

20 **Lundy DS**, Smith C, Colangelo L, Sullivan PA, Logemann JA, Lazarus CL, Newman LA, Murry T, Lombard L, Gaziano J. Aspiration: cause and implications. *Otolaryngol Head Neck Surg* 1999; **120**: 474-478

21 **Ramsey D**, Smithard D, Kalra L. Silent aspiration: what do we know? *Dysphagia* 2005; **20**: 218-225

22 Stroke Prevention and Educational Awareness Diffusion (SPREAD) Ictus cerebrale: Linee guida italiane di prevenzione e trattamento, 2007. Available from: URL: http//: www.spread.it

23 **Restivo DA**. La disfagia nelle malattie neurologiche: anatomia, fisiopatologia e diagnostica clinico-strumentale. *Neurovegetativo News* 2007; **7**: 1-7

S- Editor Cheng JX **L- Editor** Kerr C **E- Editor** Li JY

World Journal of Gastroenterology

Online Submissions: http://www.wjgnet.com/1007-9327office
wjg@wjgnet.com
doi:10.3748/wjg.v18.i23.2979

World J Gastroenterol 2012 June 21; 18(23): 2979-2987
ISSN 1007-9327 (print) ISSN 2219-2840 (online)

BRIEF ARTICLE

Diagnostic value for extrahepatic metastases of hepatocellular carcinoma in positron emission tomography/computed tomography scan

Ji Eun Lee, Jae Young Jang, Soung Won Jeong, Sae Hwan Lee, Sang Gyune Kim, Sang-Woo Cha, Young Seok Kim, Young Deok Cho, Hong Soo Kim, Boo Sung Kim, So Young Jin, Deuk Lin Choi

Ji Eun Lee, Jae Young Jang, Soung Won Jeong, Sang-Woo Cha, Young Deok Cho, Institution for Digestive Research, Digestive Disease Center, Department of Internal Medicine, Soonchunhyang University Hospital, Seoul 140-743, South Korea
Sae Hwan Lee, Hong Soo Kim, Institution for Digestive Research, Digestive Disease Center, Department of Internal Medicine, Soonchunhyang University Hospital, Cheon-an 330-721, South Korea
Sang Gyune Kim, Young Seok Kim, Boo Sung Kim, Institution for Digestive Research, Digestive Disease Center, Department of Internal Medicine, Soonchunhyang University Hospital, Bu-cheon 420-767, South Korea
So Young Jin, Department of Pathology, Soonchunhyang University Hospital, Seoul 140-743, South Korea
Deuk Lin Choi, Department of Radiology, Soonchunhyang University Hospital, Seoul 140-743, South Korea
Author contributions: Lee JE, Jang JY, Jeong SW and Choi DL wrote the paper; Lee SH, Kim SG, Cha SW, Kim YS, Cho YD, Kim HS, Kim BS and Jin SY provided clinical advice; Lee JE, Jang JY and Jeong SW performed the research.
Correspondence to: Dr. Jae Young Jang, Institute for Digestive Research, Digestive Disease Center, Department of Internal Medicine, Soonchunhyang University Hospital, 657, Hannam-dong, Yongsan-gu, Seoul 140-743, South Korea. jyjang@schmc.ac.kr
Telephone: +82-2-7099863 Fax: +82-2-7099797
Received: December 9, 2011 Revised: February 6, 2012
Accepted: February 16, 2012
Published online: June 21, 2012

Abstract

AIM: To evaluated the value of ^{18}F-fluorodeoxyglucose (FDG) positron emission tomography (PET)/computed tomography (CT) scan in diagnosis of hepatocellular carcinoma (HCC) and extrahepatic metastases.

METHODS: A total of 138 patients with HCC who had both conventional imaging modalities and ^{18}F-FDG PET/CT scan done between November 2006 and March 2011 were enrolled. Diagnostic value of each imaging modality for detection of extrahepatic metastases was evaluated. Clinical factors and tumor characteristics including PET imaging were analyzed as indicative factors for metastases by univariate and multivariate methods.

RESULTS: The accuracy of chest CT was significantly superior compared with the accuracy of PET imaging for detecting lung metastases. The detection rate of metastatic pulmonary nodule $\geqslant$ 1 cm was 12/13 (92.3%), when < 1 cm was 2/10 (20%) in PET imaging. The accuracy of PET imaging was significantly superior compared with the accuracy of bone scan for detecting bone metastases. In multivariate analysis, increased tumor size ($\geqslant$ 5 cm) (P = 0.042) and increased average standardized uptake value (SUV) uptake (P = 0.028) were predictive factors for extrahepatic metastases. Isometabolic HCC in PET imaging was inversely correlated in multivariate analysis (P = 0.035). According to the receiver operating characteristic curve, the optimal cutoff of average SUV to predict extrahepatic metastases was 3.4.

CONCLUSION: ^{18}F-FDG PET/CT scan is invaluable for detection of lung metastases larger than 1 cm and bone metastases. Primary HCC having larger than 5 cm and increased average SUV uptake more than 3.4 should be considered for extrahepatic metastases.

Key words: ^{18}F-fluorodeoxyglucose positron emission tomography/computed tomography scan; Diagnosis; Hepatocellular carcinoma; Extrahepatic metastases

Peer reviewer: Zenichi Morise, Professor, Surgery, Fujita Health University School of Medicine Banbuntane Houtokukai

Hospital, 3-6-10 Otobashi Nakagawa-ku, Nagoya, Aichi 454-8509, Japan

Lee JE, Jang JY, Jeong SW, Lee SH, Kim SG, Cha SW, Kim YS, Cho YD, Kim HS, Kim BS, Jin SY, Choi DL. Diagnostic value for extrahepatic metastases of hepatocellular carcinoma in positron emission tomography/computed tomography scan. *World J Gastroenterol* 2012; 18(23): 2979-2987 Available from: URL: http://www.wjgnet.com/1007-9327/full/v18/i23/2979.htm DOI: http://dx.doi.org/10.3748/wjg.v18.i23.2979

INTRODUCTION

Most patients with hepatocellular carcinoma (HCC) present with underlying liver disease, usually cirrhosis, hepatitis B and hepatitis C virus infection[1,2]. Screening and surveillance programmes based on periodic ultrasonography and α-fetoprotein (AFP) among high-risk patients could establish of early diagnosis and provide more effective treatments of HCC[3]. With advances in variable treatment modalities, the prognosis of HCC has been much improved[4-7]. With prolonged survival of HCC patients, the incidence of extrahepatic metastases has been reported up to 42%[8]. Precise evaluation of extrahepatic metastases of HCC is important because treatment modality could be determined belong to the results.

Positron emission tomography (PET)/computed tomography (CT) scan using ^{18}F-fluorodeoxyglucose (FDG) is now well established as a noninvasive diagnostic tool for diagnosis, staging and monitoring of a variety of malignant tumors[9,10]. However, in detection of primary HCC, the sensitivity of ^{18}F-FDG PET/CT scan has been reported not sufficiently high (50%-55%) because of its variable ^{18}F-FDG uptake pattern[11-14].

Several studies were performed for investigation of usefulness of ^{18}F-FDG PET/CT scan in detection of extrahepatic metastases of HCC. A previous study reported that the sensitivity for the detection of extrahepatic metastasis was 79%[15,16]. However, there are few detailed reports to compare ^{18}F-FDG PET/CT scan with conventional imaging modalities.

In this study, we evaluated the value of ^{18}F-FDG PET/CT scan in diagnosis of primary HCC and extrahepatic metastases. Furthermore, we suggest several clinical factors and tumor characteristics including ^{18}F-FDG PET/CT scan findings that indicate extrahepatic metastases in diagnosis of HCC.

MATERIALS AND METHODS

Patients

We conducted a retrospective chart review of patients with HCC at Soonchunhyang University Hospital who had both conventional imaging modalities and ^{18}F-FDG PET/CT scan done within at least a month between November 2006 and March 2011. During this period, all patients diagnosed with HCC who were newly diagnosed or reevaluated after treatment underwent ^{18}F-FDG PET/CT scan. A total of 138 patients were enrolled for this study. Eighty-eight patients were treatment-naïve and the other 50 patients were previously treated for HCC (tumor resection, transcatheter arterial chemoembolization, radiofrequency ablation, systemic chemotherapy). The diagnosis of primary HCC was based on contrast enhanced abdomen CT or magnetic resonance imaging (MRI), where hyperattenuation in the arterial phase and early washout in the delayed phase were considered definitely diagnostic. Elevations in tumor markers such as AFP, protein induced by vitamin K antagonist Ⅱ (PIVKA Ⅱ) levels were considered suggestive of HCC. Ultrasound-guided needle biopsy was performed when considered necessary. This study was approved by the local institutional review board and was conducted in accordance with the principles set forth in the Declaration of Helsinki.

Conventional imaging modalities

Chest X-ray and contrast enhanced chest CT for evaluation of lung metastases were performed. If there are suspicious lesions, repeated contrast enhanced chest CT was examined within 3 mo. Whole body bone scan for evaluation of bone metastases was performed. If there are suspicious lesions, bone MRI was conducted for definite diagnosis or repeated bone scan was followed within 3 mo. Regional and distant lymph node metastases were determined according to contrast enhanced CT. If there are suspicious lesions, repeated contrast enhanced CT was examined within 3 mo to observe interval size difference. Some metastatic lesions were diagnosed with pathologic confirmation, but most metastatic lesions were clinically diagnosed because of difficult access to deep lesions and too small size to do a biopsy.

Intrahepatic tumor size was measured by the greatest diameter in treatment-naïve patients, and the greatest diameter including viable portion from the first diagnosis in previously treated patients.

^{18}F-FDG PET/CT scan

^{18}F-FDG PET/CT scan was performed with a Biograph 2 (Siemens Medical Solution, Knoxville, TN, United States). All patients fasted for at least 6 h before ^{18}F-FDG injection. Serum glucose levels measured at the time of ^{18}F-FDG injection were less than 150 mg/dL in all patients. Approximately 370-500 MBq of ^{18}F-FDG was injected intravenously and an emission scan (2.5 min/bed position) was performed from the knees to the head 40 min after of ^{18}F-FDG injection in the two dimensional imaging mode. A transmission scan (3 min/bed position) was then obtained with a rotating ^{68}Ge source.

^{18}F-FDG PET images were interpreted by one over 30 years experienced nuclear medicine physician. If no significant ^{18}F-FDG uptake was detectable in the tumor compared to normal liver tissue by ^{18}F-FDG PET/CT scan, this was considered isometabolic HCC, hypermetabolic HCC for increased ^{18}F-FDG uptake, and

Table 1 Patients baseline characteristics

	n = 138	%
Age	59.6 ± 11.1 (range: 33-84)	
Sex		
M/F	114/24	82.6/17.4
Etiology of liver disease		
HBV/HCV/alcohol/unknown	89/15/10/24	64.5/10.9/7.2/17.4
AFP (ng/mL)	9512.9 ± 23 026.4	
PIVKA Ⅱ (mAU/mL)	854.2 ± 871.7	
Tumor morphology		
Nodular/infiltrating	78/60	56.5/43.6
Tumor size (mm)	69.8 ± 45.2	
Tumor number		
1/≥ 2	52/86	37.7/62.3
PVTT		
Yes	54	39.1
Child-Pugh classification		
A/B/C	77/56/5	55.8/40.6/3.6
Tumor stage[1]		
Ⅰ/Ⅱ/Ⅲ/Ⅳa/Ⅳb	7/34/26/22/49	5.1/24.6/18.8/15.9/35.5
SUV		
Iso-/hypometabolism	42/3	30.4/2.2
Hypermetabolism	93	67.4
Maximum	5.32 ± 2.38	
Average	4.03 ± 1.26	
TNR (SUV ratio)	1.60 ± 0.49	
Extrahepatic metastases	50	36.2
Lung	23	46.0
Lymph nodes	22	44.0
Bone	11	22.0
Others[2]	5	10.0

[1]Tumor stage based on the Modified Union for International Cancer Control Tumor Node Metastasis staging system; [2]Others: Adrenal gland, peritoneal carcinomatosis, Morrison's pouch. HBV: Hepatitis B virus; HCV: Hepatitis C virus; AFP: α-fetoprotein; PIVKA Ⅱ: Protein induced by vitamin K antagonist Ⅱ; PVTT: Portal vein tumor thrombosis; SUV: Standardized uptake value; TNR: Tumor-to-nontumor ratio.

hypometabolic HCC for decreased ^{18}F-FDG uptake. Isometabolic or hypometabolic HCC was excluded from quantitative evaluation. For measurement of ^{18}F-FDG uptake, region of interest (ROI) was placed over tumor lesion including the area of maximum activity. The highest value of ^{18}F-FDG uptake in ROI is defined as maximum standardized uptake value (SUV) and the average value of ^{18}F-FDG uptake in ROI is defined as average SUV. Then, ROI was placed over nontumor area sized 20 mm × 20 mm for estimation of average ^{18}F-FDG uptake of nontumor area. SUV was calculated by as follows; mean tissue activity (kBq/mL) × calibration factor × body weight (kg)/injected dose (MBq). The tumor-to-nontumor ratio (TNR, SUV ratio) was calculated by average tumor SUV/average nontumor SUV.

Histologic examination

Histologic examination was performed to assess the histologic grade of HCC (n = 50). Twenty-nine patients were indicated for tumor resection at diagnosis, the other 21 patients were performed ultrasound-guided needle biopsy. According to histologic grade, the tumors were divided into low-grade (well-differentiated and moderately-differentiated type) and high-grade (poorly-differentiated and undifferentiated type). As 4 patients were revealed as combined HCC-CC (cholangiocarcinoma), a total of 46 patients were analyzed.

Statistical analysis

Data are expressed as the mean ± SD, range, or n (%) as appropriate. When comparing the baseline characteristics of patients with 2 different groups, chi-square test and Fisher's exact test were used for categorical data, and the Student t test and U test were used for continuous variables. We performed receiver operating characteristic (ROC) curve analysis to compare the diagnostic performance of conventional and PET imaging for detection of extrahepatic metastasis. To estimate risk factors for extrahepatic metastases of HCC, univariate and subsequent multivariate logistic regression analysis were used. The overall cumulative survival rate was analyzed using the Kaplan-Meier method, and differences in survival between the groups were compared using a log-rank test. Data analysis was performed using SPSS 17.0 and MedCalc.

RESULTS

Patient characteristics

Patient characteristics are summarized in Table 1. Eighty-six patients (62.3%) had multiple lesions and 54 patients (39.1%) had portal vein thrombosis. Child-Pugh class A was 77 patients (55.8%), 56 patients (40.6%), and stage Ⅳb was 49 patients (35.5%) based on the modified Union for International Cancer Control Tumor Node Metastasis staging system.

Correlation between ^{18}F-FDG uptake and tumor differentiation

Forty-five of 138 patients (32.6%) with HCC did not have ^{18}F-FDG uptake. Therefore, SUV (maximum and average) was calculated in 93 patients (67.4%). The maximum SUV was 5.32 ± 2.38, average SUV was 4.03 ± 1.26, and tumor-to-nontumor ratio (TNR) was 1.60 ± 0.49 (Table 1). We analyzed the correlation of histologic grade in HCC with clinical factors and tumor characteristics including ^{18}F-FDG PET/CT scan findings (Table 2). Forty-six patients were performed tumor resection or ultrasound-guided needle biopsy and assessed the histologic grade.

In HCC with isometabolism, low-grade HCC was found in 14 patients and high-grade HCC in 2 patients; Isometabolic HCC tended to be histologically low-grade rather than high-grade (P = 0.061). In hypermetabolic HCC, maximum SUV value was higher in high-grade HCC than low-grade HCC (5.75 ± 2.15 *vs* 3.75 ± 0.74, P = 0.027) although average SUV and TNR (SUV ratio) was not different between two groups (Table 2).

Diagnostic value of imaging modalities for detection of extrahepatic metastases

The results of the detection rate of conventional imaging modalities and ^{18}F-FDG PET/CT scan for extrahepatic metastases in HCC are summarized in Table 3.

Table 2 Correlation of histologic grade with clinical factors and tumor characteristics *n* (%)

	Low-grade (*n* = 34)	High-grade (*n* = 12)	*P* value[1]
Age	61.7 ± 8.4	56.5 ± 6.7	0.055
Sex			0.260
M/F	32 (94.1)/2	10 (83.3)/2	
Etiology of liver disease			0.431
HBV/HCV/alcohol/unknown	21/2/2/9	9/0/1/2	
AFP (ng/mL)	2892.0 ± 9255.6	2960.5 ± 9554.0	0.930
<200/≥ 200	26 (76.5)/8	10 (83.3)/2	
PIVKA Ⅱ (mAU/mL) (*n* = 20/*n* = 7)	758.4 ± 823.1	798.6 ± 879.6	1.000
< 40/≥ 40	3 (15)/17	1 (16.7)/6	
Tumor morphology			0.441
Nodular/infiltrating	24 (70.6)/10	8 (66.7)/4	
Tumor size			0.643
< 5/≥ 5	16 (47.1)/18	7 (58.3)/5	
Tumor number			0.297
1/≥ 2	20 (58.8)/14	9 (75)/3	
PVTT			0.259
Yes	8 (23.5)	1 (8.3)	
Child-Pugh classification			0.563
A/B/C	30 (88.2)/4/0	11(91.7)/1/0	
T stage			0.537
1/2/3/4	3/15/9/7	1/7/2/2	
SUV			
Isometabolism	14 (41.2)	2 (16.7)	0.061
Hypometabolism	2	0	
Hypermetabolism (*n* = 18/*n* = 10)			
Maximum	3.75 ± 0.74	5.75 ± 2.15	0.027
Average	3.30 ± 0.42	4.15 ± 1.17	0.226
TNR (SUV ratio)	1.33 ± 0.22	1.64 ± 0.52	0.286

HBV: Hepatitis B virus; HCV: Hepatitis C virus; AFP: α-fetoprotein; PIVKA Ⅱ: Protein induced by vitamin K antagonist Ⅱ; PVTT: Portal vein tumor thrombosis; SUV: Standardized uptake value; TNR: Tumor-to-nontumor ratio. [1]Statistical significance test was done by *U* test.

Twenty-three patients were diagnosed of clinical lung metastases showing interval size increase on follow up chest CT. Fifteen patients were test positive on ^{18}F-FDG PET/CT scan, 14 patients were true positive and 1 patient turned out to be false positive revealing non-tuberculosis mycobacterium infection on percutaneous transthoracic needle aspiration (Figure 1). The detection rate of metastatic pulmonary nodule ≥ 1 cm was 12/13 (92.3%), when < 1 cm was 2/10 (20%) (P = 0.0003). The sensitivity, specificity, and accuracy for detection of lung metastases in HCC by ^{18}F-FDG PET/CT scan were 60.9%, 99.1% and 92.6%, respectively (Table 3). Contrast enhanced chest CT all detected for lung metastases in HCC and 2 lesions turned out to be false positive which did not show size increase during follow up chest CT. Therefore, the sensitivity, specificity and accuracy were 100%, 98.2% and 98.5%, respectively. The accuracy of chest CT was significantly superior compared with the accuracy of PET imaging for detecting lung metastases by comparison of ROC curves (P = 0.000, CI 0.0888-0.294) (Table 3).

Twenty-two patients were diagnosed of regional or distant lymph node metastases showing arterial phase enhancement and interval size increase on follow up contrast enhanced CT. The sensitivity of ^{18}F-FDG PET/CT scan for lymph node metastases was 90.9% showing lower than 100% in conventional imaging modalities. Both ^{18}F-FDG PET/CT scan and contrast enhanced CT detected 4 lesions as a positive test which turned out to be false positive. The accuracy of both images was not different by comparison of ROC curves (P = 0.269) (Table 3).

Table 3 Diagnostic value of ^{18}F-fluorodeoxyglucose positron emission tomography/computed tomography scan and conventional imaging modalities for detection of extrahepatic metastases

	Lung metastases (*n* = 23)		Lymph node metastases (*n* = 22)		Bone metastases (*n* = 11)	
	TP	TN	TP	TN	TP	TN
PET (+)	14	1	20	4	11	0
Conventional (+)	23	2	22	4	7	4
	PET	Conventional	PET	Conventional	PET	Conventional
Sensitivity, %	60.9	100	90.9	100	100	63.6
Specificity, %	99.1	98.2	96.5	96.5	100	96.8
Accuracy, %	92.6	98.5	95.6	97.1	100	94.1
PPV, %	93.3	92	83.3	84.6	100	63.6
NPV, %	92.5	100	98.2	100	100	96.8
Comparison of ROC curves	P = 0.000 (CI: 0.0888-0.294)		P = 0.269		P = 0.010 (CI: 0.0481-0.348)	

TP: True positive; TN: True negative; PPV: Positive predictive value; NPV: Negative predictive value; ROC: Receiver operating characteristic; PET: Positron emission tomography.

Eleven patients were diagnosed of bone metastases, ^{18}F-FDG PET/CT scan detected all of these lesions. However, bone scan failed to identify 4 patients and 4 suspicious of metastases turned out to be false positive. Therefore, the sensitivity, specificity and accuracy of ^{18}F-FDG PET/CT scan in diagnoses of bone metastases were 100%, 100% and 100%, respectively. The sensitivity, specificity and accuracy of bone scan were 63.6%, 96.8% and 94.1%, respectively. The accuracy of PET imaging was significantly superior compared with the accuracy of bone scan for detecting bone metastases by comparison of ROC curves (P = 0.010, CI: 0.0481-0.348) (Table 3).

Three patients with adrenal metastases were all detected by abdomen CT, but ^{18}F-FDG PET/CT scan failed to detect metastasis in one patient. There were 2 patients who were suspicious of cervical lymph node metastasis on both ^{18}F-FDG PET/CT scan and neck CT which turned out to be Warthin's tumor on needle biopsy.

Indicative factors for extrahepatic metastases in ^{18}F-FDG PET/CT scan

Elevated AFP (≥ 200 ng/mL), elevated PIVKA Ⅱ (≥ 40 mAU/mL), infiltrative tumor morphology, larger tumor size (≥ 5 cm), multiple tumors in liver, portal vein tumor thrombosis, advanced T stage, increased SUV uptake and high-grade HCC were associated with the presence of extrahepatic metastases of HCC (Table 4).

In multivariate analysis, increased tumor size (≥ 5 cm) (P = 0.042) and increased average SUV uptake (P = 0.028) were indicative factors for extrahepatic metastases in HCC (Table 4). Isometabolic HCC in ^{18}F-FDG PET/CT scan was inversely correlated with extrahepatic me-

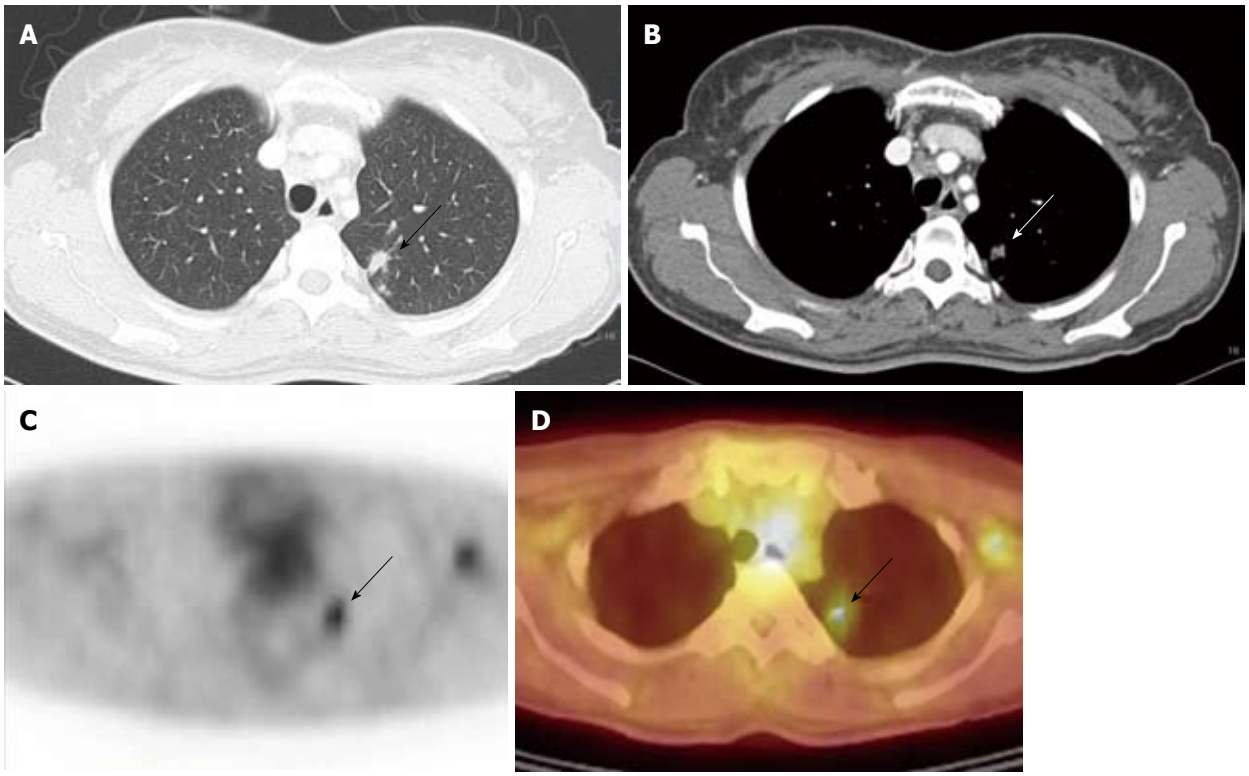

Figure 1 A 51 year-old-female with hepatocellular carcinoma was suspicious of lung metastasis (arrows) in both chest computed tomography and ^{18}F-fluorodeoxyglucose positron emission tomography/computed tomography scan which turned out to be nontuberculosis mycobacterium infection on percutaneous transthoracic needle aspiration. A: High-resolution computed tomography (CT); B: Contrast-enhanced CT; C: ^{18}F-fluorodeoxyglucose positron emission tomography (^{18}F-FDG PET); D: PET/CT scan.

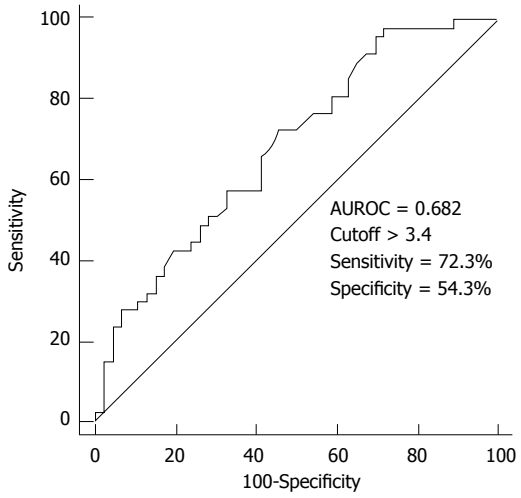

Figure 2 The area under the receiver operating characteristic curve to estimate the optimal cutoff of average standardized uptake value to predict extrahepatic metastasis. AUROC: Area under receiver operating characteristic.

tastases (P = 0.035). According to the ROC curve, the optimal cutoff of average SUV to predict extrahepatic metastases was > 3.4 (Figure 2). Therefore, when the average SUV in ROI is higher than 3.4, we should consider the possibility of extrahepatic metastases with poor prognosis.

Cumulative survival rate was studied by intrahepatic tumor size, average SUV, isometabolic HCC, and extrahepatic metastasis after dividing average SUV group into two groups by the cutoff 3.4. The survival rate was significantly higher in group with tumor size < 5 cm (1-year survival rate; 69.1% *vs* 25.9%, P = 0.000) (Figure 3A), average SUV < 3.4 (1-year survival rate; 57.1% *vs* 19.2%, P = 0.000) (Figure 3B), and isometabolic HCC (1-year survival rate; 78.0% *vs* 28.3%, P = 0.000) (Figure 3C). There were 2 clinical factors that affected survival rate of HCC by Cox proportional hazard analysis. Child-pugh class [class B: odds ratio (OR) 4.784, CI: 2.575-8.891, P = 0.000; class C: OR 10.787, CI: 3.579-32.511, P = 0.000] and metastases (OR 2.069, CI: 1.152-3.715, P = 0.015) were significantly associated with survival rate (Table 5).

DISCUSSION

Several investigators quantitatively evaluated glucose utilization in HCC with ^{18}F-FDG PET/CT scan and showed its usefulness for assessing characterization of tumor[17]. Increased tumor ^{18}F-FDG uptake is highly reflected the enzymatic activity of glucose metabolism and the histologic grading of HCC[17,18]. Well-differentiated HCC cells exhibit an ^{18}F-FDG metabolism similar to that of normal liver tissue, whereas undifferentiated HCC cells do not do so[17,19]. ^{18}F-FDG PET/CT scan was not sensitive than ultrasound and serum AFP levels for diagnosing HCC in HBV carriers[14]. Because of its limitations for intrahepatic lesions, ^{18}F-FDG PET/CT scan is not suitable as

Table 4 Clinical factors and tumor characteristics of extrahepatic metastases in hepatocellular carcinoma

	Metastasis (n = 50)	No metastasis (n = 88)	*P* value	
			Uni	Multi
Age	58.7 ± 11.1	60.1 ± 11.1	0.480	
Sex			0.285	
M/F	39/11	75/13		
Etiology of liver disease			0.215	
HBV/HCV/alcohol/unknown	31/3/4/12	58/12/6/12		
AFP (ng/mL)	15 568.8 ± 28 119.6	6072.1 ± 18 882.3	0.019	0.254
< 200/≥ 200 (%)	21/29 (58.0)	59/29 (33.0)		
PIVKA Ⅱ (mAU/mL)	1320.5 ± 784.0	630 ± 827.9	0.001	
< 40/≥ 40 (n = 25/n = 52) (%)	2/23 (92.0)	18/34 (65.4)		
Tumor morphology			0.000	0.126
Nodular/infiltrating (%)	17/33 (66.0)	61/27 (30.7)		
Tumor size	88.9 ± 40.2	58.9 ± 44.5	0.000	0.042[1]
< 5/≥ 5 (%)	7/43 (86.0)	48/40 (45.5)		
Tumor number			0.000	0.382
1/≥ 2 (%)	7/43 (86.0)	45/43 (48.9)		
PVTT			0.000	0.330
Yes (%)	30 (60.0)	24 (27.2)		
Child-Pugh classification			0.474	
A/B/C	35/11/4	68/19/1		
T stage			0.000	0.197
1/2/3/4 (%)	1/4/12/33 (66.0)	7/34/26/21 (23.9)		
SUV				
Isometabolism (%)	3 (6.0)	39 (44.3)	0.000	0.035
Hypometabolism	0	3		
Hypermetabolism (n = 47)				
Maximum	5.89 ± 2.55	4.74 ± 2.05	0.019	0.517
Average	4.38 ± 1.35	3.68 ± 1.05	0.006	0.028[2]
TNR (SUV ratio)	1.70 ± 0.51	1.50 ± 0.45	0.048	0.352
Pathology			0.042	
Low-/high-grade (n = 12/n = 34) (%)	7 (58.3)/5	27 (79.4)/7		

[1]1.06-31.8; [2]1.3-127.9. HBV: Hepatitis B virus; HCV: Hepatitis C virus; AFP: α-fetoprotein; PIVKA Ⅱ: Protein induced by vitamin K antagonist Ⅱ; PVTT: Portal vein tumor thrombosis; SUV: Standardized uptake value; TNR: Tumor-to-nontumor ratio.

Table 5 Clinical factors that affected survival by multivariate analysis

	Odds ratio	CI	*P* value
Child class B	4.784	2.575-8.891	0.000
Child class C	10.787	3.579-32.511	0.000
AFP (> 200 ng/mL)	1.825	0.998-3.338	0.051
Tumor size (> 5 cm)	1.004	1.000-1.009	0.060
Metastases	2.069	1.152-3.715	0.015

a screening tool for detection of intrahepatic recurrence after tumor resection or liver transplantation[16].

In our study, 45 of 138 patients (32.6%) with HCC did not have ^{18}F-FDG uptake. Isometabolic HCC tended to be histologically low-grade (P = 0.061) and showed superior survival rate (P = 0.000). In this aspect, ^{18}F-FDG PET/CT scan might be useful for the prediction of outcome in patients with hepatocellular carcinoma. Yang *et al*[20] reported PET imaging could be a good preoperative tool for estimating the post-LT risk of tumor recurrence. It reported the overall survival rate was significantly lower in high SUV and high TNR group. Especially, TNR was independent predictor of survival in HCC patients in multivariate analysis[18,21]. The blood glucose level is often high in patients with cirrhosis[22], affecting the SUV in the tumor region[23]. Therefore, TNR, tumor-to-nontumor SUV ratio more strongly correlated with characteristics of HCC than SUV[21]. In our study, the cumulative survival rate in the group with average SUV less than 3.4 was significantly higher than in the group with average SUV more than 3.4.

Extrahepatic metastases of HCC was occurred in 36.2% (29.5% in treatment-naïve patients) in our study which have been reported to occur in 13.5%-42%[24-27]. Major metastatic sites from HCC are the lung, lymph nodes, bone, and adrenal gland consistent with other reports[24-26,28].

It is known that lungs are both the most common site of metastases and the most common site of the first detectable metastases[16,24,25,28]. Chest X-ray is inexpensive, may serve as a baseline investigation to evaluate abnormalities, however, the detection rate of pulmonary metastases is low. Gielen *et al*[29] reported 10/19 patients with pulmonary metastases were not identified with chest X-ray in patients with colorectal cancer. To compare chest CT with ^{18}F-FDG PET/CT scan, the accuracy of chest CT was higher than ^{18}F-FDG PET/CT scan in our study. The detection rate of ^{18}F-FDG PET/CT scan was only 20% when metastatic pulmonary nodule < 1 cm. Therefore, to detect early lung metastases from

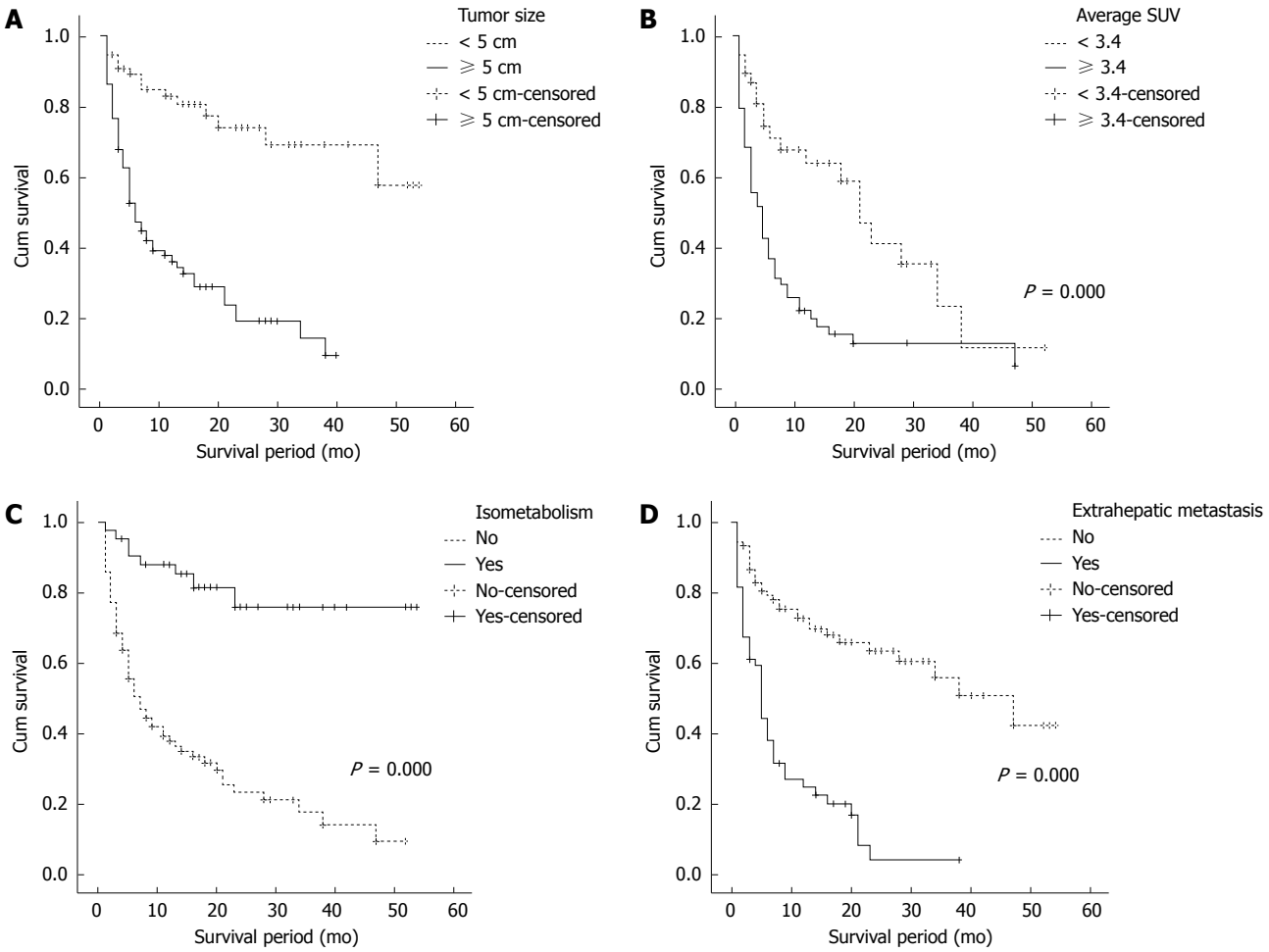

Figure 3 Cumulative survival rate in patients with hepatocellular carcinoma by intrahepatic tumor size (A), average standardized uptake value (B), isometabolic hepatocellular carcinoma (C) and extrahepatic metastasis (D). SUV: Standardized uptake value.

HCC, chest CT should be performed at regular intervals.

The diagnosis of regional or distant lymph node metastases is determined by interval size increase and arterial phase enhancement in abdomen CT/MRI, chest CT and neck CT[25]. It is well documented that patients who have cirrhosis also have benign enlarged lymph nodes[30]. In our study, 4 patients were detected for lymph node metastases, which turned out to be false positive in both ^{18}F-FDG PET/CT scan and contrast enhanced CT. Therefore, follow up CT is critical for determination of metastases even when increased ^{18}F-FDG uptake in ^{18}F-FDG PET/CT scan is observed. Lymph node metastasis is difficult to confirm due to poor accessibility for biopsy. If suspicious lesions were identified at conventional imaging or ^{18}F-FDG PET/CT scan, it should be clinically confirmed during follow-up imaging.

In our study, all bone metastases of HCC were detected by ^{18}F-FDG PET/CT scan whereas bone scan could not detect 4 lesions and 4 abnormal uptakes were false positive based on bone MRI and follow up imaging. Other studies have also reported PET imaging is more sensitive than bone scan[15,16,27]. Whole body bone scan is a routine modality in detecting bone metastases; however, lesions may remain invisible in the absence of an osteoblastic response. Furthermore, bone scan is not likely to differentiate healing fractures and degenerative disease from bone metastases[31]. Based on these results, ^{18}F-FDG PET/CT scan is more sensitive and specific diagnostic tool than bone scan for evaluation of bone metastases.

Although extrahepatic metastases of HCC are common, undergoing ^{18}F-FDG PET/CT scan in all HCC patients may not be cost-effective. Selected patients who are suspected of extrahepatic metastases of HCC should be performed of ^{18}F-FDG PET/CT scan. A previous study reported majority of patients (87%) with extrahepatic HCC had intrahepatic stage Ⅲ (10%) and stage Ⅳa (76%) tumors[25]. Natsuizaka *et al*[24] and Uka *et al*[26] also reported patients with more advanced intrahepatic tumor stage at the first diagnosis of HCC developed extraheaptic metastases more frequently. Especially, tumor diameter is a well-known predictor of extrahepatic metastases[27,28]. Our results demonstrated tumor size (⩾ 5 cm) (P = 0.042) was predictive factors for extrahepatic metastases in HCC which was strongly correlated with cumulative survival rate.

As previously mentioned, the most common site of the first detectable metastasis is lung. Our data showed that the sensitivity of ^{18}F-FDG PET/CT scan to detect

lung metastases was only 60.9%. Therefore, we suggest that patients with diagnosed of HCC should undergo chest CT at initial diagnosis of HCC. Sixteen of 22 patients (72.7%) with lymph node metastases and 6 of 11 patients (54.5%) with bone metastases were not accompanied by lung metastases, so the patients at high risk of extrahepatic metastases or who was diagnosed of lung metastases by chest CT should be considered performing ^{18}F-FDG PET/CT scan to identify other extrahepatic metastases.

Our data showed that average SUV in ^{18}F-FDG PET/CT scan is indicative factor for extrahepatic metastases, staging evaluation for metastases should be done carefully at regular interval in patients with high average SUV uptake. The SUV is well correlated with histologic differentiation and cumulative survival rate, therefore we can apply this information in clinical settings to make a decision for the treatment and predict the prognosis. PET imaging is highly sensitive for the diagnosis of bone metastases, it should be considered to be done when patients are suspicious of bone metastases, but negative results in bone scan.

There were limitations to our study. (1) It was a retrospective study; (2) We did not confirm the extrahepatic metastases by biopsy; and (3) In histologic grading of intrahepatic HCC, needle biopsy is prone to sampling error as only limited area of the tumor is analyzed microscopically.

In conclusion, ^{18}F-FDG PET/CT scan has a limitation for detection of intrahepatic tumor, but meaningful for prediction of prognosis and planning for staging evaluation. In aspect of a screening tool of extrahepatic metastasis of HCC, ^{18}F-FDG PET/CT scan is invaluable for detection of lung metastases larger than 1 cm and bone metastases. In evaluation of lymph node metastases, follow-up imaging is crucial for clinical diagnosis. We suggest that primary HCC having larger than 5 cm and increased average SUV uptake more than 3.4 should be considered for extrahepatic metastases.

COMMENTS

Background

With advances in variable treatment modalities, the prognosis of hepatocellular carcinoma (HCC) has been much improved. With prolonged survival of HCC patients, the incidence of extrahepatic metastases has been increased.

Research frontiers

Positron emission tomography (PET)/computed tomography (CT) scan using fluorodeoxyglucose (FDG) is now well established as a noninvasive diagnostic tool for diagnosis, staging and monitoring of a variety of malignant tumors. However, the role in diagnosis of primary HCC and extrahepatic metastases has not been reported sufficiently.

Innovations and breakthroughs

^{18}F-FDG PET/CT scan has a limitation for detection of intrahepatic tumor, but meaningful for prediction of prognosis and planning for staging evaluation. The detection rate of metastatic pulmonary nodule $\geq$ 1 cm was 12/13 (92.3%), when < 1 cm was 2/10 (20%) in PET imaging. The accuracy of PET imaging was significantly superior compared with the accuracy of bone scan for detecting bone metastases. In multivariate analysis, increased tumor size ($\geq$ 5 cm) (P = 0.042) and increased average standardized uptake value (SUV) uptake (P = 0.028) were predictive factors for extrahepatic metastases.

Applications

The study results suggest that ^{18}F-FDG PET/CT scan is invaluable for detection of lung metastases larger than 1 cm and bone metastases. Authors suggest that primary HCC having larger than 5 cm and increased average SUV uptake more than 3.4 should be considered for extrahepatic metastases.

Terminology

PET/CT scan: PET/CT scan depicts the spatial distribution of metabolic or biochemical activity in the body. PET/CT scan has revolutionized many fields of medical diagnosis, by adding precision of anatomic localization to functional imaging.

Peer review

This is a well-organized study in which authors analyze the substantial role in the diagnosis of extrahepatic metastases in HCC. Furthermore, the results are interesting that average SUV could suggest the prognosis of HCC. In patients with higher average SUV more than 3.4 should be carefully follow-up for the possibility of extrahepatic metastases.

REFERENCES

1 **Parkin DM**. The global health burden of infection-associated cancers in the year 2002. *Int J Cancer* 2006; **118**: 3030-3044

2 **Simonetti RG**, Cammà C, Fiorello F, Politi F, D'Amico G, Pagliaro L. Hepatocellular carcinoma. A worldwide problem and the major risk factors. *Dig Dis Sci* 1991; **36**: 962-972

3 **Trevisani F**, De NS, Rapaccini G, Farinati F, Benvegnù L, Zoli M, Grazi GL, Del PP, Di N, Bernardi M. Semiannual and annual surveillance of cirrhotic patients for hepatocellular carcinoma: effects on cancer stage and patient survival (Italian experience). *Am J Gastroenterol* 2002; **97**: 734-744

4 **Mazzaferro V**, Regalia E, Doci R, Andreola S, Pulvirenti A, Bozzetti F, Montalto F, Ammatuna M, Morabito A, Gennari L. Liver transplantation for the treatment of small hepatocellular carcinomas in patients with cirrhosis. *N Engl J Med* 1996; **334**: 693-699

5 **Arii S**, Yamaoka Y, Futagawa S, Inoue K, Kobayashi K, Kojiro M, Makuuchi M, Nakamura Y, Okita K, Yamada R. Results of surgical and nonsurgical treatment for small-sized hepatocellular carcinomas: a retrospective and nationwide survey in Japan. The Liver Cancer Study Group of Japan. *Hepatology* 2000; **32**: 1224-1229

6 **Lo CM**, Ngan H, Tso WK, Liu CL, Lam CM, Poon RT, Fan ST, Wong J. Randomized controlled trial of transarterial lipiodol chemoembolization for unresectable hepatocellular carcinoma. *Hepatology* 2002; **35**: 1164-1171

7 **Shiina S**, Teratani T, Obi S, Sato S, Tateishi R, Fujishima T, Ishikawa T, Koike Y, Yoshida H, Kawabe T, Omata M. A randomized controlled trial of radiofrequency ablation with ethanol injection for small hepatocellular carcinoma. *Gastroenterology* 2005; **129**: 122-130

8 **Si MS**, Amersi F, Golish SR, Ortiz JA, Zaky J, Finklestein D, Busuttil RW, Imagawa DK. Prevalence of metastases in hepatocellular carcinoma: risk factors and impact on survival. *Am Surg* 2003; **69**: 879-885

9 **Böhm B**, Voth M, Geoghegan J, Hellfritzsch H, Petrovich A, Scheele J, Gottschild D. Impact of positron emission tomography on strategy in liver resection for primary and secondary liver tumors. *J Cancer Res Clin Oncol* 2004; **130**: 266-272

10 **Rigo P**, Paulus P, Kaschten BJ, Hustinx R, Bury T, Jerusalem G, Benoit T, Foidart-Willems J. Oncological applications of positron emission tomography with fluorine-18 fluorodeoxyglucose. *Eur J Nucl Med* 1996; **23**: 1641-1674

11 **Khan MA**, Combs CS, Brunt EM, Lowe VJ, Wolverson MK, Solomon H, Collins BT, Di Bisceglie AM. Positron emission tomography scanning in the evaluation of hepatocellular carcinoma. *J Hepatol* 2000; **32**: 792-797

12 **Delbeke D**, Martin WH, Sandler MP, Chapman WC, Wright JK, Pinson CW. Evaluation of benign vs malignant hepatic lesions with positron emission tomography. *Arch Surg* 1998; **133**: 510-515; discussion 510-515

13 **Trojan J**, Schroeder O, Raedle J, Baum RP, Herrmann G, Jacobi V, Zeuzem S. Fluorine-18 FDG positron emission tomography for imaging of hepatocellular carcinoma. *Am J Gastroenterol* 1999; **94**: 3314-3319

14 **Jeng LB**, Changlai SP, Shen YY, Lin CC, Tsai CH, Kao CH. Limited value of 18F-2-deoxyglucose positron emission tomography to detect hepatocellular carcinoma in hepatitis B virus carriers. *Hepatogastroenterology* 2003; **50**: 2154-2156

15 **Sugiyama M**, Sakahara H, Torizuka T, Kanno T, Nakamura F, Futatsubashi M, Nakamura S. 18F-FDG PET in the detection of extrahepatic metastases from hepatocellular carcinoma. *J Gastroenterol* 2004; **39**: 961-968

16 **Kim YK**, Lee KW, Cho SY, Han SS, Kim SH, Kim SK, Park SJ. Usefulness 18F-FDG positron emission tomography/computed tomography for detecting recurrence of hepatocellular carcinoma in posttransplant patients. *Liver Transpl* 2010; **16**: 767-772

17 **Torizuka T**, Tamaki N, Inokuma T, Magata Y, Sasayama S, Yonekura Y, Tanaka A, Yamaoka Y, Yamamoto K, Konishi J. In vivo assessment of glucose metabolism in hepatocellular carcinoma with FDG-PET. *J Nucl Med* 1995; **36**: 1811-1817

18 **Seo S**, Hatano E, Higashi T, Hara T, Tada M, Tamaki N, Iwaisako K, Ikai I, Uemoto S. Fluorine-18 fluorodeoxyglucose positron emission tomography predicts tumor differentiation, P-glycoprotein expression, and outcome after resection in hepatocellular carcinoma. *Clin Cancer Res* 2007; **13**: 427-433

19 **Okazumi S**, Isono K, Enomoto K, Kikuchi T, Ozaki M, Yamamoto H, Hayashi H, Asano T, Ryu M. Evaluation of liver tumors using fluorine-18-fluorodeoxyglucose PET: characterization of tumor and assessment of effect of treatment. *J Nucl Med* 1992; **33**: 333-339

20 **Yang SH**, Suh KS, Lee HW, Cho EH, Cho JY, Cho YB, Yi NJ, Lee KU. The role of (18)F-FDG-PET imaging for the selection of liver transplantation candidates among hepatocellular carcinoma patients. *Liver Transpl* 2006; **12**: 1655-1660

21 **Shiomi S**, Nishiguchi S, Ishizu H, Iwata Y, Sasaki N, Tamori A, Habu D, Takeda T, Kubo S, Ochi H. Usefulness of positron emission tomography with fluorine-18-fluorodeoxyglucose for predicting outcome in patients with hepatocellular carcinoma. *Am J Gastroenterol* 2001; **96**: 1877-1880

22 **Megyesi C**, Samols E, Marks V. Glucose tolerance and diabetes in chronic liver disease. *Lancet* 1967; **2**: 1051-1056

23 **Langen KJ**, Braun U, Rota Kops E, Herzog H, Kuwert T, Nebeling B, Feinendegen LE. The influence of plasma glucose levels on fluorine-18-fluorodeoxyglucose uptake in bronchial carcinomas. *J Nucl Med* 1993; **34**: 355-359

24 **Natsuizaka M**, Omura T, Akaike T, Kuwata Y, Yamazaki K, Sato T, Karino Y, Toyota J, Suga T, Asaka M. Clinical features of hepatocellular carcinoma with extrahepatic metastases. *J Gastroenterol Hepatol* 2005; **20**: 1781-1787

25 **Katyal S**, Oliver JH, Peterson MS, Ferris JV, Carr BS, Baron RL. Extrahepatic metastases of hepatocellular carcinoma. *Radiology* 2000; **216**: 698-703

26 **Uka K**, Aikata H, Takaki S, Shirakawa H, Jeong SC, Yamashina K, Hiramatsu A, Kodama H, Takahashi S, Chayama K. Clinical features and prognosis of patients with extrahepatic metastases from hepatocellular carcinoma. *World J Gastroenterol* 2007; **13**: 414-420

27 **Yoon KT**, Kim JK, Kim do Y, Ahn SH, Lee JD, Yun M, Rha SY, Chon CY, Han KH. Role of 18F-fluorodeoxyglucose positron emission tomography in detecting extrahepatic metastasis in pretreatment staging of hepatocellular carcinoma. *Oncology* 2007; **72** Suppl 1: 104-110

28 **Kanda M**, Tateishi R, Yoshida H, Sato T, Masuzaki R, Ohki T, Imamura J, Goto T, Yoshida H, Hamamura K, Obi S, Kanai F, Shiina S, Omata M. Extrahepatic metastasis of hepatocellular carcinoma: incidence and risk factors. *Liver Int* 2008; **28**: 1256-1263

29 **Gielen C**, Sanli I, Stroeken L, Botterweck A, Hulsewé K, Hoofwijk A. Staging chest radiography is not useful in patients with colorectal cancer. *Eur J Surg Oncol* 2009; **35**: 1174-1178

30 **Dodd GD**, Baron RL, Oliver JH, Federle MP, Baumgartel PB. Enlarged abdominal lymph nodes in end-stage cirrhosis: CT-histopathologic correlation in 507 patients. *Radiology* 1997; **203**: 127-130

31 **Schmidt GP**, Reiser MF, Baur-Melnyk A. Whole-body MRI for the staging and follow-up of patients with metastasis. *Eur J Radiol* 2009; **70**: 393-400

S- Editor Gou SX **L- Editor** A **E- Editor** Li JY

World Journal of Gastroenterology

Online Submissions: http://www.wjgnet.com/1007-9327office
wjg@wjgnet.com
doi:10.3748/wjg.v18.i23.2988

World J Gastroenterol 2012 June 21; 18(23): 2988-2994
ISSN 1007-9327 (print) ISSN 2219-2840 (online)

BRIEF ARTICLE

Noninvasive assessment of hepatic fibrosis in Egyptian patients with chronic hepatitis C virus infection

Shawky Abdelhamid Fouad, Serag Esmat, Dalia Omran, Laila Rashid, Mohamed H Kobaisi

Shawky Abdelhamid Fouad, Serag Esmat, Department of Internal Medicine, Faculty of Medicine, Cairo University, Cairo 11562, Egypt
Dalia Omran, Department of Tropical Medicine, Faculty of Medicine, Cairo University, Cairo 11562, Egypt
Laila Rashid, Department of Biochemistry, Faculty of Medicine, Cairo University, Cairo 11562, Egypt
Mohamed H Kobaisi, Department of Pathology, National Institute of Nephrology, Cairo 35789, Egypt
Author contributions: Fouad SA, Esmat S and Omran D designed the study and collected the clinical data; Rashid L performed the laboratory analysis; Kobaisi MH performed the histopathological analysis; Fouad SA wrote the manuscript; Esmat S critically revised the manuscript for important intellectual content; all authors contributed to the selection of patients, drafting of the article and analysis of the results, and approved the version to be published.
Correspondence to: Serag Esmat, MD, Department of Internal Medicine, Faculty of Medicine, Cairo University, Cairo 11562, Egypt. seragesmat@yahoo.com
Telephone: +20-2-3646394 Fax: +20-2-3657104
Received: August 20, 2011 Revised: October 15, 2011
Accepted: October 21, 2011
Published online: June 21, 2012

Abstract

AIM: To evaluate the accuracy of specific biochemical markers for the assessment of hepatic fibrosis in patients with chronic hepatitis C virus (HCV) infection.

METHODS: One hundred and fifty-four patients with chronic HCV infection were included in this study; 124 patients were non-cirrhotic, and 30 were cirrhotic. The following measurements were obtained in all patients: serum alanine aminotransferase (ALT), aspartate aminotransferase (AST), albumin, total bilirubin, prothrombin time and concentration, complete blood count, hepatitis B surface antigen (HBsAg), HCVAb, HCV-RNA by quantitative polymerase chain reaction, abdominal ultrasound and ultrasonic-guided liver biopsy. The following ratios, scores and indices were calculated and compared with the results of the histopathological examination: AST/ALT ratio (AAR), age platelet index (API), AST to platelet ratio index (APRI), cirrhosis discriminating score (CDS), Pohl score, Göteborg University Cirrhosis Index (GUCI).

RESULTS: AAR, APRI, API and GUCI demonstrated good diagnostic accuracy of liver cirrhosis (80.5%, 79.2%, 76.6% and 80.5%, respectively); *P* values were: < 0.01, < 0.05, < 0.001 and < 0.001, respectively. Among the studied parameters, AAR and GUCI gave the highest diagnostic accuracy (80.5%) with cutoff values of 1.2 and 1.5, respectively. APRI, API and GUCI were significantly correlated with the stage of fibrosis ($P < 0.001$) and the grade of activity ($P < 0.001$, < 0.001 and < 0.005, respectively), while CDS only correlated significantly with the stage of fibrosis ($P < 0.001$) and not with the degree of activity ($P > 0.05$). In addition, we found significant correlations for the AAR, APRI, API, GUCI and Pohl score between the non-cirrhotic (F0, F1, F2, F3) and cirrhotic (F4) groups (*P* values: < 0.001, < 0.05, < 0.001, < 0.001 and < 0.005, respectively; CDS did not demonstrate significant correlation ($P > 0.05$).

CONCLUSION: The use of AAR, APRI, API, GUCI and Pohl score measurements may decrease the need for liver biopsies in diagnosing cirrhosis, especially in Egypt, where resources are limited.

Key words: Age platelet index; Aspartate aminotransferase platelet ratio index; Aspartate aminotransferase-to-alanine aminotransferase ratio; Cirrhosis discriminating score; Fibrosis evaluation; Göteborg University Cirrhosis Index; Hepatitis C virus infection; Liver fibrosis; Pohl score

Peer reviewer: Yusuf Yilmaz, MD, Department of Gastroenterology, Marmara University, School of Medicine, Fevzi Cakmak Mah, Mimar Sinan Cad. No. 41 Ust Kaynarca, Pendik,

34899 Istanbul, Turkey

Fouad SA, Esmat S, Omran D, Rashid L, Kobaisi MH. Noninvasive assessment of hepatic fibrosis in Egyptian patients with chronic hepatitis C virus infection. *World J Gastroenterol* 2012; 18(23): 2988-2994 Available from: URL: http://www.wjgnet.com/1007-9327/full/v18/i23/2988.htm DOI: http://dx.doi.org/10.3748/wjg.v18.i23.2988

INTRODUCTION

Egypt has the highest prevalence of adult hepatitis C virus (HCV) infection in the world, affecting an average of 15%-25% of the population in rural communities[1,2]. Worldwide, HCV is one of the major causes of chronic liver diseases, which include inflammation, fibrosis and cirrhosis. Furthermore, HCV has been associated with increased morbidity and mortality in hepatocellular carcinoma[3-5].

Although liver biopsy is an invasive procedure and includes a risk of complications, such as pain, pneumothorax, puncture of other viscera and hemorrhage, it is still the gold standard for grading the severity of necroinflammation and staging the extent of liver fibrosis in patients with chronic HCV infection[6-8].

In addition to the added cost, liver biopsy cannot be performed universally in all patients with impaired hemostasis of any origin[9]. The procedure is known to underestimate liver fibrosis when small tissue samples are collected, and it is prone to intra- and inter-observer variation[10-13]. Moreover, several studies have suggested that liver biopsy is far from being a perfect diagnostic tool because its accuracy in detecting pathology is dependent on the size of the biopsy[14-17]. Previous reports have proposed that a liver biopsy sample should contain a minimum of 5 portal tracts and be at least 15 mm in length to be considered adequate[18-20]. Other authors have recommended even larger samples[21]. In 2003, a French survey reported that liver biopsy may be refused by up to 59% of patients[22]. In 2005, an Italian survey reported major discrepancies among hepatologists regarding when and how to take a liver biopsy from the same subgroup of chronic hepatitis C patients[23].

Considering these limitations, many studies have recently focused on the development of non-invasive markers as surrogates of liver biopsy[24-34]. An accurate assessment of hepatic fibrosis can be achieved with various markers and indices. In this study, we aimed to assess the validity of six markers of hepatic fibrosis, including the ratio of aspartate aminotransferase (AST)/alanine aminotransferase (ALT) ratio (AAR), AST to platelet ratio index (APRI), age platelet index (API), cirrhosis discriminating score (CDS), Göteborg University Cirrhosis Index (GUCI) and Pohl score, in grading fibrosis and diagnosing early cirrhosis as an accurate alternative to liver biopsy in patients with chronic HCV infection in a country known to have a high prevalence of the disease[1,2].

MATERIALS AND METHODS

Patients

This study included 154 patients with chronic HCV infection. They were selected from the gastroenterology and hepatology clinics of the Faculty of Medicine, Cairo University, Egypt, over the period from March 2009 to November 2010. All selected patients were potential candidates for interferon therapy.

Exclusion criteria

Patients with chronic hepatitis B infection, autoimmune hepatitis, decompensated liver disease, hepatocellular carcinoma, history of previous antiviral therapy and presence of absolute contraindication for liver biopsy were excluded from this study.

Methods

All patients were subjected to full history intake, thorough physical examination and the following laboratory test measurements: serum ALT, AST, albumin, total bilirubin, prothrombin time and concentration, complete blood count, HCV antibody (anti-HCV), hepatitis B surface antigen (HBsAg), HCV-RNA by quantitative polymerase chain reaction (PCR), circulating autoantibodies (ANA, ASMA), abdominal ultrasonography and ultrasonographic guided liver biopsy.

Liver biopsies were performed using 18-20 gauge Trucut needles (GMSS.N, GHATWARY MEDICAL). To assess necroinflammation, the grade of activity was evaluated using a modified hepatic activity index: mild (0-6), moderate (7-12) and severe (13-18). Fibrosis was staged according to the METAVIR scoring system from F0 to F4. Based on the results obtained from histopathological assessment of their liver biopsies, patients were divided into two groups:the non-cirrhotic group (F0, F1, F2 and F3) and the cirrhotic group (F4).

Definition of the noninvasive indices

The following ratios, scores and indices[24-34] were calculated and compared with the results of histopathological examination: (1) AAR; (2) APRI, calculated using the following equation: (AST/upper limit of normal)/platelet count ($\times 10^9$/L) $\times$ 10; (3) API, calculated by summing the scores awarded for the following patient laboratory results (a possible value of 0-10): age (in years) < 30 = 0; 30-39 = 1; 40-49 = 2; 50-59 = 3; 60-69 = 4; ⩾ 70 = 5; platelet count ($\times 10^9$/L): ⩾ 225 = 0; 200-224 = 1; 175-199 = 2; 150-174 = 3; 125-149 = 4; < 125 = 5; (4) CDS, calculated by summing the scores awarded for the following patient laboratory results (a possible value of 0-11): platelet count ($\times 10^9$/L): > 340 = 0; 280-339 = 1; 220-279 = 2; 160-219 = 3; 100-159 = 4; 40-99 = 5; < 40 = 6. ALT/AST ratio: > 1.7 = 0; 1.2-1.7 = 1; 0.6-1.19 = 2; < 0.6 = 3. International normalized ratio (INR): < 1.1 = 0; 1.1-1.4 = 1; > 1.4 = 2; (5) GUCI, calculated using the following equation: normalized AST × INR × 100/platelet count ($\times 10^9$/L); and (6) Pohl score,which was considered positive if the AAR was ⩾ 1 and the platelet

Table 1 The demographic and laboratory data of all patients (mean ± SD)

Item	Non-cirrhotic group (F0, F1, F2 and F3) *n* (124)	Cirrhotic group (F4) *n* (30)	*P* value
Age, yr	37.19 ± 9.58	47.87 ± 7.76	0.0002
Gender, *n* (%)			
Male	86 (69.35)	18 (60)	
Female	38 (30.65)	12 (40)	
AST (IU/mL)	48.84 ± 42.7	61 ± 20.4	0.01
ALT (IU/mL)	60.235 ± 42.3	57.7 ± 24.69	0.68
Alkaline phosphatase (U/L)	81.654 ± 38.4	111 ± 42.5	0.004
Total bilirubin (mg/dL)	0.787 ± 0.30	1.003 ± 0.38	0.07
Albumin (g/dL)	5.803 ± 0.789	4.1 ± 0.42	0.004
INR	1.127 ± 0.092	1.254 ± 0.12	0.0001
Platelet count (/mm^3)	213.75 ± 66.1	151.87 ± 73.79	0.001
HCV viraemia, IU/mL	893 015.72 ± 1 571 254.86	347 974.86 ± 536 542.77	0.23

AST: Aspartate aminotransferase; ALT: Alanine aminotransferase; INR: International normalized ratio; HCV: Hepatitis C virus.

Table 2 Mean values (± SD) of aspartate aminotransferase-to-alanine aminotransferase ratio, aspartate aminotransferase-to-platelet ratio index, age platelet index, cirrhosis discriminating score and Göteborg University Cirrhosis Index in non-cirrhotic and cirrhotic groups of chronic hepatitis C virus infected patients

Variable	Non-cirrhotic group (F0, F1, F2 and F3), *n* (124)	Cirrhotic group (F4), *n* (30)	*P* value
AAR	0.84 ± 0.31	1.23 ± 0.47	0.001
APRI	0.078 ± 0.09	0.118 ± 0.07	0.02
API	2.98 ± 2.21	5.87 ± 1.99	0.0001
CDS	5.48 ± 1.36	6 ± 1.31	0.17
GUCI	0.913 ± 1.27	1.6573 ± 0.89	0.001
Pohl score	+ve 12 (9.67%)	+ve 12 (40%)	0.004
	-ve 112 (90.3%)	-ve 18 (60%)	

AAR: Aspartate aminotransferase-to-alanine aminotransferase ratio; APRI: Aspartate aminotransferase-to-platelet ratio index; API: Age platelet index; CDS: Cirrhosis discriminating score; GUCI: Göteborg University Cirrhosis Index.

count was < 150 × 10^9/L. The Ethics committee at our institution approved the study, and all patients provided informed consent before participating in this study.

Statistical analysis

Descriptive statistics included range, mean ± SD, median, frequencies (number of cases) and percentages when appropriate. Comparisons of numerical variables between the study groups were made using the Mann Whitney *U* test for independent samples. To compare categorical data, the Chi squared (χ^2) test was used.When the expected frequency was less than 5, the Exact test was used instead. Accuracy was represented using the terms sensitivity and specificity. Receiver operator characteristic analysis was used to determine the optimum cutoff value for the studied diagnostic markers. Various variables were tested for correlation using the Spearman rank correlation equation for non-normal variables. *P* values less than 0.05 were considered statistically significant. Normality of data was checked by the Kolmogorov Smirnov test. Most of our markers violated the normal assumption; therefore, the data were analyzed using non-parametric tests. Two-tailed tests were used where appropriate. Multivariate logistic regression determined only API to be significantly associated with diagnosis of cirrhosis in our cases. No other variable was found to be a significant predictor of cirrhosis. All statistical calculations were performed using the computer programs Microsoft Excel 2007 (Microsoft Corporation, NY, United States) and SPSS (Statistical Package for the Social Sciences; SPSS Inc., Chicago, IL, United States) version 15 for Microsoft Windows.

Table 3 The correlation between age and variable laboratory data, and the stage of fibrosis and grade of necroinflammatory activity

Variable	Stage of fibrosis		Grade of activity	
	Correlation coefficient	*P* value	Correlation coefficient	*P* value
Age	0.4	0.0003	0.3	0.005
AST	0.3	0.003	0.3	0.006
ALT	0.2	0.07	0.9	0.1
Alkaline phosphatase	0.3	0.006	0.2	0.08
Total bilirubin	0.2	0.07	0.3	0.003
Albumin	-0.3	0.002	-0.2	0.08
INR	0.4	0.001	0.2	0.13
Platelet count	-0.5	0.000001	-0.4	0.0002
HCV RNA load	-0.07	0.5	0.07	0.5

AST: Aspartate aminotransferase; ALT: Alanine aminotransferase; INR: International normalized ratio; HCV: Hepatitis C virus.

RESULTS

Demographic and baseline laboratory data of non-cirrhotic and cirrhotic patients are shown in Table 1.

Our findings demonstrated a statistically significant correlation for AAR, APRI, API, GUCI and Pohl score between the cirrhotic and non-cirrhotic patients; CDS was not found to be significant. Pohl score was positive (indicating cirrhosis) in 40% of cirrhotic patients, whereas it was positive in only 9.67% of non-cirrhotic patients, with a *P* value of 0.004 (Figure 1 and Table 2).

Patient age, AST and platelet count correlated significantly with both the grade of activity and the stage of fibrosis. However, neither ALT nor HCV RNA load demonstrated statistically significant correlations with the grade of activity or the stage of fibrosis. With regard to other laboratory parameters, INR, albumin and alkaline phosphatase levels were significantly correlated with stage of fibrosis but not with grade of activity, whereas serum bilirubin was significantly correlated with grade of activity but not with stage of fibrosis (Table 3).

The results of our study revealed a significant correla-

Table 4 The correlation between the aspartate aminotransferase-to-alanine aminotransferase ratio, aspartate aminotransferase- to-platelet ratio index, age platelet index, cirrhosis discriminating score and Göteborg University Cirrhosis Index and the grade of necroinflammatory activity and the stage of fibrosis

Variable	Stage of fibrosis		Grade of activity	
	Correlation coefficient	*P* value	Correlation coefficient	*P* value
AAR	0.2	0.054	0.1	0.23
APRI	0.4	0.00006	0.4	0.001
API	0.6	0.000001	0.5	0.00002
CDS	0.4	0.0002	0.2	0.056
GUCI	0.5	0.0001	0.3	0.003

AAR: Aspartate aminotransferase-to-alanine aminotransferase ratio; APRI: Aspartate aminotransferase-to-platelet ratio index; API: Age platelet index; CDS: Cirrhosis discriminating score; GUCI: Göteborg University Cirrhosis Index.

tion between APRI, API and GUCI, and both the grade of activity and the stage of fibrosis. CDS correlated significantly with the stage of liver fibrosis but not with the grade of necroinflammatory activity. In contrast, the AST/ALT ratio had no significant correlation with either the stage of fibrosis or the grade of activity (Table 4).

For non-invasive diagnosis of liver cirrhosis (F4), using AAR, APRI, API and GUCI, Table 5 and Figure 2 show the cutoff values, sensitivity, specificity, positive predictive values (PPV), negative predictive values (NPV), and area under the receiver operating characteristics curve of these parameters.

DISCUSSION

Although it is costly, requires hospitalization for at least 6-18 h, is invasive and carries a risk of complications with an associated morbidity rate between 0.3% and 0.6% and mortality rate of 0.05%, liver biopsy remains the gold standard for assessing liver histology[34-36]. However, limitations of liver biopsy include the underestimation of fibrosis stage, given that only 1/50 000 of the organ is removed[37], and the reported inter- and intra-observer discrepancies rates of 10%-20%[38,39].

In this study, we found that the optimal cutoff AAR-value for diagnosing cirrhosis was ⩾ 1.2, with a sensitivity of 46%, specificity of 88.7% and PPV and NPV of 50% and 87.3%, respectively. These results support previous findings by Giannini *et al*[40], who recommended an AAR value of ⩾ 1 as a cutoff value for diagnosing cirrhosis. However, Ehsan *et al*[41] reported a higher cutoff value (⩾ 1.5) for diagnosing cirrhosis, with a sensitivity of 44% and a specificity of 91%.

Elevation of the AST/ALT ratio in cirrhotic patients may be explained by the reduction in AST clearance, which leads to an increase in serum AST levels. In addition, advanced liver disease may be associated with mitochondrial injury, resulting in increased release of AST present in the mitochondria and cytoplasm[42].

Thrombocytopenia in patients with advanced fibrosis

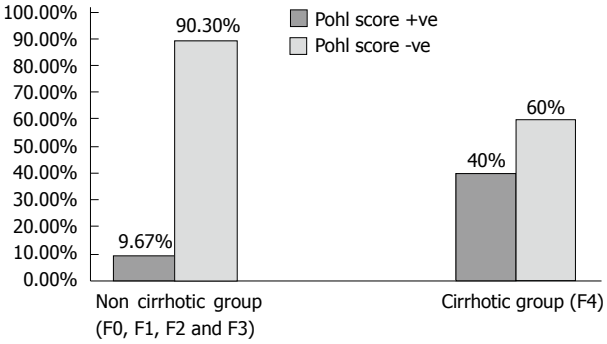

Figure 1 Positive and negative Pohl score in non-cirrhotic and cirrhotic patients with chronic hepatitis C virus infection.

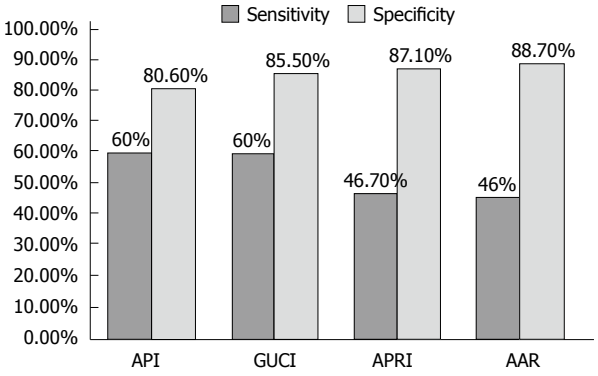

Figure 2 Sensitivity and specificity of age platelet index, Göteborg University Cirrhosis Index, aspartate aminotransferase to platelet ratio index and aspartate aminotransferase/alanine aminotransferase ratio in diagnosing cirrhosis in patients with chronic hepatitis C virus infection. API: Age platelet index; GUCI: Göteborg University Cirrhosis Index; APRI: Aspartate aminotransferase to platelet ratio index; AAR: Aspartate aminotransferase/alanine aminotransferase ratio.

may be due to reduced hepatic production of thrombopoietin, increased splenic sequestration of platelets secondary to portal hypertension or the myelosuppressive action of HCV[43,44].

Results from the current study revealed a significant correlation between APRI and both the stage of liver fibrosis and the grade of activity. The optimal cutoff APRI value for the diagnosis of cirrhosis was ⩾ 1.36, which was consistent with findings by Ichino *et al*[45] and Ehsan *et al*[41], who reported cutoff values of 1.3 and 1.5, respectively.

In the present study, we found a significant correlation between API and both the stage of fibrosis and the grade of activity ($P < 0.001$ for both). Our results revealed that the optimal AP index cutoff value for the diagnosis of cirrhosis was ⩾ 5.5, with 60% and 80.6% sensitivity and specificity, respectively, and 42.86% and 89.29% PPV and NPV, respectively. The results of the current study are in agreement with the results of previous studies by Lackner *et al*[46] and Poynard *et al*[47].

Results from this study showed that there was a significant correlation between GUCI and both the stage of liver fibrosis and the grade of activity. We recommend a GUCI value of ⩾ 1.56 as an optimal cutoff value for

Table 5 The accuracy of different ratios and indices in the diagnosis of early liver cirrhosis

Item	Cutoff value	Sensitivity (%)	Specificity (%)	PPV (%)	NPV (%)	Accuracy (%)	AUROC	*P* value
AAR	1.2	46	88.7	50	87.3	80.5	0.761	0.002
APRI	1.36	46.7	87.1	46.7	87.1	79.2	0.697	0.018
API	5.5	60	80.6	42.9	89.3	76.6	0.826	0.000
GUCI	1.56	60	85.5	50	89.8	80.5	0.783	0.001

AAR: Aspartate aminotransferase-to-alanine aminotransferase ratio; APRI: Aspartate aminotransferase-to-platelet ratio index; API: Age platelet index; GUCI: Göteborg University Cirrhosis Index; PPV: Positive predictive value; NPV: Negative predictive value; AUROC: Area under the receiver operating characteristics.

the diagnosis of cirrhosis, with 60% sensitivity, 88.7% specificity, and a PPV and NPV of 89.83% and 80.52%, respectively. These results supported those reported by Islam *et al*[48], who found a significant correlation between GUCI and both stage of fibrosis and grade of activity. Similar results were reported by Ehsan *et al*[41], who recommended a GUCI cutoff value of $\geqslant$ 1.5 for the diagnosis of cirrhosis, with 89% specificity and 74% sensitivity.

In the present study, we found a statistically significant correlation ($P = 0.004$) between positive Pohl score (AAR $\geqslant$ 1, and platelet count $< 150 \times 10^9$/L) and the presence of cirrhosis (F4). These findings supported the results of Pohl *et al*[27] and Lackner *et al*[46], who confirmed the diagnostic accuracy of the Pohl score in significant fibrosis and cirrhosis.

In our study, there was a significant correlation between CDS and stage of liver fibrosis ($P < 0.001$), but the relationship was not significant with regard to the grade of activity ($P = 0.056$). The CDS values were not significant between the cirrhotic and non-cirrhotic patients ($P = 0.17$), which disagreed with results reported by Ichino *et al*[45], who recommended a CDS value of $\geqslant$ 8 as a cutoff value for the diagnosis of cirrhosis.

Some studies showed no correlation between the histological outcome and HCV-RNA levels, while other reports suggested that the viral titer may influence the severity of liver damage and that high titer viremia correlates with the most severe liver damage[49]. The current study revealed no significant correlation between HCV RNA load as measured by quantitative PCR and both the grade of activity and fibrosis stage.

Our results agreed with the studies conducted by Lee *et al*[50] and Saleem *et al*[51]. In contrast, Kato *et al*[52] found significantly higher HCV RNA loads in patients with chronic active hepatitis and cirrhosis compared to those with chronic persistent hepatitis. These discrepancies could be attributed to the fact that serum HCV RNA load is not a stable parameter because it fluctuates[53]. In addition, a high amount of circulating HCV does not always imply a more active state of viral replication in the liver nor does it indicate a more severe degree of liver disease. HCV is known to replicate both within the liver as well as in extra-hepatic sites[54,55].

In conclusion, the API index, APRI, AST/ALT ratio and GUCI showed good accuracy, moderate sensitivity, and high specificity for the diagnosis of early cirrhosis. These measures also demonstrated significant correlation with both the stage of liver fibrosis and the grade of activity. The combination of these non-invasive biochemical markers may replace the requirement for liver biopsy, particularly for cases with cirrhosis or early cirrhotic changes in which the procedure has known limitations and complications.

COMMENTS

Background

Hepatitis C virus (HCV) is one of the major causes of chronic liver diseases worldwide. It has been associated with increased morbidity and mortality in hepatocellular carcinoma. In patients with chronic HCV infection, liver biopsy is essential to the assessment of hepatic fibrosis. Evaluating the degree of fibrosis is an important step in determining the need and priority for treatment with antiviral drugs. However, liver biopsy is a costly and invasive procedure with a risk of complications and a tendency to underestimate liver fibrosis. Hence, alternative non-invasive diagnostic tools are needed.

Research frontiers

In the area of liver cirrhosis assessment, the focus of research is on how to use biochemical markers and indices [aspartate aminotransferase (AST)/alanine aminotransferase (ALT) ratio (AAR), AST to platelet ratio index (APRI), age platelet index (API), cirrhosis discriminating score (CDS), Göteborg University Cirrhosis Index (GUCI) and Pohl score] calculated from simple routine laboratory tests, such as serum levels of bilirubin, ALT, AST, albumin and platelet count, to determine the severity of liver fibrosis and to evaluate their accuracy in comparison to liver biopsy.

Innovations and breakthroughs

The results showed that APRI, API, GUCI and CDS were significantly correlated with the degree of liver fibrosis. AAR, APRI, API, GUCI and Pohl score can accurately diagnose early liver cirrhosis. AAR and GUCI gave the highest accuracy for the diagnosis of liver cirrhosis (80.5%). These simple biochemical markers, especially when used in combination, may decrease the use of liver biopsy in the assessment of fibrosis and diagnosis of cirrhosis in patients with chronic HCV infection.

Applications

The study results suggest that these biochemical markers can identify significant fibrosis and cirrhosis in patients with chronic HCV; their combined application may decrease the need for liver biopsy, thereby reducing its associated costs and complications. Important fields for further study include the use and evaluation of these markers for repeated assessment in monitoring the progression of liver fibrosis and its regression following interferon treatment in patients with chronic hepatitis C.

Terminology

CDS, GUCI and Pohl score are indices calculated to develop noninvasive diagnostic markers of liver fibrosis depending on simple biochemical tests such as platelet count, AST and ALT.

Peer review

In this paper, the authors focused on the noninvasive assessment of liver fibrosis in Egyptian patients with chronic HCV infection using different indexes. It is potentially interesting and well-written and provides useful information in a selected population with a high prevalence of chronic HCV infection.

REFERENCES

1 **Abdel-Wahab MF**, Zakaria S, Kamel M, Abdel-Khaliq MK, Mabrouk MA, Salama H, Esmat G, Thomas DL, Strickland GT. High seroprevalence of hepatitis C infection among risk groups in Egypt. *Am J Trop Med Hyg* 1994; **51**: 563-567

2 **Frank C**, Mohamed MK, Strickland GT, Lavanchy D, Arthur RR, Magder LS, El Khoby T, Abdel-Wahab Y, Aly Ohn ES, Anwar W, Sallam I. The role of parenteral antischistosomal therapy in the spread of hepatitis C virus in Egypt. *Lancet* 2000; **355**: 887-891

3 **Shaheen AA**, Myers RP. Diagnostic accuracy of the aspartate aminotransferase-to-platelet ratio index for the prediction of hepatitis C-related fibrosis: a systematic review. *Hepatology* 2007; **46**: 912-921

4 **Sebastiani G**. Non-invasive assessment of liver fibrosis in chronic liver diseases: implementation in clinical practice and decisional algorithms. *World J Gastroenterol* 2009; **15**: 2190-2203

5 **Lin ZH**, Xin YN, Dong QJ, Wang Q, Jiang XJ, Zhan SH, Sun Y, Xuan SY. Performance of the aspartate aminotransferase-to-platelet ratio index for the staging of hepatitis C-related fibrosis: an updated meta-analysis. *Hepatology* 2011; **53**: 726-736

6 **Lewin M**, Poujol-Robert A, Boëlle PY, Wendum D, Lasnier E, Viallon M, Guéchot J, Hoeffel C, Arrivé L, Tubiana JM, Poupon R. Diffusion-weighted magnetic resonance imaging for the assessment of fibrosis in chronic hepatitis C. *Hepatology* 2007; **46**: 658-665

7 **Sebastiani G**, Halfon P, Castera L, Pol S, Thomas DL, Mangia A, Di Marco V, Pirisi M, Voiculescu M, Guido M, Bourliere M, Noventa F, Alberti A. SAFE biopsy: a validated method for large-scale staging of liver fibrosis in chronic hepatitis C. *Hepatology* 2009; **49**: 1821-1827

8 **El-Attar MM**, Rashed HG, Sewify EM, Hassan HE. A suggested algorithm for using serum biomarkers for the diagnosis of liver fibrosis in chronic hepatitis C infection. *Arab J Gastroenterol* 2010; **11**: 206-211

9 **The French METAVIR Cooperative Study Group**. Intraobserver and interobserver variations in liver biopsy interpretation in patients with chronic hepatitis C. *Hepatology* 1994; **20**: 15-20

10 **Mueller S**, Millonig G, Sarovska L, Friedrich S, Reimann FM, Pritsch M, Eisele S, Stickel F, Longerich T, Schirmacher P, Seitz HK. Increased liver stiffness in alcoholic liver disease: differentiating fibrosis from steatohepatitis. *World J Gastroenterol* 2010; **16**: 966-972

11 **Naveau S**, Gaudé G, Asnacios A, Agostini H, Abella A, Barri-Ova N, Dauvois B, Prévot S, Ngo Y, Munteanu M, Balian A, Njiké-Nakseu M, Perlemuter G, Poynard T. Diagnostic and prognostic values of noninvasive biomarkers of fibrosis in patients with alcoholic liver disease. *Hepatology* 2009; **49**: 97-105

12 **Fontana RJ**, Goodman ZD, Dienstag JL, Bonkovsky HL, Naishadham D, Sterling RK, Su GL, Ghosh M, Wright EC. Relationship of serum fibrosis markers with liver fibrosis stage and collagen content in patients with advanced chronic hepatitis C. *Hepatology* 2008; **47**: 789-798

13 **Vallet-Pichard A**, Mallet V, Nalpas B, Verkarre V, Nalpas A, Dhalluin-Venier V, Fontaine H, Pol S. FIB-4: an inexpensive and accurate marker of fibrosis in HCV infection. comparison with liver biopsy and fibrotest. *Hepatology* 2007; **46**: 32-36

14 **Bedossa P**, Carrat F. Liver biopsy: the best, not the gold standard. *J Hepatol* 2009; **50**: 1-3

15 **Poynard T**, Muntenau M, Morra R, Ngo Y, Imbert-Bismut F, Thabut D, Messous D, Massard J, Lebray P, Moussalli J, Benhamou Y, Ratziu V. Methodological aspects of the interpretation of non-invasive biomarkers of liver fibrosis: a 2008 update. *Gastroenterol Clin Biol* 2008; **32**: 8-21

16 **Bedossa P**, Dargère D, Paradis V. Sampling variability of liver fibrosis in chronic hepatitis C. *Hepatology* 2003; **38**: 1449-1457

17 **Afdhal NH**, Nunes D. Evaluation of liver fibrosis: a concise review. *Am J Gastroenterol* 2004; **99**: 1160-1174

18 **Hübscher SG**. Histological grading and staging in chronic hepatitis: clinical applications and problems. *J Hepatol* 1998; **29**: 1015-1022

19 **Schlichting P**, Hølund B, Poulsen H. Liver biopsy in chronic aggressive hepatitis. Diagnostic reproducibility in relation to size of specimen. *Scand J Gastroenterol* 1983; **18**: 27-32

20 **Scheuer PJ**. Liver biopsy size matters in chronic hepatitis: bigger is better. *Hepatology* 2003; **38**: 1356-1358

21 **Bonny C**, Rayssiguier R, Ughetto S, Aublet-Cuvelier B, Baranger J, Blanchet G, Delteil J, Hautefeuille P, Lapalus F, Montanier P, Bommelaer G, Abergel A. [Medical practices and expectations of general practitioners in relation to hepatitis C virus infection in the Auvergne region]. *Gastroenterol Clin Biol* 2003; **27**: 1021-1025

22 **Almasio PL**, Niero M, Angioli D, Ascione A, Gullini S, Minoli G, Oprandi NC, Pinzello GB, Verme G, Andriulli A. Experts' opinions on the role of liver biopsy in HCV infection: a Delphi survey by the Italian Association of Hospital Gastroenterologists (A.I.G.O.). *J Hepatol* 2005; **43**: 381-387

23 **Şirli R**, Ioan S, Bota S, Popescu A, Cornianu M. A Comparative Study of Non-Invasive Methods for Fibrosis Assessment in Chronic HCV Infection. *Hepat Mon* 2010; **10**: 88-94

24 **Yilmaz Y**, Yonal O, Kurt R, Bayrak M, Aktas B, Ozdogan O.Noninvasive assessment of liver fibrosis with the aspartate transaminase to platelet ratio index (APRI): Usefulness in patients with chronic liver disease. *Hepat Mon* 2011; **11**: 103-106

25 **Leroy V**. Other non-invasive markers of liver fibrosis. *Gastroenterol Clin Biol* 2008; **32**: 52-57

26 **Pinzani M**. Non-invasive evaluation of hepatic fibrosis: don't count your chickens before they're hatched. *Gut* 2006; **55**: 310-312

27 **Pohl A**, Behling C, Oliver D, Kilani M, Monson P, Hassanein T. Serum aminotransferase levels and platelet counts as predictors of degree of fibrosis in chronic hepatitis C virus infection. *Am J Gastroenterol* 2001; **96**: 3142-3146

28 **Sebastiani G**, Alberti A. Non invasive fibrosis biomarkers reduce but not substitute the need for liver biopsy. *World J Gastroenterol* 2006; **12**: 3682-3694

29 **Leroy V**, Halfon P, Bacq Y, Boursier J, Rousselet MC, Bourlière M, de Muret A, Sturm N, Hunault G, Penaranda G, Bréchot MC, Trocme C, Calès P. Diagnostic accuracy, reproducibility and robustness of fibrosis blood tests in chronic hepatitis C: a meta-analysis with individual data. *Clin Biochem* 2008; **41**: 1368-1376

30 **Pinzani M**, Vizzutti F, Arena U, Marra F. Technology Insight: noninvasive assessment of liver fibrosis by biochemical scores and elastography. *Nat Clin Pract Gastroenterol Hepatol* 2008; **5**: 95-106

31 **Lok AS**, Ghany MG, Goodman ZD, Wright EC, Everson GT, Sterling RK, Everhart JE, Lindsay KL, Bonkovsky HL, Di Bisceglie AM, Lee WM, Morgan TR, Dienstag JL, Morishima C. Predicting cirrhosis in patients with hepatitis C based on standard laboratory tests: Results of the HALT-C cohort. *Hepatology* 2005; **42**: 282-292

32 **Silva Jr RG**, Fakhouri R, Nascimento TV, Santos IM, Barbosa LM. Aspartate aminotransferase-to-platelet ratio index for fibrosis and cirrhosis prediction in chronic hepatitis C patients. *Braz J Infect Dis* 2008; **12**: 15-19

33 **Loaeza-del-Castillo A**, Paz-Pineda F, Oviedo-Cárdenas E, Sánchez-Avila F, Vargas-Voráckova F. AST to platelet ratio index (APRI) for the noninvasive evaluation of liver fibrosis. *Ann Hepatol* 2008; **7**: 350-357

34 **Degos F**, Perez P, Roche B, Mahmoudi A, Asselineau J, Voitot H, Bedossa P. Diagnostic accuracy of FibroScan and

comparison to liver fibrosis biomarkers in chronic viral hepatitis: a multicenter prospective study (the FIBROSTIC study). *J Hepatol* 2010; **53**: 1013-1021

35 **Poynard T**, Imbert-Bismut F, Munteanu M, Messous D, Myers RP, Thabut D, Ratziu V, Mercadier A, Benhamou Y, Hainque B. Overview of the diagnostic value of biochemical markers of liver fibrosis (FibroTest, HCV FibroSure) and necrosis (ActiTest) in patients with chronic hepatitis C. *Comp Hepatol* 2004; **3**: 8

36 **Cadranel JF**, Rufat P, Degos F. Practices of liver biopsy in France: results of a prospective nationwide survey. For the Group of Epidemiology of the French Association for the Study of the Liver (AFEF). *Hepatology* 2000; **32**: 477-481

37 **Wong JB**, Koff RS. Watchful waiting with periodic liver biopsy versus immediate empirical therapy for histologically mild chronic hepatitis C. A cost-effectiveness analysis. *Ann Intern Med* 2000; **133**: 665-675

38 **Colloredo G**, Guido M, Sonzogni A, Leandro G. Impact of liver biopsy size on histological evaluation of chronic viral hepatitis: the smaller the sample, the milder the disease. *J Hepatol* 2003; **39**: 239-244

39 **Regev A**, Berho M, Jeffers LJ, Milikowski C, Molina EG, Pyrsopoulos NT, Feng ZZ, Reddy KR, Schiff ER. Sampling error and intraobserver variation in liver biopsy in patients with chronic HCV infection. *Am J Gastroenterol* 2002; **97**: 2614-2618

40 **Giannini E**, Risso D, Botta F, Chiarbonello B, Fasoli A, Malfatti F, Romagnoli P, Testa E, Ceppa P, Testa R. Validity and clinical utility of the aspartate aminotransferase-alanine aminotransferase ratio in assessing disease severity and prognosis in patients with hepatitis C virus-related chronic liver disease. *Arch Intern Med* 2003; **163**: 218-224

41 **Ehsan N**, TawfikBadr MT, Raouf AA, Badra G. Correlation Between Liver Biopsy Findings and Different Serum Biochemical Tests in Staging Fibrosis in Egyptian Patients with Chronic Hepatitis C Virus Infection. *Arab J Gastroenterol* 2008; **9**: 7-12

42 **Okuda M**, Li K, Beard MR, Showalter LA, Scholle F, Lemon SM, Weinman SA. Mitochondrial injury, oxidative stress, and antioxidant gene expression are induced by hepatitis C virus core protein. *Gastroenterology* 2002; **122**: 366-375

43 **Peck-Radosavljevic M**. Hypersplenism. *Eur J Gastroenterol Hepatol* 2001; **13**: 317-323

44 **Dai CY**, Ho CK, Huang JF, Hsieh MY, Hou NJ, Lin ZY, Chen SC, Hsieh MY, Wang LY, Chang WY, Yu ML, Chuang WL. Hepatitis C virus viremia and low platelet count: a study in a hepatitis B & amp; C endemic area in Taiwan. *J Hepatol* 2010; **52**: 160-166

45 **Ichino N**, Osakabe K, Nishikawa T, Sugiyama H, Kato M, Kitahara S, Hashimoto S, Kawabe N, Harata M, Nitta Y, Murao M, Nakano T, Arima Y, Shimazaki H, Suzuki K, Yoshioka K. A new index for non-invasive assessment of liver fibrosis. *World J Gastroenterol* 2010; **16**: 4809-4816

46 **Lackner C**, Struber G, Liegl B, Leibl S, Ofner P, Bankuti C, Bauer B, Stauber RE. Comparison and validation of simple noninvasive tests for prediction of fibrosis in chronic hepatitis C. *Hepatology* 2005; **41**: 1376-1382

47 **Poynard T**, Bedossa P. Age and platelet count: a simple index for predicting the presence of histological lesions in patients with antibodies to hepatitis C virus. METAVIR and CLINIVIR Cooperative Study Groups. *J Viral Hepat* 1997; **4**: 199-208

48 **Islam S**, Antonsson L, Westin J, Lagging M. Cirrhosis in hepatitis C virus-infected patients can be excluded using an index of standard biochemical serum markers. *Scand J Gastroenterol* 2005; **40**: 867-872

49 **Anand BS**, Velez M. Assessment of correlation between serum titers of hepatitis C virus and severity of liver disease. *World J Gastroenterol* 2004; **10**: 2409-2411

50 **Lee YS**, Yoon SK, Chung ES, Bae SH, Choi JY, Han JY, Chung KW, Sun HS, Kim BS, Kim BK. The relationship of histologic activity to serum ALT, HCV genotype and HCV RNA titers in chronic hepatitis C. *J Korean Med Sci* 2001; **16**: 585-591

51 **Saleem N**, Mubarik A, Qureshi AH, Siddiq M, Ahmad M, Afzal S, Hussain AB, Hashmi SN. Is there a correlation between degree of viremia and liver histology in chronic hepatitis C? *J Pak Med Assoc* 2004; **54**: 476-479

52 **Kato N**, Yokosuka O, Hosoda K, Ito Y, Ohto M, Omata M. Quantification of hepatitis C virus by competitive reverse transcription-polymerase chain reaction: increase of the virus in advanced liver disease. *Hepatology* 1993; **18**: 16-20

53 **Zeuzem S**, Schmidt JM, Lee JH, Rüster B, Roth WK. Effect of interferon alfa on the dynamics of hepatitis C virus turnover in vivo. *Hepatology* 1996; **23**: 366-371

54 **Müller HM**, Pfaff E, Goeser T, Kallinowski B, Solbach C, Theilmann L. Peripheral blood leukocytes serve as a possible extrahepatic site for hepatitis C virus replication. *J Gen Virol* 1993; **74** (Pt 4): 669-676

55 **Ballardini G**, Manzin A, Giostra F, Francesconi R, Groff P, Grassi A, Solforosi L, Ghetti S, Zauli D, Clementi M, Bianchi FB. Quantitative liver parameters of HCV infection: relation to HCV genotypes, viremia and response to interferon treatment. *J Hepatol* 1997; **26**: 779-786

S- Editor Shi ZF **L- Editor** Webster JR **E- Editor** Li JY

World Journal of Gastroenterology

Online Submissions: http://www.wjgnet.com/1007-9327office
wjg@wjgnet.com
doi:10.3748/wjg.v18.i23.2995

World J Gastroenterol 2012 June 21; 18(23): 2995-3003
ISSN 1007-9327 (print) ISSN 2219-2840 (online)

BRIEF ARTICLE

Overexpression of metastasis-associated in colon cancer 1 predicts a poor outcome of hepatitis B virus-related hepatocellular carcinoma

Jian-Hui Qu, Xiu-Juan Chang, Yin-Ying Lu, Wen-Lin Bai, Yan Chen, Lin Zhou, Zhen Zeng, Chun-Ping Wang, Lin-Jing An, Li-Yan Hao, Gui-Lin Xu, Xu-Dong Gao, Min Lou, Ji-Yun Lv, Yong-Ping Yang

Jian-Hui Qu, Xiu-Juan Chang, Yin-Ying Lu, Wen-Lin Bai, Yan Chen, Lin Zhou, Zhen Zeng, Chun-Ping Wang, Lin-Jing An, Li-Yan Hao, Gui-Lin Xu, Xu-Dong Gao, Min Lou, Ji-Yun Lv, Yong-Ping Yang, Center of Therapeutic Research for Liver Cancer, The 302nd Hospital, Beijing 100039, China

Ji-Yun Lv, Yong-Ping Yang, Institute for Infectious Disease, The 302nd Hospital, Beijing 100039, China

Author contributions: Qu JH and Chang XJ contributed equally to this study; Qu JH, Chang XJ, Lv JY and Yang YP designed the research; Qu JH, Chang XJ, Lu YY, Bai WL, Chen Y, Zhou L, Zeng Z and Wang CP performed the research; Qu JH, Chang XJ, An LJ, Hao LY, Xu GL, Gao XD and Lou M analyzed the data; Qu JH and Yang YP wrote the paper.

Supported by Grants from the Key Scientific and Technological Research Foundation of the National Special-purpose Program, No. 2008ZX10002-018 and from the Capital Medical Development and Research in Beijing, China, No. 2007-1021 and 2009-2041

Correspondence to: Yong-Ping Yang, Chief, Center of Therapeutic Research for Liver Cancer, The 302nd Hospital, 100 Xi Si Huan Middle Road, Beijing 100039, China. yongpingyang@hotmail.com
Telephone: +86-10-66933429 Fax: +86-10-63879193

Received: August 4, 2011 Revised: March 22, 2012
Accepted: May 6, 2012
Published online: June 21, 2012

Abstract

AIM: To investigate the intratumoral expression of metastasis-associated in colon cancer 1 (MACC1) and c-Met and determine their clinical values associated with hepatitis B virus (HBV)-related hepatocellular carcinoma (HCC).

METHODS: A retrospective study admitted three hundred fifty-four patients with HBV-related HCC. The expression and distribution of MACC1 and c-Met were assessed by quantitative real-time polymerase chain reaction and immunohistochemistry staining. Prognostic factors influencing survival, metastasis and recurrence were assessed.

RESULTS: Intratumoral MACC1 level was found to be associated with HCC disease progression. Both median tumor-free survival (TFS) and overall survival (OS) were significantly shorter in the postoperative HCC patients with high intratumoral MACC1 expression, as compared to those with low intratumoral MACC1 levels (TFS: 34 mo *vs* 48.0 mo, $P < 0.001$; OS: 40 mo *vs* 48 mo, $P < 0.01$). Multivariable analysis indicated that high MACC1 expression or co-expression with c-Met were independent predictors for HCC clinic outcome ($P < 0.001$).

CONCLUSION: High intratumoral MACC1 expression can be associated with enhanced tumor progression and poor outcome of HBV-related HCC. MACC1 may serve as a prognostic biomarker for postoperative HCC.

Key words: Hepatocellular carcinoma; Metastasis-associated in colon cancer 1; c-Met; Prognostic factor; Recurrence

Peer reviewer: Shun-Fa Yang, PhD, Associate Professor, Institute of Medicine, Chung Shan Medical University, No. 110, Sec.1 Chien-Kuo N. Road, Taichung, 402, Taiwan, China

Qu JH, Chang XJ, Lu YY, Bai WL, Chen Y, Zhou L, Zeng Z, Wang CP, An LJ, Hao LY, Xu GL, Gao XD, Lou M, Lv JY, Yang YP. Overexpression of metastasis-associated in colon cancer 1 predicts a poor outcome of hepatitis B virus-related hepatocellular carcinoma. *World J Gastroenterol* 2012; 18(23): 2995-3003 Available from: URL: http://www.wjgnet.com/1007-9327/full/v18/i23/2995.htm DOI: http://dx.doi.org/10.3748/wjg.v18.i23.2995

INTRODUCTION

Hepatocellular carcinoma (HCC) is the fifth most common cancer and the third cause of death from cancers worldwide[1]. The incidence of HCC in China is high, and most cases are associated with chronic hepatitis B virus (HBV) infection[2]. Hepatocarcinogenesis is a complex process associated with the accumulation of multiple genetic and epigenetic changes during the initiation, progression and maturation of this fatal disease[3,4]. As such, intensive research efforts have been carried out to determine the physiological, cellular and molecular mechanisms of HCC, in the hope of developing effective preventative measures and improved treatment strategies.

The metastasis-associated in colon cancer 1 (MACC1) gene was identified by a genome-wide screen of human colon cancer samples, and its expression was closely related to the metastasis of colon cancers[5]. Subsequent clinical studies have suggested that MACC1 might be an important predictor for metastasis and recurrence of colon cancers. Further studies have revealed that MACC1-induced tumorigenesis is correlated with enhanced hepatocyte growth factor (HGF)/c-Met signaling[6,7]. MACC1 functions as a transcription factor, and one of its target promoters is that of the receptor tyrosine kinase c-Met gene. Binding of MACC1 to the promoter has been demonstrated to stimulate c-Met transcription, ultimately inducing activation of the HGF/c-Met signaling pathway and enhancing cell proliferation, motility, and metastasis[8,9]. MACC1 is normally expressed in healthy liver tissues, but marked overexpression is frequently observed in HCC clinical samples[10]. To date, however, the clinical significance of MACC1 overexpression in HCC and of the correlation between MACC1 and the c-Met signaling in the disease state remain unknown. It is intriguing to speculate that MACC1 may contribute to HCC onset and progression, and therefore may represent a readily-detectable biomarker for tumor recurrence and/or metastasis in postoperative HCC patients.

In this study, we sought to determine the expression levels of MACC1 in HBV-related HCC at different disease stages and analyze its correlation with clinical outcome. In addition, we evaluated the related levels of its transcriptional target, c-Met. Our data indicated that MACC1 expression levels represent an effective prognostic factor for HBV-related HCC patients who undergo hepatectomy.

MATERIALS AND METHODS

Patients, clinical characteristics, and tissue sampling

Tumor samples were obtained from 412 consecutive patients admitted to The 302nd Hospital (Beijing, China) with HBV-related HCC from December 2004 to June 2006. The diagnosis of HCC was based on the criteria of the European Association for the Study of the Liver[11]. By using the Barcelona Clinic Liver Cancer (BCLC) staging classification system[12], 148 patients were classified as stage A, 144 as stage B, and 120 as stage C. All patients, except for those at stage C, had undergone surgical resection. Among all patients, 36 had an incomplete resection, 12 died from other causes without recurrence, and 10 were lost to follow-up for non-medical reasons. Thus, the total study population was composed of 354 patients (Table 1). Matched non-tumor tissue samples were obtained from all surgical resected participants and were generally taken from a distance of more than 2 cm from the tumor tissue. Tumor samples from the stage C individuals were obtained by using the Single Action Biopsy Device (Promex Technologies, United States) and target tissues were identified by the following criteria: solitary lesions, or up to three nodules ⩽ 6 cm in size; partial portal vein thrombosis or vena cana invasion; absence of extrahepatic metastasis; and preserved liver function (Child-Pugh A or ⩽ B8 with serum bilirubin levels under 51.3 μmol/L). In addition, ten normal liver tissues were obtained from four cases of hepatic hemangioma and six patients with hepatic cyst, none of which had a history of viral hepatitis or liver cirrhosis.

Table 1 Basic clinical characteristics of patients with hepatitis B virus-related hepatocellular carcinoma (*n* = 354)

Clinical features	Stage A	Stage B	Stage C
Cases (*n*)	138	96	120
Median age (yr, range)	55 (24-68)	53 (29-70)	52 (21-72)
Male/female	118/20	82/14	106/14
Median tumor diameter (cm, range)	2.5 (1.5-3)	4.0 (3-5)	4.5 (2-6)
AFP (μg/L, > 400/⩽ 400)	45/93	40/56	85/35
HBV DNA (+/-)	78/60	57/39	76/44
HBeAg (+/-)	50/88	32/64	54/66
ECOG PS (0/1/2)	92/30/16	60/25/11	25/55/40
Child-Pugh (A/B)	92/46	67/29	58/62
Tumor number (single/multinodular)	123/15	56/40	67/53
Invasion of portal vein (+/-)	0/138	0/96	120/0
Tumor differentiation (high/intermediate/low)	45/66/27	27/38/31	20/50/50

HBV: Hepatitis B virus; ECOG PS: Eastern Cooperative Oncology Group Performance Status Scale; AFP: α- fetoprotein; HBeAg: HBV e antigen.

Each of the samples were divided and either prepared for histochemical staining or snap-frozen in liquid nitrogen for RNA extraction for use in subsequent reverse transcription (RT)-polymerase chain reaction (PCR). For hematoxylin and eosin (HE) and immunohistochemical staining, the tissues were fixed in 10% formalin and paraffin-embedded.

The study protocol was approved by The 302nd Hospital Research Ethics Committee, and written informed consent was obtained from all participants or their legal guardian. None of the patients had received prior treatment for HCC, including radiation or chemotherapy. Patients were followed up every 2 mo within the first postoperative year and at approximately 3-4 mo intervals thereafter. Routine evaluation included physical examination, chest roentgenography, blood chemistry analysis, HBV-DNA test, and measurement of tumor markers (carcinoembryonic antigen and α-fetoprotein). Chest

and abdominal computed tomography, brain magnetic resonance imaging and a bone scintiscan were performed every 6 mo for three years after surgery. Additional examinations were performed if any symptoms or signs of recurrence were detected.

Determination of the mRNA levels of MACC1 and c-Met

The levels of the mRNA transcripts of MACC1 and c-Met were determined by quantitative real-time PCR, as described previously[13]. β-actin mRNA expression was used as an internal control and the relative gene expression values were calculated by the $2^{-\Delta Ct}$ method using Sequence Detection System 2.1 software. Total RNA was isolated from the tissues by using an RNA isolation kit (Qiagene, Germany) and following the manufacturer's instructions. The concentration of RNA was determined by spectrophotometric measurement at A_{260}, and the purity was verified by the $A260/A280$ ratio (> 1.8 was sufficiently pure). A total of 2 μg RNA was used for the preparation of cDNA by reverse transcriptase-PCR (SYBR PrimeScript RT-PCR Kit with SYBR Premix *Ex Taq*; Takara, Japan). The following PCR primers were used: MACC1 cDNA (136 bp), 5'-TTCTTTTGATTCCTCCGGTGA-3' (F) and 5'-ACTCTGATGGGCATGTGCTG-3' (R); c-Met cDNA (173 bp), 5'-GCAGGTTGTGGTTTCTCG-3' (F) and 5'-TGCAGCCCAAGCCATTCA-3' (R); and β-actin cDNA (125 bp), 5'-CGGGAAATCGTGCGTGAC-3' (F) and 5'-AGGCAGCTCGTAGCTCTTCT-3' (R). The cDNA equivalent of 50 ng of the original RNA was used in the PCR. The 50 μL reactions for MACC1 or c-Met were run for 40 cycles as follows: predenaturation at 95 ℃ for 30 s, denaturation at 95 ℃ for 5 s, annealing and extension at 60 ℃ for 30 s. The target mRNA was normalized to the corresponding β-actin signal. Measurements were performed in triplicate.

Assessment of MACC1 and c-Met in HCC by immunohistochemistry

Paraffin-embedded tissues from resected tumor and non-tumor tissues or biopsied tumor samples were cut for serial microtome sections with 4 μm thickness. After hematoxylin and eosin staining, the samples were assessed by two independent pathologists using Edmondson criteria[14]. Samples were classified as: well differentiated, corresponding to Edmondson's Grade Ⅰ or Ⅰ-Ⅱ; moderately differentiated, corresponding to Edmondson's Grade Ⅱ or Ⅱ-Ⅲ; or poorly differentiated, corresponding to Edmondson's Grade Ⅲ or Ⅲ-Ⅳ.

Two additional serial sections from each individual were prepared for MACC1 and c-Met immunohistochemical staining. Monoclonal rabbit anti-human antibody against MACC1 (1:50; Sigma, United States) and rabbit anti-human antibody against c-Met (1:250; Abcam, Hong Kong) were used. Detection of MACC1 and c-Met was carried out with 3-amino-9-ethylcarbozole (AEC; Zhongshan Bio, China) and diaminobenzidine (DAB; R and D Systems, United States), respectively. Positive staining was indicated by a prominent brownish or red pigmentation. In each case, a negative control was prepared using phosphate buffered saline as the first antibody to ensure the specificity of immunostaining.

The extent of positive staining for MACC1 was scored as follows[15]: 0, ≤ 10%; 1, > 10%-25%; 2, > 25%-50%; 3, > 50%-75%; and 4, > 75%. The intensity of the special staining was scored as follows: 0, negative; 1+, weak; 2+, moderate; and 3+, strong. The final score was obtained by multiplying the extent scores and intensity scores, which produced values in a range from 0 to 12. Scores from 9-12 were defined as a strong staining pattern (++), scores from 0-4 were defined as negative expression (-), and scores from 6-8 were defined as an intermediate staining pattern (+). All the staining was evaluated and characterized by two independent pathologists.

Serological assays

Hepatitis B surface antigen (HBsAg), anti-HBs, HBeAg, anti-HBe and anti-HBc were detected using a commercially-available kit (Roche Diagnostics, United States) and electrochemiluminescence immunoassay analyzers (E170; Modular Analytics, Roche Diagnostics). HBV DNA was extracted from 200 μL of plasma sample from each study participant using a High Pure Viral Nucleic Acid Kit (Roche Diagnostics Applied Science, Germany) and following the manufacturer's instructions. The viral titer and genotype of HBV were determined by a real-time PCR-based method that used fluorescent hybridization probes and a LightCycler PCR machine (Roche Diagnostics). This method consisted of two steps that were carried out in a single tube: the first step used real-time PCR to quantify the viral DNA and the second step used melting curve analysis of the final PCR product to genotype the virus. Details of the design and experimental conditions of this assay are available from the manufacturer. This assay showed a broad linear distribution for HBV titers that ranged from 10^2 to 10^{11} copies/mL, with a lower detection limit of $1\text{-}5 \times 10^2$ copies/mL.

Statistical analysis

The primary endpoint of the study was tumor-free survival (TFS) and the secondary endpoint included overall survival (OS) and follow-up for over 48 mo. TFS was calculated from the date of resection to the date when tumor recurrence was diagnosed. OS was calculated from the date of commencement of resection to the date of death or last follow-up[16]. All statistical analyses were performed with SPSS version 16.0 software. Continuous data were expressed as median and range. A comparison between the groups was performed using the χ^2 test. Survival rates were estimated by the Kaplan-Meier method and compared by the log rank test. The Cox proportional hazards model was used to determine the independent factors on survival and recurrence, based on the variables selected in univariate analysis. $P < 0.05$ was considered statistically significant.

RESULTS

Increased intratumoral MACC1 mRNA is related to HCC progression

We analyzed the MACC1 mRNA levels in surgically-resected samples from 234 patients at BCLC stage A or stage B and in biopsied tumor tissues from 120 patients at BCLC stage C. MACC1 mRNA in tumor tissues was found to be increased gradually with the stage of HCC progression (Figure 1A and B). The intratumoral MACC1 mRNA levels detected in samples from HCC stage A (0.002281 ± 0.001972), B (0.003031 ± 0.003451) and C (0.009015 ± 0.004972) were about 3-, 4- and 14-fold higher than that in normal liver tissues (0.000592 ± 0.0000451), respectively. We next performed a paired comparison of gene expression for the 234 patients at stage A and stage B, for which we had matched tumor tissues and adjacent non-tumor liver tissues. The ratio of MACC1 mRNA in cancerous tissue relative to that of the matched paratumors (the T:N ratio) was about 5.4-fold higher in the stage B group than in the stage A group (1.25 ± 0.3 *vs* 0.23 ± 0.05, $P = 0.009$; Figure 1C). Thus, these data indicated that the MACC1 mRNA level in HCC tumors was associated with tumor progression.

We next determined the protein levels of MACC1 in tumor and paratumor tissues by analyzing immunohistochemistry scores. MACC1 protein levels were found to be significantly higher in malignant tissues than in paratumor tissues or normal liver tissues (both, $P < 0.001$). Compared with the corresponding peritumor tissue or normal liver tissues, tumors from 30 of 138 (22%) patients at stage A, 40 of 96 (41.6%) at stage B, and 80 of 120 (67%) at stage C displayed increased MACC1 expression (Figure 1D). Tumor cells demonstrated mild to strong positive MACC1 cytoplasmic staining (++) and apparent nuclear signals in some cases (Figure 1E).

Intratumoral MACC1 mRNA level correlates with clinical parameters in HCC patients

Patients with HCC ($n = 354$) were divided into two groups according to the median intratumoral MACC1 mRNA levels. The first group was composed of low intratumoral MACC1 mRNA (< 0.006732; range: 0.000050-0.036147) and the second of high intratumoral MACC1 mRNA (≥ 0.006732; range: 0.000050-0.036147). Following comparative analysis of these two groups, intratumoral MACC1 mRNA level was found to be associated with HCC clinical staging, age, portal vein invasion and tumor differentiation. However, no significant correlation was found between the intratumoral MACC1 mRNA level and gender, lesion number, α-fetoprotein level or Child-Pugh class (Table 2).

Intratumoral MACC1 expression is correlated with c-MET mRNA levels in HCC patients

c-Met is a well-known proto-oncogene and transcriptional target of MACC1. We next investigated whether overexpression of MACC1 corresponded to increased transcription of c-Met in HCC tissues. We found that intratumoral c-Met mRNA levels were consistent with the extent of MACC1 expression and were up-regulated in conjunction with tumor progression of HCC ($P < 0.01$; Figure 1A and B). In the 234 HCC patients with stage A and stage B, the expression of c-Met was increased in the 105 patients with high MACC1 expression, but decreased in the 129 patients with low MACC1 expression (0.058561 ± 0.017539 *vs* 0.024734 ± 0.018754, $P = 0.041$; Figure 2A). Among these 234 patients, 67 (28.6%) displayed elevated expressions of both MACC1 and c-Met, 93 (39.7%) had low expressions of both MACC1 and c-Met, and 38 (16.2%) had a high expression of MACC1 but a low expression of c-Met, while 36 (15.4%) had a high expression of c-Met but low expression of MACC1. MACC1 mRNA level was closely correlated with the corresponding intratumoral c-Met mRNA expression ($r = 0.360$, $P < 0.001$) (Figure 2B).

Further analysis of the 234 patients found that HCC patients with both MACC1 and c-Met high intratumoral co-expression had a median OS of 32 mo [95% confidence interval (CI): 25-41]. In contrast, those with both MACC1 and c-Met low intratumoral expression had a median OS of 48 mo (log-rank, $P < 0.001$; Figure 2D). Likewise, the patients with both MACC1 and c-Met high intratumoral expression had significantly shorter median TFS (28 mo, 95% CI: 22-33 mo) than those with both MACC1 and c-Met low expression (48 mo, log-rank $P < 0.001$; Figure 2C).

Increased intratumoral MACC1 expression is predictive of high risk of recurrence and poor survival in postoperative HCC patients

We followed up the 234 patients (stage A and stage B) after resection for a median of 30 mo (range: 6-48 mo). Seventy-nine of the 105 HCC patients (75.2%) with high intratumoral MACC1 mRNA levels experienced recurrent tumors, and 34 cases had extrahepatic metastasis. The 1-, 2- and 3-year recurrence-free survival rates were 81%, 67% and 39%, respectively. In contrast, only 41 of the 129 (31.8%) patients with low intratumoral MACC1 expression experienced recurrence, and 12 of those had extrahepatic metastasis. The 1-, 2- and 3-year TFS was 92%, 88% and 82%, respectively. Compared to those with low intratumoral MACC1 expression, patients with high intratumoral MACC1 had signicantly high rate of recurrence and extrahepatic metastasis (both, $P < 0.001$). Generally, the HCC patients with high intratumoral MACC1 mRNA levels had a significantly shorter median TFS (34 mo, 95% CI: 30-37 mo) than those with low intratumoral MACC1 mRNA levels (48.0 mo, log-rank $P < 0.001$; Figure 3A). In addition, post-resected patients with low intratumoral MACC1 expression had a median OS of 48 mo, while those with high intratumoral MACC1 expression had 40 mo (95% CI: 34-45 and log-rank $P < 0.01$; Figure 3B). A total of 152 patients with a ratio of T:N MACC1 expression < 1 had a median TFS of 48 mo, compared to 36 mo (95% CI: 25-47) for the 82 patients who had a ratio ≥ 1 (log-rank, $P < 0.001$; Figure 3C).

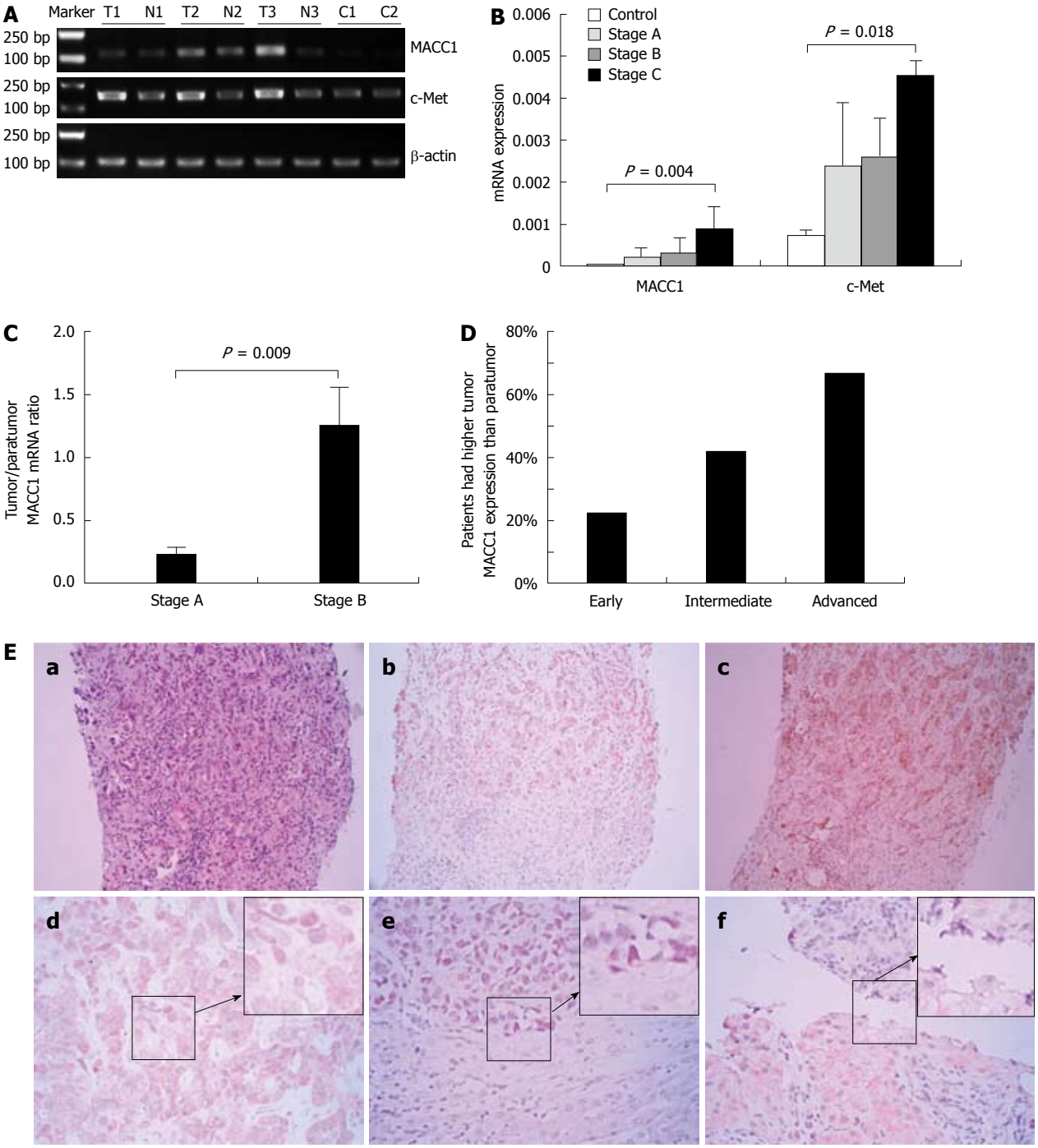

Figure 1 Analysis of metastasis-associated in colon cancer 1 and c-Met expression in liver tissues. A: Representative metastasis-associated in colon cancer 1 (MACC1) and c-Met mRNA in intratumoral [T: T1 as hepatocellular carcinoma (HCC) stage A, T2, T3 as HCC stage B] and matching paratumor tissues (N: N1, N2 and N3) and normal liver tissues (C) by reverse-transcription polymerase chain reaction (RT-PCR); B: Comparison of MACC1 and c-Met expression levels in 10 normal liver tissue, and HCC with stage A (n = 138), stage B (n = 96), stage C (n = 120) by real-time quantitative-PCR; C: The ratio for MACC1 mRNA levels in HCC stage A and stage B tumor tissues relative to matching paratumor tissues; D: Comparison of the intratumoral and peritumoral MACC1 expression in HCC stage A and stage B, as determined by immunohistochemistry; E: Immunohistochemical staining of MACC1 expression in HCC. a-c: MACC1 and c-Met expression in tumor and matching paratumor tissues in one same HCC patient (× 200). a: HE showed the tumor and paratumor cells; b: MACC1 expression was higher in tumor cytoplasm than in paratumor cells; c: c-Met was expressed on the tumor cell membrane, but no staining on nontumor liver cell membrane; d-f: Representative expression of MACC1 in HCC tumor tissues (× 400). d: MACC1 positive staining occurred mainly in the cytoplasm; e: Nuclear staining of MACC1 in cancer cells; f: Relatively weak staining of MACC1 in an early stage HCC cancer cells, as compared to paratumor cells.

Patients with a ratio of T:N MACC1 expression < 1 had a median OS of 48.0 mo, compared to 41 mo (95% CI: 36-45) for those with a ratio of T:N MACC1 expression ≥ 1 (log-rank, $P < 0.001$; Figure 3D).

Univariate statistical analysis showed that the TFS was associated with intratumoral MACC1 expression, and recurrence-free survival was related to tumor number, tumor differentiation, MACC1 expression, and co-

Table 2 Metastasis-associated in colon cancer 1 mRNA expression and clinical characteristics of hepatocellular carcinoma patients *n* (%)

Variable	Cases (*n* = 354)	MACC1 mRNA high expression group	MACC1 mRNA low expression group	*P*
Gender				0.214
Male	306	157 (88.7)	149 (84.2)	
Female	48	20 (11.3)	28 (15.8)	
Age (yr)				< 0.001
⩾ 55	185	70 (39.5)	115 (65.0)	
< 55	169	107 (60.5)	62 (35.0)	
Tumor size (cm)				0.087
⩾ 3	196	90 (50.8)	106 (59.9)	
< 3	158	87 (49.2)	71 (40.1)	
Tumor thrombus				0.007
Yes	120	72 (40.7)	48 (27.1)	
No	234	105 (59.3)	129 (72.9)	
Tumor number				0.356
Single	246	119 (67.2)	127 (71.8)	
Multinodular	108	58 (32.8)	50 (28.2)	
Stage				0.007
Early-middle	234	105 (59.3)	129 (72.9)	
Advanced	120	72 (40.7)	48 (27.1)	
Differentiation				< 0.001
High	92	21 (11.9)	71 (40.1)	
Moderate	154	92 (52.0)	62 (35.0)	
Low	108	64 (36.1)	44 (24.9)	
AFP				0.056
⩽ 400	184	83 (46.9)	101 (57.1)	
> 400	170	94 (53.1)	76 (42.9)	
HBeAg				0.190
Positive	136	62 (35.0)	74 (41.8)	
Negative	218	115 (65.0)	103 (58.2)	
HBV DNA				0.159
Positive	211	99 (55.9)	112 (63.3)	
Negative	143	78 (44.1)	65 (36.7)	
Child-Pugh				0.326
A	217	104 (58.8)	113 (63.8)	
B	137	73 (41.2)	64 (36.2)	

HBV: Hepatitis B virus; MACC1: Metastasis-associated in colon cancer 1; AFP: α-fetoprotein; HBeAg: HBV e antigen.

expression of MACC1 and c-Met. The median OS was associated with Child-Pugh class, score from Eastern Cooperative Oncology Group performance status scale (ECOG PS), tumor differentiation, MACC1 mRNA levels, co-expression of MACC1 and c-Met, tumor number, and tumor size. Further multivariate analysis using the Cox hazards model revealed that a high MACC1 expression or co-expression with c-Met was an independent poor prognostic factor for TFS and OS. The combined expression of both MACC1 and c-Met increased these prognostic values, as compared to MACC1 overexpression alone (Table 3).

DISCUSSION

Consistent with the multifactorial aetiology of HCC and the long latent period of tumor formation, a large variety of cancer genes are involved in the multistep process of human hepatocarcinogenesis[3,4]. In order to identify suitable prognostic markers and therapeutic targets, it is essential to analyze gene expression and proteomic changes by evaluating a large series of HCC patients and samples at different disease stages. Moreover, since metastasis or recurrence is the major cause of death of postoperative HCC patients, early identification of subjects at high-risk for either of these processes is necessary to improve OS rates. The clinical factors related to tumor invasiveness, such as tumor size, number, histological type and vessel invasion, are considered the most related to risk for recurrence and the most useful for prediction of HCC patient outcome[17-19]. Molecular biology studies have identified many biological factors that may act as potential tumor prognostic markers. The fact that HCC metastasis is a multistep process involving many factors[20-22] has led to attempts to develop a panel of multiple biomarkers that will facilitate tumor diagnosis and prediction of tumor metastasis and recurrence.

MACC1 was recently identified as being involved in metastasis of colon cancers, presumably by up-regulating c-Met transcription. Thus, to elucidate the MACC1-related mechanism of HCC and identify potential targets for molecular-based therapies we investigated the expression of MACC1 and c-Met in HBV-induced HCC.

We determined that intratumoral MACC1 expression was significantly up-regulated in most of the late stage HCC tissues examined. We further found that MACC1 overexpression was associated with higher c-Met expression in HCC and the intratumoral MACC1 mRNA level alone or in combination with that of c-Met can serve as an independent predictive factor for recurrence and survival of postoperative HCC patients.

We statistically analyzed the correlation of intratumoral MACC1 mRNA levels and clinical parameters of HCC patients. High intratumoral MACC1 mRNA levels were significantly associated with clinical stage, age, vessel invasion, and tumor differentiation. MACC1 mRNA levels were found to gradually increase with the progression of HCC, especially at the advanced HCC stage, and this process was accompanied by invasion of the portal vein. Shirahata *et al*[23] also showed that MACC1 expression was significantly correlated with vascular invasion, as it was in our study. Furthermore, intratumoral MACC1 protein was localized mainly in the cell cytoplasm, where the levels increased from low to robust in conjunction with tumor progression, indicating that MACC1 may represent an effective biomarker of tumor progression. Previous studies in colon cancers had also found that intratumoral MACC1 was up-regulated, as compared to levels detected in matched peritumoral or normal colon mucosa, regardless of tumor stage classification[5]. In our study of hepatic cancer, we found that the paratumor livers in some HCC patients had a relatively strong expression of MACC1; this was especially the case for those patients with TFS shorter than 6 mo after resection, implying that the pathogenesis of HCC and colon cancers is likely distinct. However, considering that all of the patients examined in our study had a background of chronic HBV

Table 3 Univariate and multivariate analyses of variables associated with tumor-free survival and overall survival

Variables	TFS				OS			
	Univariate *P*	Multivariate			Univariate *P*	Multivariate		
		Hazard ratios	95% CI	*P*		Hazard ratios	95% CI	*P*
Child-Pugh (A/B)	0.184	NA	NA	NA	0.034	1.342	1.016-1.747	0.041
Tumor differentiation (high/intermediate/low)	0.037	1.213	0.743-1.980	0.441	0.038	1.133	0.683-1.679	0.624
Tumor number (≥ 2/1)	0.021	1.012	0.675-1.517	0.354	0.040	1.107	0.732-1.575	0.630
ECOG PS (0/1/2)	0.078	NA	NA	NA	0.045	1.079	0.893-1.530	0.679
MACC1 (low/high)	< 0.001	1.489	1.071-1.801	0.013	< 0.001	1.508	1.079-1.835	0.012
MACC1 and c-Met expression (both/one)	< 0.001	1.929	1.207-3.083	0.006	< 0.001	1.539	1.172-2.208	0.010

TFS: Tumor-free survival; OS: Overall survival; ECOG PS: Eastern Cooperative Oncology Group Performance Status Scale; MACC1: Metastasis-associated in colon cancer 1; NA: Not applicable.

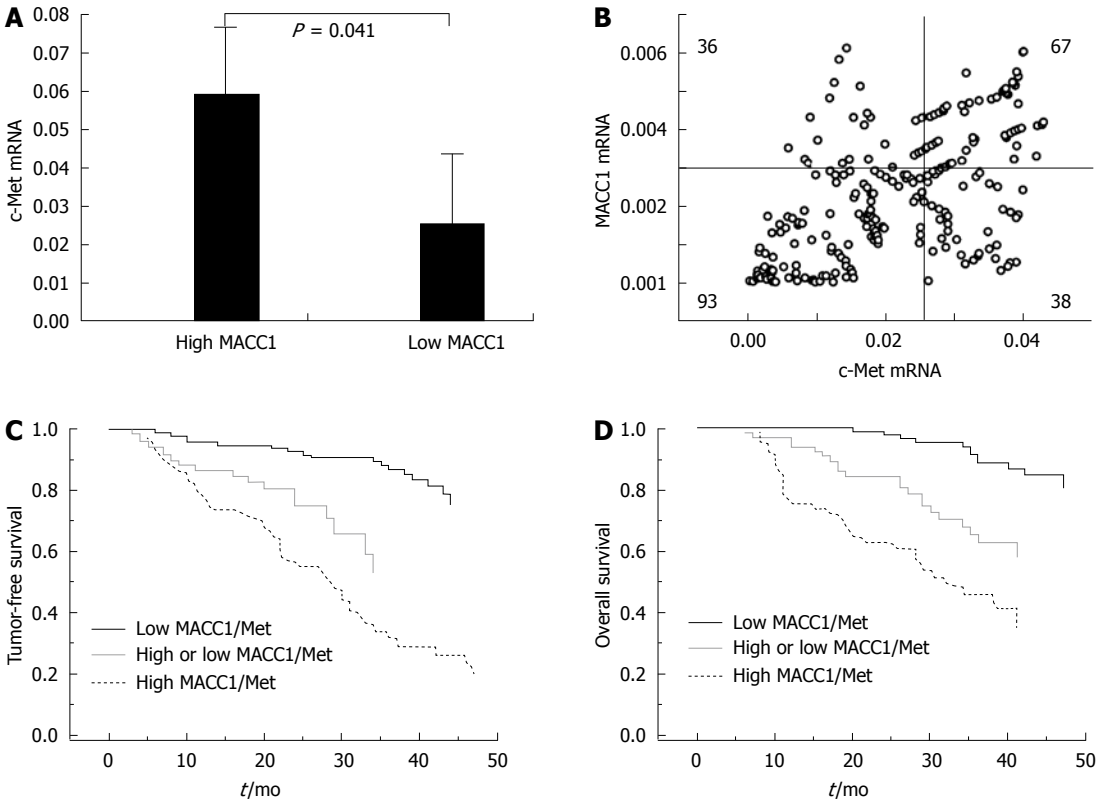

Figure 2 c-Met expression and correlation with metastasis-associated in colon cancer 1 in 234 hepatocellular carcinoma patients received resection. A: Comparison of c-Met expression level in hepatocellular carcinoma (HCC) patients with high or low intratumoral metastasis-associated in colon cancer 1 (MACC1) mRNA expression; B: c-Met level from 234 HCC patients receiving resection specimens were plottered against MACC1 levels from the same patients. Linear regression analysis showed a significant positive correlation between c-Met and MACC1 ($r = 0.360$, $P < 0.001$); C: Kaplan-Meier analysis of MACC1 and c-Met co-expression effects on tumor-free survival; D: Kaplan-Meier analysis of MACC1 and c-Met co-expression effects on overall survival.

infection and liver cirrhosis, it is possible that the above-mentioned difference is due to the chronic hepatitis B infection.

Based on our immunohistochemistry data, the over-expression rates of MACC1 in HCC ranged from 22% to 67% in patients at different stages. MACC1 staining occurred mainly in the cytoplasm of non-cancerous or cancerous cells, but some cancerous cells showed significantly strong MACC1 staining in the nucleus. Studies in colon cancer have also identified MACC1 in the nuclear compartment of cancerous cells. It has been theorized that nuclear localization of MACC1 in conjunction with high c-Met levels contribute to the later development of distant metastases[5]. The actual clinical significance of the nuclear translocation of MACC1 in HCC requires further investigation.

It has been well documented that MACC1 binds to the c-Met promoter, and this transcription regulation event is crucial for tumor metastasis as induced by HGF/c-Met signaling[9]. A regulatory feedback mechanism ex-

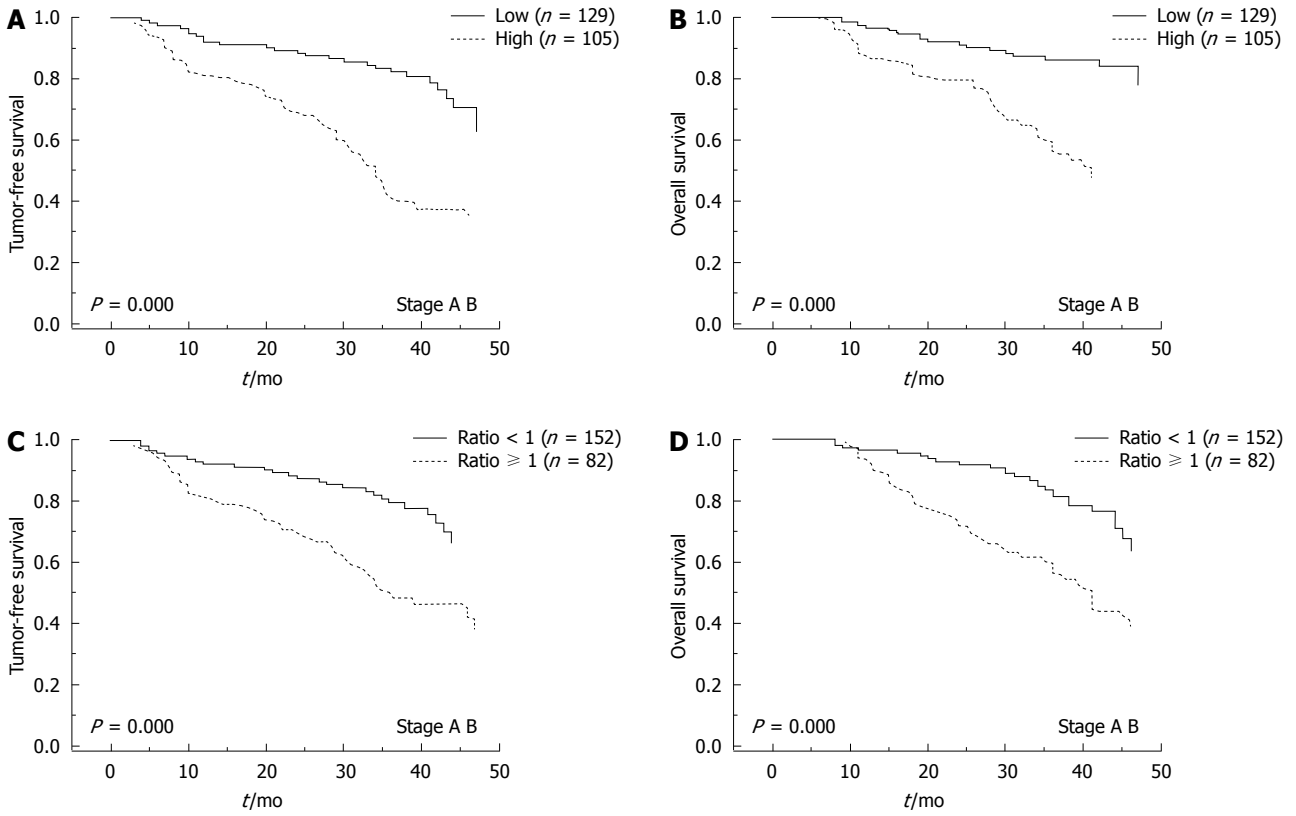

Figure 3 Metastasis-associated in colon cancer 1 expression level associated with outcomes of hepatocellular carcinoma patients receiving resection. A, B: Kaplan-Meier estimates of metastasis-associated in colon cancer 1 (MACC1) expression effects on tumor-free survival (TFS) (A) and overall survival (OS) (B); C, D: Kaplan-Meier estimates of ratio of T:N MACC1 expression effects on TFS (C) and OS (D).

ists in that HGF is able to promote the translocation of MACC1 to the nucleus, where MACC1 controls the promoter activity and hence expression of c-Met, thereby regulating c-Met-mediated signaling[6]. Our data showed that c-Met mRNA in intratumoral tissues was significantly higher than that in peritumoral tissues. Co-expression analysis showed a high consistency of MACC1 and c-Met mRNA in HCC tumors. Further investigation is required, however, to confirm whether MACC1 directly drives c-Met expression in HCC.

Previous studies on primary colon cancers indicated that the negative and positive predictions of MACC1 mRNA levels for distant metastases were 80% and 74%, respectively[5,24]. MACC1 can induce migration, invasion and proliferation of cultured cells[5], and can promote metastasis of tumor cells into liver and lung in various xenograft models. A current study in lung adenocarcinoma demonstrated that MACC1 overexpression was associated with postoperative recurrence[25]. In the present study, follow-up of 234 stage A and stage B HCC patients who received curative therapy revealed that a high intratumoral MACC1 expression level is correlated with a high rate of recurrence and extrahepatic metastasis. The median TFS and OS were much shorter in patients with high expression of both MACC1 and c-Met. High expression of intratumoral MACC1 was predictive of a poor outcome of HBV-related HCC, but when combined with high c-Met expression the predictive value for recurrence and metastasis increased.

Collectively, our data showed that intratumoral MACC1 expression is closely associated with tumor progression in HBV-induced HCC. Furthermore, elevated expression of MACC1 was statistically associated with poor outcome of these patients, suggesting that MACC1 is a novel predictor for recurrence and metastasis of postoperative HCC patients.

ACKNOWLEDGMENTS

The authors wish to thank the numerous hospital staff who conducted the baseline and follow-up surveys. We would also like to express our appreciation to Zhi-Wei Li for collecting various patient samples, Jing-Min Zhao for his enthusiastic cooperation in the pathological analysis, and Song-Shan Wang for his technical assistance in immunohistochemical staining. We thank Medjaden Bioscience Limited for assisting in the preparation of this manuscript.

COMMENTS

Background

Due to metastasis or recurrence is the major cause of death of postoperative hepatocellular carcinoma (HCC) patients, early identification of subjects at high-risk for either of these processes is necessary to improve overall survival rates. It has been known that hepatocarcinogenesis is a complex process associated with the accumulation of multiple genetic and epigenetic changes during the initiation, progression and maturation, and molecular biology studies have identified many biological factors that may act as potential tumor prognostic mark-

ers, in the hope of developing effective preventative measures and improved treatment strategies.

Research frontiers

The metastasis-associated in colon cancer 1 (MACC1) gene was identified by a genome-wide screen of human colon cancer samples, and its expression was closely related to the metastasis of colon cancers. Further studies have revealed that MACC1-induced tumorigenesis is correlated with enhanced hepatocyte growth factor/c-Met signaling.

Innovations and breakthroughs

The clinical significance of MACC1 overexpression in HCC and of the correlation between MACC1 and the c-Met signaling remain unknown. In the present study, authors sought to determine the expression levels of MACC1 in HBV-related HCC at different disease stages and analyze its correlation with clinical outcome. In addition, the authors evaluated the related levels of its transcriptional target, c-Met. The research indicated that MACC1 expression levels represent an effective prognostic factor for HBV-related HCC patients who undergo hepatectomy. The data showed that intratumoral MACC1 expression is closely associated with tumor progression in HBV-induced HCC. Furthermore, elevated expression of MACC1 was statistically associated with poor outcome of these patients.

Applications

The study results implied that the MACC1 is a novel predictor for recurrence and metastasis of postoperative HCC patients.

Terminology

The MACC1 was recently identified as being involved in metastasis of colon cancers, presumably by up-regulating c-Met transcription.

Peer review

The research is very important and the result is exciting and there is some clinical value, that is, intratumoral MACC1 expression may serve as a biomarker to predict recurrence or metastasis of postoperative HCC. The manuscript has a certain readability.

REFERENCES

1 **Parkin DM**, Bray F, Ferlay J, Pisani P. Global cancer statistics, 2002. *CA Cancer J Clin* 2005; **55**: 74-108
2 **Llovet JM**, Burroughs A, Bruix J. Hepatocellular carcinoma. *Lancet* 2003; **362**: 1907-1917
3 **Laurent-Puig P**, Zucman-Rossi J. Genetics of hepatocellular tumors. *Oncogene* 2006; **25**: 3778-3786
4 **Lee JS**, Thorgeirsson SS. Comparative and integrative functional genomics of HCC. *Oncogene* 2006; **25**: 3801-3809
5 **Stein U**, Walther W, Arlt F, Schwabe H, Smith J, Fichtner I, Birchmeier W, Schlag PM. MACC1, a newly identified key regulator of HGF-MET signaling, predicts colon cancer metastasis. *Nat Med* 2009; **15**: 59-67
6 **Stein U**, Smith J, Walther W, Arlt F. MACC1 controls Met: what a difference an Sp1 site makes. *Cell Cycle* 2009; **8**: 2467-2469
7 **Arlt F**, Stein U. Colon cancer metastasis: MACC1 and Met as metastatic pacemakers. *Int J Biochem Cell Biol* 2009; **41**: 2356-2359
8 **Birchmeier C**, Birchmeier W, Gherardi E, Vande Woude GF. Met, metastasis, motility and more. *Nat Rev Mol Cell Biol* 2003; **4**: 915-925
9 **Boccaccio C**, Comoglio PM. Invasive growth: a MET-driven genetic programme for cancer and stem cells. *Nat Rev Cancer* 2006; **6**: 637-645
10 **Stein U**, Dahlmann M, Walther W. MACC1 - more than metastasis? Facts and predictions about a novel gene. *J Mol Med* (Berl) 2010; **88**: 11-18
11 **Bruix J**, Sherman M, Llovet JM, Beaugrand M, Lencioni R, Burroughs AK, Christensen E, Pagliaro L, Colombo M, Rodés J. Clinical management of hepatocellular carcinoma. Conclusions of the Barcelona-2000 EASL conference. European Association for the Study of the Liver. *J Hepatol* 2001; **35**: 421-430
12 **Llovet JM**, Brú C, Bruix J. Prognosis of hepatocellular carcinoma: the BCLC staging classification. *Semin Liver Dis* 1999; **19**: 329-338
13 **Schmittgen TD**, Livak KJ. Analyzing real-time PCR data by the comparative C(T) method. *Nat Protoc* 2008; **3**: 1101-1108
14 **Wang C**, Lu Y, Chen Y, Feng Y, An L, Wang X, Su S, Bai W, Zhou L, Yang Y, Xu D. Prognostic factors and recurrence of hepatitis B-related hepatocellular carcinoma after argon-helium cryoablation: a prospective study. *Clin Exp Metastasis* 2009; **26**: 839-848
15 **Wang ZL**, Liang P, Dong BW, Yu XL, Yu de J. Prognostic factors and recurrence of small hepatocellular carcinoma after hepatic resection or microwave ablation: a retrospective study. *J Gastrointest Surg* 2008; **12**: 327-337
16 **Llovet JM**, Di Bisceglie AM, Bruix J, Kramer BS, Lencioni R, Zhu AX, Sherman M, Schwartz M, Lotze M, Talwalkar J, Gores GJ. Design and endpoints of clinical trials in hepatocellular carcinoma. *J Natl Cancer Inst* 2008; **100**: 698-711
17 **Lau H**, Fan ST, Ng IO, Wong J. Long term prognosis after hepatectomy for hepatocellular carcinoma: a survival analysis of 204 consecutive patients. *Cancer* 1998; **83**: 2302-2311
18 **Takenaka K**, Kawahara N, Yamamoto K, Kajiyama K, Maeda T, Itasaka H, Shirabe K, Nishizaki T, Yanaga K, Sugimachi K. Results of 280 liver resections for hepatocellular carcinoma. *Arch Surg* 1996; **131**: 71-76
19 **Livraghi T**, Bolondi L, Buscarini L, Cottone M, Mazziotti A, Morabito A, Torzilli G. No treatment, resection and ethanol injection in hepatocellular carcinoma: a retrospective analysis of survival in 391 patients with cirrhosis. Italian Cooperative HCC Study Group. *J Hepatol* 1995; **22**: 522-526
20 **Zhi H**, Zhan J, Deng QL, Huang ZM. [Postoperative detection of AFP mRNA in the peripheral blood of hepatic cellular carcinoma patients and its correlation with recurrence]. *Zhonghua Zhongliu Zazhi* 2007; **29**: 112-115
21 **Zheng Q**, Tang ZY, Xue Q, Shi DR, Song HY, Tang HB. Invasion and metastasis of hepatocellular carcinoma in relation to urokinase-type plasminogen activator, its receptor and inhibitor. *J Cancer Res Clin Oncol* 2000; **126**: 641-646
22 **Kamel L**, Nessim I, Abd-el-Hady A, Ghali A, Ismail A. Assessment of the clinical significance of serum vascular endothelial growth factor and matrix metalloproteinase-9 in patients with hepatocellular carcinoma. *J Egypt Soc Parasitol* 2005; **35**: 875-890
23 **Shirahata A**, Fan W, Sakuraba K, Yokomizo K, Goto T, Mizukami H, Saito M, Ishibashi K, Kigawa G, Nemoto H, Sanada Y, Hibi K. MACC 1 as a marker for vascular invasive hepatocellular carcinoma. *Anticancer Res* 2011; **31**: 777-780
24 **Boardman LA**. Overexpression of MACC1 leads to downstream activation of HGF/MET and potentiates metastasis and recurrence of colorectal cancer. *Genome Med* 2009; **1**: 36
25 **Shimokawa H**, Uramoto H, Onitsuka T, Chundong G, Hanagiri T, Oyama T, Yasumoto K. Overexpression of MACC1 mRNA in lung adenocarcinoma is associated with postoperative recurrence. *J Thorac Cardiovasc Surg* 2011; **141**: 895-898

S- Editor Shi ZF **L- Editor** A **E- Editor** Zheng XM

World Journal of Gastroenterology

Online Submissions: http://www.wjgnet.com/1007-9327office
wjg@wjgnet.com
doi:10.3748/wjg.v18.i23.3004

World J Gastroenterol 2012 June 21; 18(23): 3004-3007
ISSN 1007-9327 (print) ISSN 2219-2840 (online)

BRIEF ARTICLE

Investigation of the effect of military stress on the prevalence of functional bowel disorders

Xian-Zhao Yu, Hai-Feng Liu, Zhen-Xue Sun

Xian-Zhao Yu, Hai-Feng Liu, Department of Gastroenterology, General Hospital of Chinese People's Armed Police Forces, Beijing 100039, China
Zhen-Xue Sun, Authorized Outpatient Service of Chinese People's Armed Police Headquarters, Beijing 100089, China
Author contributions: Liu HF designed the study; Yu XZ, Liu HF and Sun ZX performed the research; Yu XZ contributed analytic tools; Yu XZ and Liu HF analyzed the data; Yu XZ wrote the paper.
Correspondence to: Hai-Feng Liu, MD, Professor of Medicine, Department of Gastroenterology, General Hospital of Chinese People's Armed Police Forces, No. 69 Yongding Road, Haidian District, Beijing 100039, China. haifengliu333@163.com
Telephone: +86-10-57976547 Fax: +86-10-57976549
Received: March 21, 2011 Revised: March 1, 2012
Accepted: April 2, 2012
Published online: June 21, 2012

Abstract

AIM: To investigate the morbidity of functional bowel disorders (FBD) under military stress conditions in order to lay foundations for the prevention and treatment of this disease.

METHODS: Four hundred and fifty-seven soldiers who were assigned to specified services and 471 soldiers who were assigned to routine services were enrolled using cluster sampling, with the latter as a control group. They were surveyed using the Rome Ⅲ FBD standard questionnaire. The FBD symptom questionnaire included FBD-related symptoms, severity, duration or attack time, and accompanying symptoms.

RESULTS: The morbidity of the military stress group (14.6%) was significantly higher than in the control group (9.98%) (χ^2 = 4.585, P < 0.05). The incidence of smoking, abdominal pain and acid regurgitation (χ^2 = 4.761, P < 0.05) as well as the ZUNG anxiety/depression scores (χ^2 = 7.982, P < 0.01) were also significantly higher in the military stress group compared with the control group. ZUNG anxiety (χ^2 = 11.523, P < 0.01) and depression (χ^2 = 5.149, P < 0.05) scores were higher in the FBD group compared with the non-FBD group. The differences in the ZUNG self-rated anxiety and depression scales between the 2 groups were statistically significant (χ^2 = 14.482, P < 0.01 and χ^2 = 6.176, P < 0.05).

CONCLUSION: The morbidity of FBD was higher under military stress conditions.

Key words: Military stress; Functional bowel disorders; Soldier; Self-rating anxiety; Depression scale

Peer reviewers: Javier San Martin, Chief, Gastroenterology and Endoscopy, Sanatorio Cantegril, Av. Roosevelt P 13, Punta del Este 20100, Uruguay; Ted Dinan, Professor, Department of Psychiatry and Alimentary Pharmabiotic Centre, University College Cork, Cork C1, Ireland

Yu XZ, Liu HF, Sun ZX. Investigation of the effect of military stress on the prevalence of functional bowel disorders. *World J Gastroenterol* 2012; 18(23): 3004-3007 Available from: URL: http://www.wjgnet.com/1007-9327/full/v18/i23/3004.htm DOI: http://dx.doi.org/10.3748/wjg.v18.i23.3004

INTRODUCTION

Functional bowel disorders (FBD) is the generic term for disorders of bowel motor and secretary function without organic changes, which are diagnosed according to symptoms after the exclusion of lesions such as inflammation, infection, tumor and other structural disorders[1-3]. FBD includes 5 diseases, irritable bowel syndrome, functional abdominal bloating, functional constipation, functional diarrhea and unspecified functional bowel disorder. FBD are common clinical diseases which significantly affect the quality of patients' lives and incur considerable medical costs. A large number of studies have proved that

stress is the primary induction factor of FBD. Military stress is the emotional reaction of soldiers under military conditions, and mainly manifests as a state of tension[4,5]. There are few studies regarding the effect of military stress on FBD[6], and thus this study investigated the effects of stress by comparing FBD morbidity in soldiers conducting specialized operations with those carrying out regular tasks.

MATERIALS AND METHODS

Objects

Five hundred armed soldiers (mean age 20.7 ± 1.9 years) who were transferred from one province to another in China between April 2009 and May 2010 to handle emergencies were classified as the military stress group; Five hundred armed soldiers (mean age 20.14 ± 1.65 years) from the same province who conducted routine tasks were classified as the control group. All of the soldiers were male and garrisoned in the local area at least 1 year. Both groups were comparable in age, weight, height, the length of military service, education background, duty time, training time and garrison time.

Methods

Questionnaire: The FBD symptom questionnaire including FBD-related symptoms, severity, duration or attack time, and accompanying symptoms, was made with reference to Rome Ⅲ FGIDs functional gastrointestinal disorder standard questionnaire[7], and in combination with the practical conditions of the soldiers in the Chinese People's Armed Police. Psychological factors were investigated using the ZUNG Anxiety Scale and ZUNG Depression Scale.

Quality control of the questionnaire: The questionnaires were distributed according to lists of soldiers by responsible persons in every unit, and were filled in immediately after professional staff gave instructions and answered questions. All questionnaires were checked by a specially designated person after their return. The response rate and acceptance rate were 95.20% (476/500) and (452/476), respectively, in the military stress group, and 96.20% (481/500) and (471/481), respectively, in the control group.

Statistical analysis

The results were input into Epi Info 2003 software to establish data library and analyzed by SPSS18.0 statistical software; the χ^2 test was performed on categorical data. It was statistically significant at $P < 0.05$.

RESULTS

Morbidity of FBD

The rates of FBD in the military and control groups were 14.60% (66/452) and 9.98% (47/471), respectively. The difference between the two groups was statistically significant ($P < 0.05$, Table 1).

Prevalence of primary symptoms

There were 14 primary symptoms of FBD in the questionnaire. Individuals in the sampled populations could have one or more gastrointestinal symptoms. The prevalence of the primary symptoms is presented in Table 1.

Comparison of food habits and intake in soldiers with or without FBD

The food habits of soldiers with FBD were significantly different from those without FBD ($P = 0.000$-0.001). The occurrence of bad habits such as engorgement, being particular about food, omophagia, taking cold drinks, eating hot or spicy food, drinking tea and coffee was more frequent in the FBD group than in the non-FBD group (Table 2); the proportion of soldiers who had few or no bad food habits was smaller in the FBD group compared with the non-FBD group ($P = 0.000$-0.001); the proportion of soldiers who ate a lot of vegetables and fruit was smaller in the FBD group compared with the non-FBD group, while the proportion of soldiers who ate few vegetables and fruit was higher in the FBD group compared with the non-FBD group ($P = 0.000$); the proportion of soldiers who ingested many dairy products was higher in the non-FBD group compared with the FBD group, while the proportion of soldiers who ingested few dairy products was smaller in the FBD group compared with the non-FBD group ($P = 0.000$); the proportion of soldiers who drank coffee was higher in the FBD group compared with the non-FBD group, while the proportion of soldiers who drank tea was smaller in the FBD group compared with the non-FBD group ($P = 0.000$-0.001).

Comparison of the ZUNG self-rating anxiety and depression scales

The proportion of soldiers who had a score > 40 in the ZUNG self-rating anxiety scale was higher in the military stress group (11.97%) than in the control group (5.52%), and was statistically significant ($P < 0.01$). The proportion of soldiers who had a score > 40 in the ZUNG self-rating depression scale was also higher in the military stress group (68.29%) than in the control group (58.60%), and was statistically significant ($P < 0.05$).

DISCUSSION

Military stress[8,9] is a type of emotional reaction appearing in soldiers under military conditions, and mainly manifests as tension. Military stress can be considered as a kind of stimulated or emotional state[10,11]. Military stress cannot be simplistically considered as a negative reaction. It can be understood as a psychological problem only when stress induces changes in the cognition, emotions and behavior of soldiers to severely reduce their efficiency in military missions, and is mainly manifested by an inability to take part in daily military training, to adapt to the military environment or to join in fighting[12,13].

In recent years, more studies have focused on the effect of stress on gastrointestinal function[14], but few have paid attention to the effects of military stress on

Table 1 Comparison of morbidity and prevalence of primary symptoms of functional bowel disorders in the military stress and control groups *n* (%)

	Military stress group	Control group	χ^2	*P*
Disease name				
Irritable bowel syndrome	28/452 (6.19)	16/471 (3.40)	3.972	< 0.05
Functional abdominal bloating	0/452 (0.00)	0/471 (0.00)		> 0.05
Functional constipation	23/452 (5.09)	20/471 (4.25)	0.443	> 0.05
Functional diarrhea	9/452 (1.99)	8/471 (1.70)	0.108	> 0.05
Non-specific functional bowel disorder	6/452 (1.33)	3/471 (0.64)	1.135	> 0.05
Total	66/452 (14.6)	47/471 (9.98)	4.585	< 0.05
Primary symptom (No. of person with symptoms)				
Nausea	133/452 (29.42)	74/471 (15.71)	24.931	< 0.01
Vomiting	74/452 (15.71)	53/471 (11.25)	5.849	< 0.05
Abdominal distension	145/452 (32.08)	103/471 (21.87)	12.230	< 0.01
Acid regurgitation	113/452 (25.00)	64/471 (13.59)	19.329	< 0.01
Heartburn	61/452 (13.50)	43/471 (9.13)	4.397	< 0.05
Foreign body sensation in throat	85/452 (18.81)	78/471 (16.56)	0.800	> 0.05
Substernal pain	70/452 (15.49)	47/471 (9.98)	6.312	< 0.05
Hiccough	135/452 (29.87)	82/471 (17.41)	19.899	< 0.01
Food regurgitation	101/452 (22.34)	61/471 (12.95)	14.068	< 0.01
Abdominal pain	31/452 (6.86)	13/471 (2.76)	8.483	< 0.01
Constipation	142/452 (31.42)	98/471 (20.81)	13.492	< 0.01
Diarrhea	121/452 (26.77)	86/471 (18.26)	9.602	< 0.01
Encopresis	15/452 (3.32)	9/471 (1.91)	1.808	> 0.05

Table 2 Food intake of soldiers with and without functional bowel disorders *n* (%)

Food habit	Much	Moderate	Less	Little or not	Total
With functional bowel disorder					
Engorgement	10 (15.9)	21 (32.5)	20 (31.1)	13 (20.3)	64 (100)
Omophagia	6 (8.8)	10 (15.7)	23 (34.9)	26 (40.1)	65 (100)
Particular about food	12 (18.9)	19 (29.4)	15 (22.8)	20 (30.3)	66 (100)
Cold drinks	14 (20.6)	22 (33.3)	20 (30.6)	10 (15.2)	66 (100)
Spicy food	22 (33.4)	21 (32.1)	17 (26.3)	5 (7.7)	65 (100)
Dairy products	20 (30.9)	24 (37.2)	15 (24.1)	6 (9.3)	64 (100)
Vegetables	17 (27.6)	33 (51.7)	12 (19.2)	1 (1.6)	63 (100)
Fruit	14 (22.6)	26 (39.5)	18 (28.4)	7 (10.8)	65 (100)
Without functional bowel disorder					
Engorgement	3 (5.1)	10 (16.3)	18 (29.2)	29 (48.3)	60 (100)
Omophagia	3 (5.8)	6 (10.4)	15 (24.9)	35 (59.3)	59 (100)
Particular about food	5 (8.0)	10 (17.8)	11 (19.8)	32 (55.1)	58 (100)
Cold drinks	7 (11.6)	16 (26.3)	17 (28.6)	21 (34.4)	61 (100)
Spicy food	10 (16.4)	16 (27.1)	15 (25.8)	19 (31.7)	60 (100)
Dairy products	16 (25.9)	23 (37.2)	12 (19.1)	11 (17.7)	62 (100)
Vegetables	24 (37.4)	28 (43.7)	6 (9.2)	5 (7.9)	63 (100)
Fruit	22 (34.6)	24 (37.5)	12 (18.7)	6 (9.4)	64 (100)

gastrointestinal function[15,16]. The results in this study suggested that FBD was significantly higher in the military group (14.60%) compared with the control group (9.98%). Meanwhile, the rates of smoking, abdominal pain, and acid regurgitation, and the ZUNG anxiety and depression scores were also significantly higher in the military group compared with the control group. The increased incidence of FBD under military stress might be due to the dual regulatory effects of the autonomic nervous system and the endocrine system on the movement and secretion of the alimentary tract, which are directly or indirectly affected by the central nervous system[17,18]. The anatomical structures of the nervous and endocrine system overlap with that of the emotional center[19,20], thus after tension and emotional changes induced by military stress conditions arrive at the emotional center, the gastrointestinal regulatory center will also be excited, and therefore, gastrointestinal discomfort will likely occur or be aggravated[21,22].

It has been reported[23] that there are significant differences between individuals in the length of time psychological stress is sustained. Overall, although a psychological stress reaction may be alleviated within 10 d in about 85% soldiers, it persists in about 15% soldiers after 10 d. The following measures should be adopted to deal with the increased morbidity of FBD induced by military stress: a focus on daily training activity[24,25], with simulation of various duty environments, and enhanced quality of psychological and mental preparation for emergencies; the soldiers should actively take part in the handling of an emergency situation, have a specific daily schedule

with adequate rest periods, and be given medical treatment if necessary. Non-combat casualties resulting from illness will be decreased and should guarantee that military duties will be better accomplished[26].

Overall, FBD is an old problem, but there are still areas in the pathogenesis of the disease to explore, and which may involve a wide range of research, including cell biology, neurophysiology, immunology, endocrinology, behavior and other fields of medicine and psychology. Linking the clinical problem with stress may directly lead to a clinical benefit for all patients.

COMMENTS

Background

Functional bowel disorders (FBD) is a generic name for disorders in bowel motor and secretary function without organic changes, and is diagnosed according to symptoms after the exclusion of lesions such as inflammation, infection, tumor and other structural disorders. It is a common clinical disease which significantly affects the quality of patients' lives and incurs medical costs. A large number of studies have shown that stress is the primary induction factor of FBD.

Research frontiers

There are few studies of the effect of military stress on FBD, and thus this research tried to investigate these effects through comparing the morbidity in soldiers conducting specialized tasks with those undertaking regular tasks.

Innovations and breakthroughs

Four hundred and fifty-seven soldiers who were assigned to specified services and 471 soldiers who were assigned to common services were enrolled using cluster sampling, with the latter as the control group, and then they were surveyed according to the Rome Ⅲ FBD standard questionnaire.

Applications

To provide foundations for the prevention and treatment of this disease, authors investigated the morbidity of FBD under military stress conditions.

Terminology

FBD: Disorders of bowel motor and secretary function without organic changes, diagnosed according to symptoms after the exclusion of organic lesions.

Peer review

Overall, this is an interesting study which shows clearly that the morbidity of FBD was higher under military stress conditions.

REFERENCES

1 **Keating E**, Lemos C, Monteiro R, Azevedo I, Martel F. The effect of a series of organic cations upon the plasmalemmal serotonin transporter, SERT. *Life Sci* 2004; **76**: 103-119
2 **Mykletun A**, Heradstveit O, Eriksen K, Glozier N, Øverland S, Maeland JG, Wilhelmsen I. Health anxiety and disability pension award: The HUSK Study. *Psychosom Med* 2009; **71**: 353-360
3 **Nicholl BI**, Halder SL, Macfarlane GJ, Thompson DG, O'Brien S, Musleh M, McBeth J. Psychosocial risk markers for new onset irritable bowel syndrome--results of a large prospective population-based study. *Pain* 2008; **137**: 147-155
4 **Jung IS**, Kim HS, Park H, Lee SI. The clinical course of postinfectious irritable bowel syndrome: a five-year follow-up study. *J Clin Gastroenterol* 2009; **43**: 534-540
5 **Hildrum B**, Mykletun A, Stordal E, Bjelland I, Dahl AA, Holmen J. Association of low blood pressure with anxiety and depression: the Nord-Trøndelag Health Study. *J Epidemiol Community Health* 2007; **61**: 53-58
6 **Hildrum B**, Mykletun A, Holmen J, Dahl AA. Effect of anxiety and depression on blood pressure: 11-year longitudinal population study. *Br J Psychiatry* 2008; **193**: 108-113
7 **Camilleri M**, Andrews CN, Bharucha AE, Carlson PJ, Ferber I, Stephens D, Smyrk TC, Urrutia R, Aerssens J, Thielemans L, Göhlmann H, van den Wyngaert I, Coulie B. Alterations in expression of p11 and SERT in mucosal biopsy specimens of patients with irritable bowel syndrome. *Gastroenterology* 2007; **132**: 17-25
8 **Gaman A**, Kuo B. Neuromodulatory processes of the brain-gut axis. *Neuromodulation* 2008; **11**: 249-259
9 **Boyce PM**, Talley NJ, Burke C, Koloski NA. Epidemiology of the functional gastrointestinal disorders diagnosed according to Rome II criteria: an Australian population-based study. *Intern Med J* 2006; **36**: 28-36
10 **Miao DM**. Research on Military Psychology. *Xinli Kexve Jinzhan* 2006; 14: 161-163
11 **Sperber AD**, Shvartzman P, Friger M, Fich A. A comparative reappraisal of the Rome II and Rome III diagnostic criteria: are we getting closer to the 'true' prevalence of irritable bowel syndrome? *Eur J Gastroenterol Hepatol* 2007; **19**: 441-447
12 **Drukker CA**, Heij HA, Wijnaendts LC, Verbeke JI, Kaspers GJ. Paraneoplastic gastro-intestinal anti-Hu syndrome in neuroblastoma. *Pediatr Blood Cancer* 2009; **52**: 396-398
13 **Vandvik PO**, Lydersen S, Farup PG. Prevalence, comorbidity and impact of irritable bowel syndrome in Norway. *Scand J Gastroenterol* 2006; **41**: 650-656
14 **Dunlop SP**, Jenkins D, Spiller RC. Distinctive clinical, psychological, and histological features of postinfective irritable bowel syndrome. *Am J Gastroenterol* 2003; **98**: 1578-1583
15 **Zheng PY**, Feng BS, Oluwole C, Struiksma S, Chen X, Li P, Tang SG, Yang PC. Psychological stress induces eosinophils to produce corticotrophin releasing hormone in the intestine. *Gut* 2009; **58**: 1473-1479
16 **Santos J**, Yates D, Guilarte M, Vicario M, Alonso C, Perdue MH. Stress neuropeptides evoke epithelial responses via mast cell activation in the rat colon. *Psychoneuroendocrinology* 2008; **33**: 1248-1256
17 **Heymann-Mönnikes I**, Arnold R, Florin I, Herda C, Melfsen S, Mönnikes H. The combination of medical treatment plus multicomponent behavioral therapy is superior to medical treatment alone in the therapy of irritable bowel syndrome. *Am J Gastroenterol* 2000; **95**: 981-994
18 **Demaude J**, Salvador-Cartier C, Fioramonti J, Ferrier L, Bueno L. Phenotypic changes in colonocytes following acute stress or activation of mast cells in mice: implications for delayed epithelial barrier dysfunction. *Gut* 2006; **55**: 655-661
19 **Patacchioli FR**, Angelucci L, Dellerba G, Monnazzi P, Leri O. Actual stress, psychopathology and salivary cortisol levels in the irritable bowel syndrome (IBS). *J Endocrinol Invest* 2001; **24**: 173-177
20 **La JH**, Sung TS, Kim HJ, Kim TW, Kang TM, Yang IS. Peripheral corticotropin releasing hormone mediates post-inflammatory visceral hypersensitivity in rats. *World J Gastroenterol* 2008; **14**: 731-736
21 **Rao SS**, Hatfield RA, Suls JM, Chamberlain MJ. Psychological and physical stress induce differential effects on human colonic motility. *Am J Gastroenterol* 1998; **93**: 985-990
22 **Piche T**, Barbara G, Aubert P, Bruley des Varannes S, Dainese R, Nano JL, Cremon C, Stanghellini V, De Giorgio R, Galmiche JP, Neunlist M. Impaired intestinal barrier integrity in the colon of patients with irritable bowel syndrome: involvement of soluble mediators. *Gut* 2009; **58**: 196-201
23 **Yin J**, Levanon D, Chen JD. Inhibitory effects of stress on postprandial gastric myoelectrical activity and vagal tone in healthy subjects. *Neurogastroenterol Motil* 2004; **16**: 737-744
24 **Santos J**, Saperas E, Nogueiras C, Mourelle M, Antolín M, Cadahia A, Malagelada JR. Release of mast cell mediators into the jejunum by cold pain stress in humans. *Gastroenterology* 1998; **114**: 640-648
25 **Mearin F**. Postinfectious functional gastrointestinal disorders. *J Clin Gastroenterol* 2011; **45** Suppl: S102-S105
26 **Meddings JB**, Swain MG. Environmental stress-induced gastrointestinal permeability is mediated by endogenous glucocorticoids in the rat. *Gastroenterology* 2000; **119**: 1019-1028

S- Editor Gou SX **L- Editor** Cant MR **E- Editor** Zheng XM

World Journal of Gastroenterology

Online Submissions: http://www.wjgnet.com/1007-9327office
wjg@wjgnet.com
doi:10.3748/wjg.v18.i23.3008

World J Gastroenterol 2012 June 21; 18(23): 3008-3014
ISSN 1007-9327 (print) ISSN 2219-2840 (online)

BRIEF ARTICLE

Ultrasound-guided microwave ablation for abdominal wall metastatic tumors: A preliminary study

Cai Qi, Xiao-Ling Yu, Ping Liang, Zhi-Gang Cheng, Fang-Yi Liu, Zhi-Yu Han, Jie Yu

Cai Qi, Xiao-Ling Yu, Ping Liang, Zhi-Gang Cheng, Fang-Yi Liu, Zhi-Yu Han, Jie Yu, Department of Interventional Ultrasound, The General Hospital of Chinese People's Liberation Army, Beijing 100853, China

Author contributions: Qi C, Yu XL and Liang P designed the research; Qi C, Cheng ZG and Liu FY performed the research; Han ZY carried out the statistical analysis; Yu J helped write and correct the paper; Yu XL supervised the organization process.

Correspondence to: Xiao-Ling Yu, MD, Professor of Medicine, Department of Interventional Ultrasound, The General Hospital of Chinese People's Liberation Army, 28 Fuxing Road, Beijing 100853, China. dyuxl301@yahoo.com.cn
Telephone: +86-10-66937981 Fax: +86-10-88210006
Received: November 18, 2011 Revised: February 28, 2012
Accepted: March 9, 2012
Published online: June 21, 2012

Abstract

AIM: To evaluate the feasibility, safety and efficacy of ultrasound-guided microwave (MW) ablation for abdominal wall metastatic tumors.

METHODS: From August 2007 to December 2010, a total of 11 patients with 23 abdominal wall nodules (diameter 2.59 cm ± 1.11 cm, range 1.3 cm to 5.0 cm) were treated with MW ablation. One antenna was inserted into the center of tumors less than 1.7 cm, and multiple antennae were inserted simultaneously into tumors 1.7 cm or larger. A 21 gauge thermocouple was inserted near important organs which required protection (such as bowel or gallbladder) for real-time temperature monitoring during MW ablation. Treatment outcome was observed by contrast-enhanced ultrasound and magnetic resonance imaging (MRI) [or computed tomography (CT)] during follow-up.

RESULTS: MW ablation was well tolerated by all patients. Six patients with 11 nodules had 1 thermocouple inserted near important organs for real-time temperature monitoring and the maximum temperature was 56 ℃. Major complications included mild pain (54.5%), post-ablation fever (100%) and abdominal wall edema (25%). All 23 tumors (100%) in this group were completely ablated, and no residual tumor or local recurrence was observed at a median follow-up of 13 mo (range 1 to 32 mo). The ablation zone was well defined on contrast-enhanced imaging (contrast-enhanced CT, MRI and/or contrast-enhanced ultrasound) and gradually shrank with time.

CONCLUSION: Ultrasound-guided MW ablation may be a feasible, safe and effective treatment for abdominal wall metastatic tumors in selected patients.

Key words: Abdominal wall; Microwave ablation; Neoplasm metastasis; Thermal ablation therapy; Ultrasonography

Peer reviewer: David A Iannitti, Professor, Department of General Surgery, Carolinas Medical Center, Charlotte, NC 28204, United States

Qi C, Yu XL, Liang P, Cheng ZG, Liu FY, Han ZY, Yu J. Ultrasound-guided microwave ablation for abdominal wall metastatic tumors: A preliminary study. *World J Gastroenterol* 2012; 18(23): 3008-3014 Available from: URL: http://www.wjgnet.com/1007-9327/full/v18/i23/3008.htm DOI: http://dx.doi.org/10.3748/wjg.v18.i23.3008

INTRODUCTION

Clinically, the incidence of primary abdominal wall malignant tumors is low. Usually metastasis or local infiltration is the major cause of abdominal wall metastatic tumors. A number of abdominal wall tumors occur during or after therapy, and are difficult to cure. Currently, most studies report that the main treatment for abdominal

wall tumors is resection[1], however some patients are unable to undergo resection due to tumor stage. Small subcutaneous lesions can be easily resected, whereas it is technically difficult for radical excision of large lesions, especially those which invade muscles. Moreover, surgical reconstruction is also troublesome, and a significant number of patients require abdominoplasty for larger abdominal wall tumors[2-4]. Other treatments have been used for abdominal wall tumors, such as radiotherapy, chemotherapy and thermal ablation. Radiotherapy requires patients to have optimal health status, while chemotherapy often plays an additional role and is not used as a radical cure. Thermal ablation is a minimally invasive technique, and has been widely used for the treatment of primary and metastatic liver cancer in past decades and is well established[5-8]. High intensity focused ultrasound (HIFU) and radiofrequency ablation have been used in abdominal wall metastatic tumors with curative effect[9]. Microwave (MW) ablation for the treatment of liver tumorsis relatively low-risk and has favorable therapeutic efficacy[10,11]. Compared with radiofrequency ablation, MW energy does not appear to be limited by charring and tissue desiccation, thus, thermal efficiency may be considerably higher with MW systems than with radiofrequency systems[12-15]. To our knowledge, there are no reports assessing the efficacy and safety of MW ablation for abdominal wall tumors under ultrasound guidance.

Thus, the purpose of this study was to assess the effectiveness of MW ablation for abdominal wall tumors under ultrasound guidance in the short and medium term, and to identify the possible complications that determine the rate of therapeutic success.

MATERIALS AND METHODS

Patients

From August 2007 to December 2010, eleven patients with 23 abdominal wall tumors were enrolled in this retrospective study (Table 1). The patients were 6 men and 5 women aged 35-68 years (mean age, 54.18 ± 9.14 years), and tumor size ranged from 1.3 cm to 5.0 cm in maximum diameter (mean diameter 2.59 ± 1.11 cm, range 1.3 cm to 5.0 cm). Before MW ablation, 2 patients were treated with chemotherapy, 1 patient was treated with chemotherapy and radiotherapy, and 1 patient with immunotherapy. Informed consent was obtained from all patients at enrollment. The inclusion criteria for this study were as follows: (1) The entire tumor could be clearly seen on ultrasound; (2) The tumor size was no more than 5 cm in diameter; (3) The tumor was located more than 5 mm from the skin surface; (4) The tumor had not adhered to the peritoneum or bowels; and (5) The tumor had not invaded the bones. The exclusion criteria were as follows: (1) Severe cardiopulmonary disease; (2) Severe coagulation abnormalities (prothrombin time more than 25 s, prothrombin activity higher than 40%, and platelet count higher than 40 cells × 10^9/L); and (3) Infection. All selected patients chose MW ablation on the basis of tumor stage which made them inoperable, or had comorbidities, advanced age, or refused to undergo surgery. All abdominal wall nodules were metastatic lesions. In five cases abdominal wall tumors had metastasized from hepatocellular carcinoma (HCC); two cases metastasized from adrenal glands, whose pathological types were adrenal cortical carcinoma and pheochromocytoma. The remaining four cases metastasized from lung, ovary, bladder and kidney; and the corresponding pathological types were lung adenocarcinoma, ovarian peritoneal serous papillary carcinoma, bladder transitional cell carcinoma and renal clear cell carcinoma. The primary liver lesions in five patients were treated with MW ablation, and the primary lesions in the remaining patients were resected. Abdominal wall metastatic tumors in three patients with HCC were caused by needle tract seeding, which appeared 9, 11 and 22 mo after liver puncture.

Equipment

A KY2000 MW ablation system (Kangyou Medical Instruments, Nanjing, China) consisting of two independent MW generators, two flexible coaxial cables and two water-pumping machines, which could drive two 15-gauge cooled-shaft antennae simultaneously was used. The generators are capable of producing 1-100 W of power at 2450 MHz. The cooled shaft antenna was coated with polytetrafluoroethylene to prevent adhesion, which can also be clearly seen on ultrasound. The antenna is designed to minimize power feedback and provide tissue with optimal energy deposition. Three types of antennae were applied according to the size and location of the tumor, the antennae tips were 0.5, 0.7 and 1.1 cm, respectively. For tumors smaller than 2 cm, an antenna tip of 0.5 cm was chosen, while for tumors larger than 3 cm, a tip of 1.1 cm was selected. The MW machine is also equipped with a thermal monitoring system with 21-gauge thermocouple needles, which can be placed percutaneously at a designated location to monitor the temperature during real-time ablation.

Ablation procedures

Before treatment, all patients were scanned using contrast-enhanced computed tomography (CT)/magnetic resonance imaging (MRI) and ultrasound, and an appropriate puncture route was chosen by ultrasound. After local anesthesia with 1% lidocaine, the antenna was inserted percutaneously into the tumor and placed at designated sites under ultrasound guidance. Histologic diagnoses were confirmed by guided sonography with an 18-gaugecutting-edge needle through an automated biopsy gun device before inserting the antenna, and specimens were taken from different parts of the tumor (one to three pieces). One antenna was inserted into the center of tumors less than 1.7 cm, and multiple antennae were inserted into tumors 1.7 cm or larger. General anesthesia (Propofol, 6-12 mg/kg per hour; Ketamine, 1-2 mg/kg) was applied after correct placement of

Table 1 Patient and tumor characteristics

No.	Age (yr)	Sex	Tumor type	Tumor number	Tumor size (cm)	Antenna	Antenna number	Ablation power (W)	Ablation time (min)	Session	Follow up (mo)
1	59	M	HCC	1	1.8	T11	1	50	6	1	31
2	35	M	HCC	1	2.1	T11	1	50	8	1	26
3	68	M	HCC	2	4.3	T11	2	40	5	2	19
					4.8	T11	2	50	16.5	1	19
4	57	F	Ovary serous papillary adenocarcinoma	1	2.2	T7/T11	2	45	2	2	18
5	55	F	Lung adenocarcinomas	2	1.3	T11	1	50	3.5	1	18
					1.7	T11	1	50	3.5	1	18
6	56	F	Adrenocortical carcinoma	4	4	T11	2	60	12	1	9
					3.1	T11	2	30	12	1	9
					3.3	T7/T11	2	30	16	1	9
					2.5	T5	2	50	5	1	9
7	58	M	HCC	1	1.3	T11	2	50	5	1	3
8	48	M	Bladder adenocarcinoma	2	5	T11	2	40	15	2	13
					2.1	T11	2	50	11.8	1	13
9	59	F	Renal clear cell carcinoma	5	2.2	T11	2	60	5	1	15
					2.1	T11	2	50	5.5	1	15
					2.1	T11	2	50	6	1	15
					2	T7/T11	2	45	4	1	15
					1.6	T11	1	45	3.8	1	15
10	58	F	HCC	1	2.6	T5	1	50	13	1	1
11	42	M	Adrenal pheochromocytoma	3	3.1	T7	1	50	8	1	4
					2.8	T5	2	50	6.5	1	4
					1.4	T5	1	50	1.2	1	4

M: Male; F: Female; HCC: Hepatocellular carcinoma.

antennae, and MWs were then emitted[16,17]. Two antennae were used simultaneously during MW ablation to achieve a larger ablation zone. If the tumor was adjacent to bowel, gallbladder or other important tissues, a 21 gauge thermocouple was inserted close to these tissues for real-time temperature monitoring during MW ablation. The treatment session ended if the transient hyperechoic zone between the antennae merged and covered the target region on gray-scale ultrasound. Simultaneously, according to our previous clinical experience, the temperature of the thermal needles should not exceed the target temperature to avoid heat injury in these organs[18]. For tumors with subcutaneous invasion, an ice bag was placed on the skin to avoid scalding during MW ablation.

Postprocedural observation and follow-up

After MW ablation, patients were closely monitored for possible complications such as fever, skin burns and pain which were also documented. All patients underwent contrast-enhanced ultrasound 3 d after MW ablation to assess treatment efficacy. If residual tumor (hyperenhanced area on contrast-enhanced ultrasound) was found, a further session was planned or patients entered the follow-up protocol, which consisted of contrast-enhanced CT, MRI and/or contrast-enhanced ultrasound 1, 3 and 6 mo after MW ablation, and every 6 mo thereafter. Enhanced areas on the abdominal wall were assumed to represent viable tumors. If residual or recurrent tumor on the abdominal or chest wall was detected, a further MW ablation session was planned if the lesion still met the inclusion criteria.

RESULTS

MW ablation was well tolerated by all patients. The output power ranged from 30 W to 50 W, an output setting of 50 W was routinely used during ablation sessions, relatively lower than that used in liver lesions. Four of 23 tumors were adjacent to the intestinal tract, one nodule was adjacent to the gallbladder, and 1 nodule was adjacent to the gallbladder and intestinal tract. A thermocouple was inserted adjacent to these high-risk locations for real-time temperature monitoring. In this study, we used 1 thermocouple with a maximum temperature of 56 ℃ in 6 patients with 11 nodules. The treatment time was no more than 16.5 min (mean time 7.6 ± 4.3 min, range 2 min to 16.5 min). Twenty-one of 23 tumors were successfully eradicated following one MW session. The other two tumors underwent two MW sessions; one tumor was near the adrenal gland, and the other was a tumor 5 cm in maximum diameter. All 23 tumors (100%) in this group were completely ablated which was confirmed by follow-up imaging during a period of 1-32 mo. No major complications were encountered after MW ablation. Six patients experienced grade 1 according to standardization of terms and reporting criteria for image-guided tumor ablation[19]. Post-ablation fever was encountered in all patients, but each patient's temperature was lower than 38 ℃ and no drugs were needed. No skin burns were observed in the treated area, however, the treated area was slightly swollen in 3 patients. The patients were followed up until January 20, 2011. The median survival period of the 11 patients after MW ablation was 15.0 mo. During a mean follow-up of 13 mo (range 1-32 mo), three patients died of primary

tumor progression, however, the treated tumors were unenhanced on follow-up contrast-enhanced images. In the other 8 patients, the ablation zones were well defined on contrast-enhanced images, and gradually shrank with time (Figure 1). Two patients developed distant metastases, one patient was treated with repeated sessions of MW ablation, and the other underwent HIFU.

DISCUSSION

In the past few decades, the treatment of abdominal wall tumors, especially metastasis, has evolved[9,20]. In addition to traditional surgical resection, there are many other treatments, such as transarterial embolization[20] radiofrequency ablation and HIFU[21]. Surgical resection is the first choice for abdominal tumors, although it carries a risk of hemorrhage and possible post-operative incisional hernia, and patients usually require reconstruction, such as abdominoplasty[22]. Some patients may not be surgical candidates due to poor medical conditions[23]. It is difficult to create a safety margin to eradicate possible microscopic tumor foci using transarterial embolization of the feeding vessel of the abdominal tumor, and may cause ischemic changes. Thus, it is rarely used in abdominal tumors. Compared with surgical resection, HIFU is a less invasive alternative to surgical resection. However, due to the bio-effects of focused ultrasound during the procedure, heat diffusion out of the focal region is inevitable and can damage the surrounding tissues.

We have also made some progress with the antennae used in MW ablation.Three types of antennae were used in this study according to tumor size and location, and the antennae tips were 0.5, 0.7 and 1.1 cm, respectively. According to a preliminary study, an antenna tip of 1.1 cm can ablate 2-2.6 cm *ex vivo* porcine livers with the output power of 60 W and the setting time of 10 min[24]. Based on these preliminary experiments, an antenna tip of 0.7 cm and 0.5 cm can ablate 2.4-2.6 cm and 2.2-2.4 cm *ex vivo* porcine livers with the output power of 60 W and the setting time of 10 min, respectively. The new type tips are safer, because the ablation zone is relatively small which avoids burning the skin in the superficial tumor during the procedure. Therefore, percutaneous MW ablation may be clinically feasible for superficial tumors. Based on our previous experience in MW ablation for HCC, we performed MW ablation on abdominal tumors. Treatment efficacy was encouraging. For tumors smaller than 4 cm, radical cure was achieved in all nodules within no more than 12 min and no tumor recurrence was noted during follow-up. In order to achieve the same effect, tumors larger than 4 cm needed several sessions. MW ablation, is a relatively new technique and can be used in different types of tumors[25-30], the primary effectiveness rate is equal to HIFU and radiofrequency ablation[16,31]. The favorable effectiveness of MW ablation may be attributed to its potential advantages[32], such as larger volume of ablation zone, reduced treatment time, less influence on the perfusion-mediated heat sink effect, higher thermal efficiency and the possibility of placing multiple antennae simultaneously[33-35], especially compared with radiofrequency ablation. Results suggest that, like other techniques, MW ablation may be safe and effective for abdominal wall tumors, it may also represent a competitive alternative to surgical resection and other therapies. The high effectiveness rate of MW ablation may due to the following 4 reasons: (1) The new-type antenna used in this study was capable of ablating superficial tumors more securely; (2) There were relatively strict inclusion and exclusion criteria; (3) All operations were performed by experienced doctors (Yu XL and Liang P); and (4) Real-time temperature monitoring served as an indicator for predicting reliable safety margins. No severe complications were observed in this study. Unlike the treatment of liver tumors, abdominal tumor ablation has its own complication of abdominal wall edema. We studied three patients who had abdominal wall edema and found that the ablated tumors were all located in muscles and with subcutaneous invasion. Compared with parenchymal organs, muscle tissue lacks relative capsules and can not accumulate heat. During the ablation procedure, heat overflow in the muscle bundle can readily lead to abdominal wall edema. In order to ablate completely, the actual ablation zone should be larger than the size of the tumor, which will ablate normal tissues (such as fatty tissue or muscle tissue) and cause edema in a short time. Fortunately, the abdominal wall edema seen in three patients was very mild and all patients recovered within a short time (1-3 mo) without special treatment. For the ablation of specific tumors, such as pheochromocytoma, we used low power at the beginning of MW ablation, and changed the power according to the blood pressure. The use of antihypertensive drugs during the procedure should be taken into account, as pheochromocytomas can release catecholamine which could result in blood pressure fluctuation. There are key points during MW ablation which can reduce the incidence of complications: (1) The MW antenna was inserted in the deepest area of the tumor; (2) Increasing the angle of puncture between the antenna and transducer, that is insert the antenna along the long axis of the tumor for conformable ablation; and (3) For tumors with subcutaneous invasion, the transient hyperechoic zone did not exceed the dermal layer in the gray-scan ultrasound, and an ice bag was placed on the skin to avoid scalding. Although this was not a randomized, controlled study of traditional techniques, the low complication rate, minimal side effects, rapid recovery and lower costs (compared with radiofrequency ablation in China) strongly favor MW ablation as an optional curative approach for abdominal wall tumors. This study has some limitations: (1) Only 11 patients were included in this study. More patients should be recruited in order to assess the efficacy of this treatment; (2) Follow-up was relatively short and we are uncertain of the long-term results; and (3) The study did not include a comparison with other treatments.

In conclusion, our preliminary results showed that ultrasound-guided MW ablation appeared to be effective in the treatment of abdominal wall tumors. Further stud-

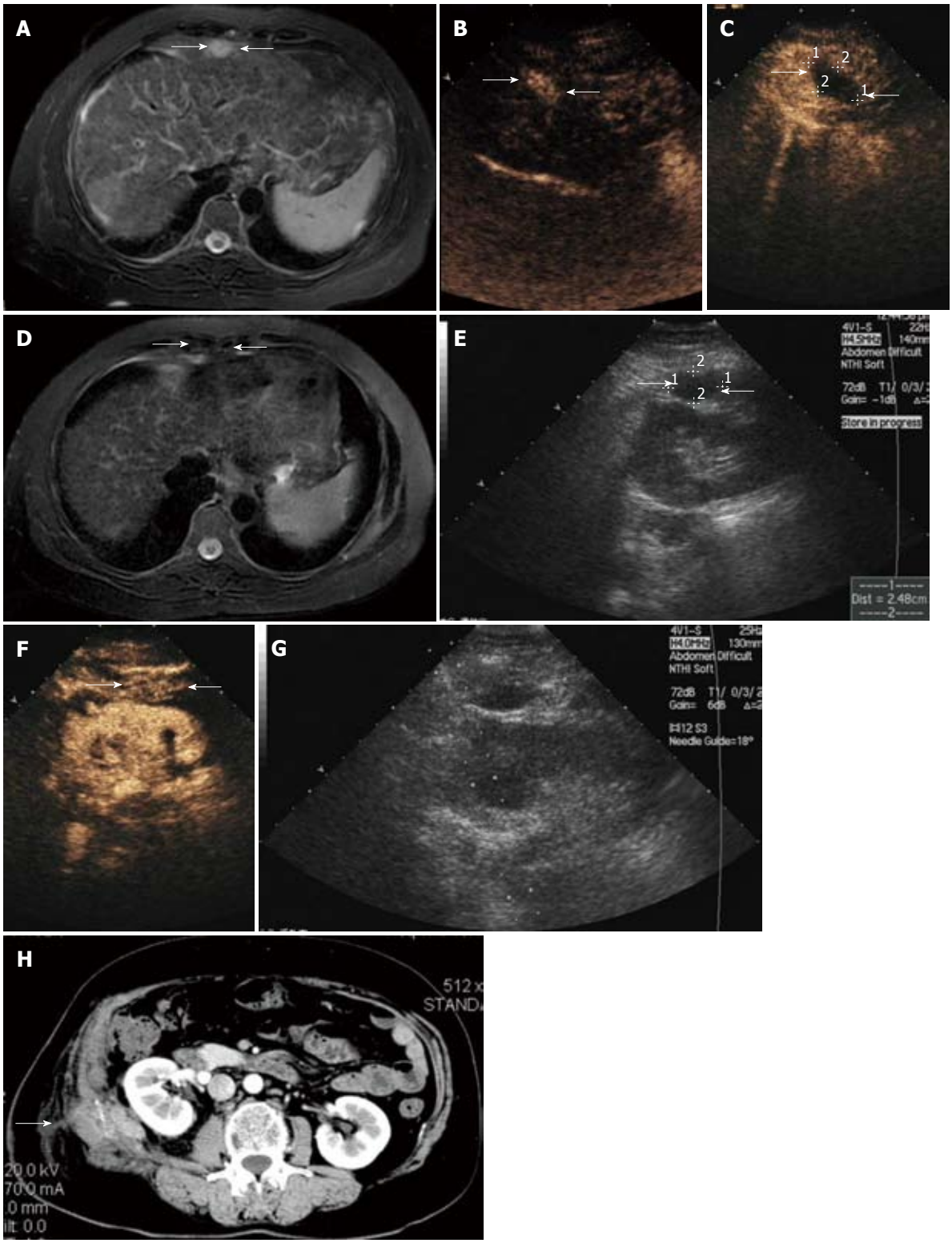

Figure 1 Ultrasound findings in a 56-year-old woman with abdominal wall tumor metastasized from liver and adrenal gland cancer. A: Contrast-enhanced magnetic resonance imaging (MRI) scan shows a lesion with hyperenhancement in T2-weighted images in the abdominal wall (arrow); B: Arterial phase in contrast-enhanced ultrasound (CEUS) shows hyperenhancement within the lesions (arrow); C: CEUS scan obtained 3 d after microwave (MW) ablation shows a hypoechoic area with no enhancement, suggestive of complete necrosis (arrow); D: Contrast-enhanced MRI scan shows a lesion with hypoenhancement in T2-weighted phase MR image obtained 1 mo after MW ablation revealing complete ablation. Contrast-enhanced MRI scan shows a lesion with hypoenhancement in T2-weighted images in the abdominal wall (arrow); E: Sonogram obtained before MW ablation shows hypoechoic nodule of 2.48 cm in maximum diameter in the abdominal wall (arrow); F: Arterial phase in CEUS shows hyperenhancement within the lesions (arrow); G: Sonogram obtained during MW ablation shows one antenna being inserted into the nodule; H: Abdominal wall edema occurred at the right lumbar in the arterial phase of contrast-enhanced CT (arrow).

ies are warranted to observe its long-term efficacy and the results should be compared with other treatments.

COMMENTS

Background

A number of abdominal wall tumors occur during or after therapy, and are difficult to cure. Currently, the main treatment for abdominal wall tumors is resection, while the excision rate is low. Microwave (MW) ablation for the treatment of liver tumors has relatively low-risk and favorable therapeutic efficacy. However, there are no reports assessing the efficacy and safety of MW ablation for abdominal wall tumors under ultrasound guidance.

Research frontiers

MW ablation, as a relatively new technique, and can be applied to different types of tumors. This research was concerned with applying MW ablation in patients with abdominal wall metastatic tumors, and to improve the effectiveness rate of this technique.

Innovations and breakthroughs

Unlike the commonly used antenna, the authors made some progress with the antennae used in this study. Three types of antennae were used according to tumor size and location, and the antennae tips used were 0.5, 0.7 and 1.1 cm, respectively. These new type tips are safer, because the ablation zone is relatively small which avoids burning the skin in the superficial tumor during the procedure. Therefore, percutaneous MW ablation may be clinically feasible for superficial tumors.

Applications

The study results suggest that ultrasound-guided MW ablation may be a feasible, safe and effective treatment of abdominal wall metastatic tumors in selected patients.

Terminology

Image-guided tumor ablation: The term tumor ablation is defined as the direct application of chemical or thermal therapies to a specific focal tumor (or tumors) in an attempt to achieve eradication or substantial tumor destruction.

Peer review

The authors present short and medium-term outcomes for ultrasound-guided MW ablation for abdominal wall metastatic tumors. The procedure was well tolerated by all patients with the most significant complication being abdominal wall edema which resolved without treatment in all cases.

REFERENCES

1 **Stojadinovic A**, Hoos A, Karpoff HM, Leung DH, Antonescu CR, Brennan MF, Lewis JJ. Soft tissue tumors of the abdominal wall: analysis of disease patterns and treatment. *Arch Surg* 2001; **136**: 70-79

2 **Lazzeri D**, Pascone C, Agostini T. Abdominal wall reconstruction: some historical notes. *Plast Reconstr Surg* 2010; **126**: 1793-1794; author reply 1794

3 **Gu Y**, Tang R, Gong DQ, Qian YL. Reconstruction of the abdominal wall by using a combination of the human acellular dermal matrix implant and an interpositional omentum flap after extensive tumor resection in patients with abdominal wall neoplasm: a preliminary result. *World J Gastroenterol* 2008; **14**: 752-757

4 **Yezhelyev MV**, Deigni O, Losken A. Management of Full Thickness Abdominal Wall Defects Following Tumor Resection. *Ann Plast Surg* 2011 May 27; Epub ahead of print

5 **Liu JG**, Wang YJ, Du Z. Radiofrequency ablation in the treatment of small hepatocellular carcinoma: a meta analysis. *World J Gastroenterol* 2010; **16**: 3450-3456

6 **Vanagas T**, Gulbinas A, Pundzius J, Barauskas G. Radiofrequency ablation of liver tumors (II): clinical application and outcomes. *Medicina* (Kaunas) 2010; **46**: 81-88

7 **Mayo SC**, Pawlik TM. Thermal ablative therapies for secondary hepatic malignancies. *Cancer J* 2010; **16**: 111-117

8 **Liang P**, Wang Y, Yu X, Dong B. Malignant liver tumors: treatment with percutaneous microwave ablation--complications among cohort of 1136 patients. *Radiology* 2009; **251**: 933-940

9 **Wang Y**, Wang W, Wang Y, Tang J. Ultrasound-guided high-intensity focused ultrasound treatment for needle-track seeding of hepatocellular carcinoma: preliminary results. *Int J Hyperthermia* 2010; **26**: 441-447

10 **Liang P**, Dong B, Yu X, Yu D, Wang Y, Feng L, Xiao Q. Prognostic factors for survival in patients with hepatocellular carcinoma after percutaneous microwave ablation. *Radiology* 2005; **235**: 299-307

11 **Martin RC**, Scoggins CR, McMasters KM. Safety and efficacy of microwave ablation of hepatic tumors: a prospective review of a 5-year experience. *Ann Surg Oncol* 2010; **17**: 171-178

12 **Wright AS**, Lee FT, Mahvi DM. Hepatic microwave ablation with multiple antennae results in synergistically larger zones of coagulation necrosis. *Ann Surg Oncol* 2003; **10**: 275-283

13 **Tanaka T**, Westphal S, Isfort P, Braunschweig T, Penzkofer T, Bruners P, Kichikawa K, Schmitz-Rode T, Mahnken AH. Microwave Ablation Compared with Radiofrequency Ablation for Breast Tissue in an Ex Vivo Bovine Udder Model. *Cardiovasc Intervent Radiol* 2011 Aug 11; Epub ahead of print

14 **Simo KA**, Sereika SE, Newton KN, Gerber DA. Laparoscopic-assisted microwave ablation for hepatocellular carcinoma: safety and efficacy in comparison with radiofrequency ablation. *J Surg Oncol* 2011; **104**: 822-829

15 **Yu J**, Liang P, Yu X, Liu F, Chen L, Wang Y. A comparison of microwave ablation and bipolar radiofrequency ablation both with an internally cooled probe: results in ex vivo and in vivo porcine livers. *Eur J Radiol* 2011; **79**: 124-130

16 **Dong BW**, Liang P, Yu XL, Zeng XQ, Wang PJ, Su L, Wang XD, Xin H, Li S. Sonographically guided microwave coagulation treatment of liver cancer: an experimental and clinical study. *AJR Am J Roentgenol* 1998; **171**: 449-454

17 **Dong B**, Liang P, Yu X, Su L, Yu D, Cheng Z, Zhang J. Percutaneous sonographically guided microwave coagulation therapy for hepatocellular carcinoma: results in 234 patients. *AJR Am J Roentgenol* 2003; **180**: 1547-1555

18 **Zhou P**, Liang P, Yu X, Wang Y, Dong B. Percutaneous microwave ablation of liver cancer adjacent to the gastrointestinal tract. *J Gastrointest Surg* 2009; **13**: 318-324

19 **Goldberg SN**, Charboneau JW, Dodd GD, Dupuy DE, Gervais DA, Gillams AR, Kane RA, Lee FT, Livraghi T, McGahan JP, Rhim H, Silverman SG, Solbiati L, Vogl TJ, Wood BJ. Image-guided tumor ablation: proposal for standardization of terms and reporting criteria. *Radiology* 2003; **228**: 335-345

20 **Shibata T**, Shibata T, Maetani Y, Kubo T, Nishida N, Itoh K. Transcatheter arterial embolization for tumor seeding in the chest wall after radiofrequency ablation for hepatocellular carcinoma. *Cardiovasc Intervent Radiol* 2006; **29**: 479-481

21 **Wu CC**, Chen WS, Ho MC, Huang KW, Chen CN, Yen JY, Lee PH. Minimizing abdominal wall damage during high-intensity focused ultrasound ablation by inducing artificial ascites. *J Acoust Soc Am* 2008; **124**: 674-679

22 **Robertson JD**, de la Torre JI, Gardner PM, Grant JH, Fix RJ, Vásconez LO. Abdominoplasty repair for abdominal wall hernias. *Ann Plast Surg* 2003; **51**: 10-16

23 **Chang S**, Kim SH, Lim HK, Kim SH, Lee WJ, Choi D, Kim YS, Rhim H. Needle tract implantation after percutaneous interventional procedures in hepatocellular carcinomas: lessons learned from a 10-year experience. *Korean J Radiol* 2008; **9**: 268-274

24 **Liu FY**, Yu XL, Liang P, Wang Y, Zhou P, Yu J. Comparison of percutaneous 915 MHz microwave ablation and 2450 MHz microwave ablation in large hepatocellular carcinoma. *Int J Hyperthermia* 2010; **26**: 448-455

25 **Yu J**, Liang P, Yu X, Wang Y, Gao Y. Ultrasound-guided percutaneous microwave ablation of splenic metastasis: report of four cases and literature review. *Int J Hyperthermia* 2011; **27**: 517-522

26 **Liang P**, Gao Y, Zhang H, Yu X, Wang Y, Duan Y, Shi W. Microwave ablation in the spleen for treatment of secondary hypersplenism: a preliminary study. *AJR Am J Roentgenol*

2011; **196**: 692-696
27 **Wang Y**, Liang P, Yu X, Cheng Z, Yu J, Dong J. Ultrasound-guided percutaneous microwave ablation of adrenal metastasis: preliminary results. *Int J Hyperthermia* 2009; **25**: 455-461
28 **Yu MA**, Liang P, Yu XL, Cheng ZG, Han ZY, Liu FY, Yu J. Sonography-guided percutaneous microwave ablation of intrahepatic primary cholangiocarcinoma. *Eur J Radiol* 2011; **80**: 548-552
29 **Liang P**, Wang Y, Zhang D, Yu X, Gao Y, Ni X. Ultrasound guided percutaneous microwave ablation for small renal cancer: initial experience. *J Urol* 2008; **180**: 844-848; discussion 848
30 **Dupuy DE**. Image-guided thermal ablation of lung malignancies. *Radiology* 2011; **260**: 633-655
31 **Espinoza S**, Briggs P, Duret JS, Lapeyre M, de Baère T. Radiofrequency ablation of needle tract seeding in hepatocellular carcinoma. *J Vasc Interv Radiol* 2005; **16**: 743-746
32 **Simon CJ**, Dupuy DE, Mayo-Smith WW. Microwave ablation: principles and applications. *Radiographics* 2005; **25** Suppl 1: S69-S83
33 **Kuang M**, Lu MD, Xie XY, Xu HX, Mo LQ, Liu GJ, Xu ZF, Zheng YL, Liang JY. Liver cancer: increased microwave delivery to ablation zone with cooled-shaft antenna--experimental and clinical studies. *Radiology* 2007; **242**: 914-924
34 **Carrafiello G**, Laganà D, Mangini M, Fontana F, Dionigi G, Boni L, Rovera F, Cuffari S, Fugazzola C. Microwave tumors ablation: principles, clinical applications and review of preliminary experiences. *Int J Surg* 2008; **6** Suppl 1: S65-S69
35 **Boutros C**, Somasundar P, Garrean S, Saied A, Espat NJ. Microwave coagulation therapy for hepatic tumors: review of the literature and critical analysis. *Surg Oncol* 2010; **19**: e22-e32

S- Editor Gou SX **L- Editor** Webster JR **E- Editor** Li JY

World Journal of Gastroenterology

Online Submissions: http://www.wjgnet.com/1007-9327office
wjg@wjgnet.com
doi:10.3748/wjg.v18.i23.3015

World J Gastroenterol 2012 June 21; 18(23): 3015-3019
ISSN 1007-9327 (print) ISSN 2219-2840 (online)

BRIEF ARTICLE

Analysis of risk factors for polypoid lesions of gallbladder among health examinees

Hua-Li Yang, Lei Kong, Li-Li Hou, Hui-Fang Shen, Yu Wang, Xin-Gang Gu, Jian-Min Qin, Pei-Hao Yin, Qi Li

Hua-Li Yang, Hui-Fang Shen, Yu Wang, Xin-Gang Gu, Department of Ultrasonography, Putuo Hospital, Shanghai University of Traditional Chinese Medicine, Shanghai 200062, China
Lei Kong, Li-Li Hou, Jian-Min Qin, Pei-Hao Yin, Department of General Surgery, Putuo Hospital, Shanghai University of Traditional Chinese Medicine, Shanghai 200062, China
Qi Li, Department of Oncology, Putuo Hospital, Shanghai University of Traditional Chinese Medicine, Shanghai 200062, China
Author contributions: Yang HL and Kong L contributed equally to this work; Yang HL, Kong L, Gu XG, Yin PH and Li Q designed and supervised the study; Kong L, Hou LL, Shen HF, Wang Y, Gu XG and Qin JM performed the experiments; Yang HL, Kong L and Yin PH wrote the manuscript; and all authors read and approved the final version to be published.
Correspondence to: Dr. Pei-Hao Yin, MD, Department of General Surgery, Putuo Hospital, Shanghai University of Traditional Chinese Medicine, No. 164, Lanxi Road, Shanghai 200062, China. yinpeihao1975@hotmail.com
Telephone: +86-21-62572723 Fax: +86-21-52665957
Received: January 28, 2012 Revised: March 20, 2012
Accepted: April 9, 2012
Published online: June 21, 2012

Abstract

AIM: To investigate the prevalence and risk factors of polypoid lesions of gallbladder (PLG) among the health examinees in the Shanghai region, China.

METHODS: A total of 11 816 subjects who underwent health examinations in our hospital between August 2010 and February 2011 were analyzed retrospectively. Among them, there were 7174 men and 4642 women. PLG was diagnosed by the real-time ultrasonography. Those with the body mass index (BMI) $\geqslant$ 28 were considered to be obese. Blood biochemical indices were detected with the fully automatic biochemical analyzer and hepatitis B surface antigen (HBsAg) was tested by the automated enzyme immunoassay. The correlations between the prevalence of PLG and age, sex, BMI, serum cholesterol (T-Cho), triglycerides (TG), blood sugar, HBsAg, high-density lipoprotein (HDL-C), low-density lipoprotein (LDL-C), gallstone and fatty liver were investigated. After univariate analysis of 11 variables, stepwise logistic regression analysis was performed to explore the risk factors of PLG.

RESULTS: There was a significant difference in sex, T-Cho, HBsAg, HDL-C, LDL-C and fatty liver between the PLG-positive group and the PLG-negative group (332/163 *vs* 6842/4479, P = 0.003; 22/473 *vs* 295/11 026, P =0.013; 92/403 *vs* 993/10 328, P = 0.001; 47/448 *vs* 332/10 989, P = 0.001; 32/463 *vs* 381/10 940, P = 0.001; 83/412 *vs* 3260/8061, P = 0.001). No significant difference was found in the age, BMI, TG, blood sugar and gallstone between the two groups (47.3 ± 26 *vs* 45.1 ± 33, P = 0.173; 59/436 *vs* 1097/10 224, P = 0.102; 52/443 *vs* 982/10 339, P = 0.158; 17/478 *vs* 295/11 026, P = 0.26; 24/471 *vs* 395/10 926, P = 0.109). Logistic regression analysis showed that the sex, HBsAg and HDL-C were independent risk factors for the development of PLG in a descending order of HDL-C > HBsAg > sex.

CONCLUSION: In healthy people, the male gender, positive HBsAg, and low HDL-C confer higher risks of PLG development.

Key words: Polypoid; Gallbladder; Risk factors; Ultrasonography; Health examination

Peer reviewers: Jai Dev Wig, MS, FRCS, Former Professor and Head, Department of General Surgery, Postgraduate Institute of Medical Education and Research, Chandigarh 160012, India; Dr. Bernardo Frider, MD, Professor, Department of Hepatology, Hospital General de Agudos Cosme Argerich, Alte Brown 240, Buenos Aires 1155, Argentina

Yang HL, Kong L, Hou LL, Shen HF, Wang Y, Gu XG, Qin JM, Yin PH, Li Q. Analysis of risk factors for polypoid lesions of gallbladder among health examinees. *World J Gastroenterol*

2012; 18(23): 3015-3019 Available from: URL: http://www.wjgnet.com/1007-9327/full/v18/i23/3015.htm DOI: http://dx.doi.org/10.3748/wjg.v18.i23.3015

INTRODUCTION

The prevalence of polypoid lesions of gallbladder (PLG), a common clinical gallbladder disease, is about 3%, with an increasing trend[1,2]. PLG is the general term of the limited abnormal accumulations of mucous membrane tissue of the gallbladder or the limited lesion projecting into the lumen of the gallbladder. Clinically, the types of polypoid growth of the gallbladder mainly includes cholesterol polypoid/cholesterosis, inflammatory polyp, cholesterosis with fibrous dysplasia of gallbladder, adenomyomatosis, hyperplastic cholecystosis and adenocarcinoma. Ultrasonography (US) is a convenient and non-traumatic modality used to profile the gallbladder and the position of the lesion. The application of US has improved significantly the detection rate of PLG. It is of great clinical significance to analyze the risk factors of PLG in an attempt to improve its prevention and diagnosis. This study retrospectively analyzed the prevalence and risk factors of PLG among 11 816 health examinees in our clinical center. Through the univariate and multivariate analyses, this study aimed to provide the first-hand evidences for the primary prevention of PLG.

MATERIALS AND METHODS

Ethics

This work was carried out in accordance with the Declaration of Helsinki (2000) of the World Medical Association. The study protocol was approved ethically by Putuo Hospital. All patients provided informed written consent.

Subjects

A total of 11 816 subjects, including 7174 men and 4642 women with an average age of 48.6 ± 31 years (range, 15-86 years) who underwent health examinations in our health center between August 2010 and February 2011, were included in this study.

Diagnosis of polypoid lesions of gallbladder

The subjects were examined with ultrasonography using a real-time scanner with a 3.5 MHz array transducer (Philips En Visor and Philips-iU22) in the early morning after fasting for about 8-12 h. They were required to stay supine or change the position when it is necessary. The gallbladder was observed through multiple cross sections to detect the size, shape, number, location, internal echo, basal part, local cyst wall and the movement of lesions with the position change.

The diagnosis of gallbladder polyps was established according to the following criteria: (1) Spherical, mulberry-like or papillary projections, derived from either pedunculated or narrow bases, and no change after position change; (2) Multiple echogenic spots which could be found in any part of the gallbladder, e.g., the gallbladder neck, body or bottom, especially in the body and bottom of the gallbladder; (3) Small echogenic spots, usually less than 10 mm; and (4) Hyperechoic (more visible) or medium echoic structures without acoustic shadow.

Measurement of body weight

We measured the body mass index (BMI) of the subjects following "The Prevention and Control Guideline for Overweight and Obesity among Chinese Adults"[3], and BMI was calculated by dividing the mean weight by the mean height squared (kg/m^2). BMI $\geqslant$ 28 was defined as obesity.

Determination of blood biochemical indices and hepatitis B surface antigen

Blood serum samples of 5 mL were routinely collected intravenously in the morning before breakfast. Cholesterol (T-Cho), triglyceride (TG), high-density lipoprotein (HDL-C), low-density lipoprotein (LDL-C) and blood glucose levels were detected and analyzed using a Hitachi 7020 Automatic Biochemical Analyzer. Hepatitis B surface antigen (HBsAg) was detected with an Italy RB 138 Automated Enzyme Immunoassay Analyzer. The reagents used were offered by the Shanghai Kehua Bioengineering Co., Ltd, Shanghai, China. The tests were undertaken strictly according to the instructions of the manufacturers.

Statistical analysis

Results were expressed as mean ± SD. We analyzed 11 variables with univariate analysis to compare the differences between the two groups. Variables (age, sex, BMI, T-Cho, TG, HDL-C, LDL-C, glucose, HBsAg, gallstones and fatty liver) were defined as independent variables and the PLG was defined as a dependent variable. They were examined in a multivariate model using forward stepwise maximum likelihood logistic regression to identify the risk factors of PLG ($\alpha = 0.05$). The variable assignment is shown in Table 1. Data were analyzed using the SPSS version 13.0 statistical software and significance was set at $P < 0.05$.

RESULTS

General data of patients with PLG

The overall prevalence of PLG found among the health examinees was 4.2% (495/11 816). The incidence of PLG was 4.6% (332/7174) in men and 3.5% (163/4642) in women. Overall, males had a significantly higher prevalence of PLG than females (4.6% *vs* 3.5%, $P = 0.003$). In this group, the incidence of obesity was 9.8% (1156/11 816); the rates of increased T-Cho, TG and LDL-C were 2.7% (317/11 816), 8.8% (1034/11 816) and 3.5% (413/11 816), respectively; the rate of high blood sugar was 2.6% (312/11 816), and the incidence of low

Table 1 Instructions of assignment of variables for polypoid lesions of gallbladder

	Female = 0	Male = 1
BMI	(< 28) = 0	(≥ 28) = 1
T-Cho	Normal or decreased = 0	Increased = 1
TG	Normal or decreased = 0	Increased = 1
HDL-C	Normal or increased = 0	Decreased = 1
LDL-C	Normal or decreased = 0	Increased = 1
Blood glucose	Normal or decreased = 0	Increased = 1
HBsAg	(-) = 0	(+) = 1
Gallstones	(-) = 0	(+) = 1
Fatty liver	(-) = 0	(+) = 1

BMI: Body mass index; T-Cho: Cholesterol; TG: Triglyceride; HDL-C: High density lipoprotein; LDL-C; Low density lipoprotein; HBsAg: Hepatitis B surface antigen.

Table 2 Results of univariate analysis of the relevant factors of polypoid lesions of gallbladder

	PLG positive	PLG negative
Age (yr)	47.3 ± 26	45.1 ± 33
Sex, male/female	332/163[a]	6842/4479
BMI, ≥ 28/< 28	59/436	1097/10 224
T-Cho, increased/normal or decreased	22/473[a]	295/11 026
TG, increased/normal or decreased	52/443	982/10 339
Glucose, increased/normal or decreased	17/478	295/11 026
HBsAg, +/-	92/403[a]	993/10 328
HDL-C, decreased/normal or increase	47/448[a]	332/10 989
LDL-C, increased/normal or decreased	32/463[a]	381/10 940
Gallstones, +/-	24/471	395/10 926
Fatty liver, +/-	83/412[a]	3260/8061

[a]$P < 0.05$ *vs* negative PLG. PLG: Polypoid lesions of gallbladder; BMI: Body mass index; T-Cho: Cholesterol; TG: Triglyceride; HBsAg: Hepatitis B surface antigen; HDL-C: High density lipoprotein; LDL-C; Low density lipoprotein.

HDL-C was 3.2% (379/11 816); and the incidence of gallstone, the fatty liver and HBsAg (+) was 3.5% (419/11 816), 28.3% (3343/11 816) and 9.2% (1085/11 816), respectively. There were significant differences in sex, T-Cho, HBsAg, HDL-C, LDL-C and fatty liver between the PLG-positive group and the PLG-negative group (332/163 *vs* 6842/4479, $P = 0.003$; 22/473 *vs* 295/11 026, $P = 0.013$; 92/403 *vs* 993/10 328, $P = 0.001$; 47/448 *vs* 332/10 989, $P = 0.001$; 32/463 *vs* 381/10 940, $P = 0.001$; 83/412 *vs* 3260/8061, $P = 0.001$). No significant difference was found in the age, BMI, TG, blood sugar and gallstone, between the two groups (47.3 ± 26 *vs* 45.1 ± 33, $P = 0.173$; 59/436 *vs* 1097/10 224, $P = 0.102$; 52/443 *vs* 982/10 339, $P = 0.158$; 17/478 *vs* 295/11 026, $P = 0.26$; 24/471 *vs* 395/10 926, $P = 0.109$) (Table 2).

Logistic regression analysis of relevant risk factors for PLG

Logistic regression analysis showed that sex, HBsAg and HDL-C were independent risk factors for PLG, in a descending order of HDL-C > HBsAg > sex. The subjects with lower HDL-C had a 3.346 times higher risk of PLG than those who had normal or higher HDL-C. The risk of PLG was 2.563 times higher in HBsAg-positive subjects than in HBsAg-negative ones. Men had a 1.843 times higher risk of PLG than women (Table 3).

Table 3 Logistic regression analysis of multiple relevant factors of polypoid lesions of gallbladder

Variables	OR	95% CI	*P* value
Sex	1.843	1.245-2.789	0.0035
HBsAg	2.563	1.875-3.418	< 0.001
HDL-C	3.346	2.932-4.133	< 0.001

OR: Odds ratio; HBsAg: Hepatitis B surface antigen; HDL-C: High density lipoprotein.

DISCUSSION

PLG, which is often neglected due to lack of significant clinical signs or symptoms, is a common disease found in the ultrasound examinations. In recent years, with changes of diet, acceleration of the pace of life, increasing health awareness and the popularity of ultrasonography, the detection rate of PLG tends to increase, and nearly 85% of PLG are detected in a routine physical examination. It is reported that the prevalence of PLG in the Western society is 1.0%-6.9%[4-6], which is significantly lower than in the Asians. Park *et al*[7] reported that PLG prevalence in the South Korea was about 6.1%. Lin *et al*[8] reported a prevalence of 9.5% in Taiwan. After the logistic regression analysis of 34 669 cases, Lin *et al*[8] showed that the male gender was an independent risk factor of PLG. The domestic studies showed a prevalence of 3% in healthy adults in our country[1,2]. The Logistic regression analysis in this study showed that the gender was an independent risk factor for PLG and males bear a significantly higher risk of PLG than females. The risk of PLG in men was 1.843 times higher than in women.

In China, hepatitis B virus carriers account for 7.2% of the population. HBsAg infection may lead to acute or chronic hepatitis. In acute hepatitis, gallbladder wall thickening, volume change and abnormal bile composition can occur and the normal systolic and diastolic functions may be disrupted[9]. Cholesterol polyp is the most common type among PLGs. Compared with non-hepatitis B patients, chronic hepatitis B patients are prone to PLG and the possible causes include: (1) Liver cell cholesterol metabolic disorders may lead to the alteration of the bile composition and quantity, and increased cholesterol in the bile of the gallbladder may easily crystallize and precipitate on the gallbladder wall, resulting in abnormal deposition; (2) Hepatitis B virus activates the immune system to produce autoimmune inflammation, leading to an increased activity of the gallbladder macrophages for cholesterol phagocytosis; (3) Gastrointestinal hormone secretion and metabolic disorder may cause tension adjustment disorder of the sphincter of Oddi, causing increased bile viscosity and poor drainage; and (4) Damages of the liver Kupffer cells may compromise the

detoxification of microbial toxins and phagocytic functions. Together with the small bile ducts and capillary damage, microorganisms and toxins can invade the gallbladder[10]. Our data showed that compared with PLG-negative group, PLG-positive group had a significantly higher incidence of hepatitis B virus infection. The logistic regression analysis showed that positive HBsAg was a risk factor for PLG. Lin *et al*[8] also reported that positive HBsAg was an independent risk factor for PLG. But there are some contrary reports[11]. The inconsistent findings may be related to the number of cases, sex ratio, ethnic differences and other factors. The role of hepatitis B virus in PLG still deserves further studies.

PLG formation mechanisms are very complicated, involving many interacting factors. The mechanisms for cholesterol polyps, the main type of PLG, have been most frequently reported. It has been reported that cholesterol polyps are related to the metabolism of cholesterol in bile. Khairy *et al*[12] found that in 74 patients with cholesterol polyps, 63 (85.1%) patients had elevated plasma cholesterol levels. However, other studies showed that higher plasma T-Cho and TG levels and the incidence of PLG were not necessarily correlated with PLG[13,14]. Ivanchenkova *et al*[15] and Zák *et al*[16] found that plasma HDL-C levels in patients with cholesterol polyps were significantly lower than in the control group, while LDL-C levels were significantly increased. Our data showed that compared with PLG-negative group, T-Cho and LDL-C levels were significantly higher in PLG-positive group while HDL-C levels were significantly lower. The TG level showed no significant difference between the two groups. Consistent with the report by Cantürk *et al*[17], our study showed that low HDL-C level was a risk factor for PLG. Currently, whether the cholesterol deposited in the gallbladder is from the plasma and the relevance between plasma TG level and PLG still remain unclear. Most studies have focused on the mechanisms of absorption and excretion of cholesterol by the mucosa of the gallbladder[18].

Although PLG is an independent disease, it is closely related to the occurrence of the gallbladder stone, which is commonly seen in PLG patients. Studies showed that PLG was often accompanied with stones, and Ito *et al*[19] reported that the rate of PLG with stones was 12%. Colecchia *et al*[20] believed that metabolic disorders of cholesterol existed in both PLG and gallbladder stones, which shared the common pathogenesis. However, these two diseases were not necessarily correlated. Our study showed that the incidence of the gallbladder stone was not significantly different between PLG-positive and PLG-negative groups.

In recent years, the prevalence of diabetes, fatty liver and obesity has been increasing year by year, affecting more and more people at younger ages. These three morbidities all belong to metabolic disorders and their roles in PLG are not consistent among previous reports[11,21,22]. Our study demonstrated that the incidences of fatty liver were not statistically different between PLG-positive and PLG-negative groups, nor the plasma glucose and obesity. The logistic regression analysis showed that diabetes, fatty liver and obesity were not risk factors of PLG.

The exact mechanisms underlying PLG pathogenesis are still not clear. This retrospective analysis has demonstrated that low HDL-C level, male gender and positive HBsAg are the risk factors for PLG, and these findings will provide the related evidence and guidance for health education, and prevention and treatment of PLG.

COMMENTS

Background

Polypoid lesions of gallbladder (PLG) are tumor or tumor-like projections, referring to any mucosal projection into the lumen of the gallbladder which is usually non-neoplastic (> 95%), but may infrequently be neoplastic (< 5%) in nature. The diagnosis of gallbladder polyps is relatively easy by ultrasonography. Although numerous studies have focused on gallbladder polyps, little has been known about factors associated with the occurrence of PLG. The authors aimed to investigate the prevalence and possible risk factors of PLG in a health screening population of Shanghai region.

Research frontiers

The incidence of PLG has an increasing tendency in recent years. The reports and analysis on the risk factors of PLG were not consistent. The literatures mostly focus on gender, lipid metabolism disorders, gallstones, hepatitis B, glucose metabolism disorders, gallbladder local inflammation and so on. Inconsistencies may be related to race, lifestyle, culture, geographic characteristics worldwide, as well as experimental design and other factors.

Innovations and breakthroughs

In China, especially in the Shanghai region, there have been few larger sample analyses on the risk factors of PLG. In this study, the authors reported that the male gender, positive hepatitis B surface antigen, and low high-density lipoprotein are high-risk factors for developing PLG in healthy people.

Applications

The study is conducive to the prevention and treatment of PLG. The relationship between gender, hepatitis B and high-density lipoprotein and PLG is worthy of further studies.

Peer review

It is an interesting topic. The authors analyzed the risk factors for polypoid lesions of gallbladder in a population of health examinees in the Shanghai region.

REFERENCES

1 **Zhou XF**. Analysis of the Incidence of polypoid lesion of gallbladder in 1124 healthy persons by hemodialysis ultrasonography. *Shenyang Yixveyuan Xvebao* 2008; **10**: 90-91

2 **Wu WQ**, Zheng DS, Ye JP, Huang FZ, Qiu SD, Chen JC. Analysis of polypoid lesion of gallbladder among people in Guangzhou in 2006. *Huanan Yufang Yixve* 2008; **34**: 56-57

3 **Xu JY**, Li XJ, Yao HH, Gu K, Li YY, Lu W. Study on the epidemiological characteristics of overweight and obesity among residents aged 15-69 yrs in Shanghai. *Zhongguo Manxingbing Yufang Yu Kongzhi* 2010; **18**: 467-469

4 **Kratzer W**, Haenle MM, Voegtle A, Mason RA, Akinli AS, Hirschbuehl K, Schuler A, Kaechele V. Ultrasonographically detected gallbladder polyps: a reason for concern? A seven-year follow-up study. *BMC Gastroenterol* 2008; **8**: 41

5 **Aldouri AQ**, Malik HZ, Waytt J, Khan S, Ranganathan K, Kummaraganti S, Hamilton W, Dexter S, Menon K, Lodge JP, Prasad KR, Toogood GJ. The risk of gallbladder cancer from polyps in a large multiethnic series. *Eur J Surg Oncol* 2009; **35**: 48-51

6 **Spaziani E**, Petrozza V, Di Filippo A, Picchio M, Ceci F, Miraglia A, Moretti V, Briganti M, Greco E, Pattaro G, De Angelis F, Salvadori C, Stagnitti F. [Gallbladder polypoid

lesions. Three clinical cases with difficult diagnosis and literature review]. *G Chir* 2010; **31**: 439-442
7 **Park JK**, Yoon YB, Kim YT, Ryu JK, Yoon WJ, Lee SH, Yu SJ, Kang HY, Lee JY, Park MJ. Management strategies for gallbladder polyps: is it possible to predict malignant gallbladder polyps? *Gut Liver* 2008; **2**: 88-94
8 **Lin WR**, Lin DY, Tai DI, Hsieh SY, Lin CY, Sheen IS, Chiu CT. Prevalence of and risk factors for gallbladder polyps detected by ultrasonography among healthy Chinese: analysis of 34 669 cases. *J Gastroenterol Hepatol* 2008; **23**: 965-969
9 **Mamos A**, Wichan P, Chojnacki J, Grzegorczyk K. [Gallbladder motor activity in patients with virus hepatitis B]. *Pol Merkur Lekarski* 2003; **15**: 507-510
10 **Zhou HB**, Wang H, Li YQ, Li SX, Wang H, Zhou DX, Tu QQ, Wang Q, Zou SS, Wu MC, Hu HP. Hepatitis B virus infection: a favorable prognostic factor for intrahepatic cholangiocarcinoma after resection. *World J Gastroenterol* 2011; **17**: 1292-1303
11 **Lim SH**, Kim DH, Park MJ, Kim YS, Kim CH, Yim JY, Cho KR, Kim SS, Choi SH, Kim N, Cho SH, Oh BH. Is Metabolic Syndrome One of the Risk Factors for Gallbladder Polyps Found by Ultrasonography during Health Screening? *Gut Liver* 2007; **1**: 138-144
12 **Khairy GA**, Guraya SY, Murshid KR. Cholesterolosis. Incidence, correlation with serum cholesterol level and the role of laparoscopic cholecystectomy. *Saudi Med J* 2004; **25**: 1226-1228
13 **Myers RP**, Shaffer EA, Beck PL. Gallbladder polyps: epidemiology, natural history and management. *Can J Gastroenterol* 2002; **16**: 187-194
14 **Sandri L**, Colecchia A, Larocca A, Vestito A, Capodicasa S, Azzaroli F, Mazzella G, Mwangemi C, Roda E, Festi D. Gallbladder cholesterol polyps and cholesterolosis. *Minerva Gastroenterol Dietol* 2003; **49**: 217-224
15 **Ivanchenkova RA**, Sviridov AV, Ozerova IN, Perova NV, Grachev SV. [High-density lipoproteins in cholesterosis of the gall bladder]. *Klin Med* (Mosk) 2000; **78**: 27-31
16 **Zák A**, Zeman M, Hrubant K, Vecka M, Tvrzická E. [Effect of hypolipidemic treatment on the composition of bile and the risk or cholesterol gallstone disease]. *Cas Lek Cesk* 2007; **146**: 24-34
17 **Cantürk Z**, Sentürk O, Cantürk NZ, Anik YA. Prevalence and risk factors for gall bladder polyps. *East Afr Med J* 2007; **84**: 336-341
18 **Strömsten A**, von Bahr S, Bringman S, Saeki M, Sahlin S, Björkhem I, Einarsson C. Studies on the mechanism of accumulation of cholesterol in the gallbladder mucosa. Evidence that sterol 27-hydroxylase is not a pathogenetic factor. *J Hepatol* 2004; **40**: 8-13
19 **Ito H**, Hann LE, D'Angelica M, Allen P, Fong Y, Dematteo RP, Klimstra DS, Blumgart LH, Jarnagin WR. Polypoid lesions of the gallbladder: diagnosis and followup. *J Am Coll Surg* 2009; **208**: 570-575
20 **Colecchia A**, Larocca A, Scaioli E, Bacchi-Reggiani ML, Di Biase AR, Azzaroli F, Gualandi R, Simoni P, Vestito A, Festi D. Natural history of small gallbladder polyps is benign: evidence from a clinical and pathogenetic study. *Am J Gastroenterol* 2009; **104**: 624-629
21 **Kratzer W**, Schmid A, Akinli AS, Thiel R, Mason RA, Schuler A, Haenle MM. [Gallbladder polyps: prevalence and risk factors]. *Ultraschall Med* 2011; **32** Suppl 1: S68-S73
22 **Lazebnik LB**, Ovsiannikova ON, Zvenigorodskaia LA, Mel'nikova NV, Samsonova NG, Khomeriki SG. [Cholesterosis of the gall bladder and atherogenic dyslipidemia: etiology, pathogenesis, clinical symptoms, diagnosis and treatment]. *Ter Arkh* 2008; **80**: 57-61

S- Editor Lv S **L- Editor** Ma JY **E- Editor** Li JY

World Journal of Gastroenterology

Online Submissions: http://www.wjgnet.com/1007-9327office
wjg@wjgnet.com
doi:10.3748/wjg.v18.i23.3020

World J Gastroenterol 2012 June 21; 18(23): 3020-3026
ISSN 1007-9327 (print) ISSN 2219-2840 (online)

BRIEF ARTICLE

WWOX induces apoptosis and inhibits proliferation of human hepatoma cell line SMMC-7721

Ben-Shun Hu, Jing-Wang Tan, Guo-Hua Zhu, Dan-Feng Wang, Xian Zhou, Zhi-Qiang Sun

Ben-Shun Hu, Guo-Hua Zhu, Dan-Feng Wang, Xian Zhou, Zhi-Qiang Sun, Department of General Surgery, Jiang Yuan Hospital affiliated to Jiangsu Institute of Nuclear Medicine, Wuxi 214063, Jiangsu Province, China
Jing-Wang Tan, Department of Hepatobiliopancreatic Surgery, Northern Jiangsu People's Hospital, Yangzhou 225001, Jiangsu Province, China
Author contributions: Hu BS and Tan JW designed the study; Hu BS, Zhu GH, Wang DF, Zhou X and Sun ZQ conducted the majority of the experiments and performed the data analysis; Hu BS wrote the manuscript; and all authors have read and approved the final manuscript.
Correspondence to: Ben-Shun Hu, MD, Department of General Surgery, Jiang Yuan Hospital affiliated to Jiangsu Institute of Nuclear Medicine, No. 20, Qianrong Road, Wuxi 214063, Jiangsu Province, China. hubenshun2008@yahoo.com.cn
Telephone: +86-510-85514482 Fax: +86-510-85514482
Received: July 11, 2011 Revised: September 28, 2011
Accepted: January 7, 2012
Published online: June 21, 2012

Abstract

AIM: To investigate the effects of the *WWOX* gene on the human hepatic carcinoma cell line SMMC-7721.

METHODS: Full-length *WWOX* cDNA was amplified from normal human liver tissues. Full-length cDNA was subcloned into pEGFP-N1, a eukaryotic expression vector. After introduction of the *WWOX* gene into cancer cells using liposomes, the WWOX protein level in the cells was detected through Western blotting. Cell growth rates were assessed by methyl thiazolyl tetrazolium (MTT) and colony formation assays. Cell cycle progression and cell apoptosis were measured by flow cytometry. The phosphorylated protein kinase B (AKT) and activated fragments of caspase-9 and caspase-3 were examined by Western blotting analysis.

RESULTS: WWOX significantly inhibited cell proliferation, as evaluated by the MTT and colony formation assays. Cells transfected with WWOX showed significantly higher apoptosis ratios when compared with cells transfected with a mock plasmid, and overexpression of WWOX delayed cell cycle progression from G1 to S phase, as measured by flow cytometry. An increase in apoptosis was also indicated by a remarkable activation of caspase-9 and caspase-3 and a dephosphorylation of AKT (Thr308 and Ser473) measured with Western blotting analysis.

CONCLUSION: Overexpression of *WWOX* induces apoptosis and inhibits proliferation of the human hepatic carcinoma cell line SMMC-7721.

Key words: WWOX; SMMC-7721; Apoptosis; Proliferation; Hepatic carcinoma

Peer reviewer: Bronislaw L Slomiany, PhD, Professor, Research Center, C-875, University of Medicine and Dentistry, New Jersey-New Jersey Dental School, 110 Bergen Street, PO Box 1709, Newark, NJ 07103-2400, United States

Hu BS, Tan JW, Zhu GH, Wang DF, Zhou X, Sun ZQ. *WWOX* induces apoptosis and inhibits proliferation of human hepatoma cell line SMMC-7721. *World J Gastroenterol* 2012; 18(23): 3020-3026 Available from: URL: http://www.wjgnet.com/1007-9327/full/v18/i23/3020.htm DOI: http://dx.doi.org/10.3748/wjg.v18.i23.3020

INTRODUCTION

The tumor suppressor gene *WWOX* is localized in a common fragile site FRA16D (locus 16q23.3-24.1). Protein encoded by *WWOX* is an oxidoreductase containing two WW protein interaction domains. The biological role of the protein is not yet defined, although there are hypotheses that it may play a part in steroid hormones me-

tabolism and ErbB4 receptor signaling pathway[1,2]. Low expression level of the *WWOX* gene has been observed in many types of cancers[3-15], possibly due to the loss of heterozygosity or epigenetic changes, such as methylation of CpG islands in promoter region. Several researches have revealed loss of heterozygosity of *WWOX* locus in gastric[7], pancreatic[6], esophageal[3] and lung[4] cancers. The role of WWOX in hepatic carcinoma is not well understood, and few studies have reported the effects of WWOX on hepatic carcinoma. In this study, we investigated the apoptotic effects of the *WWOX* gene on the human hepatic carcinoma cell line SMMC-7721.

MATERIALS AND METHODS

Materials

The eukaryotic expression vector pEGFP-N1 and *Escherichia coli* DH5α competent cells are routinely maintained by the central laboratory at our hospital. The hepatoma cell line SMMC-7721 was obtained from the Chinese Academy of Sciences (Shanghai, China). Dulbecco's modification of Eagle's medium Dulbecco (DMEM) culture medium was purchased from Gibco BRL (Gaithersburg, United States). Fetal bovine serum was obtained from Sijiqing Biological Engineering Material (Hangzhou, China). The following materials were used: RNeasy Protect Mini-kit (QIAGen Co., Germany), SMARTTM PCR cDNA synthesis kit (Clontech Co., United States), DNA gel extraction kit (Dalian TaKaRa Co., China), plasmid mini-preparation kit (Shanghai Huasun Biotechnology Co., China), KOD-Plus DNA polymerase (TOYOBO Co., United States), T4 DNA ligase and the HindⅢ and Kpn I restriction enzymes (New England Biolabs, United States), Lipofectamine 2000 (Invitrogen, United States), anti-WWOX, anti-phospho-AKT(pThr308 and Ser473), cleaved caspasse-9 and caspase-3 monoclonal antibodies (Santa Cruz Co., United States), and horseradish peroxidase-conjugated goat anti-rabbit/mouse IgG (Zhongshan Co., China). Nucleic acid sequencing was performed by Shanghai Yingjun Bioengineering Co., China. The *WWOX* and glyceraldehyde-3-phosphate dehydrogenase (GAPDH) primers were synthesized by Shanghai Yingjun Bioengineering Co., China.

Cell lines and culture conditions

SMMC-7721 cells were cultured in DMEM medium (HyClone Inc, United States) supplemented with 10% new calf bovine serum in a 37 ℃ and 5% CO_2 incubator.

Construction of pEGFP-N1-WWOX vector and establishment of cell line SMMC-7721 that stably expresses WWOX

The *WWOX* open reading frame was amplified from a cDNA clone using the forward primer 5'GGAAGCTTTTGGAGCGGGAGTGAG-3' and the reverse primer 5' GGATCCCAGCAGTTGTTGAAGTACA-3', which introduced *Kpn* I and *Hin*DⅢ restriction endonuclease sites. *WWOX* cDNA digested with *Kpn* I and *Hin*dⅢ was cloned into a pEGFP-N1 eukaryotic expression vector. The resulting vector was transfected into SMMC-7721 cells using Lipofectamine 2000 (Invitrogen, Carlsbad, CA). An empty vector of pEGFP-N1 was used as a negative control. After 24-48 h, the transient transfection efficiency was determined under an Olympus fluorescence microscope. The cells were then passaged at appropriate ratios to six-well plates. The next day, the cells were cultured in the presence of 1000-2000 g/mL G418 (Life Technology, Paisley, Scotland), which was increased in concentration in a stepwise manner over 14 d. Cells highly expressing green fluorescent protein (GFP) were selected.

Western blotting

Protein was extracted from cultured cells using lysis buffer. After a 30-min incubation on ice, the lysates were heated at 100 ℃ for 15 min and centrifuged at 12 000 × *g* for 15 min at 4 ℃. Lysates containing an equal amount of protein (25 μg) were dissolved in sodium dodecyl sulphate (SDS) sample buffer, separated on 12% SDS slab gels, and transferred electrophoretically onto polyvinylidene difluoride membranes. Equal protein loading and transfer were confirmed by Ponceau S staining. After being blocked with 5% non-fat dry milk in Tris-Buffered Saline and Tween 20 (10 mmol Ttris-HCl, pH 8.0, 100 mmol/L NaCl and 0.05% Tween), the membrane was incubated at 4 ℃ overnight with the appropriate primary antibodies. Following washing, horseradish peroxidase conjugated secondary antibody was applied to the membrane. Proteins bound by the secondary antibody were visualized by electrochemiluminescence (Amersham Bioscience) according to the manufacturer's instructions. The expression of GAPDH was measured as a control, and each experiment was performed in triplicate.

Cell growth assays

Cell growth was determined by the methyl thiazolyl tetrazolium (MTT) assay (Sigma, United States). Briefly, 1×10^4 cells were seeded onto 96-well plates with four replicates for each condition. Approximately 72 h later, MTT reagent was added to each well at 5 mg/mL in a 20 μL volume, and the reaction was incubated for another 4 h. The formazan crystals formed by viable cells were subsequently solubilized in dimethyl sulfoxide, and the absorbance (*A*) at 490 nm was measured.

Plate colony formation assay

Approximately 100 cells were added to each well of a six-well culture plate. After incubation at 37 ℃ for 15 d, cells were washed twice with phosphate-buffered saline (PBS) and stained with Giemsa solution. The number of colonies containing ⩾ 50 cells was counted under microscope [plate clone formation efficiency = (number of colonies/number of cells inoculated) × 100%]. Each experiment was performed in triplicate.

Cell cycle analysis

Forty-eight hours after treatment, logarithmically grow-

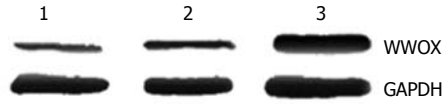

Figure 1 WWOX protein levels in SMMC-7721 cells. 1: Control group; 2: Empty vector transfection group; 3: pEGFP-*WWOX* transfection group.

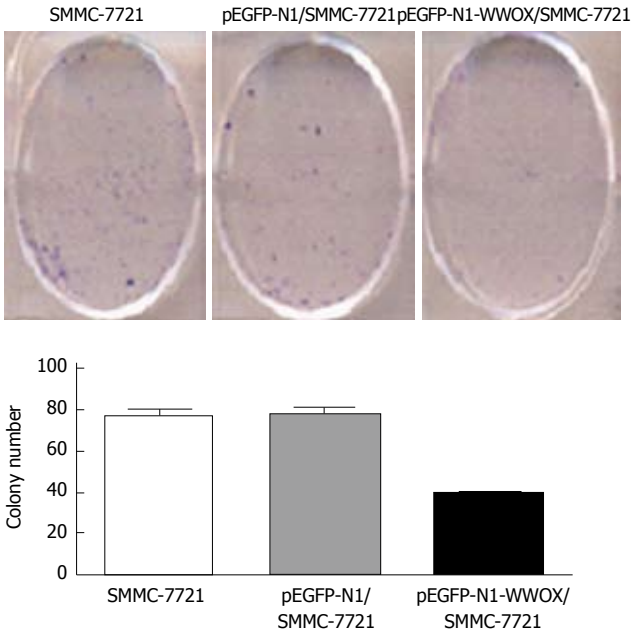

Figure 2 Growth of SMMC-7721 cells examined by plate colony formation. Overexpression of WWOX (pEGFP-N1-WWOX/SMMC-7721) resulted in a decrease in the number of formed colonies compared with the SMMC-7721 and control vector (pEGFP-N1/SMMC-7721) cells ($P < 0.05$).

ing cells were collected and washed with PBS three times and fixed with 75% ethanol at -20 ℃ for at least 1 h. After extensive washing with PBS, the cells were suspended in Hank's balanced salt solution containing 50 mg/mL RNase A (Boehringer Mannheim) and 50 mg/mL propidium iodide (PI) (Sigma-Aldrich), incubated for 1 h at room temperature, and were analyzed by FACScan (Becton Dickinson).

Apoptosis assays

Apoptosis was analyzed 48 h after treatment using the Annexin V-FITC Apoptosis Detection Kit (BD Biosciences) according to the manufacturer's instructions.

Statistical analysis

Data were presented as the mean ± SD. Comparisons of experimental values between cisplatin-treated cells and untreated controls were conducted using analysis of variance or the Kruskal-Wallis rank test. Statistical significance was defined as $P < 0.05$.

RESULTS

Overexpression of WWOX in the cell line SMMC-7721

To study the biological functions of WWOX, we introduced WWOX into SMMC-7721 cells using a pEGFP-N1 eukaryotic expression vector containing the *WWOX* gene. Seven stably transfected cell clones were obtained. Western blotting analysis with anti-GFP antibodies showed that WWOX-pGFP fusion protein in the SMMC-7721 cell clones was highly expressed compared with control cells and control-vector cells (Figure 1).

Table 1 Methyl thiazolyl tetrazolium assay

Cell line	Optical density value
SMMC-7721	1.77 ± 0.20
pEGFP-Nl/SMMC-7721	1.78 ± 0.13
pEGFP-Nl-WWOX/SMMC-7721	1.12 ± 0.23

The cell growth of parental SMMC-7721, control vector and WWOX overexpressing cells was examined by methyl thiazolyl tetrazolium assay over a 3-d period. The cell growth of the WWOX expressing cells (pEGFP-N1-WWOX/SMMC-7721) was reduced compared with the wild-type (SMMC-7721) and control vector (pEGFP-N1/SMMC-7721) cells ($P < 0.05$).

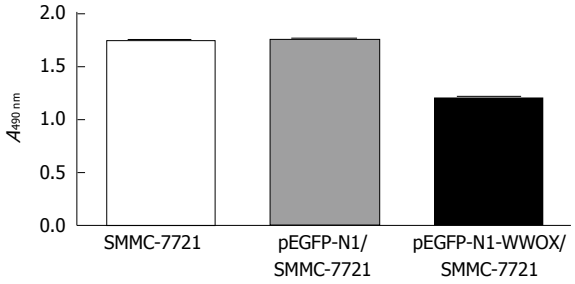

Figure 3 Overexpression of WWOX inhibits the proliferation of SMMC-7721 cells, as demonstrated by the methyl thiazolyl tetrazolium assay. There were no significant differences between the parental SMMC-7721 cell line and the control vector cell line based on the *P* values.

WWOX inhibits cell growth in vitro

To analyze the function of WWOX, we studied the rate of cell growth in the WWOX-expressing SMMC-7721 cells. The results from the colony formation assay indicated that SMMC-7721 cells overexpressing WWOX formed significantly fewer colonies than did the control clone cells and the control-vector cells ($P < 0.05$) (Figure 2). Cells transfected with *WWOX* also showed significantly decreased cell proliferation compared with control cells and control-vector cells when examined by the MTT assay (Table 1, Figure 3).

Overexpression of WWOX arrests the cell cycle in G1 and induces apoptosis of SMMC-7721 cells

To detect the effect of WWOX overexpression on the cell cycle, we measured the cell cycle distribution in WWOX-expressing SMMC-7721 cells. In these lines, there was a marked decrease in the S-phase population, while the G1 population was significantly increased compared with the control vector and wild type SMMC-7721 cells ($P < 0.05$). Neither cell lines showed significant changes in the G2 population (Figure 4, Table 2). Cells transfected with pEGFP-N1-*WWOX* demonstrated more apoptosis than did cells transfected with the mock

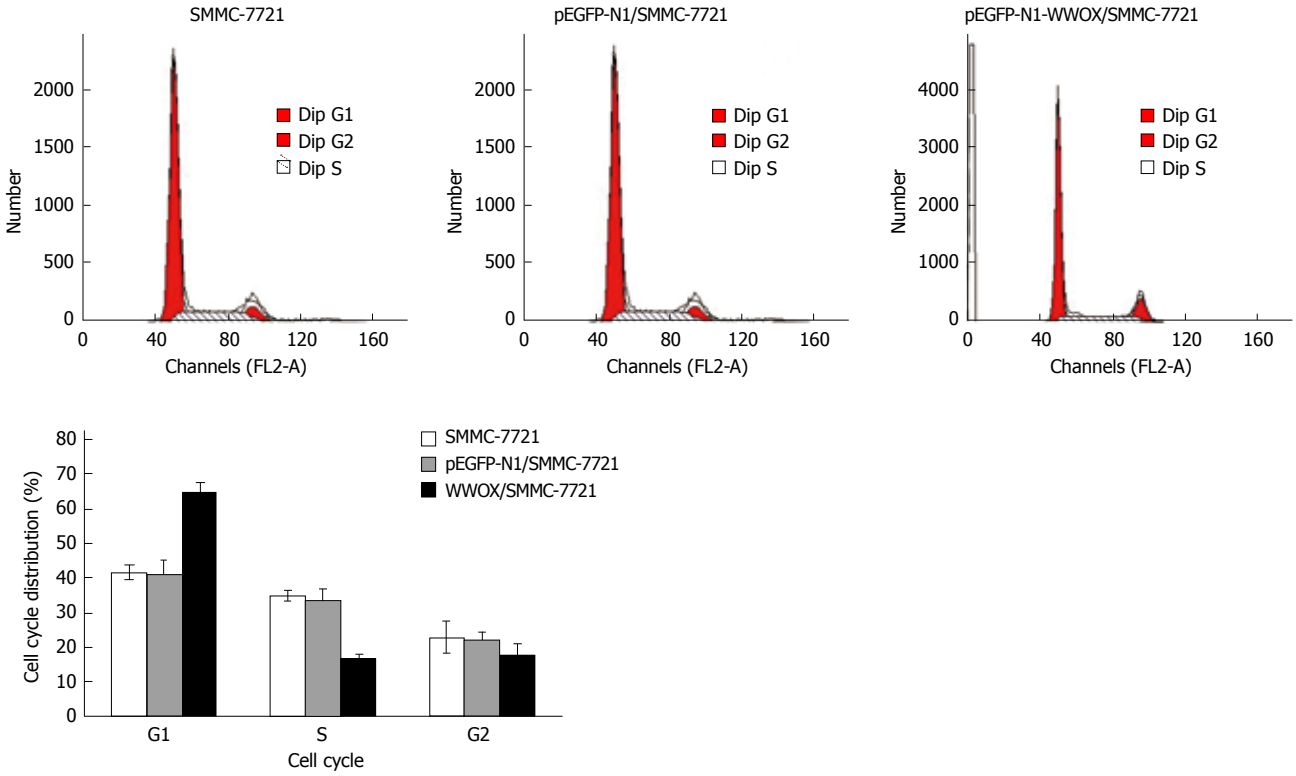

Figure 4 Cell cycle distribution of parental SMMC-7721, control vector (pEGFP-N1), and *WWOX* overexpressing (pEGFP-N1-WWOX) cells determined by fluorescently activated cell sorting caliber cytometry. The G1/S transition was inhibited in *WWOX* overexpressing cells compared with parental and control vector transformed cells ($P < 0.05$).

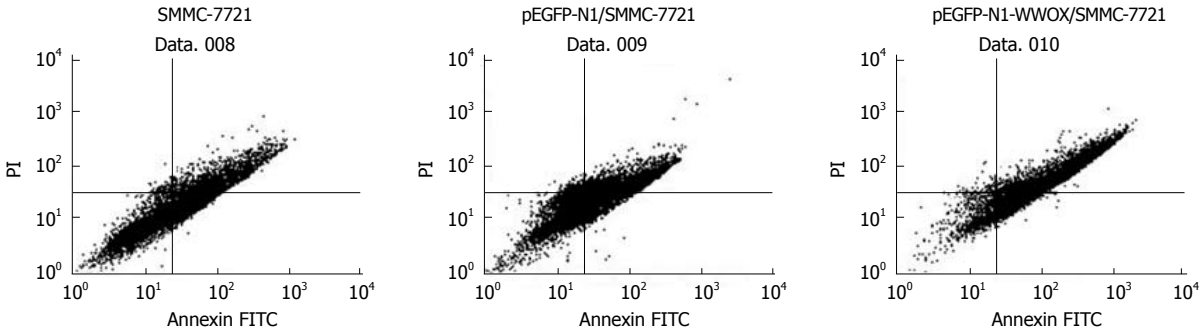

Figure 5 Cell apoptosis measured by flow cytometry using Annexin V/propidium iodide double staining. Cells transfected with pEGFP-N1-WWOX showed more apoptosis than parental cells or cells transfected with the mock plasmid ($P < 0.05$). PI: Propidium iodide; FITC: Fluorescein isothiocyanate.

Table 2 Overexpression of WWOX retards cell cycle progression from G1 to S phase

Group	Cell cycle		
	G1	S	G2
SMMC-7721	41.23 ± 2.12	34.52 ± 4.13	22.54 ± 3.12
pEGFP-Nl/SMMC-7721	40.45 ± 1.32	33.3 ± 3.11	21.24 ± 1.31
WWOX/SMMC-7721	64.23 ± 4.34	16.13 ± 2.65	17.12 ± 3.24

plasmid or the parent cells ($P < 0.05$) (Figure 5).

Caspase-9 and caspase-3 activation by WWOX

Expression of cleaved caspase-9 and caspase-3 was up-regulated, as measured by Western blotting in cells that were transfected with pEGFP-N1, compared with either the cells transfected with a control vector or parental wild-type cells (Figure 6).

Phosphorylation of Akt decreased by WWOX

To evaluate the effect of WWOX on Akt/PKB activity, the phosphorylation level at Akt Thr308 and Ser473 was examined with specific phospho-Akt antibodies. Western blot analysis showed that WWOX significantly reduced the level of Akt/PKB phosphorylation (Figure 7).

DISCUSSION

Hepatic carcinoma is a highly invasive and clinically challenging tumor, and its molecular basis remains poorly understood. We used a gain-of-function approach by

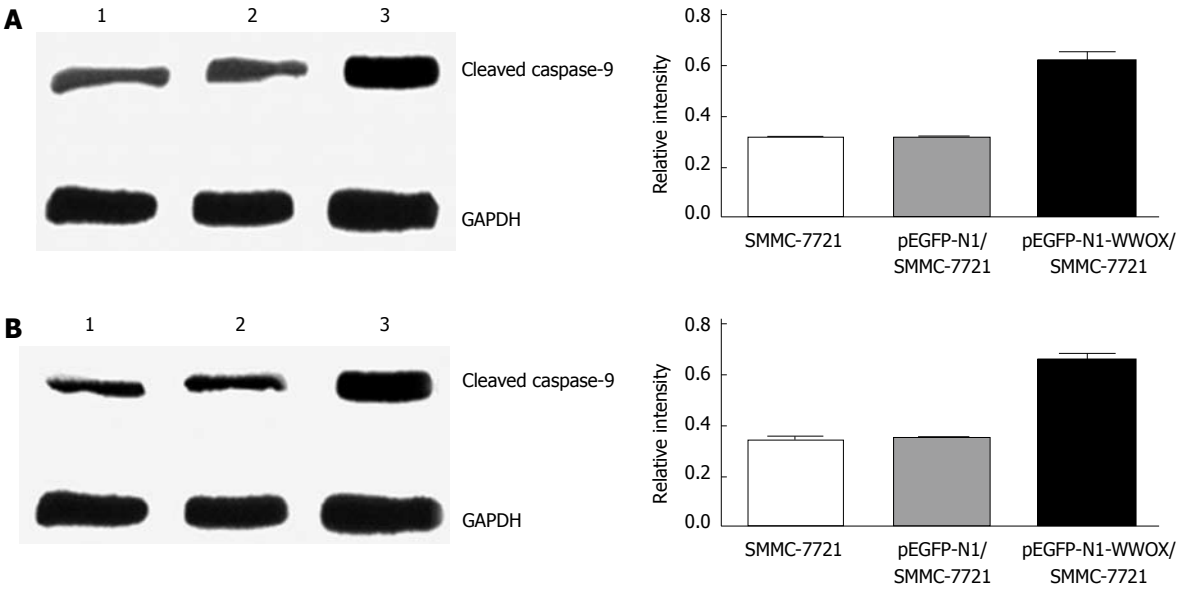

Figure 6 Overexpression of WWOX activates the expression of caspase-9 and caspase 3 protein. A: Expression of cleaved caspase-9 was upregulated in pEGFP-WWOX cells compared with parental and control vector cells; B: Protein expression of cleaved caspase 3 was upregulated in pEGFP-WWOX cells compared with control-vector cells and parental SMMC-7721. Data are presented as mean ± SD ($P < 0.05$). 1: Control group; 2: Empty vector transfection group; 3: pEGFP-WWOX transfection group. GAPDH: Glyceraldehyde-3-phosphate dehydrogenase.

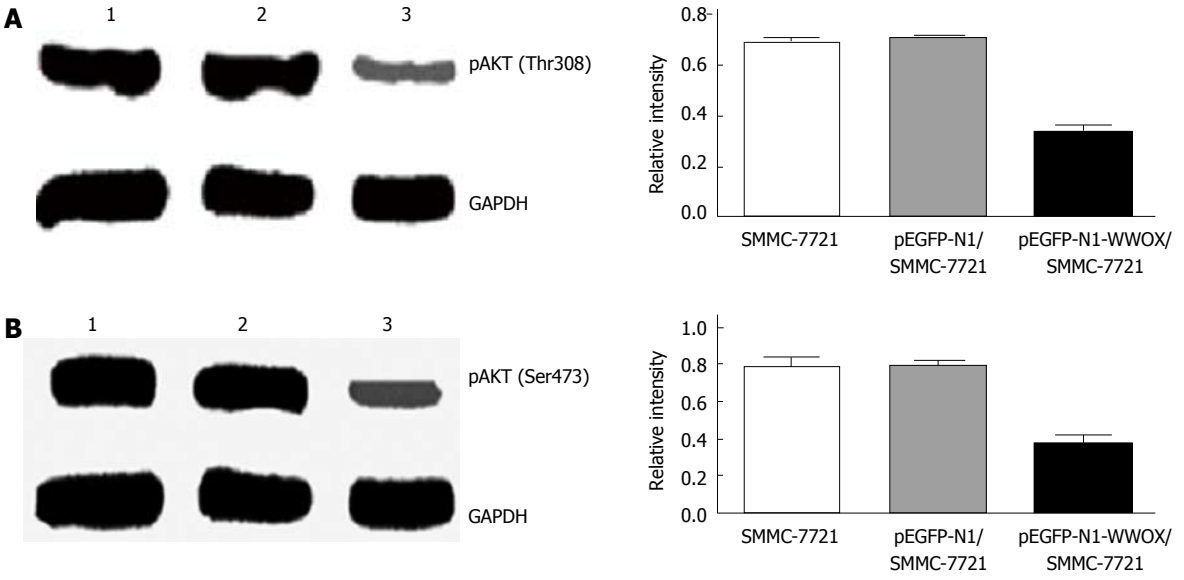

Figure 7 Overexpression of WWOX suppresses the phosphorylation of p-AKT(Thr308) and p-AKT(Ser473). A: p-AKT(Thr308) levels were decreased in pEGFP-WWOX cells compared with parental and control vector transformed cells by Western blotting analysis; B: p-AKT(Ser473) levels were decreased in pEGFP-WWOX cells compared with parental and control vector transformed cells by Western blotting analysis. Data are presented as mean ± SD ($P < 0.05$). 1: Control group; 2: Empty vector transfection group; 3: pEGFP-WWOX transfection group. GAPDH: Glyceraldehyde-3-phosphate dehydrogenase.

introducing *WWOX* into wild-type cells to investigate the effect of the *WWOX* gene on SMMC-7721, the human hepatic carcinoma cell line. Our data suggest that WWOX can significantly inhibit cell proliferation and induce cell apoptosis of the hepatic carcinoma cell line SMMC-7721. Overexpression of *WWOX* delayed the cell cycle progression from G1 into S phase, as demonstrated by flow cytometry.

Apoptosis plays a central role in tumor development, and a lack or failure of apoptosis leads to the development of many tumors, including hepatocarcinoma[16,17]. This suggests that induction of apoptosis in tumor cells might be an effective approach for delaying tumor progression. In this study, we found that overexpression of *WWOX* induces apoptosis in the hepatic carcinoma cell line SMMC-7721.

There are, at least, two broad extrinsic and intrinsic pathways that lead to apoptosis[18-20]. The extrinsic pathway begins with the binding of Fas ligand (FasL or CD95L) to the Fas receptor (CD95) and results in the

recruitment of Fas-associated protein with death domain and pro-caspase-8 to the Fas complex. This increase in the local concentration of pro-caspase-8 leads to its autocatalysis and activation. Activated caspase-8 cleaves pro-caspase-3, which then undergoes autocatalysis to form active caspase-3, a principle effector caspase of apoptosis. The intrinsic apoptosis pathway always begins with mitochondrial damage, which results in the release of cytochrome C from the damaged mitochondria. In the cytosol or on the surface of the mitochondria, cytochrome C is bound to the protein Apaf-1 (apoptotic protease activating factor), which activates the initiating caspase, caspase-9, which then activates caspase-3[21,22]. The caspase families play an important role in the apoptosis-signaling pathway. The caspases are present in the cytoplasm under normal conditions as inactive proenzymes, and most of them are activated by proteolytic cleavage when the cell undergoes apoptosis[23,24]. Both caspase-8 and caspase-9 can activate the effector caspase, caspase-3, by proteolytic cleavage, and the subsequent processes result in nuclear DNA fragmentation and the formation of apoptotic bodies. This indicates that activation of caspase-3 is a central event for the process of apoptosis. Based on these results, we speculate that WWOX allows the release of cytochrome C from mitochondria, resulting in the activation of caspase-9 and caspase-3 in sequence and finally induces apoptosis of HCC cells. Consistent with this hypothesis, the results of Western blotting showed that WWOX overexpression induced the activation of caspase-9 and caspase-3.

Our work also shows that WWOX downregulates the phosphorylation of Akt/PKB at Thr308. Akt/PKB[25,26], the major downstream effector of the PI3-kinase, is a Ser/Thr protein kinase that plays a crucial role in the regulation of several cellular signaling pathways. Akt/PKB is a regulator of cell survival and apoptosis, and its activation in a variety of cells can protect against apoptosis. Akt/PKB is phosphorylated at two regulatory sites, Thr308 and Ser473, which are essential for its activation. Activated Akt/PKB can phosphorylate BAD, IκB kinase, glycogen synthase kinase-3b, and the forkhead transcription factors[27,28], leading to their inactivation and cell survival. It has been reported that the phosphorylation of caspase-9 can regulate its activity[29]. Akt phosphorylates pro-caspase-9 at Ser196, which inhibits the proteolytic processing of pro-caspase-9.

WWOX blocks the activation of Akt, thereby attenuating the activity of a major anti-apoptotic pathway and inducing cell apoptosis. It remains unclear how WWOX affects Akt phosphorylation, as it does not affect PI3-kinase activity directly[30]. Other potential consequences of WWOX inhibition, such as the modulation of the RAS-signaling pathway, the expression of p53 and other members of the B-cell lymphoma 2 family, such as myeloid cell leukemia-1[31,32], the activation of the sphingomyelin-ceramide pathway, and interference with nuclear factor-κB[33] merit further investigation in the future.

In conclusion, WWOX may play a key role in tumor cell proliferation and carcinogenesis. Overexpression of WWOX can suppress the growth of HCC cells by inhibiting cell growth and inducing cell apoptosis. Apoptosis is induced by WWOX through the activation of the caspase cascade, which is correlated with the phosphorylation of Akt/PKB. These results suggest a potential role for WWOX as an effective chemotherapeutic and chemopreventive strategy against human liver cancer.

COMMENTS

Background

Several researches have revealed loss of heterozygosity of *WWOX* locus in gastric, pancreatic, esophageal and lung cancers. The role of *WWOX* in hepatic carcinoma is not well understood, and few studies have reported the effects of *WWOX* on hepatic carcinoma. In this study, the authors investigated the apoptotic effects of the *WWOX* gene on the human hepatic carcinoma cell line SMMC-7721.

Research frontiers

This is the first report about *WWOX* gene relevant to human hepatoma cell line SMMC-7721.

Innovations and breakthroughs

By cloning the *WWOX* gene and transferring it into hepatocellular carcinoma cell line SMMC-7721, the authors investigated the growth-inhibiting and apoptosis-inducing effects of *WWOX* gene on human hepatoma cell line SMMC-7721 and concluded that the over-expression of *WWOX* gene could induce apoptosis and inhibit the growth of hepatic carcinoma cell line SMMC-7721.

Applications

WWOX may have a potential role in development of chemotherapeutic and chemopreventive strategies against liver cancer.

Terminology

The tumor suppressor gene *WWOX* is localized in a common fragile site FRA16D (locus 16q23.3-24.1). Protein encoded by *WWOX* is an oxidoreductase containing two WW protein interaction domains.

Peer review

The manuscript describes the results of studies on the effect of tumor suppressor gene, *WWOX*, expression in SMMC-7721. This is an interesting and well presented study, with thorough introduction and the succinct discussion of the topic.

REFERENCES

1 **Aqeilan RI**, Donati V, Gaudio E, Nicoloso MS, Sundvall M, Korhonen A, Lundin J, Isola J, Sudol M, Joensuu H, Croce CM, Elenius K. Association of Wwox with ErbB4 in breast cancer. *Cancer Res* 2007; **67**: 9330-9336

2 **Aqeilan RI**, Hagan JP, de Bruin A, Rawahneh M, Salah Z, Gaudio E, Siddiqui H, Volinia S, Alder H, Lian JB, Stein GS, Croce CM. Targeted ablation of the WW domain-containing oxidoreductase tumor suppressor leads to impaired steroidogenesis. *Endocrinology* 2009; **150**: 1530-1535

3 **Kuroki T**, Trapasso F, Shiraishi T, Alder H, Mimori K, Mori M, Croce CM. Genetic alterations of the tumor suppressor gene WWOX in esophageal squamous cell carcinoma. *Cancer Res* 2002; **62**: 2258-2260

4 **Yendamuri S**, Kuroki T, Trapasso F, Henry AC, Dumon KR, Huebner K, Williams NN, Kaiser LR, Croce CM. WW domain containing oxidoreductase gene expression is altered in non-small cell lung cancer. *Cancer Res* 2003; **63**: 878-881

5 **Ishii H**, Vecchione A, Furukawa Y, Sutheesophon K, Han SY, Druck T, Kuroki T, Trapasso F, Nishimura M, Saito Y, Ozawa K, Croce CM, Huebner K, Furukawa Y. Expression of FRA16D/WWOX and FRA3B/FHIT genes in hematopoietic malignancies. *Mol Cancer Res* 2003; **1**: 940-947

6 **Kuroki T**, Yendamuri S, Trapasso F, Matsuyama A, Aqeilan RI, Alder H, Rattan S, Cesari R, Nolli ML, Williams NN, Mori M, Kanematsu T, Croce CM. The tumor suppressor

gene WWOX at FRA16D is involved in pancreatic carcinogenesis. *Clin Cancer Res* 2004; **10**: 2459-2465
7 **Aqeilan RI**, Kuroki T, Pekarsky Y, Albagha O, Trapasso F, Baffa R, Huebner K, Edmonds P, Croce CM. Loss of WWOX expression in gastric carcinoma. *Clin Cancer Res* 2004; **10**: 3053-3058
8 **Driouch K**, Prydz H, Monese R, Johansen H, Lidereau R, Frengen E. Alternative transcripts of the candidate tumor suppressor gene, WWOX, are expressed at high levels in human breast tumors. *Oncogene* 2002; **21**: 1832-1840
9 **Gourley C**, Paige AJ, Taylor KJ, Scott D, Francis NJ, Rush R, Aldaz CM, Smyth JF, Gabra H. WWOX mRNA expression profile in epithelial ovarian cancer supports the role of WWOX variant 1 as a tumour suppressor, although the role of variant 4 remains unclear. *Int J Oncol* 2005; **26**: 1681-1689
10 **Guler G**, Uner A, Guler N, Han SY, Iliopoulos D, Hauck WW, McCue P, Huebner K. The fragile genes FHIT and WWOX are inactivated coordinately in invasive breast carcinoma. *Cancer* 2004; **100**: 1605-1614
11 **Ishii H**, Furukawa Y. Alterations of common chromosome fragile sites in hematopoietic malignancies. *Int J Hematol* 2004; **79**: 238-242
12 **Paige AJ**, Taylor KJ, Taylor C, Hillier SG, Farrington S, Scott D, Porteous DJ, Smyth JF, Gabra H, Watson JE. WWOX: a candidate tumor suppressor gene involved in multiple tumor types. *Proc Natl Acad Sci USA* 2001; **98**: 11417-11422
13 **Sbrana I**, Veroni F, Nieri M, Puliti A, Barale R. Chromosomal fragile sites FRA3B and FRA16D show correlated expression and association with failure of apoptosis in lymphocytes from patients with thyroid cancer. *Genes Chromosomes Cancer* 2006; **45**: 429-436
14 **Strik H**, Deininger M, Streffer J, Grote E, Wickboldt J, Dichgans J, Weller M, Meyermann R. BCL-2 family protein expression in initial and recurrent glioblastomas: modulation by radiochemotherapy. *J Neurol Neurosurg Psychiatry* 1999; **67**: 763-768
15 **Weller M**, Malipiero U, Aguzzi A, Reed JC, Fontana A. Protooncogene bcl-2 gene transfer abrogates Fas/APO-1 antibody-mediated apoptosis of human malignant glioma cells and confers resistance to chemotherapeutic drugs and therapeutic irradiation. *J Clin Invest* 1995; **95**: 2633-2643
16 **Kerr JF**, Wyllie AH, Currie AR. Apoptosis: a basic biological phenomenon with wide-ranging implications in tissue kinetics. *Br J Cancer* 1972; **26**: 239-257
17 **Evan G**, Littlewood T. A matter of life and cell death. *Science* 1998; **281**: 1317-1322
18 **Yang J**, Liu X, Bhalla K, Kim CN, Ibrado AM, Cai J, Peng TI, Jones DP, Wang X. Prevention of apoptosis by Bcl-2: release of cytochrome c from mitochondria blocked. *Science* 1997; **275**: 1129-1132
19 **Li P**, Nijhawan D, Budihardjo I, Srinivasula SM, Ahmad M, Alnemri ES, Wang X. Cytochrome c and dATP-dependent formation of Apaf-1/caspase-9 complex initiates an apoptotic protease cascade. *Cell* 1997; **91**: 479-489
20 **Bossy-Wetzel E**, Newmeyer DD, Green DR. Mitochondrial cytochrome c release in apoptosis occurs upstream of DEVD-specific caspase activation and independently of mitochondrial transmembrane depolarization. *EMBO J* 1998; **17**: 37-49
21 **Liu X**, Kim CN, Yang J, Jemmerson R, Wang X. Induction of apoptotic program in cell-free extracts: requirement for dATP and cytochrome c. *Cell* 1996; **86**: 147-157
22 **Zou H**, Henzel WJ, Liu X, Lutschg A, Wang X. Apaf-1, a human protein homologous to C. elegans CED-4, participates in cytochrome c-dependent activation of caspase-3. *Cell* 1997; **90**: 405-413
23 **Sakai T**, Liu L, Teng X, Mukai-Sakai R, Shimada H, Kaji R, Mitani T, Matsumoto M, Toida K, Ishimura K, Shishido Y, Mak TW, Fukui K. Nucling recruits Apaf-1/pro-caspase-9 complex for the induction of stress-induced apoptosis. *J Biol Chem* 2004; **279**: 41131-41140
24 **Arnoult D**, Gaume B, Karbowski M, Sharpe JC, Cecconi F, Youle RJ. Mitochondrial release of AIF and EndoG requires caspase activation downstream of Bax/Bak-mediated permeabilization. *EMBO J* 2003; **22**: 4385-4399
25 **Dudek H**, Datta SR, Franke TF, Birnbaum MJ, Yao R, Cooper GM, Segal RA, Kaplan DR, Greenberg ME. Regulation of neuronal survival by the serine-threonine protein kinase Akt. *Science* 1997; **275**: 661-665
26 **Franke TF**, Kaplan DR, Cantley LC. PI3K: downstream AKTion blocks apoptosis. *Cell* 1997; **88**: 435-437
27 **Fang X**, Yu S, Eder A, Mao M, Bast RC, Boyd D, Mills GB. Regulation of BAD phosphorylation at serine 112 by the Ras-mitogen-activated protein kinase pathway. *Oncogene* 1999; **18**: 6635-6640
28 **Rena G**, Prescott AR, Guo S, Cohen P, Unterman TG. Roles of the forkhead in rhabdomyosarcoma (FKHR) phosphorylation sites in regulating 14-3-3 binding, transactivation and nuclear targetting. *Biochem J* 2001; **354**: 605-612
29 **Cardone MH**, Roy N, Stennicke HR, Salvesen GS, Franke TF, Stanbridge E, Frisch S, Reed JC. Regulation of cell death protease caspase-9 by phosphorylation. *Science* 1998; **282**: 1318-1321
30 **Zhou H**, Summers SA, Birnbaum MJ, Pittman RN. Inhibition of Akt kinase by cell-permeable ceramide and its implications for ceramide-induced apoptosis. *J Biol Chem* 1998; **273**: 16568-16575
31 **Hsu AL**, Ching TT, Wang DS, Song X, Rangnekar VM, Chen CS. The cyclooxygenase-2 inhibitor celecoxib induces apoptosis by blocking Akt activation in human prostate cancer cells independently of Bcl-2. *J Biol Chem* 2000; **275**: 11397-11403
32 **Lin MT**, Lee RC, Yang PC, Ho FM, Kuo ML. Cyclooxygenase-2 inducing Mcl-1-dependent survival mechanism in human lung adenocarcinoma CL1.0 cells. Involvement of phosphatidylinositol 3-kinase/Akt pathway. *J Biol Chem* 2001; **276**: 48997-49002
33 **Lee JY**, Ye J, Gao Z, Youn HS, Lee WH, Zhao L, Sizemore N, Hwang DH. Reciprocal modulation of Toll-like receptor-4 signaling pathways involving MyD88 and phosphatidylinositol 3-kinase/AKT by saturated and polyunsaturated fatty acids. *J Biol Chem* 2003; **278**: 37041-37051

S- Editor Shi ZF **L- Editor** Ma JY **E- Editor** Li JY

World Journal of Gastroenterology

Online Submissions: http://www.wjgnet.com/1007-9327office
wjg@wjgnet.com
doi:10.3748/wjg.v18.i23.3027

World J Gastroenterol 2012 June 21; 18(23): 3027-3031
ISSN 1007-9327 (print) ISSN 2219-2840 (online)

CASE REPORT

Surgical resection of a solitary para-aortic lymph node metastasis from hepatocellular carcinoma

Junji Ueda, Hiroshi Yoshida, Yasuhiro Mamada, Nobuhiko Taniai, Sho Mineta, Masato Yoshioka, Youichi Kawano, Tetsuya Shimizu, Etsuko Hara, Chiaki Kawamoto, Keiko Kaneko, Eiji Uchida

Junji Ueda, Hiroshi Yoshida, Yasuhiro Mamada, Nobuhiko Taniai, Sho Mineta, Masato Yoshioka, Youichi Kawano, Tetsuya Shimizu, Etsuko Hara, Eiji Uchida, Department of Surgery, Nippon Medical School, Tokyo 113-8603, Japan
Chiaki Kawamoto, Keiko Kaneko, Divisions of Cardiology, Hepatology, Geriatrics, and Integrated Medicine, Department of Internal Medicine, Nippon Medical School, Tokyo 113-8603, Japan
Author contributions: Ueda J, Yoshida H and Uchida E contributed equally to this work; Mamada Y, Taniai N, Mineta S, Yoshioka M, Kawano Y, Shimizu T and Hara E performed the operation; Kawamoto C and Kaneko K introduced us to this patient; All authors read and approved the final manuscript.
Correspondence to: Junji Ueda, MD, Department of Surgery, Nippon Medical School, Tokyo 113-8603, Japan. junji0821@nms.ac.jp
Telephone: +81-3-58146239 Fax: +81-3-56850989
Received: November 13, 2011 Revised: March 11, 2012
Accepted: April 9, 2012
Published online: June 21, 2012

Abstract

Lymph node (LN) metastases from hepatocellular carcinoma (HCC) are considered uncommon. We describe the surgical resection of a solitary para-aortic LN metastasis from HCC. A 65-year-old Japanese man with B-type liver cirrhosis was admitted for the evaluation of a liver tumor. He had already undergone radiofrequency ablation, transcatheter arterial chemoembolization, and percutaneous ethanol injection therapy for HCC. Despite treatment, viable regions remained in segments 4 and 8. We performed a right paramedian sectionectomy with partial resection of the left paramedian section of the liver. Six months later, serum concentrations of alpha-fetoprotein (189 ng/mL) and PIVKA-2 (507 mAU/mL) increased. Enhanced computed tomography of the abdomen revealed a tumor (20 mm in diameter) on the right side of the abdominal aorta. Fluorine-18 fluorodeoxyglucose positron emission tomography revealed an increased standard uptake value. There was no evidence of recurrence in other regions. Esophagogastroduodenoscopy and colonoscopy revealed no malignant tumor in the gastrointestinal tract. Para-aortic LN metastasis from HCC was thus diagnosed. We performed lymphadenectomy. Histopathological examination revealed that the tumor was largely necrotic, with poorly differentiated HCC on its surface, which confirmed the suspected diagnosis. After 6 mo tumor marker levels were normal, with no evidence of recurrence. Our experience suggests that a solitary para-aortic LN metastasis from HCC can be treated surgically.

Key words: Surgical resection; Lymph node metastasis; Hepatocellular carcinoma; Hepatectomy; Positron emission tomography

Peer reviewer: Dr. Masayuki Ohta, Faculty of Medicine, Oita University, 1-1 Idaigaoka, Hasama-machi, Oita 879-5593, Japan

Ueda J, Yoshida H, Mamada Y, Taniai N, Mineta S, Yoshioka M, Kawano Y, Shimizu T, Hara E, Kawamoto C, Kaneko K, Uchida E. Surgical resection of a solitary para-aortic lymph node metastasis from hepatocellular carcinoma. *World J Gastroenterol* 2012; 18(23): 3027-3031 Available from: URL: http://www.wjgnet.com/1007-9327/full/v18/i23/3027.htm DOI: http://dx.doi.org/10.3748/wjg.v18.i23.3027

INTRODUCTION

Hepatocellular carcinoma (HCC) is the fifth most common solid tumor in the world and accounts for about 500 000 deaths per year[1]. Long-term outcomes after hepatic resection remain unsatisfactory because of the high incidence of postoperative recurrence[2]. Although intrahepatic metastases are the most common type of

recurrence, extrahepatic metastases from HCC have an important impact on long-term survival[3]. The most frequent site of hematogenous metastases is the lung, followed by the adrenal gland and skeleton[4,5]. However, lymph node (LN) metastases from HCC are uncommon, with an reported prevalence of 2.2% in a series of Japanese patients who underwent hepatic resection[4]. LN metastases are usually associated with systematic metastases, and there is currently no standard treatment[6]. The 5-year survival rate of patients with LN metastases from HCC is about 20%[7], but successful resection of a solitary LN metastasis is expected to result in better outcomes[8]. We describe the surgical resection of a solitary para-aortic LN metastasis from HCC.

CASE REPORT

A 65-year-old Japanese man with B-type liver cirrhosis was admitted for the evaluation of a liver tumor. He had already undergone radiofrequency ablation, transcatheter arterial chemoembolization, and percutaneous ethanol injection therapy for HCC. Despite treatment, HCC remained viable. We therefore considered surgical resection. The patient had undergone the repair of an abdominal aortic aneurysm with a vascular prosthesis 1 year previously. Laboratory examinations revealed the serum hemoglobin concentration to be 14.7 g/dL (normal, 14 to 17 g/dL); the platelet count was $9.7 \times 10^4/\mu L$ (normal, 12 to $38 \times 10^4/\mu L$); the total bilirubin level was 2.4 mg/dL; the direct bilirubin level was 1.9 mg/dL; the albumin level was 4.1 g/dL; the serum creatinine level was 1.24 mg/dL (normal, < 1.2 mg/dL); and the prothrombin time was 90.8%, which indicated Child-Pugh class A disease. The indocyanine green clearance rate of 15 min was 3.5% (normal, < 10%). The serum concentration of PIVKA-2 was 1226 mAU/mL (normal, < 37 mAU/mL), whereas the serum concentration of alpha-fetoprotein (AFP) was 563.7 ng/mL (normal, < 10 ng/mL). Enhanced computed tomography (CT) of the abdomen revealed a tumor, 20 mm in diameter, in segment 4 of the left lobe on early-phase images, with washout on late-phase images. Abdominal CT angiography revealed a diffuse high-density area, including lesions previously treated by radiofrequency ablation, in segment 8 of the right hepatic lobe. The high-density area was visible on arterial-phase images and washed out on late-phase images (Figure 1). The tumors in both segments were diagnosed as viable HCCs. We performed hepatic right paramedian sectionectomy with partial resection of the left paramedian section of the liver. During the operation, a tumor thrombus was found in a peripheral portal vein in segment 8. Histopathologically, the tumor contained broad areas of necrosis and fibrosis, and the HCC had a moderate-grade funicular structure. Poorly differentiated HCC was present in some parts of the tumor. The diagnosis was moderately to poorly differentiated HCC (T2N0M0, pStage Ⅱ UICC TNM classification). Peripheral portal vein invasion was detected (Figure 2). The postsurgical course was uneventful, and

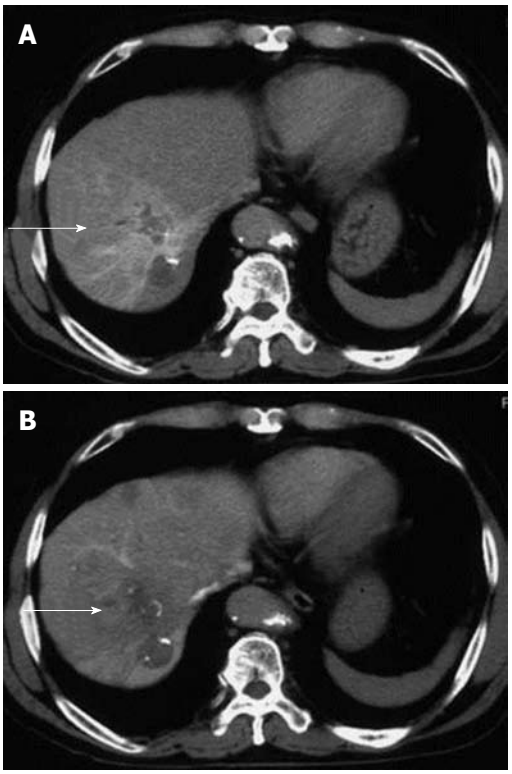

Figure 1 An abdominal computed tomography angiographic scan, showing a diffuse high-density area. A: An abdominal computed tomography angiographic scan including a lesion previously treated by radiofrequency ablation in segment 8 of the right hepatic lobe, in the arterial phase (arrow); B: The area was washed out on late-phase images (arrow).

the patient was discharged on postoperative day 14. After the operation, the serum concentration of PIVKA-2 decreased to 439 mAU/mL, whereas the concentration of AFP fell to 25.5 ng/mL after the operation. Upper gastrointestinal endoscopy revealed the presence of mild esophageal varices without gastric varices (Li, Cw, F1, RC0, according to the General Rules for Recording Endoscopic Findings of Esophagogastric Varices[9]).

Six months later, serum concentrations of PIVKA-2 (507 mAU/mL) and AFP (189 ng/mL) rose again. Enhanced CT of the abdomen revealed a tumor (20 mm in diameter with slight enhancement) on the right side of the abdominal aorta (Figure 3). Magnetic resonance imaging of the abdomen revealed a high-intensity tumor in the right para-aortic region on T2-weighted images. Fluorine-18 fluorodeoxyglucose positron emission tomography (FDG-PET) revealed an increased standard uptake value (SUV) in this tumor (Figure 4). There was no evidence of recurrence in any other region. Upper-gastrointestinal endoscopy and colonoscopy showed no evidence of a malignant tumor in the gastrointestinal tract. The tumor was diagnosed as a para-aortic LN metastasis from HCC because of the increased tumor marker level and increased SUV on FDG-PET. We performed lymphadenectomy. At the time of the operation, the surface of the tumor was smooth and slightly adhesive. Histopathological examination showed that the tumor was largely necrotic, with poorly differentiated HCC

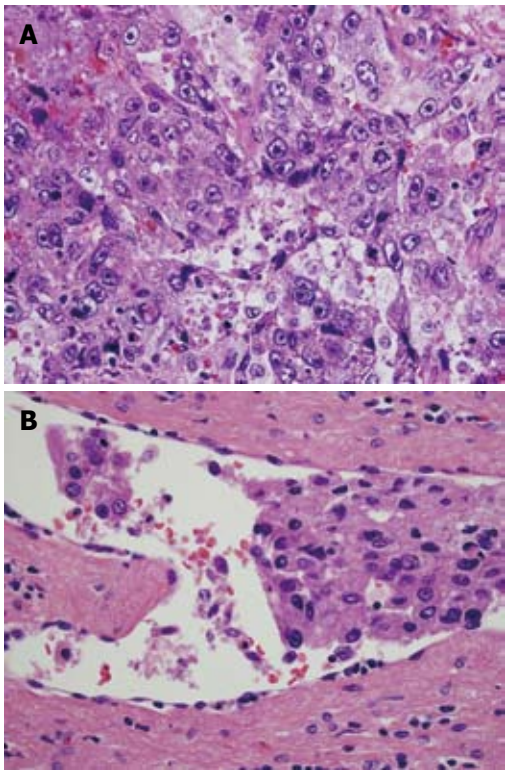

Figure 2 Histopathological examination revealed the presence of considerable necrosis and fibrosis in the tumor. The hepatocellular carcinoma (HCC) was graded as moderate-grade funicular type. A: Poorly differentiated HCC was present in some regions; B: Peripheral portal vein invasion was detected (hematoxylin and eosin, ×600).

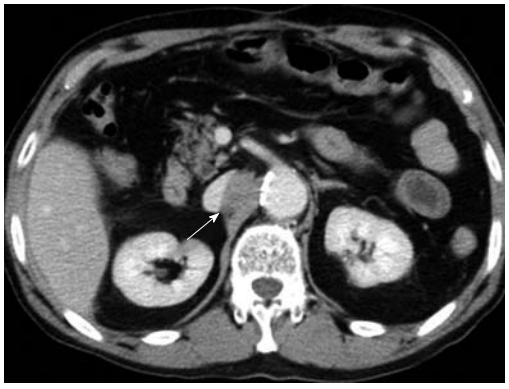

Figure 3 An enhanced computed tomographic scan of the abdomen revealed a tumor (20 mm in diameter, arrow) on the right side of the abdominal aorta.

on its surface (Figure 5). The invasion of lymphocytes was noted. The tumor was diagnosed as a para-aortic LN metastasis from HCC. Recovery was uneventful, and the patient was discharged on postoperative day 17. After 6 mo, the levels of tumor markers remained normal, with no evidence of recurrence.

DISCUSSION

LN metastasis is an important risk factor for the progression and recurrence of many malignant tumors[10]. LN status is an established prognostic factor in oncologic surgery, with a major impact on long-term survival[7]. LN metastasis also plays an important role in the outcomes of patients with HCC, in whom its presence is related to poorer survival and a higher risk of tumor recurrence[7]. Even after lymphadenectomy, patients with LN metastases still have poorer disease-free survival and overall survival than those without LN metastases[11].

The most common site of LN metastases from HCC is the hepatic pedicle node, followed by the retropancreatic space and common hepatic artery station. These nodes appear to be key stations for lymphatic spread from liver tumors toward regional and more distant nodes[12]. However, solitary para-aortic LN metastasis from HCC is relatively rare. Some HCCs can lead to what has been termed "skip LN metastases", LN metastases at distant sites without metastases in the hepatoduodenal ligament[13-16]. Moreover, peritumoral vascular or lymphatic invasion, tumor multifocality, or distal obstruction of the lymphatics by tumor metastasis can change the direction of lymph flow to alternative routes[17]. In our patient, skipping LN metastasis might have been caused by liver cirrhosis or an operation altering the direction of lymph flow.

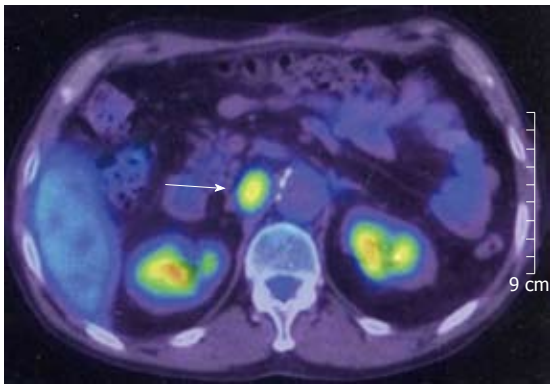

Figure 4 Fluorine-18 fluorodeoxyglucose positron emission tomography revealed that the tumor had an elevated standard uptake value (arrow).

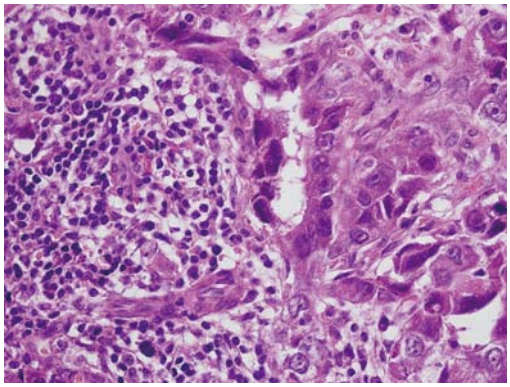

Figure 5 Histopathological examination revealed that the tumor consisted of a broad region of necrosis with poorly differentiated hepatocellular carcinoma on its surface (hematoxylin and eosin, ×600).

Previous studies have reported that patients with more advanced intrahepatic tumors or vessel invasion at initial diagnosis are more likely to have extrahepatic metastases[18]. A primary tumor size of > 5 cm has been associated with the presence of extrahepatic metastasis in HCC[19]. In our patient, the primary HCC was associated with peripheral portal vein invasion.

No standard treatment for extrahepatic metastases developing after hepatic resection of HCC is available[3]. Most patients with recurrent HCC have multiple extrahepatic metastases. The median survival time after the diagnosis of extrahepatic metastases is about 5 mo[20]. Patients with a solitary metastasis from a controlled intrahepatic tumor can be treated surgically, and good outcomes have been reported[8]. In our patient, the para-aortic LN metastasis was solitary, and there was no tumor in the residual liver or evidence of other extrahepatic metastases. We therefore resected the solitary LN metastasis.

A recent study reported that FDG-PET is a useful imaging technique for identifying extrahepatic metastases[19]. The sensitivity of FDG-PET for the detection of extrahepatic metastases was 79%. The detection rate was influenced by the size of metastatic lesions: it was 83% for metastatic lesions larger than 1 cm and 13% for lesions less than or equal to 1 cm[21]. FDG-PET is considered a very useful noninvasive imaging technique for diagnosis, staging and monitoring the treatment response in a variety of malignant tumors[22,23]. In patients with HCCs that produce AFP, an unexplained rise of the serum AFP level after treatment is an early sign of tumor recurrence or extrahepatic metastasis[24]. One study reported that tumor restaging by FDG-PET can detect and localize disease recurrence among patients with no or mild symptoms and elevated levels of tumor markers[25]. As well as being a useful tool for the preoperative staging of HCC, FDG-PET is also better than conventional diagnostic modalities for follow-up, especially staging and re-staging after hepatectomy[24]. In our patient, the serum AFP level increased after hepatectomy, and para-aortic LN metastasis was detected on FDG-PET. We therefore recommend FDG-PET for the screening of metastasis from HCC after hepatectomy.

In conclusion, our experience suggests that a solitary para-aortic LN metastasis from HCC can be treated surgically.

ACKNOWLEDGMENTS

The Department of Surgery for Organ and Biological Regulation, Nippon Medical School, performed the histological examination of the hepatocellular carcinoma and lymph node metastases and played a crucial role in producing this manuscript.

REFERENCES

1 **Parkin DM**, Bray F, Ferlay J, Pisani P. Estimating the world cancer burden: Globocan 2000. *Int J Cancer* 2001; **94**: 153-156

2 **Tung-Ping Poon R**, Fan ST, Wong J. Risk factors, prevention, and management of postoperative recurrence after resection of hepatocellular carcinoma. *Ann Surg* 2000; **232**: 10-24

3 **Shoji F**, Shirabe K, Yano T, Maehara Y. Surgical resection of solitary cardiophrenic lymph node metastasis by video-assisted thoracic surgery after complete resection of hepatocellular carcinoma. *Interact Cardiovasc Thorac Surg* 2010; **10**: 446-447

4 Primary liver cancer in Japan. Clinicopathologic features and results of surgical treatment. Liver Cancer Study Group of Japan. *Ann Surg* 1990; **211**: 277-287

5 **Katyal S**, Oliver JH, Peterson MS, Ferris JV, Carr BS, Baron RL. Extrahepatic metastases of hepatocellular carcinoma. *Radiology* 2000; **216**: 698-703

6 **Yamashita H**, Nakagawa K, Shiraishi K, Tago M, Igaki H, Nakamura N, Sasano N, Siina S, Omata M, Ohtomo K. Radiotherapy for lymph node metastases in patients with hepatocellular carcinoma: retrospective study. *J Gastroenterol Hepatol* 2007; **22**: 523-527

7 **Xiaohong S**, Huikai L, Feng W, Ti Z, Yunlong C, Qiang L. Clinical significance of lymph node metastasis in patients undergoing partial hepatectomy for hepatocellular carcinoma. *World J Surg* 2010; **34**: 1028-1033

8 **Une Y**, Misawa K, Shimamura T, Ogasawara K, Masuko Y, Sato N, Nakajima Y, Uchino J. Treatment of lymph node recurrence in patients with hepatocellular carcinoma. *Surg Today* 1994; **24**: 606-609

9 **Tajiri T**, Yoshida H, Obara K, Onji M, Kage M, Kitano S, Kokudo N, Kokubu S, Sakaida I, Sata M, Tajiri H, Tsukada K, Nonami T, Hashizume M, Hirota S, Murashima N, Moriyasu F, Saigenji K, Makuuchi H, Oho K, Yoshida T, Suzuki H, Hasumi A, Okita K, Futagawa S, Idezuki Y. General rules for recording endoscopic findings of esophagogastric varices (2nd edition). *Dig Endosc* 2010; **22**: 1-9

10 **Roukos DH**. Extended (D2) lymph node dissection for gastric cancer: do patients benefit? *Ann Surg Oncol* 2000; **7**: 253-255

11 **Sun HC**, Zhuang PY, Qin LX, Ye QH, Wang L, Ren N, Zhang JB, Qian YB, Lu L, Fan J, Tang ZY. Incidence and prognostic values of lymph node metastasis in operable hepatocellular carcinoma and evaluation of routine complete lymphadenectomy. *J Surg Oncol* 2007; **96**: 37-45

12 **Ercolani G**, Grazi GL, Ravaioli M, Grigioni WF, Cescon M, Gardini A, Del Gaudio M, Cavallari A. The role of lymphadenectomy for liver tumors: further considerations on the appropriateness of treatment strategy. *Ann Surg* 2004; **239**: 202-209

13 **Watanabe J**, Nakashima O, Kojiro M. Clinicopathologic study on lymph node metastasis of hepatocellular carcinoma: a retrospective study of 660 consecutive autopsy cases. *Jpn J Clin Oncol* 1994; **24**: 37-41

14 **Uehara K**, Hasegawa H, Ogiso S, Sakamoto E, Ohira S, Igami T, Mori T. Skip lymph node metastases from a small hepatocellular carcinoma with difficulty in preoperative diagnosis. *J Gastroenterol Hepatol* 2003; **18**: 345-349

15 **Magari S**. Hepatic lymphatic system: structure and function. *J Gastroenterol Hepatol* 1990; **5**: 82-93

16 **Taniai N**, Yoshida H, Mamada Y, Mizuguchi Y, Fujihira T, Akimaru K, Tajiri T. A case of recurring hepatocellular carcinoma with a solitary Virchow's lymph node metastasis. *J Nihon Med Sch* 2005; **72**: 245-249

17 **Sandrucci S**, Mussa A. Sentinel lymph node biopsy and axillary staging of T1-T2 N0 breast cancer: a multicenter study. *Semin Surg Oncol* 1998; **15**: 278-283

18 **Natsuizaka M**, Omura T, Akaike T, Kuwata Y, Yamazaki K, Sato T, Karino Y, Toyota J, Suga T, Asaka M. Clinical features of hepatocellular carcinoma with extrahepatic metastases. *J Gastroenterol Hepatol* 2005; **20**: 1781-1787

19 **Yoon KT**, Kim JK, Kim do Y, Ahn SH, Lee JD, Yun M, Rha

SY, Chon CY, Han KH. Role of 18F-fluorodeoxyglucose positron emission tomography in detecting extrahepatic metastasis in pretreatment staging of hepatocellular carcinoma. *Oncology* 2007; **72** Suppl 1: 104-110

20 **Uka K**, Aikata H, Takaki S, Shirakawa H, Jeong SC, Yamashina K, Hiramatsu A, Kodama H, Takahashi S, Chayama K. Clinical features and prognosis of patients with extrahepatic metastases from hepatocellular carcinoma. *World J Gastroenterol* 2007; **13**: 414-420

21 **Sugiyama M**, Sakahara H, Torizuka T, Kanno T, Nakamura F, Futatsubashi M, Nakamura S. 18F-FDG PET in the detection of extrahepatic metastases from hepatocellular carcinoma. *J Gastroenterol* 2004; **39**: 961-968

22 **Rigo P**, Paulus P, Kaschten BJ, Hustinx R, Bury T, Jerusalem G, Benoit T, Foidart-Willems J. Oncological applications of positron emission tomography with fluorine-18 fluorodeoxyglucose. *Eur J Nucl Med* 1996; **23**: 1641-1674

23 **Iglehart JK**. The new era of medical imaging--progress and pitfalls. *N Engl J Med* 2006; **354**: 2822-2828

24 **Sun L**, Guan YS, Pan WM, Chen GB, Luo ZM, Wu H. Positron emission tomography/computer tomography in guidance of extrahepatic hepatocellular carcinoma metastasis management. *World J Gastroenterol* 2007; **13**: 5413-5415

25 **Liu FY**, Chen JS, Changchien CR, Yeh CY, Liu SH, Ho KC, Yen TC. Utility of 2-fluoro-2-deoxy-D-glucose positron emission tomography in managing patients of colorectal cancer with unexplained carcinoembryonic antigen elevation at different levels. *Dis Colon Rectum* 2005; **48**: 1900-1912

S- Editor Gou SX **L- Editor** A **E- Editor** Li JY

World Journal of Gastroenterology

Online Submissions: http://www.wjgnet.com/1007-9327office
wjg@wjgnet.com
doi:10.3748/wjg.v18.i23.3032

World J Gastroenterol 2012 June 21; 18(23): 3032-3034
ISSN 1007-9327 (print) ISSN 2219-2840 (online)

Effect of discounting on estimation of benefits determined by hepatitis C treatment

Andrea Messori, Valeria Fadda, Dario Maratea, Sabrina Trippoli

Andrea Messori, Sabrina Trippoli, Laboratorio SIFO di Farmacoeconomia, Area Vasta Centro Toscana, 59100 Prato, Italy
Valeria Fadda, Dario Maratea, Department of Pharmaceutical Sciences, University of Firenze, 50019 Sesto Fiorentino, Italy
Author contributions: All authors were involved in data collection, study design, data analysis and interpretation and all authors were involved in writing of the manuscript.
Correspondence to: Dr. Andrea Messori, PhD, Laboratorio SIFO di Farmacoeconomia, c/o Area Vasta Centro Toscana, Regional Health System, Via Guimaraes 9-11, 59100 Prato, Italy. andrea.messori.it@gmail.com
Telephone: +39-347-6053933 Fax: +39-574-701319
Received: December 23, 2011 Revised: February 27, 2012
Accepted: March 20, 2012
Published online: June 21, 2012

Abstract

The combination of either boceprevir or telaprevir with ribavirin and interferon (triple therapy) has been shown to be more effective than ribavirin+interferon (dual therapy) for the treatment of genotype 1 hepatitis C. Since the benefit of these treatments takes place after years, simulation models are needed to predict long-term outcomes. In simulation models, the choice of different values of yearly discount rates (e.g., 6%, 3.5%, 2%, 1.5% or 0%) influences the results, but no studies have specifically addressed this issue. We examined this point by determining the long-term benefits under different conditions on the basis of standard modelling and using quality-adjusted life years (QALYs) to quantify the benefits. In our base case scenario, we compared the long-term benefit between patients given a treatment with a 40% sustained virologic response (SVR) (dual therapy) and patients given a treatment with a 70% SVR (triple therapy), and we then examined how these specific yearly discount rates influenced the incremental benefit. The gain between a 70% SVR and a 40% SVR decreased from 0.45 QALYs with a 0% discount rate to 0.22 QALYs with a 6% discount rate (ratio between the two values = 2.04). Testing the other discounting assumptions confirmed that the discount rate has a marked impact on the magnitude of the model-estimated incremental benefit. In conclusion, the results of our analysis can be helpful to better interpret cost-effectiveness studies evaluating new treatment for hepatitis C.

Key words: Boceprevir; Telaprevir; Cost-effectiveness; Markov model; Hepatitis C

Peer reviewers: Chao-Hung Hung, Kaohsiung Chang Gung Memorial Hospital, 123 Ta Pei Road, Niao Sung, Kaohsiung 833, Taiwan, China; Faisal M Sanai, Hepatobiliary Sciences, King Abdulaziz Medical City, King Abdulaziz Medical City, Riyadh 11462, Saudi Arabia

Messori A, Fadda V, Maratea D, Trippoli S. Effect of discounting on estimation of benefits determined by hepatitis C treatment. *World J Gastroenterol* 2012; 18(23): 3032-3034 Available from: URL: http://www.wjgnet.com/1007-9327/full/v18/i23/3032.htm DOI: http://dx.doi.org/10.3748/wjg.v18.i23.3032

TO THE EDITOR

The review by Tsubota *et al*[1] has examined the main options available for the treatment of hepatitis C, including two antiviral drugs that have recently been marketed in many countries. Focusing more thoroughly on these two innovative agents is worthwhile because boceprevir and telaprevir, along with other innovative agents, are thought to be an important advancement in the treatment of this disease[2], although at a high cost.

Hepatitis C virus (HCV) genotype 1, which accounts for 60% of all HCV-infected patients[3-5], is the target at which these two new agents are directed in combination with ribavirin + interferon. Considering that the combination of either boceprevor or telaprevir with ribavirin+interferon (triple therapy) has been shown

Table 1 Main characteristics of the Markov models[1]

Authors	Modelling details (base case)	Expected outcome		
		No treatment	Interferon monotherapy	Dual treatment
Bennett *et al*[16] 1997	Age = 35 yr; time horizon = lifetime; discount rate = 0% per year	36.2 LYs	37.7 LYs	NR
Bennett *et al*[16] 1997	Age = 35 yr; time horizon = lifetime; discount rate = 5% per year	16.2 LYs	16.4 LYs	NR
Bennett *et al*[16] 1997	Age = 35 yr; time horizon = lifetime; discount rate = 0% per year	28.0 QALYs	31.7 QALYs	NR
Shepherd *et al*[17] 2004	Age = 36 yr; time horizon = 30 yr; discount rate = 1.5% per year	21.464 QALYs	NR	23.417 QALYs
Shepherd *et al*[18] 2007	Age = 40 yr; time horizon = lifetime; discount rate = 1.5% per year	20.17 QALYs	NR	From 20.94 to 22.48 QALYs
Hartwell *et al*[19] 2011[2]	Age = 40 yr; time horizon = lifetime; discount rate = 3.5% per year, dual therapy with PEG-interferon alpha-2α	NR (naïve patients), 10.74 QALYs (previously treated patients)	NR	15.68 QALYs (naïve patients), 11.05 QALYs (previously treated patients)
Hartwell *et al*[19] 2011[2]	Age = 40 yr; time horizon = lifetime; discount rate = 3.5% per year, dual therapy with PEG-interferon alpha-2β	NR (naïve patients), 10.74 QALYs (previously treated patients)	NR	13.89 QALYs (naïve patients), 11.14 QALYs (previously treated patients)

LY: Life year; QALY: Quality-adjusted life year; PEG: Pegylated; NR: Not reported. [1]In a preliminary search on PubMed, we identified 47 articles describing a simulation model for hepatitis C; the complete references for these studies can be obtained from the authors upon request; [2]This study assessed also the shortened duration regimen of PEG-interferon + ribavirin, the data of which have not been reported in this table.

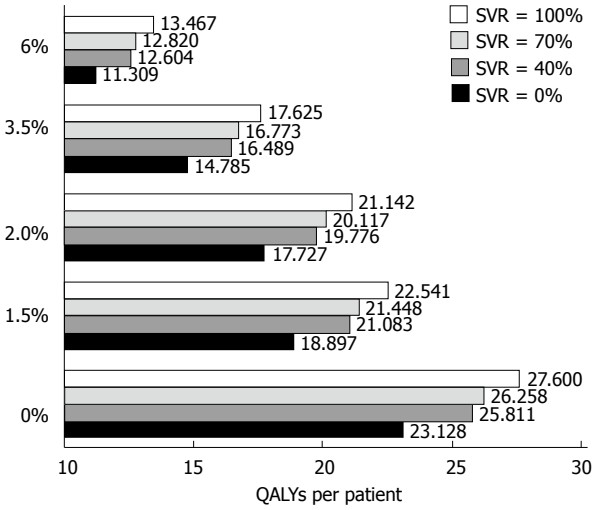

Figure 1 Estimation of the values of quality-adjusted life expectancy per patient under different modelling assumptions (time horizon = 30 years). The y-axis shows five different assumptions of yearly discount rate. QALYs: Quality-adjusted life years; SVR: Sustained virologic response.

to be more effective than ribavirin + interferon (dual therapy) in genotype 1[1-3], in the near future the dual therapy is expected to be replaced by the triple therapy in a certain proportion of these cases. The debate is still ongoing to set appropriate criteria to identify the best candidates for the triple therapy, and this selection will depend on a number of factors including pretreated *vs* naive condition[3] and interleukin 28B polymorphism[6].

The economic impact of this new approach to HCV treatment can be very substantial since it has been estimated that around 120 million euros per year are needed in a country with 60 million inhabitants[5], and this figure seems to be confirmed by the recent sales in the United States where these "third" drugs have already been available[7].

The predicted expenditure for the "third" drug (irrespective of whether it is boceprevir or telaprevir) is likely to be at least 20 000 euros per patient[5]. Since this is also the typical expenditure for target therapies in oncologic patients, decision-makers will have to face the competition for the same pharmaceutical budget between oncologic innovative treatments approved recently (e.g., ipilimumab for metastatic melanoma) and the triple therapy for genotype-1 hepatitis C.

The typical benefit of the latest oncologic treatments is a gain of 2-4 mo of survival per patient[8]; their pharmacoeconomic profile suggests an expenditure of 20 000 euros to gain up to a 4-mo survival, i.e., a cost-effectiveness ratio of 5000 euros per month or 60 000 euros per year.

Contrasting the cost-effectiveness between oncologic treatment and the triple therapy implies the need to compare the short-term benefits observed in oncologic patients (e.g., survival prolongation in metastatic melanoma from 6 mo without ipilimumab to 10 mo with ipilimumab) with the benefits in HCV patients that are instead known to take place at least 10 years after treatment.

The discount rate is the typical method employed in cost-effectiveness studies to convert future clinical benefits into their present value[9-14]. In the United States, rates around 5% or 6% per year were suggested nearly 20 years ago, but later various panels of experts revised this suggestion by proposing an annual rate of 3%[9,10]. In the United Kingdom, the National Institute of Clinical Excellence initially chose to use 3.5% per year[11], but in August 2011 this value was re-determined as 1.5% per year at least in some cases[15].

Several years ago, the pharmacoeconomic studies comparing dual therapy *vs* interferon alone led to the development of numerous models[16-19] based on the Markov technique that were aimed at predicting the natural history of the disease with or without achievement of post-treatment sustained virologic response (SVR). Although the number of simulation models for hepatitis C published in the past is exceedingly high, the systematic review by Hartwell *et al*[19] confirms that the models initially developed by Bennett *et al*[16] and by Shepherd *et al*[17,18] remain still valid to carry out a thorough comparative assessment of the new *vs* old treatments.

The choice of specific values of yearly discount rates

is the key factor influencing the model's outcome (Table 1). For this reason, we have summarized the different effects determined by the choice of different discount rates using a single simulation model among those reported in the literature.

The results of our analysis are shown in Figure 1. The values of quality-adjusted life years (QALYs) per patient have been calculated by examining five different assumptions of yearly discount rates (6%, 3.5%, 2%, 1.5% and 0%) and four SVR rates (0%, 40%, 70% and 100%). With regard to the SVR rates, the assumption of a 100% SVR has, of course, a purely hypothetical function, whereas the assumption of 0% SVR represent the option of no treatment. More importantly, the assumption of 40% SVR represents the typical outcome of dual treatment while 70% SVR is used to estimate the outcome of triple treatment, as well as other treatments that are currently under investigation, but will become available quite soon[2].

The information shown in Figure 1 clearly indicates that the effect of choosing different discount rates is very substantial. The gain between 100% SVR and 0% SVR (a purely hypothetical comparison) decreases from 4.47 QALYs with a 0% discount rate to 2.16 QALYs with a 6% discount rate (ratio between the two values =2.07). On the other hand, the gain between 70% SVR and 40% SVR decreases from 0.45 QALYs with a 0% discount rate to 0.22 QALYs with a 6% discount rate (ratio between the two values =2.04). These simulations have a general validity because they are only based on the clinical end-point of SVR, and therefore do not rely on specific assumptions in the patients whether are naive or pretreated. As shown in Figure 1, we could compute the value of QALYs per patient for any intermediate value of SVR ($SVR_{NN\%}$) in a range from 0% to 100% according to the equation: $QALYs_{SVRNN\%} = [QALY_{SVR100\%} \times NN + QALY_{SSVR0\%} \times (100\text{-}NN)]/100$. It should be noted that, in real practice as well as in model-based estimations, the favorable economic results of these treatments do not result only from the economic countervalue of the clinical benefit, but also from the savings derived from reduced morbidity. However, the latter factor was beyond the purposes of the present study.

In conclusion, our analysis has exclusively focused on the consequences of choosing different discount rates in estimating the magnitude of the clinical benefit of treatments for hepatitis C. Our results indicate that varying the discount rate within commonly accepted values can produce more than 2-fold variations in the estimates of the incremental benefit. This point should be kept in mind when regulatory agencies or third-part payers will be asked to determine the value-based price for the new treatments in this area.

ACKNOWLEDGMENTS

We thank Professor Americo Cicchetti and Professor Antonio Gasbarrini (both from the Università Cattolica, Policlinico Gemelli, Rome, Italy), coordinators of the WEF group (Workshop in Epatologia e Farmacoeconomia).

REFERENCES

1 **Tsubota A**, Fujise K, Namiki Y, Tada N. Peginterferon and ribavirin treatment for hepatitis C virus infection. *World J Gastroenterol* 2011; **17**: 419-432
2 **Chung RT**. A watershed moment in the treatment of hepatitis C. *N Engl J Med* 2012; **366**: 273-275
3 **Butt AA**, Kanwal F. Boceprevir and telaprevir in the management of hepatitis C virus-infected patients. *Clin Infect Dis* 2012; **54**: 96-104
4 **Messori A**, Del Santo F, Maratea D. First-line treatments for hepatitis C. *Aliment Pharmacol Ther* 2011; **33**: 1383-1385
5 **Maratea D**, Messori A, Fadda V. Nationwide prediction of future expenditure for protease inhibitors in chronic hepatitis C. *Dig Liver Dis* 2012; **44**: 86-87
6 **Miyamura T**, Kanda T, Nakamoto S, Wu S, Fujiwara K, Imazeki F, Yokosuka O. Hepatic STAT1-nuclear translocation and interleukin 28B polymorphisms predict treatment outcomes in hepatitis C virus genotype 1-infected patients. *PLoS One* 2011; **6**: e28617
7 **Cohen B**. Vertex score big with hepatitis drug in America (September 2011). Available from: URL: http: //www.hepctrust.org.uk/News_Resources/news/2011/September/Vertex score big with hepatitis drug in America accessed on 20 December 2011
8 **Fojo T**, Grady C. How much is life worth: cetuximab, non-small cell lung cancer, and the $440 billion question. *J Natl Cancer Inst* 2009; **101**: 1044-1048
9 **Krahn M**, Gafni A. Discounting in the economic evaluation of health care interventions. *Med Care* 1993; **31**: 403-418
10 **Siegel JE**, Torrance GW, Russell LB, Luce BR, Weinstein MC, Gold MR. Guidelines for pharmacoeconomic studies. Recommendations from the panel on cost effectiveness in health and medicine. Panel on cost Effectiveness in Health and Medicine. *Pharmacoeconomics* 1997; **11**: 159-168
11 **Torgerson DJ**, Raftery J. Economic notes. Discounting. *BMJ* 1999; **319**: 914-915
12 **West RR**, McNabb R, Thompson AG, Sheldon TA, Grimley Evans J. Estimating implied rates of discount in healthcare decision-making. *Health Technol Assess* 2003; **7**: 1-60
13 **Brouwer WB**, Niessen LW, Postma MJ, Rutten FF. Need for differential discounting of costs and health effects in cost effectiveness analyses. *BMJ* 2005; **331**: 446-448
14 **Claxton K**, Paulden M, Gravelle H, Brouwer W, Culyer AJ. Discounting and decision making in the economic evaluation of health-care technologies. *Health Econ* 2011; **20**: 2-15
15 **Anonymous**. NICE changes discount rate methods (7 August 2011). Available from: URL: http: //scharrheds.blogspot.com/2011/08/nice-changes-discount-rate-methods.html accessed on 20 December 2011
16 **Bennett WG**, Inoue Y, Beck JR, Wong JB, Pauker SG, Davis GL. Estimates of the cost-effectiveness of a single course of interferon-alpha 2b in patients with histologically mild chronic hepatitis C. *Ann Intern Med* 1997; **127**: 855-865
17 **Shepherd J**, Brodin H, Cave C, Waugh N, Price A, Gabbay J. Pegylated interferon alpha-2a and -2b in combination with ribavirin in the treatment of chronic hepatitis C: a systematic review and economic evaluation. *Health Technol Assess* 2004; **8**: iii-iv, 1-125
18 **Shepherd J**, Jones J, Hartwell D, Davidson P, Price A, Waugh N. Interferon alpha (pegylated and non-pegylated) and ribavirin for the treatment of mild chronic hepatitis C: a systematic review and economic evaluation. *Health Technol Assess* 2007; **11**: 1-205, iii
19 **Hartwell D**, Jones J, Baxter L, Shepherd J. Peginterferon alfa and ribavirin for chronic hepatitis C in patients eligible for shortened treatment, re-treatment or in HCV/HIV co-infection: a systematic review and economic evaluation. *Health Technol Assess* 2011; **15**: i-xii, 1-210

S- Editor Gou SX **L- Editor** Ma JY **E- Editor** Li JY

World Journal of Gastroenterology

Online Submissions: http://www.wjgnet.com/1007-9327office
wjg@wjgnet.com
www.wjgnet.com

World J Gastroenterol 2012 June 21; 18(23): I
ISSN 1007-9327 (print) ISSN 2219-2840 (online)

Acknowledgments to reviewers of *World Journal of Gastroenterology*

Many reviewers have contributed their expertise and time to the peer review, a critical process to ensure the quality of *World Journal of Gastroenterology*. The editors and authors of the articles submitted to the journal are grateful to the following reviewers for evaluating the articles (including those published in this issue and those rejected for this issue) during the last editing time period.

Edward J Ciaccio, PhD, Research Scientist, Department of Medicine, HP 804, Columbia University, 180 Fort Washington Avenue, New York, NY 10032, United States

William Dickey, Professor, Altnagelvin Hospital, Londonderry, BT47 6SB, Northern Ireland, United Kingdom

Yasuhiro Fujino, MD, PhD, Director, Department of Surgery, Hyogo Cancer Center, 13-70 Kitaoji-cho, Akashi 673-8558, Japan

Markus Gerhard, Professor, Laboratory of Molecular Gastroenterology 3K52, Second Medical Department, Klinikum rechts der Isar, Technical University of Munich, Ismaningerstr. 22, 81675 Munich, Germany

Luis Grande, Professor, Department of Surgery, Hospital del Mar, Passeig Marítim 25-29, 08003 Barcelona, Spain

Kevin Cheng-Wen Hsiao, MD, Assistant Professor, Colon and Rectal Surgery, Tri-Service General Hospital, No. 325, Sec. 2, Cheng-Kung Rd, Nei-Hu district, Taipei 114, Taiwan, China

Dr. Selin Kapan, Associate Professor of General Surgery, Department of General Surgery, Dr. Sadi Konuk Training and Research Hospital, Kucukcekmece, 34150 Istanbul, Turkey

Hyo-Cheol Kim, MD, Clinical Assistant Professor in Vascular Intervention Section, Department of Radiology, Seoul National University Hospital, 28 Yongon-dong, Chongno-gu, Seoul 110-744, South Korea

Takashi Kobayashi, MD, PhD, Department of Surgery, Showa General Hospital, 2-450 Tenjincho, Kodaira, Tokyo 187-8510, Japan

Richard A Kozarek, MD, Executive Director, Digestive Disease Institute, Virginia Mason Medical Center 1100 Ninth Avenue, PO Box 900, Seattle, WA 98111-0900, United States

Sang Kil Lee, MD, Assistant Professor, Department of Gastroenterology, Yonsei University College of Medicine, 134 Shinchon-dong, Seodaemun-gu, Seoul 120-752, South Korea

Jong H Moon, MD, PhD, Professor of Medicine, Digestive Disease Center, Soon Chun Hyang University Bucheon Hospital, 1174 Jung-Dong, Wonmi-Ku, Bucheon 420-767, South Korea

Vittorio Ricci, MD, PhD, Department of Physiology, Human Physiology Section, University of Pavia Medical School, Via Forlanini 6, 27100 Pavia, Italy

Francisco Rodriguez-Frias, PhD, Proteins Hepatitis Molecular Genetics Unitat, Biochemistry Department, Vall d'Hebron Unicersitary Hospital, 08035 Barcelona, Spain

Ji Kon Ryu, Professor, Department of Internal Medicine, Seoul National University College of Medicine, 28 Yeongeon-dong, Jongno-gu, Seoul 110-744, South Korea

George Sgourakis, MD, PhD, FACS, 2nd Surgical Department and Surgical Oncology Unit, Red Cross Hospital, 11 Mantzarou Str, Neo Psychiko, 15451 Athens, Greece

Branko Stefanovic, PhD, Department of Biomedical Sciences, College of Medicine, Florida State University, 1115 W.Call st, Tallahassee, FL 32306-4300, United States

Masahiro Tajika, MD, PhD, Department of Endoscopy, Aichi Cancer Center Hospital, 1-1 Kanokoden, Chikusa-ku, Nagoya 464-8681, Japan

Naoki Tanaka, MD, PhD, Department of Metabolic Regulation, Shinshu University Graduate School of Medicine, Asahi 3-1-1, Matsumoto 390-8621, Japan

Dr. Shinji Tanaka, Director, Department of Endoscopy, Hiroshima University Hospital, 1-2-3 Kasumi, Minami-ku, Hiroshima 734-8551, Japan

Yucel Ustundag, Professor, Department of Gastroenterology, Zonguldak Karaelmas University School of Medicine, 67600 Zonguldak, Turkey

Fang Yan, MD, PhD, Research Associate Professor, Division of Gastroenterology, Department of Pediatrics, Hepatology, and Nutrition, Vanderbilt University Medical Center, 2215 Garland Avenue, MRB Ⅳ, Room 1035J, Nashville, TN 37232, United States

Lin Zhang, PhD, Associate Professor, Department of Pharmacology and Chemical Biology, University of Pittsburgh Cancer Institute, University of Pittsburgh School of Medicine, UPCI Research Pavilion, Room 2.42d, Hillman Cancer Center, 5117 Centre Ave., Pittsburgh, PA 15213-1863, United States

World Journal of Gastroenterology

Online Submissions: http://www.wjgnet.com/1007-9327office
wjg@wjgnet.com
www.wjgnet.com

World J Gastroenterol 2012 June 21; 18(23): I
ISSN 1007-9327 (print) ISSN 2219-2840 (online)

Events Calendar 2012

January 13-15, 2012
Asian Pacific *Helicobacter pylori* Meeting 2012
Kuala Lumpur, Malaysia

January 19-21, 2012
American Society of Clinical Oncology 2012 Gastrointestinal Cancers Symposium
San Francisco, CA 3000, United States

January 19-21, 2012
2012 Gastrointestinal Cancers Symposium
San Francisco, CA 94103, United States

January 20-21, 2012
American Gastroenterological Association Clinical Congress of Gastroenterology and Hepatology
Miami Beach, FL 33141, United States

February 3, 2012
The Future of Obesity Treatment
London, United Kingdom

February 16-17, 2012
4th United Kingdom Swallowing Research Group Conference
London, United Kingdom

February 23, 2012
Management of Barretts Oesophagus: Everything you need to know
Cambridge, United Kingdom

February 24-27, 2012
Canadian Digestive Diseases Week 2012
Montreal, Canada

March 1-3, 2012
International Conference on Nutrition and Growth 2012
Paris, France

March 7-10, 2012
Society of American Gastrointestinal and Endoscopic Surgeons Annual Meeting
San Diego, CA 92121, United States

March 12-14, 2012
World Congress on Gastroenterology and Urology
Omaha, NE 68197, United States

March 17-20, 2012
Mayo Clinic Gastroenterology and Hepatology
Orlando, FL 32808, United States

March 26-27, 2012
26th Annual New Treatments in Chronic Liver Disease
San Diego, CA 92121, United States

March 30-April 2, 2012
Mayo Clinic Gastroenterology and Hepatology
San Antonio, TX 78249, United States

March 31-April 1, 2012
27th Annual New Treatments in Chronic Liver Disease
San Diego, CA 92121, United States

April 8-10, 2012
9th International Symposium on Functional GI Disorders
Milwaukee, WI 53202, United States

April 13-15, 2012
Asian Oncology Summit 2012
Singapore, Singapore

April 15-17, 2012
European Multidisciplinary Colorectal Cancer Congress 2012
Prague, Czech

April 18-20, 2012
The International Liver Congress 2012
Barcelona, Spain

April 19-21, 2012
Internal Medicine 2012
New Orleans, LA 70166, United States

April 20-22, 2012
Diffuse Small Bowel and Liver Diseases
Melbourne, Australia

April 22-24, 2012
EUROSON 2012 EFSUMB Annual Meeting
Madrid, Spain

April 28, 2012
Issues in Pediatric Oncology
Kiev, Ukraine

May 3-5, 2012
9th Congress of The Jordanian Society of Gastroenterology
Amman, Jordan

May 7-10, 2012
Digestive Diseases Week
Chicago, IL 60601, United States

May 17-21, 2012
2012 ASCRS Annual Meeting-American Society of Colon and Rectal Surgeons
Hollywood, FL 1300, United States

May 18-19, 2012
Pancreas Club Meeting
San Diego, CA 92101, United States

May 18-23, 2012
SGNA: Society of Gastroenterology Nurses and Associates Annual Course
Phoenix, AZ 85001, United States

May 19-22, 2012
2012-Digestive Disease Week
San Diego, CA 92121, United States

June 2-6, 2012
American Society of Colon and Rectal Surgeons Annual Meeting
San Antonio, TX 78249, United States

June 18-21, 2012
Pancreatic Cancer: Progress and Challenges
Lake Tahoe, NV 89101, United States

July 25-26, 2012
PancreasFest 2012
Pittsburgh, PA 15260, United States

September 1-4, 2012
OESO 11th World Conference
Como, Italy

September 6-8, 2012
2012 Joint International Neurogastroenterology and Motility Meeting
Bologna, Italy

September 7-9, 2012
The Viral Hepatitis Congress
Frankfurt, Germany

September 8-9, 2012
New Advances in Inflammatory Bowel Disease
La Jolla, CA 92093, United States

September 8-9, 2012
Florida Gastroenterologic Society 2012 Annual Meeting
Boca Raton, FL 33498, United States

September 15-16, 2012
Current Problems of Gastroenterology and Abdominal Surgery
Kiev, Ukraine

September 20-22, 2012
1st World Congress on Controversies in the Management of Viral Hepatitis
Prague, Czech

October 19-24, 2012
American College of Gastroenterology 77th Annual Scientific Meeting and Postgraduate Course
Las Vegas, NV 89085, United States

November 3-4, 2012
Modern Technologies in Diagnosis and Treatment of Gastroenterological Patients
Dnepropetrovsk, Ukraine

November 4-8, 2012
The Liver Meeting
San Francisco, CA 94101, United States

November 9-13, 2012
American Association for the Study of Liver Diseases
Boston, MA 02298, United States

December 1-4, 2012
Advances in Inflammatory Bowel Diseases
Hollywood, FL 33028, United States

World Journal of Gastroenterology

Online Submissions: http://www.wjgnet.com/1007-9327office
wjg@wjgnet.com
www.wjgnet.com

World J Gastroenterol 2012 June 21; 18(23): I-VI
ISSN 1007-9327 (print) ISSN 2219-2840 (online)

GENERAL INFORMATION

World Journal of Gastroenterology (*World J Gastroenterol*, *WJG*, print ISSN 1007-9327, online ISSN 2219-2840, DOI: 10.3748) is a weekly, open-access (OA), peer-reviewed journal supported by an editorial board of 1352 experts in gastroenterology and hepatology from 64 countries.

The biggest advantage of the OA model is that it provides free, full-text articles in PDF and other formats for experts and the public without registration, which eliminates the obstacle that traditional journals possess and usually delays the speed of the propagation and communication of scientific research results. The open access model has been proven to be a true approach that may achieve the ultimate goal of the journals, i.e. the maximization of the value to the readers, authors and society.

Maximization of personal benefits

The role of academic journals is to exhibit the scientific levels of a country, a university, a center, a department, and even a scientist, and build an important bridge for communication between scientists and the public. As we all know, the significance of the publication of scientific articles lies not only in disseminating and communicating innovative scientific achievements and academic views, as well as promoting the application of scientific achievements, but also in formally recognizing the "priority" and "copyright" of innovative achievements published, as well as evaluating research performance and academic levels. So, to realize these desired attributes of *WJG* and create a well-recognized journal, the following four types of personal benefits should be maximized. The maximization of personal benefits refers to the pursuit of the maximum personal benefits in a well-considered optimal manner without violation of the laws, ethical rules and the benefits of others. (1) Maximization of the benefits of editorial board members: The primary task of editorial board members is to give a peer review of an unpublished scientific article via online office system to evaluate its innovativeness, scientific and practical values and determine whether it should be published or not. During peer review, editorial board members can also obtain cutting-edge information in that field at first hand. As leaders in their field, they have priority to be invited to write articles and publish commentary articles. We will put peer reviewers' names and affiliations along with the article they reviewed in the journal to acknowledge their contribution; (2) Maximization of the benefits of authors: Since *WJG* is an open-access journal, readers around the world can immediately download and read, free of charge, high-quality, peer-reviewed articles from *WJG* official website, thereby realizing the goals and significance of the communication between authors and peers as well as public reading; (3) Maximization of the benefits of readers: Readers can read or use, free of charge, high-quality peer-reviewed articles without any limits, and cite the arguments, viewpoints, concepts, theories, methods, results, conclusion or facts and data of pertinent literature so as to validate the innovativeness, scientific and practical values of their own research achievements, thus ensuring that their articles have novel arguments or viewpoints, solid evidence and correct conclusion; and (4) Maximization of the benefits of employees: It is an iron law that a first-class journal is unable to exist without first-class editors, and only first-class editors can create a first-class academic journal. We insist on strengthening our team cultivation and construction so that every employee, in an open, fair and transparent environment, could contribute their wisdom to edit and publish high-quality articles, thereby realizing the maximization of the personal benefits of editorial board members, authors and readers, and yielding the greatest social and economic benefits.

Aims and scope

The major task of *WJG* is to report rapidly the most recent results in basic and clinical research on esophageal, gastrointestinal, liver, pancreas and biliary tract diseases, *Helicobacter pylori*, endoscopy and gastrointestinal surgery, including: gastroesophageal reflux disease, gastrointestinal bleeding, infection and tumors; gastric and duodenal disorders; intestinal inflammation, microflora and immunity; celiac disease, dyspepsia and nutrition; viral hepatitis, portal hypertension, liver fibrosis, liver cirrhosis, liver transplantation, and metabolic liver disease; molecular and cell biology; geriatric and pediatric gastroenterology; diagnosis and screening, imaging and advanced technology.

Columns

The columns in the issues of *WJG* will include: (1) Editorial: To introduce and comment on major advances and developments in the field; (2) Frontier: To review representative achievements, comment on the state of current research, and propose directions for future research; (3) Topic Highlight: This column consists of three formats, including (A) 10 invited review articles on a hot topic, (B) a commentary on common issues of this hot topic, and (C) a commentary on the 10 individual articles; (4) Observation: To update the development of old and new questions, highlight unsolved problems, and provide strategies on how to solve the questions; (5) Guidelines for Basic Research: To provide guidelines for basic research; (6) Guidelines for Clinical Practice: To provide guidelines for clinical diagnosis and treatment; (7) Review: To review systemically progress and unresolved problems in the field, comment on the state of current research, and make suggestions for future work; (8) Original Article: To report innovative and original findings in gastroenterology; (9) Brief Article: To briefly report the novel and innovative findings in gastroenterology and hepatology; (10) Case Report: To report a rare or typical case; (11) Letters to the Editor: To discuss and make reply to the contributions published in *WJG*, or to introduce and comment on a controversial issue of general interest; (12) Book Reviews: To introduce and comment on quality monographs of gastroenterology and hepatology; and (13) Guidelines: To introduce consensuses and guidelines reached by international and national academic authorities worldwide on basic research and clinical practice gastroenterology and hepatology.

Name of journal

World Journal of Gastroenterology

ISSN and EISSN
ISSN 1007-9327 (print)
ISSN 2219-2840 (online)

Editorial office
World Journal of Gastroenterology
Editorial Department: Room 903, Building D,
Ocean International Center,
No. 62 Dongsihuan Zhonglu,
Chaoyang District, Beijing 100025, China
E-mail: wjg@wjgnet.com
http://www.wjgnet.com
Telephone: +86-10-59080039
Fax: +86-10-85381893

Indexed and abstracted in
Current Contents®/Clinical Medicine, Science Citation Index Expanded (also known as SciSearch®), Journal Citation Reports®, Index Medicus, MEDLINE, PubMed, PubMed Central, Digital Object Identifier, and Directory of Open Access Journals. ISI, Thomson Reuters, 2010 Impact Factor: 2.240 (35/71 Gastroenterology and Hepatology).

Published by
Baishideng Publishing Group Co., Limited

SPECIAL STATEMENT

All articles published in this journal represent the viewpoints of the authors except where indicated otherwise.

Biostatistical editing
Statistical review is performed after peer review. We invite an expert in Biomedical Statistics from to evaluate the statistical method used in the paper, including *t* test (group or paired comparisons), chi-squared test, Ridit, probit, logit, regression (linear, curvilinear, or stepwise), correlation, analysis of variance, analysis of covariance, *etc*. The reviewing points include: (1) Statistical methods should be described when they are used to verify the results; (2) Whether the statistical techniques are suitable or correct; (3) Only homogeneous data can be averaged. Standard deviations are preferred to standard errors. Give the number of observations and subjects (*n*). Losses in observations, such as drop-outs from the study should be reported; (4) Values such as ED50, LD50, IC50 should have their 95% confidence limits calculated and compared by weighted probit analysis (Bliss and Finney); and (5) The word 'significantly' should be replaced by its synonyms (if it indicates extent) or the *P* value (if it indicates statistical significance).

Conflict-of-interest statement
In the interests of transparency and to help reviewers assess any potential bias, *WJG* requires authors of all papers to declare any competing commercial, personal, political, intellectual, or religious interests in relation to the submitted work. Referees are also asked to indicate any potential conflict they might have reviewing a particular paper. Before submitting, authors are suggested to read "Uniform Requirements for Manuscripts Submitted to Biomedical Journals: Ethical Considerations in the Conduct and Reporting of Research: Conflicts of Interest" from International Committee of Medical Journal Editors (ICMJE), which is available at: http://www.icmje.org/ethical_4conflicts.html.

Sample wording: [Name of individual] has received fees for serving as a speaker, a consultant and an advisory board member for [names of organizations], and has received research funding from [names of organization]. [Name of individual] is an employee of [name of organization]. [Name of individual] owns stocks and shares in [name of organization]. [Name of individual] owns patent [patent identification and brief description].

Statement of informed consent
Manuscripts should contain a statement to the effect that all human studies have been reviewed by the appropriate ethics committee or it should be stated clearly in the text that all persons gave their informed consent prior to their inclusion in the study. Details that might disclose the identity of the subjects under study should be omitted. Authors should also draw attention to the Code of Ethics of the World Medical Association (Declaration of Helsinki, 1964, as revised in 2004).

Statement of human and animal rights
When reporting the results from experiments, authors should follow the highest standards and the trial should conform to Good Clinical Practice (for example, US Food and Drug Administration Good Clinical Practice in FDA-Regulated Clinical Trials; UK Medicines Research Council Guidelines for Good Clinical Practice in Clinical Trials) and/or the World Medical Association Declaration of Helsinki. Generally, we suggest authors follow the lead investigator's national standard. If doubt exists whether the research was conducted in accordance with the above standards, the authors must explain the rationale for their approach and demonstrate that the institutional review body explicitly approved the doubtful aspects of the study.

Before submitting, authors should make their study approved by the relevant research ethics committee or institutional review board. If human participants were involved, manuscripts must be accompanied by a statement that the experiments were undertaken with the understanding and appropriate informed consent of each. Any personal item or information will not be published without explicit consents from the involved patients. If experimental animals were used, the materials and methods (experimental procedures) section must clearly indicate that appropriate measures were taken to minimize pain or discomfort, and details of animal care should be provided.

SUBMISSION OF MANUSCRIPTS

Manuscripts should be typed in 1.5 line spacing and 12 pt. Book Antiqua with ample margins. Number all pages consecutively, and start each of the following sections on a new page: Title Page, Abstract, Introduction, Materials and Methods, Results, Discussion, Acknowledgements, References, Tables, Figures, and Figure Legends. Neither the editors nor the publisher are responsible for the opinions expressed by contributors. Manuscripts formally accepted for publication become the permanent property of Baishideng Publishing Group Co., Limited, and may not be reproduced by any means, in whole or in part, without the written permission of both the authors and the publisher. We reserve the right to copy-edit and put onto our website accepted manuscripts. Authors should follow the relevant guidelines for the care and use of laboratory animals of their institution or national animal welfare committee. For the sake of transparency in regard to the performance and reporting of clinical trials, we endorse the policy of the ICMJE to refuse to publish papers on clinical trial results if the trial was not recorded in a publicly-accessible registry at its outset. The only register now available, to our knowledge, is http://www.clinicaltrials.gov sponsored by the United States National Library of Medicine and we encourage all potential contributors to register with it. However, in the case that other registers become available you will be duly notified. A letter of recommendation from each author's organization should be provided with the contributed article to ensure the privacy and secrecy of research is protected.

Authors should retain one copy of the text, tables, photographs and illustrations because rejected manuscripts will not be returned to the author(s) and the editors will not be responsible for loss or damage to photographs and illustrations sustained during mailing.

Online submissions

Manuscripts should be submitted through the Online Submission System at: http://www.wjgnet.com/1007-9327office. Authors are highly recommended to consult the ONLINE INSTRUCTIONS TO AUTHORS (http://www.wjgnet.com/1007-9327/g_info_20100315215714.htm) before attempting to submit online. For assistance, authors encountering problems with the Online Submission System may send an email describing the problem to wjg@wjgnet.com, or by telephone: +86-10-5908-0039. If you submit your manuscript online, do not make a postal contribution. Repeated online submission for the same manuscript is strictly prohibited.

MANUSCRIPT PREPARATION

All contributions should be written in English. All articles must be submitted using word-processing software. All submissions must be typed in 1.5 line spacing and 12 pt. Book Antiqua with ample margins. Style should conform to our house format. Required information for each of the manuscript sections is as follows:

Title page

Title: Title should be less than 12 words.

Running title: A short running title of less than 6 words should be provided.

Authorship: Authorship credit should be in accordance with the standard proposed by ICMJE, based on (1) substantial contributions to conception and design, acquisition of data, or analysis and interpretation of data; (2) drafting the article or revising it critically for important intellectual content; and (3) final approval of the version to be published. Authors should meet conditions 1, 2, and 3.

Institution: Author names should be given first, then the complete name of institution, city, province and postcode. For example, Xu-Chen Zhang, Li-Xin Mei, Department of Pathology, Chengde Medical College, Chengde 067000, Hebei Province, China. One author may be represented from two institutions, for example, George Sgourakis, Department of General, Visceral, and Transplantation Surgery, Essen 45122, Germany; George Sgourakis, 2nd Surgical Department, Korgialenio-Benakio Red Cross Hospital, Athens 15451, Greece.

Author contributions: The format of this section should be: Author contributions: Wang CL and Liang L contributed equally to this work; Wang CL, Liang L, Fu JF, Zou CC, Hong F and Wu XM designed the research; Wang CL, Zou CC, Hong F and Wu XM performed the research; Xue JZ and Lu JR contributed new reagents/analytic tools; Wang CL, Liang L and Fu JF analyzed the data; and Wang CL, Liang L and Fu JF wrote the paper.

Supportive foundations: The complete name and number of supportive foundations should be provided, e.g. Supported by National Natural Science Foundation of China, No. 30224801

Correspondence to: Only one corresponding address should be provided. Author names should be given first, then author title, affiliation, the complete name of institution, city, postcode, province, country, and email. All the letters in the email should be in lower case. A space interval should be inserted between country name and email address. For example, Montgomery Bissell, MD, Professor of Medicine, Chief, Liver Center, Gastroenterology Division, University of California, Box 0538, San Francisco, CA 94143, United States. montgomery.bissell@ucsf.edu

Telephone and fax: Telephone and fax should consist of +, country number, district number and telephone or fax number, e.g. Telephone: +86-10-59080039 Fax: +86-10-85381893

Peer reviewers: All articles received are subject to peer review. Normally, three experts are invited for each article. Decision for acceptance is made only when at least two experts recommend an article for publication. Reviewers for accepted manuscripts are acknowledged in each manuscript, and reviewers of articles which were not accepted will be acknowledged at the end of each issue. To ensure the quality of the articles published in *WJG*, reviewers of accepted manuscripts will be announced by publishing the name, title/position and institution of the reviewer in the footnote accompanying the printed article. For example, reviewers: Professor Jing-Yuan Fang, Shanghai Institute of Digestive Disease, Shanghai, Affiliated Renji Hospital, Medical Faculty, Shanghai Jiaotong University, Shanghai, China; Professor Xin-Wei Han, Department of Radiology, The First Affiliated Hospital, Zhengzhou University, Zhengzhou, Henan Province, China; and Professor Anren Kuang, Department of Nuclear Medicine, Huaxi Hospital, Sichuan University, Chengdu, Sichuan Province, China.

Abstract

There are unstructured abstracts (no less than 256 words) and structured abstracts (no less than 480). The specific requirements for structured abstracts are as follows:

An informative, structured abstracts of no less than 480 words should accompany each manuscript. Abstracts for original contributions should be structured into the following sections.

AIM (no more than 20 words): Only the purpose should be included. Please write the aim as the form of "To investigate/study/…"; MATERIALS AND METHODS (no less than 140 words); RESULTS (no less than 294 words): You should present *P* values where appropriate and must provide relevant data to illustrate how they were obtained, e.g. 6.92 ± 3.86 *vs* 3.61 ± 1.67, $P < 0.001$; CONCLUSION (no more than 26 words).

Key words

Please list 5-10 key words, selected mainly from *Index Medicus*, which reflect the content of the study.

Text

For articles of these sections, original articles and brief articles, the main text should be structured into the following sections: INTRODUCTION, MATERIALS AND METHODS, RESULTS and DISCUSSION, and should include appropriate Figures and Tables. Data should be presented in the main text or in Figures and Tables, but not in both. The main text format of these sections, editorial, topic highlight, case report, letters to the editors, can be found at: http://www.wjgnet.com/1007-9327/g_info_20100315215714.htm.

Illustrations

Figures should be numbered as 1, 2, 3, *etc.*, and mentioned clearly in the main text. Provide a brief title for each figure on a separate page. Detailed legends should not be provided under the figures. This part should be added into the text where the figures are applicable. Figures should be either Photoshop or Illustrator files (in tiff, eps, jpeg formats) at high-resolution. Examples can be found at: http://www.wjgnet.com/1007-9327/13/4520.pdf; http://www.wjgnet.com/1007-9327/13/4554.pdf; http://www.wjgnet.com/1007-9327/13/4891.pdf; http://www.wjgnet.com/1007-9327/13/4986.pdf; http://www.wjgnet.com/1007-9327/13/4498.pdf. Keeping all elements compiled is necessary in line-art image. Scale bars should be used rather than magnification factors, with the length of the bar defined in the legend rather than on the bar itself. File names should identify the figure and panel. Avoid layering type directly over shaded or textured areas. Please use uniform legends for the same subjects. For example: Figure 1 Pathological changes in atrophic gastritis after treatment. A:...; B:...; C:...; D:...; E:...; F:...; G: …*etc.* It is our principle to publish high resolution-figures for the printed and E-versions.

Tables

Three-line tables should be numbered 1, 2, 3, *etc.*, and mentioned clearly in the main text. Provide a brief title for each table. Detailed legends should not be included under tables, but rather added into the text where applicable. The information should complement, but not duplicate the text. Use one horizontal line under the title, a second under column heads, and a third below the Table, above any footnotes. Vertical and italic lines should be omitted.

Notes in tables and illustrations

Data that are not statistically significant should not be noted. $^{a}P < 0.05$, $^{b}P < 0.01$ should be noted ($P > 0.05$ should not be noted). If there are other series of *P* values, $^{c}P < 0.05$ and $^{d}P < 0.01$ are used. A third series of *P* values can be expressed as $^{e}P < 0.05$ and $^{f}P < 0.01$. Other notes in tables or under illustrations should be expressed as ^{1}F, ^{2}F, ^{3}F; or sometimes as other symbols with a superscript (Arabic numerals) in the upper left corner. In a multi-curve illustration, each curve should be labeled with ●, ○, ■, □, ▲, △, *etc.*, in a certain sequence.

Acknowledgments

Brief acknowledgments of persons who have made genuine contributions to the manuscript and who endorse the data and conclusions should be included. Authors are responsible for obtaining written permission to use any copyrighted text and/or illustrations.

REFERENCES

Coding system

The author should number the references in Arabic numerals according to the citation order in the text. Put reference numbers in square brackets in superscript at the end of citation content or after the cited author's name. For citation content which is part of the narration, the coding number and square brackets should be typeset normally. For example, "Crohn's disease (CD) is associated with increased intestinal permeability[1,2]". If references are cited directly in the text, they should be put together within the text, for example, "From references[19,22-24], we know that...".

When the authors write the references, please ensure that the order in text is the same as in the references section, and also ensure the spelling accuracy of the first author's name. Do not list the same citation twice.

PMID and DOI

Pleased provide PubMed citation numbers to the reference list, e.g. PMID and DOI, which can be found at http://www.ncbi.nlm.nih.gov/sites/entrez?db=pubmed and http://www.crossref.org/SimpleTextQuery/, respectively. The numbers will be used in E-version of this journal.

Style for journal references

Authors: the name of the first author should be typed in boldfaced letters. The family name of all authors should be typed with the initial letter capitalized, followed by their abbreviated first and middle initials. (For example, Lian-Sheng Ma is abbreviated as Ma LS, Bo-Rong Pan as Pan BR). The title of the cited article and italicized journal title (journal title should be in its abbreviated form as shown in PubMed), publication date, volume number (in black), start page, and end page [PMID: 11819634 DOI: 10.3748/wjg.13.5396].

Style for book references

Authors: the name of the first author should be typed in boldfaced letters. The surname of all authors should be typed with the initial letter capitalized, followed by their abbreviated middle and first initials. (For example, Lian-Sheng Ma is abbreviated as Ma LS, Bo-Rong Pan as Pan BR) Book title. Publication number. Publication place: Publication press, Year: start page and end page.

Format

Journals

English journal article (list all authors and include the PMID where applicable)

1 **Jung EM**, Clevert DA, Schreyer AG, Schmitt S, Rennert J, Kubale R, Feuerbach S, Jung F. Evaluation of quantitative contrast harmonic imaging to assess malignancy of liver tumors: A prospective controlled two-center study. *World J Gastroenterol* 2007; **13**: 6356-6364 [PMID: 18081224 DOI: 10.3748/wjg.13.6356]

Chinese journal article (list all authors and include the PMID where applicable)

2 **Lin GZ**, Wang XZ, Wang P, Lin J, Yang FD. Immunolog-

ic effect of Jianpi Yishen decoction in treatment of Pixudiarrhoea. *Shijie Huaren Xiaohua Zazhi* 1999; **7**: 285-287

In press

3 **Tian D**, Araki H, Stahl E, Bergelson J, Kreitman M. Signature of balancing selection in Arabidopsis. *Proc Natl Acad Sci USA* 2006; In press

Organization as author

4 **Diabetes Prevention Program Research Group**. Hypertension, insulin, and proinsulin in participants with impaired glucose tolerance. *Hypertension* 2002; **40**: 679-686 [PMID: 12411462 PMCID:2516377 DOI:10.1161/01.HYP.0000035706.28494.09]

Both personal authors and an organization as author

5 **Vallancien G**, Emberton M, Harving N, van Moorselaar RJ; Alf-One Study Group. Sexual dysfunction in 1, 274 European men suffering from lower urinary tract symptoms. *J Urol* 2003; **169**: 2257-2261 [PMID: 12771764 DOI:10.1097/01.ju.0000067940.76090.73]

No author given

6 21st century heart solution may have a sting in the tail. *BMJ* 2002; **325**: 184 [PMID: 12142303 DOI:10.1136/bmj.325.7357.184]

Volume with supplement

7 **Geraud G**, Spierings EL, Keywood C. Tolerability and safety of frovatriptan with short- and long-term use for treatment of migraine and in comparison with sumatriptan. *Headache* 2002; **42** Suppl 2: S93-99 [PMID: 12028325 DOI:10.1046/j.1526-4610.42.s2.7.x]

Issue with no volume

8 **Banit DM**, Kaufer H, Hartford JM. Intraoperative frozen section analysis in revision total joint arthroplasty. *Clin Orthop Relat Res* 2002; (**401**): 230-238 [PMID: 12151900 DOI:10.1097/00003086-200208000-00026]

No volume or issue

9 Outreach: Bringing HIV-positive individuals into care. *HRSA Careaction* 2002; 1-6 [PMID: 12154804]

Books

Personal author(s)

10 **Sherlock S**, Dooley J. Diseases of the liver and billiary system. 9th ed. Oxford: Blackwell Sci Pub, 1993: 258-296

Chapter in a book (list all authors)

11 **Lam SK**. Academic investigator's perspectives of medical treatment for peptic ulcer. In: Swabb EA, Azabo S. Ulcer disease: investigation and basis for therapy. New York: Marcel Dekker, 1991: 431-450

Author(s) and editor(s)

12 **Breedlove GK**, Schorfheide AM. Adolescent pregnancy. 2nd ed. Wieczorek RR, editor. White Plains (NY): March of Dimes Education Services, 2001: 20-34

Conference proceedings

13 **Harnden P**, Joffe JK, Jones WG, editors. Germ cell tumours V. Proceedings of the 5th Germ cell tumours Conference; 2001 Sep 13-15; Leeds, UK. New York: Springer, 2002: 30-56

Conference paper

14 **Christensen S**, Oppacher F. An analysis of Koza's computational effort statistic for genetic programming. In: Foster JA, Lutton E, Miller J, Ryan C, Tettamanzi AG, editors. Genetic programming. EuroGP 2002: Proceedings of the 5th European Conference on Genetic Programming; 2002 Apr 3-5; Kinsdale, Ireland. Berlin: Springer, 2002: 182-191

Electronic journal (list all authors)

15 Morse SS. Factors in the emergence of infectious diseases. Emerg Infect Dis serial online, 1995-01-03, cited 1996-06-05; 1(1): 24 screens. Available from: URL: http://www.cdc.gov/ncidod/eid/index.htm

Patent (list all authors)

16 **Pagedas AC**, inventor; Ancel Surgical R&D Inc., assignee. Flexible endoscopic grasping and cutting device and positioning tool assembly. United States patent US 20020103498. 2002 Aug 1

Statistical data

Write as mean ± SD or mean ± SE.

Statistical expression

Express *t* test as *t* (in italics), *F* test as *F* (in italics), chi square test as χ^2 (in Greek), related coefficient as *r* (in italics), degree of freedom as υ (in Greek), sample number as *n* (in italics), and probability as *P* (in italics).

Units

Use SI units. For example: body mass, m (B) = 78 kg; blood pressure, p (B) = 16.2/12.3 kPa; incubation time, t (incubation) = 96 h, blood glucose concentration, c (glucose) 6.4 ± 2.1 mmol/L; blood CEA mass concentration, p (CEA) = 8.6 24.5 μg/L; CO_2 volume fraction, 50 mL/L CO_2, not 5% CO_2; likewise for 40 g/L formaldehyde, not 10% formalin; and mass fraction, 8 ng/g, *etc.* Arabic numerals such as 23, 243, 641 should be read 23 243 641.

The format for how to accurately write common units and quantums can be found at: http://www.wjgnet.com/1007-9327/g_info_20100315223018.htm.

Abbreviations

Standard abbreviations should be defined in the abstract and on first mention in the text. In general, terms should not be abbreviated unless they are used repeatedly and the abbreviation is helpful to the reader. Permissible abbreviations are listed in Units, Symbols and Abbreviations: A Guide for Biological and Medical Editors and Authors (Ed. Baron DN, 1988) published by The Royal Society of Medicine, London. Certain commonly used abbreviations, such as DNA, RNA, HIV, LD50, PCR, HBV, ECG, WBC, RBC, CT, ESR, CSF, IgG, ELISA, PBS, ATP, EDTA, mAb, can be used directly without further explanation.

Italics

Quantities: *t* time or temperature, *c* concentration, *A* area, *l* length, *m* mass, *V* volume.

Genotypes: *gyrA*, *arg* 1, *c myc*, *c fos*, *etc.*

Restriction enzymes: *Eco*RI, *Hin*dI, *Bam*HI, *Kbo* I, *Kpn* I, *etc.*

Biology: *H. pylori*, *E coli*, *etc.*

Examples for paper writing

Editorial: http://www.wjgnet.com/1007-9327/g_info_20100315220036.htm

Frontier: http://www.wjgnet.com/1007-9327/g_info_20100315220305.htm

Topic highlight: http://www.wjgnet.com/1007-9327/g_info_20100315220601.htm

Observation: http://www.wjgnet.com/1007-9327/g_info_20100312232427.htm

Guidelines for basic research: http://www.wjgnet.com/1007-9327/g_info_20100315220730.htm

Guidelines for clinical practice: http://www.wjgnet.com/1007-9327/g_info_20100315221301.htm

Review: http://www.wjgnet.com/1007-9327/g_info_20100315221554.htm

Original articles: http://www.wjgnet.com/1007-9327/g_info_20100315221814.htm

Brief articles: http://www.wjgnet.com/1007-9327/g_info_20100312231400.htm

Case report: http://www.wjgnet.com/1007-9327/g_info_20100315221946.htm

Letters to the editor: http://www.wjgnet.com/1007-9327/g_info_20100315222254.htm

Book reviews: http://www.wjgnet.com/1007-9327/g_info_20100312231947.htm

Guidelines: http://www.wjgnet.com/1007-9327/g_info_20100312232134.htm

RESUBMISSION OF THE REVISED MANUSCRIPTS

Please revise your article according to the revision policies of *WJG*. The revised version including manuscript and high-resolution image figures (if any) should be re-submitted online (http://www.wjgnet.com/1007-9327office/). The author should send the copyright transfer letter, responses to the reviewers, English language Grade B certificate (for non-native speakers of English) and final manuscript checklist to wjg@wjgnet.com.

Language evaluation

The language of a manuscript will be graded before it is sent for revision. (1) Grade A: priority publishing; (2) Grade B: minor language polishing; (3) Grade C: a great deal of language polishing needed; and (4) Grade D: rejected. Revised articles should reach Grade A or B.

Copyright assignment form

Please download a Copyright assignment form from http://www.wjgnet.com/1007-9327/g_info_20100315222818.htm.

Responses to reviewers

Please revise your article according to the comments/suggestions provided by the reviewers. The format for responses to the reviewers' comments can be found at: http://www.wjgnet.com/1007-9327/g_info_20100315222607.htm.

Proof of financial support

For paper supported by a foundation, authors should provide a copy of the document and serial number of the foundation.

Links to documents related to the manuscript

WJG will be initiating a platform to promote dynamic interactions between the editors, peer reviewers, readers and authors. After a manuscript is published online, links to the PDF version of the submitted manuscript, the peer-reviewers' report and the revised manuscript will be put on-line. Readers can make comments on the peer reviewer's report, authors' responses to peer reviewers, and the revised manuscript. We hope that authors will benefit from this feedback and be able to revise the manuscript accordingly in a timely manner.

Science news releases

Authors of accepted manuscripts are suggested to write a science news item to promote their articles. The news will be released rapidly at EurekAlert/AAAS (http://www.eurekalert.org). The title for news items should be less than 90 characters; the summary should be less than 75 words; and main body less than 500 words. Science news items should be lawful, ethical, and strictly based on your original content with an attractive title and interesting pictures.

Publication fee

WJG is an international, peer-reviewed, Open-Access, online journal. Articles published by this journal are distributed under the terms of the Creative Commons Attribution Non-commercial License, which permits use, distribution, and reproduction in any medium, provided the original work is properly cited, the use is non commercial and is otherwise in compliance with the license. Authors of accepted articles must pay a publication fee. The related standards are as follows. Publication fee: 1300 USD per article. Editorial, topic highlights, book reviews and letters to the editor are published free of charge.

World Journal of Gastroenterology®

Volume 18 Number 23
June 21, 2012

Published by Baishideng Publishing Group Co., Limited
Room 1701, 17/F, Henan Building,
No. 90 Jaffe Road, Wanchai, Hong Kong, China
Fax: +852-31158812
Telephone: +852-58042046
E-mail: bpg@baishideng.com
http://www.wjgnet.com

ISSN 1007-9327

ISSN 1007-9327 CN 14-1219/R Local Post Offices Code No. 82-261